

University of South Wales
Faculty of Computing, Engineering & Science
School of Engineering

***PERFORMANCE ENHANCEMENT OF CONCRETE PRODUCED WITH
TREATED DEMOLITION WASTE AGGREGATES***

QUSAI FANDI AL-WAKED

Supervised by:

Director of Studies: Dr. Jiping Bai

Prof. John Kinuthia

Dr. Paul Davies

*A Thesis Submitted to The University of South Wales as Fulfilment of The Requirements of
The Degree of Doctor of Philosophy in Civil Engineering*

JUNE 2022

DECLARATION

Statement of Originality & Data Protection

I hereby declare that this thesis, together with the work contained herein, was produced entirely by myself, and contains no materials that have been accepted for the award of any other degree or diploma in any university. To the best of my knowledge and belief, this thesis contains no material previously published or written by another person except where due acknowledgement to others has been made.

I Qusai Fandi Al-Waked, hereby give my consent for data protection purposes to the release, within the confines of the University of South Wales, of my dissertation **“PERFORMANCE ENHANCEMENT OF CONCRETE PRODUCED WITH TREATED DEMOLITION WASTE AGGREGATES”** year 2022, to students and others in pursuit of their studies for inspection. I accept that all other legal rights pertaining to my dissertation are hereby unaffected.

.....

Signature/Date

Qusai Fandi Al-Waked

CERTIFICATE OF RESEARCH

This is to certify that, except where a specific reference is made, the work described in this thesis is the result of work carried out by the candidate. Neither this thesis nor any part of it has been presented or is currently submitted in candidature for any other degree at any other university.

..... Date
Qusai Fandi Al-Waked
(P.hD. Candidate)

..... Date
Dr. Jiping Bai
(Director of studies)

..... Date
Professor John Kinuthia
(Supervisor)

..... Date
Dr. Paul Davies
(Supervisor)

List of Publications

- Al-Waked, Qusai; Bai, Jiping; Kinuthia, John; Davies, Paul, 2022. Enhancing the aggregate impact value and water absorption of demolition waste coarse aggregates with various treatment methods. *Case studies in construction materials*, volume 17, p. e01267, <https://doi.org/10.1016/j.cscm.2022.e01267>
- Al-Waked, Qusai; Bai, Jiping; Kinuthia, John; Davies, Paul, 2022. Enhancement of Mechanical Properties of Concrete with Treated Demolition Waste Aggregate. *Journal of Building Engineering*, p. 105047, <https://doi.org/10.1016/j.jobe.2022.105047>
- Al-Waked, Qusai; Bai, Jiping; Kinuthia, John; Davies, Paul, 2022. Durability and Microstructural Analyses of Concrete Produced with Treated Demolition Waste Aggregates, *Construction and Building Materials*, volume 347, p. 128597, <https://doi.org/10.1016/j.conbuildmat.2022.128597>

DEDICATION

This research is devoted to my beloved parents, Dr. Fandi Al-Waked and Mrs. Fatimeh ALattari, who have been my non-stopping source of inspiration. It is also lovingly dedicated to my soul mate wife, Mrs. Balqis Alabsi and my baby daughter Maria.

They have given me the drive to tackle my research with determination and enthusiasm. Without their constant love and support, this work would not have been accomplished.

All praise is due to Allah, by whose favour good deeds are accomplished, I praise Him for all His favours and ask Him for an excess of His bounty and generosity.

ACKNOWLEDGEMENT

First and foremost, I would like to praise Allah the Almighty, the Most Merciful, and the Most Gracious for His given blessing to me throughout my work and in successfully completing this thesis.

I want to express my gratitude to my director of studies, Dr. Jiping Bai, for being an outstanding supervisor. His active supervision, encouragement, helpful suggestions, valuable comments, remarks, advice, and assistance made this work successful.

I would also like to thank Prof. John Kinuthia and Dr. Paul Davies for accepting to be members of the supervisory team. Their valuable comments and feedback efficiently enhanced the quality of this work.

Furthermore, I would like to appreciate the crucial role of the laboratory technical staff in Civil Engineering, Mr. Stephen Ngigi, and Mr. Darren Crocker, who gave their support and have willingly shared their precious time during the process of the experimental studies.

I want to express my most profound appreciation to Dr. Fandi Al-Waked, for his outstanding efforts. I can't say thanks enough for his tremendous support and help; I feel motivated and encouraged every time I attend a conversation with him. Without his encouragement and guidance, this project would not have materialised.

I'm incredibly grateful to my close friends, whose support and encouragement helped me organise my project, especially writing this thesis.

Finally, I owe special gratitude to my family, my uncle Ahmed Al-Attari, and my wife for their continuous and unconditional support during my postgraduate years. This thesis would indeed not have existed without them.

ABSTRACT

Recently, the utilisation of recycled aggregate from construction and demolition waste in civil engineering applications has proved to be an eco-friendly approach to overcome the current environmental concerns. Nevertheless, the poor quality of recycled aggregate and the high uncertainty of recycled aggregate concrete structural performance have limited its utilisation in structural applications. The current literature showed only a few studies on the use of treated recycled aggregate from construction and demolition waste and its effect on the different engineering properties of concrete.

The main thrust of this research is to evaluate the effects of different enhancement and treatment methods in enhancing the mechanical properties, durability properties, and microstructure of concrete produced with 100% recycled aggregate from construction and demolition waste, with the overall aim of promoting the use of recycled aggregate in the construction industry. In view of this, an innovative regime of various treatment methods, batching techniques, and their combinations were developed to enhance the engineering properties of recycled aggregate and recycled aggregate concrete. This research studied the geometrical, physical, and mechanical characteristics of the supplied recycled aggregate. It examined the effects of various treatments on Aggregate Impact Value and Water Absorption properties of recycled aggregate. It also investigated the effects of different treatments methods, batching techniques, and their combinations on mechanical performance (workability, density, compressive strength, flexural strength, tensile splitting strength, and modulus of elasticity), durability (water absorption, resistance to freeze-thaw, and resistance to sulphate attack), and the microstructure of recycled aggregate concrete.

The treated recycled aggregate demonstrated an enhanced Aggregate Impact Value of 15% and reduced Water Absorption of 3% compared to the untreated recycled aggregate with 17% and 6.1% Aggregate Impact Value and Water Absorption, respectively. The enhanced recycled aggregate concrete mixes showed an increase in the 28-day compressive strength of up to 46MPa suitable for structural applications, compared to the control untreated recycled aggregate concrete that exhibited 35MPa. The enhanced recycled aggregate concrete mixes also achieved enhanced tensile splitting strength, flexural strength, elastic modulus, and sulphate and freeze-thaw resistance. The improved engineering performance of the treated recycled aggregate concrete is attributed to the strengthened interfacial transition zone, better overall interlocking of the treated recycled aggregate with the new cement paste, filled-up

pores and micro-cracks, reduced porosity, and compacted dense microstructure. The application of the proposed innovative regime of enhancement methods is anticipated to promote the use of recycled aggregate in the construction industry and provide a better and deeper scientific understanding of the performance of concrete produced with 100% treated recycled aggregate from the construction and demolition waste for structural applications.

TABLE OF CONTENTS

ITEM	PAGE NO.
DEDICATION	III
ACKNOWLEDGEMENT	IV
LIST OF PUBLICATIONS.....	V
ABSTRACT	VI
TABLE OF CONTENTS	VIII
LIST OF ABBREVIATIONS & SYMBOLS	XI
LIST OF FIGURES.....	XIII
LIST OF TABLES.....	XVIII
LIST OF EQUATIONS	XX

CHAPTER ONE - INTRODUCTION

1.1 Introduction	22
1.2 Problem Statement	25
1.3 Aims & Objectives	26
1.4 Research Methodology	27
1.5 Contribution to the Existing Knowledge.....	28
1.6 Structure of the Thesis	29

CHAPTER TWO - LITERATURE REVIEW

2.1 Background	32
2.2 Recycled Aggregate (RA).....	33
2.2.1 Composition of RA.....	33
2.2.2 Processing & recovery of construction and demolition waste aggregate.....	33
2.2.3 Specifications & standards	36
2.2.4 Classification of recycled aggregates	36
2.2.5 Interfacial transition zone (ITZ) and adhered mortar of RA	38
2.2.6 Engineering characteristics of recycled aggregate	40
2.2.6.1 Particle properties of RA	40
2.2.6.2 Water absorption of RA	40
2.2.6.3 Aggregate impact value of RA	41
2.2.7 Summary of studies on properties of RA	41
2.3 Engineering Properties of Recycled Aggregate Concrete (RAC)	42

2.3.1 Consistency of fresh RAC	42
2.3.2 Mechanical properties of RAC	45
2.3.2.1 Compressive strength	45
2.3.2.2 Split tensile strength & flexural strength.....	48
2.3.2.3 Modulus of elasticity & stress-strain behaviour	50
2.3.3 Durability properties of RAC	51
2.3.3.1 Water absorption	52
2.3.3.2 Resistance to freeze & thaw	52
2.3.3.3 Sulphate attack	53
2.3.4 Summary of studies on properties of RAC.....	54
2.4 Treatment Methods for Recycled Aggregate	60
2.4.1 Self-healing.....	60
2.4.2 Water washing	60
2.4.3 Water saturation.....	60
2.4.4 Carbonation treatment	60
2.4.5 Soaking RA in sodium silicate - silica fume solution	63
2.4.6 Coating RA with cement slurry or cement-silica fume slurry.....	64
2.4.7 Soaking RA in cement-pozzolan solution	64
2.5 Batching Techniques for Recycled Aggregate Concrete.....	65
2.5.1 Stone enveloped with pozzolan powder (SEPP)	65
2.5.2 Two-stage mixing approach (TSMA).....	65
2.5.3 Sand enveloped mixing approach (SEMA).....	66
2.5.4 Mortar mixing approach (MMA)	66
2.6 Summary of the Current Enhancement Methods for RA and RAC	66
2.7 Research Gaps	71

CHAPTER THREE - MATERIALS

3.1 Portland Cement (PC).....	72
3.2 Pozzolan Materials	73
3.2.1 Pulverised fuel ash.....	73
3.2.2 Silica fume.....	73
3.2.3 Ground granulated blastfurnace slag	73
3.2.4 Metakaolin.....	73
3.3 Aggregates	77
3.3.1 Natural aggregate (NA)	77
3.3.2 Recycled aggregate (RA)	77
3.3.3 Fine aggregate.....	77
3.4 Other Materials.....	81
3.4.1 Sodium silicate	81

3.4.2 Calcium hydroxide	82
3.4.3 Sodium sulphate	82
3.4.4 Dentstone plaster	82
3.4.5 Superplasticiser (SP)	82
CHAPTER FOUR – EXPERIMENTAL METHODOLOGY	
4.1 Experimental Testing Program.....	83
4.2 Aggregate Characterisation.....	86
4.2.1 Sampling of aggregates	86
4.2.2 Composition of recycled aggregates.....	86
4.2.3 Geometrical properties of aggregates used in the current study.....	87
4.2.3.1 Particle size distribution [BS EN 933-1:2012]	87
4.2.3.2 Particle shape [BS EN 933-3:2012] & [BS EN 933-4:2008]	88
4.2.4 Physical and mechanical properties of aggregates	90
4.2.4.1 Particle density and water absorption [BS EN 1097-6:2013]	90
4.2.4.2 Resistance to fragmentation [BS EN 1097-2:2020]	90
4.3 Treatments and Batching Techniques Used for RA & RAC.....	92
4.3.1 Regime A – Water treatment methods	92
4.3.1.1 Water washing of RA	93
4.3.1.2 Water saturation (pre-saturation of RA)	93
4.3.1.3 Self-healing of RA.....	94
4.3.2 Regime B - Strengthening the adhered mortar methods.....	94
4.3.2.1 Accelerated carbonation treatment (AC)	95
4.3.2.2 Soaking RA in sodium silicate - silica fume solution	97
4.3.2.3 Coating with cement slurry or cement-silica fume slurry	97
4.3.2.4 Soaking in different cement-pozzolan solutions (SCP).....	100
4.3.3 Regime C - Batching techniques	101
4.3.3.1 Sand envelope mixing approach (SEMA).....	101
4.3.3.2 Mortar mixing approach (MMA).....	101
4.3.3.3 Stone enveloped with pozzolan powder (SEPP).....	101
4.3.3.4 Two-stage mixing approach (TSMA).....	102
4.3.4 Combination of different treatments with batching techniques	102
4.3.4.1 Bi-combination of SCP and AC.....	102
4.3.4.2 Bi-combination of SCP + SE.....	102
4.3.4.3 Bi-combination of AC + SE.....	103
4.3.4.4 Triple combination of SCP + AC + SE	103
4.4 Concrete Mix Design	103
4.4.1 Preliminary trial concrete mixture compositions	103
4.4.2 Batching techniques mixture compositions.....	104
4.4.3 Optimised mixture compositions.....	105
4.5 Specimen Preparation & Testing of Concrete	107
4.5.1 Specimen preparation & curing condition.....	107

4.5.2 Consistency of fresh concrete [BS EN 12350-2: 2019]	110
4.5.3 Mechanical properties of the hardened concretes.....	111
4.5.3.1 Density of hardened concrete [BS EN 12390-7: 2009].....	111
4.5.3.2 Compressive Strength [BS EN 12390-3: 2009].....	112
4.5.3.3 Tensile splitting strength [BS EN 12390-6: 2009]	113
4.5.3.4 Flexural strength [BS EN 12390-5: 2009]	114
4.5.3.5 Modulus of elasticity [BS EN 12390-13:2021]	115
4.5.4 Durability properties.....	116
4.5.4.1 Water absorption [BS 1881-122:2011+A1:2020]	116
4.5.4.2 Resistance to freeze-thaw [PD CEN/TS 12390-9:2016]	116
4.5.4.3 Resistance to sulphate attack [BS EN 206:2013+A2: 2021]	117
4.5.5 Microstructure investigations	119
4.5.5.1 Scanning Electron Microscopy (SEM) investigation.....	119
4.5.5.2 Energy-dispersive X-ray spectroscopy (EDS)	121

CHAPTER FIVE – RESULTS & DISCUSSION

5.1 Effects of Treatment Methods on Properties of RA.....	123
5.1.1 Effects of Regime A – Water treatment methods on AIV & WA of RA.....	123
5.1.2 Effects of Regime B – Strengthening the adhered mortar on AIV & WA of RA	126
5.2 Effects of Regime C Batching Techniques on Properties of RAC	141
5.2.1 Consistency – slump of fresh RAC with batching techniques	141
5.2.2 Density of hardened RAC with batching techniques.....	142
5.2.3 Compressive strength of RAC with batching techniques.....	143
5.3 Initial Criteria Matrix for Selection of Treatment & Batching Techniques.....	146
5.4 Effects of Treatment & Batching Techniques on Properties of RAC.....	153
5.4.1 Consistency - slump	153
5.4.2 Density of hardened concretes.....	158
5.4.3 Compressive strength	158
5.5 Second Criteria Matrix for Selection of Treatment & Batching Techniques	168
5.6 Effects of Treatment & Batching Techniques on Other Mechanical Performance .	170
5.6.1 Tensile splitting strength	170
5.6.2 Flexural strength.....	173
5.6.3 Modulus of elasticity	178
5.7 Correlation Analysis & Comparison with Design Codes.....	182
5.7.1 Tensile splitting strength vs. flexural strength.....	183
5.7.2 Compressive Strength vs. modulus of elasticity.....	183
5.7.3 Compressive strength vs. tensile splitting strength	184
5.7.4 Compressive strength vs. flexural strength	184
5.8 Effects of Treatment & Batching Techniques on Durability Performance of RAC	186

5.8.1 Water absorption.....	186
5.8.2 Resistance to freeze-thaw cycles	187
5.8.2.1 Visual inspection	188
5.8.2.2 Mass change of treated RACs after freeze-thaw cycles.....	188
5.8.2.3 Compressive strength loss of treated RACs after freeze-thaw cycles.....	190
5.8.3 Sulphate attack resistance	192
5.8.3.1 Visual inspection	193
5.8.3.2 Mass change after sulphate attack	193
5.8.3.3 Compressive strength loss after exposure to sulphate	195
5.9 Effects of Treatment & Batching Techniques on the Microstructure of RAC	198
5.9.1 SEM analyses	198
5.9.2 EDS analysis.....	206
5.10 Practical Implications of the Research	209
5.11 Cost Analysis.....	211
CHAPTER SIX - CONCLUSIONS & RECOMMENDATIONS	
6.1 Conclusions	213
6.1.1 Effects of different treatments on the AIV & WA of RA	213
6.1.2 Effects of batching techniques on the compressive strength of RAC	215
6.1.3 Consistency and compressive strength of the enhanced RAC	216
6.1.4 Flexural, tensile splitting, and modulus of elasticity of the enhanced RACs.....	217
6.1.5 Durability performance of the enhanced RACs	218
6.1.6 Microstructure analyses of the enhanced RACs.....	218
6.2 Recommendations for Further Research	220
REFERENCES	221
APPENDICES.....	256
APPENDIX A.....	256
Appendix A-1: data table for Figures 5.1. & 5.2.....	256
Appendix A-2: data table for Figures 5.3 & 5.4.....	256
Appendix A-3: data table for Figures 5.6 & 5.7.....	256
Appendix A-4: data table for Figures 5.9 & 5.10.....	257
Appendix A-5: data table for Figures 5.11 & 5.12.....	257
Appendix A-6: data table for Figure 5.15	258
APPENDIX B.....	258
Appendix B-1: data table for Figure 5.20.....	258
APPENDIX C.....	259

Appendix C-1: <i>Data table for Figure 5.21</i>	259
Appendix C-2: <i>Data table for Figure 5.23</i>	259
Appendix C-3: <i>Data table for Figure 5.26</i>	259
APPENDIX D	260
Appendix D-1: <i>Data table for Figure 5.29</i>	260
Appendix D-2: <i>Data table for Figures 5.33 & 5.32</i>	260
Appendix D-3: <i>Data table for Figures 5.36 & 5.35</i>	262
APPENDIX E-JOURNAL PUBLICATIONS	263

LIST OF ABBREVIATIONS & SYMBOLS

RA	Recycled aggregate
RAC	Recycled aggregate concrete
NAC	Natural aggregate concrete
NA	Natural aggregate
RCA	Recycled concrete aggregate
C&DW	Construction and demolition waste or demolition waste aggregates
WRAP	Waste & Resources Action Programme
ITZ	Interfacial transition zone
AM	Adhered mortar
AIV	Aggregate Impact Value
WA	Water Absorption
NAC1	Natural aggregate concrete mixture (1 st control)
RAC2	Untreated recycled aggregate concrete mixture (2 nd control)
SCP	Concrete mixture produced with 100% treated recycled aggregate via soaking in a cement-pozzolan solution
SE	Concrete mixture produced with 100% untreated recycled aggregate via Sand Enveloped Mixing Approach
AC	Concrete mixture produced with 100% treated recycled aggregate via accelerated carbonation technique
SCP+SE	Concrete mixture produced with 100% recycled aggregate treated with soaking in cement-pozzolan solution and mixed using Sand Enveloped Mixing approach
AC+SE	Concrete mixture produced with 100% recycled aggregate treated via accelerated carbonation technique and mixed using Sand Enveloped Mixing Approach
SCP+AC	Concrete mixture produced with 100% treated recycled aggregate via soaking in cement-pozzolan solution followed by accelerated carbonation technique
SCP+AC+SE	Concrete mixture produced with 100% treated recycled aggregate via soaking in cement-pozzolan solution followed by accelerated carbonation technique and

	mixed using Sand Enveloped Mixing Approach
TSMA	Two-stage Mixing Approach
SEPP	Stone Enveloped with Pozzolanic Powder
MMA	Mortar Mixing Approach
SEMA	Sand Enveloped Mixing Approach
SEM	Scan Electron Microscopy
C-S-H	Calcium Silicate Hydrates gel
PC	Portland cement
PFA	Pulverised Fuel Ash
GGBS	Ground Granulated Blast-furnace Slag
SF	Silica Fume
M	Metakaolin
SP	Superplasticiser
CO₂	Carbon Dioxide gas
CH	Calcium Hydroxide
<i>f_{ck}</i>	Compressive strength
<i>f_{cu}</i>	Tensile splitting strength
<i>f_{ct}</i>	Flexural strength
<i>E</i>	Modulus of Elasticity
<i>w/c</i>	Water to cement ratio

LIST OF FIGURES

Figure 1.1: (a) NA, (b) RA from C&DW	29
Figure 1.2: Building rubble in Jordan (Qasrawi, 2017).....	30
Figure 2.1: Arrangements for inert waste received to produce RA (WRAP, 2015).....	41
Figure 2.2: Processing of C&DW to obtain recycled aggregates (Abukersh, 2009).....	42
Figure 2.3: Comparison of total aggregate vs C&DW quantity and recycled aggregate production of some European countries in 2015 (after Tam et al., 2018).....	43
Figure 2.4: Influence of different RA moisture states on the consistency of RAC over time (Poon et al., 2004)	52
Figure 2.5: Effects of utilising superplasticisers on the flowability of recycled aggregate concrete (Barbudo et al., 2013)	53
Figure 2.6: Relationship between RA replacement levels and concrete strength at different w/c ratios (Limbachiya et al., 2000).....	55
Figure 2.7: The effects of different RA replacement levels on the tensile strength of RAC at different w/c ratios (Barbudo et al., 2013)	57
Figure 2.8: Comparison between 100% RAC and 100% NAC in terms of modulus of elasticity presented by different researchers (Barbudo et al., 2013; Fonseca et al., 2011; Malešev et al., 2010; Casuccio et al., 2008; Limbachiya et al., 2011) respectively.....	59
Figure 2.9: Stress-strain trends of RAC (Xiao et al., 2005)	59
Figure 2.10: Schematic diagram of the mechanism of carbonation treatment method after to Pu et al. (2021)	70
Figure 3.1: (a) SEM image of PC, (b) PC used, (c) EDS peaks chemical analysis for PC compositions, (d) PC oxide compositions by EDS	82
Figure 3.2: (a) SEM image of PFA, (b) PFA used, (c) EDS peaks chemical analysis for PFA compositions, (d) PFA oxide compositions by EDS	83

Figure 3.3: (a) SEM image of SF, (b) SF used, (c) EDS peaks chemical analysis for SF compositions, (d) SF oxide compositions by EDS	83
Figure 3.4: (a) SEM image of GGBS, (b) GGBS used, (c) EDS peaks chemical analysis for GGBS compositions, (d) GGBS oxide compositions by EDS	84
Figure 3.5: (a) SEM image of MK, (b) MK used, (c) EDS peaks chemical analysis for MK compositions, (d) MK oxide compositions by EDS	84
Figure 3.6: (a) NA used in this research, (b) SEM image of surface texture for one particle of NA of 10mm size.....	86
Figure 3.7: (a) RA used, (b) SEM image of RA of 10mm size.....	86
Figure 3.8: (a) sand, (b) SEM image of sand particles	86
Figure 3.9: Particle size distribution of coarse RA and coarse NA.....	88
Figure 3.10: (a) sodium silicate used, (b) SEM image for sodium silicate	89
Figure 4.1: Breakdown structure of the experimental testing program utilised for this research	93
Figure 4.2: Sieve shaker device for determination of particle size distribution	96
Figure 4.3: Thickness gauge for determination of flakiness index	97
Figure 4.4: Chart used for determining roundness and sphericity of particles (based on Powers, 1953).....	97
Figure 4.5: Aggregate Impact Value (AIV) test apparatus.....	99
Figure 4.6: Los Angeles test machine for testing resistance to fragmentation.....	100
Figure 4.7: Conventional concrete mixer machine for recycled aggregates water washing treatment.....	102
Figure 4.8: Self-healing of recycled aggregates	102
Figure 4.9: CO ₂ incubator used for the CO ₂ treatment of recycled aggregates	104
Figure 4.10: Croker Cumflow RP100 XD MK2 rotating pan mixer.....	117

Figure 4.11: (a) various moulds oiled and prepared for fresh concrete casting, (b) some of the hydrated concrete test specimens, (c) test specimens cured in a water tank with controlled temperature	118
Figure 4.12: (a) slump test apparatus, (b) slump test for one of the designated concrete mixtures	119
Figure 4.13: Density testing regime for hardened concrete mixtures.....	120
Figure 4.14: Compression testing machine used for testing compressive strength of concrete	121
Figure 4.15: (a) framed steel, (b) tensile splitting strength test, (c) splitting of cylinder specimen	122
Figure 4.16: (a) flexural strength test, (b) flexural failure of prismatic concrete beam	123
Figure 4.17: (a) preparation of the cylinder specimen, (b) steel frame with attached strain gauge, (c) modulus of elasticity test	124
Figure 4.18: Sulphate attack test on some of the concrete samples	127
Figure 4.19: Block diagram of a typical SEM unit (courtesy of University of South Wales)	128
Figure 4.20: (a) Agor Auto sputter gold coater, (b) specimen prior to coating, (c) specimen after coating with gold layer	128
Figure 4.21: Specimens mounted on the specimens' stand in the SEM chamber	129
Figure 5.1: Effects of water treatment methods on the AIV of RA, note; NA-natural aggregate, URA – untreated recycled coarse aggregate	131
Figure 5.2: Effects of the various water treatment methods on the WA of RA	131
Figure 5.3: The impact of carbonation treatment at different concentration levels and CO ₂ exposure time on the AIV of the RA shown in (a) clustered column chart, and (b) scatter chart, note: NA – natural coarse aggregate, URA – untreated recycled coarse aggregate	134
Figure 5.4: The impact of carbonation treatment at different concentration levels and CO ₂ exposure times on the WA of RA shown in (a) clustered column chart, and (b) scatter chart, note: NA – natural aggregate, URA – untreated recycled aggregate	136

Figure 5.5:(a) untreated RA, (b) treated RA with soaking in sodium silicate-silica fume solution	138
Figure 5.6: (a) effects of soaking the RA in sodium silicate-silica fume solution at various replacement levels and soaking times on the AIV of the RA, (b) enhancement values in the AIV relative to the untreated RA.....	138
Figure 5.7: effects of soaking the RA in sodium silicate-Silica Fume solution at various replacement levels and soaking times on the WA of the RA, (b) enhancement values in the WA relative to the untreated RA	138
Figure 5.8: (a) untreated RA, (b) treated RA with coating with cement-silica fume slurry...	142
Figure 5.9: (a) the effects of the different coating with cement and/or cement-SF methods on the AIV of the RA, (b) enhancement values in the AIV relative to the untreated RA.....	142
Figure 5.10: (a) the effects of the different coating with cement and/or cement-SF methods on the WA of the RA, (b) enhancement values in the WA relative to the untreated RA.....	142
Figure 5.11: (a) untreated RA (URA), (b) treated RA with soaking in PC-PFA+SF solution, (c) treated RA with soaking in PC-PFA+MK, (d) treated RA with soaking in PC-SF+MK .	145
Figure 5.12: (a) the effects of different soaking solutions at different replacement levels and soaking times on the AIV of the RA, (b) enhancement values in the AIV relative to the untreated RA.....	145
Figure 5.13: (a) the effects of different soaking solutions at different replacement levels and soaking times on the WA of the RA, (b) enhancement values in the WA relative to the untreated RA.....	145
Figure 5.14: The effects of the different batching techniques on consistency of the RAC....	149
Figure 5.15: Development of compressive strength of batching technique concrete mixtures	152
Figure 5.16: The effects of batching techniques on strength of RAC at different curing ages	152
Figure 5.17: Results of slump test for the RACs produced with different treatment methods at various w/c ratios.....	161

Figure 5.18: Slump test for some of the concrete mixes	162
Figure 5.19: Strength development of the various RAC mixes produced with different selected treatments, in comparison with NAC1 at different w/c ratios: (a) w/c= 0.4, (b) w/c= 0.45, (c) w/c= 0.5, (d) w/c= 0.55, (e) w/c= 0.6.....	168
Figure 5.20: Effects of the different treatment methods on the relative compressive strength of concrete at 28-day.....	169
Figure 5.21: Variation in tensile strength development at 28-day for treated RACs mixes at different w/c ratios, compared to NAC1 and RAC2	177
Figure 5.22: Effects of the finally selected treatment methods on the relative tensile strength of RAC at different w/c ratios	177
Figure 5.23: Flexural strength development for treated RAC mixes at different w/c ratios, compared to NAC1 mixes and untreated RAC2 mixes.....	180
Figure 5.24: Effects of the finally selected treatment methods on the relative flexural strength of the RAC at different w/c ratios	181
Figure 5.25: Flexural failure mode of some of the RAC beams.....	181
Figure 5.26: Variations in modulus of elasticity of the different treated RACs mixes in comparison with untreated RAC2 and NAC1 mixes.....	184
Figure 5.27: Relative modulus of elasticity of the treated RACs at different w/c ratios.....	185
Figure 5.28: Correlation and regression relationships between the different engineering properties of treated RACs, Eurocode 2, and ACI, (a) flexural strength vs. tensile splitting strength, (b) modulus of elasticity vs. compressive strength, (c) tensile splitting strength vs. compressive strength, (d) flexural strength vs. compressive strength.....	191
Figure 5.29: Results of the water absorption of the enhanced RACs in comparison with the untreated RAC2 and NAC1, (a) w/c ratio=0.4, (b) w/c ratio=0.5, (c) w/c ratio=0.6	192
Figure 5.30: Concrete cube test specimens after 20 successive freeze-thaw cycles, (a) RAC2 specimen, (b) SCP+SE specimen, (c) NAC1 specimen	194

Figure 5.31: Mass change (Loss or gain) due to freeze-thaw cycles, (a) w/c ratio of 0.4, (b) w/c ratio of 0.5, and (c) w/c ratio of 0.6	195
Figure 5.32: Residual compressive strength of the different concretes at 4 weeks and 20 weeks due to freeze-thaw cycles, (a) w/c ratio of 0.4, (b) w/c ratio of 0.5, and (c) w/c ratio of 0.6.	197
Figure 5.33: Some of the test specimens after 20 weeks of exposure to sulphate, (a) NAC1 specimen, (b)SCP+SE specimen, (c) RAC2 specimen	199
Figure 5.34: Mass change (loss or gain) of the treated RACs due to sulphate attack. (a) w/c = 0.4, (b) w/c = 0.5, (c) w/c = 0.6	200
Figure 5.35: Residual compressive strength of the treated RACs due to sulphate exposure, (a) w/c=0.5, (b) w/c=0.5, (c) w/c=0.6	202
Figure 5.36: SEM images of NAC1 sample, (a) microstructure of NAC1 sample, (b) SEM image for the hydrated compounds developed in NAC1 sample	205
Figure 5.37: SEM images of RAC2 sample, (a) microstructure of RAC2 sample, (b) SEM image for the hydrated compounds developed in RAC2 sample	205
Figure 5.38: SEM images for SCP sample, (a) microstructure of SCP sample, (b) SEM image for the hydrated compounds developed in SCP sample	208
Figure 5.39: SEM images for SE sample, (a) microstructure of SE sample, (b) SEM image for the hydrated compounds developed in SE sample	208
Figure 5.40: SEM images for SCP+SE sample, (a) microstructure of SCP+SE sample, (b) SEM image for the hydrated compounds developed in SCP+SE sample	208
Figure 5.41: EDS analysis, (a) NAC1 sample, and (b) untreated RAC2 sample	212
Figure 5.42: EDS analysis, (a) SE sample, (b) SCP sample, (c) SCP+SE sample.....	214
Figure 5.43: Technical guidelines for processing RA via WRAP protocol and then treating RA onsite procedure	218
Figure 5.44: Technical guidelines for processing RA via WRAP protocol and then enhancing RA and RAC performance by the RA producer or end user	218

Figure 5.45: Technical guidelines for RAC performance enhancement by the RA producer or end user..... 219

Figure 5.47: Cost analysis of the various enhancement methods: (a) cost vs. compressive strength after 20 cycles of freezing-thawing, (b) cost vs. water absorption, (c) cost vs. compressive strength after exposure to sulphate attack, (d) cost vs. environmental impact, (e) cost vs. 28-day compressive strength, (f) other influencing factors.....219

LIST OF TABLES

Table 2.1: Classification of RA according to some countries and standards (McNeil & Kang, 2013).....	44
Table 2.2: Classification of the constituents of coarse recycled aggregates (BS EN 12620:2002+A1:2008)	46
Table 2.3: Summary of RA properties.....	49
Table 2.4: Some of the engineering properties of the RA and NA utilised in Poon et al. (2004)51	
Table 2.5: Summary of research on mechanical properties of RAC	64
Table 2.6: Previous studies on the effects of RA from the C&DW on concrete mechanical and durability property	66
Table 2.7: Previous research on removing the adhered mortar treatment methods	76
Table 2.8: Previous research on strengthening the adhered mortar treatment methods	77
Table 2.9: Previous studies on improving the whole matrix of RAC.....	78
Table 3.1: Oxide compositions and physical properties of Portland cement and different pozzolanic materials used throughout this study	83
Table 3.2: Characteristics of the RA compared with NA and relevant BS EN standards	88
Table 3.3: Roundness and sphericity results of RA and NA	89
Table 3.4: Constituents of recycled aggregates in this study (BS 8500-2:2015 +A2: 2019) ...	90
Table 4.1: Classification of the constituents of recycled aggregates (BS EN 12620:2002+A1:2008)	96
Table 4.2: proposed solution ingredient for soaking RA in sodium silicate-SF solution.....	107
Table 4.3: The surface area of the different aggregate particle sizes	108
Table 4.4: Proportions of treatment solutions for 1000 g of RA prepared in this study	110

Table 4.5: Preliminary trial concrete mixtures for recycled aggregate concrete and natural aggregate concrete (1m ³)	113
Table 4.6: Design mix proportion for batching techniques (1m ³).....	114
Table 4.7: Optimised mix proportions for various RAC produced with various treatments at variations of w/c ratios for testing mechanical properties	116
Table 4.8: Mix proportions for various RAC produced with various treatments at variations of w/c ratios for testing mechanical performance (flexural strength, tensile splitting strength, and modulus of elasticity) and durability performance.....	117
Table 4.9: Detailed description of the experimental program utilised for all the test specimens	119
Table 5.1: Results of density of hardened RAC produced with different batching techniques	153
Table 5.2: Summary of the effects of Regime A and Regime B treatments on the AIV and the WA of the RA, along with the effects of Regime C treatments on the compressive strength of RAC	160
Table 5.3: Selective analysis and the points-based system working mechanism.....	161
Table 5.4: Selective analysis using selection matrix for the best treatments nominations from Regime A, Regime B, and Regime C treatments	162
Table 5.5: Consistency assessment and 28-day density of the RACs produced with different treatment methods at different w/c ratios	166
Table 5.6: 2nd Selective analysis for nominating the final best sole treatments for further investigations.....	179
Table 5.7: 2nd Selective analysis for nominating the final best combination of treatments for further investigations	180
Table 5.8: Description of the visual inspection of damage/defect endured by the different concrete cube specimens during and at the end of the freeze and thaw cycles	198
Table 5.9: Price breakdown of the different concrete mixes and the associated embodied carbon dioxide footprint.....	213

Table 6.1: Summary of the effects of different treatment methods on the AIV and WA of RA228

LIST OF EQUATIONS

(Equation 4.1) Sodium Silicate Powder/Silica Fume Powder = 0.6.....	84
(Equation 4.2) $V_{ca} = W_{ca}/r_{ca}$	86
(Equation 4.3) $S_{agg} = V_{ca} \times S_m$	86
(Equation 4.4) $V_p = S_{agg} \times t_{th}$	87
(Equation 4.5) $r_p = (W_c + W_w + W_p) / (W_c/Y_c + W_w/Y_w + W_p/Y_p)$	87
(Equation 4.6) $W_p = V_p \times r_p$	87
(Equation 4.7) $f_{cm} = f_{ck} + k \times s$	91
(Equation 4.8) Water content = $\frac{2}{3} \times W_f + \frac{1}{3} \times W_{ca}$	93
(Equation 4.9) $\rho_p = M_3 / V_F - V_w$	104
(Equation 4.10) $WA = 100 \times M_4 - M_5/M_5$	104
(Equation 4.11) $AIV = W_2/W_1 \times 100\%$	105
(Equation 4.12) $LA = 5000 - M / 50$	106
(Equation 4.13) $\Delta_{mF-T} = m_{ni} - m_{oi} / m_{oi} \times 100$	114
(Equation 4.14) $f_{ci,rel} = 100 \times (1 - f_{ci,n}^m / f_{cr,n}^m)$	114
(Equation 4.15) $\Delta m_{n,SA} = m_{ni} - m_{oi} / m_{oi} \times 100$	116
(Equation 4.16) $f_{n,SA} = 100 \times (1 - f_{ci,n}^m / f_{cr,n}^m)$	116
(Equation 5.1) $f_{ct} = 1.64f_{ctm} - 0.65$	148
(Equation 5.2) $E_{cm} = 0.26f_{ck} + 19.91$	148
(Equation 5.3) $f_{ctm} = 0.06f_{ck} + 1.14$	148
(Equation 5.4) $f_{ct} = 0.11f_{ck} + 1.08$	148
(Equation 5.5) (EC2) $f_{ct} = \max (1.6 - h/1000) f_{ctm}$	149
(Equation 5.6) (ACI) $f_{ct} = 1.1f_{ctm}$	149
(Equation 5.7) (EC2) $E_{cm} = 9.5(0.8f_{ck} + 8)^{(1/3)}$	149
(Equation 5.8) (ACI) $E_{cm} = 4127f_{ck}^{0.5}$	149
(Equation 5.9) (EC2) $f_{ctm} = 0.3f_{ck}^{(2/3)} \leq C50/60$	150

(Equation 5.10) (ACI) $f_{ctm} = 0.49f_{ck}^{0.5}$	150
(Equation 5.11) (EC2) $f_{ct} = 0.35f_{ck}^{(2/3)}$	150
(Equation 5.12) (ACI) $f_{ct} = 0.54\sqrt{f_{ck}}$	150
(Equation 6.1) $\text{Ca(OH)}_2 + \text{CO}_2 \longrightarrow \text{CaCO}_3 + \text{H}_2\text{O}$	173
(Equation 6.2) $\text{C-S-H} + \text{CO}_2 \longrightarrow \text{CaCO}_3 + \text{SiO}_2 \cdot n\text{H}_2\text{O}$	173
(Equation 6.3) $\text{Na}_2\text{SiO}_3 + \text{Ca(OH)}_2 + \text{H}_2\text{O} \longrightarrow \text{C-S-H} + \text{NaOH}$	175
(Equation 6.4) Pozzolanic reaction: $\text{Ca(OH)}_2 + \text{S} \longrightarrow \text{C-S-H}$	178
(Equation 6.5) Cement reaction: $\text{C}_3\text{S} + \text{H} \longrightarrow \text{C-S-H} + \text{CH}$	178

CHAPTER ONE - INTRODUCTION

This chapter presents the background of the research, its problem statement, aims and objectives, research significance, research contribution to knowledge, and ends with briefly describing the structure of the thesis.

1.1 Introduction

The rise in global warming has become one of the significant issues and concerns worldwide due to the massive carbon dioxide emission (Lu et al., 2019). The estimation of the average increase in temperature is 1.1 °C due to the industrial revolution (Lu et al., 2019). The construction industry contributes approximately 39% of the annual global carbon dioxide (Ali et al., 2020).

Concrete has become a versatile leading material for various construction purposes in the past century. Its utilisation includes buildings, roads, dams, piping, lighting poles and retaining structures. Its annual global production is around 20 billion tons, making it the most widely used artificial material globally (Tošić et al., 2017). Concrete's high production accounts for 8% of the overall global carbon dioxide gas emissions (Timperley, 2018). Natural aggregate occupies three-quarters of concrete volume, and its enormously consumed as one of the primary constituents of concrete (Naqi & Jang, 2019; Neville, 2011).

Moreover, because of the ripple impacts of the rapid and extensive growth of the construction industry, massive landscaping problems, deforestation, excessive waste, environmental pollution, ecological discontinuity, and imbalance in biodiversity have surfaced (de Brito & Saikia, 2013; Ghanbari et al., 2017).

The construction industry activities generate large amounts of waste, and according to Redling (2018), about 3 billion tonnes of construction and demolition waste (C&DW) is generated globally every year. Europe produces approximately 850 million tons of C&DW (Tošić et al., 2017), while, nearly 18.8 and 21.2 million tonnes of hard demolition waste were generated in the UK in 2014 and 2015, respectively, and this quantity is predicted to continue to increase annually (Sharman, 2018). Wales generates about 3.4 million tonnes of C&DW, according to a study carried out by Flynn (2012).

The dumping and landfilling of C&DW have rapidly and enormously led to a series of issues to the environment because C&DW may contain hazardous materials (Lu, 2019). Even

though several countries recycle around 80% of C&DW, such as Japan, Netherlands, Germany etc., developing countries have an average recycling rate of 20% to 40% (Tam et al., 2018). Accordingly, promoting the use of recycled aggregate (RA) from the C&DW into new concrete as a replacement for natural aggregate (NA) is an essential priority. This would reduce carbon dioxide emissions and contribute significantly towards preserving the environment by minimising the depletion of natural resources (Silva et al., 2014).

Rodrigues et al. (2013) stated that the construction industry could achieve its sustainable development if the reduction in the consumption of natural aggregates is to be carried out simultaneously with the increase in the utilisation of the C&DW materials. Recently, the utilisation of RA from the C&DW in civil engineering applications has gained a huge interest worldwide, and studies on their possible use in new concrete have been carried out extensively over the last two decades.

With the advances in technology in the manufacture of crusher machines and the developed recycling process of plants, it is now possible to obtain RA from large portions of C&DW at a reasonable cost. Figure 1.1 is an example of RA, while Figure 1.2 shows some building rubble in Jordan that could be recycled for new concrete production.

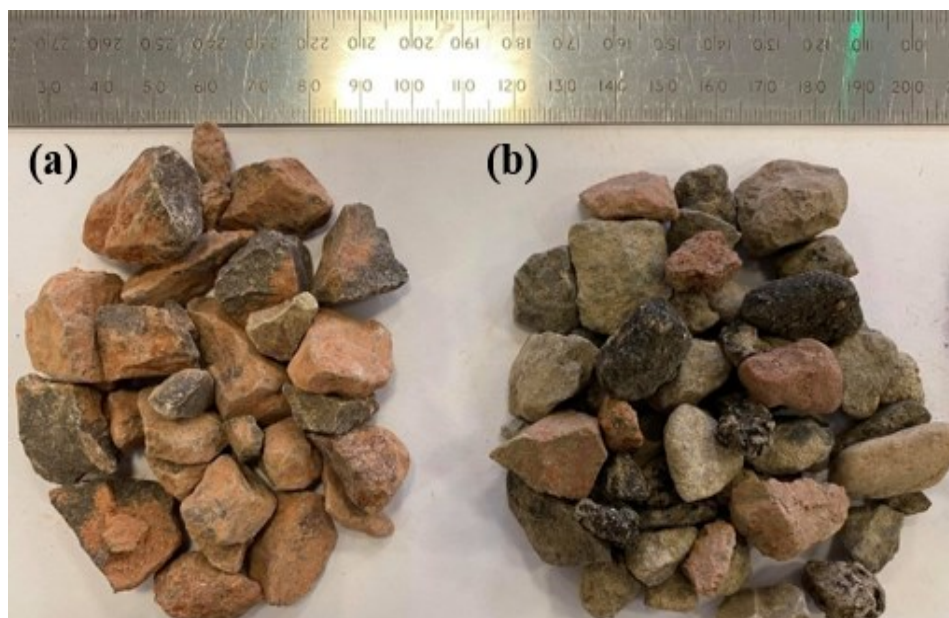


Figure 1.1: The coarse aggregate used in this study (a) natural coarse aggregate, (b) recycled aggregate from the construction and demolition waste



Figure 1.2: Building rubble in Jordan (Qasrawi, 2017)

The vast majority of recycled aggregate plants in the UK follow WRAP protocol, which is a guideline established by Smiths & Sons (Bletchington) under the guidance of the Environmental Agency and WRAP (Waste & Resource Action Programme) and DEFRA Guidance for notes (Smiths & Sons, 2015). It aims at ensuring the quality of the produced aggregates from the inert waste by demonstrating the framework procedures to produce recycled aggregate. Nonetheless, currently, there is no clear statement on the performance criteria with limitations or any performance-related approach or technical guidelines that demonstrate the utilisation of RA in the British and European standards, which highlights the lack of codified provisions and uncertainty on the incorporation of recycled aggregates in concrete production. If RA is to be successfully utilised in the construction industry in high-grade applications, further research is required to establish a better understanding of the enhancement of the structural performance of RAC.

A significant number of studies examined the effects of RA on concrete (Batayneh et al., 2007; Behera et al., 2014; Etxeberria et al., 2007; Sagoe-Crentsil et al., 2001; Rahal, 2007), revealed that replacing NA with RA in concrete reduces the compressive strength of concrete by 30% to 40%. This is ascribed mainly to the poor engineering properties of RA due to numerous factors, primarily the presence of the adhered mortar and the weak old interfacial transition zone (ITZ) on the RA surface (Gonzalez & Etxeberria, 2014). Other factors include pre-loading, accelerated weathering, processing costs, and the constituent of different materials with different engineering properties (i.e., bricks, glass, rounded stones, recycled concrete aggregates) (Gonzalez & Etxeberria, 2014). Therefore, RA possesses low density, low strength, high water absorption, weak ITZ, weak bonding, micropores, and microcracks compared to NA (Bru et al., 2014). This negative effect of RA on concrete resulted its use

only in non-structural applications such as road bases, blinding concrete, footpaths etc. (Tam, 2009). Consequently, studies with the aim of enhancing the quality of RA and RAC have been carried out extensively over the past decade to produce high-quality RA and ultimately expand RAC application into high-grade concrete.

1.2 Problem Statement

Although there are considerable amounts of studies and findings that deal with the use of recycled aggregates in concrete production either as partial or full replacement for natural aggregate (Katz, 2003; Etxeberria et al., 2007; Ajdukiewicz & Kliszczewicz, 2002; Poon et al., 2002; Talamona & Tan, 2012; Tam et al., 2007; Kou et al., 2011), recycled aggregates constitute less than three percent of all aggregates used worldwide at present, due to the poor quality of their properties and lack of technical specifications (Collery et al., 2015). Moreover, based on the literature, it is currently well-established that the incorporation of recycled aggregate at high replacement levels in concrete leads to significant adverse effects on concrete properties, including strength, durability, and structural performance (Agrela et al., 2013; Omrane et al., 2017; Liu et al., 2019).

Consequently, techniques including processing (Pepe et al., 2014; Bru et al., 2014), treatment methods including removing the adhered mortar and strengthening the adhered mortar (Gracia-Gonzalez et al., 2014; Ismail & Ramli, 2004; Zhu et al., 2013; Shayan & Xu, 2003; Al-Bayati et al., 2016), batching techniques (Elhakam et al., 2012; Qiu, 2003; Tam et al., 2005; Xu et al., 2018), and incorporating of mineral admixtures (Ann et al., 2008; Bui et al., 2018; Nuaklong et al., 2018; Omrane et al., 2017) have been introduced recently to recycled aggregate concrete to enhance its quality. Nevertheless, the present scientific understanding of the effects of replacing 100% RA from the C&DW treated with different treatments such as removing the adhered mortar, strengthening the adhered mortar, batching techniques, and combination of these treatments on the mechanical, durability, and microstructural properties of recycled aggregate concrete (RAC) is quite limited.

Furthermore, the vast majority of the previous studies investigated the replacement of recycled concrete aggregate (RCA), whilst minimal studies examined the incorporation of recycled aggregates from the C&DW at 100% replacement level. Accordingly, there is still an urgent need to investigate different types of treatment methods, utilising different batching techniques, explore the combination of existing treatment methods, and examine their effects

on enhancing the mechanical, durability, and structural reliability of C&DW RAC, which in turn would help to overcome the present high level of uncertainty associated with the structural application of such material in concrete production.

The overall significance of this research stems from achieving sustainable development through resolving the environmental issues associated with the construction industry activities is one of the main benefits of utilising RA in concrete production. The vast majority of the previous studies examined recycled concrete aggregate produced in the laboratory or recycled concrete aggregate produced by crushed concrete members (i.e., slabs, beams, columns). Nevertheless, scant studies are available in the literature in terms of the effects of utilising RA from the C&DW on concrete properties.

It is anticipated that the outcome of this research will undoubtedly add promising and enriching data to the literature and specifically to the construction industry regarding the effects of different enhancement and treatment methods and their combinations on the performance of concrete produced with 100% RA from the C&DW.

1.3 Aims & Objectives

To highly promote the utilisation of RA in the construction industry, the overall aim of this research is to (i) enhance the water absorption (WA) and aggregate impact value (AIV), (ii) enhance the mechanical performance of RAC, (iii) enhance the durability performance of RAC, and (iv) enhance the microstructure of RAC.

In pursuit of the stated aims, the following specific objectives were set:

- To investigate the sourced RA's geometrical, mechanical, and physical characteristics compared to natural aggregate.
- To evaluate the effects of treatment methods on enhancing the properties of RA by testing the aggregate impact value and water absorption of RA after the application of the treatments selected.
- To investigate the mechanical properties, including workability, hardened density, compressive strength, tensile splitting strength, flexural strength, and the modulus of elasticity of RAC produced with 100% treated RA and batching techniques.

- To determine the optimal and practical treatment methods based on their performance under different criteria by means of selective analysis.
- To examine the durability performance, including water absorption, resistance to freeze-thaw, and sulphate attack of concrete produced with 100% treated RA.
- To critically investigate and evaluate the microstructure of RACs produced with treated RA and understand the microstructural changes to the RAC microstructure that could lead to enhancement in strength, durability, and structural performance of RAC produced with 100% RA from the construction and demolition waste.
- To develop technical guidelines for the manufacturers of RA and end-users based on the performance of treated RA and enhanced RAC via different treatments and batching techniques.

1.4 Research Methodology

The present study involved the examination of the following six main phases, as shown in the breakdown structure of the experimental methodology adopted:

Phase I Carried out preliminary tests on the sourced recycled aggregates, which included particle size distribution, Aggregate Impact Value (AIV), Water absorption (WA), density, particle shape by flakiness index, particle shape by shape index, LA abrasion coefficient, roundness and sphericity, constituent of recycled aggregate.

Phase II Investigated the influence of the different treatment methods adopted from Regime A (water treatment methods) and Regime B (strengthening the adhered mortar) on Aggregate Impact Value (AIV) and Water Absorption (WA) of recycled aggregate. It also involved evaluating the best performed batching techniques on the main mechanical properties of plain concrete, properties of the fresh concrete (workability; slump and compaction index), and properties of the hardened concrete (i.e., compressive strength and density).

Once Phase II was completed, selective analysis of the best performed treatments was carried out to select the best treatments for further experimental investigations. The effects of trials of a combination of treatment methods were also included.

- Phase III** This phase examined the mechanical properties of concretes produced with the different select treatments from Phase II, i.e., slump, density, and compressive strength at various water to cement ratios, 0.4, 0.45, 0.5, 0.55, and 0.6. Afterwards, further selective analysis was conducted to select the best treatment methods for further experimental investigations.
- Phase IV** Examined the mechanical and structural performance of plain concretes produced with the finally selected treatments. It involved slump, density, compressive strength, tensile splitting strength, flexural strength, modulus of elasticity at three water to cement ratios, 0.4, 0.5, and 0.6.
- Phase V** Evaluated the durability performance, water absorption, resistance to freeze-thaw, and sulphate attack of concretes produced with the finally selected treatment methods at 0.4, 0.5, and 0.6 water to cement ratios.
- Phase VI** Included investigations on the microstructure of the finally selected treatments by means of two main techniques, namely, direct observation by scanning electron microscope (SEM) and Energy Dispersive Spectrometer (EDS), to provide a deep understanding of the link between engineering behaviour, composition, and microstructure of treated recycled aggregate concretes.

1.5 Contribution to the Existing Knowledge

The main scientific contribution of this research is demonstrated by achieving the set key aims through the successful completion of the objectives of this research. Thus, better agreement and understanding on the engineering performance of concrete produced with 100% treated RA from the C&DW. Although there are extensive amounts of studies in the literature that dealt with the performance enhancement of RAC using different treatment methods (Ahmad, et al., 2017; Ahmed & Lim, 2021; Alqarni et al., 2021; Bui et al., 2018; Fang et al., 2021; Hanumesh et al., 2018), this research however is considered one of the earliest attempts at investigating the effects of different sole treatments and combination of other treatments, on the mechanical, durability, and microstructural properties of concretes produced with 100% treated RA from the C&DW. Wang et al. (2021) argued that the influence of RA with different constituent (i.e., recycled concrete aggregate, recycled clay brick aggregate, bitumen, and natural stone) on the short-term performance (compressive strength, tensile, and flexural strength) and the long-term performance including the durability

properties of RAC should be investigated. Accordingly, the contribution to knowledge in this research is demonstrated by enriching the literature review with full-scale study data on the performance enhancement of concrete produced with 100% recycled aggregates from the C&DW using a developed innovative regime of various treatment methods batching techniques, and their combinations. The material performance of treated RA and RAC produced with treated RA is considered a great asset to the construction industry, recycling plants, and relevant institutions to help promote RA utilisation in new concrete.

1.6 Structure of the Thesis

This experimentally laboratory-based research evaluated different parameters to achieve the aims and the objectives of this study properly. The present work was organised into seven chapters, followed by references and appendices. Each of these chapters is subdivided into sections and sub-sections. The following gives a brief overview of each chapter for better clearance:

CHAPTER ONE:

This chapter starts with a discussion of the background of the research. It moves over to the state of the problems associated with the RA in terms of its incorporation into concrete along with the research gaps in the literature. Chapter one also presents the significance of the current work and justifies the need to carry out the research. This chapter also outlines the aims of this research and the objectives of the methodology, which are the key to the successful completion of this research. It also presents the anticipated contribution to the existing knowledge. Finally, this chapter ends with an overview of the methodology adopted and the breakdown structure of the thesis. Chapter one will help the reader easily navigate the entire thesis and get a better overview of the research outlines.

CHAPTER TWO:

This is the literature chapter that includes a comprehensive review of the existing studies and work on the RA and RAC background, available relevant standards, associated problems, RA constituents, effects of incorporating RA on the mechanical, structural, durability properties of concrete. In addition, this chapter outline a summary of

the existing treatments used to enhance the engineering properties of RA. It also includes an overview of the existing research gaps in the literature and more importantly the contribution of the current work to the knowledge.

CHAPTER THREE: Chapter three gives a detailed description of the sources of the material, reasons for using each material, chemical compositions, and some of the physical properties. Scanning Electron Microscopy (SEM) microstructural images and Energy Dispersive Spectrometer (EDS) chemical analysis have also been presented in this chapter for all the materials used. This chapter classified the materials utilised into four main categories, binding materials, aggregates (coarse and fine), pozzolan materials, and other materials. The binding material used was Portland cement (CEM IIB), the utilised aggregates were subdivided into fine aggregates (river sand), and coarse aggregates (natural limestone aggregates and recycled aggregates), while the pozzolan materials used were (Silica Fume – SF, Granulated Blast Furnace Slag – GGBS, Pulverised Fuel Ash – PFA, and Metakaolin – MK), the other materials used were sodium silicate, sodium sulphate, limewater, Dentstone plaster, and superplasticiser.

CHAPTER FOUR: This chapter demonstrates the details of the analytical techniques and methods within the experimental program utilised in the present research. Chapter four involved the preliminary investigations used to evaluate the materials characteristics of the recycled aggregate in comparison with natural aggregate. It also includes the experimental procedures for mix design, sample preparation, treatment methods used, density, slump, compressive strength, tensile splitting strength, flexural strength, and modulus of elasticity. The experimental investigation also included durability investigations, water absorption, sulphate attack, and resistance to freeze-thaw cycles. Scanning Electronic Microscopy (SEM) and Energy Dispersive Spectrometer (EDS) are also presented in this chapter for microstructural investigations.

CHAPTER FIVE: This chapter gives the detailed experimental results obtained from the AIV and WA on treated RA via Regime A and Regime B treatments and on the mechanical properties of hydrated RAC produced with different batching techniques (Regime C) during the initial treatment phase of RA. It also includes a description of the first and second detailed selective analysis to select different treatments. This chapter further describes the results of mechanical properties, structural performance, durability, and microstructure investigations of RAC produced with different treatment methods.

CHAPTER SIX: Chapter six discusses and interprets the research results given in chapter five. This chapter has been divided into five sections. Section 1 discusses the first stage evaluation of the performance of the treatments selected in enhancing the AIV and WA of RA (Regime A and Regime B), along with the performance of the devised batching techniques in improving the mechanical properties of RAC (Regime C), Section 1 also includes the selection matrix and its interpretation for selecting the best treatment methods for further investigations. Section 2 discusses the performance of the treatment methods selected from Section 1 in terms of mechanical properties of concretes produced at different w/c ratios, a second selection matrix is also included in Section 2 to select the final best treatment methods for further investigations. Section 3 discusses the structural performance of the final selected treatment methods. Section 4 discusses the durability assessment of the final selected treatments. Section 5 interprets the results of the microstructural investigations. An overall practical implication of the current research, along with the analysis of the environmental and economic benefits, is also included in the present chapter.

CHAPTER SEVEN: The overall target of the present research was to overcome the current issues associated with RAC in terms of its limited use to non-structural applications. Thus, the primary aim was to develop recycled aggregate concrete is suitable for structural application by

investigating different treatment methods to enhance the RAC quality. Accordingly, the current chapter presents the conclusions of this research. This chapter also suggests recommendations for future work to get better scientific understanding of the RAC field

CHAPTER TWO - LITERATURE REVIEW

Chapter two presents the state-of-the-art of RA and RAC by reviewing the existing studies in the literature. This chapter is a key to getting a better understanding of the current knowledge on RA in terms of the current challenges and up to date solutions to overcome the current associated technical obstacles to the use of RA in concrete applications. This chapter establishes the present research gaps in the literature and identifies the potential contribution of the current research to the existing knowledge.

According to Bruntland's report (1987), sustainable development is defined as development that meets the needs at present without compromising the needs of future generations to meet their own needs. The primary outcome of Bruntland's report is to outline guidelines and draw a strategy for governments, local authorities, and the construction industry for the management and consumption of natural mineral resources, controlling the waste, promoting the utilisation of recycled waste materials and by-products in the construction industry, and reducing the risk of deteriorating the environment. To overcome the current challenges facing prompting the application of RA in the world market, it is necessary to have a deep understanding of RA effects on RAC and the structural performance of concrete produced with demolished aggregates. This chapter presents a comprehensive review of the previous research on utilising RA in new concrete, RA properties, RAC mechanical and durability properties, the structural performance of RAC, and the different previously applied treatments to RA to enhance the engineering performance of concrete produced with treated demolition waste aggregates.

2.1 Background

According to BS EN 12620: 2013, recycled aggregate is aggregates resulting from the processing of inorganic or mineral materials previously utilised in construction. Glushge initiated the first experimental investigation on the utilisation of recycled demolished concrete in Russia in 1946 (Xiao et al., 2006). The Germans used recycled aggregates to build dwelling units to meet the large demand for the reconstruction of residential buildings (DeVenny, 1999). In the late 70's, the International Union of Laboratories and Experts in Construction Materials, Systems and Structures (RILEM) and several universities, along with research centres in Europe and other parts of the world, started numerous research projects on the potential use of recycled aggregates in construction (Tam et al., 2018). Since the beginning of the 80's, there has been significant progress in C&DW utilisation in terms of the management

system. The outcome of the carried out research work has demonstrated a promising solution as a replacement of natural aggregate in concrete.

In the UK, Building Research Establishment (BRE) published a report known as Digest 433 recycled aggregates in 1998. It mainly aimed to improve the quality of recycled aggregate to promote its use in higher grade applications such as structural concrete (BRE, 1998). The research on recycled aggregate has rapidly increased worldwide in the following years. Studies were mainly engaged in the processing approach, design of mix-proportion, durability investigations, structural performance, and properties enhancement methods.

2.2 Recycled Aggregate (RA)

2.2.1 Composition of RA

RA is typically obtained through processing the C&DW at recycling plants, i.e., demolished concrete structures, waste concrete, rejected precast concrete members, masonry, roadbeds of concrete, asphalt pavement, concrete waste from ready mix concrete plants, and waste generated from testing laboratories (Behera et al., 2014). According to Tam et al. (2018), recycled aggregate from the C&DW may contain, concrete, bricks, tiles and ceramics, wood, glass, plastic bituminous mixtures and tars, metals (ferrous & non-ferrous), soils and stones, gypsum-based materials including plasterboard, waste electronic and electrical equipment, chemicals, hazardous substances, cardboards materials and in some cases asbestos.

2.2.2 Processing & recovery of construction and demolition waste aggregate

With the advance in technology, recycling of the C&DW is currently readily accessible and generally inexpensive. The most commonly used approach for recycling the C&DW involves crushing and screening by utilising mobile sorters and crushers such as impact and jaw crushers. The vast majority of recycled aggregate plants in the UK follow the set quality protocol established by the Waste and Resources Action Programme (WRAP), the Environment Agency, and the Department for Environment, Food and Rural Affairs (DEFRA) in consultation with the construction industry (WRAP, 2015). The protocol guidelines are established to ensure the quality of the produced aggregates from the inert waste, which must also conform to the European standard. Their guidelines demonstrate the framework procedures to produce recycled aggregate that starts with inert waste accepting procedures, followed by the production process and then a testing regime is to be met (weekly, monthly, and

annually) on aggregates properties. Figure 2.1 demonstrates the WRAP quality protocol regarding RA's production process flow diagram.

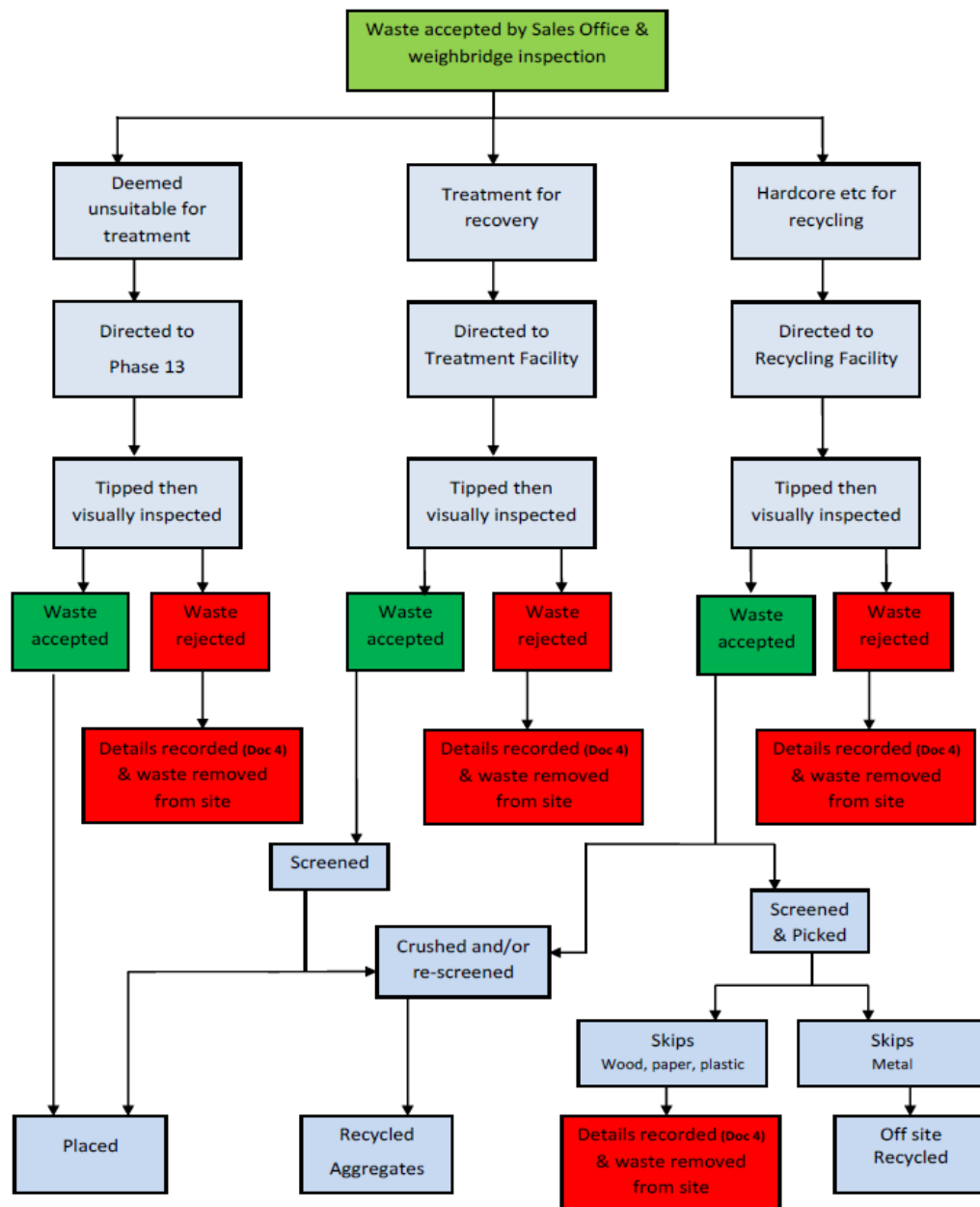


Figure 2.1: Arrangements for inert waste received to produce RA (WRAP, 2015)

Statistics from a survey on managing C&DW in Wales conducted by Flynn (2012) indicate that about 44 percent was prepared for reuse, 31 percent was recycled, 19 percent was disposed of via landfill, and 4 percent was sent for backfilling. In the United Kingdom, it is estimated that 52 million tonnes of aggregates are obtained annually from the C&DW. This figure represents a significant percentage of the total of 248 million tonnes used annually in

the UK (WRAP, 2015). Figure 2.2 shows the processing of C&DW to produce recycled aggregates.



Figure 2.2: Processing of C&DW to obtain recycled aggregates (Abukersh, 2009)

Figure 2.3 indicates the best estimates for 2015, according to Tam et al. (2018), the total natural aggregate production, C&DW quantity produced, and the quantity of recycled aggregates production from the C&DW of some European Union countries.

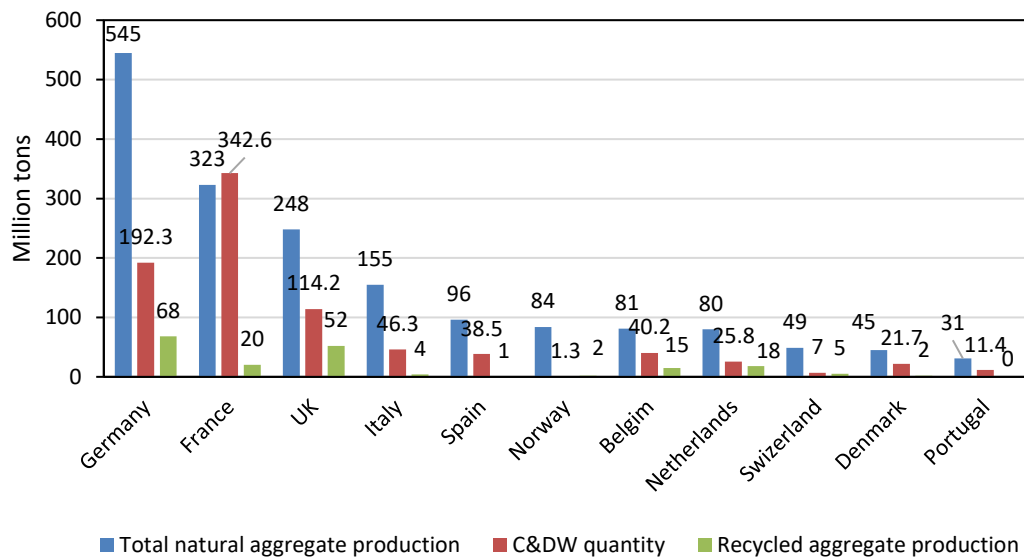


Figure 2.3: Comparison of total aggregate vs C&DW quantity and recycled aggregate production of some European countries in 2015 (after Tam et al., 2018)

2.2.3 Specifications & standards

Specifications on the use of recycled aggregates, whether it is from construction and demolition waste or coarse crushed concrete aggregates (recycled concrete aggregates), have been stated in the provisions of the British Standards BS EN 933-11:2009, and BS 8500-2:2015+A2:2019. The first standard discusses the tests for geometrical properties of aggregates and the classifications for the constituents of coarse recycled aggregate. The latter one is a complementary British Standard to BS EN 206, demonstrating the specifications for constituent materials and concrete with recycled aggregates. According to BS EN 206-1:2013, the European standard for the specification of concrete, Type A aggregates from a known source may be used in exposure classes to which the original concrete was designed with a maximum percentage of replacement of 30%. BS 8500-1:2015+A1:2016 and BS 8500-2:2015 only specify the use of crushed concrete aggregate in concrete with limitations up to 20% replacement by mass and up to C40/50 strength class, excluding structures exposed to chlorides.

BS EN 8500 part 2: 2006 has stated that at least 87%, by weight, of RA shall be sourced from crushed concrete members. Whereas BS EN 12620: 2013 classifies the constituents of coarse recycled aggregates. Nonetheless, there is still a lack of codified provisions in terms of design procedures nationally and internationally regarding RAC structural members in which design engineers are faced with a high level of uncertainty to design structural RAC members (Silva

et al., 2014). Consequently, if recycled aggregates utilisation needs to succeed in the construction industry, further research studies are required to better understand the engineering properties of recycled aggregates from the C&DW and their key effects on concrete structural performance.

2.2.4 Classification of recycled aggregates

According to Silva et al. (2014) recycled aggregates from C&DW can be classified into four main categories:

- Recycled concrete aggregates (RCA): RA to be considered as RCA, it must consist of a minimum of 90%, by mass, of Portland cement-based materials.
- Recycled masonry aggregates (RMA): consists of a minimum of 90%, by mass, of clay-based materials, blast-furnace slag bricks and blocks, sand-lime bricks.
- Mixed recycled aggregates (MRA): this category comprises a mixture of crushed concrete and masonry rubble. It must compose of less than 90%, by mass, of Portland cement-based materials. Therefore, it may consist of masonry-based materials such as ceramic.
- Construction & demolition waste aggregates (C&DW): where it is not possible to properly categorise RA, they are deemed C&DW aggregates. In other words, it may also consist of asphalt, glass, plastic, and wood. If RA has not undergone proper sorting or screening, it may contain variable materials.

Some countries classified RA according to its characteristics, i.e. water absorption, density, porosity, shape, particle distribution, and strength. Table 2.1 demonstrates the classification of RA according to some countries and standards.

Table 2.1: Classification of RA according to some countries and standards (McNeil & Kang, 2013)

Country/ standard	Type/class of RA	Constituents of RA	Density (kg/m ³)	WA (%)
Germany (DIN 4226-100) (DIN 2002)	Type 1	Concrete chipping + crusher sand	≥ 2000	≤10
	Type 2	Construction chipping + crusher sand	≥ 2000	≤15
	Type 3	Masonry chipping + crusher sand	≥ 1800	≤20
	Type 4	Mixed chipping + crusher sand	≥ 1500	No limit

Australia (AS1141.6.2) (AS 1996)	Class 1A	No more than 0.5% brick	≥ 2100	≤ 6
	Class 1B	No more than 30% brick	≥ 1800	≤ 8
RILEM (1994)	Type 1	Masonry Rubble	≥ 1500	≤ 20
	Type 2	Concrete rubble	≥ 2000	≤ 10
	Type 3	NA (min 80%) + RA (20%)	≥ 2500	≤ 3
Spain (EHE 2000)	Minimum requirement	—	≥ 2500	≤ 3

Recently, BS EN 12620:2002+A1(2008) classified recycled aggregates according to their constituents into the following categories shown in Table 2.2. There are four main categories into which RA from the C&DW can be classified depending on the composition of RA according to the BS EN 12620:2002+A1(2008). These are RC (concrete-based materials), Rc+Ru (unbound aggregate, natural stone, and hydraulically bound aggregate), Rb (clay-based materials), and Ra (bituminous aggregate).

Table 2.2: Classification of the constituents of coarse recycled aggregates (BS EN 12620:2002+A1:2008)

Constituents	Content percentage (by mass)	Category
RC (Concrete, concrete products, mortar, concrete masonry units)	≥ 90	Rc ₉₀
	≥ 80	Rc ₈₀
	≥ 70	Rc ₇₀
	≥ 50	Rc ₅₀
	< 50	Rc _{Declared}
	No requirement	Rc _{NR}
Rc+Ru (Unbound aggregate, natural stone, hydraulically bound aggregate)	≥ 95	Rcu ₉₅
	≥ 90	Rcu ₉₀
	≥ 70	Rcu ₇₀
	≥ 50	Rcu ₅₀
	< 50	Rcu _{Declared}
	No requirement	Rcu _{NR}
Rb (Clay masonry units <i>i.e.</i> bricks and tiles, calcium silicate masonry unit, aerated non-floating concrete)	≤ 10	Rb ₁₀
	≤ 30	Rb ₃₀
	≤ 50	Rb ₅₀
	> 50	Rb _{Declared}
	No requirement	Rb _{NR}
Ra (Bituminous materials)	≤ 1	Ra ₁
	≤ 5	Ra ₅
	≤ 10	Ra ₁₀
X+Rg X: others such as cohesive (<i>i.e.</i> clay and soils). Miscellaneous: metals (ferrous and non-ferrous), non-floating wood, plastic and rubber, gypsum plaster. Rg: glass	≤ 0.5	XRg _{0.5}
	≤ 1	XRg ₁
	≤ 2	XRg ₂
FL	$\leq 0.2^a$ (cm ³ /kg)	FL _{0.2}
	≤ 2	FL ₂
	≤ 5	FL ₅

^a The ≤ 0.2 category is intended for special applications requiring high quality surface finish.

2.2.5 Interfacial transition zone (ITZ) and adhered mortar of RA

The external layer of residual cement mortar coated on the surface of the RA plays a vital role in altering the properties of RAC. The old mortar is generally considered the primary cause of poorer characteristics of RA compared to NA (Butler et al., 2011; Etxeberria et al., 2006; Oikonomou, 2005). The attached mortar contains micro-cracks because of processing and deterioration, which makes it very porous, less dense, and inhomogeneous, not to mention RA has a weak strength because of the previous loading and processing (Behera et al., 2014). This affects RA quality compared to NA, as RA has higher water absorption, lower density, lower strength, poor shape, lower specific gravity, weak bonding with the new cementitious paste with concrete structure (Duan & Poon, 2014).

The quantity of the adhered mortar on the surface of RA varies depending on the aggregate particle size. According to Behera et al. (2014), the volume of the adhered mortar increases with a decrease in the RA particle size, for instance, it is estimated to be 20% by weight for

RA particle sizes ranging from 20 to 30mm and higher for RA particle size between 10 and 4mm. Likewise, Hansen & Narud (1983) concluded that the quantity of the adhered mortar is about 60%, 40%, and 35% for RA particle sizes of 4-8 mm size, 8-16 mm size, and 16-32 mm, respectively.

Unlike natural aggregate concrete having one ITZ, RAC possesses two ITZs. One is between the adhered mortar and the RA surface (old ITZ). The other is between the new cement paste and the adhered mortar (new ITZ), as shown in Figure 2.4. Due to the presence of the two ITZs and the porous nature of RA, along with its poor quality, the porosity of RAC is usually higher than the corresponding NAC resulting in inferior mechanical and durability properties of RAC compared to NAC (Wang et al., 2021).

In addition, the compressive strength, and moduli of elasticity of the adhered mortar are lower than that of the RA, and the presence of microcracks on the adhered mortar is generated during the crushing process of producing RA (Verian, 2012). It is believed that the old ITZ in RAC plays a significant role in the bonding behaviour of RA with the cement mixture. Failure of loading can be observed in the part of the old ITZ in RAC due to the weak bonding of the old ITZ with the new cement mixture within the concrete matrix (Lee & Choi, 2013).

It has also been reported that the load-carrying capacity of ITZ is always lower than the cement paste, due to the higher number of small grains and voids in the ITZ (Scrivener et al., 2004). According to Wang et al. (2021), no clear boundary can be identified between the old cement past (the adhered mortar) and the new cement paste at the microstructure level due to the progressive transition from the new ITZ to the new cement paste.

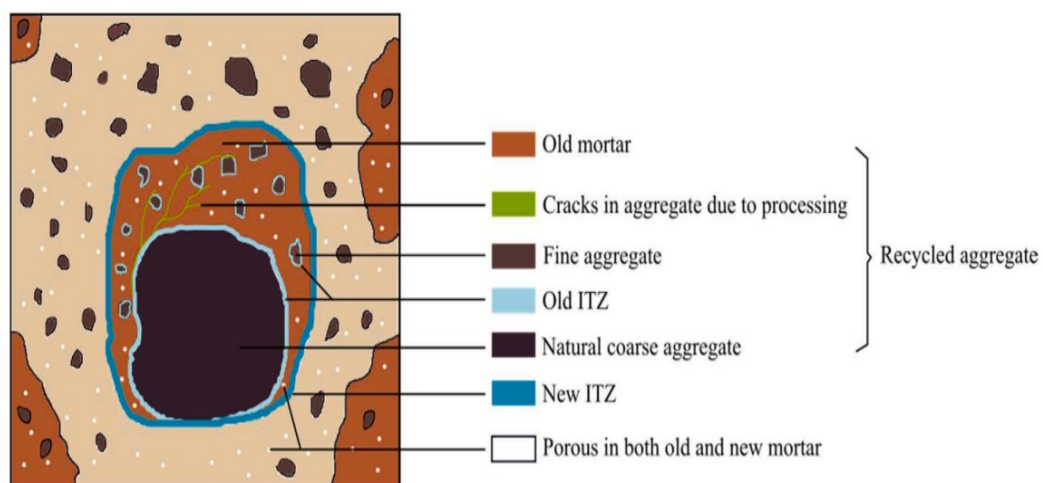


Figure 2.4: Typical illustration of RA within RAC (Wang et al., 2021)

2.2.6 Engineering characteristics of recycled aggregate

The characteristics of RA sourced from different recycling plants vary depending on their compositions, the parent concrete's quality, the effectiveness of the crushing process, and the crushing method used (Behera et al., 2014).

2.2.6.1 Particle properties of RA

RA is generally poorly graded because of its poor distribution of particle size as it may be too coarse or too fine due to the processing and crushing process (McNeil & Kang, 2013). The presence of the adhered mortar on the RA surface results in the formation of an old interfacial transition zone (ITZ), as can be seen in Figure 2.4. The old ITZ is relatively weak in nature due to the presence of the developed micro-cracks, fissures, and minute pores (Kou & Poon, 2012). According to Behera et al. (2014), RA typically has a rough surface texture, mostly rounded in nature, and irregular shape due to the adhered mortar, processing, and crushing.

2.2.6.2 Water absorption of RA

According to Poon et al. (2003), RA has 2-3 times higher water absorption capacity than NA, and in some cases, the water absorption of RA may go up to 13%. Behera et al. (2014) pointed out that the water absorption capacity of RA is higher for smaller particle sizes as the greater the specific surface area of the aggregate particle size, the greater the adhered mortar content. This is in line with Kou and Poon (2019) who reported water absorption values for RA of 6.23% and 7.76% for 20mm and 10mm aggregate particle size, respectively, while the NA had water absorption of 0.68% and 0.87% for 20mm and 10mm aggregate size, respectively. This higher water absorption capacity of RA generally leads to higher water absorption of RAC.

Furthermore, Kazmi et al. (2019) reported five times higher water absorption of RA compared to NA, which may be attributable to the presence of the adhered mortar on the RA surface. Similarly, Verian et al. (2018) pointed out that the water absorption of RA is typically between 0.5% to 14.75% and 0.34% to 3.0% for NA. This is in agreement with Kisku et al. (2017) who concluded that the water absorption capacity of RA is higher than NA by 3-12%, while Hansen and Henrik (1983) stated that the water absorption of RA is typically 2.3-4.6 times higher than NA.

2.2.6.3 Aggregate impact value of RA

Behera et al. (2014) pointed out that RA is inferior to natural aggregate (NA) in terms of crushing strength, aggregate impact value, and abrasion resistance. Kazmi et al. (2019) reported a lower aggregate impact value of RA by 13% compared to NA. This is in line with Kisku et al. (2017) who concluded that the AIV of RA was 33% and 45% higher than that of NA for 10-20 mm and 10-4.75 mm sized aggregate, respectively. Similarly, Mistri et al. (2020) investigated the aggregate impact value of RA and NA and concluded that the AIV of NA is 13.98%, whereas it is 21.78% for RA. Behera et al. (2014) stated that RA's inferior aggregate impact value performance is mainly due to the presence of the adhered mortar, pre-loading, and possibly processing.

2.2.7 Summary of studies on properties of RA

Table 2.2 summarises the engineering characteristics of RA, including aggregate impact value (AIV), crushing value (CR), abrasion value (Abr), water absorption (WA), moisture content (MC), and specific gravity (SG).

Table 2.3: Summary of RA properties

Reference	Aggregate type	AIV (%)	CR (%)	Abr (%)	WA (%)	MC (%)	SG
Katz (2004)	Recycled concrete aggregate				5.5	0.5-0.6	2.41
	NA			29	2.5		2.52
Dimitriou et al. (2018)	Recycled concrete aggregate			32	7.2	2.7-2.9	2.28
Pepe et al. (2014)	NA				1.28		2.634
	Recycled concrete aggregate				4.94		2.268
Ismail & Ramli (2013)	NA	13.98	24.32		0.6		2.6
	Recycled concrete aggregate	21.78	29.15		4.44		2.33
Al-bayati et al. (2016)	Recycled concrete aggregate		27.42	23.57	5.91		2.295
Kou & Poon (2012)	NA (10 mm)				1.12		2.62
	NA (20 mm)				1.11		2.62
	RA (10 mm)				4.26		2.49
	RA (20 mm)				3.52		2.58
Kou & Poon (2010)	NA (20 mm)				0.68		2.662
	Recycled concrete aggregate (20 mm)				6.23		2.423
Li et al. (2017)	RA (5-10 mm)				6.22		2.611
	RA (10-20 mm)		27.8		6.19		2.583
Singh et al. (2018)	NA	20.32	20.06		0.65		2.62
	Recycled concrete aggregate	26.89	26.51		1.4		2.2
Kazmi et al. (2019)	NA		27		1.3		2.66
	RA		31		6.85		2.55
Parthiban & Mohan (2017)	NA			14.2	0.77		2.72
	Recycled concrete aggregate			20.3	14.2		2.44
Abera (2022)	NA	25.22			2.78	2.89	2.58
	RA	24.11			3.21	1.02	1.02
	Recycled concrete aggregate	23.27			3.64	1.12	1.12
	RA	23.86			4.26	1.15	1.14
Tang et al. (2022)	NA				0.9		
	RA				7.7		

2.3 Engineering Properties of Recycled Aggregate Concrete (RAC)

2.3.1 Consistency of fresh RAC

The fresh state of normal concrete, such as workability and wet density, are affected by several factors such as, characteristics of the aggregates used (type of aggregate, size of aggregate, aggregate water absorption, shape of aggregate, and surface texture), water content, water to cement ratio. Recycled aggregate concrete (RAC) exhibits lower slump and higher slump loss than natural aggregate concrete (Kou and Poon, 2009). Given its porous nature, RAC requires more water than conventional concrete to obtain similar workability, and hence it is quite challenging to meet the workability requirements.

It has been reported that RAC requires 10% of additional water to obtain a similar slump as natural aggregate concrete (NAC) (Tabsh & Abdelfatah, 2009). Fathifazl (2008) stated that RA type and quantity could significantly affect the workability of RAC even at the same water to cement ratio as NAC. In general, the fresh state of RAC has a granular and harsher texture compared to NAC as a result of the existing adhered mortar, which leads to a more angular aggregate, higher demand for water and higher energy for compaction due to the friction of the inner particles (Etxeberria et al., 2007).

This is in line with Sagoe-Crentsil et al. (2001) study, which reported that commercially processed RA with a smoother surface leads to better workability than RA produced in laboratories. Ridzuan et al. (2001) argued that smaller RA sizes require more water than bigger sizes due to the increased quantity of the adhered mortar. Therefore, it is not easy to control the properties of fresh RAC, and thus, this significantly influences the strength and durability of RAC.

The workability of fresh RAC gets hampered if RA is used in a dried state, depending on the quantity of RA. The loss in a slump in RAC is greatly prominent at a higher amount of RA replacement, i.e., exceeding 50% (Behera et al., 2014). During mixing of concrete, RA tends to absorb the free water from the mixture because of the adhered mortar, this causes higher demand for water to maintain the desired workability.

In view of this issue, several studies have been carried out aiming to overcome this concern. Some researchers adopted the use of RA at surface saturated dry condition (SSD), and it was reported when RA was utilised in SSD state, an increase in the initial concrete slump was

observed, this is attributed to the high absorption capacity of RA resulting in a larger amount of initial free water (Poon et al., 2004). Nevertheless, this may result in bleeding of concrete and an increase in the w/c ratio of the fresh concrete matrix. In the study of Poon et al. (2004), RA was added into concrete at three different moisture states, oven-dry (OD), air dry (AD) and saturated surface dry (SSD), to examine the effects of different moisture states of RA on the workability of RAC.

The utilised RA in Poon et al. (2004) study was sourced from demolished reinforced structures and concrete runways. 12.4% and 22.6% extra amount of water was added to the RAC mixtures with RA at OD state and AD state, respectively, whereas concrete mixtures with RA at SSD condition had no extra water. Table 2.4 shows some of the engineering properties of natural aggregates and recycled aggregates utilised in the study of Poon et al. (2004).

Table 2.4: Some of the engineering properties of the RA and NA utilised in Poon et al. (2004)

Agg type	Nominal size (mm)	Water absorption (%)	Porosity (%)	Density (kg/m ³)	Strength (kN)
Crushed granite	20	1.24	—	2620	—
RA	10	1.25	1.6	2620	159
	20	6.28	—	2370	—
	10	7.56	10.45	2330	117

Poon et al. (2014) study showed that mixtures produced with 100% oven-dried RA obtained the highest initial slump values, as shown in Figure 2.4. This was ascribed due to the extra amount of water added to the mixture to compensate for the water loss due to the high-water absorption nature of RA. Recycled aggregates initially had not absorbed the additional water, resulting in a higher effective w/c ratio when the slump test was carried out. All the mixtures obtained similar slump values after 15-30 minutes, indicating that RAs absorbed additional mixing water.

These results were in line with Brand et al. (2015) who stated that concrete mixtures with oven-dried state RA achieved the highest initial slump values compared to the SSD state and air-dried ones. According to Brand et al. (2015), this was ascribed to the additional amount of water added to the mixtures as compensation for the water being absorbed by the RA during mixing and hence, maintaining an equivalent effective w/c ratio for all the mixtures.

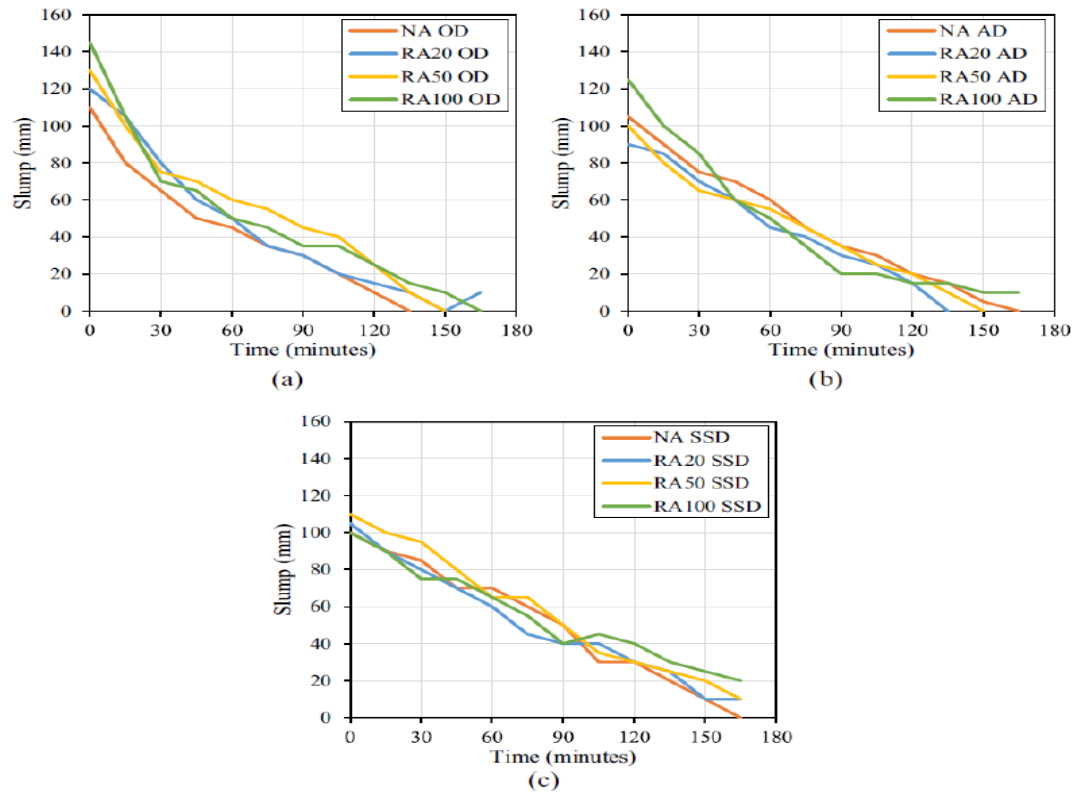


Figure 2.4: Influence of different RA moisture states on the consistency of RAC over time (Poon et al., 2004)

Another suggested method in the literature to overcome the poor workability of RAC is the use of superplasticisers which can compensate for the water demand. The utilisation of water-reducing agents in concrete has recently gained a lot of attention because of its capability to enhance the workability of concrete mixtures, accelerate concrete setting time, and enhance air content (Matias et al., 2013).

Barbudo et al. (2013) examined the effects of utilising superplasticisers on the workability of RAC. 1% superplasticiser of cement weight was used in the study, three groups of mixtures were produced with different replacement ratios of 0%, 20%, 50%, and 100% of natural aggregates weight. The utilised RA was recycled concrete aggregates sourced from crushed 30-day old concrete. The reference concrete mixture was designated with w/c of 0.54 and a slump value of 125 mm, whereas the RAC mixtures were designated with w/c ratio of 0.4. It was found that the incorporation of superplasticiser reduced the amount of water needed in the mix to obtain the required consistency. Figure 2.5 shows the influence of utilising water-reducing agents on the workability of RAC. These results align with Kumar and Dhinakaran (2012) who reported that the water demand for RAC during mixing could be reduced by 12.5% by using superplasticiser while maintaining the desired workability.

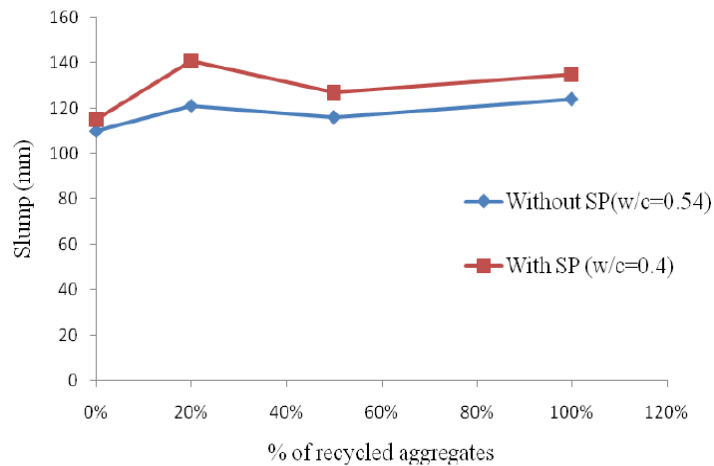


Figure 2.5: Effects of utilising superplasticisers on the flowability of recycled aggregate concrete (Barbudo et al., 2013)

2.3.2 Mechanical properties of RAC

The hardened properties of recycled aggregate concrete include the following mechanical properties, compressive strength, flexural strength, split tensile strength, and elastic modulus. These mechanical properties depend on various parameters such as the characteristics of the RA used, the w/c ratio of the RAC mix, and the microstructure of RAC. RA was reported to have lower resistance to mechanical actions due to the poor link between the adhered mortar and RA surface, the presence of micro-cracks and fissures, and the presence of weak and porous adhered mortar (Behera et al., 2014). The mechanical performance of RAC depends on the replacement level of RA (Kou & Poon, 2012; Kwan et al., 2012), quality of RA (Crentsil et al., 2001; Bazaz & Khayati, 2012), the quantity of the adhered mortar (de Juan & Gutierrez, 2009), w/c ratio used in the design, and the moisture condition of RA (Behera et al., 2014).

2.3.2.1 Compressive strength

The compressive strength of RAC is influenced by various factors such as, the replacement level of RA, the w/c ratio, the moisture state of RA, the physical and mechanical characteristics of RA (the crushing and impact strength), and the constituent of RA (Kou & Poon, 2012). The vast majority of previous studies on RAC reported that the compressive strength of RAC is significantly affected by the increment of the replacement level of RA at the same w/c ratio (Behera et al., 2014). The reduction in compressive strength of RAC was widely reported to be up to 30% at 100% replacement level compared to NAC at the same w/c ratio (Hansen & Narud, 1983; Butler et al., 2011; Tam et al., 2005). Some studies concluded

that the reduction in strength is in the range of 12% to 25% at 100% replacement level (Hansen, 1992; Etxeberria et al., 2007; Rahal, 2007). Other studies reported 60% (Bairagi et al., 1993) and 76% (Katz, 2003) reduction in compressive strength at 100% replacement level compared to conventional concrete.

According to Limbachiya et al. (2000), RA can be incorporated into concrete at 30% replacement level without affecting concrete strength while maintaining the same w/c ratio as the NAC. The utilised RA in their study were sourced from a demolished precast concrete with 20-10mm and 10-15mm aggregate size, and water absorption of 4.9% and 5.2%, respectively. As shown in Figure 2.6, concrete mixtures with 30% RA have similar strength values as mixtures with 100% natural aggregates at the same w/c ratio. In comparison, concrete mixtures with 100% RA obtained lower strength than the 100% NA concrete mixtures by almost 5 N/mm². Similarly, Beltran et al. (2014), found that RA can replace NA in concrete at up to 25% without affecting concrete strength, taking into account the quality of the utilised RA, for instance, concretes produced with high-quality RA sourced from a demolished precast structural member can achieve similar strength performance as NAC at 30% replacement level. This is in line with the studies of Barbudo et al. (2013) and Mefteh et al. (2013). Likewise, Etxeberria et al. (2007) stated that by adjusting the w/c ratio of concretes produced with 25% RA, similar strength to NAC can be achieved. The British standard BS 8500-2:2015+A2:2019 limited the use of RA in structural concrete to 20% and permitted 100% incorporation of RA in the application of roadbase, trench fill, and unreinforced concrete.

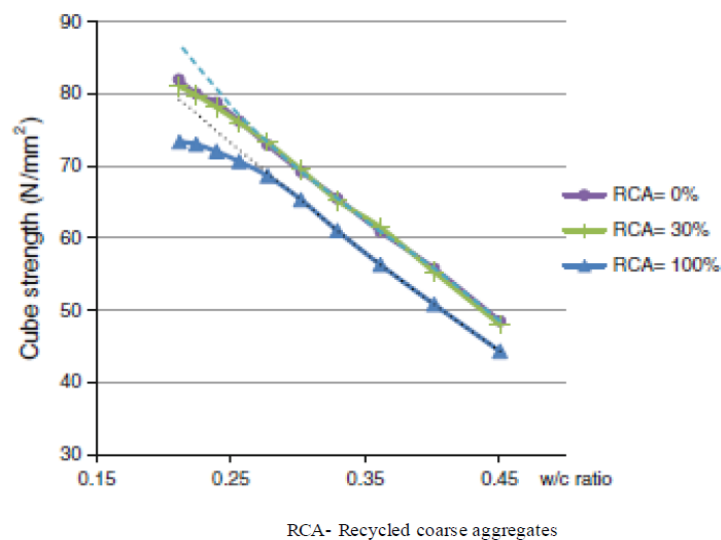


Figure 2.6: Relationship between RA replacement levels and concrete strength at different w/c ratios (Limbachiya et al., 2000)

The literature showed that the strength of RAC tends to decrease with the increase of the w/c ratio, following the same trend as that of NAC (Behera et al., 2014). Hansen (1983) reported that the compressive strength of RAC is dependent on the w/c ratio of parent concrete (original concrete) and the w/c ratio of RAC, while keeping the other factors identical.

Nonetheless, Li (2004) concluded that the compressive strength of RAC decreased with the increase in water to cement ratio at all replacement levels of RA except for the 50% replacement level. The reason behind this non-linearity behaviour between compressive strength and w/c ratio at 50% replacement level was not clear. On the contrary, two studies concluded that the compressive strength of RAC is sometimes greater than the corresponding NAC (Ridzuan et al., 2001; Yoda et al., 1985). This may be attributed to the lowered effective w/c ratio combined with a high rate of water absorption capacity of RA, which might cause an increase in strength.

Otsuki et al. (2003) reported that the compressive strength of RAC is equal to the strength of NAC at higher water to cement ratios, i.e., 0.6 and 0.7. This is due to the new interfacial transition zone formed that governs the compressive strength performance of RAC at higher w/c ratio. In contrast, the strength performance of RAC at lower w/c ratio is governed by the old interfacial transition zone (Behera et al., 2014). According to Domingo-Cabo et al. (2009), when RA is used in dry state, the compressive strength of RAC increases with the increase of the replacement level. This is due to the reduced effective w/c ratio due to the higher water absorption capacity of dry RA. It was also concluded by Etxeberria et al. (2007) that the early compressive strength gain of RAC at 7-day is more than NAC.

Furthermore, Poon et al. (2004) stated that the moisture condition of RA affects the strength of RAC. Poon et al. (2004) concluded that oven dried RA exhibited higher strength than air dried and surface saturated dried RA. This is associated with the high water absorption capacity and rough texture of RA in the case of oven dried condition, which in turn leads to better interlocking between the RA and the new mixture.

According to Etxeberria et al. (2007), by adjusting the w/c ratio of RAC to be 4 to 10% lower than NAC or using more cement content of 5 to 10%, the desired compressive strength of RAC can be achieved. In addition, Saravan and Dhinakaran (2012) concluded that by using superplasticiser combined with 20% of fly ash, a compressive strength of 5% lower than NAC could be obtained.

2.3.2.2 *Split tensile strength & flexural strength*

The other possible inferior mechanical property of RAC is the tensile splitting strength which shows a similar trend of mechanical behaviour as compressive strength in terms of replacement levels of RA. The splitting tensile strength of concrete produced with RA decreases with an increase in RA replacement level. This is ascribed to the presence of the adhered mortar on the RA surface. Nevertheless, the percentage of reduction in tensile strength of RAC is lower than that of compressive strength of RAC (Barbudo et al., 2013; Sato et al., 2007; Gonzalez-Fonteboa et al., 2011; Ajdukiewicz & Kliszczewicz, 2002). Sato et al. (2007) stated that although the adhered mortar on the RA surface forms a weak area under compression, a small quantity can help transfer load under tension. However, a significant amount of adhered mortar will reduce the tensile strength and compressive strength of RAC.

The tensile splitting strength of RAC exhibits similar behaviour as compressive strength. Nonetheless, the effect of RA on tensile splitting strength is less than compressive strength. Several studies showed that the reduction in tensile splitting strength is up to 10% at 100% replacement level (Ajdukiewicz & Kliszczewicz, 2002; Hansen, 1992; Yang et al., 2008; Malesev et al., 2010). According to Rao et al. (2011), the reduction of tensile splitting strength of RAC is about 24% at 100% replacement level.

In general, it has been observed that the tensile splitting strength and flexural strength of RAC is mainly governed by the quality and the surface characteristic of RA (Sonawane & Pimplikar, 2013; Malesev et al., 2010; Abbas et al., 2006). Likewise, several studies reported that the tensile splitting strength of RAC is dependent on a variety of aspects, water to binder ratio, mixing methods, cement type, curing age, and quality of RA (Kou & Poon, 2013; Elhakam et al., 2012; Kou et al., 2011; Zega & Di Maio, 2011). On the contrary, some authors reported that the tensile splitting strength of RAC exhibits similar performance to NAC (McNeil & Kang, 2013), wherein some cases, it was reported that it had better performance compared to NAC (Etxeberria et al., 2007).

Etxeberria et al. (2007) pointed out that this higher split tensile strength of RAC may be attributed to the higher water absorption capacity of RA, which leads to mortar clinging and results in the development of proper bonding with the cement matrix. According to Matias et al. (2013), the increase in tensile splitting strength may be ascribed to the rough surface, of

RA, leading to better interlocking with the cement paste. Rao (2005) argued that the adhered mortar acts like a weak link that fails under compressive load and results in lower split tensile strength. Bairagi et al. (1993) reported that the split tensile strength of RAC is about 40% less than that of NAC. It was also reported that the split tensile strength is enhanced as the curing age increases (Etxeberri et al., 2007; Kou & Poon, 2008; Sagoe-Crentsil et al., 2001).

Sivakumar et al. (2014) pointed out that lower water-binder ratio results in higher tensile splitting strength of RAC compared to higher water to binder ratios. Overall, it can be stated that the bonding strength between the RA and the cement matrix greatly influences the split tensile strength of RAC. Figure 2.7 shows the results of splitting tensile strength of various recycled aggregate concretes (RC) produced with different RA levels at different w/c ratios.

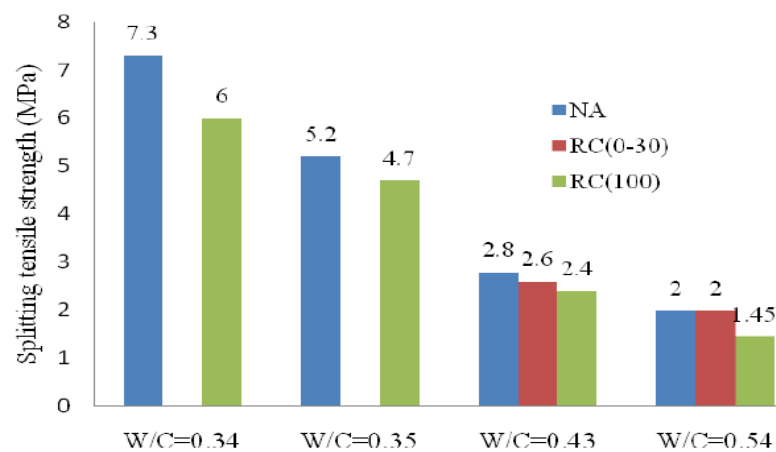


Figure 2.7: The effects of different RA replacement levels on the tensile strength of RAC at different w/c ratios (Barbudo et al., 2013)

Flexural strength, also known as modulus of the rupture of concrete, is another aspect affecting the mechanical performance of RAC; it is mainly governed by the moisture state of RA, curing age and condition, the constituent of RA, and water to binder ratio etc. Similar to compressive strength and tensile splitting strength, RAC exhibits lower flexural strength than NAC. It has been reported that the flexural strength of RAC is mainly dependent on the curing of concrete and the water to binder ratio.

The flexural strength of RAC has been observed to be lower by 26% than that of normal concrete at 100% replacement level. Behra et al. (2014) pointed out the reduction in the flexural strength of RAC is mainly ascribed to the poor quality of the ITZ between the adhered mortar on the RA surface and the new cement paste matrix. Topcu & Sengel (2004) found that the flexural strength of RAC is less than NAC by 10%. Similar to tensile splitting

strength, the increase in the water to binder ratio has been observed to have variable effects on the flexural strength of RAC. Mas et al. (2012) studied the effects of three water to cement ratios of 0.65, 0.72, and 0.45 on the flexural strength of RAC and reported a reduction in flexural strength by 20%, 13%, and 30%, respectively. Yang et al. (2008) argued that incorporating RA with lower water absorption capacity leads to better flexural strength in RAC.

2.3.2.3 Modulus of elasticity & stress-strain behaviour

The elastic modulus of concrete can be defined as the ratio of the stress to the strain of concrete under loads. It is governed by several parameters, concrete strength, aggregate, cement paste, moduli of elasticity of concrete's ingredients, cement paste, mix proportion, and the characteristics of the transition zone (Neville, 2011).

Results from previous research in the literature indicate that the elastic modulus of RAC decreased with an increase in recycled aggregate replacement levels (Dilbas et al., 2014; Limbachiya et al., 2011; Barbudo et al., 2013; Sato et al., 2007; Ignjatovic et al., 2013; Malešev et al., 2010; Duan & Poon, 2014; Rahal, 2007; Casuccio et al., 2008; Fonseca et al., 2011). The researchers explained this behaviour due to the poor quality of RA, which is because of the formed micro-cracks during processing, weathering, pre-loading, high-water absorption, and the poor ITZ of RA. Figure 2.8 demonstrates a comparison of modulus of elasticity values between concretes produced with 100% RA and conventional concretes at 28-day of curing. From Figure 2.11, it can be seen there is a reduction of about 30% in modulus of elasticity in concretes produced with 100% RA compared to NAC.

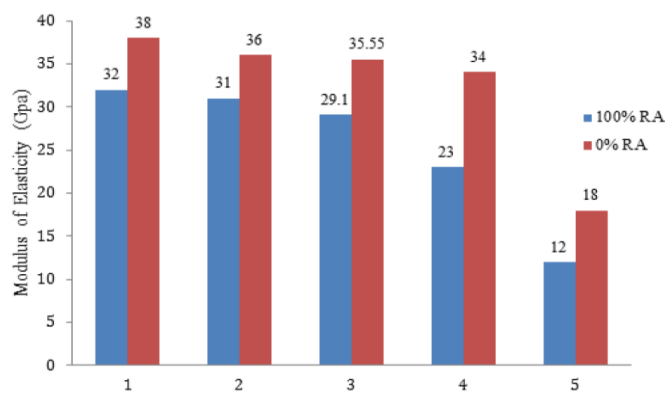


Figure 2.8: Comparison between 100% RAC and 100% NAC in terms of modulus of elasticity presented by different researchers (Barbudo et al., 2013; Fonseca et al., 2011; Malešev et al., 2010; Casuccio et al., 2008; Limbachiya et al., 2011) respectively.

Figure 2.9, presented by Xiao et al. (2005) study shows a comparison between concretes produced with different RA replacement levels (RC) and conventional concrete (NC) in terms of stress-strain behaviour. Although there is a similar stress-strain trend for RACs and conventional concrete, RAC obtained lower strains values at the same stress values because of the lower elastic modulus. Xiao et al. added, incorporating RA in concrete negatively affects concrete making it more brittle.

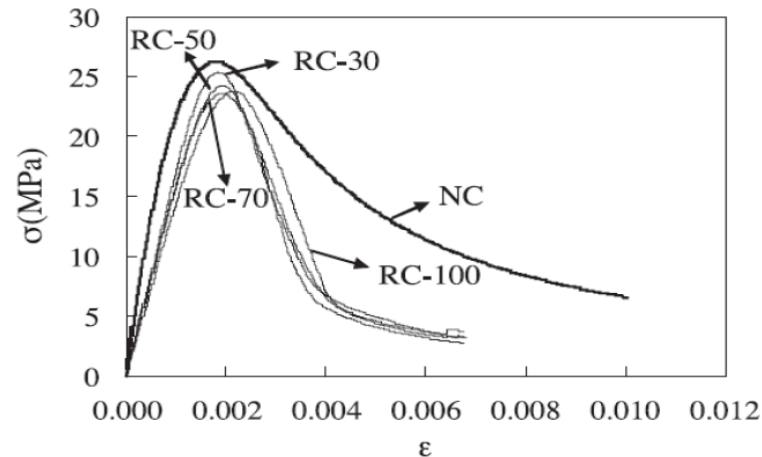


Figure 2.9: Stress-strain trends of RAC (Xiao et al., 2005)

2.3.3 Durability properties of RAC

Durability is a crucial aspect of concrete engineering performance, a durable material contributes significantly toward sustainable development as it helps reduce waste, and conserves resources. The durability of concrete can be defined as the ability to withstand weathering actions, physical and chemical actions while maintaining the desired engineering performance. Concrete durability is mainly dependent on the quality of concrete and its ingredient, mixing proportion, curing conditions, and any utilised admixtures (Kisku et al., 2017). Consequently, because of the poor quality of RA, as mentioned before, the durability performance of RAC is a major concern (Kou & Poon, 2012; Manzi et al., 2013; Richardson et al., 2011; Yadav & Pathak, 2018). This part will review the previous research on the durability performance of RAC in terms of water absorption, freeze and thaw resistance, and sulphate attack.

2.3.3.1 Water absorption

Concrete water absorption can be defined as the flow process of foreign materials through concrete pores. As RA is porous in nature due to the existing micro-cracks on its surface,

concretes produced with a full replacement or partial replacement of RA exhibit higher water absorption compared to NAC (Tam & Tam, 2007). On the other hand, Kwan et al. (2012) concluded that RAC with 15% and 30% replacement levels exhibited similar water absorption values, nevertheless, water absorption proportionally increased with an increase of RA replacement levels above 30%. Previous research indicated that there are similar trends for capillary water absorption in RAC, caused by the presence of higher osmosis pressure, porous adhered mortar, and the high capacity of water absorption of RA (Kou & Poon, 2012; Corinaldesi & Moriconi, 2009) (Debieb & Kenai, 2008; Thomas et al., 2013; Leemann et al., 2015). Thomas et al. (2013) stated that water absorption of RAC tends to significantly increase as the size of RA decreases due to the increased quantity of the adhered mortar. Thomas et al. added that the water absorption of RAC is governed by the quality of RA, constituent of RA, and the source of RA.

2.3.3.2 Resistance to freeze & thaw

Neville (2012) stated that concrete exhibits irreparable loss of strength caused by the expansion associated with the formation of ice due to the occurrence of freezing before the development of desirable strength. RAC resistance to freeze and thaw is dependent on RA replacement levels, the utilisation of air entraining admixtures, and the quality of RA (Tuyan et al., 2014). Similar to other durability properties, freeze and thaw resistance of RAC decreases with an increase in RA replacement levels, and most of the previous studies indicated considerable reduction in RAC mass as high as 0.6% after 150 cycles (Rao et al., 2011; Gokce et al., 2004; Medina et al., 2013). This behaviour is attributed to the existence of air void content in the adhered mortar that significantly changes the pores system in RAC to a partial non-air-entrained void system which in turn would cause profound durability loss under frost attack (Gokce et al., 2004).

2.3.3.3 Sulphate attack

Sulphate attack is one of the major durability concerns of concrete due to the expansion and degradation/ deterioration caused upon concrete exposure to sulphate-rich environment. The phenomenon of loss in strength and increase in mass for all the concrete specimens after exposure to the sulphate solution is due to the ettringite formed within the concrete sample microstructure that causes internal stresses that leads to a loss in strength. Ettringite is formed due to the reaction occurring between the hydrated cement products and the sulphate ions in the sulphate solutions, leading to gypsum production. This gypsum converts the tricalcium

aluminate (C_3A) to ettringite [$Ca_6Al_2(SO_4)_3(OH)_{12} \cdot 26H_2O$] (Mullauer et al., 2013; Bizzozero et al., 2014). The growth rate of sulphate concentration by penetration through the micropores in the first 4 weeks is low and slow because of the low water absorption of concrete, and then it increases with time, as the porosity of concrete decreases due to the reaction occurring between the sulphate ions and the hydrated cementitious products.

The gypsum and ettringite formed in the micropores of concrete via this chemical reaction can delay the penetration process during the first 4 weeks of sulphate exposure. Nonetheless, this process accelerates with time as a result of increased concrete porosity due to the generated micro-cracks because of the internal crystallisation pressure applied on the pore walls of concrete by the ettringite formed. Additionally, another reason that could accelerate the penetration process of sulphate into concrete is the leaching of calcium ions as it increases the porosity of concrete by enlarging concrete capillary pores during the leaching process (Euml et al., 2003; Rozière et al., 2009).

Similar to other durability properties of RAC, the high-water absorption of RAC leads to lower resistance to sulphate attack. This inferior durability property of RAC is mainly due to the high absorption capacity of RA because of the presence of the adhered mortar, pores and microcracks. The literature showed a limited number of studies on the effects of sulphate attack on RAC. Limbachiya et al. (2012) pointed out that RAC exhibits lower sulphate attack resistance than NAC. This is in line with Zuo et al. (2012) study who stated that the higher strength loss observed and higher mass increase for RAC samples after 20 weeks of exposure time compared with the first 4 weeks of exposure is due to the rise in the concentration of sulphate with time and decrease in depth of the concrete sample during exposure to sulphate solution. The decrease in sulphate content with depth of concrete is because sulphate ions need to transfer to the interior structure of the unsaturated concrete by either diffusion, capillary sorption, and penetration. Similarly, Kazmi et al. (2019) reported 1.5% higher increase in mass and 9.5% higher loss in strength for RAC in comparison with NAC upon exposure to sulfate solution. This is also in line with the results of Xie et al. (2020) study, which showed that the mass gain of RACs increased slightly up to 0.69% by 40 weeks of exposure to sulphate due to the ettringite and gypsum (expansion products) formed by the chemical reaction between the sulphate ions and the hydrated cement products.

Furthermore, Bulatovic et al. (2017) reported higher strength loss for the RACs than the NACs by 23% and 3%, after 180 days of exposure to sulphate solution, at 0.55 and 0.38 w/c

ratios, respectively. Moreover, after 365 days of exposure time, RACs exhibited higher strength loss than NAC by 9% and 3%, at 0.55 and 0.38 w/c ratios, respectively. This is also in agreement with Xie et al. (2020) who examined the effects of sulphate attack on recycled aggregate concrete for up to 40 weeks, the results showed that the RACs exposed to sulphate attack showed higher strength loss by 20% compared RACs without sulphate, after 40 weeks of exposure time. In addition, the RACs started to exhibit a loss in strength after 22 weeks of exposure time. Xie et al. (2020) explained these results as the internal pressure caused by the crystallisation of ettringite exceeded the tensile strength of the capacity of concrete, resulting in internal propagated microcracks and damage.

2.3.4 Summary of studies on properties of RAC

Table 2.5 shows a summary of the previous studies on the mechanical properties of RAC with detailed information on RA source, water absorption of RA used, moisture condition, and replacement level for each study, whereas Table 2.6 demonstrates a summary of previous studies on the effect of RA on RAC mechanical and durability properties. It can be summarised from Tables 2.5 and 2.6 that the compressive strength, modulus of elasticity, flexural strength, and tensile splitting strength of RAC generally show a descending tendency with an increase in the RA replacement level. At 100% replacement level, RAC shows an average reduction of up to 40%, 40%, 20%, and 40% in compressive strength, elastic modulus, flexural strength, and tensile splitting strength, respectively, compared to the corresponding conventional concrete. Nevertheless, it can also be established that up to 20% replacement level, the effect of RA on RAC mechanical properties is not prominent.

Furthermore, it can be well summarised that the influence of RA replacement level on compressive strength is significantly higher than other mechanical properties. It can also be concluded that the mechanical properties of RAC depend more or less on the w/c ratio deployed of RAC, quality of RA, source of RA, RA composition and replacement level of RA. The workability of RAC also follows a similar descending tendency to other mechanical properties with an increase in RA replacement level, nonetheless, with the utilisation of pre-wet RA prior to mixing along with the incorporation of superplasticisers, the desired workability can be achieved.

Table 2.6 shows that the durability performance of RAC is inferior to that of conventional concrete. It also can be noted that the higher the replacement level of RA, the poorer the durability performance of RAC. Similar to the mechanical properties of RAC, the durability

performance of RAC depends on the quality of RA deployed, the source of RA, the composition of RA, and the replacement level.

Table 2.5: Summary of research on mechanical properties of RAC

Authors	Coarse RA source/size	Coarse NA source/size	RA Replacement level	Water absorption RA/NA (%)	w/c ratio	RA moisture condition	Compressive strength (MPa)	Flexural strength (MPa)	Splitting tensile strength (MPa)	Modulus of elasticity (GPa)		
Prince & Singh (2013)	Laboratory concrete cubes/ 12.5mm	Crushed limestone/12.5mm	0%	6/0.98	0.54	SSD	36.9	—	—	—		
			25%				28.88					
			50%				24					
			57%				26.2					
			100%				24.7					
Xiao & Falkner (2007)	Processed waste concrete/ 12mm	Crushed limestone/ 12mm	0%	9.25/0.4	0.43	Pre-soaked	43.5	—	—	—		
			50%				39.3					
			100%				34.6					
			100%				34.6					
Ignjatovic et al.(2013)	Demolished old bridge/ 31.5-8mm	Natural river gravel/31.5-8mm	0%	3.8/0.5	0.52	Oven dried	44.2	—	3.2	26.6		
			50%				43.7		3.1	26.2		
			100%				42.5		2.7	25.4		
			100%				42.5		2.7	25.4		
Manzi et al. (2013)	Processed 15years old concrete/ 25-15mm	Natural gravel 25-16mm	0%	7/1.2	0.48	Air dried	41.3	6.4	3.8	31.4		
			27%				44.7	5.8	4.1	30.3		
			37%				45.6	4.8	3.2	26.9		
			64%				51.4	4.9	3.0	24.9		
			100%				51.4	4.9	3.0	24.9		
Topçu & Şengel (2004)	Crushed concrete cubes of 14MPa/32-4mm	Natural gravel 32-4mm	0%	—	0.57	Pre-soaked	20	2.2	—	—		
			30%				18.2	2				
			50%				17.8	1.7				
			70%				16.5	1.7				
			100%				14	1.6				
Xiao et al. (2005)	Processed concrete from airport runway/20-6mm	Natural gravel/20-6mm	0%	9.25/0.4	0.43	Pre-soaked	35.9	—	—	27		
			30%				34.1			15		
			50%				29.6			16		
			70%				30.3			16		
			100%				26.7			17		
Etxeberria et al. (2007)	Unknown/25-4mm	Unknown/25-4mm	0%	—	0.55	Pre-wetted	29	—	2.49	32.56		
			25%		0.55		28		2.97	31.3		
			50%		0.52		29		2.7	28.6		
			100%		0.5		28		2.72	27.8		
Casuccio et al. (2008)	Crushed 2 years of concrete of different strengths/30-6mm	Crushed natural granitic/30-6mm	0%	0.5	—	—	48.4	—	7.3	39.9		
			100%				3.9		0.35	44.4	6	34.2
			100%				3.9		0.35	43.8	5.8	32.7
			100%				3.8		0.34	35.7	5.3	28.8
			100%				3.8		0.34	36.4	4.1	28.2

(Continue) of Table 2.5: Summary of previous research on mechanical properties of RAC

Authors	Coarse RA source/size	Coarse NA source/size	RA Replacement level	Water absorption RA/NA (%)	w/c ratio	RA moisture condition	Compressive strength (MPa)	Flexural strength (MPa)	Splitting tensile strength (MPa)	Modulus of elasticity (GPa)	
Limbachiya et al. (2000)	Recycling plant/ 20-5mm	Natural gravel/20mm	0%	5.3/0.61	—	SSD	45	5	—	19	
			30%				40	5.1		15	
			50%				38	4.6		14	
			100%				32	4.9		12.5	
Fonseca et al. (2011)	Laboratory crushed concrete waste/25mm	Crushed Natural limestone/25mm	0%	6.1/1.3	0.43	Air-dried	51	—	2.8	36	
			20%				48.8		2.6	35	
			50%				51.2		2.8	35.5	
			100%				51.3		2.4	31	
Beltran et al. (2014)	Crushed concrete blocks/20-4mm	Unknown/16-4mm	0%	6.93/1.53	0.6	Air-dried	42.02	4.71	—	27.3	
			20%				42.86	4.65		26.2	
			50%				42.51	4.68		25.9	
			100%				40.86	4.8		25.1	
Kou & Poon (2012)	Recycling plant/10mm	Crushed granite/20mm	0%	3.52/1.11	0.55	Air-dried	48.6	—	—	—	
			20%				45.3			—	—
			50%				42.5			—	—
			100%				38.1			—	—
Dilbas et al. (2014)	Processed from demolished building/32-4mm	Crushed basalt/32-8mm	0%	4.3/0.6	0.5	Pre-soaked	35.8	—	2.25	28.1	
			100%				34.1		2.41	25.2	
Barbudo et al. (2013)	Crushed 30 days concrete blocks/25-4mm	Crushed Natural limestone/20-12mm	0%	7.34/1.25	0.54	Air-dried	50	—	11	38	
			20%				52		9	37	
			50%				48		8	36	
			100%				46		8	32	
Mefteh et al. (2013)	Processed demolished precast structural element/20-5mm	Crushed limestone/20-5mm	0%	5.3/2.4	0.54	SSD	31	—	2	—	
			20%				33		2	—	
			60%				25.5		1.9	—	
			80%				25		1.65	—	
Chakradhara et al. (2010)	Processed demolished 15 years concrete/20mm	Crushed dolomite/20mm	0%	3.92/0.2	0.43	SSD	50	5.23	2.67	31.22	
			25%				45	4.17	2.03	20.35	
			50%				46.6	4.42	2.05	21.54	
			100%				43	4.17	2.33	23.57	
			100%				—	—	1.45	—	

Table 2.6: Previous studies on the effects of RA from the C&DW on concrete mechanical and durability property

Reference	Mix design adopted	Properties tested	Main findings
Ferriz-Papi & Thomas (2017)	(1) 80% of NA was replaced with coarse and fine RA. (2) Control specimen of 100% NA. (3) w/c ratio was 0.6 for specimen A and 1 for specimen B (cement content is constant)	Workability, absorption, and compressive strength	Significant reduction of the 28-day compressive strength of 60% in specimen A and 71% in specimen B compared to the control mix. Both samples exhibited a substantial increase at about three times the reference sample in terms of absorption. Slump values were 13cm for the control mix, 2.5cm for sample A and 23 cm for sample B, this indicates that RAC with a lower W/C ratio exhibits lower workability than that of a higher w/c ratio.
Alexandridou et al. (2018)	0%, 25%, and 75% of NA were replaced with coarse RA	Compressive strength, absorption, sorptivity, freeze and thaw resistance,	Compressive strength values decrease as the replacement of RA increases. 37% reduction in compressive strength was observed at 75% replacement. Likewise, the durability properties seem to be negatively affected at higher replacement levels.
Bravo et al. (2015)	Coarse and fine RA were collected from 5 different recycling plants. 10%, 25%, 50% and 100%, replaced fine and coarse natural aggregate	Workability, density, absorption	The use of RA resulted in dry mixtures in terms of workability, reduced density, and poor durability performance. Mixtures with fine RA exhibited the worse results due to the high clay content in fine RA.
Bravo et al. (2015)	Coarse and fine RA were collected from 5 different recycling plants. 10%, 25%, 50% and 100%, replaced fine and coarse natural aggregate	Compressive strength, tensile splitting strength, modulus of elasticity, and abrasion resistance.	Concretes with fine RA exhibited the worse compressive strength and tensile splitting strength. Reduction in compressive strength and tensile strength varied from one sample to another depending on their source, RA composition (specifically clay content), and quality of the adhered mortar. Modulus of elasticity tends to decrease with replacement of RA with a loss of 40% at 100% replacement. Reduction in abrasion resistance was also observed, and the authors concluded the main reason behind that is the size of RA utilised.
Kou et al. (2004)	20%, 50% and 100% recycled coarse aggregate replaced NA	Compressive strength at 7-, 28- and 90-day	RAC mixtures exhibited losses in compressive strength of 33%, 37% and 31%. However, the adverse effects of RA incorporation seem to fade over time.
Poon et al. (2007)	10%, 20%, 50%, 80% and 100% replacement ratio	Compressive strength at 3-, 7-, 28- and 90-day	24%, 16%, 19% and 10% were the loss in compressive strength at 100% replacement level at 3,7,28, and 90 days respectively.
Medina et al. (2014)	C&DW aggregate with high content of asphalt and floating matter.	Compressive strength	A Loss of 18% in compressive strength was recorded at a 50% replacement level.
Zaharieva et al. (2003)	Recycled fine aggregates and recycled coarse aggregate were used	Water absorption	At the full replacement level, water absorption of RAC increased by 16%, whereas the combination of recycled aggregate (fine and coarse) increased water absorption by 42%.

Continue of Table 2.6: Previous studies on the effects of RA from the C&DW on concrete mechanical and durability properties.

Reference	Mix design adopted	Properties tested	Main findings
Cantero et al. (2018)	20%, 25%, 50%, 75% and 100% were the replacement levels, water-base polycarboxylate superplasticiser was added to the mix.	Workability, density, air content, compressive strength, flexural, and splitting tensile	All the RAC mixtures exhibited slightly similar workability compared to that of NAC. 6.9% decline in the density of 100% replacement and 36.7% rise in air content at the same replacement level. Under 50% of replacement, neither compressive strength nor flexural strength exhibited reductions, however, at higher replacement levels, there were significant reductions. i.e., 7% compressive, 4% tensile and 19% flexural of reduction at 100% replacement level. Nonetheless, it was concluded that this type of C&DW aggregates could be used in concrete for structural application with $f_{ck} > 30$ MPa.
Seara-Paz et al. (2016)	20%, 50% and 100% replacement levels with two w/c ratios of 0.5 and 0.65, RA were pre-saturated in water for 10 mins prior to batching, superplasticiser SIKAMENT 500 HE was added as a water-reducing admixture	Consistency, density, water absorption, compressive strength at 28- and 42-day, modulus of elasticity	RACs showed slightly better performance at all replacement levels than NAC in terms of consistency due to pre-saturation and the use of admixtures. The density of hardened RACs showed a reduction in values as the replacement levels increased. Water absorption of RACs increases as the replacement level increases. W/c ratio of 0.5 showed better compressive strength results for all RACs. Compressive strength decreases as the RA replacement level increases, likewise to the modulus of elasticity. At 100% level and 28 days curing age, there was a loss of 29% in compressive strength.
Hadavand & Imaninasab (2019)	10%, 20%, 30% and 50% replacement. W/c ratio of 0.4, 0.45, 0.5.	Workability, compressive at 7- and 28-days strength, tensile, and flexural strength	The workability of mixes increases as the w/c ratio increase and decreases with an increase in RA replacement level. Compressive strength tends to decrease with the rise in replacement level and w/c ratio. At the replacement level of 50%, tensile strength exhibited a 10% reduction compared to the control mix. Likewise, the introduction of RA to concrete decreases the flexural strength. It was concluded that, under 50% replacement level, there were no significant effects on compressive, tensile, and flexural strength.

2.4 Treatment Methods for Recycled Aggregate

2.4.1 Self-healing

The self-healing treatment aims at allowing the un-hydrated adhered mortar on the RA surface to undergo a hydration process while it is in contact with water for a long period of time. This treatment involved soaking RA in water for 30 days prior to its incorporation into concrete. Elhakam et al. (2012) studied the effects of self-healing treatment on the RAC mechanical properties and reported enhanced compressive strength of RAC by more than 30%.

2.4.2 Water washing

The water washing method resembled a prolonged Los Angeles test, that removed a significant amount of the adhered mortar along with any fractured or weaker aggregates, hence keeping only stronger and sounder ones which are the results of the RA colliding into each other in the presence of water. Dimitriou et al. (2018) studied the influence of water washing and reported 50% enhancement to the WA after water washing treatment.

2.4.3 Water saturation

The water saturation method aims mainly to prevent the recycled aggregates from consuming the effective mixing water, which is needed for cement hydration. Ferreira et al. (2011) recommended that 90% of saturation level can be achieved by immersing the aggregates in water for 5 mins prior to mixing. Ferreira et al. (2011) reported that, 90% of saturation level is ideal, whereas 100% of saturation may cause a detrimental effect on concrete.

2.4.4 Carbonation treatment

The carbonation treatment method is composed of two main treatments, accelerated carbonation treatment, and cyclic carbonation treatment/cyclic lime-water-accelerated carbonation treatment. The efficiency of accelerated carbonation treatment in enhancing the properties of the RA stems from the chemical reaction of CO₂ with the hydrated products within the adhered mortar on the RA surface. The pores and micro-cracks of the RA can be filled with hydration products through carbonation (Mistri et al., 2020). Pu et al. (2021) reported 9.14% reduction in the AIV of the RA after carbonation treatment at 20% CO₂ concentration level for seven days of carbonation. Zhang et al. (2015), Li (2014), and Ying et al. (2017), reported 22.6-40.3% enhancement in water absorption after carbonation treatment

at various CO₂ concentration levels. Zhan et al. (2017), observed that carbonated RA achieved 44% enhancement in AIV after pre-soaking, followed by accelerated carbonation. Whilst Zhan et al. (2017) reported that a 50% reduction in water absorption could be achieved when cyclic carbonation treatment is repeated for three cycles.

Fang et al. (2021) reported 6.5% and 10% enhancement in the 7-day and 28-day compressive strength of the RAC, respectively, after carbonation treatment. A similar trend was observed by Lu et al. (2019) who concluded in their study that incorporating carbonated RA into RAC enhanced the 28-day and the 90-day compressive strength of RAC by 24.1% and 26.8%, respectively. Lu pointed out that the treated RAC produced with carbonated RA exhibited denser ITZ, lower porosity, and fewer cracks due to the calcium carbonate and silica gel formed, which filled in the pore structure of RAC, these factors contributed significantly to better strength development of the treated RAC. Pu et al. (2021) pointed out the superior compressive strength of carbonated RAC to non-carbonated or untreated RAC is due to the lower amount of water used in the case of carbonated RAC, which led to reducing the effective water to cement ratio and hence, enhanced compressive strength. In addition, the improved AIV and density of carbonated RA compared to non-carbonated RA has also led to improved compressive strength.

Shi et al. (2018) stressed that the enhanced compressive strength of RAC produced with treated RA by accelerated carbonation might be attributed to the generated secondary calcium silicate hydrates (C-S-H) by the production of silica gel which further produced calcium silicate hydrates due to the chemical reaction between carbon dioxide and calcium silicate hydrates at later age of curing. Figure 2.10 shows the schematic diagram of the mechanism of the carbonation treatment method according to Pu et al. (2021).

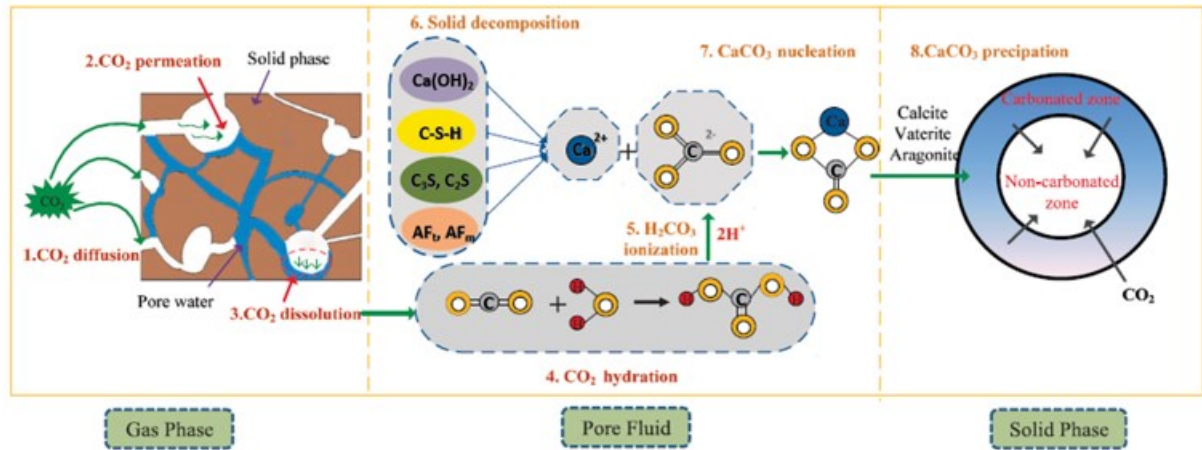


Figure 2.10: Schematic diagram of the mechanism of carbonation treatment method after to Pu et al. (2021)

According to Liang et al. (2020), there are several impact factors and variable parameters affecting the efficiency of RA carbonation treatment:

1. **Pre-treatment method:** the main reason behind the quality improvement of RA by carbonation treatment is the production of CaCO_3 . Therefore, supplying an additional source of Ca^{+2} through the pre-treatment method might result in further enhancement of RA properties. According to Zhan et al. (2017), presoaking RA in CaCl_2 solution prior to carbonation treatment resulted in 38.8% and 60% enhancement in crushing value and water absorption, respectively. They also stated that, pre-soaking RA in $\text{Ca}(\text{NO}_3)_2$ solution led to 40% and 65% further enhancement in crushing value and water absorption, respectively.
2. **Water content of RA:** the water content of RA promotes the efficiency of the carbonation reaction, because it dissolves the CO_2 gas and Ca^{+2} contained in RA. The lower water content of RA means insufficient amount of water that participates in the carbonation process, whereas higher water content delays the penetration of CO_2 . Zhan et al. (2016) and Pan et al. (2017) suggested that the optimum water content for RA ranged from 4% to 6.5%.
3. **CO_2 gas concentration:** the concentration of CO_2 is another key factor in RA carbonation treatment. Once the CO_2 concentration exceeds the optimum value, the improvement of the carbonation efficiency cannot be increased with the further increase in the CO_2 level. Pan et al. (2017) found that the water absorption values of RA after the carbonation treatment with a CO_2 levels of 20%, 70%, and 100% were

2.00%, 1.65%, and 2.00%, respectively. They concluded that, the optimum CO₂ concentration for carbonation treatment ranges from 40-60%.

4. **CO₂ gas pressure:** the gas pressure of CO₂ got a distinct effect on the efficiency of the carbonation of treatment. Zhan et al. (2017) reported that the water absorption of RA decreased when the CO₂ pressure increased from 0 MPa to 0.5 MPa, however, the water absorption increased when the CO₂ pressure increased to 1.5 MPa. Excessive CO₂ pressure leads to higher porosity and water absorption of RA, which might be due to the formation of new cracks in the adhered mortar of the RA (Tam et al., 2016). Furthermore, when applying a high carbonation pressure, a needle-shaped calcium carbonate product is formed, while a particle-shaped calcium carbonate is generated in RA when it is carbonated under a low gas pressure (Zhan et al., 2016).
5. **Time of CO₂ curing:** with the increase in CO₂ curing time, the carbonation percentage of RA tends to increase until the RA is completely carbonated. Zhan et al. (2014) found that, at the first 2 hrs of carbonation, RA carbonation percentages rapidly increased and obtained 25.06% carbonation percentage, while it just attained 28.47% carbonation percentage when the curing time was extended to 4 hrs. In other words, RA attained a significant improvement at the preliminary stage of carbonation in terms of its properties, whereas this improvement was slow with a further increase in carbonation time.
6. **RA components & the availability of the adhered mortar:** another major key aspect is the components of RA. The efficiency of carbonation treatment mainly relies on the chemical reaction between Ca(OH)₂ and CO₂. This means the quantity of the adhered mortar plays a significant role in achieving a better-quality RA through carbonation treatment. In other words, constituents of RA affect the efficiency of the carbonation treatment, RA with a higher quantity of recycled concrete aggregates (aggregates with cement-based external layer) obtains a better quality after CO₂ treatment.

2.4.5 Soaking RA in sodium silicate - silica fume solution

Immersing the RA in a pozzolanic solution can improve the microstructure and the engineering properties of the RA in two aspects; pozzolana acts as a micro-filler that fills in the pores and micro-cracks of RA, these materials will form C-S-H gel through reacting with CH crystals in RA that fill up the voids with RA. A thin layer called water repellent is formed

by impregnating the RA in sodium silicate-silica fume solution for a specific time, resulting in filling the pores and the voids within the adhered mortar when. When RA is immersed in this solution, both materials can react with the calcium hydroxide existing in the adhered mortar to form C-S-H gel (Yang et al., 2016).

Yang et al. (2016) soaked RA in water glass (sodium silicate) solution of different concentrations of 3%, 5%, 8%, 10%, 20%, and 40% for 10 min, 1h, 2h, and 5h. They found that the RA obtained enhanced water absorption by 36% when RA was soaked in a water-glass solution with 40% concentration for 1 hour, whereas soaking the RA in a water-glass solution with 5% for 1 hour achieved the best performance in terms of concrete 3-, 7-, and 28-day compressive strength at about 22%, 28% and 29% enhanced performance respectively. Bui et al. (2018) soaked RA in three main solutions; solution type G, solution type S, and sodium silicate SS. Solution type G included; GFA (fly ash + NaSiO_3 + NaOH), GSF (silica fume + NaSiO_3 + NaOH), GMK (metakaolin + Na_2SiO_3 + NaOH). Solution type S included; SFA (fly ash + Na_2SiO_3), SSF (Silica fume + Na_2SiO_3), and SMK (metakaolin + Na_2SiO_3). Solution type SS was sodium silicate. RA was soaked for 24 hours and at three different solution concentrations 10%, 20%, and 30%. Among all the treatment solutions, RA soaked with sodium silicate (SS) solution at 30% concentration achieved the best performance in terms of water absorption, RA attained 34% enhanced water absorption. Bui et al. stated that, among all the utilised solutions, the combination between silica fume and sodium silicate achieved the best 28-day compressive strength, concrete produced with treated RA in silica fume-sodium silicate solution achieved 36% enhancement.

2.4.6 Coating RA with cement slurry or cement-silica fume slurry

Overall, this surface treatment method aims at altering the micro surface structure of RA and then strengthen it by the touch-up of new materials (i.e., cement, silica fume, fly ash) and coating of the older material via patching and bonding of the smaller pores on the surface of RA to enhance its quality and properties, hence, reinforcing the bonding force and mechanical strength of the interface between coating materials and RA (Lee et al., 2011). It can also be added that, the basic premise of this treatment is to coat RA with hydrated cement film, which is thick enough to act as a shield on the surface of RA. Kareem et al. (2018) found that coating the individual RA at 0.1 mm coating thickness with cement only slurry resulted in better AIV by 7% enhancement compared to 0.05, 0.2, 0.4 mm coating thicknesses. Lee et al. (2011) reported a 12% enhancement in the RA AIV via coating with cement slurry at 0.25%

coating thickness. Zhihui et al. (2013) reported 9% enhancement in AIV of RA after coating the total combined RA size fraction with cement slurry.

2.4.7 Soaking RA in cement-pozzolan solution

The main principle behind this treatment is to cover the RA surface with a thin layer of hydration products, hence strengthening RA engineering properties. After the treatment, a dense coated layer is formed around the RA surface after the reaction of the pozzolanic materials with the $\text{Ca}(\text{OH})_2$ in the adhered mortar. Shaban et al. (2019) reported an approximate reduction of 40% and 51.4% in AIV and WA, respectively, after soaking RA in cement-pozzolan solutions. Li et al. (2009) examined the effect of soaking of RA by pozzolanic powder (fly ash, silica fume, and GGBS) and found that the combination of Portland cement along with fly ash and silica fume is more efficient for high strength recycled aggregate concrete with better packing density and denser interfacial transition zone. Limited studies investigated coating/soaking of RA in cement-pozzolan slurry prior to mixing, while the vast majority of studies examined the effects of coating RA with cement and/or pozzolan slurry during mixing. According to Tam et al. (2021), very few studies dealt with treating RA by coating and/ or soaking in pozzolan solution or slurry prior to mixing. Liang et al. (2015) examined the effects of treating RA by soaking in cement-SF solution, and reported a 29% increase in the 28-day compressive strength of RAC, compared to the untreated RAC.

2.5 Batching Techniques for Recycled Aggregate Concrete

2.5.1 Stone enveloped with pozzolan powder (SEPP)

Li et al. (2009) demonstrated that the stone enveloped with pozzolan powder (SEPP) batching method utilises surface coating with pozzolanic powder prior to mixing, this process offers improvement in RAC strength due to the formed thin cement-pozzolan layer on the surface of the RA along with the effects of pozzolan which is well-known for its effectiveness in strength growth. The authors reported that Silica Fume is most effective in densifying the cementitious matrix than other pozzolanic materials due to the pore-filling effects and wider distribution of its particles. The incorporation of Silica Fume in the surface coating of recycled aggregate prior to the SEPP batching technique contributes significantly toward the higher strength development of the RAC because SF is more prone to obtain a maximum packing density.

2.5.2 Two-stage mixing approach (TSMA)

Tam et al. (2007) stated that during the first stage of mixing in the two-stage mixing approach (TSMA), a thin layer of cement slurry on the RA surface is developed, leading to filling up the micro-cracks and voids in the adhered mortar of the RA. The strength improvement comes in the second stage of mixing where the added remaining water contributes to the completion of the hydration process of cement and hence improving the strength of the concrete mixture (Elhakam et al., 2012).

2.5.3 Sand enveloped mixing approach (SEMA)

Liang et al. (2015) reported that, the strength improvement in the sand enveloped mixing approach (SEMA) is mainly governed by enhancing the adhered mortar quality. Liang et al. (2015) also added, the benefits of utilising the SEMA method is that it involves mixing sand, cement and three-quarters of the total mixing water prior to the incorporation of RA, which allows the sand particles to mix more readily with cement and water and hence the RA will absorb less water.

2.5.4 Mortar mixing approach (MMA)

The concept of the mortar mixing approach (MMA) batching technique is preventing the adhered mortar on the surface of the RA from consuming the effective mixing water, hence sufficient water will be available for cement hydration which in return leads to an enhancement in compressive strength (Liang et al., 2015).

2.6 Summary of the Current Enhancement Methods for RA and RAC

The vast majority of the previously utilised approaches and techniques in the literature that dealt with the treatment and enhancement of RA and RAC quality, can be fundamentally classified into three main categories: (i) removing the adhered mortar, (ii) strengthening the adhered mortar, and (iii) improving the whole matrix of RAC. The latter mainly includes, batching techniques, incorporation of mineral admixtures, and the addition of superplasticisers. Tables 2.7, 2.8, and 2.9 summarise the enhancement methods obtained from the existing literature. The assessment of these methods is also provided.

As shown in Tables 2.7, 2.8, and 2.9, it can be concluded that the literature showed extensive studies on the effects of treatment methods on improving the quality of RA, however, it should be noted that when considering the type of treatment to be utilised, several key factors

should be taken into considerations; the feasibility of applying the selected treatment method in the construction industry and recycling plants, cost efficiency, efficiency, environmental concerns, and simplicity.

Mechanical grinding treatment of RA is not an efficient method since it might weaken RA microstructure. All water-based treatment methods are cost-effective, applicable and straightforward, but their efficiency needs to be tested on the structural performance of RAC members. Pre-soaking in acid increases the production cost and may introduce micro-cracks to RA.

Polymer impregnation is not an effective approach since it did not show any significant improvement. Coating or impregnating with cement and supplementary cementitious materials is one of the best approaches to treat RA, but caution must be taken regarding the cost perspective. Carbonation might be the best treatment method since it combines all the key factors and no adverse effects have been encountered, but its impact on the structural performance of RAC beams must be carried out to obtain a better scientific agreement when choosing such a treatment method. Moreover, batching techniques are promising methods for improving RAC engineering performance, and it can be combined with other treatment approaches to obtain better results.

Table 2.7: Previous research on removing the adhered mortar treatment methods

Treatment Method	Method Used	Reference	Positive Results	Negative Results
Mechanical Grinding	Autogenous cleaning	Pepe et al., 2014; Montgomery, 1998	Simple, produce high-quality RCA, improve the shape of aggregates due to collision and peeling-off effects, a progressive decrease of the water absorption capacity up to 50%.	RCA could be damaged due to collision and grinding by introducing micro-cracks.
	Selective heat grinding combined with autogenous cleaning.	Bru et al., 2014	Effective removal of adhered mortar. Improved quality of RCA.	RCA could be damaged due to collision and grinding by introducing micro-cracks.
	Heating and rubbing/scrubbing combined with autogenous cleaning	Fathifazl et al., 2009, Al-Bayati et al., 2016, Tateyashiki et al., 2001	Improving various physical properties, including water absorption, specific gravity, porosity and freezing and thawing.	Aggregate suffers from thermal expansion followed by internal stresses due to exposure to a high temperature between 400°C and 600°C. Whereas there is serious microcracking of the cement matrix when the material is exposed to a higher temperature range between 600°C and 800°C, resulting in degradation, breakdown and mass loss of aggregate.
Pre-soaking in water/ Ultrasonic water cleaning	_____	Gracia-Gonzalez, et al., 2014; Katz, 2004	Effective in washing away loose, weak adhered mortar, and increases the compressive strength of the recycled aggregate concrete; but the strength increase was about 7% at 28-day	Stronger mortar cannot be removed.
Self-healing	_____	Elhakam et al., 2012	Improved mechanical properties of recycled aggregates concrete, especially for low cement content	_____
Pre-soaking in acid	Hydrochloric acid (HCl), sulfuric acid (H ₂ SO ₄) and phosphoric acid (H ₃ PO ₄)	Tam et al., 2007	Reduced water absorption and improved mechanical properties for the recycled aggregate concrete. HCl is the most effective acid. some reaction products of H ₂ SO ₄ tended to crystallise, and the products of H ₃ PO ₄ were unstable	The process increases concrete production costs, which is the obstacle to implementing this approach. Possibilities to introduce micro-cracking and acid corrosion.
	Immersing in HCl and impregnating with calcium metasilicate (CaSiO ₃) solution	Ismail & Ramli, 2004	Improved mechanical properties, reduced water absorption and improved bond strength at the contact between the aggregate surface and the cement matrix because of coating with calcium metasilicate.	
	Immersing in both hydrochloric acid (HCl) and acetic acid (C ₂ H ₄ O ₂)	Al-Bayati et al., 2016	Using weak acid is more efficient than the strong acid to decrease the influence of acid attacks	
	Hydrochloric acid (HCl), nitric acid (HNO ₃) and sulfuric acid (H ₂ SO ₄)	Saravanakumar et al., 2016	Silica fume impregnation after chemical immersion treatment gave better densified recycled aggregate.	

Table 2.8: Previous research on strengthening the adhered mortar treatment methods

Treatment Method	Method used	Reference	Positive Results	Negative Results
Polymer emulsion/impregnation, or water-repellent post-treatment.	Immersing in Polyvinyl alcohol (PVA) solution	Kou & Poon, 2010,	The polymer molecules can fill the pores of the adhered mortar and seal the surfaces of the RCA. Improved physical and workability, and durability properties. Decreased water absorption. Increase the bonding strength between the cement paste and the aggregate, and reduce the water-to-cement ratio in the ITZs. improved workability, compressive strength, and drying shrinkage	Reduce the compressive strength of the concrete. The reasons might be that the positive polymer groups permeate into the cement paste and make it hydrophobic, which hinders the hydration of the un-hydrated cement in the paste. At the same time, the formation of water-repellent film weakens the bonding strength between the aggregate and cement matrix.
	Silicon-based water-repellent polymers: silane-based polymer	Zhu et al., 2013	It has been found that the surface coating treatment was more efficient in reducing the water absorption of concrete compared with the integral treatment.	
	Alkylalkoxysilanes (silane), polydiorganosiloxanes (siloxane) or both with impregnation in sodium silicate solution PVA and naphthalene superplasticiser	Spaeth & Tegguer, 2013 Qiu, 2003	significant reduction of water absorption capacity. efficient and resistant in an alkali environment Both used materials reduced the water absorption of RCA. Superplasticizer treatment could improve the bonding strength between the aggregate and the cement matrix compared with PVA.	
Immersing/impregnated in Pozzolan Slurry or Mineral Admixture Solution	Impregnation in silica fume solution	Katz, 2004	Fill the pores and voids inside the adhered mortars, and then react with calcium hydroxide to form C-S-H gel. Improve the microstructure of both ITZs in RCA and improved durability.	Minor adverse effects on the mechanical properties. _____ _____ Sodium silicate treatment might introduce alkalis, which increases the risk of an alkali-silica reaction. _____ _____
	Immersing in lime solution and silica fume solution	Shayan & Xu, 2003	The microstructure of RCA was much denser and the ITZs were obviously improved. Strengthened the weak structure of the RA. Improved durability	
	Nano-SiO ₂ solution	Singh et al., 2013	Efficient in improving the properties of RCA due to small size and high reactivity.	
	Sodium silicate solution	Chen et al. 2006	Sodium silicate solution can react with calcium hydroxide to form C-S-H gel.	
Surface improvement through coating	Paraffin based material: oil-type agent and silane-type agent	Tsujino et al., 2007	Water absorption of RCA is reduced with the number of spraying and drying cycles. Oil-type agent performs better than a silane-type agent in terms of mechanical properties and strength enhancement as well as cracking resistance.	_____
	Pozzolanic powder	Li et al., 2009	Significant improvement in the mechanical performance of recycled aggregate concrete, denser ITZ structure.	_____
Calcium carbonate bio-deposition. Carbonation	S. pasteurii cell (Sp. cell)	Grabiec et al., 2012	Reduction in the water absorption of aggregate	_____
	Carbon dioxide treatment	Kou et al., 2014; Zhang et al., 2015; Li et al., 2017	Increasing CO ₂ concentration and pressure would accelerate carbonation and increase the strength development rate of concrete. carbonation increased the density and decreased the water absorption and crushing values of the RCA. enhance adhered mortars and both the original and new ITZs around the RCA. CO ₂ treatment is lower in cost Improved durability.	No adverse results have been encountered

Table 2.9: Previous studies on improving the whole matrix of RAC

Treatment method	Method used	Reference	Positive Results	Negative Results
Batching technique	Two-stage mixture approach (TSMa)	Tam et al., 2005	Can improve RAC properties, that's because the RCA will be coated with mortar of a lower water-binder ratio in the premix process, which can lead to a stronger interfacial transition zone (ITZ).	
	Two-stage mixing approach (silica fume) TSMAs, and Two-stage mixing approach (silica fume and cement): TSMAsc	Tam & Tam, 2008	TSMAs and TSMAsc can provide alternative methodologies for further improvement in the quality of this recyclable material and provide an effective method for enhancing the strength behaviour of RAC when compared with TSMa.	
	Triple mixing method	Kong et al., 2010	Enhanced compressive strength and chloride ions penetration, improve the microstructure of the ITZ.	
	Stone enveloped with pozzolanic powder (SEPP). Scattering-filling coarse aggregate (SFCA)	Li et al., 2009 Xu et al., 2018	Significant improvement in the mechanical performance of recycled aggregate concrete. A denser ITZ structure. The properties of SFRA concrete are better than the ordinary concrete and conventional RAC. reduce the drying shrinkage and chloride penetration. The frost resistance of SFRA is comparable with conventional concrete. improving ITZ between the aggregate and cement paste in RAC	
	Recycled Woven Plastic Sack fibre and recycled PET bottle fibre. combination of Silica Fume (SF) and RPET fibre Polypropylene fibres (PP)	Bui et al., 2018 Hanumesh et al., 2018	Post-cracking behaviour of RAC was improved, improved compressive strength, elastic modulus, splitting strength, shear strength. RPET performed better than RWS fibres. For 100% RAC with 1% PP fibre volume, compressive strength, split tensile strength and shear strength increased by 15.68%, 34.84% and 38.32%, respectively, compared with reference mixes. For 100% RAC with 2% PP fibre volume, compressive strength, split tensile strength and shear strength increase by 35.7%, 85.6% and 38.32% ,respectively, when compared with reference mixes.	
Blending with SCMs and other materials.	Two types of cement and admixtures (polycarboxylate and ether polycarboxyliquet)	Tahar et al., 2017	There is no reduction in a slump of recycled aggregates concrete (RAC) up to 30% of recycled aggregates (RA).	Decrease in density and strength of recycled aggregates concrete (RAC).
	superplasticisers: polycarboxylic-based and lignosulfate-based ones	Bravo et al., 2017	The efficiency of polycarboxylic superplasticisers on concrete made with recycled aggregates was satisfactory	
	Blending with Nano-silica sodium hydroxide (NH) and sodium silicate (NS) as alkaline activators	Nuaklong et al., 2018	The addition of Nano-silica showed great potential to enhance the mechanical properties of recycled aggregate geopolymer concrete. OPC-fly ash blend mixture exhibited the highest compressive strength of 48.7 MPa	
	1- coupling effects of silica fume and steel fibres 2- silica fume and polypropylene fibres	Xie et al., 2018	Improvement in the compressive and flexural behaviour of the fibre reinforced RAC. The coupling effect of silica fume and steel fibre was better than that of the silica fume and PPF and enhanced RAC flexural resistance.	
	Rice husk ash	Padhi et al., 2018	Concrete mixes containing 100% coarse recycled concrete aggregates and 10–15% rice husk ash satisfies the design requirements for application in the construction industry.	

2.7 Research Gaps

It is established that the incorporation of RA in new concrete negatively affects the engineering properties of concrete. The quality of RAC depends on various parameters, the quality of RA, RA components, and the quality of the recycling process of RA. The effects of incorporating recycled concrete aggregate in new concrete are extensively studied in the literature. However, less focus has been given to utilising RA from C&DW. Although there are significant numbers of previous studies investigating the mechanical performance of RAC, the number of studies that deal with the mechanical performance of RAC from the C&DW is scarce, and some contradicting outcomes in the literature have been noticed. Whereas some authors reported that the tensile splitting and flexural strength of RAC are lower than that of NAC, others have concluded that there is no significant difference between RAC and NAC. Consequently, more full-scale research is required to establish a good agreement on the engineering performance of concrete produced with treated RA from the C&DW (Seara-Paz et al., 2018).

After reviewing the current state of the literature on the RAC field, the following research gaps can be drawn:

- Most previous studies examined the effects of recycled concrete aggregates on concrete performance. Nevertheless, scant studies have been carried out on the effects of utilisation of RA from the C&DW on RAC engineering performance.
- Based on the literature review, no studies examined the effects of the combination of treatment/enhancement methods on the mechanical, durability, and microstructural properties of concrete produced with RA from the C&DW.
- Minimal studies have covered the effects of different batching techniques on RAC compressive strength, durability, and structural performance.
- Limited number of studies examined the durability performance of RAC with treated aggregate from the C&DW, including, freeze-thaw resistance and sulphate attack.
- Scant studies investigated the effects of different treatment methods on the AIV and the WA of RA from the C&DW.

- There is no full-scale research covering the mechanical, durability, and microstructural of concrete produced with treated RA from the C&DW.

CHAPTER THREE - MATERIALS

This Chapter gives detailed information on the raw materials used throughout this study. It describes the materials sources, reasons for using each material, chemical compositions, and some of the physical properties. Scanning Electron Microscopy (SEM) microstructural images and Energy Dispersive Spectrometer (EDS) chemical analysis have also been presented in this chapter for all the raw materials used. This chapter classified the materials utilised into four main categories, binding materials, aggregates (coarse and fine), pozzolan materials, and other materials. The binding material used was Portland cement (CEM I), the utilised aggregates were sub-divided into fine aggregates (river sand), and coarse aggregates (natural aggregates and recycled aggregates), while the pozzolan materials utilised were Silica Fume – SF, Ground Granulated Blastfurnace Slag – GGBS, Pulverised Fuel Ash – PFA, and Metakaolin – MK. The other materials used were sodium silicate, sodium sulphate, limewater, Dentstone plaster, and superplasticiser.

3.1 Portland Cement (PC)

A commercially available Portland cement (CEM I-42.5 N) manufactured in accordance with BS EN 197-1: 2011, was used throughout the study. The CEM I was sourced from Jewson UK limited, based in Caerphilly, South Wales, UK. The oxide and physical composition of the cement used are given in Table 3.1, while other relevant parameters such as SEM image and EDS analysis are shown in Figures 3.1. Portland cement was used throughout this research mainly as a binder to produce concrete, and in most of the strengthening, the adhered mortar treatment methods.

Portland cement is a traditional hydraulic binder that comes in a finely grey ground powder. It is manufactured from grinding limestone/chalk and clay/shale. These raw materials are mixed intermittently in pre-determined proportions to form a slurry in case of the wet process and powder in case of the dry process. The materials then are burned in a large rotary kiln at a temperature of 1450 °C. After that, the slurry formed exhibits some chemical and physical changes that lead to its partial fusion into balls known as clinker. The clinker is an assemblage of ferrite (C₃AF), aluminite (C₃A), belite (C₂S), and alite (C₃S). The clinker is then cooled down and grounded with gypsum leading to the formation of the widely used construction material Portland cement (Neville, 2011).

3.2 Pozzolan Materials

3.2.1 Pulverised fuel ash

The Pulverised Fuel Ash (PFA) used throughout this study was compliant with BS EN 450-1:2012. It was supplied by Aberthaw power station in Wales. PFA is a by-product material supplied from coal-fired power stations and is produced when pulverised coal is fed into the boilers and burnt at a temperature of about 1400°C (Oti et al., 2020). The oxide composition and some physical properties of PFA are given in Table 3.1. The SEM images and EDS analysis for the PFA used in this study are shown in Figure 3.2.

3.2.2 Silica fume

The Silica Fume utilised throughout this study was an un-densified Silica Fume with a commercial code 971U and was to the conformity of BS EN 13263-2:2005+A1:2009. It was manufactured by Elkem Silicon Materials based in Norway and had a 97.1% purity. SF is a commercial by-product of the silicon and ferro-silicon industries, and it is a highly reactive pozzolanic material. The procedures for producing SF are as follows, when high purity quartz is reduced to silicon at a temperature of up to 2000°C, SiO is then produced as vapour. This vapor is then oxidised and condensed at low temperature to ultra-fine particles, consisting of 85-99% non-crystalline silica (SiO₂), known as un-densified Silica Fume (Billong et al., 2021). The oxide composition and some physical properties of SF are shown in Table 3.1. The SEM image and EDS chemical analysis of SF are presented in Figure 3.3.

3.2.3 Ground granulated blast-furnace slag

Ground Granulated Blast-furnace Slag (GGBS) is also a by-product material, generated from the iron-making industry, and was supplied from the Port Talbot steel works in South Wales, UK. GGBS was in compliance with BS EN 15167-1:2006. The oxide composition and some physical properties of GGBS can be seen in Table 3.1. The SEM image and EDS analysis of GGBS are shown in Figure 3.4.

3.2.4 Metakaolin

Metakaolin (MK) was an industrial type of the Metastar 501 brand manufactured by IMERYS company in the UK. MK is produced by heating natural clay mineral kaolin at a temperature of 650°C and 800°C. The oxide composition and some physical properties of MK can be seen in Table 3.1. The SEM image and EDS analysis of GGBS are shown in Figure 3.5.

Table 3.1: Oxide compositions and physical properties of Portland cement and different pozzolanic materials used throughout this study (data taken from the suppliers of the different materials, Jewson UK limited (PC), Aberthaw power station (PFA), ELKEM (SF), Port Talbot steel works (GGBS), IMERYS (MK))

Oxide	Composition by (wt%)				
	PC	SF	PFA	GGBS	MK
CaO	61.49	–	0.22	37.99	0.07
SiO ₂	18.84	97.1	59.04	35.54	52.1
Al ₂ O ₃	4.77	0.1	34.08	11.46	41.0
MgO	3.54	0.15	0.43	8.78	0.19
Fe ₂ O ₃	2.87	0.2	2.00	0.42	4.32
Mn ₂ O ₃	0.05	–	–	0.43	–
SO ₃	3.12	0.06	0.05	1.54	–
TiO ₂	0.26	–	–	0.70	0.81
K ₂ O	0.57	–	1.26	0.43	0.63
Na ₂ O	0.02	–	1.26	0.37	0.26
P ₂ O ₅	0.1	–	–	0.02	–
V ₂ O ₅	0.06	–	–	0.04	–
BaO	0.05	–	–	0.09	–
L.O. I	4.30	0.08	–	2.00	0.6

Physical properties					
Colour	Grey	Dark Grey	Light Grey	Off-white	Off-white
Bulk density (kg/m ³)	1400	120-220	800-1000	1200	500
Specific gravity (Mg/m ³)	3.16	2.20	2.90	2.85	2.50

Note: PC - Portland cement, SF - Silica Fume, PFA - Pulverised Fuel Ash, GGBS - Granulated Blast-furnace Slag, MK - Metakaolin

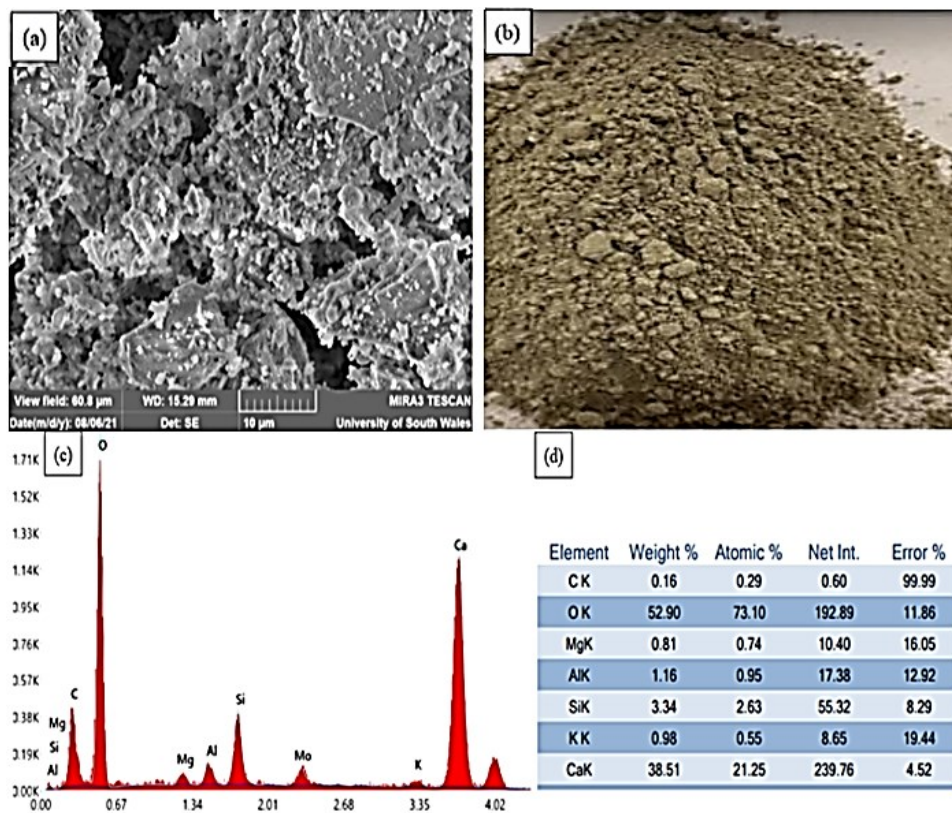


Figure 3.1: (a) SEM image of PC, (b) PC used, (c) EDS peaks chemical analysis for PC compositions, (d) PC oxide compositions by EDS

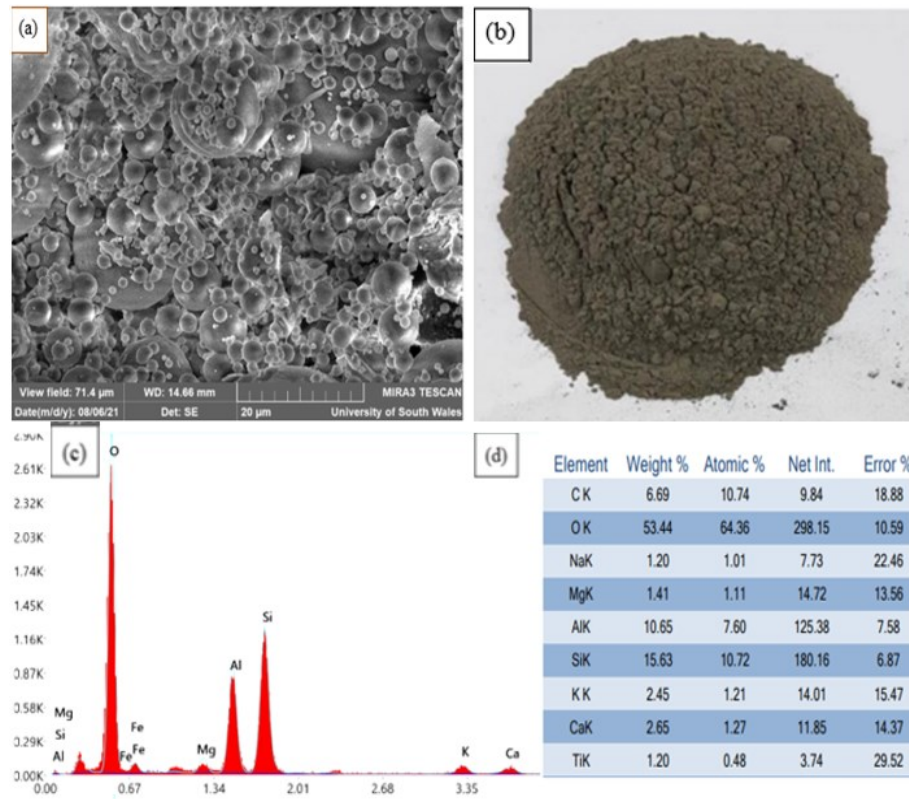


Figure 3.2: (a) SEM image of PFA, (b) PFA used, (c) EDS peaks chemical analysis for PFA compositions, (d) PFA oxide compositions by EDS

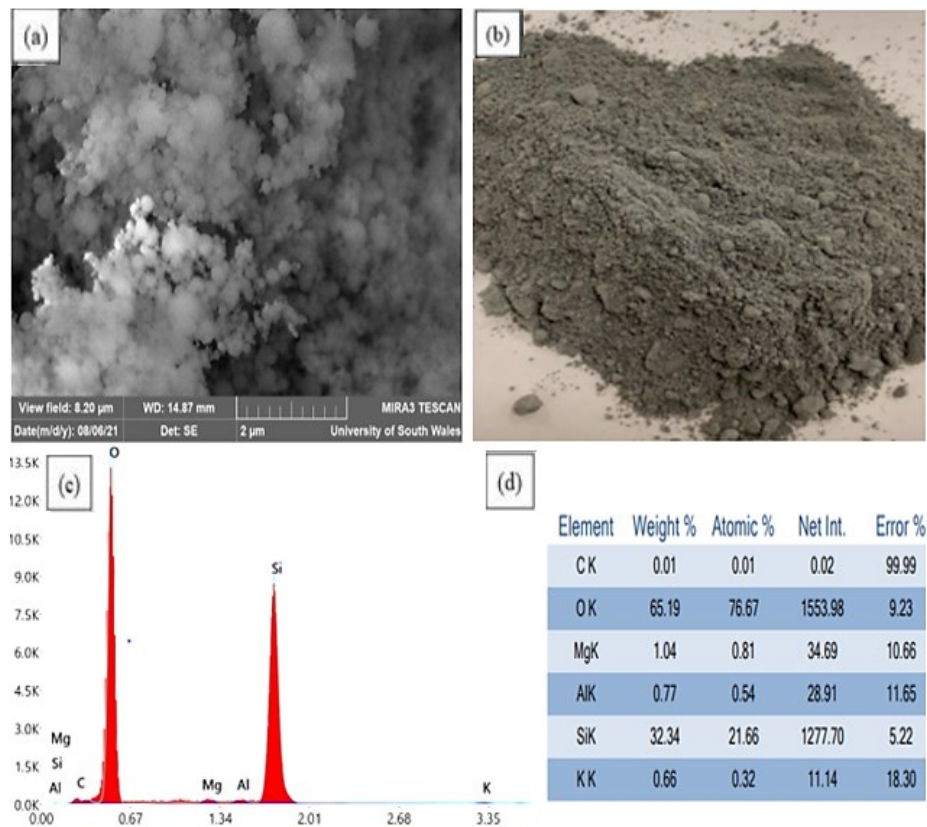


Figure 3.3: (a) SEM image of SF, (b) SF used, (c) EDS peaks chemical analysis for SF compositions, (d) SF oxide compositions by EDS

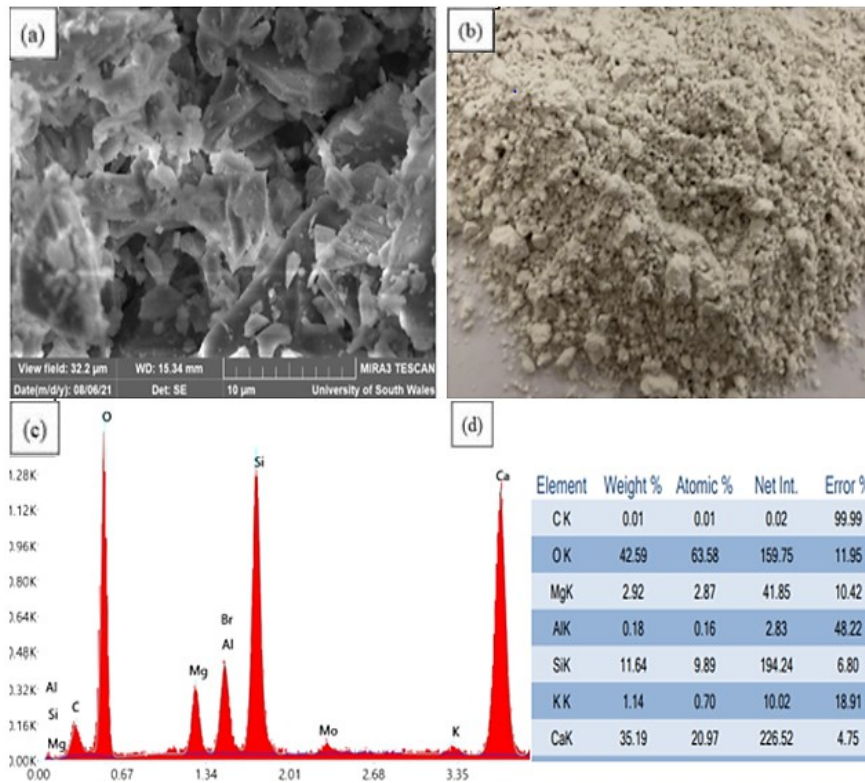


Figure 3.4: (a) SEM image of GGBS, (b) GGBS used, (c) EDS peaks chemical analysis for GGBS compositions, (d) GGBS oxide compositions by EDS

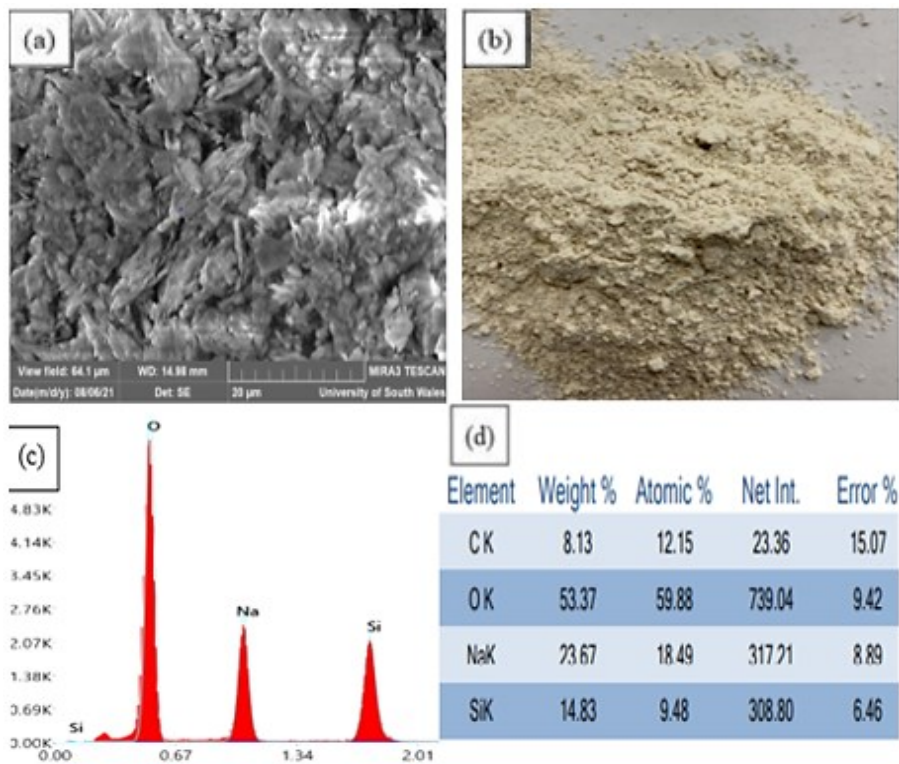


Figure 3.5: (a) SEM image of MK, (b) MK used, (c) EDS peaks chemical analysis for MK compositions, (d) MK oxide compositions by EDS

3.3 Aggregates

3.3.1 Natural aggregate (NA)

Two particle sizes of crushed limestone coarse aggregate (NA) were used throughout this study, 20/10 mm, and 10/4 mm. The limestone aggregate was sourced in bulk from Jewson UK Limited in Caerphilly, South Wales, UK, confirming BS EN 12620:2002+A1 and PD 6682-1:2009. The NA was quarried from crushed sedimentary rocks and consisted mainly of fossils and carbonated minerals, including calcite and/ or dolomite (Alexander and Mindess, 2005). NA was used to produce natural aggregate concrete (conventional concrete) and marked as 1st control compared to recycled aggregate concrete (RAC). SEM image for NA is shown in Figure 3.6. The geometrical, physical, and mechanical properties of the natural limestone coarse aggregate are presented in Table 3.2. The particle size distribution of NA is shown in Figure 3.9.

3.3.2 Recycled aggregate (RA)

The recycled aggregate (RA) utilised was sourced from Derwen Group, Neath Abbey, UK. It is a mix of construction and demolition waste with a size range of clean 20/10 mm and 10/4mm. According to Derwen Group, the RA provided was produced to industry standards, in accordance with WRAP Quality protocol and the BS EN 13242: 2013 specifications (Derwen Group, 2016). RA consisted of different recycled materials, i.e., brick, glass, bituminous, rounded stones, and recycled concrete aggregates. RA was the primary study focus and was used at 100% replacement level of natural aggregate to produce recycled aggregate concrete and undergone various treatments methods. The SEM image for recycled aggregate is shown in Figure 3.7. The composition of the RA used throughout this research is presented in Table 3.4, the particle size distribution of recycled coarse aggregate is shown in Figure 3.9, and the geometrical, physical, and mechanical properties are shown in Table 3.2.

3.3.3 Fine aggregate

The fine aggregate utilised in this study was natural sea-dredged sand sourced from the Bristol Channel, and it complies with the standards of BS EN 1097-6, BS EN 933-4 and BS 812-112. The sand particles were mostly fine-grained particles passing the BS sieve size of 2mm by 99.2%, and were supplied by Jewson UK Limited, based in Caerphilly, South Wales,

UK. Sand was used to produce RAC and NAC throughout the experimental work. The SEM image of the river sand is shown in Figure 3.8.

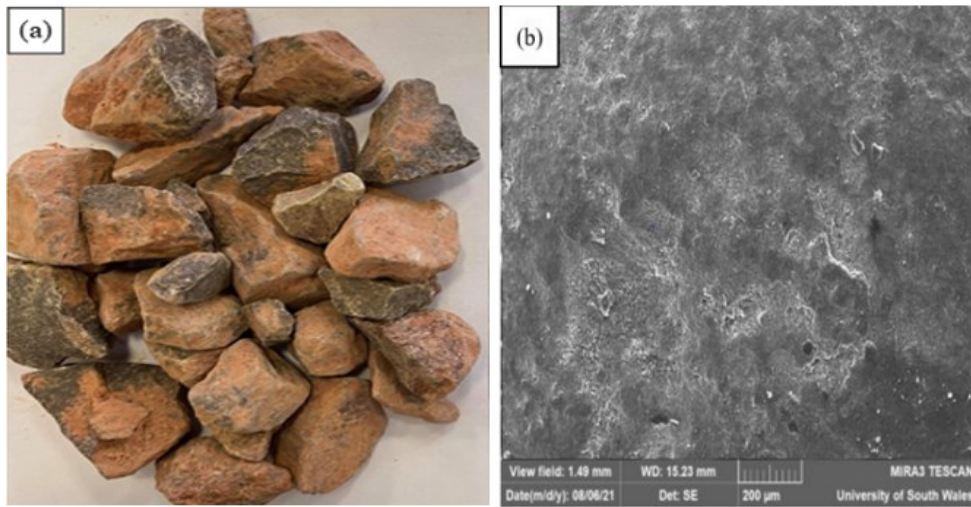


Figure 3.6: (a) NA used in this research, (b) SEM image of surface texture for one particle of NA of 10mm size

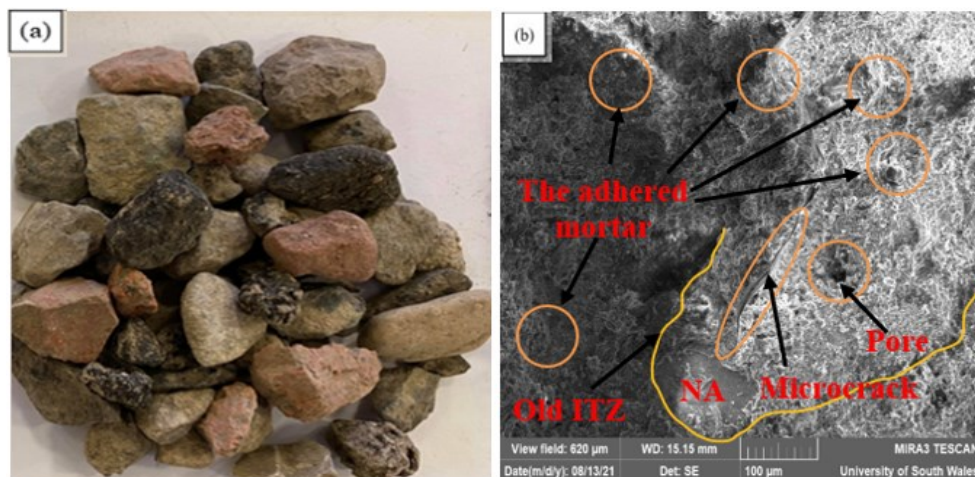


Figure 3.7: (a) RA used, (b) SEM image of RA (recycled concrete aggregate) of 10mm size.

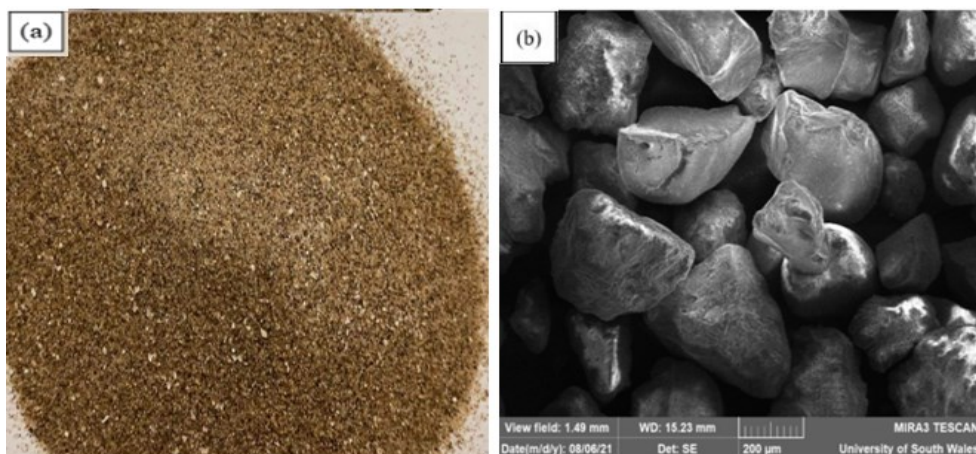


Figure 3.8: (a) sand, (b) SEM image of sand particles

Table 3.2: Characteristics of the RA compared with NA and relevant BS EN standards

Characteristic	NA	RA	BS limits	Standard
Flakiness Index (FI) (%)	18	27	< 40	BS EN 933-3:2012
Shape Index (SI) (%)	12	18	< 55	BS EN 933-4:2008
Water Absorption (WA) (%)	1.5	6.1	< 8	BS EN 1097-6:2013
Particle density mg/kg ³	2.48	2.12	–	BS EN 1097-6:2013
Aggregate Impact Value (AIV) (%)	14	17	< 32	BS EN 1097-2:2020
LA (%)	18	26	< 50	BS EN 1097-2: 2010

The results of the tests carried out on the characteristics of both recycled aggregates and natural aggregates in Table 3.2 are the average of three measurements. As expected, the NA performed better than the RA, as shown in Table 3.2. The lower performance of the RA is thought to be attributable to the presence of the adhered mortar, the presence of microcracks and pores, processing, weathering, and the source of the recycled aggregates, among other possible reasons (Medina et al., 2014).

The results from the particle shape tests indicated that, RA demonstrated a higher flakiness index and shape index compared to NA but within acceptable values conforming with the British standards limitations of BS EN 933-3:2012 and BS EN 933-4:2018. This finding is consistent with Muduli & Mukharjee (2019) and Chakradhara Rao et al. (2011).

The RA in this research was found to have higher water absorption values than the NA mainly due to the porous microstructure of RA, but it is still within the permissible limits as per BS EN 1097-6:2013. This is in line with Levy and Helen (2004) study, who reported that the WA of RA was within a range of 0.5 to 14.75% and 0.34 to 3% for NA.

The RA exhibited a lower resistance to fragmentation and AIV compared to NA, this may be attributed to the presence of micro-cracks within RA because of the crushing process, weathering, pre-loading, and the weak old interfacial transition zone, as shown in the SEM image of RA in Figure 3.7. Similarly, Shinde et al. (2013) observed that RA showed lower performance in AIV by 60% compared to NA. Nonetheless, these two parameters were well within the permissible limits as per standard provisions of BS EN 1097-2:2020 and BS EN 1097-2:2010. The particle size distribution of the three test RA samples as per BS EN 933-1:2012, along with the grading of the NA in Figure 3.9 shows that the RA grading curves approximately followed the same pattern as the NA, and both lie within the fine- medium

gravel classification. The RA fall within the limits of BS 12620:2002+A1: 2008, with one of the test samples coming close to the maximum limit.

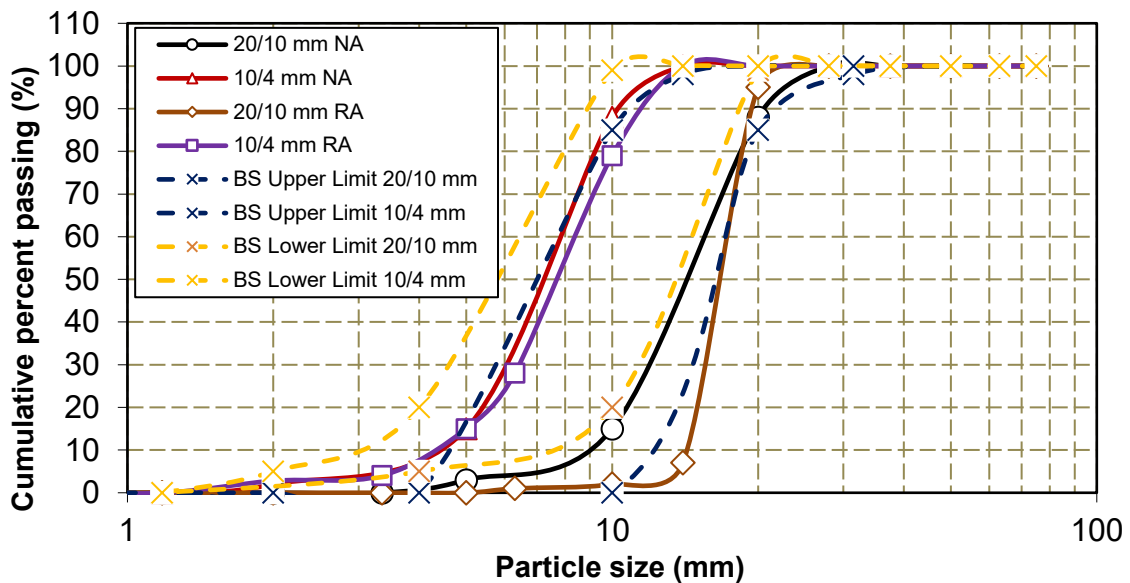


Figure 3.9: Particle size distribution of coarse RA and coarse NA

Table 3.3 shows the results of the classifications of the RA in terms of roundness and sphericity. The results indicate that the RA showed higher sphericity and angularity than NA, this may be due to the use of an on-site crusher type that can produce different particles of different shapes, in addition, the existence of the adhered mortar on the RA particle surfaces which can alter the angularity of RA. The results also showed that RA had a rough texture. These results are in agreement with the findings by Xu et al. (2018) who used an aggregate image measurement system in their study and found that RA showed similar surface toughness to NA, but it has a higher sphericity, higher angularity, less flat and elongated particles than NA.

Table 3.3: Roundness and sphericity results of RA and NA

Roundness & Sphericity Category	NA	RA
High sphericity – angular %	3	46
High sphericity – sub-angular %	7	13
Low sphericity – angular %	0	13

The classification results for the composition of the particles comprising the recycled aggregates used throughout this research were carried out in accordance with BS 8500-2:2015

+A2: 2019, as shown in Table 3.4. Based on the BS 8500-2:2015 +A2: 2019 and the composition of RA, RA can be labelled as R_{cuNR} . The constituents of the supplied RA for the present study, in terms of the permissible foreign materials, have met the outlined British standard.

Table 3.4: Constituents of recycled aggregates in this study (BS 8500-2:2015 +A2: 2019)

	R_c (%)	R_u (%)	R_b (%)	R_g (%)	R_a (%)	X (%)
Sample 1	49.14	29.47	12.51	0.17	8.38	0.34
Sample 2	47.5	28.06	11.5	1.12	11.00	0.48
Sample 3	50.6	25.8	13.4	0.00	9.5	0.37
BS limits	–	–	–	–	≤10%	≤1%
Mean	49.08	27.78	12.47	0.42	9.6	0.39

Notes: R_c refers to any cement-based products, R_u are the unbounded aggregates and natural stones, R_b refers to any clay masonry units, i.e., bricks and tiles, calcium silicate masonry unit, R_a are bituminous materials, and X refers to any miscellaneous materials and non-floating wood, plastic, and rubber, R_g refers to crushed glass.

3.4 Other Materials

3.4.1 Sodium silicate

Sodium Silicate, known as water-glass or Sodium Metasilicate, was used to treat RA. It was supplied by Fisher Scientific, Leicestershire, the UK, as a commercial white powder with a molar ratio $SiO_2/Na_2O = 2$. The SEM image of Sodium Silicate is given in Figure 3.10.

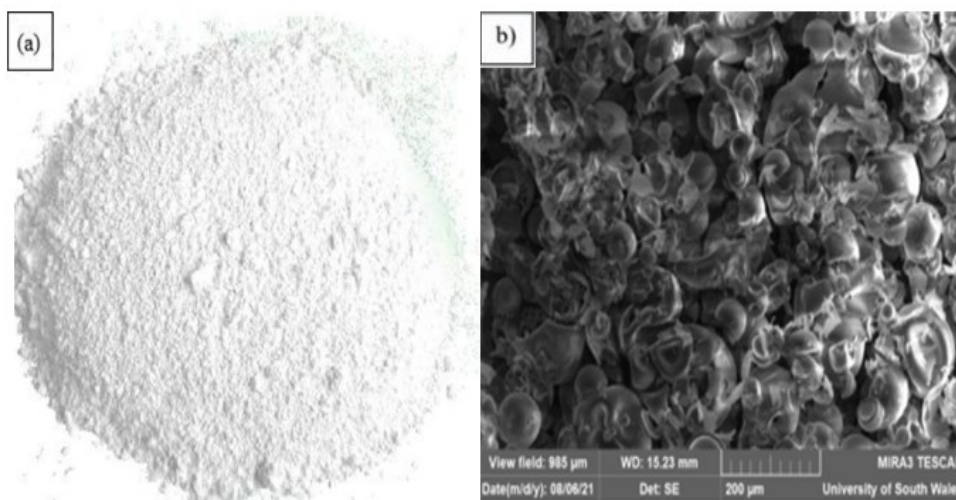


Figure 3.10: (a) sodium silicate used, (b) SEM image for sodium silicate

3.4.2 Calcium hydroxide

Commercially available calcium hydroxide white powder with a purity of 99.995% and 2.24g/mL density, was also supplied by fisher scientific, Leicestershire, UK. It was used to treat RA prior to accelerated carbonation treatment as the main component of limewater solution. Limewater solution was prepared by mixing 1.65g of calcium hydroxide in 1L of water at 25° C.

3.4.3 Sodium sulphate

Commercially available sodium sulphate granular powder ACS Reagent grade with a purity of 99%, specific gravity of 2.68kg per litre, and 5.2 – 9.2 pH level, was also supplied by fisher scientific, Leicestershire, UK. Chemical compositions of sodium sulphate are, 99% sodium sulphate 0.001% iron, 0.005% magnesium, 0.001% phosphate, 0.001% chloride, 0.5% loss on ignition, and 0.01% potassium. It was used in this study to simulate and evaluate the effects of sulphate attack on concretes produced with untreated recycled aggregate and treated recycled aggregate.

3.4.4 Dentstone plaster

Commercially available Dentstone KD pastel yellow powder was used in this study as a coating layer on the top surface of the concrete cylinder specimens prior to the modulus of elasticity test. It is a formulated hemihydrate plaster produced from naturally occurring gypsum minerals.

3.4.5 Superplasticiser (SP)

Commercially available ADVA Flow-340 superplasticiser (SP) amber/ straw liquid was used in this study to enhance the consistency of untreated recycled aggregate concrete at a low w/c ratio.

CHAPTER FOUR – EXPERIMENTAL METHODOLOGY

This chapter demonstrates the details of the analytical techniques and methods within the experimental program utilised in the present research. Chapter four involved the preliminary investigations used to evaluate the materials characteristics of the recycled aggregate in comparison with natural aggregate. It also includes the experimental procedures for mix design, sample preparation, treatment methods used, density, slump, compressive strength, tensile splitting strength, flexural strength, and modulus of elasticity. The experimental investigations also included durability investigations, water absorption, sulphate attack, and resistance to freeze-thaw cycles. Scanning Electronic Microscopy (SEM) and Energy Dispersive Spectrometer (EDS) are also presented in this chapter for microstructural investigations.

4.1 Experimental Testing Program

The present study involved the examination of the following six main phases, as shown in the breakdown structure in Figure 4.1 of the experimental testing program adopted:

Phase I Carried out preliminary tests on the recycled aggregates sourced in this research, which included, particle size distribution, Aggregate Impact Value (AIV), Water absorption (WA), density, particle shape by flakiness index, particle shape by shape index, LA abrasion coefficient, roundness and sphericity, and constituent of recycled aggregate.

Phase II Investigated the influence of the treatment methods adopted from Regime A (water treatment), and Regime B (strengthening the adhered mortar), on Aggregate Impact Value (AIV) and Water Absorption (WA) of recycled aggregate. It also involved evaluating the best performed batching techniques from Regime C on the main mechanical properties of plain concrete, fresh concrete properties (workability; slump and compaction index), and properties of the hardened concrete (i.e., compressive strength and density).

Once Phase II was completed, selective analysis of the best performed treatments was carried out to select the best treatments to be utilised in further experimental investigations. The effects of trials of a combination of treatment methods were also included.

Phase III Examined the mechanical properties of concretes produced with the different selected treatments from Phase II, i.e., slump, density, and compressive strength at various water to cement ratios, 0.4, 0.45, 0.5, 0.55, and 0.6.

Afterwards, further selective analysis was conducted to select the best treatment methods for further experimental investigations.

Phase IV Examined the mechanical and structural performance of plain concretes produced with the selected treatments from phase III. It involved, slump, density, compressive strength, tensile splitting strength, flexural strength, modulus of elasticity at three water to cement ratios, 0.4, 0.5, and 0.6.

Phase V Evaluated the durability performance, water absorption, resistance to freeze-thaw, and sulphate attack of concretes produced with the selected treatment methods from phase III, at 0.4, 0.5, and 0.6 water to cement ratios.

Phase VI Included investigations on the microstructure of concretes produced with the selected treatments from phase III by means of two main techniques, namely, direct observation by scanning electron microscope (SEM), and Energy Dispersive Spectrometer (EDS), to provide a deep understanding of the link between engineering behavior, composition, and microstructure of treated recycled aggregate concretes.

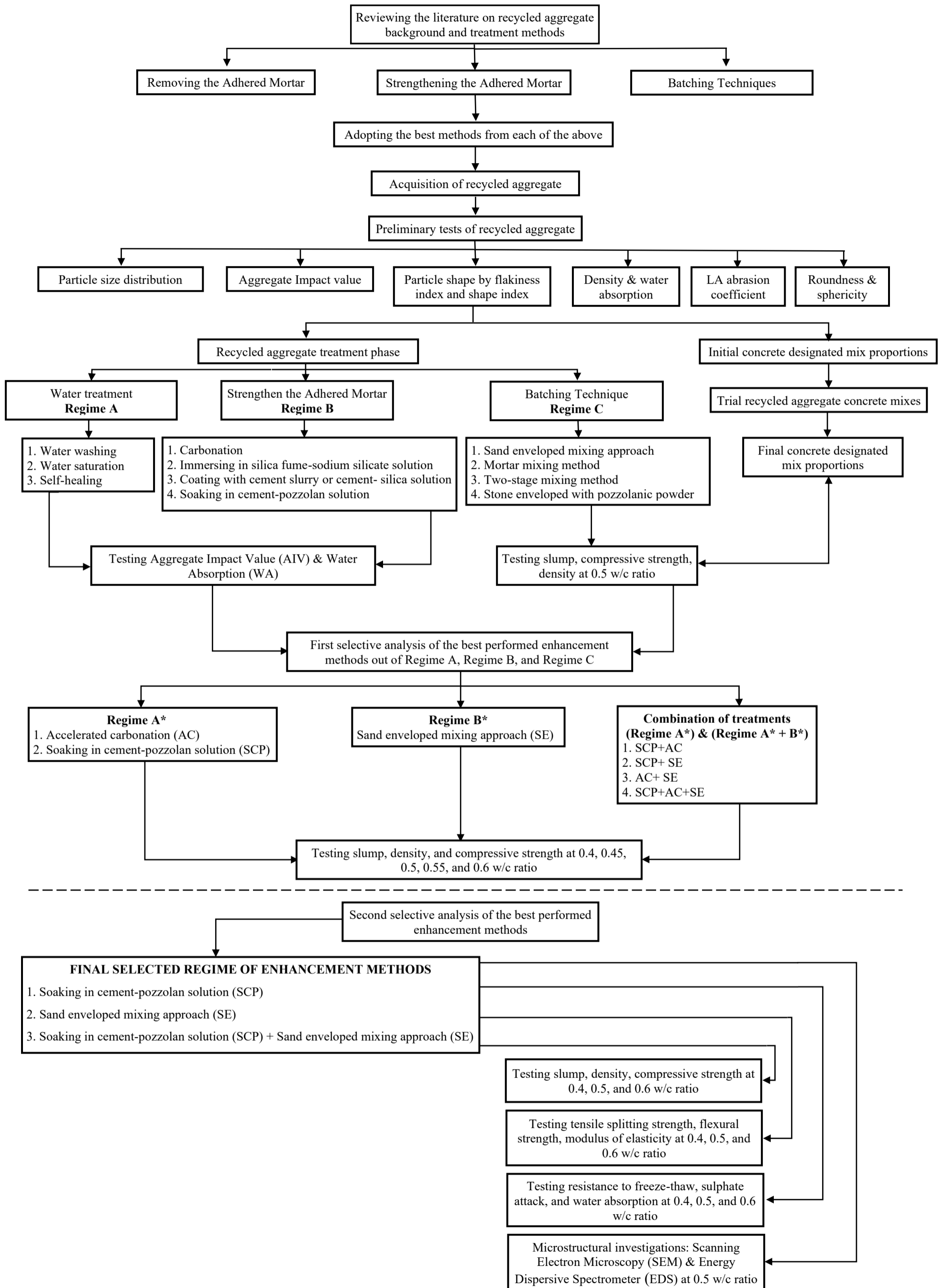


Figure 4.1: Breakdown structure of the experimental testing program utilised for this research

4.2 Aggregate Characterisation

The aggregate quality in a concrete mixture plays an indispensable role in altering concrete's strength, durability, and structural performance. Aggregates in this study, were tested to investigate their various properties for concrete production, to ensure that they satisfy the requirements of the current standards.

The present study of untreated recycled aggregate and natural aggregate properties included geometrical tests (Flakiness Index (FI), Shape Index (SI), particle size distribution, roundness and sphericity), physical, and mechanical properties tests (particle density and Water Absorption (WA), resistance to fragmentation by Aggregate Impact Value (AIV), and LA abrasion). Constituents of recycled aggregates were also studied to determine the compositions of recycled aggregates.

The characteristics of the recycled aggregate were compared with those of the natural aggregate prescribed by British standards of BS EN 12620:2013 and BS 8500-2:2015+A2:2019. It should be noted that the natural aggregates were dried at (110 ± 5) °C to constant weight prior to testing, whereas the recycled aggregates were dried at (40 ± 5) °C. The results of aggregate characterisation are given in Chapter 3, Section 3.3.

4.2.1 Sampling of aggregates

Prior to carrying out any preliminary test, the aggregates used throughout this study were reduced and riffled in accordance with BS EN 932-1:1997 to obtain representative samples. The samples were divided into two equal portions to decrease the sample size to a practical quantity.

4.2.2 Composition of recycled aggregates

The composition of recycled aggregate was carried out in compliance with BS EN 12620:2002+A1(2008). Table 4.1 was followed as a guideline to determine the composition of recycled aggregates used throughout this study. Three samples of 1000g each of recycled aggregates were selected to undergo classification based on the components. Thereafter, hand sorting of recycled aggregate was carried out to classify the recycled aggregate depending on their source (i.e., cement-based product - Rc, unbounded aggregate – Ru, clay masonry unit – Rb, and bituminous materials Ra) in accordance with BS EN 12620:2002+A1(2008) given in

Table 4.1. Once sorting was completed, the percentage by weight of each constituent was determined.

Table 4.1: Classification of the constituents of recycled aggregates (BS EN 12620:2002+A1:2008)

Constituents	Content percentage (by mass)	Category
RC (Concrete, concrete products, mortar, concrete masonry units)	≥ 90	Rc ₉₀
	≥ 80	Rc ₈₀
	≥ 70	Rc ₇₀
	≥ 50	Rc ₅₀
	< 50	Rc _{Declared}
	No requirement	Rc _{NR}
Rc+Ru (Unbound aggregate, natural stone, hydraulically bound aggregate)	≥ 95	Rcu ₉₅
	≥ 90	Rcu ₉₀
	≥ 70	Rcu ₇₀
	≥ 50	Rcu ₅₀
	< 50	Rcu _{Declared}
	No requirement	Rcu _{NR}
Rb (Clay masonry units <i>i.e.</i> bricks and tiles, calcium silicate masonry unit, aerated non-floating concrete)	≤ 10	Rb ₁₀
	≤ 30	Rb ₃₀
	≤ 50	Rb ₅₀
	> 50	Rb _{Declared}
	No requirement	Rb _{NR}
Ra (Bituminous materials)	≤ 1	Ra ₁
	≤ 5	Ra ₅
	≤ 10	Ra ₁₀
X+Rg X: others such as cohesive (<i>i.e.</i> clay and soils). Miscellaneous: metals (ferrous and non-ferrous), non-floating wood, plastic and rubber, gypsum plaster. Rg: glass	≤ 0.5	XRg _{0.5}
	≤ 1	XRg ₁
	≤ 2	XRg ₂
FL	≤ 0.2 ^a (cm ³ /kg)	FL _{0.2}
	≤ 2	FL ₂
	≤ 5	FL ₅

^a The ≤ 0.2 category is intended for special applications requiring high quality surface finish.

4.2.3 Geometrical properties of aggregates used in the current study

4.2.3.1 Particle size distribution [BS EN 933-1:2012]

Grading of recycled aggregates and natural aggregates was carried out by using the dry sieve method in accordance with BS EN 933-1:2012. The test involved the following, the aggregates were poured into the top of a series of BS test sieves stack. Then the aggregates were shaken using a sieve shaker for 10 mins (Figure 4.2). Thereafter the aggregates retained in every sieve were poured into a metal tray, and the amount of aggregates retained in each sieve was weighed to determine the mass retained for each sample. The values of mass retained were then written in a data table. Finally, the results obtained were plotted on a semi logarithmic chart to determine the grading of the aggregates.



Figure 4.2: Sieve shaker device for determination of particle size distribution

4.2.3.2 Particle shape [BS EN 933-3:2012] & [BS EN 933-4:2008]

The analysis of aggregate particle shape was performed due to the significance of this characteristic in influencing the workability and engineering properties of concrete. It was carried out to evaluate the percentage of flaky, elongate, round, and angular aggregates in the bulk aggregates used in the present study for both the natural aggregate and the recycled aggregate. The determination of particle shape was carried out using three methods, Flakiness Index (FI), Shape Index (SI), and roundness and sphericity.

Determination of particle shape by flakiness index [BS EN 933-3:2012]

The flakiness index can be explained as the percentage of flaky particles by weight in a sample. It can be determined by expressing the percentage of the flaky particles by weight to the total weight of the sample. Prior to the test, sieve analysis of the aggregate sample was performed using a sieve shaker, as mentioned in the previous section. The samples retained on each sieve were then weighed and categorised into groups depending on their particle size. Thereafter, each group was tested using the thickness gauge (Figure 4.3), where each particle was passed through a slot of specified thickness along the least dimension. Finally, the weight of the particles that passed the specified thickness gauge slot was recorded for each group/fraction.

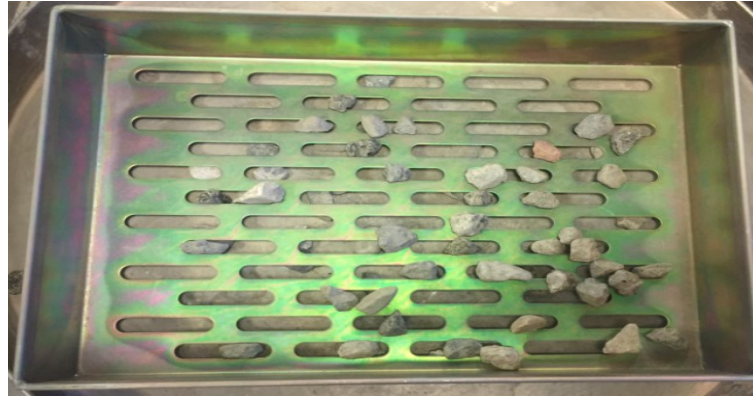


Figure 4.3: Thickness gauge for determination of flakiness index

Determination of particle shape by Shape Index [BS EN 933-4:2008]

The shape index was used to determine the elongation of aggregate particles. A special slide gauge was used to determine the category for each aggregate particle. Two categories are recognised for shape index, cubical and non-cubical. The non-cubical category reflects on the particles where the thickness is less than one-third of the length. The aggregates length and thickness were measured using the special made particle slide gauge. The shape index was expressed as the ratio between the weight of non-cubical particles to the total mass of the test sample.

Roundness & sphericity

Rounded, angular and non-hollow cylindrical aggregate particle shapes were individually examined using the visual comparison chart developed by Powers (1953) to determine their two-dimensional particle shape by comparing them with particles of known roundness and sphericity.













Roundness classes	Very Angular	Angular	Sub-angular	Sub-rounded	Rounded	Well Rounded
High Sphericity						
Low Sphericity						
Roundness indices	0.12 to 0.17	0.17 to 0.25	0.25 to 0.35	0.35 to 0.49	0.49 to 0.70	0.70 to 1.00

Figure 4.4: Chart used for determining roundness and sphericity of particles (based on Powers, 1953)

4.2.4 Physical and mechanical properties of aggregates

4.2.4.1 Particle density and water absorption [BS EN 1097-6:2013]

Particle density indicates the mass of a unit volume of particles, excluding the void spaces. The test was carried out in compliance with set test procedures in BS EN 1097-6:2013. Water absorption is an essential characteristic of recycled aggregate since it is highly sensitive to water giving to its porous condition. It measures the total absorbed water of aggregate after placing it in a container filled with water for 24 hours, then drying it to constant weight in an oven at 105 ± 5 °C. The following equations were used to determine particle density and water absorption of the aggregate utilised throughout this study in accordance with BS EN 1097-6:2013.

$$\rho\rho = \frac{M_3}{V_{(F)} - V_{(w)}} \quad \text{Equation 4.1}$$

Where, $\rho\rho$ - particle density, mg/kg^3 , M_3 - mass of dry aggregate, g, $V_{(F)}$ - volume of water and aggregate in container A, ml, V_w - volume of water in container B, ml

$$\text{WA} = 100 \times \frac{M_4 - M_5}{M_5} \quad \text{Equation 4.2}$$

Where, M_4 = mass of the saturated surface-dry aggregate in the air, g, M_5 = mass of the oven dried sample, g

4.2.4.2 Resistance to fragmentation [BS EN 1097-2:2020]

Determination of resistance of aggregate to fragmentation was investigated through two test methods, Aggregate Impact Value (AIV), and Los Angeles abrasion. It measures the ability of

aggregate to withstand wearing, scraping, and shattering by impact or friction. It reflects on the aggregate quality and generally resistance to degradation as results of mixing, handling, or stockpiling.

Aggregate Impact Value (AIV) [BS EN 1097-2:2020]

Aggregate resistance to impact was performed on coarse aggregate passing the 12.5 mm sieve and retaining on the 10 mm BS test sieve. The test specimen was then poured into a cylindrical cup, followed by subjecting to 25 gentle blows with a tamping rod to get it compacted at three layers. Thereafter, any surplus aggregates were stuck off, and the net weight of the aggregate was determined as (W_1). The aggregates were then poured into another cylindrical cup attached to the impact apparatus base, where 25 strokes were then applied with a tamping rod to compact the test sample. The hammer of the machine was raised until its lower face was 380 mm above the upper surface of the test sample in the cup and was allowed to fall freely on the test sample for 15 blows (see Figure 4.5). The crushed test sample was then removed and sieved through the 2.36 mm BS sieve, and the passing particles were weighed (W_2). The Aggregate Impact Value (AIV) was calculated according to the following equation.

$$AIV = \frac{W_2}{W_1} \times 100\% \quad \text{Equation 4.3}$$

Where, W_1 = total weight of dried sample, g, W_2 = weight of sample passing 2.36 mm sieve, g



Figure 4.5: Aggregate Impact Value (AIV) test apparatus

LA Abrasion BS EN [1097-2:2020]

The Los Angeles abrasion test was applied on aggregates with size range from 10 to 14mm. The test involved, placing 11 spherical steel balls in the LA abrasion machine (see Figure 4.6), then the test sample portion was added. The machine cover was then shut and rotated for 500 revolutions at a constant speed between 31 r/min and 33 r/min for 15 mins. Thereafter, the drum content was discharged into a tray placed under the drum, the crushed particles were collected and sieved using 1.6 mm BS test sieve, and the retained particles were removed and dried to constant weight and let to be cooled. Finally, the mass of the dried crushed test sample was recorded. The following equation was used to determine the value of LA abrasion.

$$LA = \frac{5000 - M}{50} \quad \text{Equation 4.4}$$

Where, M = the mass of crushed test sample retained on the 1.6 mm BS test sieve



Figure 4.6: Los Angeles test machine for testing resistance to fragmentation

4.3 Treatments and Batching Techniques Used for RA & RAC

Based on the literature review given in Chapter two Section 2.9, the following treatment methods and batching techniques were selected in this research for recycled aggregate and recycled aggregate concrete performance enhancement. The methods utilised were categorised into three main categories, (i) water treatment, (ii) strengthening the adhered mortar, (iii) batching techniques.

The effects of water treatment methods and the effects of strengthening the adhered mortar treatment methods, were initially evaluated by testing the Aggregate Impact Value (AIV) and Water absorption (WA) of treated recycled aggregates. The performance of batching techniques was assessed by examining their effects on the mechanical properties (density, slump, and compressive strength) of recycled aggregate concrete.

4.3.1 Regime A – Water treatment methods

Regime A water treatment methods were selected based on their merit in terms of simplicity, cost efficiency, and feasibility. Three treatment methods were adopted in the current research as water treatments, water washing, water saturation, and self-healing. The effects of these treatments were examined by testing the AIV and WA of RA after these treatments were applied.

4.3.1.1 Water washing of RA

Recycled aggregates were placed into a conventional concrete mixer (Figure 4.7), then the mixer was rotated for 2 hrs, while a sufficient amount of water was being added. After that, the aggregates were then placed in the oven to dry them to constant mass. Two approaches were carried out after that; (i) discarding any aggregates with sizes smaller than 4mm, and (ii) keeping the grading as it is.

Since RA may come with particle sizes smaller than 4mm, discarding these sizes was carried out after water washing treatment to examine the effects on the AIV and WA of RA. Water washing treatment aimed to remove any dust, fine particles, and any loose weaker adhered mortar on the RA surface by RA collision with water during the treatment process.

4.3.1.2 Water saturation (pre-saturation of RA)

Two types of water saturation treatment methods were used, (i) full saturation, and (ii) partial saturation.

Full saturated condition

In this method, the recycled aggregates were immersed in water for about 24 hours to reach saturated surface dry condition. It basically aimed to reduce the exchange of water between the cement paste and the recycled aggregates as much as possible, or nearly cancelling out

any water absorbed by the aggregate during batching. It improves the aggregate's water content homogeneity and avoids having the effective w/c ratio of the cement-paste affected at any time.

Partially saturated condition

Similar to the full saturation method, the only difference in this method is that recycled aggregates were immersed in water for a short interval of time of 4 mins prior to testing.



Figure 4.7: Conventional concrete mixer machine for recycled aggregates water washing treatment

4.3.1.3 Self-healing of RA

The recycled aggregates were soaked in water for 30 days allowing the un-hydrated adhered mortar on the aggregate surfaces to undergo hydration process while it is in contact with water.



Figure 4.8: Self-healing of recycled aggregates

4.3.2 Regime B - Strengthening the adhered mortar methods

The performance of strengthening the adhered mortar approach treatment methods was initially evaluated by testing Aggregate Impact Value (AIV) and Water Absorption (WA) of treated RA via the following treatments, carbonation (accelerated carbonation and cyclic carbonation), immersing RA in sodium silicate-silica fume solution, coating RA with cement slurry or cement-silica fume slurry, and soaking RA in cement-pozzolan solution.

4.3.2.1 Accelerated carbonation treatment (AC)

This study also examined the effects of (i) accelerated carbonation treatment, and (ii) cyclic carbonation treatment on Aggregate Impact Value (AIV) and Water Absorption (WA) of demolition waste RA.

Accelerated carbonation treatment

After reviewing the key factors affecting the efficiency of CO₂ treatment which were mentioned in the literature review, the following key factors were analysed, and the relevant key factors values were selected for the RA accelerated carbonation treatment method:

- **Pre-treatment method:** the lime-water solution was selected for pre-treating by pre-soaking RA prior to carbonation treatment. The main key contribution of the adopted limewater saturation process is to artificially introduce the additional calcium hydroxide into the pores of the recycled aggregate, resulting in more CO₂ uptake and

more calcium carbonate precipitates, consequently further improvement can be achieved.

- **Water content of RA:** RA was air-dried prior to carbonation and monitored to achieve a water content of 5%, as recommended by Zhan et al. (2016) and Pan et al. (2017), this value will offer sufficient amount of water for the carbonation process and will enhance the penetration of CO₂.
- **CO₂ gas concentration:** in order to select the optimum CO₂ gas concentration for the carbonation treatment, three levels of CO₂ concentration were selected, 20%, 50% and 100%. These values were selected for comparison purposes and to select the optimal CO₂ gas concentration.
- **CO₂ gas pressure:** the utilised CO₂ gas pressure for the carbonation treatment was set at +0.1 bar. As an excessive gas pressure will lead to adverse effects on RA properties.
- **Time, temperature and relative humidity of CO₂ curing:** carbonation time has complex effects on the efficiency of the carbonation treatment, therefore, in order to understand the effects of carbonation time on RA engineering properties and to be able to select the optimum carbonation time, there was a need to have 7 days of carbonation and tests on RA engineering properties were carried out from day 1 to day 7. As it was recommended by Zhan et al. (2016) to have a relatively low temperature for the carbonation process, 20 ± 2 °C was selected.

The effects of two key accelerated carbonation treatment parameters, CO₂ gas concentration level and carbonation time on the performance of the RA were investigated. Accelerated carbonation treatment examined three different CO₂ gas concentration levels 20%, 50%, and 100% for up to 7 days. The accelerated carbonation device used in the present work (Fig 4.9) is a Galaxy 170 R CO₂ incubator, consisting mainly of an air-tight carbonation chamber with volume capacity of 170 litres, control PCB graphics display which carries out all control functions, CO₂ sensor with automatic auto-zero pump and pressure detector, four curve-matched thermistors that measure temperature, graphics display with fluorescent backlighting and inverter, 8-position shelving rack with 4 shelves, and a commercially supplied CO₂ storage tank with a purity of 99.5% and an attached regulator and pressure controller.

Prior to carbonation treatment, the RA was firstly preconditioned in a drying room at room temperature for about 3 days to maintain the desired moisture content of 5% for the required experimental work, with a view to accelerating the carbonation reaction through dissolving

CO₂ gas and Ca⁺² contained in RA (especially in the adhered mortar), while reducing the moisture content of the recycled aggregates. The RA was then placed on the shelves in the chamber. The carbonation process included an auto-zeroing stage that was carried out before the injection of CO₂. A sufficient quantity of silica gel was placed at the bottom of the chamber to remove the evaporated water from the aggregates during the carbonation process.



Figure 4.9: CO₂ incubator used for the CO₂ treatment of recycled aggregates

Cyclic limewater-CO₂ treatment

In this treatment approach, the following steps are for one cycle and repeated for 3 cycles, where one cycle includes, (1) RA were pre-soaked in limewater solution for about three days, and then (2) pre-dried in a chamber at a $20 \pm 2^\circ\text{C}$ and relative humidity of $50 \pm 5\%$ for 3 days. (3) The RA was then placed in the CO₂ chamber under 100% CO₂ concentration level at a pressure of +0.1 bar for 24 h.

4.3.2.2 Soaking RA in sodium silicate - silica fume solution

The recycled aggregates were impregnated in sodium silicate and silica fume solution for 1 hr, 4 hrs, and 24 hrs to form a thin layer called water repellent that fills the pores and voids inside the adhered mortar, hence improving the properties of the recycled aggregates. The solutions selected for this treatment were prepared with three different replacement levels in which sodium silicate-silica fume replaced water at 5 wt% ,10 wt%, and 15wt%, and the mixing proportion of these two combined materials was worked out using Equation 4.5.

$$\frac{\text{Sodium Silicate Powder}}{\text{Silica Fume Powder}} = 0.6$$

Equation 4.5

Table 4.2 is a sample mix proportion design of the solution for 1000g recycled aggregate:

Table 4.2: proposed solution ingredient for soaking RA in sodium silicate-SF solution

Replacement level %	Sodium Silicate (g)	Silica Fume (g)	Water (g)
5%	19	31	950
10%	37.5	63	900
15%	56	94	850

The methodology adopted involved the following procedures, the recycled aggregates were first dried in an oven for 24 h at 105 °C, and then cooled at room temperature. After the sodium silicate-silica fume solution was prepared, it was stirred for 2 mins to reach homogeneity and ensured an appropriate diffusion of sodium silicate and silica fume particles. The recycled aggregates were then immersed in the solutions prepared for 1 hr, 4 hrs, and 24 hrs. Thereafter, the aggregates were then drained for 10 min. Finally, the recycled aggregates were dried in an oven at 105 °C for 24 hrs and cooled down at a room temperature for one day.

4.3.2.3 Coating with cement slurry or cement-silica fume slurry

This treatment method involved the following procedures, firstly, the cement slurry or cement-silica fume slurry was prepared with the required cement or cement-silica fume and water, then properly stirred. RA was then added to the slurries prepared and properly mixed using a mixer machine for 10 mins. The aggregates coated were then placed on trays to dry for 1 day and then cured in water for 7 days holding time to ensure the cement paste of the coated RA was fully hydrated. The basic premise of this treatment method is to coat the RA surface with hydrated cement film, which is thick enough to act as a shield around the surface of RA. This coating cement layer should not be very thick, causing sticking among particles and forming lumps between RA. Hence, three parameters should be considered to obtain the ideal coating thickness for RA, (1) the amount of cement required for efficiently coating RA with a uniform cement film, (2) the required water/cement ratio to reach the optimum coating process and cement hydration, and (3) the optimum hydration time needed to obtain a permanent bond of the coated cement paste film onto the surface of RA.

In this present study, RA was coated with cement slurry or cement-silica fume slurry to reinforce its ability in resisting impact and enhancing its water absorption, hence, enhancing the engineering properties of RAC containing RA. Two methods of coating RA with cement

were adopted in this study: (i) coating of individual RA size fractions separately, and (ii) coating of the total combined RA particle size fraction.

Coating the individual size fractions with cement and cement/silica fume slurry

The surface area (SA) of RA was used as a key representing count in designing the fabrication of RA with cement coating, hence, assuming that the RA is spherical grain, the BS ISO 3310-2:2013 standard sieve sizes were used to reflect surface area values of RA, as shown in Table 4.3.

Table 4.3: The surface area of the different aggregate particle sizes

Sieve size ^a (mm)	<i>d</i> (mm)	S _m ^b (m ² / m ³)
20.00 – 14.00	17	352.9
14.00 – 12.50	13.25	452.8
12.50 – 10.00	11.25	533.3
10.00 - 6.30	8.15	736.2
6.30 – 5.00	5.65	1061.9
5.00 – 3.35	4.175	1437.1
3.35 – 2.36	2.86	2097.9
2.36 – 1.18	1.77	3389.8
1.18 – 0.60	0.89	6741.6

^a The standard size of coarse aggregate that shall comply with BS ISO 3310-2:2013

^b S_m = 6000/*d*

The total surface areas (SA) of the different RA size fractions were needed to determine the required volume of coating paste for coating the surface of RA, which is the relationship between the required quantity of RA to be coated and the content of the binder paste. The calculation steps that were set by Lee et al., (2011), to determine the required volume of the coating paste for coating RA, were followed in this research. The water-to-binder ratio for the preparation of the slurries was set at 0.45. Silica fume replaced 15% of cement weight in the cement-silica fume slurry. When the coating paste around RA of 4.75mm size exceeds the designated theoretical thickness of 0.65 mm, then the coating paste may get cemented into lumps and cannot be separated easily, while the coating paste cannot entirely coat the surface of RA when the coating paste around the surface of RA of 12.5 mm size is less than 0.25 mm of the coating thickness.

Consequently, there is a certain effective coating range that should be obtained for the needed volume of coating pastes under different theoretical coating thicknesses for the various granular sizes of RA. For the present research, three different theoretical thicknesses (*t*_{th})

were proposed to coat RA; 0.1 mm, 0.2 mm, and 0.3 mm. The following steps are the calculations required to fabricate RA with cement coating treatment (Lee et al., 2011):

1. Select the theoretical coating thickness of RA, t_{th} , for each aggregate size fraction.
2. Compute the volume of the RA that is required to coat:

$$V_{ca} = W_{ca} / \gamma_{ca} \quad \text{Equation 4.6}$$

3. Compute the S_{agg} of RA based on the surface area representing value (S_m) for each aggregate size fraction:

$$S_{agg} = V_{ca} \times S_m \quad \text{Equation 4.7}$$

4. Compute the coating volume of RA for each size fraction:

$$V_p = S_{agg} \times t_{th} \quad \text{Equation 4.8}$$

5. Compute the specific gravity of the coating paste:

$$\gamma_p = \frac{W_c + W_w + W_p}{\frac{W_c}{\gamma_c} + \frac{W_w}{\gamma_w} + \frac{W_p}{\gamma_p}} \quad \text{Equation 4.9}$$

6. Compute the coating paste weight (W_p) based on the theoretical coating thickness (t_{th}) for each RA size fraction:

$$W_p = V_p \times \gamma_p \quad \text{Equation 4.10}$$

Where, t_{th} is the theoretical coating thickness, V_{ca} is the volume of RA, W_{ca} is the weight of RA, γ_{ca} is the unit weight of RA, S_m is the representing value of the SA for each RA size fraction given in Table 4.2, V_p is the volume of coating paste, γ_p is the unit weight of coating paste, W_c is the weight of cement, W_w is the weight of coating mixing water, W_p is the weight of pozzolan, γ_c is unit weight of cement, γ_w is unit weight of mixing water, γ_p is unit weight of pozzolan.

Coating the total combined gradation with cement or cement-silica fume slurry

In this technique, the total combined gradation of RA was coated with a coating level of 5% of cement content by the weight of the utilised RA. The set water-to-binder ratio for the coating slurry was 0.55. After preparing the slurry by mixing the required cement and water,

RA was added to the mix and then appropriately mixed by a small mixing machine and then it was left to dry before soaking it with water for curing for about 7 days to ensure proper hydration of cement and hence, efficiently coating RA with a cemented layer. Similar to the previously mentioned technique, silica fume replaced 15% of the cement-silica fume slurry.

4.3.2.4 Soaking in different cement-pozzolan solutions (SCP)

Recycled aggregates were treated via soaking method in different types of cement-pozzolan solutions with the aim of strengthening the weak adhered mortar. The main principle behind this treatment is to cover the RA surface with a thin layer of hydration products, hence strengthening RA engineering properties. Different solutions were designed for RA treatment at different dosages as given in Table 4.4. The selected ingredients for the different solutions were Portland cement (PC), silica fume (SF), metakaolin (MK), and pulverised fuel ash (PFA). These pozzolan materials were selected with the aim of fulfilling the environmental and economic criteria. The solutions were prepared by blending the materials with water (twice the weight of RA) for several minutes. Then recycled aggregate was added into each solution and soaked for 1 hr and 4 hrs at 5%, 10% and 15% concentrations. Thereafter, recycled aggregates were removed from the solution bath and let drain for 10 min and then air-dried at room temperature for 24 hrs prior to testing.

Table 4.4: Proportions of treatment solutions for 1000 g of RA prepared in this study

Notation	Treatment solutions	Binder (g)				Aggregate (g)	Water (g)	Replacement level
		PC	FA	SF	M			
Group 1	PC+PFA+MK	40	30	—	30	1000	1900	5%
	PC+ PFA+SF	40	30	30	—	1000	1900	5%
	PC+MK+SF	40	—	30	30	1000	1900	5%
Group 2	PC+PFA+MK	80	60	—	60	1000	1800	10%
	PC+ PFA+SF	80	60	60	—	1000	1800	10%
	PC+MK+SF	80	—	60	60	1000	1800	10%
Group 3	PC+PFA+MK	120	90	—	90	1000	1700	15%
	PC+ PFA+SF	120	90	90	—	1000	1700	15%
	PC+MK+SF	120	—	90	90	1000	1700	15%

Note: PC - Portland cement, PFA - pulverised fuel ash, SF - silica fume, MK - metakaolin

4.3.3 Regime C - Batching techniques

The batching techniques selected with the aim of strengthening the whole RAC matrix were, (i) sand enveloped mixing approach (SEMA), (ii) mortar mixing approach (MMA), (iii) stone enveloped with pozzolan powder (SEPP), and (iv) two-stage mixing approach (TSMA).

4.3.3.1 Sand envelope mixing approach (SEMA)

Sand was first mixed with 75% of the mixing water for 30 seconds, cement was then added to the mix and mixed for 45 seconds, thereafter, the recycled aggregate was added to the mixture with the rest of the mixing water and mixed for 90 seconds.

4.3.3.2 Mortar mixing approach (MMA)

Mortar mixing approach involved the following mixing procedures. Sand and cement were firstly added to the mixer, 75% of the mixing water was then added to the mixture, and the mixture was mixed then for 90 seconds. Thereafter, the recycled aggregate was added to the mix along with 25% of the mixing water and mixed for 90 seconds.

4.3.3.3 Stone enveloped with pozzolanic powder (SEPP)

The pozzolanic powder was firstly mixed with a certain portion of water w_1 for 60 seconds, then recycled aggregates were added to the mix and mixed for 60 seconds. Cement, sand and w_2 were thereafter added to the mixture and mixed for 120 seconds. The water to pozzolanic powder ratio was 0.35, and the total binder to water ratio was fixed depending on the mix proportion. The first portion of water w_1 was calculated knowing the weight of the binder and the selected water to pozzolanic powders ratio. The rest of the required water w_2 was then added with sand and Portland cement. This treatment method aimed to coat the recycled aggregate with a lower water to binder ratio than the total water to binder ratio. The pozzolanic powders used replaced 25% of Portland cement by weight, Silica Fume (SF) and Ground Granulated Blastfurnace Slag (GGBS) were selected as pozzolanic powders for this devised mixing approach.

4.3.3.4 Two-stage mixing approach (TSMA)

In this batching technique, sand and recycled aggregate were first added to the mixer and mixed for 60 seconds, then half of the mixing water was added to the mix and mixed for 60 seconds, thereafter cement was added to the mix and mixed for another 60 seconds. Finally, the other half of the mixing water was added to the mix and mixed for 120 seconds.

4.3.4 Combination of different treatments with batching techniques

The combination of treatments or the synergistic effects of different treatments was carried out after selective analysis of the selected treatments, the following section discusses

combinations of treatments utilised for investigating the possibilities of further enhancements of RA and RAC engineering properties.

4.3.4.1 Bi-combination of SCP and AC

The untreated RAs were first dried to constant mass, then soaked in the pre-prepared cement-SF+PFA solution for 4 hrs, and then air-dried at room temperature for 3 days. Once this treatment was completed, the treated RA were removed to the accelerated carbonation device and underwent accelerated carbonation treatment at a 50% CO₂ concentration level for 5 days of carbonation time. The aim here was to introduce more carbonatable compounds around the RA surface prior to carbonation treatment for further enhancement of RAC. This treatment method was labelled as SCP+AC in the current study.

4.3.4.2 Bi-combination of SCP + SE

The untreated RA was firstly dried to constant mass and then soaked in the pre-prepared cement-SF+PFA solution for 4 hrs, and then air-dried at room temperature for 3 days. Thereafter, the treated RA was incorporated into the mixing design of RAC and mixed via the sand envelope batching technique. This treatment was labelled as SCP+SE.

4.3.4.3 Bi-combination of AC + SE

In this combination of treatments, the untreated RA was first air dried for 3 days to achieve the desired moisture content, the RA was then treated via accelerated carbonation treatment for 5 days of carbonation time at a 50% CO₂ concentration level. Thereafter, the treated RA was then incorporated into the concrete mix and mixed via the sand envelope mixing approach. This treatment method was labelled as AC+SE.

4.3.4.4 Triple combination of SCP + AC + SE

The untreated RA were first dried to constant mass, then soaked in the pre-prepared cement-SF+PFA solution for 4 hrs, and then air-dried at room temperature for 3 days. Once this treatment was completed, the treated RA was removed to the accelerated carbonation device and underwent accelerated carbonation treatment at a 50% CO₂ concentration level for 5 days of carbonation time. Thereafter, the treated RA via the previous two treatments was incorporated into the concrete mix and mixed via the sand envelope mixing approach. This treatment method was labelled as SCP+AC+SE.

4.4 Concrete Mix Design

The main focus of the present study was on enhancing the quality of RA via various treatment methods and enhancing the engineering performance of RAC by the use of batching approaches, as was reviewed in Section 4.2. Recycled aggregate concrete mix and natural aggregate concrete mix were initially proportioned using the concrete mix design of the British method of mix design (DOE) (Department of Environment, 1988) presented by Neville (2012).

The DOE method gives considerations the durability of concrete and is convenient for mix proportioning conventional concrete mixtures produced with Portland cement and any incorporation of pozzolan materials. Five main key factors govern the DOE method in the following order, maximum size of aggregates, grading of aggregates, specific gravity of aggregates, required workability, and density of fully compacted fresh concrete.

4.4.1 Preliminary trial concrete mixture compositions

DOE concrete design method was used to develop eight concrete trial mixtures with a satisfactory workability with a range of S1 to S2 slump class for natural aggregate concrete (1st control) and untreated recycled aggregate concrete (2nd control). The prime aim for carrying out trial concrete mixtures was to obtain an engineering understanding of the performance of the untreated recycled aggregate (2nd control) in terms of workability and 7-day strength in comparison with conventional concrete (1st control).

The designated concrete trial mixtures pose various water contents, various cement contents, two water to cement ratio (0.5, and 0.6), different slump classes. Table 4.5 shows the mix proportions of the 8 trial mixtures with the results of workability and 7-day strength.

Table 4.5: Preliminary trial concrete mixtures for recycled aggregate concrete and natural aggregate concrete (1m³)

Mix code	PC (kg/m ³)	Water (kg/m ³)	w/c ratio	FA (kg/m ³)	Coarse aggregate		Slump mm	Slump class	7 days strength (MPa)
					NA (kg/m ³)	RA (kg/m ³)			
W050/NAC1-1	380	190	0.5	677	1257	----	60	S2	35.6
W050/RAC2-1	380	190	0.5	677	----	1206	35	S1	28.8
W050/NAC1-2	340	170	0.5	677	1257	----	45	S2	32.4
W050/RAC2-2	340	170	0.5	677	----	1206	25	S1	24.6
W060/NAC1-1	320	190	0.6	677	1257	----	90	S2	20.5
W060/RAC2-1	320	190	0.6	677	----	1206	65	S2	14.3
W060/NAC1-2	285	170	0.6	677	1257	----	70	S2	18.7
W060/RAC2-2	285	170	0.6	677	----	1206	55	S2	12.8

Note: NAC - natural aggregate concrete (1st control), RAC2 – untreated recycled aggregate concrete (2nd control), FA - natural fine aggregate, NA - natural coarse aggregate, RA - recycled coarse aggregate, w/c -water to cement ratio, PC - Portland cement

As can be seen from Table 4.5 RAC produced with untreated RA obtained a lower performance in terms of workability and 7-day compressive strength compared to the 1st control mix. This is due to the poor engineering properties of RA as discussed in Chapter 2. The next stage was to evaluate the performance of the various batching techniques adopted in enhancing the engineering properties of recycled aggregate concrete, as discussed in Section 4.2. Mix no. 3 and 4 were selected to develop concretes for further investigations on evaluating the effects of batching techniques on RAC performance.

4.4.2 Batching techniques mixture compositions

Table 4.6 shows the mixing proportions utilised to evaluate the performance of the different utilised batching techniques. The pozzolan materials in Table 4.6 (PC, SF, and GGBS) were utilised as part of the batching techniques mixing steps.

Table 4.6: Design mix proportion for batching techniques (1m³)

Mix Code	Water (kg/m ³)	Binder (kg/m ³)			Coarse aggregate (kg/m ³)		FA (kg/m ³)	Mixing method
		PC	SF	GGBS	NA	RA		
NAC1	170	340	0	0	1257	0	677	NMA
RAC2	170	340	0	0	0	1206	677	NMA
SEMA	170	340	0	0	0	1206	677	SEMA
MMA	170	340	0	0	0	1206	677	MMA
TSMA	170	340	0	0	0	1206	677	TSMA
SEPP _(SF)	170	255	85	0	0	1206	677	SEPP
SEPP _(GGBS)	170	255	0	85	0	1206	677	SEPP

Note: NAC1 - natural aggregate concrete (1st control), RAC2 – untreated recycled aggregate concrete (2nd control), NMA - normal mixing approach / conventional mixing, SEMA - sand enveloped mixing approach, MMA - mortar mixing approach, TSMA - two-stage mixing approach, SEPP_(SF) - stone enveloped with pozzolanic powder (Silica Fume), SEPP_(GGBS) - stone enveloped with pozzolanic powder (Ground Granulated Blast-furnace Slag).

4.4.3 Optimised mixture compositions

Table 4.7 shows concretes mix proportions produced with the various selected treatments at 5 different water to cement ratios, 0.4, 0.45, 0.5, 0.55, and 0.6. The aim here was to evaluate the effects of different treatments at variations of water to cement ratio on the mechanical

properties of recycled aggregate concrete in comparison with natural aggregate concrete. Accordingly, 45 different concrete mixtures were developed to produce 9 concrete cubes per mixture and tested for the slump, density, and compressive strength at 7-, 14-, and 28-day. Superplasticiser was only used for concretes produced with 0.4 w/c ratio at a certain dosage in real-time to achieve satisfactory workability.

Table 4.7: Optimised mix proportions for various RAC produced with various treatments at variations of w/c ratios for testing mechanical properties

Specimen Designation	PC (kg/m ³)	Water (kg/m ³)	w/c ratio	NA (kg/m ³)	RA (kg/m ³)	FA (kg/m ³)	Mixing Method	Notes
W040/NAC1	450	180	0.4	1257	0	677	NMA	Natural aggregate concrete (control 1)
W040/RAC2	450	180	0.4	0	1206	677	NMA	Un-treated recycled aggregate concrete (Control 2)
W040/SCP	450	180	0.4	0	1206	677	NMA	Soaking RA in cement-SF+FA solution
W040/AC	450	180	0.4	0	1206	677	NMA	Accelerated carbonation treatment
W040/SE	450	180	0.4	0	1206	677	SEMA	Untreated RA
W040/SCP+SE	450	180	0.4	0	1206	677	SEMA	Soaking RA in cement-SF+FA + SEMA
W040/AC + SE	450	180	0.4	0	1206	677	SEMA	Carbonation treatment +SEMA
W040/SCP+AC	450	180	0.4	0	1206	677	NMA	Soaking RA in cement-SF+FA solution + carbonation treatment
W040/SCP+AC+SE	450	180	0.4	0	1206	677	SEMA	Soaking RA in cement-SF+FA solution + carbonation treatment + SEMA
W045/NAC1	400	180	0.45	1257	0	677	NMA	Natural aggregate concrete (control 1)
W045/RAC2	400	180	0.45	0	1206	677	NMA	Un-treated recycled aggregate concrete (Control 2)
W045/SCP	400	180	0.45	0	1206	677	NMA	Soaking RA in cement-SF+FA solution
W045/AC	400	180	0.45	0	1206	677	NMA	Accelerated carbonation treatment
W045/SE	400	180	0.45	0	1206	677	SEMA	Untreated RA
W045/SCP+SE	400	180	0.45	0	1206	677	SEMA	Soaking RA in cement-SF+FA + SEMA
W045/AC + SE	400	180	0.45	0	1206	677	SEMA	Carbonation treatment +SEMA
W045/SCP+AC	400	180	0.45	0	1206	677	NMA	Soaking RA in cement-SF+FA solution + carbonation treatment
W045/SCP+AC+SE	400	180	0.45	0	1206	677	SEMA	Soaking RA in cement-SF+FA solution + carbonation treatment + SEMA
W050/NAC1	350	175	0.5	1257	0	677	NMA	Natural aggregate concrete (control 1)
W050/RAC2	350	175	0.5	0	1206	677	NMA	Un-treated recycled aggregate concrete (Control 2)
W050/SCP	350	175	0.5	0	1206	677	NMA	Soaking RA in cement-SF+FA solution
W050/AC	350	175	0.5	0	1206	677	NMA	Accelerated carbonation treatment
W050/SE	350	175	0.5	0	1206	677	SEMA	Untreated RA
W050/SCP+SE	350	175	0.5	0	1206	677	SEMA	Soaking RA in cement-SF+FA + SEMA
W050/AC + SE	350	175	0.5	0	1206	677	SEMA	Carbonation treatment +SEMA
W050/SCP+AC	350	175	0.5	0	1206	677	NMA	Soaking RA in cement-SF+FA solution + carbonation treatment
W050/SCP+AC+SE	350	175	0.5	0	1206	677	SEMA	Soaking RA in cement-SF+FA solution + carbonation treatment + SEMA
W055/NAC1	300	165	0.55	1257	0	677	NMA	Natural aggregate concrete (control 1)
W055/RAC2	300	165	0.55	0	1206	677	NMA	Un-treated recycled aggregate concrete (Control 2)
W055/SCP	300	165	0.55	0	1206	677	NMA	Soaking RA in cement-SF+FA solution
W055/AC	300	165	0.55	0	1206	677	NMA	Accelerated carbonation treatment
W055/SE	300	165	0.55	0	1206	677	SEMA	Untreated RA
W055/SCP+SE	300	165	0.55	0	1206	677	SEMA	Soaking RA in cement-SF+FA + SEMA
W055/AC + SE	300	165	0.55	0	1206	677	SEMA	Carbonation treatment +SEMA
W055/SCP+AC	300	165	0.55	0	1206	677	NMA	Soaking RA in cement-SF+FA solution + carbonation treatment
W055/SCP+AC+SE	300	165	0.55	0	1206	677	SEMA	Soaking RA in cement-SF+FA solution + carbonation treatment + SEMA
W060/NAC1	250	150	0.60	1257	0	677	NMA	Natural aggregate concrete (control 1)
W060/RAC2	250	150	0.60	0	1206	677	NMA	Un-treated recycled aggregate concrete (Control 2)
W060/SCP	250	150	0.60	0	1206	677	NMA	Soaking RA in cement-SF+FA solution
W060/AC	250	150	0.60	0	1206	677	NMA	Accelerated carbonation treatment
W060/SE	250	150	0.60	0	1206	677	SEMA	Untreated RA
W060/SCP+SE	250	150	0.60	0	1206	677	SEMA	Soaking RA in cement-SF+FA + SEMA
W060/AC + SE	250	150	0.60	0	1206	677	SEMA	Carbonation treatment +SEMA
W060/SCP+AC	250	150	0.60	0	1206	677	NMA	Soaking RA in cement-SF+FA solution + carbonation treatment
W060/SCP+AC+SE	250	150	0.60	0	1206	677	SEMA	Soaking RA in cement-SF+FA solution + carbonation treatment + SEMA

Table 4.8 shows concretes mix proportions produced with the final selected treatments at 3 different water to cement ratios, 0.4, 0.5, and 0.6. The aim here was to evaluate the effects of the final selected treatments at variations of water to cement ratios on the structural performance and durability of recycled aggregate concrete in comparison with natural aggregate concrete.

Accordingly, 15 different concrete mixtures were developed to produce 8 concrete cubes (100mm × 100mm × 100mm), 2 cylinders (100mm × 200mm), 2 cylinders (150mm × 300mm), 2 beams (500mm × 100mm × 100mm) per concrete mixture and tested for mechanical performance, slump, density, compressive strength, structural performance, tensile splitting strength, flexural strength, and modulus of elasticity. Durability performance tests included water absorption, sulphate attack, and resistance to freeze-thaw. Superplasticiser was only used for concretes produced with 0.4 water to cement ratio.

Table 4.8: Mix proportions for various RAC produced with various treatments at variations of w/c ratios for testing mechanical performance (flexural strength, tensile splitting strength, and modulus of

Specimen Designation	PC (kg/m ³)	Water (kg/m ³)	NA (kg/m ³)	RA (kg/m ³)	Sand (kg/m ³)	Mixing Method	Notes
W040/NAC1	450	180	1257	0	677	NMA	Natural aggregate concrete
W040/RAC2	450	180	0	1206	677	NMA	Un-treated recycled aggregate concrete
W040/SCP	450	180	0	1206	677	NMA	Soaking RA in cement-SF+FA solution
W040/SE	450	180	0	1206	677	SEMA	Untreated RA
W040/SCP+SE	450	180	0	1206	677	SEMA	Soaking RA in cement-SF+FA + SEMA
W050/NAC1	350	175	1257	0	677	NMA	Natural aggregate concrete
W050/RAC2	350	175	0	1206	677	NMA	Un-treated recycled aggregate concrete
W050/SCP	350	175	0	1206	677	NMA	Soaking RA in cement-SF+FA solution
W050/SE	350	175	0	1206	677	SEMA	Untreated RA
W050/SCP+SE	350	175	0	1206	677	SEMA	Soaking RA in cement-SF+FA + SEMA
W060/NAC1	250	150	1257	0	677	NMA	Natural aggregate concrete
W060/RAC2	250	150	0	1206	677	NMA	Un-treated recycled aggregate concrete
W060/SCP	250	150	0	1206	677	NMA	Soaking RA in cement-SF+FA solution
W060/SE	250	150	0	1206	677	SEMA	Untreated RA
W060/SCP+SE	250	150	0	1206	677	SEMA	Soaking RA in cement-SF+FA + SEMA

elasticity) and durability performance

4.5 Specimen Preparation & Testing of Concrete

4.5.1 Specimen preparation & curing condition

Various test specimens were prepared, mixed, cast, and cured under laboratory conditions, Table 4.9 shows the detailed description of the test specimens utilised for different testing throughout this study. All the materials needed to produce natural aggregate concrete and recycled aggregate concrete were kept dry at room temperature and were used in their

supplied condition except for recycled aggregate which were treated as discussed in Section 4.2.

Depending on the designated concrete mixture, the needed materials for the fabrication of the required number of concrete test specimens were prepared and weighed prior to mixing. Croker Cumflow RP100 XD MK2 rotating pan mixer with 1131 - 163kg nominal max input capacity and 16RPM pan mixing speed, was used for concrete mixing as shown in Figure 4.10.

The following procedures were followed to produce fresh concrete mixtures, the mixing raw materials were first added to the rotating pan mixer. The pre-weighed mixing water was then added slowly into the mixer and mixed for 3 minutes. The mixer was then opened, and the fresh concrete formed was scooped out from the edges back to the middle of the mixer pan using a hand-held scope.

Once this stage was finished, workability test by means of slump was carried out, prior to cast concrete into the moulds. Thereafter, the fresh concrete was removed and cast into the various moulds i.e., cubes, cylinders, and beams, and compacted using a vibrating table. The test specimens were then placed on worktops and air cured for 24 hrs at room temperature of 20 ± 3 °C.

It is worth mentioning that no segregation or bleeding were observed in any of the concrete mixes during the casting of different specimens. After 24 hrs of air curing, the test specimens were demoulded and placed into water curing tanks with a controlled temperature of 20 ± 3 °C and cured until the testing day, in compliance with BS EN 12390-2:2009. Some of the test specimens are presented in Figures 4.11a and 4.11b, while Figure 4.11c shows the test specimens cured in a water tank.

Table 4.9: Detailed description of the experimental program utilised for all the test specimens

Type of mould	Dimensions	Test aspect	No. of test specimens	Testing age	Notes
Cube	100mm × 100mm × 100mm	Compressive strength & density	63	7, 14, and 28 days	Evaluating 7 various mixtures including developed batching techniques at 0.5 w/c ratio
	100mm × 100mm × 100mm	Compressive strength & density	405	7, 14, and 28 days	Evaluating 9 different mixtures including various treatment methods at 0.4, 0.45, 0.5, 0.55, and 0.6
	100mm × 100mm × 100mm	Compressive strength	30	28 days	Determining the compressive strength for 5 different mixtures including the various treatment mixtures for modulus of elasticity calculations, at 0.4, 0.5, and 0.6
	100mm × 100mm × 100mm	Water absorption, sulphate attack, freeze-thaw	90	28 days	Durability tests for 5 mixtures including various treatment mixtures at 0.4, 0.5, and 0.6
	100mm × 200mm	Tensile splitting Strength	30	28 days	Tensile splitting strength test was for 5 mixtures including the various treatments used at 0.4, 0.5, and 0.6
	150mm × 300mm	Modulus of elasticity	30	28 days	Modulus of elasticity test was for 5 mixtures including the various treatments used at 0.4, 0.5, and 0.6
	500mm × 100mm × 100mm	Flexural strength	30	28 days	Flexural strength test was for 5 mixtures including the various treatments used at 0.4, 0.5, and 0.6
	Total number of cubes			588	
Total number of small cylinders			30		Tensile splitting strength
Total number of large cylinders			30		Modulus of elasticity
Total number of beams			30		Flexural strength
Total test specimens throughout this study			678		Including all types of moulds



Figure 4.10: Croker Cumflow RP100 XD MK2 rotating pan mixer

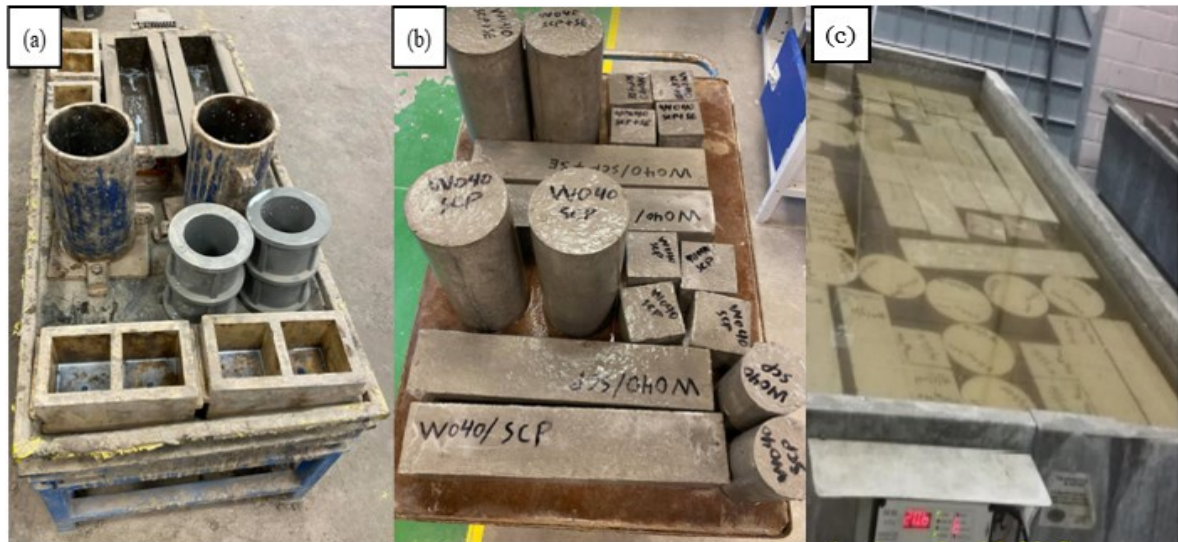


Figure 4.11: (a) various moulds oiled and prepared for fresh concrete casting, (b) some of the hydrated concrete test specimens, (c) test specimens cured in a water tank with controlled temperature

4.5.2 Consistency of fresh concrete [BS EN 12350-2: 2019]

Consistency also known as workability of concrete define the fresh state of the concrete mixture in terms of mobility and compactability. It also determines the degree of concrete mixture wetness, within the standard limits, wet concretes are more workable/ flowable than dry concretes. Consistency of the fresh natural aggregate concrete (1st control), and untreated recycled aggregate concrete (2nd control), along with the different treated concrete mixtures at the different water to cement ratios were measured by the slump test in accordance with BS EN 12350-2: 2019.

The slump test is quite popular because of its simplicity, it is usually utilised, indirectly to check if the correct amount of water has been added to the mix. The apparatus used for slump test comprise of (i) a metal hollow cone shaped with 300 mm high, 200 mm wide at the bottom and 100 mm wide at the top opening, (ii) scoop, (iii) tamping or compacting rod, (iv) smooth non-absorbent base steel plate, and (v) steel ruler for measurement. Figure 4.12 shows the slump test for one of the concrete mixtures.

The experimental procedures included the following, the cone was placed on a flat and smooth horizontal surface while ensuring the cone was planted firmly on the ground by standing on the footholds either side. The cone was then filled in three layers where every layer was approximately one-third of the cone height when compacted. Each layer was compacted or tamped 25 times in an even and uniformed manner using the steel tamping rod.

Once the cone was filled, any overflowing fresh concrete was removed from the top. Any spilled concrete on the base of the cone was also removed. Thereafter, the cone was slowly lifted vertically until the cone was clear of concrete. The cone was then placed upside down on the surface plate next to the concrete. Once the concrete subsided, the steel rod was placed across the top of the upturned cone, so it overhung concrete. The slump was then measured and recorded by determining the difference between the height of the cone and that of the highest point of the slumped test sample. Finally, the level of slump was measured by a ruler to the nearest 10mm, as shown in Figure 4.12.

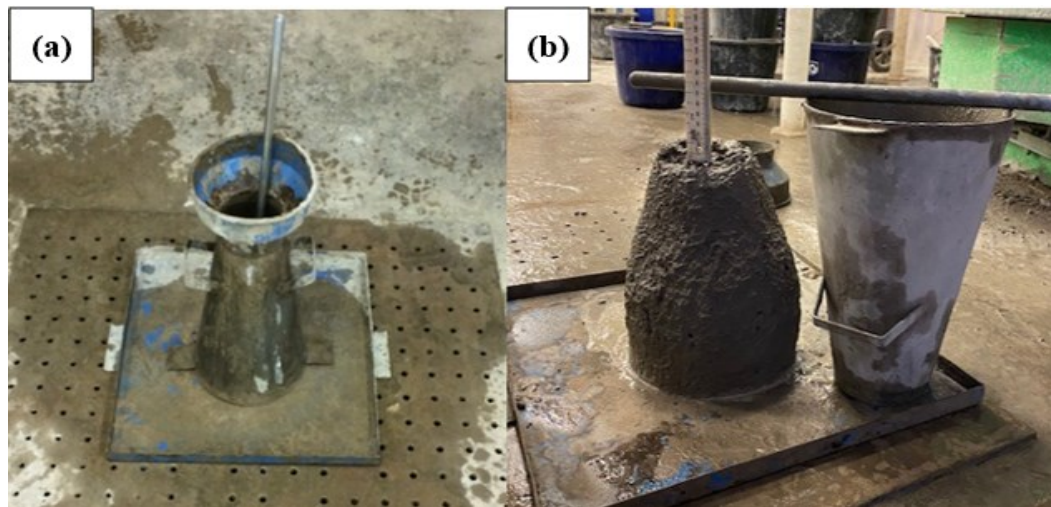


Figure 4.12: (a) slump test apparatus, (b) slump test for one of the designated concrete mixtures

4.5.3 Mechanical properties of the hardened concretes

4.5.3.1 Density of hardened concrete [BS EN 12390-7: 2009]

The apparent density of hardened concrete refers to the ratio of the mass to the volume occupied by the tested solid including the hollow space. It is dependent on the form of the constituent particles, the constituent of the solid components, and the curing method. Density is one of the hardened concrete properties that can influence strength and durability. The density of the two control concretes and the treated concretes at the different water to cement ratios were determined by the water displacement method in accordance with BS EN 12390-7: 2009. The utilised comprehensive testing system for testing density was an electronic DENSION-MAYES hydrostatic weight balance which was connected to a computer monitor as shown in Figure 4.13. The weight balance comprised of a water tank with mechanical

lifting device, steel support frame, and a stirrup suspended below the balance system for holding the tested sample.



Figure 4.13: Density testing regime for hardened concrete mixtures

After 28 days of water curing, the hardened concrete specimens were removed from water curing tanks and then they underwent density test, the experimental procedures followed for testing density of hardened concretes involved the following, the concrete specimen was first placed on the stirrup and the water tank was raised up by the lifting device until the specimen is totally immersed in water. The weight of the concrete specimen in air and in water was then automatically determined by the weight balance and displayed on the computer screen. Finally, the density value was automatically measured to the nearest 10 kg/m^3 . Once the density test was finished, any excess of water and extraneous materials on the surface of the tested specimens were wiped off by a dried cloth, prior to compressive strength test.

4.5.3.2 Compressive Strength [BS EN 12390-3: 2009]

The unconfined compression strength test was used to investigate the ability of the treated concrete mixtures to gain strength at 7, 14, and 28 curing ages and at the various utilised water to cement ratios, the results were compared to those of the natural aggregate concrete (1st control) and the untreated recycle aggregate concrete (2nd control). The investigation was carried out on cubic specimens of dimensions $100 \text{ mm} \times 100 \text{ mm} \times 100 \text{ mm}$ in accordance with BS EN 12390-3:2009 using a compression testing machine type DENSION-MATEST 7225 with a Digital indicator of 0 to 2000 kN in increments of 0.04 kN and complied with EN 12390-3: 2009 as shown in Figure 4.14.

Three cubes per concrete mixture were used in the compressive strength test and their arithmetic average value was taken as the representative strength result. Prior to the test, any loose grit on the bearing surfaces of the testing machine were wiped off and cleaned, then the concrete specimen was placed between the upper and the lower platens in a way that the force was applied perpendicularly to the surface of casting. The test started with applying a vertical axial load at a constant increasing rate of $0.06 \pm 2 \text{ N/mm}^2$ per sec on the test concrete specimen until failure is reached, then the strength value was automatically determined and displayed on the testing machine screen.



Figure 4.14: Compression testing machine used for testing compressive strength of concrete

4.5.3.3 Tensile splitting strength [BS EN 12390-6: 2009]

To measure the resistance of the control mixes and the treated recycled aggregate concretes to splitting under tension, the tensile splitting strength of 100mm in diameter and 20000 height cylindrical concrete specimens at 28 curing age was carried out in accordance with the indirect method given in the specifications of BS EN 12390-6: 2009 using the DENSION-MATEST 7225 testing machine illustrated in Figure 4.15.

The cylindrical concrete specimens were first placed into a framed steel, then two plywood strips were fitted to cover the cylinder from the top and bottom in between the loading platens

of the steel frame to allow for distributional uniformly applied load along the specimen length until failure is reached. After that, the load was applied at a constant and rate of 1.57 kN/sec, until the cylindrical specimen reached failure by splitting into two halves along with their vertical planes. The results of tensile splitting strength test of the concrete cylinders in this study are the mean of two measured values per concrete mixture.

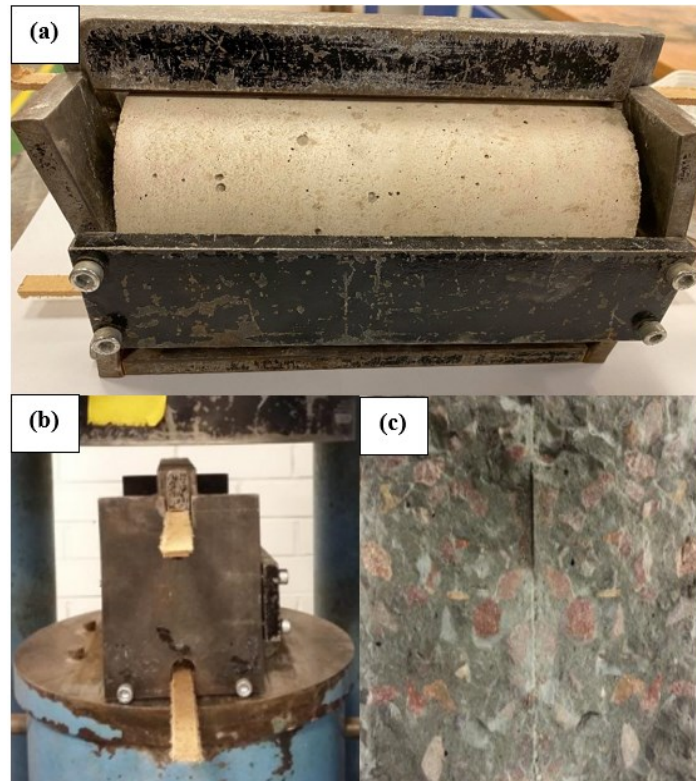


Figure 4.15: (a) framed steel, (b) tensile splitting strength test, (c) splitting of cylinder specimen

4.5.3.4 Flexural strength [BS EN 12390-5: 2009]

The flexural strength test was carried out on prismatic concrete beams of 500mm × 100mm × 100mm, in accordance with BS EN 12390-5: 2009, using a four-points loading test as shown in Figure 4.16a. The flexural strength test procedure involved the following, the upper and supporting rollers were wiped and cleaned while their capability of rotating freely was ensured.

The prismatic beam was then marked from both sides and placed on the rollers while ensuring an equal distance between both sides of the beam and the rollers. Thereafter, the beam specimen was adjusted on the machine to make sure the force was applied perpendicularly to the surface of casting. The load was then applied in a constant increased rate of 10 kN/min

until failure is occurred (Figure 4.16b). The results of flexural strength test of the concrete prismatic beams in this study are the mean of two measured values per concrete mixture.

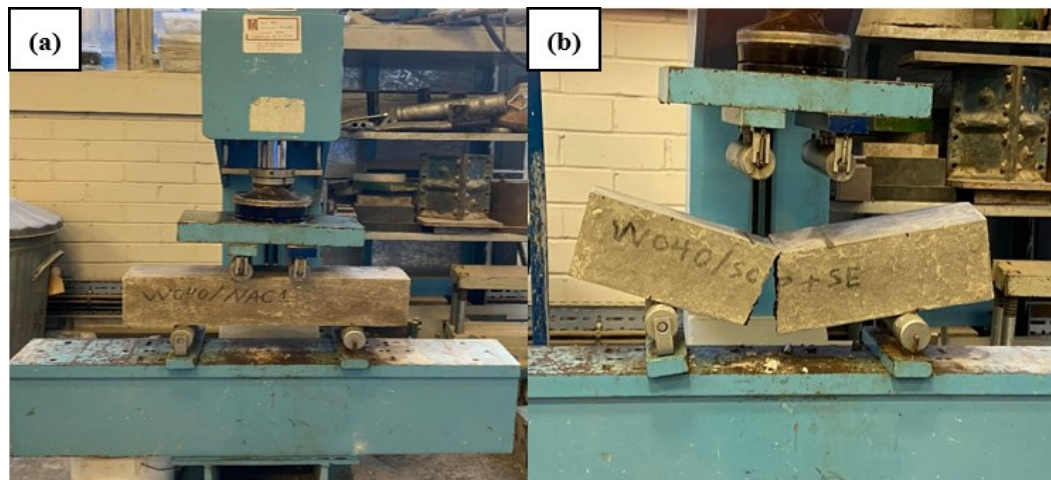


Figure 4.16: (a) flexural strength test, (b) flexural failure of prismatic concrete beam

4.5.3.5 Modulus of elasticity [BS EN 12390-13:2021]

Modulus of elasticity was carried out on cylindrical concrete specimen with 150mm diameter and 300mm height in accordance with BS EN 12390-13:2021 as shown in Figure 4.17c. The test was carried out using a compression machine with the ability of holding, increasing, and decreasing the load at a constant rate of 636 kN/min.

The test involved the following procedures, first, a coating slurry was prepared by mixing a Dentstone KD adhesive powder with water. The upper surface of cylinders was then coated with a thick layer of this slurry to minimise friction and allow for a proper distributed load on the cylinder surface. The coated layer was covered with a glass panel and then levelled by a Driak circular spirit level which was placed on top of the glass panel and moved around until the desired level was achieved (Figure 4.17a). After the coating layer dried, the panel glass was removed, and the cylindrical specimen was then placed into an aluminium frame attached with strain measuring gauge (Figure 4.17b). The specimen was centred in a way that both upper and lower frame at similar distance from both ends of the cylinder. Thereafter, the frame screws on the top and bottom were tightened while the pivot rods were removed.

The cylinder specimen was placed into the compression machine and three cycles of loading and unloading was applied at a constant rate of 636 kN/min. One cycle involved of 10 kN stress and one third of the compression strength stress, which was obtained from the previous

compressive strength test for the same concrete batch. During the test, the strain at each loading and unloading cycled was recorded. The modulus of elasticity of the specimen was calculated after the end of the three cycles.

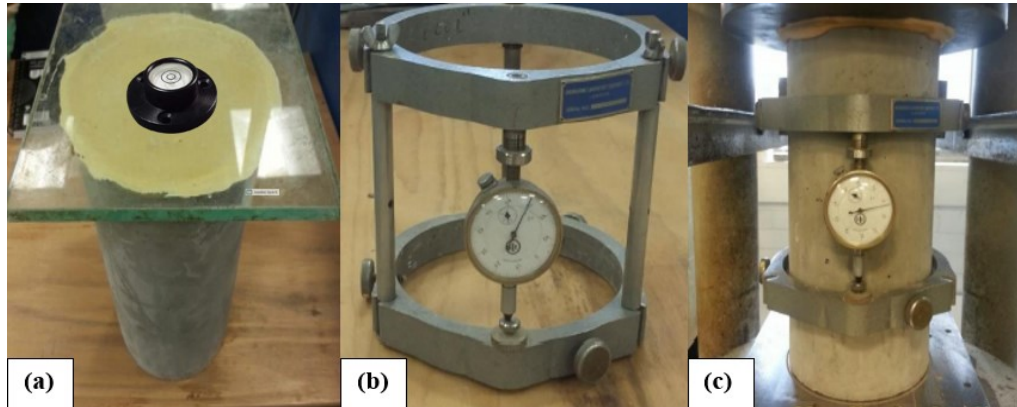


Figure 4.17: (a) preparation of the cylinder specimen, (b) steel frame with attached strain gauge, (c) modulus of elasticity test

4.5.4 Durability properties

The durability performance evaluation for the natural aggregate concrete (1st control), the untreated recycled aggregate concrete (2nd control), the various treated recycled aggregate concretes at 0.4, 0.5, and 0.6 water to cement ratio included the followings tests, (i) water absorption, (ii) resistance to freeze and thaw, and resistance to sulphate attack.

4.5.4.1 Water absorption [BS 1881-122:2011+A1:2020]

Water absorption test of the natural aggregate concrete (1st control), untreated recycled aggregate concrete (2nd control), and the various treated recycled aggregate concrete specimens were carried out in compliance with the specifications set in BS 1881-122:2011+A1:2020. The test was carried out on two concrete cubes of dimensions 100mm × 100mm × 100mm. The water absorption was measured as the change in weight of the test specimen immersed in water for 28 days and the oven dry weight at 105°C to constant weight, expressed as percentage of the dry weight.

4.5.4.2 Resistance to freeze – thaw [PD CEN/TS 12390-9:2016]

Resistance of concrete to freezing and thawing is often used as an evaluation index of concrete durability. It can be addressed by measuring concrete weight loss rate, and strength loss rate after concrete exposure to repeated freezing and thawing cycles. In general, water

content, porosity, aggregate type, and environmental conditions affect this durability property. In this study, the resistance to freeze and thaw repeated cycles was investigated to evaluate the ability of the various treated recycled aggregate concretes to resist damage when exposed to successive freeze and thaw cycles in compliance with PD CEN/TS 12390-9:2016. The test was carried out in a Prior Clave LCH/600/25 model with 0.7m³ volume capacity environmental chamber, in accordance with BS 5628-3: 2005 and BS 6073-2: 2008. Four concrete cubes per mix of dimensions 100mm × 100mm × 100mm underwent freeze-thaw cycles.

The specimens were firstly immersed (cured) in water after demoulding at 20 ±2°C for 7 days prior to freezing-thawing test. Thereafter, the freeze-thaw cycles started with the concrete cubic specimens being removed from the water bath and placed into the freezing chamber for seven days at a temperature of -15°C and then removed to be thawed for one hour in a water bath with a controlled temperature at 20±2°C. This cycle was repeated for twenty times and the strength losses of the two control concrete specimens and the various treated recycled aggregate concrete specimens for 28 days (3 cycles) and 140 days (20 cycles) were recorded. In addition, weight gain/ losses were recorded at the end of each cycle. Visual inspections were also carried out to report and scaling, spalling, cracking, or chipping that may have occurred to any of the test concrete specimens. The mass change (Δm_{F-T}) and the residual compressive strength ($f_{ci,rel}^m$) were empirically calculated using the following equations, respectively:

$$\Delta m_{F-T} = \frac{m_{ni} - m_{0i}}{m_{0i}} \times 100 \quad \text{Equation 4.11}$$

Where i and n represent the specimen number and the freeze-thaw cycles respectively; m_{0i} is the initial mass, and m_{ni} is the mass after n freeze-thaw cycles.

$$f_{ci,rel}^m = 100 \times \left(1 - \frac{f_{ci,n}^m}{f_{cr,n}^m}\right) \quad \text{Equation 4.12}$$

Where, $f_{ci,n}^m$, and $f_{cr,n}^m$ are the compressive strength after n cycles (3 and 20 repeated cycles) of freeze-thaw, and the compressive strength of the reference concrete test specimen cured in water, respectively.

4.5.4.3 Resistance to sulphate attack [BS EN 206:2013+A2: 2021]

Sulphate attack is the deterioration of concrete due to the physical-chemical interactions between the hydrated cementitious products and sulphate found in soil, seawater, aggregates, and cements. These interactions result in expansion, cracking, spalling and disintegration of concrete. In addition, external sulphate attack may also cause other deterioration mechanisms such as softening of concrete as a result of leaching of cement hydration products, and salt exfoliation. In this study, sulphate attack was carried out to evaluate the performance of the various treated recycled aggregate concretes to withstand sulphate attack and in comparison, with the conventional concrete. The test of sulphate attack in this study involved the following procedures, concrete specimens were first cured in water bath at controlled temperature of 20 ± 2 °C for 7 days. Seawater saline solution was selected for concrete specimen immersion and poured into a lidded plastic container in accordance with BS EN 206:2013+A2: 2021.

After 7 days of water curing, the concrete specimens were removed and placed into the lidded container for sulphate attack investigations. The use of lidded plastic container offered protection against various environment exposure such as frost action, wetting or drying, abrasion, and different moisture content that may occur between the surface and the core of the tested concrete specimens. Thus, limiting the interactions to only the ions presented in the solution and the immersed concrete specimens.

Four $100\text{mm} \times 100\text{mm} \times 100\text{mm}$ concrete cubes per concrete mixture were utilised for sulphate attack investigations (Figure 4.18). Deterioration due to sulphate attack was investigated in terms of loss/gain in weight at every 7 days and loss in compressive strength at 28 days and 140 days relative to the reference specimen. In addition, any visible physical damage to the concrete specimens after sulphate attack was recorded via visual inspections. The mass change ($\Delta m_{n,SA}$) and the residual compressive strength ($f_{n,SA}$) after for the sulphate attack were empirically calculated using the following equations, respectively:

$$\Delta m_{n,SA} = \frac{m_{ni} - m_{0i}}{m_{0i}} \times 100 \quad \text{Equation 4.13}$$

Where m_{0i} and m_{ni} are the initial mass, the mass n days after sulphate attack, respectively.

$$f_{n,SA} = 100 \times \left(1 - \frac{f_{ci,n}^m}{f_{cr,n}^m}\right) \quad \text{Equation 4.14}$$

Where $f_{ci,n}^m$ and $f_{cr,n}^m$ are the compressive strength after n days (28 and 140 days) of sulphate attack, and the compressive strength of the reference test specimen at n days (28 and 140 days) immersed in tap water, respectively.



Figure 4.18: Sulphate attack test on some of the concrete samples

4.5.5 Microstructure investigations

4.5.5.1 Scanning Electron Microscopy (SEM) investigation

In order to get a better detailed scientific understanding of the morphology of the cementitious materials, materials composition, and surface texture of the microstructure of the treated recycled aggregate concretes, SEM investigations were employed and compared to those of the natural aggregate concrete (1st control) and the untreated recycled aggregate concrete (2nd control). The SEM operates by scanning an electron beam across a specimen, hence offering high resolution images of the morphology or topography of the tested specimen with great depth field, at either very low or very high magnifications depending on the requirements.

The SEM unit requires the specimen to be placed into a specimen chamber that is pre-evacuated. It then produces a beam of electrons in the vacuum. The electronic beam is collimated by electromagnetic condenser lenses, focussed by an objective lens, and scanned across the specimen surface by electromagnetic deflection coils. The main imaging method stems from collecting secondary electrons that are released by the specimen. The secondary electrons are detected by a scintillation material that generates flashes of light from the electrons. Thereafter, the light flashes are detected and amplified by a photomultiplier tube and converted into electric signals, thus processed to produce an image on the SEM monitor. Figure 4.19 shows a typical diagram of the SEM unit.

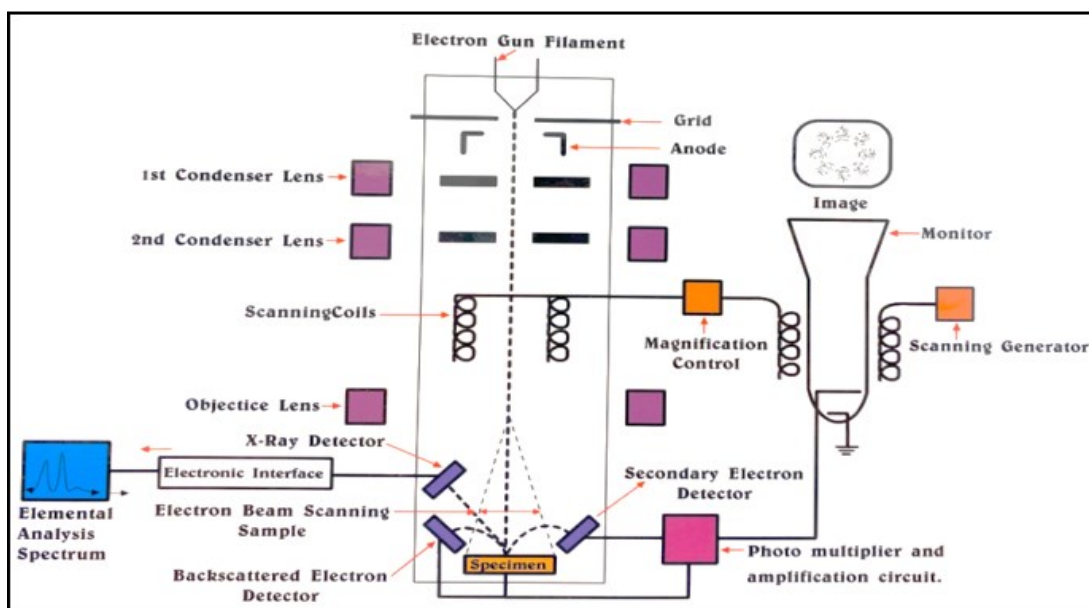


Figure 4.19: Block diagram of a typical SEM unit (courtesy of University of South Wales)

In the present study, the preparation of test specimens for microstructural investigations involved the following procedures, after 28 days of water curing, the concrete cubic specimens were removed from the water curing tanks and placed in a desiccator to be dried at low temperature of a 40 °C. This drying process was accelerated by incorporating silica gel, which was constantly replenished through drying in an oven to expel any absorbed moisture. A diamond wheel cutter was utilised to cut the concrete cube specimens into small slices of dimensions 5mm thickness × 10mm length × 10mm width. The slices were then polished and metallised with a gold layer to produce a specimen with electrically conductive surface (Figure 4.20). Thereafter, the specimens were impregnated into a double-sided stub with a sticky tab to hold the specimen. The stubs were then fitted on the sample stands in the SEM chamber prior to the start of the SEM analysis (Figure 4.21).

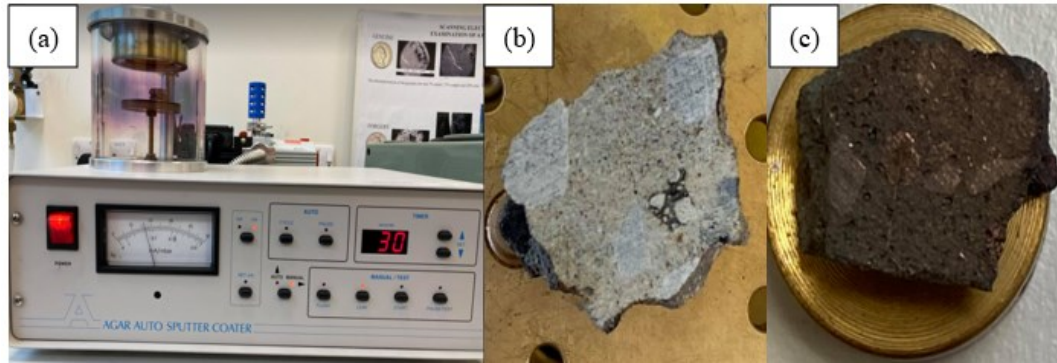


Figure 4.20: (a) Agor Auto sputter gold coater, (b) specimen prior to coating, (c) specimen after coating with gold layer

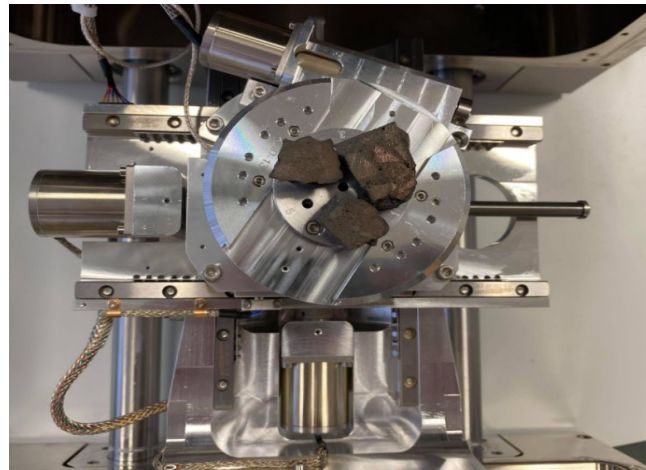


Figure 4.21: Specimens mounted on the specimens' stand in the SEM chamber

The specifications of the SEM machine are the following, a MIRA3 TESCAN Scanning Electron Microscope (SEM), fitted with a Solid-state Backscattered (electron) Detector (SBD). Several fragments were taken from different parts of the dried concrete specimen and examined to give better representation of the whole hydrated concrete specimens. Two areas of interest were initially visually selected to be further studied with the SEM unit, (i) the ITZ between the old aggregate and the adhered mortar, and (ii) the ITZ between new cementitious paste and the adhered mortar.

4.5.5.2 Energy-dispersive X-ray spectroscopy (EDS)

The SEM unit was also equipped with an INCA-SUITE version 4.01 Oxford Instrument connected to an Ametek Energy Dispersive X-ray spectrometer (EDS), and it is used as a material analyser for chemical composition analysis and additional identification of crystalline phases.

CHAPTER FIVE – RESULTS & DISCUSSION

Chapter five gives the results and discussion of the detailed experimental works obtained from the Aggregate Impact Value and Water Absorption on treated RA via Regime A and Regime B treatments and on the mechanical properties of hydrated RAC produced with different batching techniques (Regime C) during the initial treatment phase of RA. This Chapter further presents the results and the discussion of mechanical properties, durability, and microstructure investigations of RAC produced with different treatment methods. This chapter has been divided into 9 sections. Section 1 present the results and discussion of the first stage evaluation of the performance of the treatments selected in enhancing the AIV and WA of RA (Regime A and Regime B). Section 2 includes the results and discussion of the performance of the batching techniques in enhancing the mechanical properties of RAC (Regime C). Section 3 presents the first selection matrix and its interpretation for selecting the best treatment methods for further investigations. Section 4 gives the results and discussion of the performance of the treatment methods selected from Section 3 in terms of mechanical properties of concretes produced at different w/c ratios. Section 5 gives a second selection matrix to select the final best treatment methods for further investigations. Section 6 presents the results and discussion of the mechanical performance of the final selected treatment methods in terms of flexural strength, tensile splitting strength, and modulus of elasticity. Section 7 includes correlation & linear regression analysis along with description of comparison with design codes of the different criteria examined in this research. Section 8 presents the results and discussion of the durability assessment of the final selected treatments. Section 9 includes the results and interpretation of the microstructural investigations.

5.1 Effects of Treatment Methods on Properties of RA

5.1.1 Effects of Regime A – Water treatment methods on AIV & WA of RA

Figure 5.1 shows the AIV of the treated RA after water treatment methods utilised in comparison with untreated RA and NA. The results of the effects of the water treatment methods on the WA of the RA are presented in Figure 5.2. The results indicated little or insignificant enhancements in the AIV achieved by water washing and partial saturation treatments. The highest enhancement in the AIV was recorded for water washing with discarded any RA with particle size < 4mm. Nevertheless, the RA treated with self-healing

and water saturation not only showed no enhancement in the AIV, but there was an adverse effect of these treatments on the AIV.

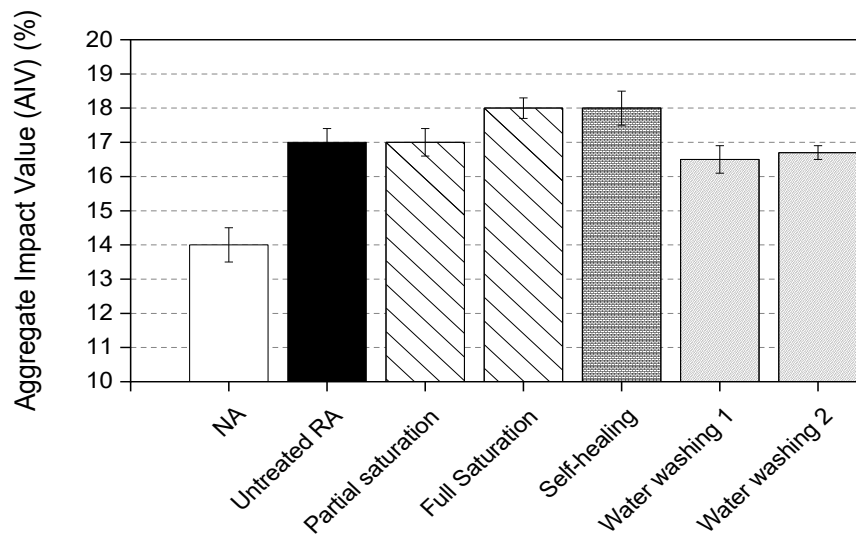


Figure 5.1: Effects of water treatment methods on the AIV of RA before and after water treatment methods, note; NA-natural aggregate, URA – untreated recycled coarse aggregate

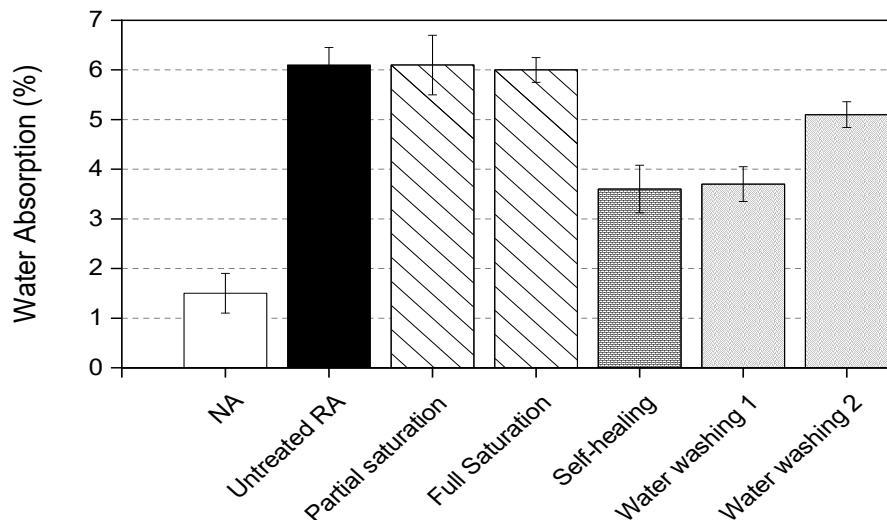


Figure 5.2: Effects of the various water treatment methods on the WA of RA before and after water treatment methods

The effects of water treatment methods on the WA of the RA were significant and more evident. The highest enhancement was achieved by self-healing treatment method. Self-healing of the RA for over 30 days of soaking in water managed to enhance the WA of the RA from 6.1% to 3.6%. Likewise, water washing also exhibited significant enhancement of 6.1% to 3.7% and from 6.1% to 5.1% for water washing with any aggregate with particle size < 4mm being discarded, and water washing with all aggregate particle sizes, respectively. Full

saturation of the RA in water showed insignificant enhancement in WA, while partial saturation of the RA in water showed no enhancement in the WA. It can be concluded that the best treatment method in Regime A was water washing, nonetheless, the enhancement achieved by this treatment in the AIV was yet insignificant.

The findings of the effects of water treatment methods on the AIV and WA of RA indicate that, the self-healing treatment approach showed no enhancement to the AIV of the RA, this might be due to the fact that the supplied recycled aggregates consisted of various materials that have different engineering characteristics with about 50% recycled concrete aggregate of its constituents, which significantly reduced the efficiency of the self-healing treatment, not to mention the previous exposure to weathering, loading, and crushing process. In addition, another possible reason could be that treatment utilised such as self-healing directly influence the water absorption property of RA by filling the voids and pores on RA surface through further hydration (Munir et al., 2022). On the other hand, the AIV of RA is mainly controlled by various factors, such as the strength of the parent concrete, the composition of RA (source), and the type of crushed used on-site (Munier et al., 2022).

The enhancement achieved by self-healing method in the WA property of RA might be due to the further hydration of the un-hydrated cement particles (the adhered mortar) which provided an extra calcium silicate hydrate (C-S-H) gel that blocked some of the existing pores on the RA surface, hence reducing the high-water absorption of recycled aggregates (Elhakam et al., 2012). Elhakam et al. (2012) studied the effects of self-healing treatment on the RAC mechanical properties. The test RACs were produced with recycled concrete aggregate (RCA). Elhakam et al. (2012) study concluded that, treating RCA with self-healing method enhanced the compressive strength of RAC by more than 30%.

The water washing method showed slight enhancement to the AIV of the RA and significant enhancement to the WA of the RA. This method resembled a prolonged Los Angeles test, that removed a significant amount of the adhered mortar along with any fractured or weaker aggregates, hence keeping only stronger and sounder ones which are the results of the RA colliding into each other's in the presence of water. Discarding any RA with size lower than 4mm reduced the AIV from 17% to 16.5% and the WA from 6.1% to 3.7%, while keeping the grading sizes as it is reduced the AIV from 17% to 16.7% and the WA from 6.1% to 5.1%. This is maybe ascribed to the higher mortar content of lower sizes of RA compared to that of the higher sizes as explained by Dimitriou et al. (2018) who recorded 50% enhancement to

the WA after water washing treatment, which may be attributal to the extended water washing process of about 5 hrs.

The aim of the water saturation method is mainly to prevent the recycled aggregates from consuming the effective mixing water or the w/c ratio, which is needed for cement hydration, hence it is desirable to be used prior to mixing of recycled aggregate concrete. The full saturation and partial saturation of RA showed insignificant or no enhancement to the AIV and the WA of the RA. These results can be explained as the nature of the WA test includes drying the test samples to constant weight prior to soaking water for 24 hrs which leads to eliminating the efficiency of water saturation. On the other hand, Ferreira et al. (2011) recommended that 90% of saturation level can be achieved by immersing the aggregates in water for 5 mins, reported that, 90% of saturation level is ideal whereas 100% of saturation may cause a detrimental effect on concrete.

Overall, it can be observed that none of the water treatment methods have shown significant enhancement to the AIV of the RA, and this shows the very poor state of the supplied RA in this study, arising from previous loading, weathering, and crushing process of these aggregates, which resulted in weakening their strength. The following points on the overall performance of water treatment methods can be summarized as follows:

- Self-healing water method enhanced the WA of RA from 6.1% to 3.6%, however it did not improve the AIV of RA.
- Water washing treatment method showed slight enhancement in the AIV of RA and reduced the WA from 6.1% to 3.7%.
- Water saturation method showed no enhancement in the AIV nor WA of RA.
- Overall, treated RA using water treatment methods exhibited better performance in terms of the WA, however, the AIV did not improve.

5.1.2 Effects of Regime B – Strengthening the adhered mortar on AIV & WA of RA

Regime B treatment methods included the following treatments, carbonation treatment, soaking RA in sodium silicate-silica fume solution, coating RA with cement and/or cement-silica fume slurry, soaking RA in cement-pozzolan solutions.

(ii) Accelerated carbonation treatment (AC)

Figure 5.3 shows the effects of different CO₂ concentration levels on the aggregate impact value (AIV) of the RA. Figure 5.3 showed various enhancements achieved in the AIV of RA after accelerated carbonation treatment.

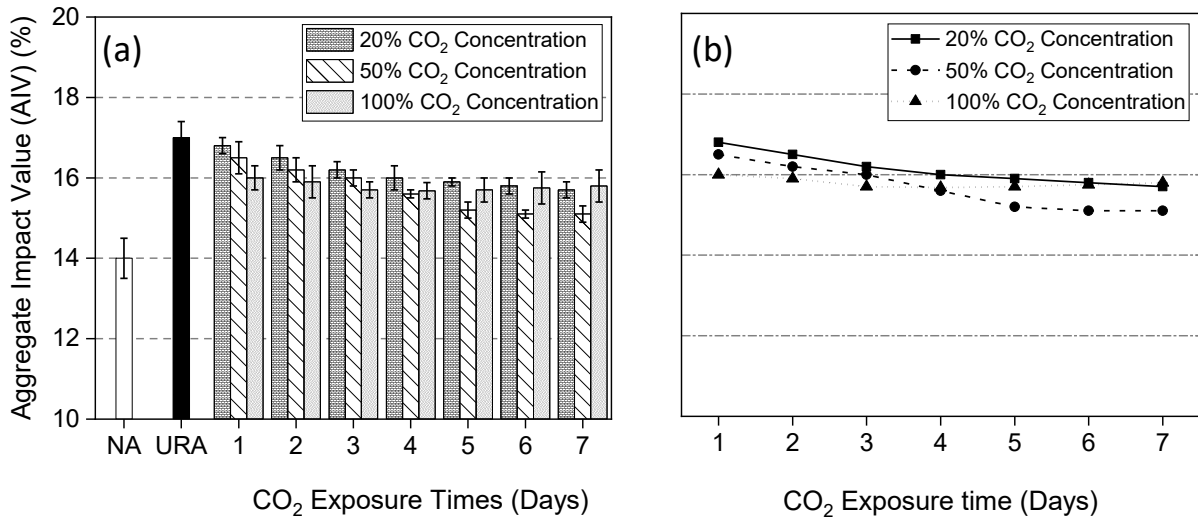


Figure 5.3: The impact of carbonation treatment at different concentration levels and CO₂ exposure time on the AIV of the RA shown in (a) clustered column chart, and (b) scatter chart, note: NA – natural coarse aggregate, URA – untreated recycled coarse aggregate

During the first 3 days of carbonation treatment, the AIV of the RA treated with 100% CO₂ concentration showed the highest reduction from 17% to 15.7%. This can be explained as the diffusion rate of CO₂ is influenced by the concentration level of CO₂ and the transport paths. Thus, a higher CO₂ concentration level such as 100% is more beneficial for the diffusion of CO₂ prior to the pores being blocked up by calcium carbonates. Moreover, during the initial period of reaction, carbonation occurs intensely in a rapid growth stage. These two aspects contributed to a higher enhancement of 100% concentration level during the first 3 days of carbonation (Pu et al., 2021).

Accordingly, the results demonstrate that the observed optimal CO₂ exposure time for 100% CO₂ concentration was 3 days. After three days of CO₂ carbonation, there was no further improvement in the AIV at a 100% CO₂ concentration level. Anstice et al. (2005) and Hyvert et al. (2010) confirmed that increased concentration in CO₂ level may lead to C-S-H gel decalcification, while increasing the CO₂ level up to 100% may lead to complete disappearance of C-S-H gel, which results in adverse effects on the RA properties. Similarly, Kashef-Haghighi et al. (2015) also observed that there was no further increase in RA carbonation percentages when the CO₂ concentration level reached 100%.

After 3 days of carbonation, RA treated with 50% CO₂ concentration started to achieve lower AIV compared to the RA treated with 100% and 20% CO₂ concentration levels. This can be attributed to the high concentration level of CO₂ which increased the degree of decalcification of calcium-silicate-hydrate. Thus, a large amount of CO₂ was allowed to react with C-S-H which formed a phase of a lower Ca/Si ratio, hence achieving better enhancement in AIV. The highest AIV enhancement at 50% CO₂ concentration level was reached at 6 days of carbonation, the AIV was reduced from 17% to 15.1%. Thus, the optimal CO₂ exposure time at a 50% CO₂ concentration level is at 6 days of carbonation.

Treating RA with a 20% CO₂ concentration level offered better quality results over time but with slow AIV enhancements because of the lower CO₂ concentration level. The highest AIV enhancement at a 20% CO₂ concentration level was recorded at 7 days of CO₂ exposure time, where the AIV of RA was reduced from 17% to 15.9%. This is thought to be due to carbonation treatment that led to a denser particle surface of the RA which in turn reduced the rate of diffusion of CO₂ into RA pores, hence slowing down the efficiency with time. This is in line with Pu et al. (2021) who reported a 9.14% reduction in the AIV of the RA after carbonation treatment at a 20% CO₂ concentration level for 7 days of carbonation.

Generally, the main reason behind the enhancement/ reduction of the AIV value of the RA after carbonation treatment is that the old ITZ was filled by the calcium carbonate that was produced during the carbonation treatment. Furthermore, the efficiency of accelerated carbonation treatment in enhancing the properties of the RA stems from the chemical reaction of CO₂ with the hydrated products within the adhered mortar on the RA surface. The pores and micro-cracks of the RA can be filled through the process of carbonation (Mistri et al., 2020). At the start of carbonation, the carbonation of Ca(OH)₂ starts first, and it is rate initially higher compared to that of C-S-H as it is shown in Equation 5.1. The reaction between CO₂ and C-S-H begins (Equation 5.2) with decalcification, in which the Ca²⁺ reacts within the interlayer with CO₃²⁻ (Borges et al., 2010).



Figure 5.4 demonstrates the effects of the different CO₂ concentration levels on the enhancement of the water absorption (WA) of the RA.

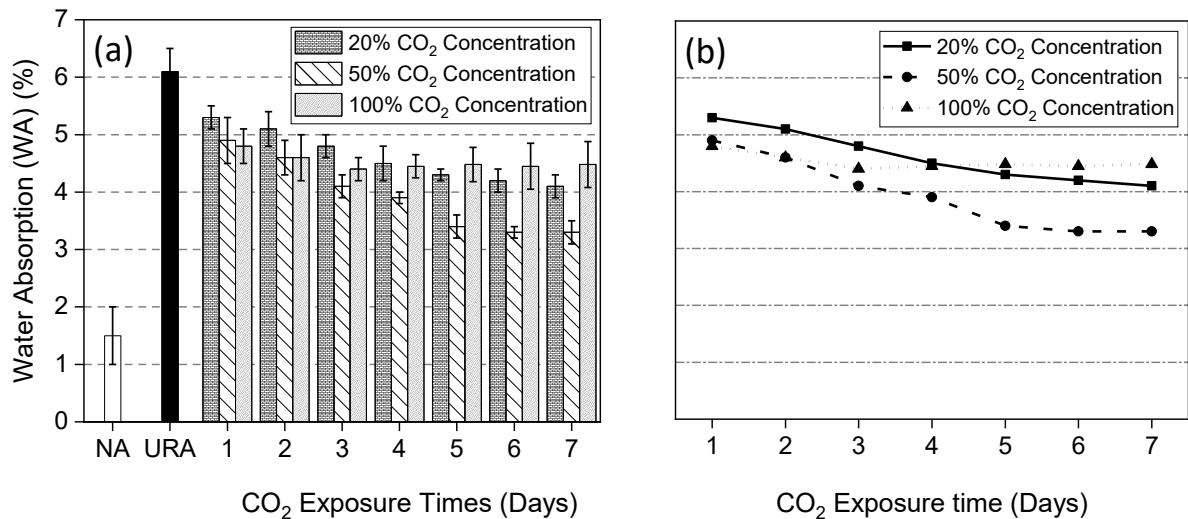


Figure 5.4: The impact of carbonation treatment at different concentration levels and CO₂ exposure times on the WA of RA shown in (a) clustered column chart, and (b) scatter chart, note: NA – natural aggregate, URA – untreated recycled aggregate

The RA treated at a 100% CO₂ concentration level achieved the highest reduction in the WA value from 6.1% to 4.4% during the first day of carbonation. The highest reduction in the WA was at a 50% CO₂ concentration level at 6 days of carbonation, the WA of the RA was reduced from 6.1% to 3.3%. At a 20% CO₂ concentration level and 7 days of carbonation, the WA was reduced from 6.1% to 4.1%. It can be concluded that the optimal CO₂ concentration level was 50% at an optimal CO₂ exposure time of 5 days. These results can be attributed to the reduction of the porosity of the cement paste after carbonation treatment, the refinement of pore structures, the transformation of portlandite into calcite, and the formation of amorphous carbonation products during accelerated carbonation treatment. A similar observation was reported by Zhang et al. (2015), Li (2014), and Ying et al. (2017), who reported a 22.6-40.3% enhancement in water absorption after carbonation treatment at various CO₂ concentration levels.

(ii) Cyclic limewater-accelerated carbonation treatment

Aggregates treated with three cyclic limewater-accelerated carbonation treatment achieved further and better improvement compared to the sole use of accelerated CO₂ at 100% concentration level for 3 days. The AIV of RA was reduced from 17% to 15.4% and water absorption was reduced from 6.1% to 3.9%. Aggregates treated with three cyclic limewater-accelerated carbonation treatment achieved further and better improvement compared to the sole use of accelerated CO₂ at 100% concentration level for 1 day. The AIV of RA was

reduced from 17% to 15.4% and water absorption was reduced from 6.1% to 3.9%. This is mainly due to the introduction of limewater pre-soaking technique resulting in additional carbonatable compounds into the pores of the RA, thus leading to more CO₂ uptake and more calcium carbonate precipitates, hence, resulting in a denser microstructure of the adhered mortar on the RA surface (Zhan et al., 2018). These findings are in consistent with the previous finding of Zhan et al. (2017), who observed that carbonated RA achieved 44% enhancement in AIV after pre-soaking followed by accelerated carbonation. Zhan et al. (2018) reported that 50% reduction in water absorption can be achieved when cyclic carbonation treatment is repeated for three cycles.

The following points can be summarised on the performance of carbonation treatment in enhancing the AIV and WA of RA:

- There are several key factors affecting the efficiency of the carbonation treatment, where the CO₂ concentration level and carbonation time are the more critical factors.
- Accelerated carbonation treatment at 50% CO₂ concentration level for six days of carbonation time achieved the best results. The optimal carbonation treatment conditions were found to be as 50% CO₂ concentration level at 6 days of carbonation.
- Recycled aggregates treated with three cyclic periods of pre-soaking in limewater followed by accelerated carbonation at 100% CO₂ concentration level for 24 hours, exhibited better improvement in AIV and WA compared to a sole use of accelerated carbonation treatment at the same carbonation conditions.

Soaking in sodium silicate-Silica fume solution (SS-SF)

Figure 5.5 shows RA after soaking in sodium silicate-silica fume solution. Figures 5.6 and 5.7 show the effects of soaking RA in different solution concentration and time on the AIV and the WA of the RA, respectively.

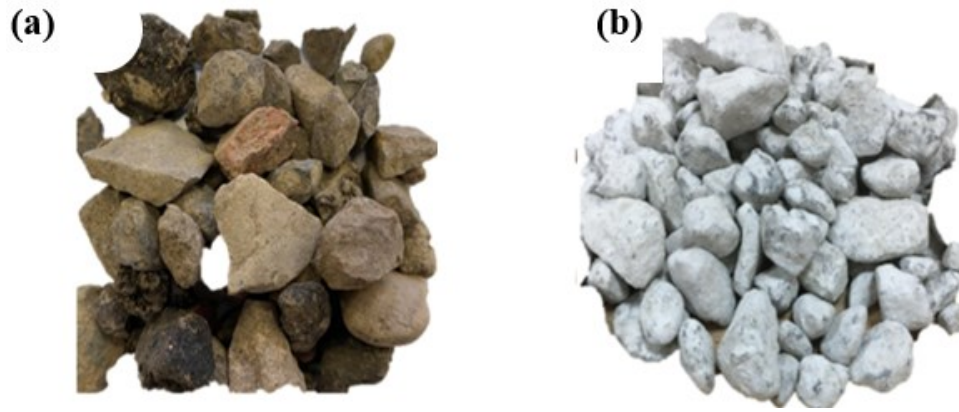


Figure 5.5:(a) untreated RA, (b) treated RA with soaking in sodium silicate-silica fume solution

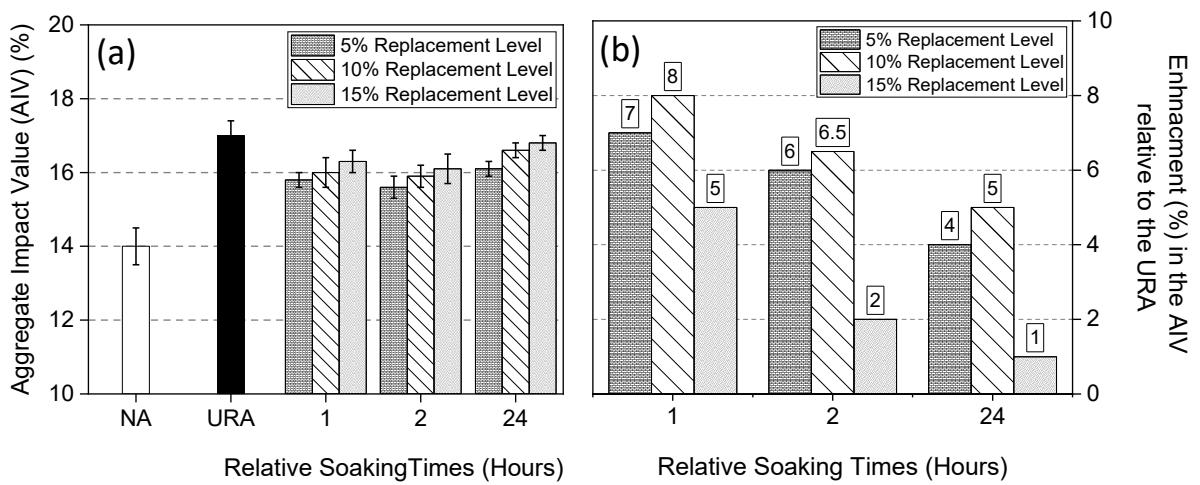


Figure 5.6: (a) effects of soaking the RA in sodium silicate-silica fume solution at various replacement levels and soaking times on the AIV of the RA, (b) enhancement values in the AIV relative to the untreated RA

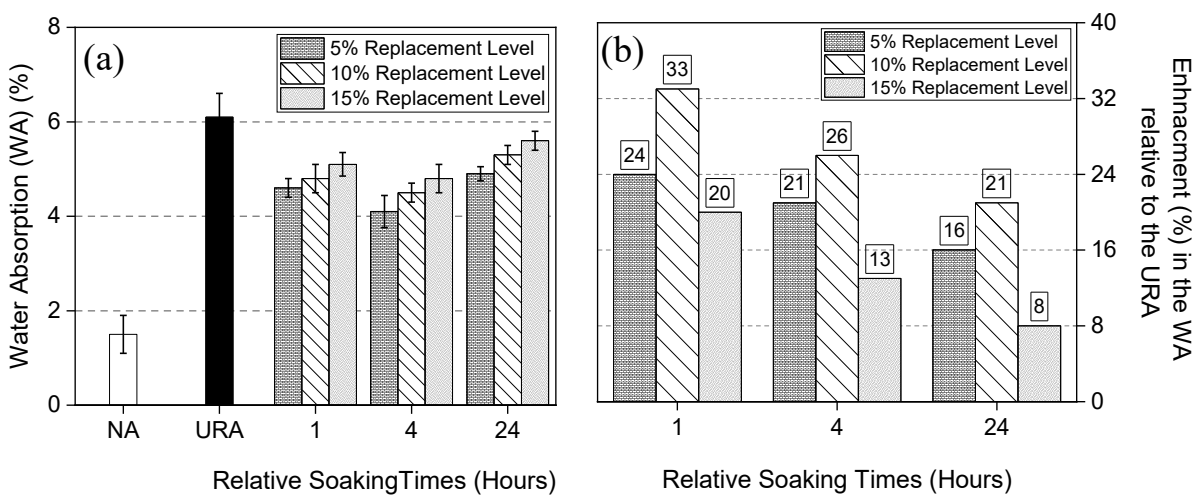


Figure 5.7: effects of soaking the RA in sodium silicate-Silica Fume solution at various replacement levels and soaking times on the WA of the RA, (b) enhancement values in the WA relative to the untreated RA

During the first 1 hour of soaking treatment, the AIV of the RA treated in the sodium silicate-silica fume solution with a 5% replacement level showed the highest reduction from 17% to 15.8%, whereas the AIV of the RA treated in the solution with 15% replacement level, recorded the lowest enhancement, the AIV was reduced from 17% to 16.3%. After 4 hours of soaking, an increase in the reduction trend of the AIV of the RA is evident for all the solutions with different replacement levels. The highest AIV enhancement was obtained by the solution with a 5% replacement level, the AIV was reduced from 17% to 15.6%. Further soaking times of up to 24 hours showed lower enhancements in the AIV of the RA compared to 1 hour and 4 hours soaking times.

A similar trend can be seen for the WA of the RA with a significant reduction in the WA after treating RA by soaking in sodium silicate – silica fume solution. At the first hour of soaking, a solution with a 5% replacement level showed the highest reduction in the WA, the WA of the RA treated in this solution was reduced from 6.1% to 4.6%. A significant increase in the reduction of the WA can be observed after 4 hours of soaking for all the solutions with different replacement levels. The highest reduction in the WA at this soaking time was obtained by the solution with a 5% replacement level, where the WA was significantly reduced from 6.1% to 4.1%. Further observations also indicated that, after 24 hours of soaking time, lower enhancement can be seen in the WA for all the prepared solutions with different sodium silicate-Silica Fume replacement levels, compared to 1 hour and 4 hours soaking times. It can be concluded that, among all the concentration solutions utilized, the solution with a 5% replacement level achieved the best enhancements in the AIV and the WA of the RA, whereas solutions with a higher replacement level of 15% achieved the lowest enhancement results. Among all the soaking times, soaking for 4 hours achieved the highest enhancements. Consequently, soaking in solution with a replacement level of 5% for 4 hours of soaking time is considered to be optimum.

Immersing RA in a pozzolanic solution can improve the microstructure and the engineering properties of the RA in two aspects; pozzolana acts as a micro-filler that fills in the pores and micro-cracks of RA, these materials will form C-S-H gel through reacting with CH crystals in RA that fill up the voids with RA. A thin layer called water repellent is formed by impregnating the RA in sodium silicate-silica fume solution for a certain time, resulting in filling the pores and the voids within the adhered mortar when. When RA is immersed in this

solution, both materials can react with the calcium hydroxide existing in the adhered mortar to form C-S-H gel, according to equation 5.3 (Yang et al., 2016):



Furthermore, further improvement can be achieved in this method, as a result of the pozzolanic reaction between silica fume and the $\text{Ca}(\text{OH})_2$ which produces secondary C-S-H gel, hence a stronger interfacial transition zone will be developed on the RA surface.

Soaking RA in sodium silicate-silica fume solution significantly enhanced the AIV and the WA of the RA. This may be ascribed to the thin film layer formed of sodium silicate and pozzolana particles on the surface of RA through consuming the CH product in the AM which in return made RA a denser structure by filling up and sealing the pores and cracks of RA. This is in line with the outcome of Shaban et al. (2019) study who stated that soaking RA in sodium silicate solution significantly reduced the WA of the RA. They added that this is attributed to the silicic acid that filled up the pores and voids of the RA surface along with the chemical reaction between the sodium silicate and CH that produced C-S-H gel which enhanced the bond between the adhered mortar and RA.

Among all the utilized concentration solutions, solutions with 5% concentration achieved the best performance, whereas solutions with a higher concentration of 15% achieved the lowest enhancement results. Among all the soaking periods of time, soaking for 4 hours achieved the highest enhancement values in terms of RA engineering properties. This might be because the pozzolan materials could not penetrate deeply into the surface of RA and efficiently strengthen it in the case of short soaking times (Shaban et al., 2019). Moreover, long soaking times i.e., 24 hours would result in removing the hydration products and eroding the surface of RA and thus lower enhancements to the AIV and WA of RA will be achieved (Ouyang et al., 2020). Higher concentration levels also are not beneficial to the enhancement of RA as the solution may be too thick to penetrate the surface of RA and it would also reduce the degree of hydration of the pozzolan products. Ouyang et al. (2020) stated that excessive treatment methods should be avoided, such as high concentration of the treatment solutions, and long soaking times, which could erode the surface of RA, leading to reducing the efficiency of the treatment employed.

This is in line with Yang et al. (2016) who soaked RA in water-glass (sodium silicate) solution with different concentrations of 3%, 5%, 8%, 10%, 20%, and 40% for 10 min, 1h, 2h, and 5h. Yang et al. (2016) found that the treated RA obtained enhanced water absorption by 36% when RA was soaked in water-glass solution with 40% concentration for 1 hour, whereas soaking the RA in water-glass solution with 5% for 1 hour achieved the best performance in terms of concrete 3-, 7-, and 28-day compressive strength at about 22%, 28% and 29% enhanced performance respectively.

Bui et al. (2018) soaked RA in three main solutions; solution type G, solution type S, and sodium silicate SS. Solution type G included; GFA (fly ash + NaSiO_3 + NaOH), GSF (silica fume + NaSiO_3 + NaOH), GMK (metakaolin + Na_2SiO_3 + NaOH). Solution type S included; SFA (fly ash + Na_2SiO_3), SSF (Silica fume + Na_2SiO_3), and SMK (metakaolin + Na_2SiO_3). Solution type SS was sodium silicate. RA was soaked for 24 hours and at three different solution concentrations 10%, 20%, and 30%. Among all the treatment solutions, RA soaked with sodium silicate (SS) solution at 30% concentration achieved the best performance in terms of water absorption, RA attained 34% enhanced water absorption. Bui et al. (2018) stated that, among all the utilized solutions, the combination between silica fume and sodium silicate achieved the best 28-day compressive strength, whereas concrete produced with treated RA in silica fume-sodium silicate solution achieved 36% enhancement.

The overall performance of soaking RA in sodium silicate-silica fume solution treatment on enhancing the AIV and WA of RA can be concluded as follows:

- Soaking RA in in sodium silicate-silica fume solution with 5% replacement level for 4 hrs soaking time was found to be optimal.
- Treated RA by soaking in sodium silicate-silica fume solution reduced the WA and AIV of RA from 6.1% to 4.1% and from 17% to 15.6%, respectively.

Coating with cement or cement-silica fume slurry

The RA was treated by coating with cement and cement-silica fume by two different methods, (i) Coating of the individual size fractions of recycled aggregate separately with cement and cement/silica fume slurry, and (ii) Coating of the total combined gradation of recycled aggregate with cement and cement-silica fume slurry. The coating of the individual particle size fraction involved three coating thicknesses, 0.1mm, 0.2mm, and 0.3mm, the coating was

carried out by Portland cement slurry or by Portland cement-silica fume slurry. Figure 5.8 shows RA before and after coating with cement-silica fume slurry.

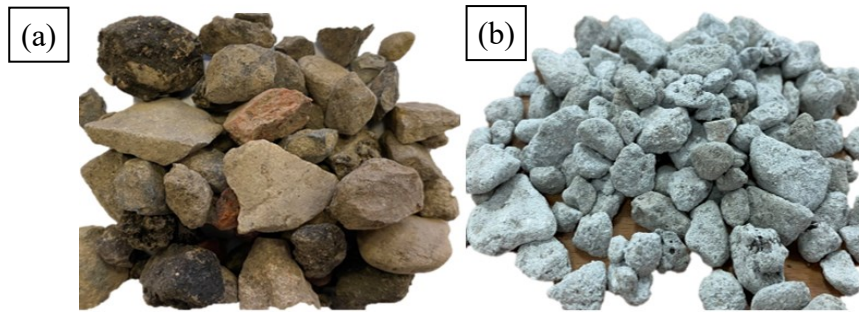


Figure 5.8: (a) untreated RA, (b) treated RA with coating with cement-silica fume slurry

Figures 5.9 and 5.10 show the effects of coating the individual particle size fraction with cement slurry or cement-silica fume slurry, along with the effects of coating the total combined gradation of RA, on the AIV and the WA of the RA, respectively.

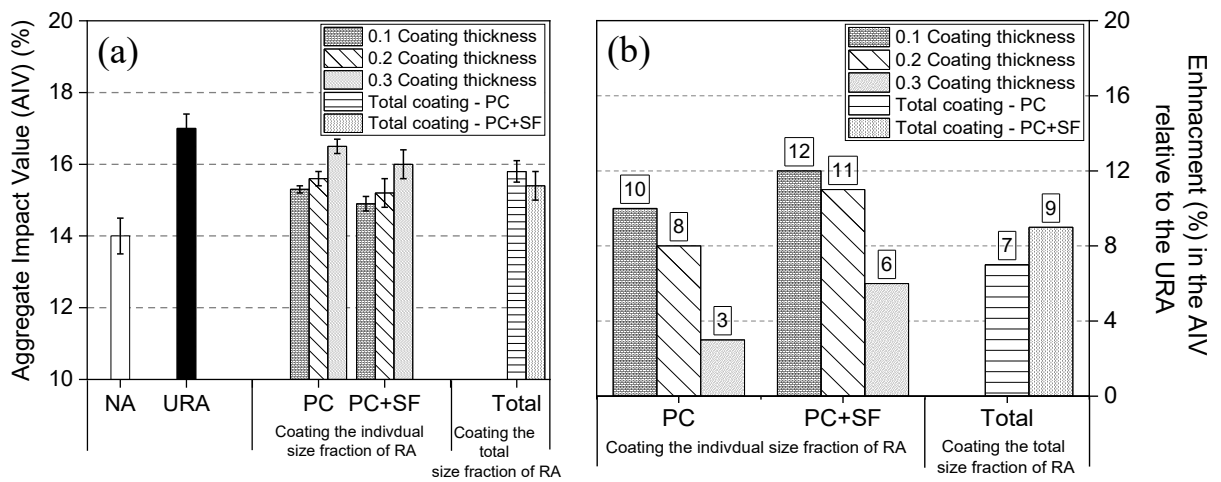


Figure 5.9: (a) the effects of the different coating with cement and/or cement-SF methods on the AIV of the RA, (b) enhancement values in the AIV relative to the untreated RA

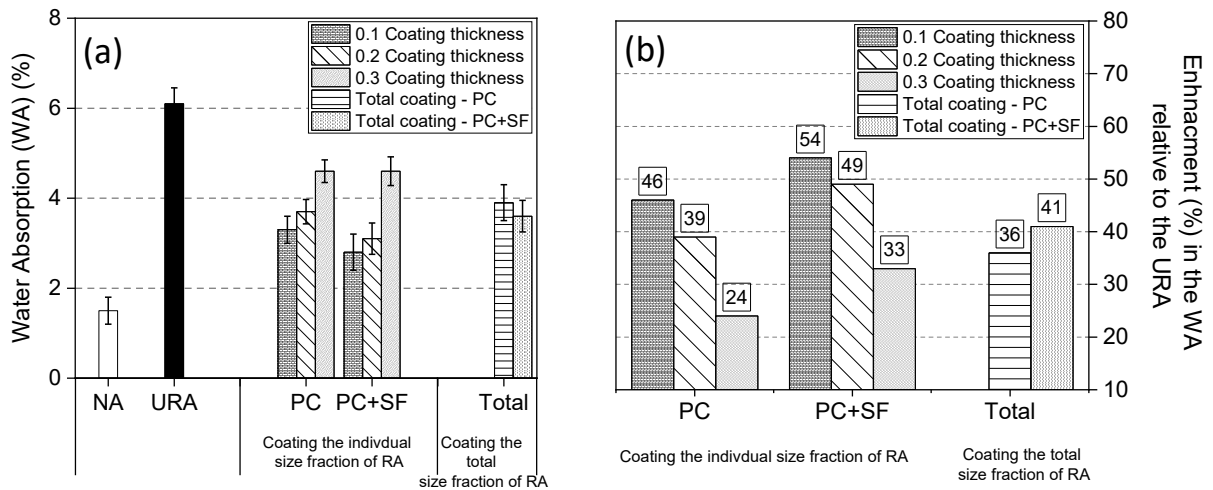


Figure 5.10: (a) the effects of the different coating with cement and/or cement-SF methods on the WA of the RA, (b) enhancement values in the WA relative to the untreated RA

As can be seen from Figures 5.9 and 5.10, among all the coating thicknesses and coating materials, the treated RA with cement-silica fume slurry and coating thickness of 0.1mm recorded the highest reduction in the AIV and the WA, from 17% to 14.9%, and from 6.1% to 2.8%, respectively, compared to the other coating thicknesses. In addition to that, via visual inspection, coating RA particles smaller than 10 mm with a thickness of 0.3 mm, results in getting the RA cemented to each other and hence, they cannot be separated easily. According to Lee et al. (2011), when the coating paste around RA of 4.75mm size exceeds the designated theoretical thickness of 0.65 mm, then the coating paste may get cemented into lumps and cannot be separated easily, while the coating paste cannot entirely coat the surface of RA when the coating paste around the surface of RA of 12.5 mm size is less than 0.25 mm of the coating thickness.

Accordingly, based on these results, it can be concluded that 0.1mm is the optimum coating thickness to coat the individual RA grain sizes. This may be attributed to the small coating thickness resulting in filling the pores/cracks and thus leading to strengthening the weak RA particles. These findings are in line with Kareem et al. (2018) who found that coating the individual RA at 0.1 mm coating thickness with cement slurry resulted in better AIV by 7% enhancement compared to 0.05, 0.2, and 0.4 mm coating thicknesses. RA treated with cement-silica fume slurry showed better AIV and WA compared to the ones treated with cement slurry only, this may be attributed to the additional produced C-S-H gel which effectively filled the pores and voids in the weak adhered mortar (Lee et al., 2011).

Coating the total combined RA with cement slurry only reduced the AIV and WA of RA from 17% to 15.8% and from 6.1% to 3.9%, respectively. Whereas coating with cement and silica fume slurry offered slightly higher reduction of in the AIV from 17% to 15.4% and from 6.1% to 3.6% for WA. Overall, the results of the effects of different coating methods on the AIV and the WA of the RA indicated significant enhancement in the AIV and the WA for all the coated RA with cement and/or cement-silica fume slurry regardless of the coating method.

It was also found that the increase in coating thickness layer results in adverse effects on the AIV and the WA. The RA treated with cement-silica fume slurry showed better enhancements in the AIV and the WA compared to the ones treated with cement slurry only. The method of coating the RA particle size fraction individually performed better in enhancing the AIV and the WA of the RA, in comparison with the method of coating the total gradation of the RA. This is in line with Zhihui et al. (2013) who reported a 9% enhancement in AIV and a 39% enhancement in the WA of RA after coating the total combined RA size fraction with cement slurry.

Overall, this surface treatment method aims at altering the micro-surface structure of RA and then strengthen it by the touch-up of new materials (i.e., cement, silica fume, fly ash) and coating of the older material via patching and bonding of the smaller pores on the surface of RA to enhance its quality and properties, hence, reinforcing the bonding force and mechanical strength of the interface between coating materials and RA (Lee et al., 2011). It can also be added that the basic premise of this treatment is to coat RA with hydrated cement film which is thick enough to act as a shield on the surface of RA.

The overall effects of coating RA with cement slurry or cement-silica fume slurry treatment can be summarised as follows:

- Coating the individual size fraction of RA achieved better enhancement in the AIV and the WA compared with coating the whole size fraction of RA.
- Among all the coating thicknesses, coating RA at 0.1 mm coating thickness obtained the highest enhancement values.
- Coating RA with cement and silica fume slurry was observed to provide better enhancement in the AIV and the WA, compared to coating RA with only cement slurry.

- Coating the individual size fraction of RA with cement/silica fume slurry at 0.1mm coating thickness led to the best enhancements of 12% and 54% in the AIV and the WA, respectively.

Soaking RA in different cement-pozzolan solutions

Figure 5.11 shows RA after soaking in different cement-pozzolan solutions. The results shown in Figures 5.12 and 5.13 show the effects of soaking RA in different cement-pozzolan solutions on the AIV and WA of RA, respectively.

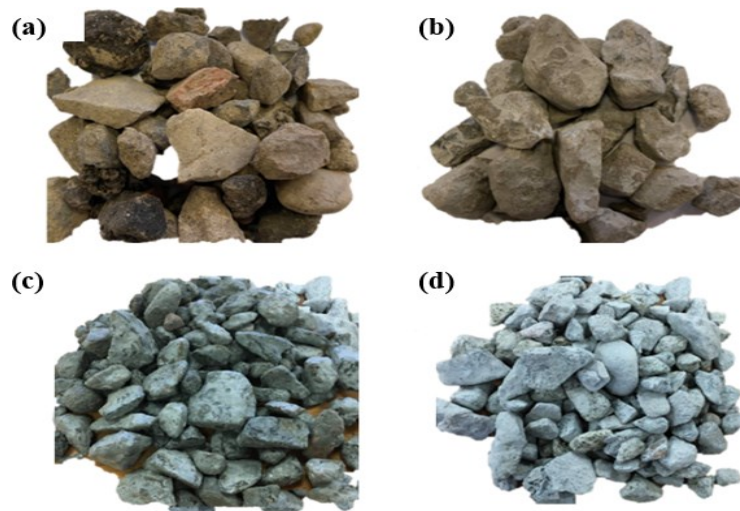


Figure 5.11: (a) untreated RA (URA), (b) treated RA with soaking in PC-PFA+SF solution, (c) treated RA with soaking in PC-PFA+MK, (d) treated RA with soaking in PC-SF+MK

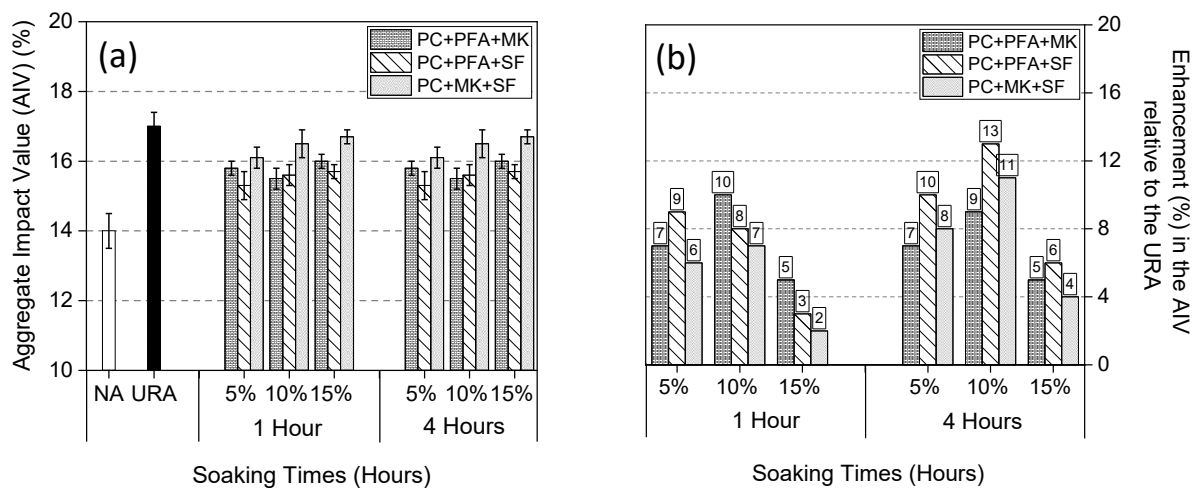


Figure 5.12: (a) the effects of different soaking solutions at different replacement levels and soaking times on the AIV of the RA, (b) enhancement values in the AIV relative to the untreated RA

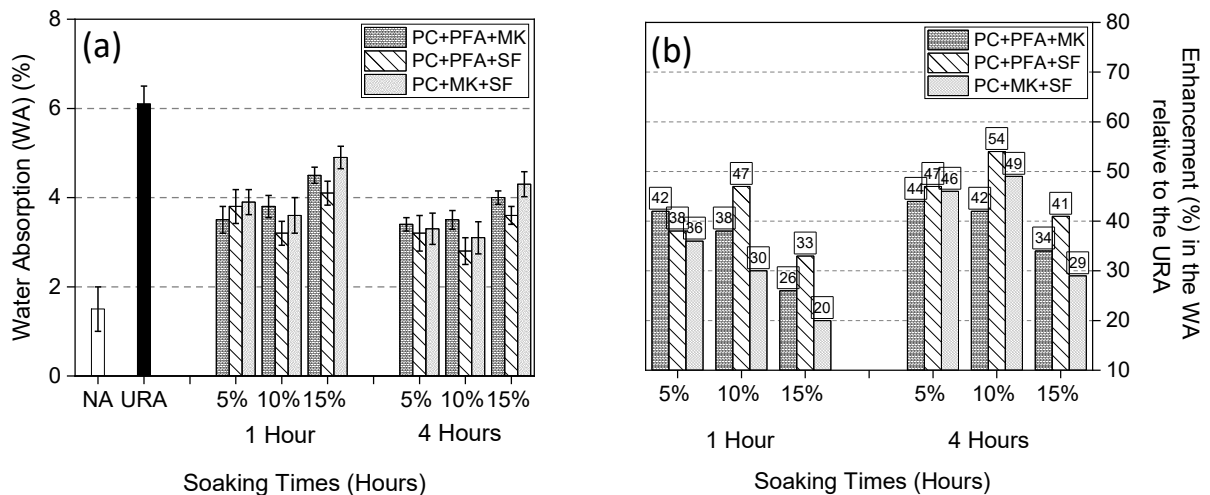


Figure 5.13: (a) the effects of different soaking solutions at different replacement levels and soaking times on the WA of the RA, (b) enhancement values in the WA relative to the untreated RA

At the first 1 hour of soaking time, the RA treated with the combination of PFA+MK solution with a 10% replacement level exhibited the highest reduction in the AIV, the AIV was reduced from 17% to 15.3%. Whereas the RA treated with the combination of PFA+SF solution with a 10% replacement level, recorded the highest reduction in the WA, the WA was reduced from 6.1% to 3.2%. These results are ascribed to the pozzolan thin layer formed on the RA surface after the treatment which filled the pores and the micro-cracks of the RA.

Further soaking time of the RA for up to 4 hours resulted in better enhancement in the AIV and the WA of the RA regardless of the replacement level and combination of materials, compared to 1 hour of soaking. This might be because the pozzolanic materials need a longer time to deeply penetrate the adhered mortar and efficiently strengthen it. This finding is in line with Shaban et al. (2019) who reported a 51.4% reduction in water absorption of RA after soaking in pozzolan solution. Li et al. (2009) examined the effect of soaking of RA by pozzolanic powder (fly ash, silica fume, and GGBS), and found that the combination of Portland cement along with fly ash and silica fume is more efficient for high strength recycled aggregate concrete with better packing density and denser interfacial transition zone.

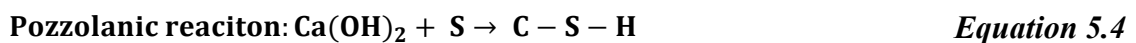
The highest reduction in the AIV and the WA was obtained by the PFA+SF solution at a 10% replacement level. The AIV was reduced from 17% to 14.7%, while the WA was reduced from 6.1% to 2.8%. This may be attested to the high reactivity of this pozzolan solution

(Mistri et al., 2020). A similar finding was observed by Shaban et al. (2019), who reported an approximate reduction of 40% in AIV after soaking RA in cement-pozzolan solutions.

Overall, it can be seen that soaking the RA in the solutions adopted for 4 hours provided better enhancements in the AIV and the WA of the RA regardless of solutions replacement levels, compared to the 1 hour of soaking time. Among all the replacement levels used, solutions with a 10% replacement level offered higher enhancements in the AIV and the WA of the RA, in comparison with solutions prepared with 5% and 15% replacement levels. In addition, the AIV and the WA of the RA soaked in the solutions prepared with a 15% replacement level exhibited lower enhancement values compared to solutions prepared with a 5% and 10% replacement levels regardless of the soaking time and the materials used. Consequently, it can be concluded that the optimal soaking time is 4 hours, and the optimal replacement level is 10%. Among all the combinations of materials used for solution preparation, the solution prepared with PFA+SF solution achieved somewhat the best results regardless of soaking time and replacement level.

The main principle behind soaking RA in cement-pozzolan treatment is to cover the RA surface with a thin layer of hydration products, hence strengthening RA engineering properties. After the treatment, a dense coated layer is formed around the RA surface after the reaction of the pozzolanic materials with the Ca(OH)_2 in the adhered mortar.

According to Singh et al. (2013), the additional hydrated calcium silicate (C-S-H) gel fills the pores and voids of the adhered mortar as shown in Equation 5.4. The incorporation of cement in the solutions is important for the treatment because it releases additional (C-S-H) gel and Ca(OH)_2 during hydration, as given in Equation 5.5.



This additional production of C-S-H gel efficiently fills the voids and pores of the weak adhered mortar, resulting in a much denser microstructure of RA. Singh et al. (2013) stated that particle size, the content of calcium hydroxide in the adhered mortar, the alkalinity of pore solution, and the reactivity of the pozzolanic materials are the main factors affecting the efficiency of the pozzolan solution treatment. The overall performance of soaking RA in

cement-pozzolan solution treatment in enhancing the AIV and WA of RA can be concluded in the following points:

- Soaking RA in 10% replacement level for 4hrs soaking time was found to be optimal.
- Soaking RA in Portland cement-PFA+SF solution obtained the best reduction in the AIV and WA.

5.2 Effects of Regime C Batching Techniques on Properties of RAC

Untreated RA was incorporated in concrete mixtures at certain mixing proportions given in Chapter 4, Section 4.4 and mixed via 5 different batching techniques. Four different batching techniques were utilised to produce concrete mixtures, sand enveloped mixing approach (SEMA), mortar mixing approach (MMA), two-stage mixing approach (TSMA), and stone enveloped with pozzolanic powder (SEPP). SEPP batching technique involved two pozzolanic powder, Silica Fume (SF), and Ground Granulated Blast-furnace Slag (GGBS), hence they were labelled as SEPP_{SF} and SEPP_{GGBS}. Another two mixtures were also included and mixed via normal/conventional mixing method, natural aggregate concrete (NAC1/1st control) and untreated recycled aggregate concrete (RAC2/2nd control). The effects of the different batching techniques used were evaluated by testing slump, density, and compressive strength, and the results were compared to the 1st control and the 2nd control mixtures.

5.2.1 Consistency – slump of fresh RAC with batching techniques

The effects of the different utilised batching techniques on the consistency (slump) of the developed concrete mixtures are given in Figure 5.14. As was expected, NAC1 mixture achieved the highest slump value of 70 mm, whereas RAC2 attained the lowest slump of 30 mm. These results are in line with results of Verian et al. (2018) and Lotfi et al. (2014) who reported significant reduction in consistency of RAC compared to NAC at the same mix composition. This reduction in slump of the RAC2 mixture is ascribed to the rougher surface and irregular shape of RA, and the higher absorption capacity of RA (Kurda et al., 2017).

Observations also indicate that all the utilised batching techniques provided improvements in slump values. The best performed batching technique was recorded for stone enveloped with pozzolanic powder (SEPP_{SF}) mix, with 100% increase in slump value. This can be ascribed to the coated thin layer formed of silica fume powder around the RA surface during mixing, which resulted in hampering the water absorption behaviour of RA, hence the workability was

enhanced (Li et al., 2009). The observed high improvement in slump value of the mix SEPP_{SF} is in line with the study carried out by Li et al. (2009), which suggest that the inclusion of mineral admixtures in mixing of RAC intends to produce a tighter and denser interfacial transition zone (ITZ) and hampers the water absorption behaviour of RA via the developed thin coated film which in return governs the improvement in workability compared to the non-pozzolanic mixtures.

The second best performed batching technique was the SEMA mixture. SEMA managed to increase the slump from 30mm to 55mm. The SEMA mixing procedure involved mixing sand, cement, and three quarter of the total mixing water prior to the addition of RA, hence allowing the sand particle to get mixed more readily with cement and enough water for hydration, and ultimately preventing RA from absorbing the effective mixing water. These results are in line with Liang et al. (2015), who studied the influence of three batching techniques (MMA, SEMA, TSMA) on the mechanical properties of RAC. They reported 125 mm, 150 mm, and 75 mm slump value for MMA, SEMA, and TSMA mixtures, respectively.

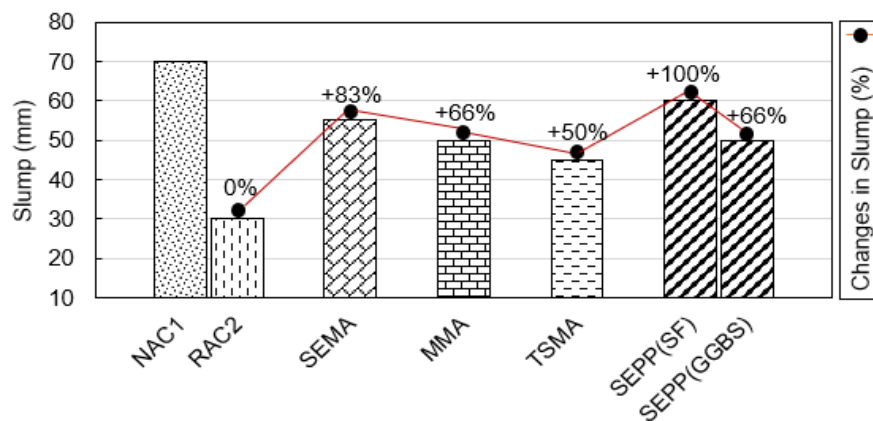


Figure 5.14: The effects of the different batching techniques on consistency of the RAC

Overall, the results of the slump tests indicate that the slump of NAC1 mixture falls in S2 class in accordance with BS EN 206:2013+A2:2021, while the mix with 100% untreated RA and no utilised batching technique (RAC2) was classed as S1 dry mix. Close observation shows that, all the batching techniques utilised managed to change the slump class of the RAC2 mix from S1 to S2. This suggests that the poor workability of RAC can be overcome via the utilisation of batching techniques. It should be noted that all the concrete mixtures showed true slump shape during performing of the slump test. Generally, the results of the slump tests indicated that the NAC1 is a S2 Standard mix, while the RAC2 was classed as a

S1 Dry Mix, in accordance with BS EN 12350-2. Close observation showed that, all the utilised batching techniques managed to change the slump class of the RAC2 mix from S1 to S2. This suggests that the poor workability of RAC can be overcome via the utilisation of the batching techniques.

5.2.2 Density of hardened RAC with batching techniques

The density of an average of three cubes of 100 mm³ size under the standard curing conditions of 7-, 14-, and 28-day was taken. The results were rounded to the nearest 10 kg/m³ and are presented in Table 5.1. The results from Table 5.1 show that, all the mixtures produced with 100% untreated RA exhibited lower density values regardless of curing age, compared to that of the 1st control mixture regardless of the batching technique utilised.

The density of RACs produced with different modified batching techniques were in the range of 2340 – 2370 kg/m³. The results also indicate that the measured densities of all the hydrated RAC specimens regardless of the batching technique utilised, fall within the specified density range for normal weight concrete in accordance with BS EN 206:2013+A2:2021. This may be attributed to the lower specific gravity and the adhered mortar of the RA which contributes to the lower density of RAC. These results are in line with Etxeberria et al. (2007) who stated that the density of RAC is lower than NAC by 3.3%.

Table 5.1: Results of density of hardened RAC produced with different batching techniques

Mix code	Density (kg/m ³)		
	7 days	14 days	28 days
NAC1 (1st control)	2390	2410	2410
RAC2 (2nd control)	2350	2360	2360
SEMA	2340	2340	2350
MMA	2350	2340	2350
T SMA	2330	2330	2340
SEPP_(SF)	2340	2360	2350
SEPP_(GGBS)	2360	2370	2370

5.2.3 Compressive strength of RAC with batching techniques

Figure 5.15 shows the results of the 7-, 14-, and 28-day compressive strength of the batching techniques used, in comparison with untreated RAC (RAC2) and natural aggregate concrete (NAC1), whilst Figure 5.16 demonstrates the effects of the batching techniques on the

compressive strength of the RAC at 7-, 14-, and 28-day. The results at each curing day are the average of 3 readings of concrete cubes per mixture.

It can be seen that the highest 7-, 14- and 28-day compressive strength was achieved by the NAC1 mix of 29.5, 33.5, and 39.2 MPa, respectively, across all the concrete mixtures, whereas the RAC2 mixture had considerably the lowest 7-, 14-, and 28-day compressive strength value of 19, 24.3, and 28.9 MPa, respectively, among all the test hardened concrete mixtures. This is mainly due to the poor quality of RAC resulted from the higher water absorption, high porosity, weak bonding of the interfacial transition zone between the RA and the new cement paste (Tam & Tam, 2008). These results are in agreement with the study of Etxeberria et al. (2007) who reported that the compressive strength of concrete produced with 100% RA is lower by 20% to 25% compared to natural aggregate concrete at 28-day produced with the same mix composition.

The results also indicate that the effects of the batching techniques on RAC strength enhancements are quite prominent. It can be seen all the batching techniques utilised offered various strength enhancements to the RAC with a marginal increase in 7-, 14-, and 28-days compressive strength compared to the untreated RAC2 mixtures. The highest increase in compressive strength at 7-, 14-, and 28-day was produced by SEPP_(SF) mixture, the strength was increased from 19 to 25.8 MPa (36% enhancement), 24.3 to 30.9 MPa, and 28.9 to 35.6 MPa, respectively. Among all the batching techniques concrete mixes, SEPP_(SF) mix was able to achieve a compressive strength of 35.6MPa at 28-day which is comparable to the control mix. These results can be explained by the work of Li et al. (2009) who demonstrated that, SEPP batching method utilises surface coating with pozzolanic powder prior to mixing, this process offers improvement in RAC strength due to the formed thin cement-pozzolan layer on the surface of the RA along with the effects of pozzolan which is well-known for its effectiveness in strength growth. Li et al. (2009) reported that Silica Fume is most effective in densifying the cementitious matrix than other pozzolanic materials due to the filling effects and wider distribution of its particles. The incorporation of Silica Fume in surface coating of recycled aggregate prior to SEPP batching technique contributes significantly towards the higher strength development of the RAC because SF is more prone to obtain a maximum packing density.

SEPP_(GGBS) and SEMA mixtures experienced slightly lower strength enhancement at 7-, 14-, and 28-day compared to SEPP_(SF) mix. Liang et al. (2015) reported that, the strength

improvement in the MMA mixture and SEMA mixture is mainly governed by the enhancement of the quality of mortar. The concept of MMA batching technique is preventing the adhered mortar on the surface of the RA to consume the effective mixing water, hence sufficient water will be available for cement hydration which in return leads to an enhancement in compressive strength. Liang et al. (2015) also added, the beneficial of utilising SEMA method is it mixes sand, cement and three quarters of the total mixing water prior to the incorporation of RA which allow the sand particles to mix more readily with cement and water and hence the RA will absorb less water.

Tam et al. (2007) stated that in during the first stage of mixing in TSMA method, a thin layer of cement slurry on RA surface is developed which leads to filling up the micro-cracks and voids in the adhered mortar of the RA. The strength improvement comes in the crystallisation mixing where the added remaining water contributes to the completion of the hydration process of cement and hence improving the strength of the concrete mixture (Elhakam et al., 2012).

Overall, it can be observed that, a similar trend of compressive strength enhancements occurred for all the batching technique concrete mixtures at 7-, 14- and 28-day. This shows that the effects of the batching techniques on strength enhancement of RAC is significant. It can be concluded that all the batching techniques managed to change the strength class of RAC by increasing the 28-day compressive strength of RAC up to a minimum of 30 MPa, and hence all are classified as concretes suitable for structural applications.

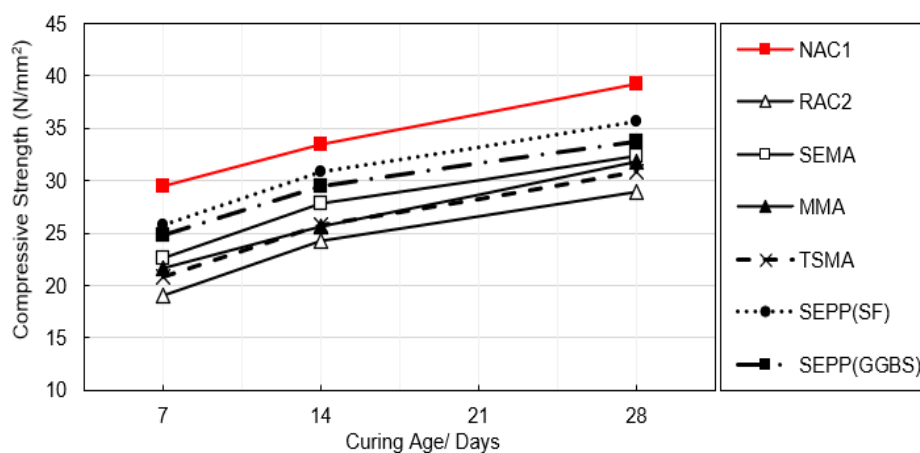


Figure 5.15: Development of compressive strength of batching technique concrete mixtures

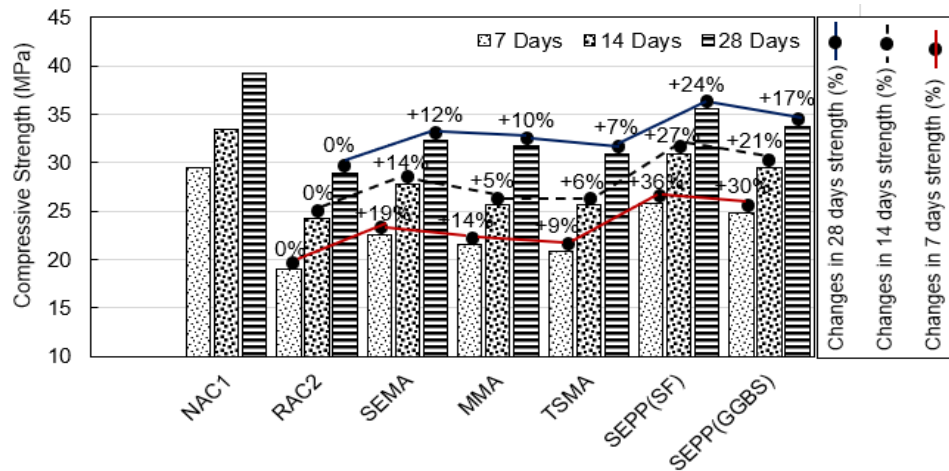


Figure 5.16: The effects of batching techniques on strength of RAC at different curing ages

According to Li et al. (2009), the utilisation of batching techniques can improve the strength of the RAC due to the following possible aspects; (i) it improves the bond behaviour between the new cement paste and the existing adhered mortar, (ii) it seals the porous voids in the adhered mortar, hence it saves the mixing water to be absorbed by the RA and gives sufficient amount of water for hydration reaction, (iii) the relatively lower water to binder ratio in the coating slurry contributes significantly towards a denser interfacial transition zone and thus higher strength of RAC, (iv) inner bleeding of water within the RAC mixture is prevented due to the formation of the pozzolanic coated layer on RA surface that acts as a barrier.

The overall performance of the batching techniques in enhancing the compressive strength of RAC can be summarised as follow:

- All the batching techniques utilised managed to enhance the compressive strength and slump of RAC.
- Among all the batching techniques used, SEPP_{SF} and SEMA methods achieved the highest enhancement in the 28-day compressive strength of 26% and 22%, at 0.5 w/c ratio, respectively.

5.3 Initial Criteria Matrix for Selection of Treatment & Batching Techniques

In order to select the best treatment methods to undergo further investigations, a selection matrix was formulated as shown in Table 5.2. The selection matrix was based on several criteria/aspects which included, property enhancement (efficiency), feasibility, cost-effectiveness, application time, simplicity, and environmental impact. Each criteria was given

a score of 10 points except for the efficiency criteria which was given 20 points in weight score. The score points-based system was established as an indicator to better describe the drawback/effect of each treatment on the different given criteria/aspect, the higher the scored number the better the treatment, with 10 points being the highest and 0 point the lowest. The total score of each treatment was given as a maximum of 70 points, hence the selected treatments were selected based on the highest collected total scored points out of 70 points. The following description of each criteria was provided to give a better understanding on the criteria utilised and how the overall selection matrix works.

1. **Property enhancement/ efficiency:** this is the major key aspect that was used for the selection of the best treatment method. The ability of each treatment method utilised in enhancing the RA AIV and WA (Regime A and Regime B), and the strength of RACs (Regime C only), was utilised as an indicator to reflect on the efficiency of the treatment utilised. Accordingly, the scored points for a given treatment shows how efficient is this treatment in providing enhancement to a given engineering property, the higher the scored points the better the treatment. This criteria was given a total of 20 points weight since it is the most important aspect.

2. **Feasibility:** this criteria describes how easy or difficult the application of a given treatment. The 0 to 10 points here shows how doable to perform this treatment, with 10 points being the most feasible and 0 points shows the impracticality of the treatment. In addition, feasibility criteria takes into consideration the feasibility of the application of a given treatment on bulk recycled aggregates and on site production.

3. **Cost-effectiveness:** cost efficiency here only include the cost of the application of the treatment and discard the total cost of the production of concrete. Accordingly, the higher the scored point for each treatment, the better the cost efficiency, and vice versa.

4. **Application time:** the duration of application of treatment whether it's a process or holding time for retrieving the treated RA. The higher the scored point, the better the treatment, or in other words, the shorter the time/ holding time of the application of the treatment is more desirable.

5. **Simplicity:** the simplicity of a given treatment is relatively similar to its feasibility, but it reflects more on how complicated the treatment to be performed, in terms of man power and the necessity for sophisticated advanced machine/ equipment. The more simple and straight forward the treatment the higher the scored point.

6. **Environmental impact:** this criteria is quite important as it reflects on the main concern and the reason why this study was carried out. Environmental friendly is another terms that has been constantly used throughout the literature to describe the impact of construction materials on the environment and carbon dioxide footprint emission to be exact. It is related to sustainability and the sustainable development of the construction industry. The environmental impact of each treatment was used to evaluate the impact of the application of each treatment on the environment in terms of its contribution to carbon dioxide footprint. The higher the scored point the more friendly of the application of a given treatment to the environment.

The treatments with highest scored points out of 70 points were selected based in their merits to undergo further investigations. Comparison in terms of scored points were measured firstly between Regime A and Regime B treatments since their efficiency were evaluated by testing their effects on enhancing the RA AIV and WA, whilst Regime C treatments were given scored points in comparison with each other since their efficiency were evaluated by testing their effects on enhancing the compressive strength of RAC. Accordingly, the selection matrix for group C treatments was given seperatly. Table 5.2 summarises the effects of Regime A and Regime B treatments on the AIV and the WA of RA, along with the effects of Regime C treatments on the compressive strength of RAC. The interpretation of each treatment method and their given score points in Table 5.4 is given in Table 5.3.

Based on the selection matrix in Table 5.4 and the points score system provided, the following treatments achieved the highest points in the efficiency criteria and in the total score points out of a maximum of 70 points:

1. Accelerated carbonation treatment: 54/70
2. Soaking in Portland cement-pulverised fuel ash + silica fume solution: 58/70
3. Sand enveloped mixing approach (SEMA): 66/70

These treatments were selected mainly based on their efficiency in enhancing the AIV and the WA of the RA (Regime B treatments) and in enhancing the compressive strength of RAC (Regime C methods) and secondly on their overall scored points out of 70. It is worth mentioning that soaking of RA in sodium silicate-silica fume solution achieved a total score of 56/70 and 17/20 in the efficiency criteria, nonetheless, this treatment may result in adverse effects in terms of the durability of RAC, as sodium silicate might introduce alkalis which

could increase the risk of alkali–silica reaction. Thus, it was removed out of the nomination treatments.

Although the stone enveloped with pozzolanic powder (SEPP_{SF}) achieved the highest score points of 18/20 across all the batching techniques in the efficiency criteria, it was removed since the addition of silica fume might be the reason behind its significant enhancement to the compressive strength of the RAC, hence, it was not possible to judge its overall performance as a batching technique compared to other batching techniques such as SEMA method.

Accordingly, the previous three treatment methods were selected for further investigations along with the following suggested combinations to be investigated too:

1. Soaking in cement-PFA+SF (SCP) + accelerated carbonation treatment (AC); SCP+AC
2. Soaking in cement-PFA+SF (SCP) + sand enveloped mixing approach (SE): SCP+SE
3. Accelerated carbonation treatment (AC) + sand enveloped mixing approach (SE): AC+SE
4. Soaking in cement-PFA+SF (SCP) + accelerated carbonation treatment (AC) + sand enveloped mixing approach (SE): SCP+AC+SE

These treatments and their combinations underwent investigations through evaluating their effects on mechanical properties of RAC, consistency, 7-and 28-day compressive strength at 0.4, 0.45, 0.5, 0.55, and 0.6 w/c ratios.

Table 5.2: Summary of the effects of Regime A and Regime B treatments on the AIV and the WA of the RA, along with the effects of Regime C treatments on the compressive strength of RAC

Treatment Regime	Treatment	Type of treatment	AIV value (%)	WA value (%)	Notes
Untreated RA	—	—	17	6.1	—
Regime A treatments	Self-healing	—	18	3.6	—
	Water washing	Water washing 1	16.5	3.7	Discarding any RA particle size < 4mm Keeping the same grading
		Water washing 2	16.7	5.1	
	Water saturation	Full saturation	18	6	—
Partial saturation		17	6.1	—	
Regime B treatments	Carbonation	Accelerted carbonation	15.2	3.4	Carbonating RA at 50% CO ₂ concentration level for 5 days of carbonation time
		Cyclic carbonation	15.4	3.9	—
	Soaking in SS/ SF solution	—	15.6	4.1	Soaking RA in sodium silicate-silica fume solution at 5% replacement level for 4hrs of soaking time
	Coating with Cement & cement-SF slurry	Coating of the individual particle size fraction	14.9	2.8	Coating with cement/silica fume slurry at 0.1 coating thickness
		Coating of the total combined particle sizes	15.4	3.6	Coating with cement-silica fume slurry
Soaking in cement - pozzolan solutions	Soaking in cement-PFA+SF solution	14.7	2.8	Soaking RA in cement/pulverized fuel ash and silica fume solution at 10% replacement level for 4hrs of soaking time	
Treatment Regime	Batching approach	Type of mixing approach	28-Day compressive strength (MPa)	Enhancement in the 28-day strength (%)	Notes
Untreated RAC	Conventional mixing approach	NMA	29.8	—	Normal Mixing approach
Regime C treatments	Sand enveloped mixing approach	SEMA	36.4	22	SEMA mixing approach
	Mortar mixing approach	MMA	34.8	17	MMA mixing approach
	Two-stage mixing approach	TSMA	33.7	13	TSMA mixing approach
	Stone enveloped with pozzolanic powder	SEPP _{SF}	37.6	26	Stone enveloped with silica fume powder mixing approach
		SEPP _{GGBS}	35.5	19	Stone enveloped with ground granulated blast-furnace powder mixing approach

Table 5.3: Selective analysis and the points-based system working mechanism

Treatment method	Type of the treatment	Efficiency	Feasibility	Cost- Efficiency	Application time	Simplicity	Environmental impact
Self – healing	—	Did not show any enhancement to the AIV	Only need water and curing tank	Only water is needed for the treatment	High time consuming	Straight forward treatment	Environmentally friendly
Water washing	Water washing 1	Did not show significant enhancement	Only need a mixer machine	Cost of the mixer machine	4 min	Straight forward treatment but needs higher size than 4mm	RA with smaller size than 4mm could be sent to landfill
	Water washing 2	Did not show significant enhancement	Only need a mixer machine	Cost of the mixer machine	4 mins	Simple treatment	—
Carbonation	Accelerated carbonation	Significant enhancement	Needs a special device to simulate the carbonation machine on site for mass production of carbonated RA	Cost of the carbonation device	4 to 5 holding days to achieve desirable results	Simple treatment	Environmentally friendly treatment due to the use of CO ₂ in the process of treatment
	Cyclic carbonation	Significant enhancement	Needs a special device and pre-soaking in limewater solution	Cost of limewater and the carbonation device	15 to 20 holding days	Relatively simple treatment	Use of limewater
Soaking in SS + SF solution	—	Significant enhancement	Only needs a curing tank	Cost of SF and SS	4 hrs	Simple straightforward treatment	Relatively environmentally friendly treatment
Soaking in PC/PFA+SF solution	—	Significant enhancement	Only needs a curing tank	Cost of materials	4 hrs	Simple treatment	The use of Portland cement
Coating with PC/SF slurry	Coating the individual RA	Significant enhancement	Coating the RA particle size individually might be a challenge for mass production	Cost of materials	7 days holding time	Simple treatment to an extent	The use of Portland cement
	Coating the total RA	Significant enhancement	Relatively feasible treatment	Cost of materials	7days holding time	Simple treatment	The use of Portland cement
Treatment method	Type of the treatment	Efficiency	Feasibility	Cost- Efficiency	Application time	Simplicity	Environmental impact
SEMA	—	Efficient method	Can be carried out anywhere	Cost efficient method	2-3mins mixing	Highly straightforward method	No impact on the environment
MMA	—	Efficient method	Can be carried out anywhere	Cost efficient method	2-3mins mixing	Highly straightforward method	No impact on the environment
TSMA	—	Efficient method	Can be carried out anywhere	Cost efficient method	2-3mins mixing	Highly straightforward method	No impact on the environment
SEPP	SEPP _{SF}	Efficient method	Can be carried out anywhere	Cost of SF	2-3mins mixing	Highly straightforward method	Energy consumption to produce SF
	SEPP _{GGBS}	Efficient method	Can be carried out anywhere	Cost of GGBS	2-3mins mixing	Highly straightforward method	Energy consumption of GGBS

Table 5.4: Selective analysis using selection matrix for the best treatments nominations from Regime A, Regime B, and Regime C treatments

Treatment method	Type of the treatment	Efficiency	Feasibility	Cost-Efficiency	Application time	Simplicity	Environmental impact	Total score
Self – healing	—	2/20	10/10	10/10	0/10	10/10	10/10	42/70
Water washing	Water washing 1	6/20	8/10	8/10	9/10	9/10	9/10	50/70
	Water washing 2	4/20	9/10	9/10	10/10	10/10	9/10	51/70
Carbonation	Accelerated carbonation	16/20	7/10	7/10	7/10	8/10	9/10	54/70
	Cyclic carbonation	14/20	5/10	6/10	2/10	7/10	6/10	40/70
Soaking in SS + SF solution	—	17/20	8/10	6/10	8/10	9/10	8/10	56/70
Soaking in PC/PFA+SF solution	—	18/20	8/10	6/10	8/10	9/10	9/10	58/70
Coating with PC/SF slurry	Coating the individual RA	17/20	3/10	4/10	4/10	7/10	7/10	42/70
	Coating the total RA	15/20	7/10	6/10	6/10	8/10	8/10	50/70
Treatment method	Type of the treatment	Efficiency	Feasibility	Cost-Efficiency	Application time	Simplicity	Environmental impact	Total score
SEMA	—	16/20	10/10	10/10	10/10	10/10	10/10	66/70
MMA	—	15/20	10/10	10/10	10/10	10/10	10/10	65/70
TSMA	—	14/20	10/10	10/10	10/10	10/10	10/10	64/70
SEPP	SEPP _{SF}	18/20	10/10	8/10	9/10	10/10	9/10	64/70
	SEPP _{GGBS}	15/20	10/10	7/10	9/10	10/10	9/10	60/70

Notes: SS - sodium silicate, SF - silica fume, PC - Portland cement, PFA - pulverised fuel ash, SEMA - sand enveloped mixing approach, MMA - mortar mixing approach, TSMA - two-stage mixing approach, SEPP - stone-enveloped with pozzolanic powder.

5.4 Effects of Treatment & Batching Techniques on Properties of RAC

This section presents the results of mechanical properties of various RAC mixtures produced with different selected treatment methods from Section 5.3 (sole treatments and combination of treatments) with 5 different water to cement ratios (i.e., 0.4, 0.45, 0.5, 0.55, and 0.6). The treatments investigated in this section were selected based on various aspects (see Chapter 6) using a selective analysis system in the 1st phase. The mechanical properties tested were workability, density, 7- and 28-day compressive strength. Three treatments were selected for further investigations, accelerated carbonation (AC), sand enveloped mixing approach (SE), and soaking in cement- SF+PFA (SCP). Four combinations of these treatments were also suggested for further investigations, AC+SE, SCP+AC, SCP+SE, and SCP+AC+SE.

5.4.1 Consistency - slump

The results for the consistency of the fresh RACs produced with various treatment methods at different water to cement ratios and measured through the slump test are given in Figure 5.17. Figure 5.18 shows the slump test for one of the concrete mixtures. Table 5.5 shows the assessment of consistency of the fresh RACs produced with the selected and suggested treatments, including slumps classes and shapes in accordance with BS EN 206:2013+A1:2016. The slump value observed for the NAC1 mix recorded the highest slump values across all the concrete mixes and regardless of the water to cement ratio used, whereas the RAC2 mix experienced the lowest slump values among all the fresh concrete mixes irrespective of water to cement ratio. This is mainly because of the porous nature of RA which reflects on its higher ability to absorb water compared to NA, and hence the slump values of the RAC2 mixes are lower than the NAC1 mixes.

This in line with Malesev et al. (2010) and Kou & Poon (2009), who reported higher slump loss for RAC compared with NAC. Kurda et al. (2017) stressed out that the reduced consistency of RAC is mainly ascribed to the higher water absorption capacity of RA, the rougher surfaces and more angularity of RA compared to NA. Nonetheless, the poor consistency of the RAC2 mixture at low w/c ratio of 0.4 was improved by the addition of superplasticiser, and this is because of the efficiency of superplasticiser in increasing the concrete workability. This is in line with Matias et al. (2013) who stated that the poor consistency of RAC can be overcome by the use of superplasticisers.

The designated treated RACs mixes, SCP, SE, AC, SCP+SE, SCP+AC, AC+SE, and SCP+AC+SE showed variations in slump values, depending on the treatment method used, and the design mix proportions. These treated RAC mixes showed consistency enhancement and higher slump values compared to RAC2 mix at all the different water to cement ratios.

The highest increase (enhancement) in slump value was observed with SCP+SE mix (soaking RA in cement-PFA+SF solution combined with mixing via sand enveloped mixing approach) across all the designated treated RAC mixes regardless of the w/c ratios, the synergetic effects of the combined treatments presented in SCP+SE mix increased the slump value by 33% (from 45mm to 60mm) at 0.4 water to cement ratios.

The triple combination of treatments presented in W040/SCP+AC+SE, W045/ SCP+AC+SE, W050/ SCP+AC+SE, W055/ SCP+AC+SE, and W060/ SCP+AC+SE RAC mixes, showed closed increase in slump values compared to the SCP+SE mixes. The AC mixture (sole use of accelerated carbonation of RA) showed little or no enhancement in the consistency of the fresh RAC in some cases, regardless of w/c ratios. The effects of the utilisation of superplasticiser (SP) in the mixes of 0.4 w/c ratio, can be observed in the consistency of W040/RAC2. The incorporation of SP managed to produce a S2 class of W040/RAC2.

The sole utilisation of the batching technique (SEMA) presented in W040/SE RAC mixtures, resulted in slightly higher enhancements in slump values, compared to the sole use of the selected soaking RA in cement-PFA+SF solution treatment (SCP) presented in W040/SCP.

Overall, it can be concluded that the poor consistency of untreated RAC can be overcome by the incorporation of either superplasticisers, or the treatments and batching techniques selected. The best performed treated RAC mixes in terms of consistency are the mixes with the combination of SCP+SE treatment. It should be mentioned that, whilst the mixing of the concrete and during performing of the slump tests, there was no segregation of concrete observed in any of the concrete mixes.

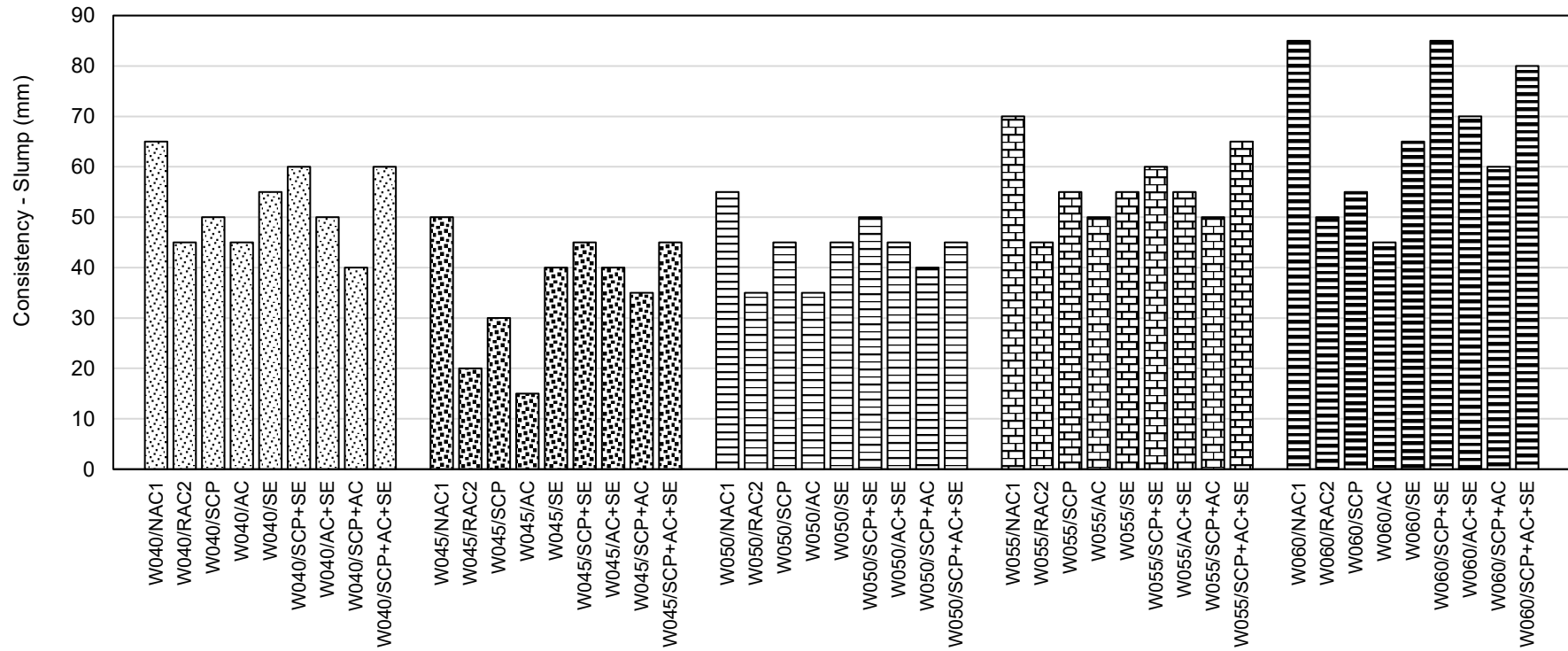


Figure 5.17: Results of slump test for the RACs produced with different treatment methods at various w/c ratios

Table 5.5: Consistency assessment and 28-day density of the RACs produced with different treatment methods at different w/c ratios

Designated mix	Consistency		Hardened concrete	Designated mix	Consistency		Hardened concrete
	Slump (mm)	Slump class	Density (kg/m ³)		Slump (mm)	Slump class	Density (kg/m ³)
W040/NAC1	65	S2	2420	W045/NAC1	50	S2	2410
W040/RAC2	45	S2	2340	W045/RAC2	20	S1	2350
W040/SCP	50	S2	2350	W045/SCP	30	S1	2340
W040/AC	45	S2	2350	W045/AC	15	S1	2360
W040/SE	55	S2	2340	W045/SE	40	S1	2330
W040/SCP+SE	60	S2	2340	W045/SCP+SE	45	S2	2340
W040/AC+SE	50	S2	2320	W045/AC+SE	40	S1	2350
W040/SCP+AC	40	S1	2350	W045/SCP+AC	35	S1	2340
W040/SCP+AC+SE	60	S2	2340	W045/SCP+AC+SE	45	S2	2350
W050/NAC1	55	S2	2400	W055/NAC1	70	S2	2380
W050/RAC2	35	S1	2360	W055/RAC2	45	S2	2280
W050/SCP	45	S2	2350	W055/SCP	55	S2	2290
W050/AC	35	S1	2330	W055/AC	50	S2	2270
W050/SE	45	S2	2320	W055/SE	55	S2	2230
W050/SCP+SE	50	S2	2340	W055/SCP+SE	60	S2	2340
W050/AC+SE	45	S2	2350	W055/AC+SE	55	S2	2250
W050/SCP+AC	40	S1	2350	W055/SCP+AC	50	S2	2230
W050/SCP+AC+SE	45	S2	2340	W055/SCP+AC+SE	65	S2	2270
W060/NAC1	85	S2	2350	W060/SCP+SE	85	S2	2220
W060/RAC2	50	S2	2270	W060/AC+SE	70	S2	2250
W060/SCP	55	S2	2290	W060/SCP+AC	60	S2	2280
W060/AC	45	S2	2250	W060/SCP+AC+SE	80	S2	2240
W060/SE	65	S2	2230				



Figure 5.18: Slump test for some of the concrete mixes

The improved slump achieved by the SCP treatment (soaking RA in cement-PFA+SF solution) mixes is mainly ascribed to the strengthened adhered mortar by the coated pozzolana layer/ film around the RA surface that filled up all the micro pores and cracks of the RA, and ultimately preventing the RA to absorb high amount of mixing water, thus the workability was improved. Li et al. (2009) examined the effects of coating the RA with different pozzolanic powder i.e., fly ash, silica fume, and GGBS. It was found that the combination of Portland cement combined with fly ash and silica fume achieved the best enhancements in terms of the mechanical properties of RAC due to the better packing density and denser formed ITZ due to the better packing of these pozzolan in terms of pores filling.

Similarly, the improved slump loss value for the AC (accelerated carbonation) mixes can be ascribed to the blocked pores by a dense coating layer with the hydration products mainly calcium carbonates due to the chemical reaction between the calcium hydroxide and the carbon dioxide from one side, and between the calcium silicate hydrates and carbon dioxide from another side. Consequently, the incorporation of carbonated RA into concrete can prevent the RA from absorbing the effective mixing water, and thus the consistency of RAC can be improved. This is in line with Li et al. (2017) study who stated that the inclusion of carbonated RA into concrete enhanced its fresh state properties.

The utilisation of sand enveloped mixing approach (SEMA) presented in SE mixes was able to enhance the workability of RAC because of the mixing process of SEMA method involves firstly mixing sand with water and cement to forms a mixture of cement paste and mortar, and then the RA is added to the mixture resulting in its pores and cracks filled with this premixed cement than water. Liang et al. (2015) proposed this mixing method, and reported that the consistency of RAC was enhanced significantly after using SEMA.

All the combined treatments achieved better consistency than the sole use of the aforementioned treatments, this shows that the coupled effects of combined treatments are more efficient in enhancing the properties of RA and RAC, compared to the sole use of treatments. This is in line with the results of Liang et al. (2015) who combined soaking of RA in cement-SF solution with different mixing techniques and concluded that, RAC produced with combination of soaking RA cement-SF+PFA solution followed by SEMA method achieved better mechanical properties compared to the sole use of either soaking in cement-SF+PFA or SEMA method.

5.4.2 Density of hardened concretes

The densities of 28-day hardened RACs produced with different treatments at various w/c ratios are given in Table 5.5. The density results presented are the arithmetic averages of three concrete cubic test specimens per mix.

The results show that, the highest density values were achieved by NAC1 across all the concrete mixes with range of densities from 2350 – 2420 kg/m³. All the concrete mixtures produced with 100% RA including concretes produced with treated RA and batching techniques and their combinations obtained variations in densities with a range from 2220 – 2360 kg/m³, but lower density values compared to NAC1 regardless of any treatments applied. Nonetheless, the results indicate that the measured densities of all the hydrated RAC specimens, fall within the specified density range for normal weight concrete in accordance with BS EN 206:2013+A2:2021.

The density results of the hardened concrete specimens showed variation in density values for all the treated RACs. The lower density of the RAC2 specimens compared to the NAC1 specimens can be ascribed to mainly the poor quality of RA given to the attached adhered mortar being porous in nature, the lower density and lower specific gravity of RA. This in line with Silva et al. (2018) who stated that the average hardened density of RAC is lower by 5% than that of the NAC. Fang et al. (2021) reported 7% lower density value for the RAC compared to that of the NAC.

5.4.3 Compressive strength

The compressive strength results of the different RAC mixtures with different treatment methods and batching techniques and their combinations investigated in the current research at various water to cement ratios, are given in Figure 5.19. Figure 5.20 shows the relative compressive strength of the different RACs mixtures with treatment methods and batching techniques compared to untreated RAC2 and NAC1. The compressive strength results per curing age are the arithmetic averages of three concrete cubic test specimens per mix. The compressive strength results given were for the strength development observed in the various water cured concrete cube specimens for 7- and 28-day, in comparison with untreated RAC2 and NAC1.

NAC1 mixtures showed the highest initial compressive strengths among all the concrete mixtures with a range of 18.4MPa to 38.9MPa, at different w/c ratios, whilst RAC2 mixtures produced the lowest early compressive strengths of a range of 9.1MPa to 29MPa. Among all the treated RAC mixes, the coupled effects of soaking in cement-PFA+SF and sand enveloped mixing approach labelled as SCP+SE showed the highest increase in the initial strength of treated RAC. For instance, the 7-day compressive strength of SCP+SE mixes increased from 29 to 36.7MPa, and from 18.2 to 26.8MPa (47% enhancement), at 0.4 and 0.5 w/c ratios, respectively.

The combination of soaking RA in cement-PFA+SF, accelerated carbonation, and sand enveloped mixing approach presented in SCP+AC+SE RAC mixes, showed slightly similar increase in the initial strength of RAC compared to SCP+SE mixes. The SCP+AC+SE mixes increased the initial compressive strength from 29 to 36MPa, 18.2 to 25.2MPa, at 0.4 and 0.5 w/c ratios, respectively. RAC mixes produced with soaking RA in cement/PFA+SF followed by accelerated carbonation (SCP+AC), showed better enhancements in the initial compressive strength of RAC compared to RAC mixes produced with RA treated by accelerated carbonation and mixed via sand enveloped mixing approach (AC+SE). SCP+AC mixes managed to enhance the 7-day strength of RAC by 18% and 37% at 0.4 and 0.5 w/c ratios, respectively.

Among all the treated RAC mixes via the sole use of treatments labelled as AC, SE, and SCP, RAC mixes produced with soaking RA in cement-PFA+SF prior to mixing presented in SCP mixes, showed the best enhancements in the 7-day compressive strength. SCP mixes increased the 7-day strength of RAC from 29 to 32.5MPa, and from 18.2 to 21.8MPa at 0.4 and 0.5 w/c ratios, respectively. The sole use of accelerated carbonation (AC) showed the lowest enhancements in the initial compressive strength compared to the sole use of sand enveloped mixing approach (SE) and the sole use of soaking in cement-PFA+SF (SCP), regardless of the w/c ratio used.

Similar observations/trends to the results of the 7-day compressive strength were noticed in the 28-day compressive strength for all the concrete mixes. After 28 days of water curing, NAC1 mixtures further developed the highest strengths across all the concrete mixtures. NAC1 developed strength with a range of 28.2MPa to 48.80MPa, at different w/c ratios. In contrast, RAC2 mixtures exhibited the lowest 28-day compressive strength gain amongst all the designated concrete mixes. The 28-day compressive strength results for untreated RAC

were with a range of 17.6MPa to 37.2MPa, at different w/c ratios. The synergetic effects of soaking RA in cement-PFA+SF prior to mixing and sand enveloped mixing approach labelled as SCP+SE showed the highest increase in the 28-day strength of RAC across all the treated RAC mixes. The 28-day compressive strength of SCP+SE mixes was increased from 37.2 to 46.3MPa and from 27.4 to 36.5MPa at 0.4 and 0.5 w/c ratios, respectively.

The triple combinations of soaking RA in cement-PFA+SF prior to mixing followed by accelerated carbonation, and mixed using sand enveloped mixing approach, presented in SCP+AC+SE RAC mixes, showed close increase in the 28-day compressive strength of RAC in comparison with SCP+SE mixes. The SCP+AC+SE RAC mixes were able to increase the 28 -days compressive strength from 37.2 to 44.1MPa and from 27.4 to 35.8MPa at 0.4 and 0.5 w/c ratios, respectively.

RAC mixes produced with soaking RA in cement-PFA+SF followed by accelerated carbonation (SCP+AC), showed slightly better enhancements/ developments in the 28-day compressive strength of RAC in comparison with RAC mixes produced with RA treated by the combinations of accelerated carbonation and sand enveloped mixing approach (AC+SE). The SCP+AC mixes increased the 28-day compressive strength of RAC by 17% and 25% at 0.4 and 0.5 w/c ratios, respectively. Among all the treated RAC mixes via the sole use of treatments labelled as AC, SE, and SCP, SCP mixes produced with the sole use of treating RA by soaking in cement-PFA+SF prior to mixing led to the best enhancements in the 28-day compressive strength. SCP mixes enhanced the 28-day compressive strength from 37.2 to 41MPa and from 27.4 to 32.6MPa at 0.4 and 0.5 w/c ratios, respectively.

Furthermore, the sole use of accelerated carbonation (AC) resulted in the lowest enhancements in the 28-day compressive strength compared to the sole use of sand enveloped mixing approach (SE) and the sole use of soaking in cement-PFA+SF (SCP), regardless of the w/c ratio used.

Overall, RAC2 mixtures and all the RAC mixtures produced with the different selected treatment methods (AC, SE, SCP, AC+SE, SCP+AC, SCP+SE, SCP+AC+AC) demonstrated similar trend to NAC1 in terms of strength development with an increase in curing age of the test specimens. Likewise, an increase in 7- and 28-day compressive strength occurred when the w/c ratio of the concrete mix was reduced for all the RAC1 mixes and the treated RACs

mixes specimens. This indicates that the RAC whether it was treated or untreated shows similar trend in strength development compared to natural aggregate concrete.

All the utilised treatment methods and the combination of them showed early and later strength enhancement in RAC mixes. The strength enhancement achieved by the applied selected treatment methods was more significant and obvious at the initial stage of compressive strength compared to the 28-day compressive strength. The best treatment method in terms of 7-day and 28-day strength enhancement was recorded for the combination of soaking RA in cement-PFA+SF and sand enveloped mixing approach (SCP+SE). All the selected treatment methods and the combination of them were able to increase the 28-day compressive strength of RAC from 27MPa to a minimum of 30MPa, at 0.5 w/c ratio, hence changing its classification to concrete suitable for structural application, except for the sole use of accelerated carbonation treatment (AC) mixes.

It can also be concluded that, the sole use of accelerated carbonation treatment (AC) did not show significant enhancement compared to the other treatments, as it needs to be combined with other treatments to work more efficiently. In other words, accelerated carbonation needs to be either combined with a batching approach i.e., sand enveloped mixing approach, or with a strengthening the adhered mortar method i.e., soaking in cement-pozzolan solution, in order to increase its efficacy, and hence better outcome within RAC engineering properties can be achieved. In conclusion, the lower compressive strength of RAC can be overcome by applying one of the selected treatments, that can enhance the properties of RAC and widen its application in the construction industry to be utilised in structural members.

Based on the results given so far, a 2nd phase of selective analysis (selection matrix) was carried for selecting the best performed treatments for further investigations including, mechanical performance (tensile splitting strength, flexural strength, and modulus of elasticity), durability performance (water absorption, resistance to freeze-thaw cycles, and sulphate attack), and microstructural investigations including SEM imaging and EDS chemical analysis. Accordingly, Chapter 6 will discuss in detail the process of the 1st phase and 2nd phase selective analysis for selecting the best treatment methods based on different criteria.

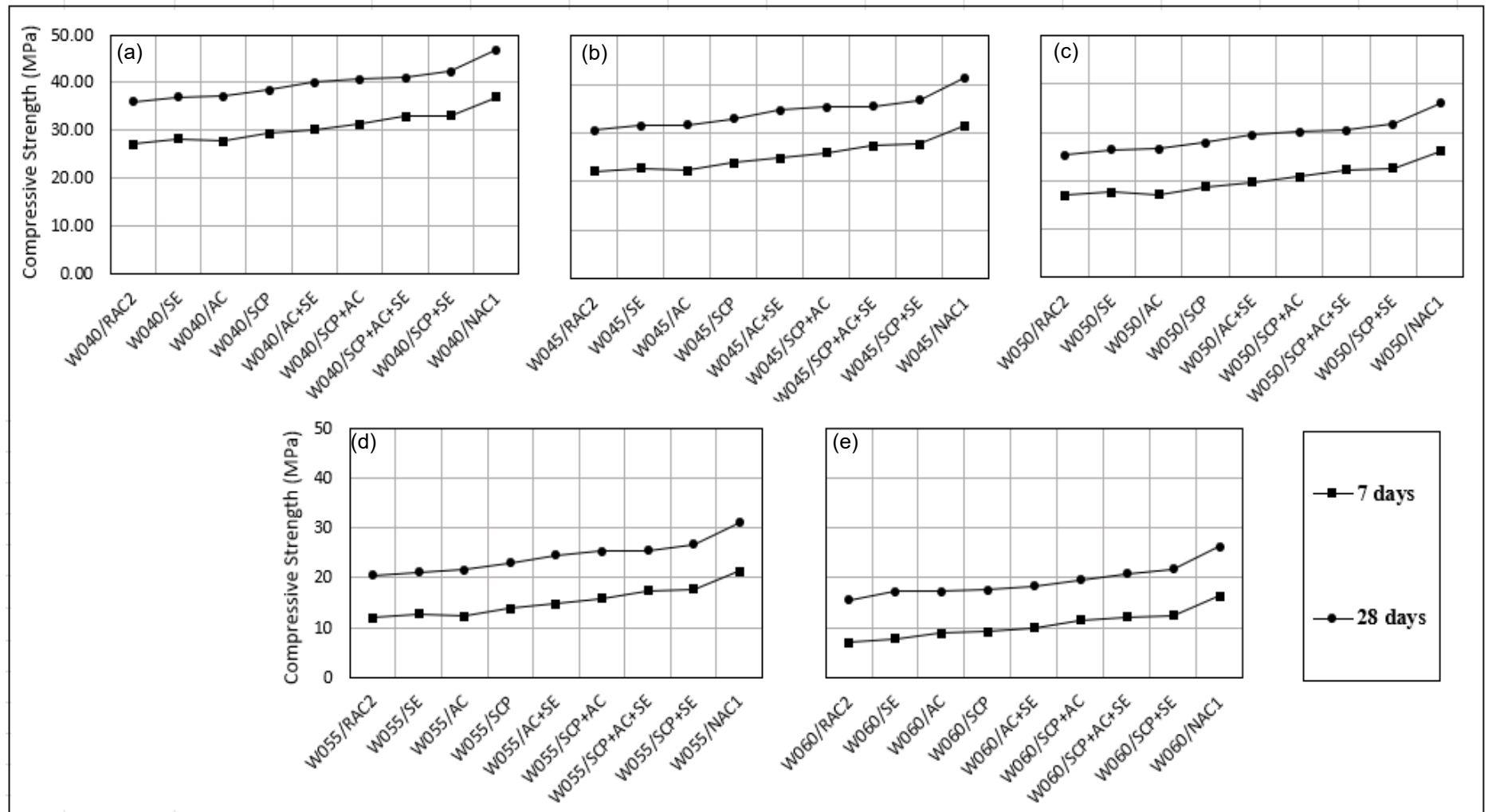


Figure 5.19: Strength development of the various RAC mixes produced with different selected treatments, in comparison with NAC1 at different w/c ratios: (a) w/c= 0.4, (b) w/c= 0.45, (c) w/c= 0.5, (d) w/c= 0.55, (e) w/c= 0.6

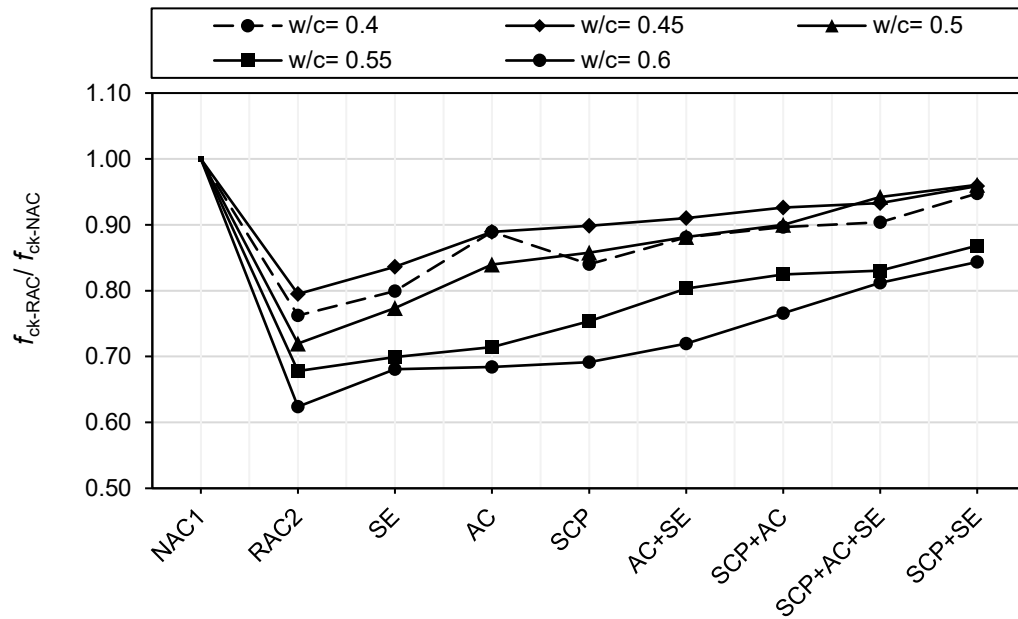


Figure 5.20: Effects of the different treatment methods on the relative compressive strength of concrete at 28-day

The results of the 7-day and 28-day compressive strength of the hydrated NAC1, untreated RAC2, and the RACs specimens with different treatments and batching techniques, at 0.4, 0.45, 0.5, 0.55, and 0.6 w/c ratio, showed variation in compressive strength values.

The untreated RAC2 specimens showed lower 7-day and 28-day compressive strength values compared to the NAC1 specimens, at the same designed mix parameters. This inferior compressive strength property of the RAC arises from various factors such as, the poor bonding between the adhered mortar and the RA from one side and between the RA and the cement paste within concrete matrix from another side, the presence of microcracks and fissures on the RA surface due to processing, and the porous nature of the adhered mortar, the higher water absorption capacity of RA, the different composition of RA, the poor engineering properties of RA, the presence of two ITZ (interfacial transition zone) in RAC, and the weak old ITZ, (Behera et al., 2014).

The literature shows that the widely reported reduction in compressive strength of the RAC compared to the NAC at 100% replacement level is up to 30% (Butler et al., 2011; Tam et al., 2005; Poon et al., 2004; Hansen & Narud, 1983; Xiao et al., 2012; Ravindraiah et al., 1987). Whilst some researchers reported reduction in compressive strength between 12% and up to 25% at 100% replacement level (Evangelista & de Brito, 2007; Rahal, 2007; Yang et al., 2008; Etzeberria et al., 2007; Sanchez et al., 2004). Other studies such as Bairagi et al. (1993),

reported 60% reduction in compressive strength of the RAC compared to the conventional concrete, whereas Katz (2003) concluded about 76% reduction in compressive strength of the RAC at 100% replacement level in comparison with the normal concrete. Nonetheless, these results obtained from the literature are incomparable to each other, but agreed on the lower compressive strength of the RAC compared to the NAC, this could be ascribed to the fact that the strength of the RAC may vary depending on various parameters such as but not limited to, the constituent of the RA used, the quality of the RA used, the w/c ratio deployed, the type of cement used, and the mix design used (Behera et al., 2014).

The results of the compressive strength also showed that, all the enhanced RACs with different treatments and batching techniques showed prominent enhancement in the 7-day strength and the 28-day compressive strength of the RAC, regardless of the used w/c ratio.

The enhancement in the 7-day and the 28-day compressive strength achieved by the AC (accelerated carbonation treatment) mixes can be ascribed to the enhanced hydration of the new cement at the interface due to the calcium carbonate formed on the carbonated RA surface as a result of the chemical reaction between the calcium hydroxide presented in the adhered mortar and the carbon dioxide from one side, and between the calcium aluminate hydrates and the carbon dioxide from other side (Matshei, et al., 2007). This is in line with the work of Fang et al. (2021) who reported 6.5% and 10% enhancement in the 7-day and 28-day compressive strength of the RAC, respectively, after carbonation treatment. Lu et al. (2019) concluded in his study that incorporating carbonated RA into RAC enhanced the 28-day and the 90-day compressive strength of RAC by 24.1% and 26.8%, respectively.

Lu pointed out that the treated RAC produced with carbonated RA exhibited denser ITZ, lower porosity, and less cracks due to the calcium carbonate and silica gel formed which filled in the pore structure of RAC, these factors contributed significantly towards better strength development of the treated RAC. Pu et al. (2021) pointed out the superior compressive strength of carbonated RAC to non-carbonated or untreated RAC is due to the lower amount of water being used in the case of carbonated RAC which led to reducing the effective water to cement ratio and hence, enhanced compressive strength. In addition, the enhanced AIV and density of carbonated RA compared to non-carbonated RA has also led to improved compressive strength. Shi et al. (2018) stressed out that the enhanced compressive strength of RAC produced with treated RA by accelerated carbonation might be attributed to the generated secondary calcium silicate by the production of silica gel which further produced calcium

silicate hydrates due to the chemical reaction between carbon dioxide and calcium silicate hydrates at later age of curing.

The enhanced 7-day and 28-day compressive strength of the SCP mixes (soaking RA in cement-PFA+SF solution treatment) can be ascribed to the strengthened the adhered mortar, enhanced particle density, enhanced AIV, improved water absorption of RA, and strengthened bond in the existing ITZ after this treatment. The enhanced compressive strength of the SCP mixes can further be explained as the adhered mortar on the RA surface consists of a significant amount of calcium hydroxide which can react with the pozzolana materials (SF and PFA) and form a dense coating layer around the RA surface, the formation of the additional calcium silicate hydrates and calcium aluminate hydrates due to the presence of aluminate in PFA, leads to filling in the pores and the voids of the adhered mortar (Wang et al., 2021). In addition, the presence of cement in the treatment solution can lead to additional formation of calcium silicate hydrates which in turn effectively fills in the pores and microcracks in the weak ITZ and the adhered in the RA surface, leading in a much denser microstructure of RA. It is also worth noting that given to the fine particles' nature of SF, filler effect, high specific surface area, better packing density, it can efficiently fill the pores and voids in the adhered mortar, and ultimately enhance the compressive strength of RAC (Shaban et al., 2019).

Limited studies investigated the coating/soaking RA in cement-pozzolan slurry prior to mixing, while the vast majority of studies examined the effects of coating RA with cement and/or pozzolan slurry during mixing. According to Tam et al. (2021), there are very scant studies in the literature to date that dealt with treating RA by coating and/ or soaking in pozzolan solution or slurry, prior to mixing. Liang et al. (2015) examined the effects of treating RA by soaking in cement-SF solution, and reported 29% increase in the 28-day compressive strength of RAC, compared to the untreated RAC, Liang pointed out that this surface pretreatment method can strengthen the adhered mortar by forming a thick coating layer filling in great extent of pores and voids, and thus reducing the water absorption of RA during mixing stage, not to mention providing an enhanced interface bond and ITZ between RA and the surrounding cement paste. This is also in line with the results of Alqarni et al. (2021) who investigated the effects of soaking RA in cement-silica fume solution, in which it was reported an enhanced 28-day compressive strength by 66% and 32% for treated RAC produced with 10mm and 20mm RA size, respectively.

Wang et al. (2020) treated RA with cement and PFA solution, and concluded 5% and 4% increase in the 28-day and the 7-day compressive strength, respectively, compared to untreated RAC. Shaban et al. (2019) treated RA prior to mixing in three different solutions with different replacement levels, the solutions were, PFA+SF, PFA+PC, and nano-silica. The study of Shaban did not investigate the effects of these treatment solutions on the compressive strength, but rather on the engineering properties of RA themselves, i.e., WA, AIV, porosity, crushing resistance value, particle density, and abrasion value. The findings of Shaban study indicated that all the treatment solutions enhanced the engineering properties of RA, and among these treatment solutions treating RA with nano-silica solution obtained the best enhancements, owing to the higher filling effects of nano-silica and smaller particle size, compared to SF and PFA. The combination of cement and PFA performed better than the combination of PFA and SF due to the formation of further calcium silicate hydrates. It is worth noting that, the efficacy of the pozzolan slurry treatment is governed by the particle size of the used pozzolan, calcium hydroxide content in the adhered mortar, the reactivity of the used pozzolan, and the alkalinity of the pore solution (Singh et al., 2013).

Mixing RA using sand enveloped mixing approach (SEMA) presented in the SE mixes has also managed to enhance/ increase the 7-day and the 28-day compressive of the RAC. This mixing technique or sequential mixing technique was established by Liang et al. (2015) and the enhanced compressive strength of the SE mixes can be ascribed to the sequential mixing process of this mixing approach, as sand and 3/4 of the total mixing and cement are mixed first for a certain period of time which allow to form a cement paste prior to the addition of RA, hence less water (effective mixing water) will be absorbed by the RA. To the best of the author knowledge, the only study that dealt with the use of SEMA is the study carried out by Liang et al. (2015). Liang et al. (2015) study did not show the effects of this mixing approach on the compressive strength of RAC in comparison with RAC produced with normal/conventional mixing approach, but only reported its effects on compressive strength of RAC compared with mortar mixing approach (MMA) and two-stage mixing approach (TSMA), in which SEMA performed better than both MMA and TSMA. Nonetheless, for comparative purposes, the effects of the some of the mixing approaches on the compressive strength of RAC, that have been reported in the literature will be discussed here.

The two-stage mixing approach (TSMA) was initially established by Tam et al. (2005) and then by Tam & Tam (2007). TSMA was found to enhance the 7-, 28-, and-56 day

compressive strength of the test concrete mixes produced with 30% RA replacement level by 20%, 14%, and 6.44%, respectively, compared to the reference concrete mixes. Mortar mixing approach (MMA) was also developed by Liang et al. (2015) who reported that SEMA method is better in enhancing the compressive strength of RAC compared to MMA method, at the same w/c ratio. Another mixing approach was developed by Li et al. (2009), this mixing approach is referred to as stone enveloped with pozzolanic powder (SEPP), since it aims at strengthen the adhered mortar of the RA with a coating layer of pozzolan material (i.e., SF, GGBS, PFA) during mixing. The enhancement in the properties of RAC produced with modified mixing approach may be attributed to the incorporation of pozzolan materials rather than the mixing approach itself, thus, the effects of such mixing method can not be compared to SEMA, MMA, and TSMA.

The sole use of the SCP treatment achieved higher enhancement in the compressive strength than the sole use of the SE and the AC treatments. Soaking RA in cement-pozzolan solution prior to mixing managed to strengthen the adhered mortar of the RA better than accelerated carbonation treatment due to the fact that, the calcium hydroxide content is the main factor affecting the efficiency of the sole use of accelerated carbonation, as this treatment relies on chemical reaction between carbon dioxide and calcium hydroxide presented in the adhered mortar, and in this present research case RA consists of variety of materials with about 50% recycled concrete aggregate of its constituent. Accordingly, the efficiency of the accelerated carbonation treatment is reduced due to the low quantity of the recycled concrete aggregate (Kikuchi & Kuroda, 2011). In addition, it was reported that the reaction of calcium hydroxide with carbon dioxide is incomplete, this might be ascribed to the ability of carbon dioxide in penetrating the surface of stronger adhered mortar on the RA surface that was produced with parent concrete of a low w/c ratio with different type of cement (Zhang et al., 2015; Xuan et al., 2016). Consequently, there is uncertainty about accelerated carbonation treatment for RA with lower content of calcium hydroxide and pore distribution within concrete matrix (Otsuki et al., 2003; Li et al., 2019).

The sole use of the batching technique presented in SE mixes (sand enveloped mixing approach), experienced lower enhancements in the compressive strength of the RAC, compared to the sole use of the SCP mixes. This can be explained as the SEMA method aims at only limiting the amount of the absorbed water by the RA during mixing, whilst the SCP

treatment mechanism aims at strengthening the adhered mortar on the RA surface prior to mixing, which in return ultimately results in higher compressive strength enhancement.

Overall, all of the combined treatment methods presented in the SCP+SE, SCP+AC, AC+SE, and the SCP+AC+SE mixes achieved better enhancements in the 7-day and 28-day compressive strength of RAC, compared to the sole use of these treatments. This finding can be ascribed to the coupled effects of these combined treatments on the development of the compressive strength of the RAC. The literature showed that there are limited studies have investigated the synergetic effects of two treatments on the RAC properties. According to Tam et al. (2021), combining two treatment methods can be a promising superior hybrid methodology to the sole use of any treatments, nevertheless, the effects of such hybrid methods have not been investigated in detail in the literature.

To sum up the consistency and compressive strength performance of RAC produced with different treatment methods, the following key points can be concluded:

- The untreated recycled aggregate concrete showed inferior compressive strength compared to the natural aggregate concrete at the same mix design parameters.
- All the utilised treatment methods showed variations of enhancements in the slump, the 7-day compressive strength and the 28-day compressive strength of RAC. In addition, all the treatment methods utilised, and their combinations managed to obtain at least 30MPa which is suitable for structural applications.
- Among all the combination of treatment methods utilised, the combination of SCP+SE treatments exhibited the highest 28-day compressive strength of 42.3MPa at 0.4 w/c ratio.
- the sole use of SCP treatment showed the highest the compressive strength of 38.5MPa at 0.4 w/c ratio across all the sole use of treatments.

5.5 Second Criteria Matrix for Selection of Treatment & Batching Techniques

The second-final criteria matrix was developed in similar procedures to the initial selection matrix in Section 5.3. The purpose of the 2nd- final selection matrix is to selected the final best performed treatment methods to undergo further investigations which included, splitting tensile strength, flexural strength, modulus of elasticity, water absorption, resistance to freezing and thawing, resistance to sulphate attack, and microstructural investigations.

The 2nd and final selection matrix shown in Table 5.6 is for the sole use of treatment methods, while Table 5.7 is for the combination of the treatment methods. The given score points per each criteria in Table 5.6 was in comparison with the performance of each treatment within Table 5.6 (sole treatments), whilst the given weight score in Table 5.7 for each combination treatments was given based on the performance of these treatments compared to each other. The results of the selective analysis in Table 5.6 shows that, the SE scored the highest total points of 63/70, whilst the AC treatment scored the lowest total points of 50/70, and the SCP treatment had 56/70 points. In terms of efficiency, the SCP treatment scored the highest points 18/20, whilst the AC treatment 13/20 points.

The results of the selective analysis in Table 5.7 for the combination of treatments showed that, the combination of the SCP+SE treatment scored the highest total points of 56/70 and the highest efficiency points of 18/20 points, whilst the combination of the SCP+AC scored the lowest total points of 42/70, and the combination of the AC+SE scored the lowest efficiency points of 13/20. Based on the results of the selective analysis, it can be indicated that, the AC (accelerated carbonation treatment) achieved lower points compared to the SCP and the SE treatments.

In addition, as was discussed earlier, there is uncertainty about accelerated carbonation treatment for the RA with lower content of calcium hydroxide and pore distribution within concrete matrix. The accelerated carbonation treatment may seem like a great choice of treatment selection in terms of the environmental impact perspective, but it needs a special device for bulk treatments of the RA, not to mention, it needs prior pre-surface treatment to boost its efficiency. Consequently, the AC treatment was eliminated from the final treatment methods nomination, whilst the SCP, the SE, and their combination have undergone further investigations.

Table 5.6: 2nd Selective analysis for nominating the final best sole treatments for further investigations

Treatment abbreviation	Efficiency	Feasibility	Cost-Efficiency	Application time	Simplicity	Environmental impact	Total score
SCP	18/20	8/10	6/10	7/10	9/10	8/10	56/70
SE	16/20	10/10	9/10	10/10	9/10	9/10	63/70
AC	13/20	7/10	7/10	5/10	8/10	10/10	50/70

Table 5.7: 2nd selective analysis for nominating the final best combination of treatments for further investigations

Type of the treatment	Efficiency	Feasibility	Cost-Efficiency	Application time	Simplicity	Environmental impact	Total score
SCP+SE	18/20	8/10	6/10	7/10	9/10	8/10	56/70
SCP+AC	15/20	6/10	4/10	4/10	6/10	7/10	42/70
AC+SE	13/20	7/10	7/10	5/10	8/10	10/10	50/70
SCP+AC+SE	17/20	6/10	4/10	3/10	6/10	9/10	45/70

5.6 Effects of Treatment & Batching Techniques on Other Mechanical Performance of RAC

5.6.1 Tensile splitting strength

The tensile splitting strength results of the cylindrical treated RACs specimens water cured for 28 days are given in Figure 5.21. Whereas Figure 5.22 shows the relative tensile strength of RACs produced with SCP and SE methods compared to untreated RAC2 and NAC1. The tensile strength results w/c ratios are the arithmetic averages of two concrete cylinders test specimens per mix.

The results indicate that the tensile splitting strength of all the test cylindrical specimens increased when the w/c ratio was decreased. The highest tensile strength values across all the test concretes were recorded for NAC1 mixes, whilst RAC2 mixes obtained the lowest tensile strength values regardless of the w/c ratio. NAC1 mixes achieved tensile strength of 3.8, 3.4, and 2.8MPa, at 0.4, 0.5, and 0.6 w/c ratios, respectively, whereas RAC2 mixes attained tensile strength values of 3.3, 2.85, and 1.9 MPa, at 0.4, 0.5, and 0.6 w/c ratios, respectively.

Among all the finally selected treatments, RAC mixes produced with the combination of soaking in cement-PFA+SF followed by mixing using sand enveloped mixing approach presented in SCP+SE mixes, achieved the highest tensile strength enhancement. SCP+SE mixes increased the tensile strength of RAC from 3.3 to 3.65MPa, 2.85 to 3.3MPa, and 1.9 to 2.4MPa, at 0.4, 0.5, and 0.6 w/c ratios, respectively. Overall, all the finally selected treatments led to enhancements in the tensile strength of RAC, but the enhancements were not as high as was in the case of compressive strength.

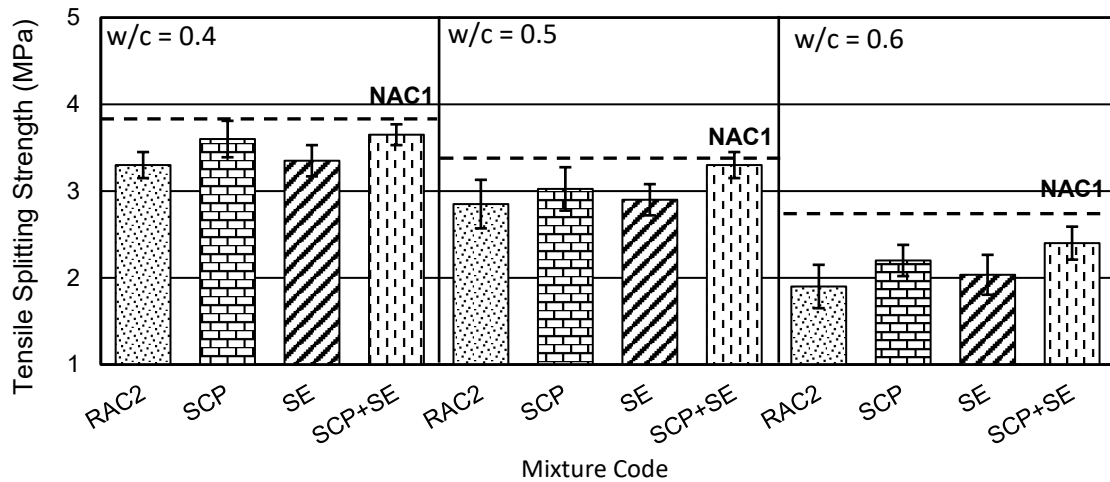


Figure 5.21: Variation in tensile strength development at 28-day for treated RACs mixes at different w/c ratios, compared to NAC1 and RAC2

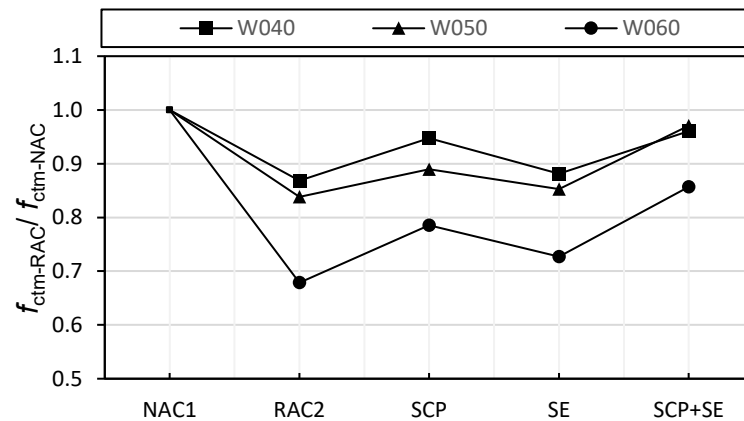


Figure 5.22: Effects of the finally selected treatment methods on the relative tensile strength of RAC at different w/c ratios

Tensile splitting strength is one of the most well-known indirect methods for testing tensile strength of concrete. It has been established that the tensile splitting strength of RAC is governed by various factors, water to binder ratio, mixing methods, curing age, type of cement used, quality of the RA, bonding strength of the RA with the cement matrix, and the quality of the ITZ (Nayak & Dutta, 2017).

The results of the tensile splitting strength of the different cylindrical concretes showed that the tensile splitting strength of the untreated RAC2 specimens experienced similar behaviour to the compressive strength. Nonetheless, the effect of the RA on the split tensile strength of concrete is less than that on the compressive strength. The RAC2 specimens exhibited lower

28-day tensile splitting strength compared to the NAC1 specimens at the same mix design parameters. McKeil and Kang (2013) stated that the lower tensile splitting strength of the RAC compared to the NAC is mainly ascribed to the poor quality of RA especially the adhered mortar which acts as a weak point that fail under compressive load and lead to a lower split tensile strength. This is in line with Bairagi et al. (1993) who reported 40% reduction in tensile splitting strength of RAC, compared with NAC. Katz (2003) reported 6% lower split tensile strength of the RAC compared to the NAC, while other studies reported up to 10% reduction in tensile splitting strength of RAC in comparison with NAC (Verian et al., 2018). Rao et al. (2011) concluded 24% loss in the split tensile strength of the RAC compared to the NAC. Another study of Alqarni et al. (2021) showed a reduction in the split tensile strength of 52% and 39% compared with conventional concrete, for 10mm aggregate size and 20mm aggregate size, respectively, the author added, this reduction was due to the excessive amount of the porous adhered mortar on the RA surface.

Wang et al. (2021) pointed out that the maximum reduction in the split tensile strength of the RAC is about 16% compared to ordinary concrete. In the contrary, some researchers reported siliar tor better performance in tensile splitting strength of RAC compared to NAC (McNeil & Kang, 2013; Butler et al., 2013). According to Etxeberria et al. (2007), the higher water absorption capacity of RA leads to a proper bonding bewtween the RA and the cement matrix, hence, resulting in higher tensile splitting strength of RAC. Matias et al. (2013) pointed out that increase in the split tensile strength of the RAC can be attributed to the RA rough surface which enhance the adherence to the cement matrix. All the test concrete specimens experienced similar trend of development higher tensile splitting strength values with decrease in w/c ratio, this in line with the work of Sivakumar et al. (2014) who stated that the tensile splitting strength of RAC increases with decrease in water to binder ratio.

The use of the soaking RA in cement- PFA+SF solution treatment prior to mixing, managed to enhance the split tensile strength of the RAC. This can be attributed to the strengthend adhered mortar on the RA surface and especially the ITZ being densified after this treatment. Behera et al. (2014) pointed out the enhancement in the ITZ of the RAC have greated influence on the split tensile strength compared to the compressive strength. Kukadia et al. (2017) treated the RA by soaking in cement solution, and reported 20% enhancement in the tensile splitting strength of concrete produced with 30% RA and 70% NA. Whereas, Alqarni et al. (2021) treated the RA with cement- silica fume slurry, and concluded 8% enhancement

in the split tensile strength. Ahmed & Lim (2021) investigated the effects of treated RA with cement-PFA+SF solution prior to mixing, and reported 14% enhancement in the splitting tensile strength of RAC produced with RA treated via this treatment.

The SE mixes also exhibited enhancement in the split tensile strength, as the sand enveloped mixing approach (SEMA) procedures involved adding the untreated RA to the initially premixed sand-rich mortar during the first stage of mixing. Under these circumstances, the water that will be absorbed by the RA during mixing will be limited. This sand-rich mortar coated the RA surface, and ultimately strengthened the adhered mortar by sealing the RA surface (Sarvanakumar et al., 2021). The literature showed that very limited studies carried out on the effects of the batching approaches on the tensile splitting strength of RAC. Jagan et al. (2021) in their investigations, mixed the RAC using sand enveloped mixing approach (SEMA), and stated that the tensile splitting tensile strength was enhanced by 14% after using SEMA method.

The combination of soaking RA in cement-PFA+SF solution prior to mixing followed by sand enveloped mixing approach presented in the SCP+SE mixes in enhancing the tensile splitting strength followed the same trend of enhancement to the compressive strength. The SCP+SE mixes obtained the highest enhancement in the tensile splitting strength of the RAC, this can be explained as the coupled effects of both SCP and SEMA, ultimately enhanced the RA properties and the RAC matrix. To the best of the author knowledge, there is no studies to be found in the literature that examined the couple effects of these treatment methods on the tensile splitting strength of the RAC.

5.6.2 Flexural strength

The results of the flexural strengths of the different RACs produced with the three selected enhancement methods are given in Figure 5.23, whilst the effects of the selected treatment methods on the relative flexural strength of RACs is given in Figure 5.24. The mean flexural strength obtained from the average of two beams/ prismatic specimen per mix was taken. Similar trend to tensile strength development was noticed in the 28-day development of the different RACs flexural strength. Likewise, an increase in w/c ratio led to decrease in the flexural strength for all the RACs specimens and the natural aggregate concrete.

NAC1 mixes exhibited the highest flexural strength of 6.44, 4.6, and 3.96 MPa, among all the concrete mixes specimens, at 0.4, 0.5, and 0.6 w/c ratios. In contrast, RAC2 mixes seems to

develop significantly lower flexural strength compared to NAC1. Untreated RAC2 mixes obtained 4.6, 3.89, and 2.49 MPa flexural strengths, at 0.4, 0.5, and 0.6 w/c ratios, respectively.

All the finally selected treatment methods utilised were able to enhance the flexural strength of RAC. Amongst all the finally selected treatments utilised, the combination of soaking in cement-PFA+SF followed by mixing via sand enveloped mixing approach presented in SCP+SE mixes, provided the best enhancements in the flexural strength. The synergetic effects of SCP+SE treatment resulted in significant increase in the flexural strengths of RAC from 4.62 to 5.36MPa, from 3.89 to 4.46MPa, from 2.49 to 3.06MPa.

The sole use of soaking RA in cement-PFA+SF presented in SCP mixes showed close enhancements in the flexural strength of RA to SCP+SE mixes and showed better enhancements compared to SE mixes. Mixing RAC via the sand enveloped mixing approach presented in SE mixes, has also led to flexural strength enhancements but not as high as SCP+SE and SCP mixes. Figure 5.25 shows the flexural failure of some of the test specimens.

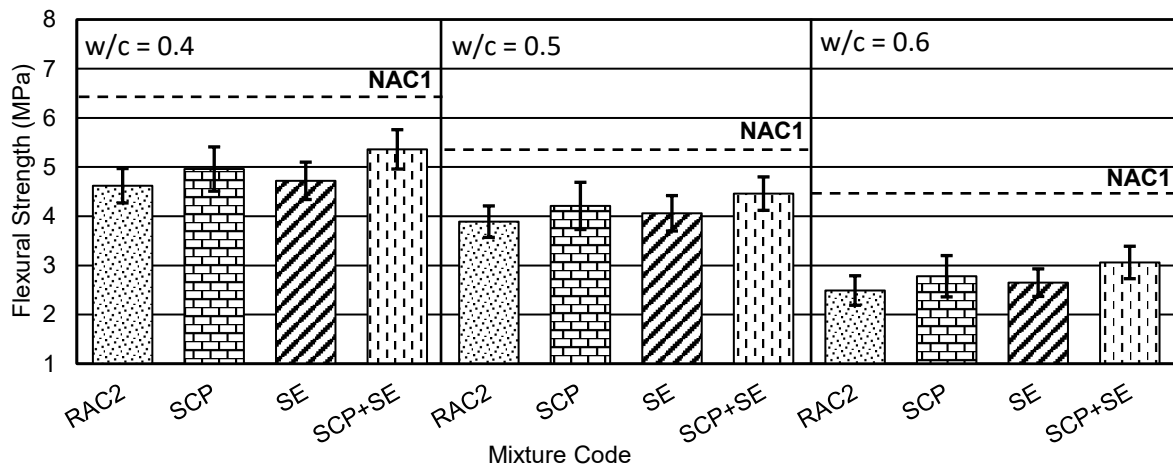


Figure 5.23: Flexural strength development for treated RAC mixes at different w/c ratios, compared to NAC1 mixes and untreated RAC2 mixes

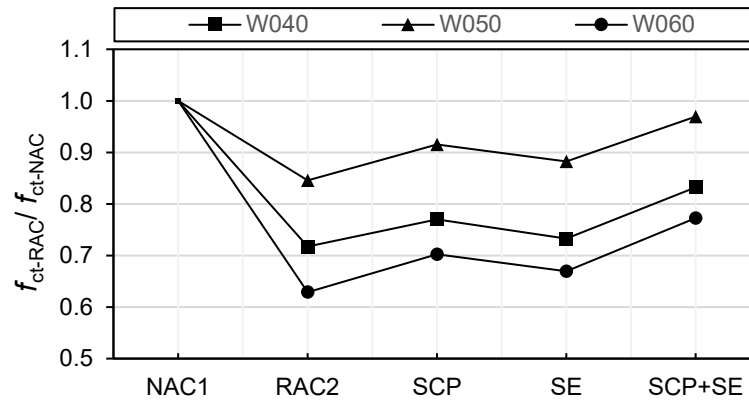


Figure 5.24: Effects of the finally selected treatment methods on the relative flexural strength of the RAC at different w/c ratios



Figure 5.25: Flexural failure mode of some of the RAC beams

The flexural strength of the RAC2 beam specimens under the three-point bending test, followed similar declining pattern to the compressive strength and tensile splitting strength, compared to the NAC1 specimens, at the same mix design parameters.

This trend of reduction in flexural strength can be attributed to the weak bonding between the RA and the new cement paste within the concrete matrix owing to the poor quality of the adhered mortar on the RA surface and the poor quality of the developed ITZ (Limbachiya et al., 2012). Majhi et al. (2018) concluded 6.5% reduction in the flexural strength of the RAC in comparison with NAC. Similarly, Katz (2003) reported a reduction in the flexural strength of up to 10% for RAC in comparison with ordinary concrete. Some researchers reported a reduction up to 10% in the flexural strength of the RAC compared to the NAC (Ajdukiewicz

& Kliszczewicz, 2002; Malesev et al., 2010; Yang et al., 2008). In the contrary, some studies have reported no significant difference encountered in the flexural strength of concrete produced with 100% RA compared to ordinary concrete (Rao et al., 2011; Ravindrajah & Tam, 1985). This can be attributed to the rough texture and angular shape of the RA, which might lead to a better adhesion bond and interlock between the cement paste and the RA particles (Kazemain et al., 2019).

It was also observed that the flexural strength of all the concrete specimens including the enhanced and untrated RAC2 specimens, showed increase in flexural strength with decrease in w/c ratio. This is in line with the results of Bairagi et al. (1993) who observed that the flexural strength of the RAC increased with decrease in water to cement ratio, and pointed out that the flexural strength of RAC is 26% lower than that of ordinary concrete. According to Yang et al. (2008), the incorporation of RA with lower or enhanced water absorption capacity results in better flexural strength of RAC, the authors also pointed out that, the flexural strength of RAC is observed to increase with increase in grade of RAC.

The results of the flexural strength also showed that all the treated RAC specimens presented in the SCP, the SE, and the SCP+SE specimens, followed similar flexural strength enhancement patterns to tensile splitting strength and compressive strength. Nonetheless, the percentage of enhancements in the tensile splitting strength and flexural strength is lower compared to the compressive strength.

Soaking RA in cement-PFA+SF solution which is presented in the SCP specimens, managed to enhance the flexural strength of RAC by different percentages depending on the used w/c ratio, as shown in the results section. This can be attributed to the denser developed ITZ after the treatment of the RA resulting in a better bonding between the RA and the cement paste. It is worth noting that, the literature showed limited studies on the effects of coating/ soaking RA with cement-pozzolan slurry/ solution on the flexural strength of the RAC. Similar findings were observed by Ahmed & Lim (2021) who coated the RA with pozzolan slurry and reported 13% enhancement in the flexural strength of the RAC. Ahmad and Lim, pointed out that the enhancement in the flexural strength after the use of the pozzolan slurry, is mainly attributed to the counteracting the microstructural deficiencies by the formation of the secondary calcium silicate hydrates which contributed to the enhancement of the flexural strength of the RAC.

This in line with Shaban et al. (2019) who pointed out that soaking RA in cement-pozzolan solution leads to filling the pores and voids in the RA surface and densify the pore structure of RAC. The authors added that SF is most effective to densify cementitious matrix due to its better packing density in terms of wider distribution of its particle. It was also added, that the coupled effects of PFA and SF is more prone to achieve a maximum packing density, that significantly contributes to the enhancement of the flexural strength of the RAC (Li et al., 2009).

The use of sand enveloped mixing approach presented in the SE specimens has also showed enhancement in the flexural strength of the RAC, but lower than that of the SCP specimens. This indicates that, the SCP treatment is more prone to strengthening the adhered mortar and the ITZ of the RA, owing to the pre-treatment of the RA prior to mixing, which ultimately densified the ITZ and the bonding strength of the RAC. The enhancement in flexural strength obtained by the SE specimens can be explained to the developed stiff non-porous sand-rich cement paste that coated the surface of the RA during mixing, which led to strengthening the ITZ of the RAC and reduced its porosity.

There are scarce studies that deal with the effects of the sand enveloped mixing approach on the flexural strength of the RAC. Jagan et al. (2021a) reported 11% enhancement in the flexural strength of RAC after mixing using sand enveloped mixing approach (SEMA). Same authors on a different study indicated that, RAC produced with sand enveloped mixing approach exhibited about 16% enhancement in flexural strength in comparison with RAC produced with normal mixing approach (Jagan et al., 2021b). Jagan et al. (2021b) pointed out that, this enhancement in flexural strength by SEMA method is mainly ascribed to the strengthened ITZ between the cement paste and the RA, which tends to resist more loading under the action of bending.

The combination of soaking RA in cement- PFA+SF solution prior to mixing followed by mixing using sand enveloped mixing approach obtained better enhancement compared to the sole use of the each method. This can be explained as the coupled effects of the two methods significantly strengthened the adhered mortar on the RA surface and densified the ITZ resulting in a stronger bonding between the RA and the cement paste within the RAC matrix. To the best of the author knowledge, there are no studies that examined the synergetic effect of these two methods on the flexural strength of the RAC.

5.6.3 Modulus of elasticity

The results of the elastic modulus of the treated RACs cylindrical specimens after 28 days of water curing are presented in the Figure 5.26. Figure 5.27 shows the relative modulus of elasticity of the treated RACs. As a general trend of modulus of elasticity developments of all the concrete mixes, when the w/c ratio decreased, the modulus of elasticity increased. The highest modulus of elasticity was recorded for NAC1 mixes, with ranges between 27–33.5GPa, whilst untreated RAC2 mixes exhibited lower modulus of elasticity values, ranging from 23.5–28.6GPa.

The treated RACs via the selected three treatments showed variations in modulus of elasticity. The effects of these treatments have led to little enhancements compared to the enhancements observed in compressive strength, tensile strength, and flexural strength. Following the same enhancements trend observed in the compressive strength, tensile strength, and flexural strength, the highest enhancements in the modulus of elasticity of RAC were recorded for SCP+SE mixes. The coupled effects of SCP+SE treatment obtained the highest modulus of elasticity values compared to the untreated RAC2 mix, the SCP, and the SE mixes. Whereas SCP and SE mixes showed close enhancements in the modulus of elasticity of RACs, but slightly lower compared to SCP+SE mixes.

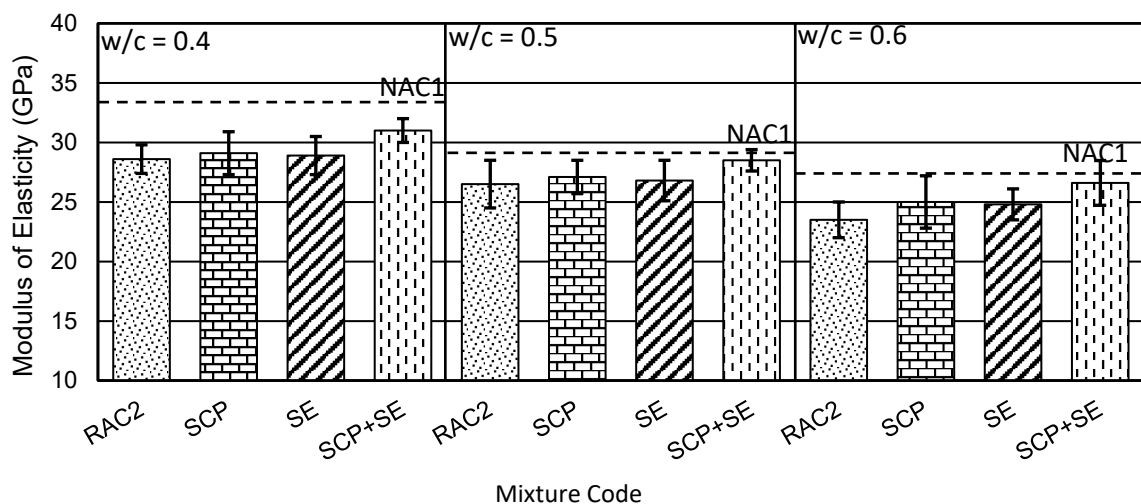


Figure 5.26: Variations in modulus of elasticity of the different treated RACs mixes in comparison with untreated RAC2 and NAC1 mixes

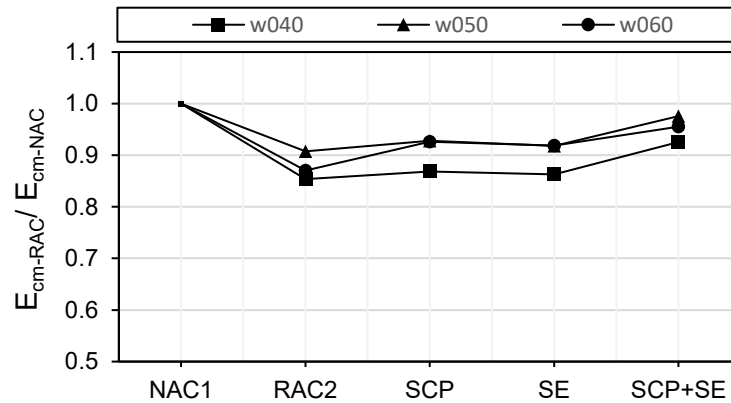


Figure 5.27: Relative modulus of elasticity of the treated RACs at different w/c ratios

The modulus of elasticity also known as elastic modulus and Young's modulus is another crucial engineering property that indicates the concrete stiffness and influences its deflection. According to Behera et al. (2014), the modulus of elasticity of a given RAC specimen is governed by various aspects such as the strength of the RAC specimen, quality of the RA i.e., porosity and density, constituent of the RA, the characteristics of the transition zone, the mix design of the RAC specimen, the RAC specimen age, and the curing condition. It was also pointed out by Li et al. (2009) that the porosity and density of the RA determines the stiffness of the bulk matrix. Li also stressed out that the reduction in the elastic modulus of RAC is decreased when a better quality of RA is used.

Like the compressive strength, the tensile splitting strength, and the flexural strength, similar reduction trend has also been observed for the modulus of elasticity of the RAC2 specimens compared to the NAC1 specimens. The untreated RAC2 specimens exhibited lower modulus of elasticity values compared to the NAC1 specimens, at the same mix design parameters. This is possibly ascribed to the higher water absorption capacity of RA due to the porous adhered mortar, lower density and the weak bonding between the old ITZ and the new ITZ because of the presence of pores and micro-cracks around the RA (Behera et al., 2014).

The literature showed variations in the reduction of the modulus of elasticity of RAC compared with ordinary concrete. Some studies reported a reduction of up to 45% in the modulus of elasticity of RAC compared to the NAC (Rao et al., 2011; Ajdukiewicz & Kliszczewicz, 2002; Rahal, 2007; Yang et al., 2008; Poon et al., 2003; Malesev et al., 2010; Xiao et al., 2012; Kwan et al., 2012; Xiao et al., 2005). Kheder & Al-Windawi (2005)

indicated that it is lower by 20 to 25%, whilst Bairagi et al. (1993) reported it was lower by 39%.

In addition, it was also indicated that the RAC modulus of elasticity is 10% to 33% less than that of the conventional concrete (Verian et al., 2018). Interestingly noting, a study by Topcu & Guncan (1995) reported that its 80% lower than normal concrete. According to Limbachiya et al. (2012), RAC shows higher brittle failure behaviour compared to conventional concrete. The authors added that, the lower modulus of elasticity of RAC compared to NAC is attributed to the inferior quality of the RA compared to the NA, whereas, Xiao et al. (2012) pointed out that the reduction in elastic modulus of the RAC is due to the porous RA surface owing to the adhered mortar with a relatively lower elastic moduli to the RA.

According to Belen et al. (2011), the RA adversely affects both the longitudinal and the transverse modulus of elasticity and owing to the lower elastic moduli of the RA, the peak strain and ultimate strain of RAC is increased, thus, large deformation in the RAC is endured. This was confirmed by Casuccio et al. (2008) who indicated that the inclusion of RA into concrete decreases concrete stiffness and increases concrete brittleness due to the reduced modulus of elasticity.

All the utilised treatment methods, soaking RA in cement-PFA+SF solution (SCP), sand enveloped mixing approach (SE), and the combination of both of them (SCP+SE), managed to enhance the modulus of elasticity of the RAC. There are very limited studies on the effects of soaking RA in cement-pozzolan solution and sand enveloped mixing approach on the Young's modulus of RAC.

The enhanced modulus of elasticity of RAC achieved by the SCP specimens can be ascribed to the enhanced modulus of elasticity of RA after soaking in cement-PFA+SF solution along with the enhanced compressive strength and other related mechanical properties. Wang et al. (2020) studied the effects of slurry wrapping RA with cement-PFA slurry on the dynamic elastic modulus of RAC. The dynamic elastic modulus reflects on the internal compactness of concrete matrix via the transmission of the characteristic waves. The dynamic modulus of elasticity of concrete is mainly affected by internal pores and voids, interfacial characteristics, and the presence of micro-cracks.

The results of Wang et al. (2020) study showed that the dynamic modulus of elasticity of RAC was mainly related to the apparent density of RA and the actual effective water to binder ratio. The authors argued that the slurry wrapping treatment increased the modulus of elasticity of RAC by 4%, as a result of the reduced the porosity of RA, and the increased amount of the cementitious materials within the concrete matrix, which led to enhanced mechanical properties of the RAC, and thus enhanced modulus of elasticity.

Mixing RAC using sand enveloped mixing approach presented in the SE specimens has also enhanced the modulus of elasticity of the RAC. This is possibly attributed to the formed pre-mixed stiff matrix during the first stage of SEMA method which filled the pores and micro-cracks of the RA, resulting in stiffer and enhanced modulus of elasticity of the RA. Jagan et al. (2021a) investigated the effects of sand enveloped mixing approach on the elastic modulus of RAC, and reported 12% and 14.8% enhancement in the modulus of elasticity of RAC at 28-day and 90-day, respectively. Jagan et al. (2021b) reported 1.5% and 1.2% enhancement in the modulus of elasticity of RAC produced with sand enveloped mixing approach, at 28- and 90-day, respectively. The authors pointed out it that this enhancement in the elastic modulus was due to the improved stiffness of bonding of RA with the new cementitious paste. In addition, the enhanced porosity of RA led to increased stiffness in the RAC and thus increased modulus of elasticity.

Similar to compressive strength, tensile splitting strength, and flexural strength, the combination of SCP+SE resulted in further enhancement in the modulus of elasticity compared to the sole use of each treatment. To the best of the author knowledge, no studies to be found on the synergetic effects of these two treatments on the modulus of elasticity of RAC.

Nonetheless, it can be argued that the coupled effects of SCP+SE resulted in better modulus of elasticity of RA, enhanced porosity of RA, better bonding and interlocking between the RA and the cement paste, and enhanced ITZ, which ultimately led to better modulus of elasticity of RAC treated with the combination of soaking in cement- PFA+SF solution followed by sand enveloped mixing approach.

To summarise the tensile splitting strength, flexural strength, and modulus of elasticity performance of RAC produced with different treatment methods, the following points can be concluded:

- The untreated recycled aggregate concrete showed inferior flexural strength, tensile splitting strength, and modulus of elasticity performance compared to the natural aggregate concrete.
- Soaking RA in cement-PFA+SF prior to mixing achieved better enhancements than sand enveloped mixing approach, whereas the combination of SCP and SEMA led to the best results.
- The combination of SCP+SE treatment achieved the best modulus of elasticity performance.

5.7 Correlation Analysis & Comparison with Design Codes

The correlation analysis/ relationships of the different treated RACs properties are given in Figure 5.28. It involves, (i) flexural strength vs. tensile splitting strength, (ii) modulus of elasticity vs. compressive strength, (iii) tensile splitting strength vs. compressive strength, (iv) flexural strength vs. compressive strength. The results of the flexural strength of the untreated RAC2 and the treated RACs (SCP, SE, and SCP+SE) were plotted against the corresponding splitting tensile strength, the results of the compressive strength were plotted against the corresponding elastic modulus, the results of the compressive strength were also plotted against the corresponding flexural strength, and the results of the compressive were also plotted against the corresponding tensile splitting tensile strength, as shown in Figure 5.28.

It can be seen from the liner regression analysis results that a direct relationship exists between the all the untreated and treated RAC mechanical properties investigated in this work. It can be indicated that all the relationships between the different mechanical properties plotted in Figure 5.28 are proportional to each other. For instance, the more tensile splitting strength results in more flexural strength in the test concrete mixes and vice versa. The correlation between the different mechanical properties was obtained from the maximum correlation coefficient and can be expressed as follows:

$$f_{ct} = 1.64 f_{ctm} - 0.65 \quad \text{Equation 5.6}$$

$$E_{cm} = 0.26 f_{ck} + 19.91 \quad \text{Equation 5.7}$$

$$f_{ctm} = 0.07f_{ck} + 1.06 \quad \text{Equation 5.8}$$

$$f_{ct} = 0.11f_{ck} + 1.08 \quad \text{Equation 5.9}$$

Where f_{ct} is the flexural strength and f_{ctm} is the splitting tensile strength, E_{cm} is the modulus of elasticity, and f_{ck} is the cube compressive strength. The R-factor of all the above derived correlations was above 0.9, which indicates the accuracy of the experimental works and soundness of the analysis.

5.7.1 Tensile splitting strength vs. flexural strength

The American Concrete Institute (ACI) and the Eurocode (EC2) provided the relationship between flexural strength and tensile splitting strength in the following equations:

$$\text{(EC2) } f_{ct} = \max\left(1.6 - \frac{h}{1000}\right) f_{ctm} \quad \text{Equation 5.10}$$

$$\text{(ACI) } f_{ct} = 1.1f_{ctm} \quad \text{Equation 5.11}$$

The ACI and EC equations are plotted in Figure 5.28a to indicate the compliance of the test concretes with these equations. The plotted design codes show that, the EC2 prediction equation seems more representative of the current work results, as it slightly over-estimates the flexural strength of the lower-grade RACs and estimates relatively well for higher grade RACs, whilst the ACI prediction equation under-estimates the flexural strength of RACs. The maximum difference between the predicted values and the corresponding experimental values are 14% and 35%, for EC2 and ACI, respectively.

5.7.2 Compressive Strength vs. modulus of elasticity

The EC2 and the ACI give the following equations to express the relationship between the cube compressive strength and the modulus of elasticity of concrete, and these equations were also plotted in Figure 5.28b.

$$\text{(EC2) } E_{cm} = 9.5(0.8f_{ck} + 8)^{(1/3)} \quad \text{Equation 5.12}$$

$$(ACI) E_{cm} = 4127f_{ck}^{0.50} \quad \text{Equation 5.13}$$

It can be observed from Figure 5.28 that the ACI prediction equation tends to largely under-predicts the modulus of elasticity whereas, the EC2 equation over-estimates the modulus of elasticity. The maximum difference between the estimated values and the corresponding experimental values are 11% and 31%, for EC2 and ACI, respectively.

5.7.3 Compressive strength vs. tensile splitting strength

The prediction equations of both the EC2 and the ACI for the relationship between the compressive strength and tensile splitting strength were plotted in Figure 5.28c, the following equations were used.

$$(EC2) f_{ctm} = 0.3f_{ck}^{(2/3)} \leq C50/60 \quad \text{Equation 5.14}$$

$$(ACI) f_{ctm} = 0.49f_{ck}^{0.5} \quad \text{Equation 5.15}$$

It can be seen that, the EC2 equation slightly underestimates the tensile splitting strength of RACs, whilst the ACI equation largely underestimated the tensile splitting strength of RACs. The maximum difference between the estimated values and the corresponding experimental values are 9% and 16%, for EC2 and ACI, respectively.

5.7.4 Compressive strength vs. flexural strength

The EC2 and the ACI provide the following equations to estimate the flexural strength of normal aggregate concrete based on the cube compressive strength:

$$(EC2) f_{ct} = 0.35f_{ck}^{(2/3)} \quad \text{Equation 5.16}$$

$$(ACI) f_{ct} = 0.54\sqrt{f_{ck}} \quad \text{Equation 5.17}$$

It can be observed from Figure 5.28d that both the EC2 and the ACI equations under-predicts the flexural strength of the RACs. The maximum difference between the estimated values and the corresponding experimental values are 31% and 42%, for EC2 and ACI, respectively.

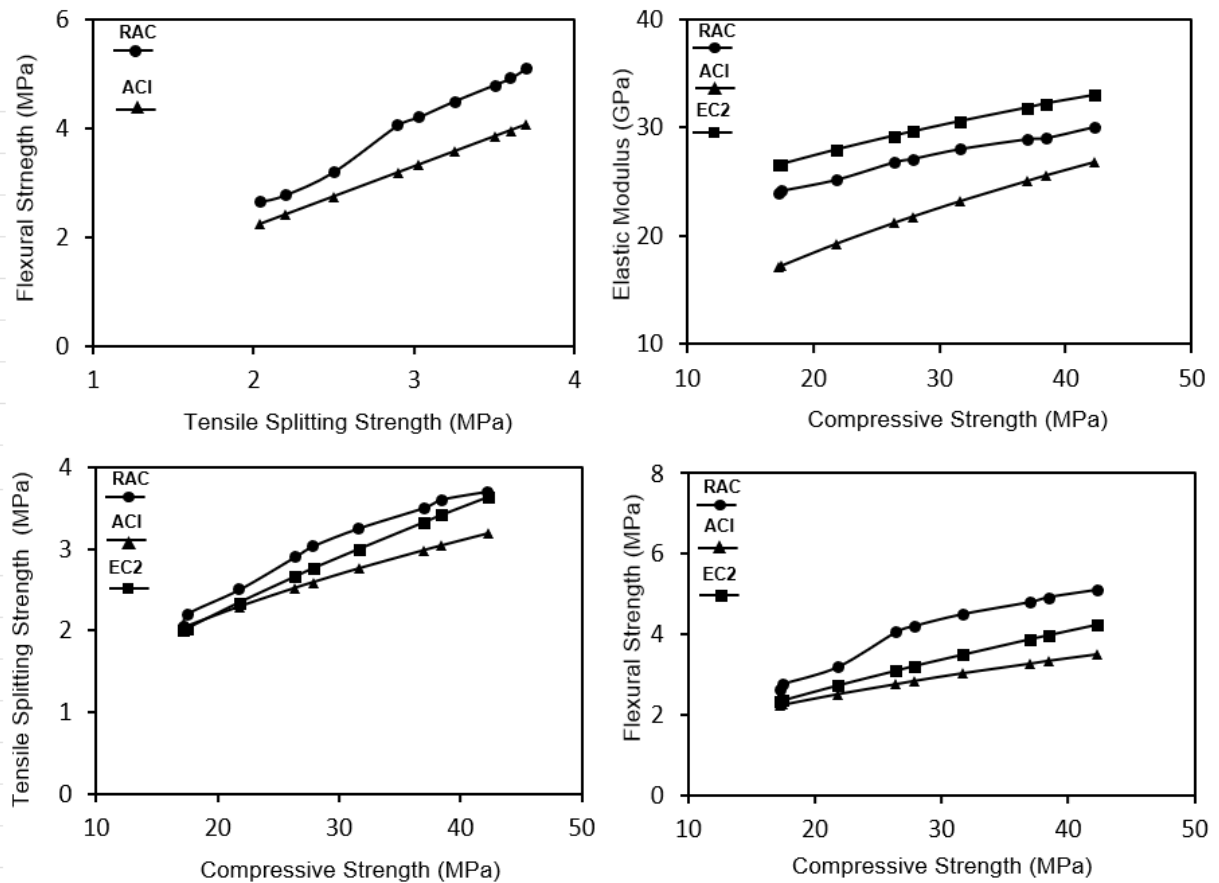


Figure 5.28: Correlation and regression relationships between the different engineering properties of treated RACs, Eurocode 2, and ACI, (a) flexural strength vs. tensile splitting strength, (b) modulus of elasticity vs. compressive strength, (c) tensile splitting strength vs. compressive strength, (d) flexural strength vs. compressive strength

Overall, it can be seen from Figure 5.28 that none of the design codes equations provided by the ACI and EC can predict the mechanical properties of the enhanced RACs. This might be mainly due to the lower mechanical properties of the enhanced RACs compared to natural aggregate concrete. Nonetheless, the provided prediction equations can be used to predict the mechanical properties of the enhanced RACs. Furthermore, it is suggested that further

research is required on the effects of treatment methods on the mechanical properties of RACs to establish better understanding on the scientific knowledge of the performance of the enhanced RACs. This would also enrich the literature with further data on the performance of the enhanced the RACs.

5.8 Effects of Treatment & Batching Techniques on Durability Performance of RAC

5.8.1 Water absorption

Figure 5.29 shows the results of the water absorption of the enhanced RACs in comparison with the untreated RAC2 and NAC1 mixes, at 0.4, 0.5, and 0.6 w/c ratios. As a general trend for all the test concretes specimens, the lower the w/c ratio the lower was the water absorption.

NAC1 mixes recorded the lowest water absorption values across all the test concrete mix specimens, at all w/c ratios, whilst RAC2 mixes exhibited the highest water absorption values at all w/c ratios. It can also be seen that all the treatment methods varied in the enhancement of the water absorption of RAC.

The bi-combination of soaking RA in cement-PFA+SF prior to mixing and batching using the sand envelope mixing approach, presented in SCP+SE mixes, produced the highest enhancement in water absorption.

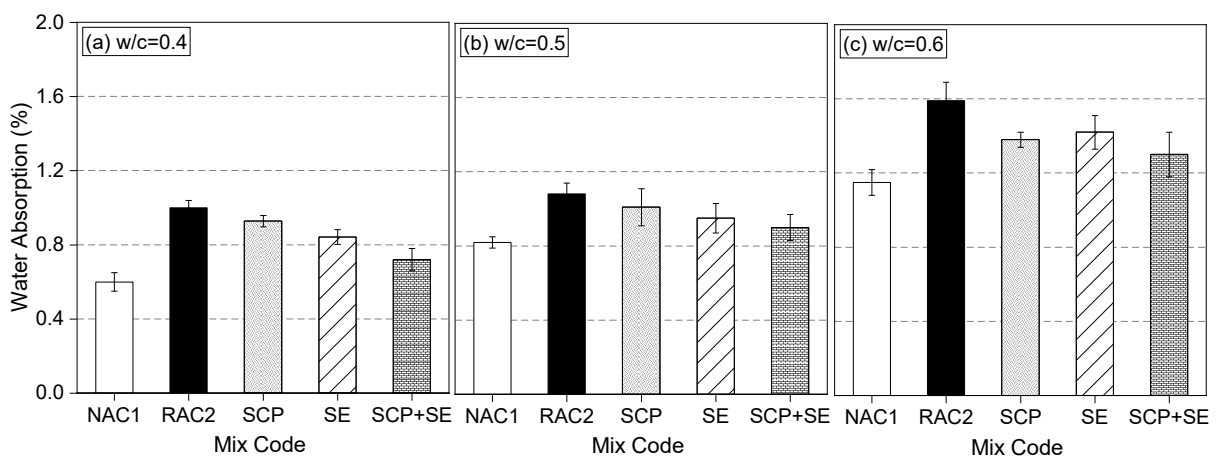


Figure 5.29: Results of the water absorption of the enhanced RACs in comparison with the untreated RAC2 and NAC1, (a) w/c ratio=0.4, (b) w/c ratio=0.5, (c) w/c ratio=0.6

The water absorption of a given test concrete specimen reflects on its porosity state, hence the higher the porosity of concrete, the higher its water absorption property (Le & Bui, 2020). The water absorption for all the designed concrete in general increased with an increase in w/c ratio. This is mainly ascribed to the increased pores and voids and lesser dense microstructure of lower strength concrete. This is in line with the work of Thomas et al. (2013) who stated that higher-strength concrete tends to show lower water absorption compared to concrete of lower-strength. According to Lotfi et al. (2015), designing concrete with a low water/cement ratio and higher cement content reduces the capillary voids, and thus a reduction in the water absorption can be achieved. The current test results showed higher water absorption of the untreated RAC2 mixes compared to NAC1 mixes, this is because of the porous nature of RA given to the attached adhered mortar around the RA surface which consists of micro-cracks and pores that are formed during the preparation of RA.

Similar observations were given in the study of Debieb et al. (2010) who argued that the water absorption of RAC is significantly lower than that of NAC by 0.4% to 0.6%. Kwan et al. (2012) stated that due to the porous nature of RA and the developed micro-cracks during the crushing process, its incorporation in concrete significantly increases the permeability.

Lotfi et al. (2015) stated that the adverse effects of RA on the high water absorption of the RAC can be mitigated by utilizing lower water to binder ratio. Tam & Tam (2007) stressed that mixing RAC using batching approach increase the RAC resistance to water absorption due to the reduced water absorption. In this study, the enhanced water absorption by SE mixes using the SE method (sand enveloped mixing approach) can be ascribed to the process of the SE mixing approach, in which the RA is covered with premixed cement/ mortar slurry that filled up the cracks and pores of RAC, hence enhancing its resistance to water absorption (Wang et al., 2021).

The enhanced water absorption provided by the SCP mixes (soaking RA in cement-PFA+SF solution) can be explained by the formation of a thin coated pozzolanic layer that blocked the pores and micro-cracks, thus enhancing the ITZ of RA, and lowering the porosity of RAC (Shaban et al., 2019).

5.8.2 Resistance to freeze-thaw cycles

The capability of the hydrated treated RACs specimens to withstand frost damage via simulation of freeze-thaw repeated cycles, was evaluated by testing mass change and strength loss at the end of 4 cycles and 20 cycles. Visual inspections of any physical damage endured by the test specimens was made in successive freeze-thaw cycles and after the end of the 20th cycle was also determined.

5.8.2.1 Visual inspection

Table 5.8 shows the description of defect/damage endured by the different concrete mixes via the visual inspection after the freezing and thawing repeated cycles. Figure 5.30 shows some of the test specimens after freeze-thaw cycles.

Table 5.8: Description of the visual inspection of damage/defect endured by the different concrete cube specimens during and at the end of the freeze and thaw cycles

Description of Damage	Visual Remarks
Fractures	No fractures were encountered for all the concrete specimens investigated after the end of the 20 th freeze-thaw cycle.
Scaling/ Peeling	Minimal scaling was observed on all the NAC1 specimens during and after the end of the freeze-thaw cycles. RAC2 specimens exhibited prominent scaling after the 8 th freeze-thaw cycle. The treated RAC specimens experienced minor to medium scaling on all the concrete cubes faces during the freeze-thaw cycles.
Hairline Cracks <0.2mm	No hairline cracks were noticed on any of the concrete test specimens throughout the freeze-thaw cycles.
Surface Crack >0.2mm	No surface cracks were observed on any of the concrete specimens throughout the freeze-thaw cycles up to 20 cycles.
Chipping	Chipping of concrete edges was observed on all the concrete specimens throughout the freeze-thaw cycles. Minor chippings were observed on the NAC1 specimens, whilst the RAC2 specimen exhibited prominent chippings along its edges. Treated RAC specimens showed somewhat minor chippings along the edges throughout the freeze-thaw cycles.
Craters	Visual inspections showed no craters in any of the concrete specimens throughout the freeze-thaw cycles.
Major Spalling/ Delamination	Observations showed no major spalling nor delamination occurred on any of the concrete specimens during the freeze-thaw cycles.

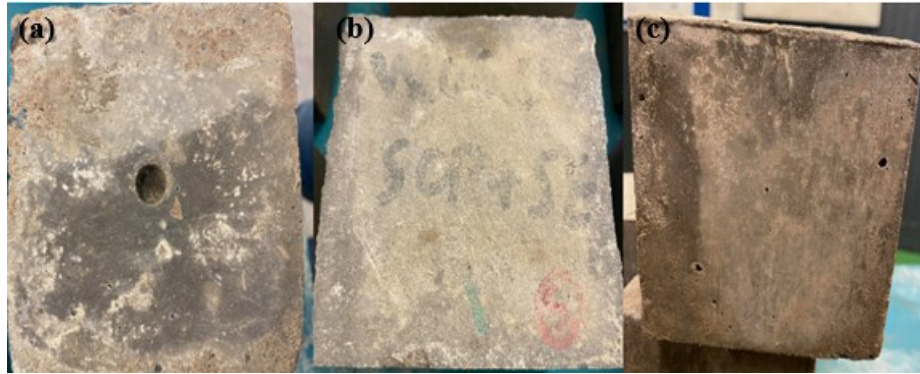


Figure 5.30: Concrete cube test specimens after 20 successive freeze-thaw cycles, (a) RAC2 specimen, (b) SCP+SE specimen, (c) NAC1 specimen

5.8.2.2 Mass change of treated RACs after freeze-thaw cycles

A typical profile of the effects of freezing and the thawing cycles on the mass change of the NAC1, RAC2 and the enhanced RAC specimens is shown in Figure 5.31.

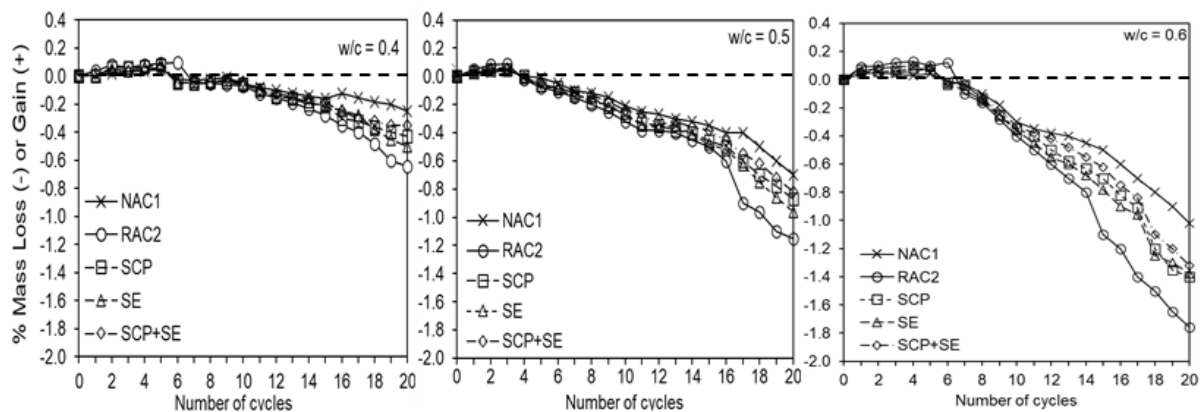


Figure 5.31: Mass change (Loss or gain) due to freeze-thaw cycles, (a) w/c ratio of 0.4, (b) w/c ratio of 0.5, and (c) w/c ratio of 0.6

At the start of the freezing and thawing cycles, all the concrete specimens showed mass gain regardless of the w/c ratio, with no further mass gain after the 4th and 6th cycles. This can be explained by the filling of the enclosed pores with water within the concrete matrix caused by the freezing action of water. At the end of the 6th cycle, the highest mass gain was observed for RAC2 specimens across all the concrete specimens, whilst the lowest recorded mass gain was for the NAC1 specimens. This is in line with the study of Salem et al. (2003) who stated that the higher mass gain of the untreated RAC2 specimens at the start of the freeze-thaw cycles can be ascribed to the penetrated water into the inner cracks and pores of the RAC after exposure to freeze-thaw filling all the pores and interfacial transition zone (ITZ). The

enhanced RAC specimens given in SCP, SE, and SCP+SE mixes showed reductions in mass gain compared to the RAC2 specimens. This can be ascribed to the enhanced water absorption of RAC after these enhancement methods.

A general trend of mass loss occurred after around 4 to 6 freeze-thaw cycles for all the concrete specimens, and the degree of the mass loss increased with increase in w/c ratio and increased in the freezing and thawing cycles. This is attributed to the higher number of capillary pores, average aperture and porosity of higher w/c ratios. The NAC1 specimens recorded the lowest mass loss across all the concrete specimens after the end of the 20th freezing and thawing cycles. Whereas the RAC2 specimens experienced the highest mass loss. This is mainly attributed to the high water absorption of RA which can drain into the cement paste and then lead to more intense frost damage. The absorbed water within the concrete matrix gets frozen upon exposure to freeze-thaw cycles, leading to internal cracks and pressure, hence resulting in the spalling of mortar and loss of mass (Kazmi et al., 2020). Wu et al. (2017) concluded that the RAC specimens endured lower resistance to freeze and thaw cycles in terms of mass loss, compared to NAC specimens due to internal cracks developed and pressure endured. This is also in line with the work of Kazmi et al. (2020) who stated that the higher mass loss for RAC specimens is ascribed to the additional pores of RAC compared to NAC, which results in a rise in the water ingress through these pores leading to further internal pressure and micro-cracks of RAC. Similarly, Li et al. (2017) stated that the observed higher mass loss for the RAC compared with the NAC after the action of freezing and thawing, is related to the pop-out effect, due to the disintegration of the cement paste surrounding the concrete specimen and the expansion of the saturated RA (due to the high absorption of RA) near the surface of the concrete sample. Li et al. (2017) added, due to the frost action, the generated internal pressure leads to failing of the RA surrounding the cement paste. In addition, given the porous nature of RA, they absorb significant amount of water during the mixing stage of the fresh paste. This would result in delaying the drying of the concrete specimen and increasing the level of saturation of the RAC specimen. Thus, ultimately resulting in higher frost damage and lower resistance to freeze-thawing cycles.

All the treated RAC specimens showed a reduction in mass loss compared to RAC2 mixes. Among all the treated RAC specimens, the SCP+SE mixes showed the lowest mass loss. This is mainly attributed to the strengthening of the attached adhered mortar via the combination of these enhancement methods, which resulted in reduced porosity, lesser cracks and denser

microstructure of the enhanced RAC specimens (Kazmi et al., 2019). It is also attributed to the formed thin coating film of pozzolanic powder around the RA surface that filled up all the pores and reduced the high water absorption of RA (Li et al., 2009). In addition, the use of sand envelop mixing approach further reduced the water absorption of RA during mixing. This is in line with the work of Liang et al. (2015) who reported improved properties of the untreated RAC after using SEMA mixing method. It should be noted that scant studies are available on the effects of treatment methods on the resistance to freeze-thaw of RAC.

5.8.2.3 Compressive strength loss of treated RACs after freeze-thaw cycles

Figure 5.32 shows the effects of freezing and thawing cycles on the compressive strength of the NAC1 specimens, RAC2 specimens and the treated RAC specimens at 4 weeks and 20 weeks exposure time.

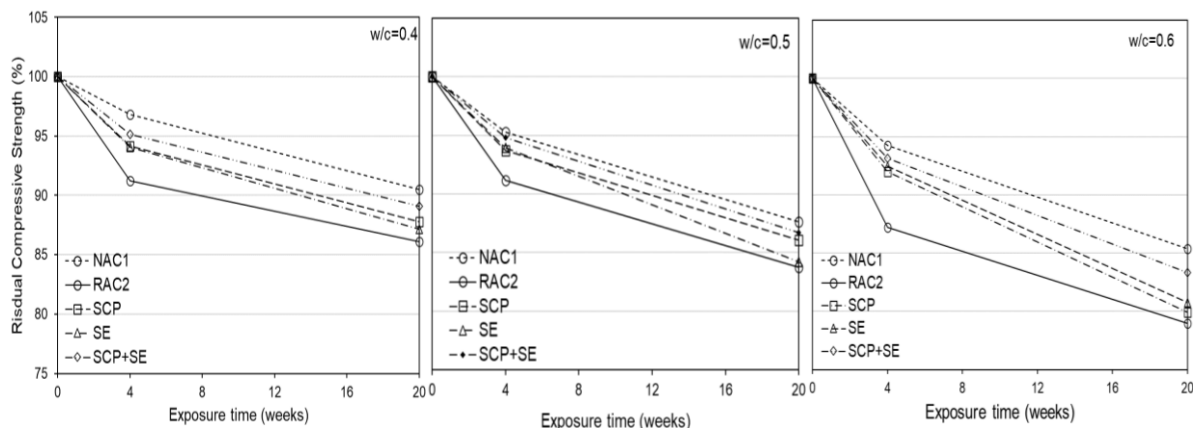


Figure 5.32: Residual compressive strength of the different concretes at 4 weeks and 20 weeks due to freeze-thaw cycles, (a) w/c ratio of 0.4, (b) w/c ratio of 0.5, and (c) w/c ratio of 0.6

Frost damage or freezing and thawing are normally used as an assessment index of durability of concrete. In this study, the frost resistance of the designed concrete specimens was evaluated by measuring the mass loss rate and compressive strength loss rate after exposure to freezing and thawing cycles. According to Guo et al. (2018), the ability of concrete to resist frost damage is mainly governed by porosity, water content, w/c ratio, the environmental conditions, and the aggregate types of the test concrete.

Observations showed a general trend of strength loss across all the concrete specimens after 4 weeks and 20 weeks of freeze-thaw cycles. The strength loss was more prominent in higher w/c ratio concrete mixes and at higher freeze-thaw cycles. This is in line with Wu et al. (2017) study who stated that strength loss of RAC and NAC specimens increased when the freezing

and thawing cycles increased and when the w/c ratio increased. This is also in line with Bogas et al. (2016) study, who reported that the strength losses in high-strength RAC were much lower than those observed in the lower-strength RAC. Rangel et al. (2020) examined the freeze-thaw performance of C35 concrete and C60 concrete for 150 and 300 cycles, and concluded that C35 concrete exhibited higher strength loss values than C60 concretes, due to the higher porosity of C35 and the lower resistance of its internal structure to frost damage. According to Kisku et al. (2017), the phenomenon of concrete strength loss during freeze-thaw cycles is attributed to the exposure of concrete to frost action before the development of desirable strength. The occurred expansion is associated with the formation of ice which leads to disruption and hence, irreparable strength loss.

At the end of the 20th freezing and thawing cycles, all the concrete specimens endured higher compressive strength loss compared to the 4 weeks strength loss. The highest strength losses at the end of the freezing and thawing cycles were exhibited by the RAC2 specimens. The higher reduction observed in the strength of the RAC specimen is mainly ascribed to the inner cracks evolved in the cement paste and the ITZ, which loosened the paste and weakened the bond between the aggregates and the cement paste. Another possible reason is the high water absorption of RA which can drain into the cement paste and then lead to more intense frost damage. Kazmi et al. (2019) stated that the higher strength loss in RAC compared to NAC after freezing and thawing cycles could be the results of many factors, i.e., higher water absorption of RA, mineralogical types of aggregates, higher porosity of RAC, w/c ratio, and air content. Similarly, Wu et al. (2017) concluded that the RAC specimens endured lower resistance to freeze and thaw cycles in terms of cubic compressive strength and mass loss, compared to NAC specimens due to internal cracks developed and pressure endured.

All the treated RAC specimens were able to minimize the strength losses of the untreated RAC. The best-performed treatment in terms of enhancing the frost resistance of untreated RAC was for the SCP+SE mixes. This could be explained as the coupled effects of these two methods resulted in higher quality RAC compared to the sole use of these two enhancement methods. The literature showed no studies on the effects of bi-combination enhancement methods on the resistance of RAC to freezing-thawing cycles.

The improved frost resistance of the SCP mixes is mainly attributed to the formation of a thin coating film of pozzolanic powder around the RA surface that occupied all the pores and reduced the high water absorption of RA (Li et al., 2009). The enhanced strength loss of the

SE mixes can be ascribed to the use of this batching technique (SE) which stems from allowing the sand particles in the mixture to mix more readily with water and cement, thus reducing the water absorbed by the RA. This is in line with the work of Liang et al. (2015) who reported improved properties of the untreated RAC after using the SE mixing method.

5.8.3 Sulphate attack resistance

The physical and mechanical degradations of the NAC1 specimens, the untreated RAC2 specimens, and the enhanced RAC specimens due to sulphate attack was evaluated in terms of mass change and compressive strength change. The main test specimens were soaked in sodium sulphate-based solution to test the effects of sulphate attack on the strength change rate at 28-day (4 weeks) and 140-day (20 weeks) of the test specimens, compared to the reference specimens which were soaked in tap water, at 0.4, 0.5, and 0.6 w/c ratio. In addition, the study also included the mass change rate, which was measured every 4 weeks at 0.4, 0.5, and 0.6 w/c ratio. Visual inspection was also carried out to examine any physical damage/ defects to the test specimens due to sulphate attack.

5.8.3.1 Visual inspection

Figure 5.33 shows some of the test specimens after 20 weeks of exposure to sulphate attack. The results of the visual inspection for any physical change to the test specimens showed that there were no observed changes in terms of expansion in dimension or any spalling in any of the test specimens after immersing in sodium sulphate solution for 20 weeks. Crystallized salt and efflorescence were observed covering the upper surface of the test specimens after exposure to the sulphate environment. The degree of the crystallized salt was observed to increase with increased time of immersion in a sulphate solution.

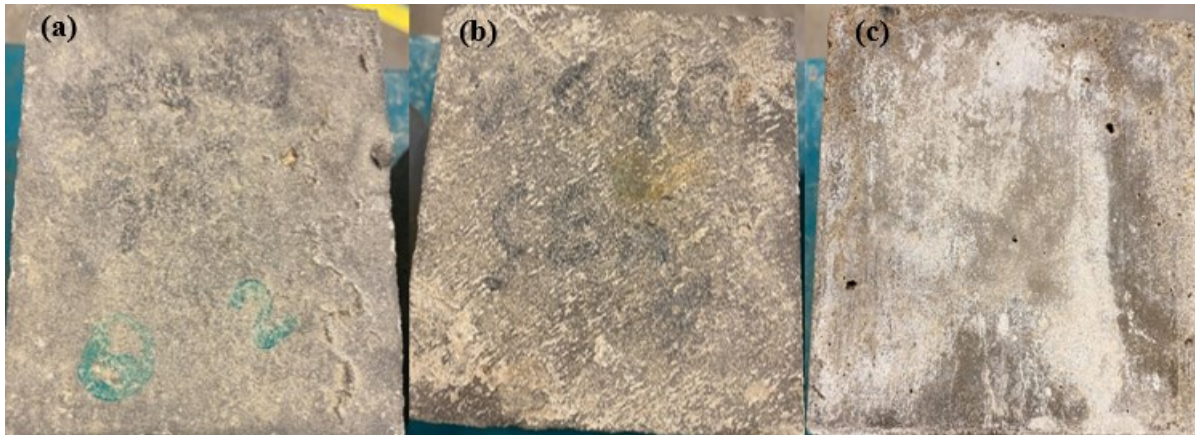


Figure 5.33: Some of the test specimens after 20 weeks of exposure to sulphate, (a) NAC1 specimen, (b) SCP+SE specimen, (c) RAC2 specimen

5.8.3.2 Mass change after sulphate attack

The results of the mass change rate of the NAC1, RAC2, SCP, SE, SCP+SE concrete specimens under sulphate attack for 20 weeks are shown in Figure 5.34.

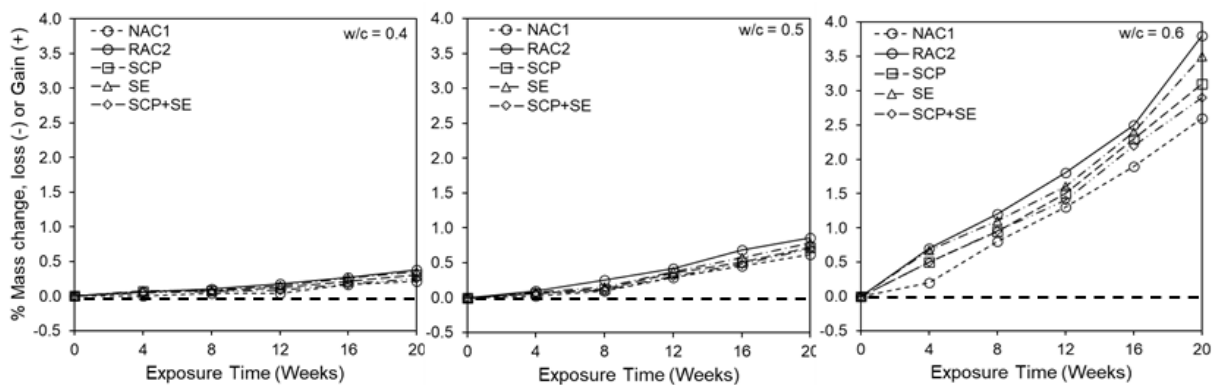


Figure 5.34: Mass change (loss or gain) of the treated RACs due to sulphate attack. (a) $w/c = 0.4$, (b) $w/c = 0.5$, (c) $w/c = 0.6$

Sulphate attack is one of the major durability concerns of concrete due to the expansion and degradation/ deterioration caused upon concrete exposure to sulphate-rich environment. The results showed a general trend of mass increase for all the concrete specimens after exposure to sulphate solution at all w/c ratios. This is due to the formed ettringite within the concrete

structure that causes internal stresses that leads to the loss of strength. Ettringite formed as the result of the occurred reaction between the hydrated cement products and the sulphate ions in the sulphate solutions, leading to the production of gypsum. This produced gypsum converts the tricalcium aluminate (C_3A) to ettringite (Mullauer et al., 2013; Bizzozero et al., 2014).

The growth rate of sulphate concentration by penetration through the micropores in the first 4 weeks is low and slow because of the low water absorption of concrete. The decrease in sulphate content with depth of concrete is also because sulphate ions needs to transfer to the interior structure of the unsaturated concrete by either diffusion, capillary sorption, and penetration (Zuo et al., 2012).

The growth rate of sulphate concentration then increases with time, as the porosity of concrete increases due to the occurred reaction between the sulphate ions and the hydrated cementitious products. The gypsum and ettringite formed in the micropores of concrete via this chemical reaction can delay the diffusion process during the first 4 weeks of sulphate exposure. Nonetheless, this diffusion process accelerates with time as a result of increased concrete porosity due to the generated micro-cracks because of the internal crystallisation pressure applied on the pore walls of concrete by the ettringite formed. Additionally, another reason that could accelerate the diffusion process is the leaching of calcium (Euml et al., 2003; Rozière et al., 2009).

After 20 weeks of sulphate exposure, the NAC1 specimens exhibited the lowest mass gain across all the concrete specimens, whilst the untreated RAC2 specimens endured the highest mass gain. This can be ascribed to the poor quality of RA compared to NA. RA is porous in nature, hence it absorbed a significant amount of water during mixing. This resulted in higher porosity of concrete which in turn leads to higher penetration of sulphate ion. Thus, higher uptake of gypsum and greater formation of ettringite was obtained, and ultimately greater damage to sulphate attack. This is in line with the results of Xie et al. (2020) study, which showed that the mass gain of RAC increased slightly up to 0.69% by 40 weeks of exposure to sulphate due to the ettringite and gypsum (expansion products) formed by the chemical reaction between the sulphate ions and the hydrated cement products

All the enhanced RACs showed a lesser gain in mass and enhanced sulphate resistance after 20 weeks of exposure to sulphate, compared to the untreated RAC2 specimens. The bi-combination of SCP+SE showed the lowest gain in mass compared to the sole use of SCP

method and the sole use of SE method. This could be explained by the enhanced porosity due to the pozzolan coated layer formed around the RA surface that filled the micropores and the micro-cracks of RA. In addition, the use of the SE mixing method resulted in further enhancement due to the efficiency of the sand enveloped batching technique in reducing the water absorption of RA during mixing, and hence strengthening the whole matrix (Wang et al., 2017). The literature showed little research on the effects of bi-combination of enhancement methods on the resistance to sulphate attack of RAC. Kazmi et al. (2019) reported lesser mass gain for treated RACs compared with untreated RACs, after 10 weeks of sulphate exposure.

5.8.3.3 Compressive strength loss after exposure to sulphate

Figure 5.35 shows the residual compressive strength of the NAC1, the untreated RAC2, and the enhanced RACs after exposure of sulphate solution for up to 20 weeks. Overall, all the test concrete specimens endured compressive strength loss after exposure to sulphate solution. The strength loss rate is higher at the end of the 20 weeks exposure and higher w/c ratios. None of the test concrete specimens showed significant reduction in compressive strength after 4 weeks of exposure to sulphate solution except for the untreated RAC2 specimen. Xie et al. (2020) examined the effects of sulphate attack on untreated recycled aggregate concrete for up to 40 weeks, the results showed that the RACs exposed to sulphate attack showed higher strength loss by 20% compared to RACs without sulphate, after 40 weeks of exposure time.

In addition, the RACs started to exhibit a loss in strength after 22 weeks of exposure time. Xie et al. (2020) explained these results as the internal pressure caused by the crystallisation of ettringite exceeded the tensile strength capacity of concrete, resulting in internal propagated microcracks and damage.

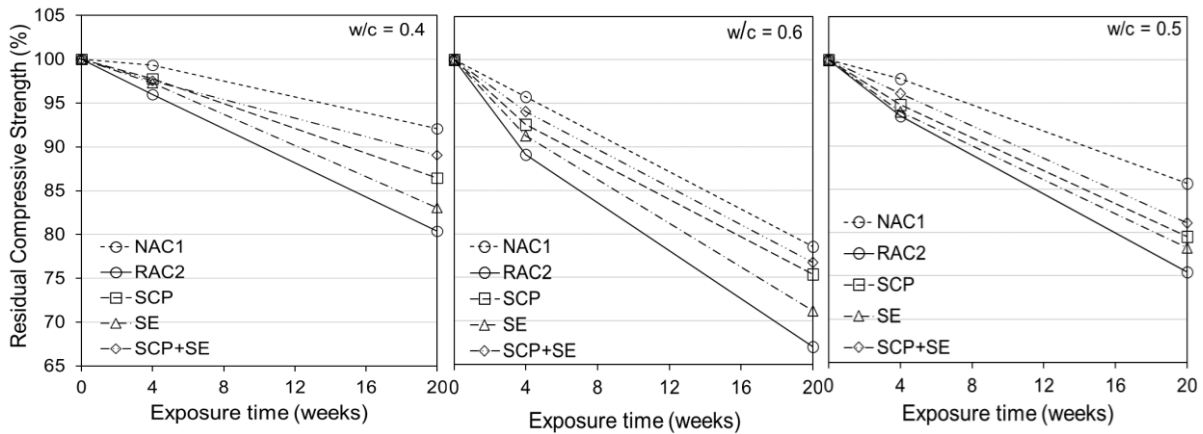


Figure 5.35: Residual compressive strength of the treated RACs due to sulphate exposure, (a) $w/c=0.5$, (b) $w/c=0.5$, (c) $w/c=0.6$

All the enhanced RACs specimens showed a lesser reduction in the 4 weeks strength compared to the untreated RAC2 specimens. The combined treatments given in SCP+SE specimens showed the lowest reduction in compressive strength after 4 weeks of exposure time compared to the SE and SCP specimens.

After 20 weeks of immersion in sulphate solution, all the concrete specimens showed a higher reduction in compressive strength loss compared to the 4 weeks of sulphate attack. Amongst all the concrete specimens, the NAC1 specimens recorded the lowest loss in compressive strength after 20 weeks of exposure to sulphate solution, whereas the RAC2 specimens exhibited the highest strength loss. This can be attributed to the poor quality of RA compared to NA. RA is porous in nature, hence it absorbed significant amount of water during mixing. This would result in higher porosity of concrete which in turn leads to higher penetration of sulphate ion. Hence, the increase in porosity resulted in higher uptake of gypsum and greater formation of ettringite, and ultimately greater damage to sulphate attack. This in line with the work of Kazmi et al. (2019) who reported 9.5% higher loss in strength for RAC in comparison with NAC. Similarly, Bulatovic et al. (2017) reported higher strength loss for the RACs than the NACs by 23% and 3%, after 180 days of exposure to sulphate solution, at 0.55 and 0.38 w/c ratios, respectively. Moreover, after 365 days of exposure time, the untreated RACs exhibited higher strength loss than NAC1 by 9% and 3%, at 0.55 and 0.38 w/c ratios, respectively.

Xie et al. (2020) examined the effects of sulphate attack on recycled aggregate concrete for up to 40 weeks, the results showed that the RACs exposed to sulphate attack showed higher

strength loss by 20% compared RACs without sulphate, after 40 weeks of exposure time. In addition the RACs started to exhibit loss in strength after 22 weeks of exposure time. The authors explained these results as the internal pressure caused by the crystallisation of ettringite exceeded the tensile strength of the capacity of concrete, resulting in internal propagated microcracks and damage.

The results also indicated enhanced sulphate resistance achieved by the enhanced RACs in terms of strength loss after 20 weeks of sulphate exposure. The SCP+SE showed the lowest reduction in compressive strength after 20 weeks of exposure to sulphate. This could be attributed to the synergetic effects of the bi-combination of SCP+SE. The enhanced sulphate resistance of the SCP specimens could be attributed by the enhanced water absorption due to the pozzolan coated layer formed around the RA surface that filled the micropores and the micro-cracks of RA. The enhanced resistance to sulphate attack of the SE specimens can be attributed to the efficacy of the sand envelope batching technique in reducing the water absorption of RA during mixing, and hence densifying the whole matrix (Wang et al., 2017).

The literature shows that concrete under sulphate exposure exhibited a higher increase in its compressive strength up to 22 to 25 weeks compared to water cured concretes, and then the compressive strength tends to decrease rapidly at later ages of exposure to sulphate. Xie et al. (2020) reported about a 10% to 12% higher increase in compressive strength for untreated recycled aggregate concrete exposed to sulphate solution compared with concretes cured in water after 22 weeks of curing age. This higher increase in compressive strength can be ascribed due to the pore structure being filled by the expansion products. Nonetheless, this was not observed in the current study and this could be because the present study has only examined the compressive strength loss of the concrete test specimens after 4 weeks and 20 weeks of sulphate attack.

The overall durability performance of RAC produced with soaking in cement-PFA+SF and sand enveloped batching technique and the combination of both of them can be summarised in the following points:

- The untreated RAC exhibited lower durability performance in terms of water absorption, freeze-thaw resistance, and sulphate attack, compared to NAC.
- The sole use of soaking in cement-PFA+SF solution exhibited better durability performance compared to the sole use of sand enveloped mixing approach.

- The combination of SCP+SE achieved the best results in terms of resistance to freeze-thaw, resistance to sulphate attack, and water absorption.
- The combination of SCP+SE treatment reduced the loss in compressive strength by 4% and 6%, after 20 freeze-thaw cycles, and 140 days of sulphate attack, respectively, at 0.5 w/c ratio.
- The SCP+SE treatment has also reduced the water absorption of RAC by 16.6%, at 0.5 w/c ratio.

5.9 Effects of Treatment & Batching Techniques on the Microstructure of RAC

The microstructural investigation is a key parameter to validate the results of the investigated effects of the different used treatments on the mechanical, structural, and durability properties. It plays an important role to provide deep scientific understanding on the mechanism behind the enhanced properties of RAC after the utilisation of treatments.

Microstructural investigation was carried out using Scan Electron Microscopy (SEM) images of the morphology and the microstructure of the different components of the enhanced RAC specimens. It also was used to identify cementitious hydrate compounds developed during the hydration reaction in comparison with the visual images obtained for the untreated RAC specimen. It also showed any changes occurred to the old and the new ITZ after the applications of the enhancement methods utilised.

5.9.1 SEM analyses

- *SEM observation for the microstructure of NAC1 vs. RAC2*

Figure 5.36 shows SEM images of NAC1, while Figure 5.37 shows SEM images of the untreated RAC2 samples. The SEM observations for the NAC1 specimen revealed that the microstructure of the NAC1 is well-formed with good interlocking behaviour between the cement paste and the natural aggregate, specifically at the interfacial zones. Whereas the SEM observations for the untreated RAC2 specimens showed that the microstructure of the RAC2 specimen is quite different and complicated structure than that of the NAC1 specimen. This is due to the presence of the adhered mortar on the RA surface which leads to the formation of two interfacial transition zones (ITZ). The first ITZ is between the RA and the adhered mortar, while the 2nd ITZ is between the adhered mortar and the new cement paste. This is in line with work of Poon et al. (2004), Otsuki et al. (2003), and Li et al. (2012).

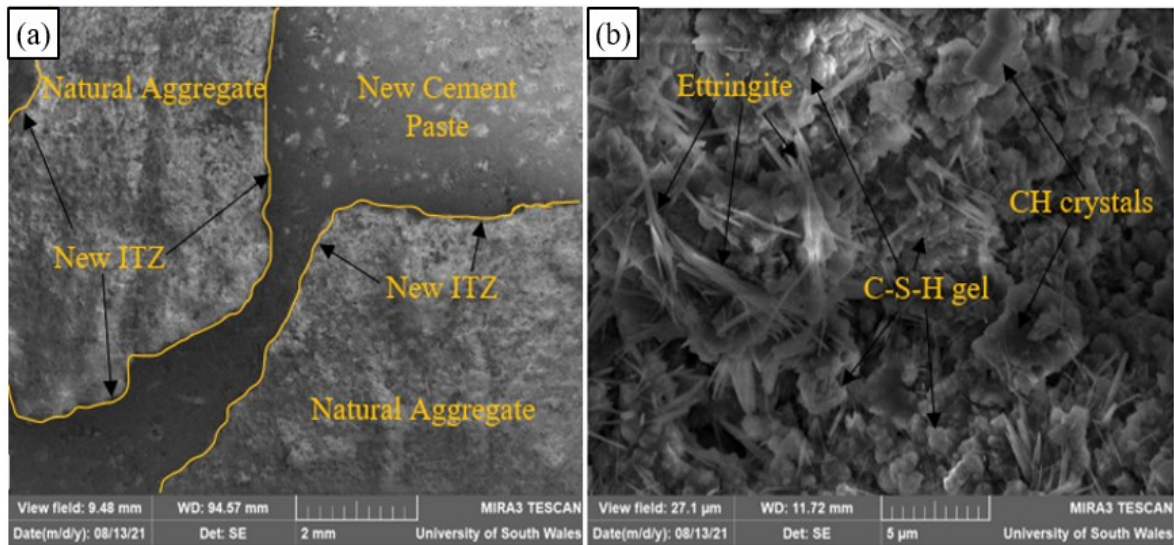


Figure 5.36: SEM images of NAC1 sample, (a) microstructure of NAC1 sample, (b) SEM image for the hydrated compounds developed in NAC1 sample

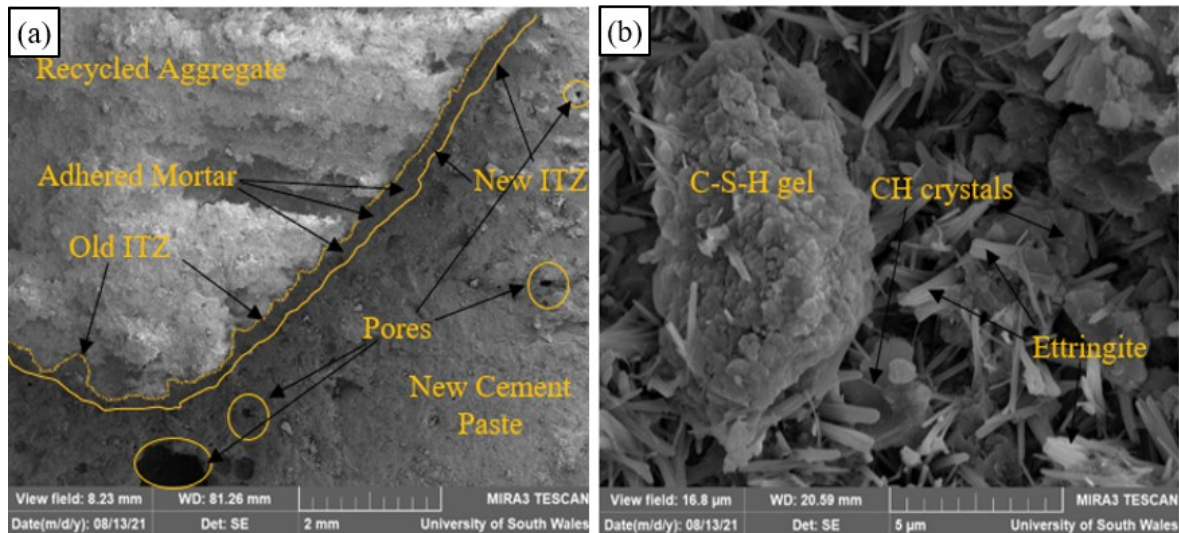


Figure 5.37: SEM images of RAC2 sample, (a) microstructure of RAC2 sample, (b) SEM image for the hydrated compounds developed in RAC2 sample

Furthermore, the SEM observation for NAC1 specimen showed that the constructed cement paste in the designed mix possess strong coherence. Whilst the SEM observation for RAC2 specimen indicates the appearance of pores, voids, cavities, and hollow spaces. The presence of the clustered pores, and micro-cracks around the interfacial transition zone, indicated that the cement paste was not sufficiently compacted. These porous zones and cavities ultimately weaken the bond between the aggregates and the cement paste, which may possibly explain the lowered strength of RAC2 specimens compared to the NAC1 specimen (Poon et al., 2004).

The old interfacial transition zone in RAC matrix plays a vital role in defining the quality of RAC compared to the new interfacial transition zone. Otsuki et al. (2003) stated that at high water to cement ratios, if the characteristics of the old interfacial transition zone is better than the new interfacial transition zone, the strength of the RAC is comparable to the of NAC. Whilst at low water to cement ratios, a weaker old interfacial transition zone results in lower strength of RAC compared to NAC. According to Xiao et al. (2013), an increase in the ratio of the mechanical properties of the old interfacial transition zone (i.e., elastic modulus and strength), leads to higher strength but reduced ductility.

Accordingly, it can be argued that the old interfacial transition zone formed the weakest link in the RAC2 matrix. The old interfacial transition zone resulted in more fragile microstructure of RAC due to its porous nature, weak bonding with the new cement paste, the presence of the loose particles, voids, pores, and micro-cracks (Nayak & Dutta, 2017). In addition, the adhered mortar has a lower modulus of elasticity to that of the RA, which resulted in lower modulus of elasticity of the RAC2 compared to NAC1 (Otsuki et al., 2003).

The characteristics of the old interfacial transition zone is governed by the quality of the adhered mortar, and the type of aggregate. For instance, the old interfacial transition zone was found to be thicker and better for recycled limestone aggregate than recycled gravel aggregate (Xiao et al., 2013). Xiao et al. (2013) argued that the old interfacial transition zone acts as the weakest link that limits the strength phase in RAC as it forms a barrier wall between the cement paste phase and the RA phase within concrete. The old interfacial transition zone also prevents transferring the loads in RAC as the cracks develops first near the old interfacial transition zone (Tam et al., 2005; Otsuki et al., 2003; Mehta & Monterio, 1986).

Poon et al. (2004) pointed out that the interfacial transition zone acts as a gradual transition zone in which its thickness is influenced by the degree of hydration and the content of the adhered mortar on the RA surface. Behera et al. (2014) argued that the interfacial transition zone is highly porous and consists of less unhydrated products, higher concentration of calcium hydroxide, and ettringite. Poon et al. (2004) added that the interfacial transition zone comprised of numerous minute intrinsic pores, voids, micro-cracks, and fissures.

According to Thomas et al. (2013), Xiao et al. (2013a), and Xiao et al. (2013b), the porous nature of interfacial transition zone leads to lower strength and reduced modulus of elasticity around the surrounded cement paste matrix. The authors added that, owing to the very poor

microstructure of interfacial transition zone, the RAC stiffness is lowered and does not withstand the transferred stresses.

Khalaf & DeVenny (2004) argued that the cement paste can only partially penetrate the RA surface due to the variation in sizes of the existing pores and cracks on the RA surface. However, water can easily penetrate these pores which explains the higher water absorption of RA. Khalaf & DeVenny (2004) also stated that, number of fine flake-like and whisker like crystals was observed in the pores and voids of the interfacial transition zone. Behera et al. (2014) revealed that, the incomplete formation of hydration calcium hydroxide crystals attached to the surface of the RA, leads to the development of a highly porous structure in the interfacial transition zone. This was due to the accumulation of water film in the surrounding area to the RA surface. Accordingly, this may explain the poor durability performance of the RAC2 specimen, as it was associated with the porous nature of RA, the higher absorption capacity, and the poor old interfacial transition zone.

It can also be seen that similar produced hydration compounds were developed in both NAC1 and RAC2 samples as shown in Figures 5.36b and 5.37b, respectively. The hydrated compounds observed were identified based on the EDS analysis given in Section 5.9.2. The hydrated compounds observed in the NAC1 and the RAC2 samples composed of column-shaped crystals known as portlandites or calcium hydroxide hydrates $\text{Ca}(\text{OH})_2$, and smaller but greater in growth crystals globular-like particles clumped together with no definite shape (honeycomb) known as C-S-H and/or C-A-H (cement silicates and aluminates hydration) gels. In addition, another hydration compound was identified as needle shaped ettringite crystals $[\text{Ca}_6\text{Al}_2(\text{SO}_4)_3(\text{OH})_{12}\cdot 26\text{H}_2\text{O}]$, precipitates in both the NAC1 and the RAC2 samples.

- ***SEM observation for the microstructure of SCP, SE, SCP+SE vs. RAC2***

Figures 5.38, 5.39, and 5.40 show SEM images of the SE concrete sample, the SCP concrete sample, and the SCP+SE concrete sample, respectively.

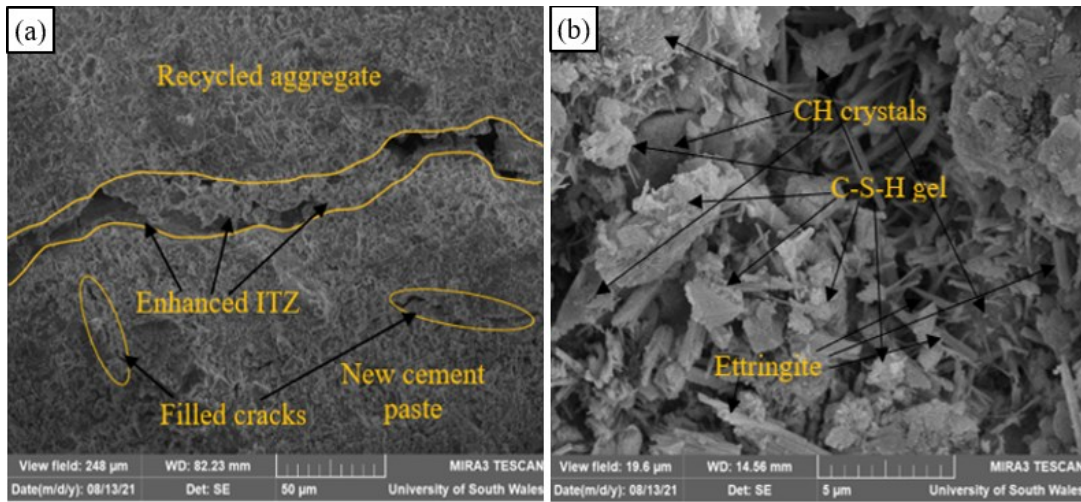


Figure 5.38: SEM images for SCP sample, (a) microstructure of SCP sample, (b) SEM image for the hydrated compounds developed in SCP sample

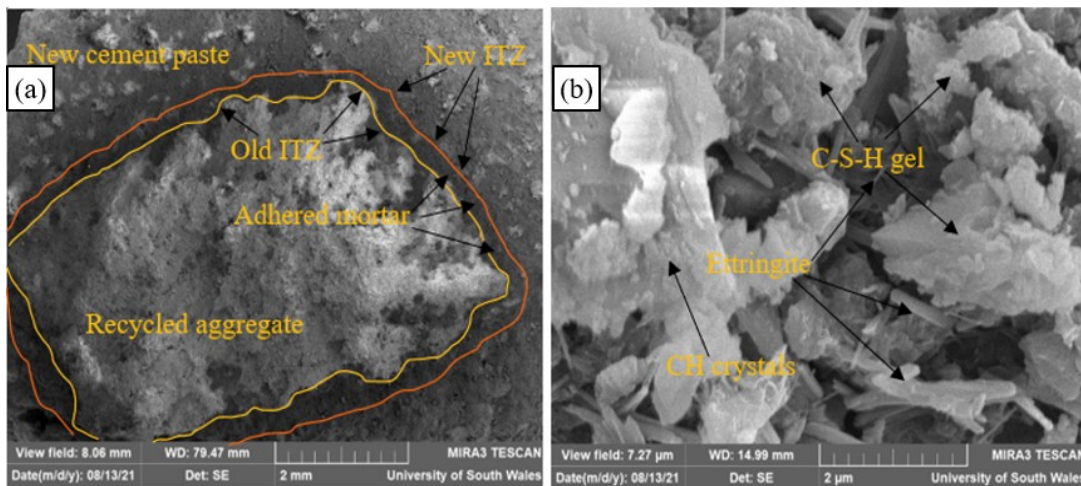


Figure 5.39: SEM images for SE sample, (a) microstructure of SE sample, (b) SEM image for the hydrated compounds developed in SE sample

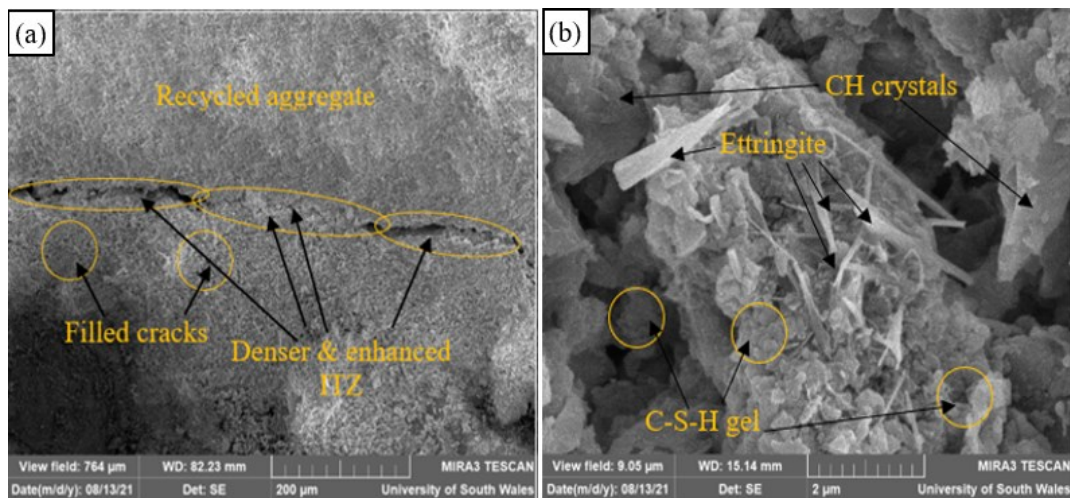


Figure 5.40: SEM images for SCP+SE sample, (a) microstructure of SCP+SE sample, (b) SEM image for the hydrated compounds developed in SCP+SE sample

SEM analysis – SCP sample: the SEM observations for the SCP specimen (Figure 5.38a) showed that, the interfacial transition zone was much tighter and more compacted, and the width and number of the micro-cracks were reduced, compared to the untreated RAC2 specimen. It was also observed that the number of pores and voids were reduced which reflects on the reduced porosity. This was possibly due to the larger amount of the calcium silicate hydrates and calcium hydroxide products that filled the pores and the micro-cracks. In addition, other possible reasons behind the microstructure enhancement of RAC after coating with cement-PFA+SF solution are as follow, (i) the relatively lower water to binder ratio of coated layer on the RA surface leads to denser and stronger interfacial transition zone, thus higher strength of RAC. (ii) the use of micro-fillers SF and PFA tend to flocculate due to their overwhelming specific area and better packing density. (iii) the coated cement- pozzolan layer on the RA surface forms a barrier that reduces inner bleeding of water. (iv) the incorporation of the treated RA in RAC limits the amount of the absorbed effective mixing water during mixing.

This in line with the study of Wang et al. (2020) who treated RA with cement and fly ash slurry. The results of the SEM observations in Wang et al. (2020) showed lesser and smaller micro-cracks and pores at the interfacial transition zone zone, compared to the untreated RAC specimen. Wang et al. (2020) added that, the new ITZ was filled with overlaid hydration products, the micro-cracks got disappeared and the old interfacial transition zone was enhanced. Consequently, the results indicated that the slurry wrapping treatment can optimize the interfacial transition zone coating paste. Similarly, Kong et al. (2010) stated that coating and/or soaking RA in pozzolanic slurry/ solution leads to the consumption of the calcium hydroxide accumulated in the voids, micro-pores, and micro-cracks on the surface of the adhered mortar. Thus, this would generate new hydration products, that further enhance the microstructure of the ITZ.

According to Duan et al. (2013), the micro filling of aggregate by the pozzolan stems from the reaction between the pozzolan and the un-hydrated calcium hydroxide which leads to the production of calcium silicate hydrates that improves the weak structure of RA. Shannag (2000) stressed out that the reaction caused by the pozzolan combined with the filler effect of SF and PFA effectively occupied the pores, the microcracks, and the interfacial transition zone of the RA, thus, this resulted in a denser microstructure of RA and enhanced interfacial transition zone.

According to Mistri et al. (2020) the macro-micro pores have to be filled with fine materials that not only will act as inert filler but will also contribute to the hydration process i.e., secondary hydration, thus, a superior quality RA can be obtained by coating RA with pozzolan solution. Li et al. (2009) examined the effects of treating RA with different pozzolan solutions (fly ash, silica fume, and GGBS) and found that the combination of fly ash and silica fume is more effective for better enhancement in RAC strength due to its packing density in terms of pore filling and denser interfacial transition zone.

Ahmed & Lim (2021) carried out SEM investigations on treated RA with cement-PFA+SF solution and found that non-treated RA have inferior microstructure quality consisting of several cavities, microcracks, and micropores. Ahmed & Lim (2021) also reported that there was a weak bonding between the cement paste and the non-treated RA due to the presence of the adhered mortar, these defects in the microstructure resulted in lowered mechanical performance of RAC. Ahmed & Lim (2021) stated that the SEM observations of the treated RAC by cement-pozzolan solution showed an improved microstructure quality due to the pozzolan effects. The filling-sealing effects of pozzolan effectively counteracted the weaknesses in the RAC microstructure by the production of the secondary calcium silicate hydroxide and enhanced interfacial transition zone. In addition, the cement paste showed enhanced bonding behaviour with the RA, which later resulted in enhanced mechanical performance.

SEM analysis – SE sample: the SEM observations for the SE specimen (Figure 5.39a) also showed a better compacted structure of RAC. It also demonstrated fewer cracks and lesser pores around the interfacial transition zone due to the coated RA with the sand-rich mortar during the initial stage of mixing. The literature showed limited studies on the microstructure investigations of RAC produced with sand enveloped mixing approach. Jagan et al. (2021) studied the effects of mixing RAC using sand enveloped mixing approach on the microstructure of RAC. The results of the SEM investigations in Jagan et al. (2021) study showed that the microstructure of RAC was enhanced with lesser cracks and pores and better bonding behaviour due to the non-porous stiff sand-rich mortar.

SEM analysis – SCP+SE sample: the SEM images for the SCP+SE specimen (Figure 5.40a) showed the best enhanced microstructure compared to SCP and SE specimen. This was mainly the result of the coupled effects of soaking RA in cement-pozzolan solution followed by mixing using sand enveloped mixing approach. The SCP+SE specimen showed the fewest

cracks and pores and the densest interfacial transition zone. In addition, the microstructure of SCP+SE specimen achieved an excellent combination, and highly strengthened interfacial transition zone with excellent interlock and bonding between the RA and the cement paste. The literature showed no studies on the microstructure investigations of RAC produced with 100% treated RA by soaking in cement-PFA+SF solution combined with sand enveloped mixing approach.

General trend of crystalline components phase (Figures 5.38b, 5.39b, and 5.40b) was found in all the treated RAC samples and similar to that of NAC1 sample and RAC2 sample, with some variations in numbers of the developed crystals. SEM observations showed that the amount of CH and ettringite are less in the SE sample compared to the other samples, whilst the SCP and the SCP+SE samples developed higher numbers of C-S-H gels compared to the other samples. The findings of SEM analyses support the laboratory test results which demonstrated that the SCP+SE mixes achieved the highest enhancements in the compressive strength, tensile splitting strength, flexural strength, modulus of elasticity, water absorption, freeze-thaw resistance, and sulphate attack. The overall microstructural performance of RAC produced with different treatments can be concluded in the following points:

- The microstructure of the RAC had two interfacial transition zones, whereas the microstructure of the NAC had one interfacial transition zone. The SEM images have also indicated that the microstructure of the untreated RAC was poorly compacted with obvious pores, cavities, microcracks, and weak bonding between the RA and the cement paste.
- The observed SEM images for the SCP, the SE, and the SCP+SE specimen showed a better microstructure compared to the untreated RAC.
- Soaking RA in cement-PFA+SF solution presented in the SCP samples showed better compacted microstructure, lesser pores and microcracks, denser interfacial transition zone, and better interlocking behaviour between the RA and the new cement paste.
- The sole use of sand enveloped mixing approach has also resulted in a better compacted and formed microstructure, but the presence of the voids and micro-cracks was more evident compared to the SCP specimen.
- The combination of the SCP+SE enhancement method resulted in the most desired microstructure of the RAC. The synergetic effects of these two methods led to a

relatively stronger and compacted microstructure with the fewest pores and microcracks, stronger and denser ITZs.

5.9.2 EDS analysis

The EDS analysis was carried out for mineralogical assessment of the different studied concrete specimens. The EDS was used for elemental identification and quantitative composition of the chemical elements on material surfaces. The EDS given in this study did not show the compound compositions/ crystalline such as C-S-H gels, CH, and ettringite [$\text{Ca}_6\text{Al}_2(\text{SO}_4)_3(\text{OH})_{12}\cdot 26\text{H}_2\text{O}$], but only showed the chemical oxide compositions / elements of the test concrete samples in terms of single element peaks. The EDS analyses the chemical compositions at a given point on the test concrete sample. Therefore, the atomic weight/ concentration per oxide composition may differ from a point to another within the test sample.

It also should be noted that the EDS device picked up some chemical elements that are irrelevant to the test concrete samples, such as Au (gold) which was picked up in all the test samples in the EDS analysis due to its applications as a coating layer for producing a conductive surface of the test specimen. As (Arsenic) is also an irrelevant chemical element and was also encountered in some of the test samples. Figures 5.41a and 5.41b show the EDS peaks/ patterns of NAC1 sample, and RAC2 sample, respectively.

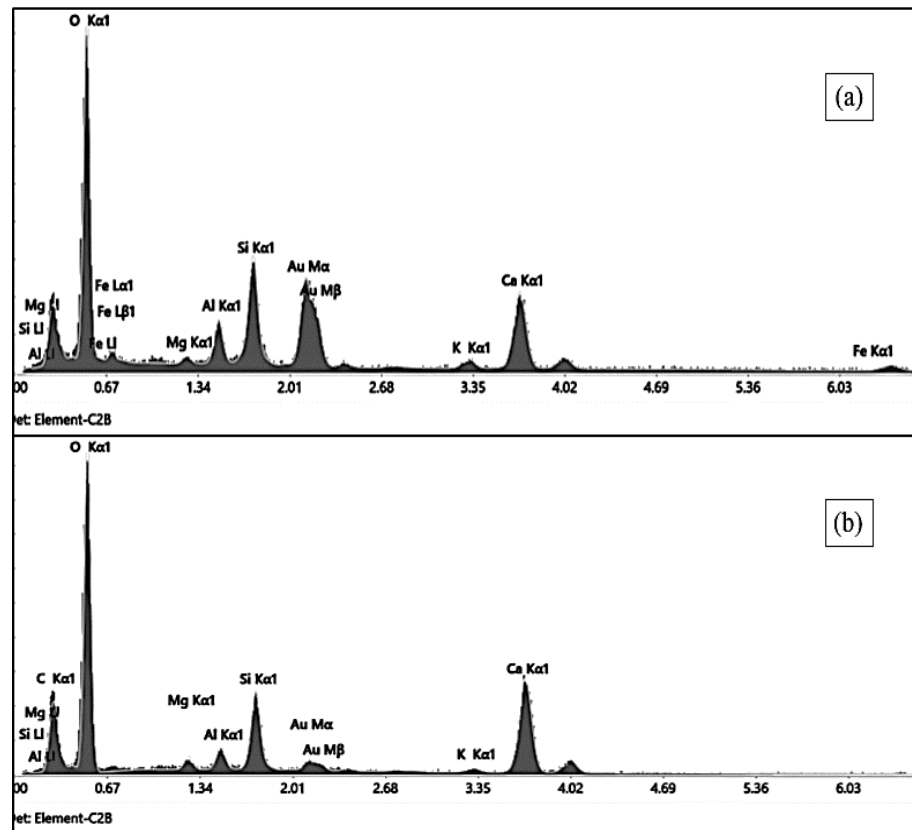


Figure 5.41: EDS analysis, (a) NAC1 sample, and (b) untreated RAC2 sample

The ED spectra of the NAC1 and RAC2 samples (Figures 5.41a, and 5.41b), showed good numbers of distinct sharp peaks of elements of silicon (Si), calcium (Ca), and oxygen (O) being the highest. The RAC2 sample in Figure 5.42b, shows slightly increased intensities for silicon and calcium, this may be ascribed to the presence of the adhered mortar on the RA surface which consists of un-hydrated cement particles that further hydrates upon contact with water. All these elements include in the formation of the compounds of CH, ettringite, and C-S-H gel. Along with these elements, the EDS analysis showed peaks of aluminium (Al), magnesium (Mg), and iron (Fe), for both NAC1 and RAC2 samples.

Figures 5.42a, 5.42b, and 5.42c present the EDS peaks/ patterns for SE sample, SCP sample, and SCP+SE sample, at 0.5 w/c ratio and 28 days of curing, respectively. The EDS analysis for SE sample in Figure 5.42a, showed similar peaks of chemical elements to RAC2 sample. SCP sample and SCP+SE sample in Figures 5.42b and 5.42c produced similar chemical elements peaks, but with increased intensities of silicon (Si) and calcium (Ca), compared to the other concrete samples. SCP sample and SCP+SE sample included coated RA in cement-PFA+SF solution prior to mixing, which explains the increased intensities in silicon and calcium in these both samples. Li et al. (2009) reported that the hydrates in the treated RA

with cement- pozzolan were mainly composed of uniform calcium silicate hydrates and large amount of calcium hydroxide crystals, along with the formation of ettringite.

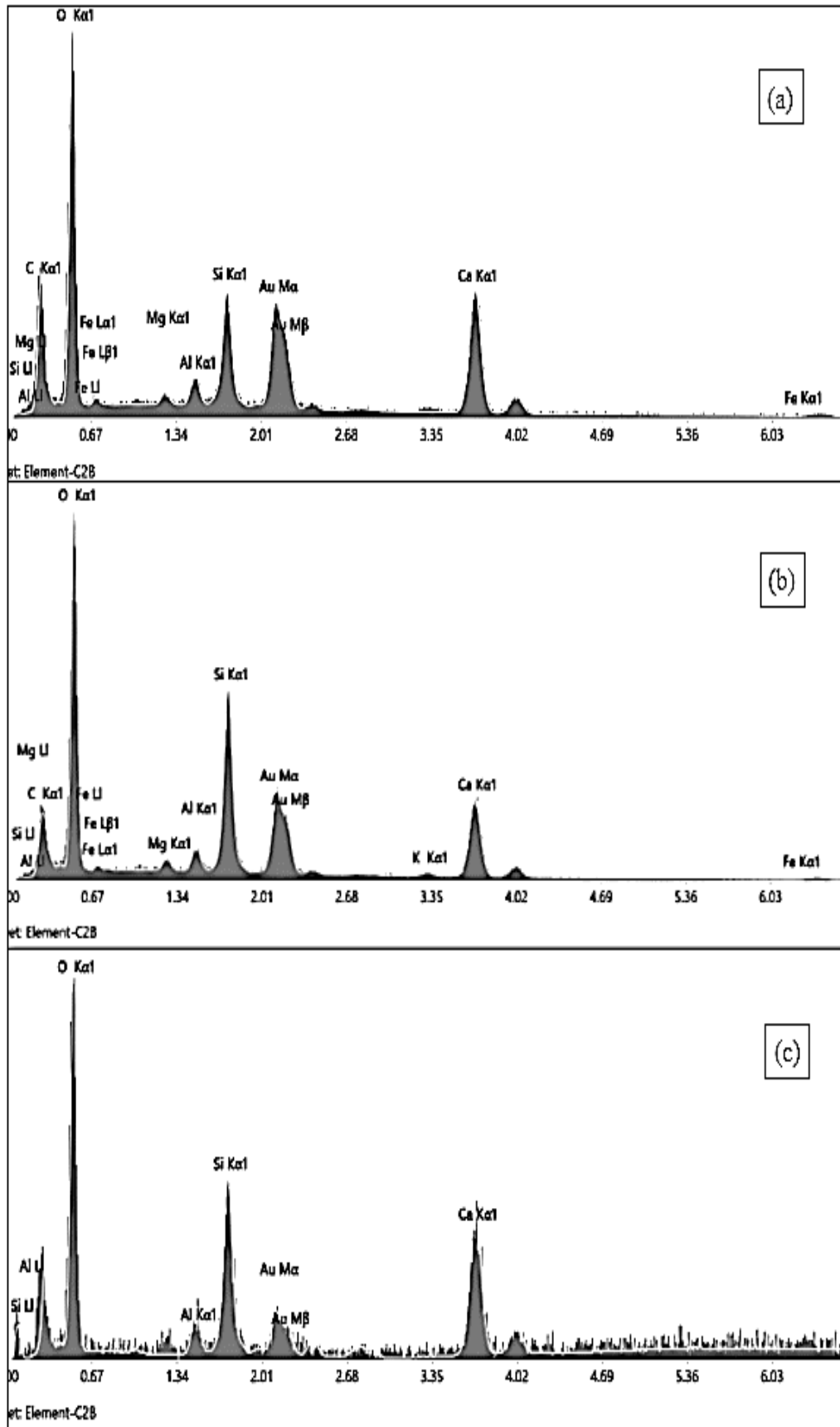


Figure 5.42: EDS analysis, (a) SE sample, (b) SCP sample, (c) SCP+SE sample

5.10 Practical Implications of the Research

The reuse of recycled aggregate or waste aggregate from the construction and demolition waste greatly influences the environment as the process of demolition consumes around 2-3% of energy, and about 2% of carbon emissions are generated during the demolition process (Pu et al., 2021). Thus, the reuse of recycled aggregate can contribute significantly to the preservation of natural resources.

The enormous and rapid growth in the construction industry world wide in the last century in terms of urbanisation has resulted in a significant rise in the amount of waste. Consequently, the use of RA from the construction and demolition waste can be a promising and sustainable option for the construction industry, which would help in achieving sustainable development.

Furthermore, the successful use of RA into new concrete can save the environment by protecting soil and avoid contamination of ground water by reducing or eliminating landfilling of the construction and demolition waste, and hence going towards cleaner and greener environment.

Nonetheless, the current main application field for RA and RAC is limited to non-structural applications due to the inferior quality and engineering performance of RA and RAC compared with NA and NAC. For instance the RA was generally used as filling material, substratum improvement for roads, pavement, and gabions, in Germany. In the United Kingdom, the RA was mainly used for bulk fills, base or fill for drainage structures, road construction, pavements, curbing, noise barriers and embankments, and as foundations for bridges. In Australia, the RA was also widely utilised for path, footpath, cyclepath, and parking bays (Wang et al., 2020).

Nevertheless, the results of the present study showed that using the adopted treatment methods can significantly enhance the engineering properties of the RAC, and expand its application to structural concrete. The findings of the present research can be of great interest to stakeholders, such as recycling plants owners, relevant government sectors and bodies, the construction industry, design engineers, and researchers.

There are a number of research gaps in the literature such as the lack of studies on the effects of utilising RA from the C&DW on RAC engineering performance, very limited studies on

the effects of different batching techniques on RAC compressive strength, durability, and structural performance.

Furthermore, there are limited number of studies examined the durability performance of RAC with treated aggregate from the C&DW including, freeze-thaw resistance and sulphate attack. Accordingly, the results of the current study can be added to the current literature and contribute to the current knowledge by filling these research gaps found in the literature.

The sole use of the treatment method of soaking RA in cement-PFA+SF solution can be adopted by the recycling plants on site for mass production. Whilst the sand enveloped mixing approach can be carried out anywhere such as end users to produce a better quality RAC for structural applications.

To this end, Figure 5.44 and 5.45 show a flow chart that can be adopted by either RA producers or end user to use enhanced RA properties that can be suitable for structural applications. The flowchart firstly follow the WRAP protocol in processing of RA and then proceeds with guidelines on treating RA and/or enhancing RACs.

5.11 Cost analysis

Several factors play significant role in promoting the use of recycled aggregate in the construction industry in comparison with natural aggregate. These are cost efficiency, environmental impact, performance, sustainability, and durability. Table 5.9 shows the price breakdown per concrete mix. It is clearly notable that the untreated RAC mix have a lower carbon footprint and lower price per cubic meter compared to NAC. Nevertheless, based on the durability performance in this study, the untreated RAC exhibited poor durability properties compared to NAC.

Therefore, there was a need to carry out treatment/ enhancement methods in order to enhance the quality of RAC. However, several factors should be considered when selecting the type of the enhancement methods. As shown in Table 5.9, soaking RA in cement-pozzolan solution prior to mixing (SCP mix) increased the cost and the associated carbon footprint of the end product by 93% and 17%, respectively, compared to the untreated RAC. In the contrary, the utilization of sand envelop batching technique (SE mix) kept the same cost and the same carbon footprint compared to the untreated RAC.

Table 5.9: Price breakdown of the different concrete mixes and the associated embodied carbon dioxide footprint

Mix	Constituent						Concrete cost (£/m ³) ^a	Cost /NAC1	Cost/ RAC2	kg CO ₂ e / m ³ concrete ^b
	OPC	PFA	SF	NA	Sand	RA				
Estimated Price (£/t)	150	650	550	40	40	15	-	-	-	-
NAC1 (£/m ³)	67	-	-	58	27	-	152	100%	-	450
RAC2 (£/m ³)	67	-	-	-	27	19	113	74%	100%	437
SCP (£/m ³)	83	48	41	-	27	19	218	143%	193%	530
SE (£/m ³)	67	-	-	-	27	19	113	74%	100%	437
SCP+SE (£/m ³)	83	48	41	-	27	19	218	143%	193%	530

^a Tentative price for each concrete ingredient including SF and PFA were obtained from searching through trading local suppliers.

^b The estimated embodied carbon footprint was calculated based on the data given in ICE (2019) and excluding transportation.

Figure 5.46 shows the cost analysis of the various enhancement methods against several aspects related to untreated RAC. It can be seen the use of bi-combination of enhancement methods (SCP+SE) obtained the best performance in terms of durability properties and compressive strength at 28-days. Nevertheless, the sole use of batching technique (SE) seemed a better choice in terms of other influencing factors such as cost efficiency, carbon dioxide footprint, simplicity, application time, and feasibility.

In view of this discussion, it is quite important to consider the cost-efficiency, sustainability, and efficiency of enhancement method for RA and RAC. Although treatments such as soaking RA in cement-pozzolan may increase the cost and CO₂ emission for RAC, it is still a better choice compared to other treatments utilized by other researchers, i.e., acid treatment, and heating treatment. To this end, in order to successfully promote the use of RA in the construction industry, several factors should be considered specifically the feasibility of the treatment method to be used in practice at bulk production.

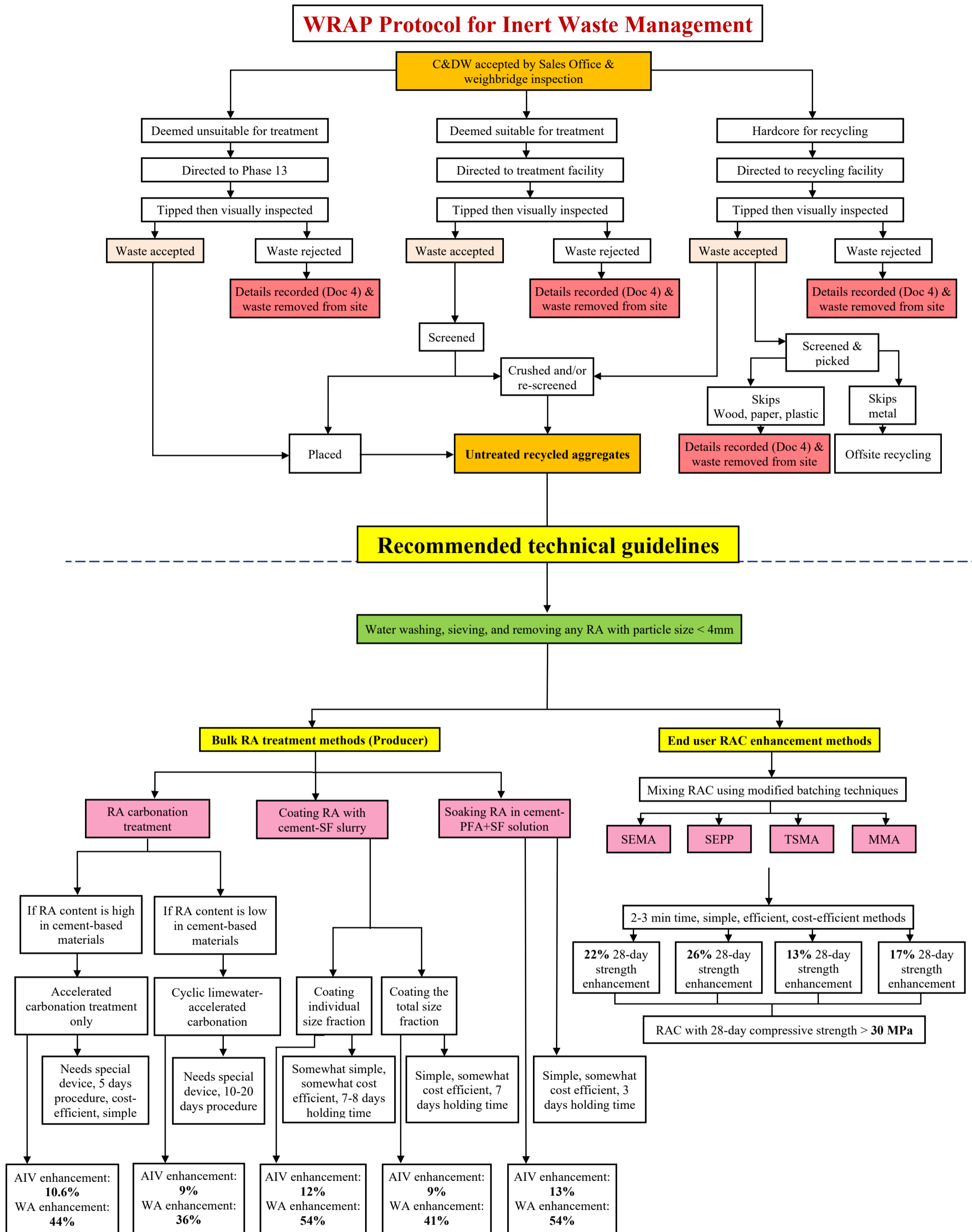


Figure 5.44: Technical guidelines for processing RA via WRAP protocol and then enhancing RA and RAC performance by the RA producer or end user

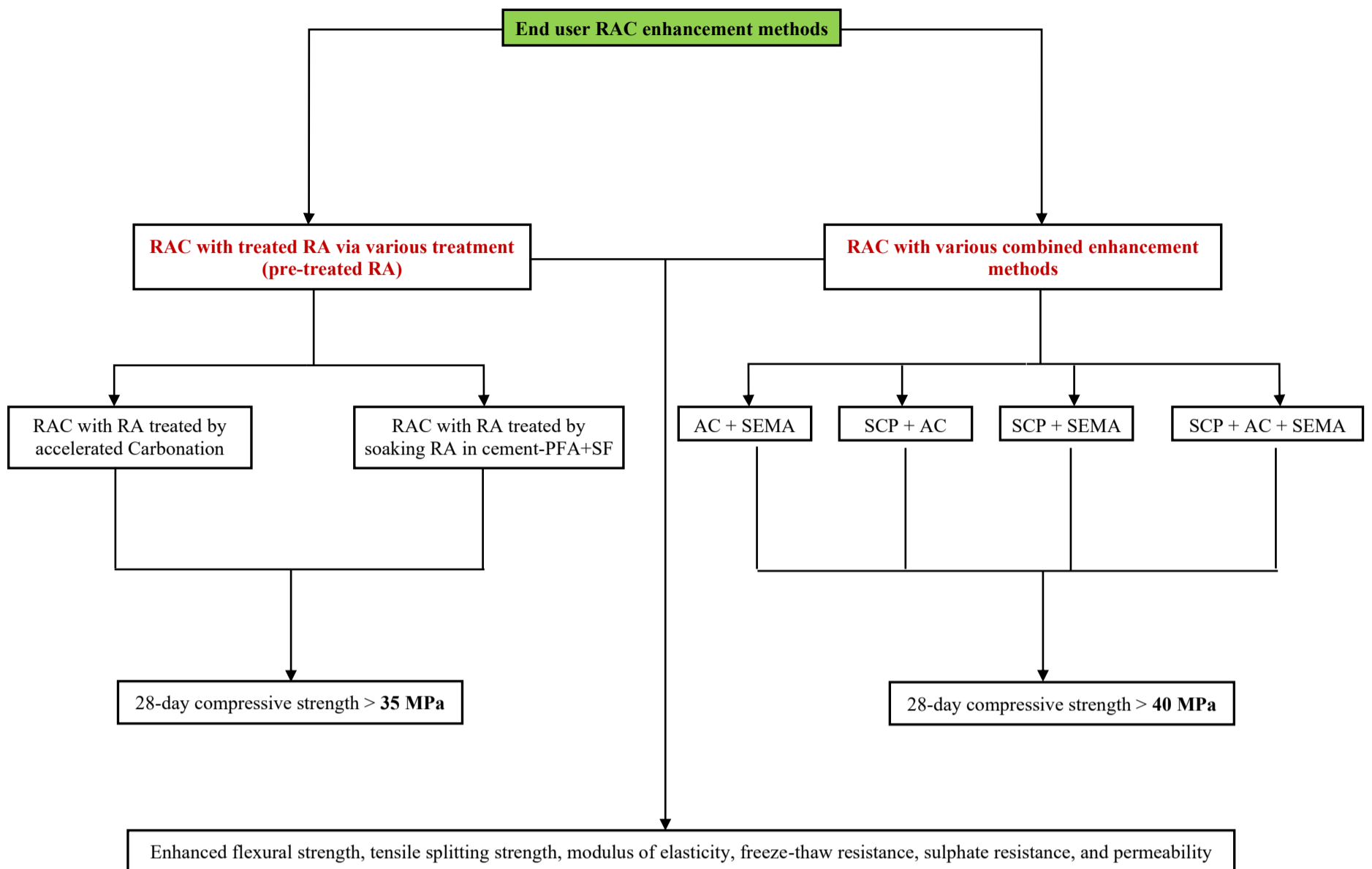


Figure 5.45: Technical guidelines for RAC performance enhancement by the RA producer or end user

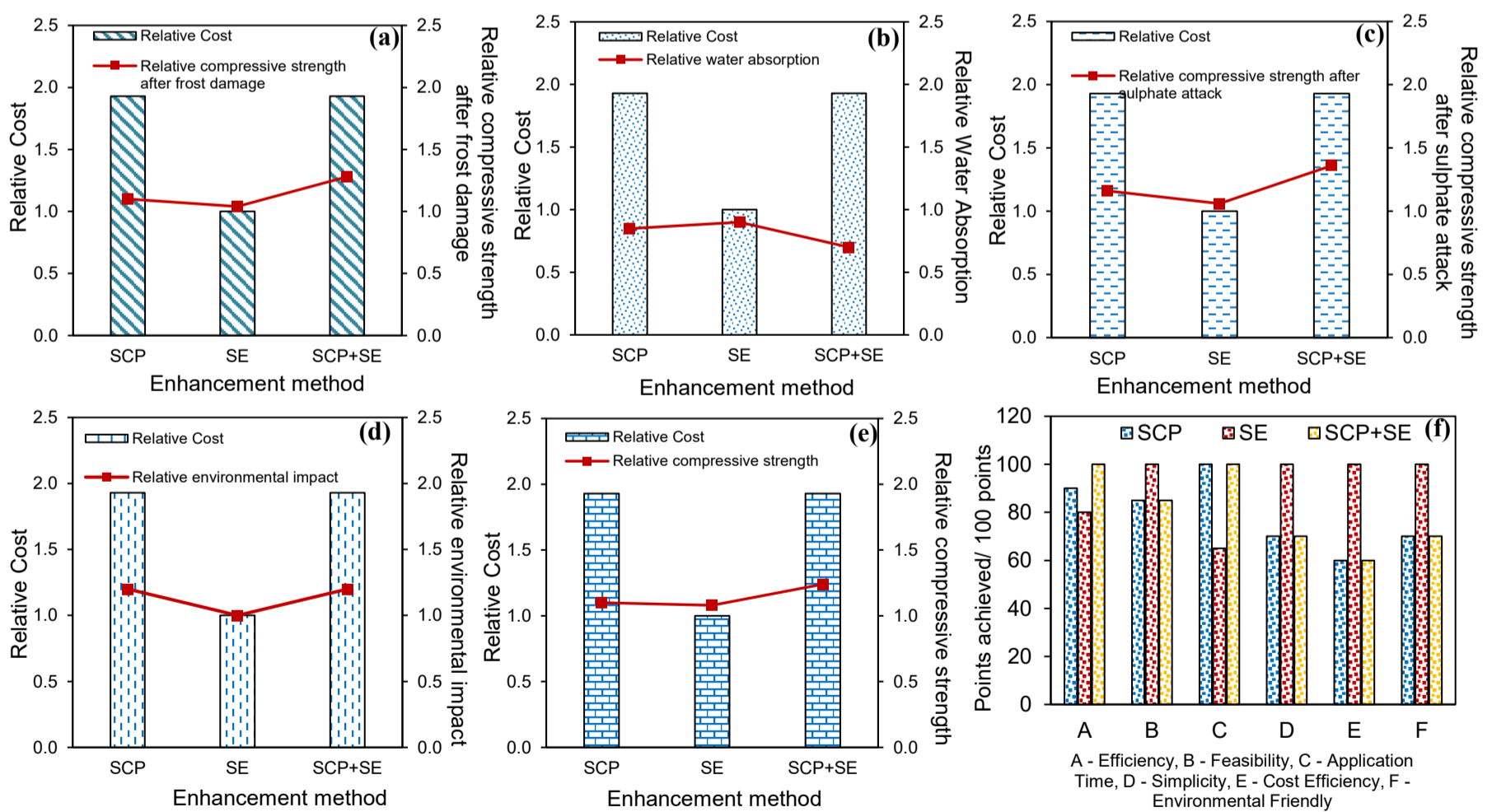


Figure 5.46: Cost analysis of the various enhancement methods: (a) cost vs. compressive strength after 20 cycles of freezing-thawing, (b) cost vs. water absorption, (c) cost vs. compressive strength after exposure to sulphate attack, (d) cost vs. environmental impact, (e) cost vs. 28-day compressive strength, (f) other influencing factors.

CHAPTER SIX - CONCLUSIONS & RECOMMENDATIONS

The overall target of the present research was to overcome the current issues associated with RAC in terms of its limited use to non-structural applications. Thus, the primary aim was to develop a recycled aggregate concrete that is suitable for structural applications by investigating different treatment methods to enhance the RAC quality. Accordingly, this chapter presents the conclusions of this research. Chapter 6 also suggests recommendations for future work to get better scientific understanding and wider applications of RAC.

6.1 Conclusions

Untreated RA and RAC have demonstrated low-quality engineering performance compared to NA and NAC in terms of aggregate characteristics and concrete mechanical, durability, and microstructural properties due to several factors. Two of the main factors is the adhered mortar on the RA surface and the old weak ITZ which results in weak interfacial transition zone and weak bonding within the recycled aggregate concrete matrix. Other concerns include variation in composition, previous loading, processing, and weathering compared to freshly crushed natural aggregates. This research has presented experimental laboratory-based investigations on the effects of different treatment and enhancement methods on enhancing the engineering properties of the untreated RA and RAC. Accordingly, based on the data presented, the following specific conclusions can be drawn:

6.1.1 Effects of different treatments on the AIV & WA of RA

- **Water treatment:** treated RA using water treatment methods exhibited better performance in terms of the WA, however, none of them significantly improved the AIV of RA. Among these methods, self-healing of RA obtained the best results.
- **Carbonation:** carbonation is a viable treatment method for enhancing the engineering properties of RA. There are several key factors affecting the efficiency of the carbonation treatment, where the CO₂ concentration level and carbonation time are the more critical factors. The RA was treated at three CO₂ concentration level of 20%, 50%, and 100% for up to 7 days carbonation time. Carbonation treatment at 50% CO₂ concentration level for six days of carbonation time achieved the best results. The optimal CO₂ concentration level was found to be 50% at 6 days of carbonation. Recycled aggregates treated with three cyclic periods of pre-soaking in limewater

followed by carbonation at 100% CO₂ concentration level for 24 hours, exhibited better improvement in AIV and WA compared to a sole use of accelerated carbonation treatment at the same carbonation conditions. The observed enhancements in the AIV and the WA after accelerated carbonation treatment was mainly due to the carbonation process through the chemical reactions between the available calcium hydroxide on the RA surface and the CO₂ from one side and between the calcium silicate hydrates and CO₂ from other sides. This carbonation process filled the pores and the cracks on the RA surface and sealed its surface.

- ***Soaking RA in sodium silicate-silica fume solution:*** treating RA with soaking in sodium silicate-silica fume solution has also achieved enhancement in the AIV and WA of RA. Soaking RA in in sodium silicate-silica fume solution with 5% replacement level for 4 hrs soaking time was found to be optimal. This was ascribed to the produced C-S-H gel by the chemical rection between sodium silicate and calcium hydroxide with the presence of water and between silica fume and calcium hydroxide simultaneously. The produced C-S-H gel and the secondary C-S-H gel effectively filled the micro-pores, voids, and micro-cracks on the RA surface, which reflected on the reduced WA and enhanced AIV.
- ***Coating RA with cement or cement-silica fume slurry:*** coating the individual size fraction of RA achieved better enhancement in the AIV and the WA compared with coating the whole size fraction of RA. Among all the coating thicknesses, coating RA at 0.1 mm coating thickness obtained the highest enhancement values. Coating RA with cement and silica fume slurry was observed to provide better enhancement in the AIV and the WA, compared to coating RA with only cement slurry. Coating the individual size fraction of RA with cement-silica fume slurry at 0.1mm coating thickness led to the best reduction in the AIV and WA of RA. The observed reduction in water absorption and enhancement in the AIV was mainly due to the RA surface being covered with a thick layer of hydration products and C-S-H gel that acted as a shield that strengthened the adhered mortar and reduced its porosity.
- ***Soaking RA in cement-pozzolan solution:*** soaking RA in different cement-pozzolan solutions were carried out on three different solutions, Portland cement-PFA+SF, Portland cement- PFA+MK, and Portland cement- SF+MK. The RA was soaked in

three prepared solutions with different replacement levels, 5%, 10%, and 15%, for two soaking times 1hr and 4hrs. Among these conditions, soaking in 10% replacement level for 4hrs soaking time was found to be optimal. It was argued that the filling and sealing pores effects of soaking RA in cement- pozzolan solutions resulted in enhanced AIV and WA of RA.

Table 6.1: Summary of the effects of different treatment methods on the AIV and WA of RA

Treatment Regime	Treatment	Type of treatment	AIV value (%)	WA value (%)
Untreated RA	—	—	17	6.1
Regime A treatments	Self-healing	—	18	3.6
	Water washing	Water washing 1	16.5	3.7
		Water washing 2	16.7	5.1
	Water saturation	Full saturation	18	6
		Partial saturation	17	6.1
Regime B treatments	Carbonation	Accelearted carbonation	15.2	3.4
		Cyclic carbonation	15.4	3.9
	Soaking in SS/ SF solution	—	15.6	4.1
	Coating with cement-SF slurry	Coating of the individual size fraction	14.9	2.8
		Coating of the total combined particle sizes	15.4	3.6
	Soaking in cement -pozzolan solutions	Soaking in cement-PFA+SF solution	14.7	2.8

6.1.2 Effects of batching techniques on the compressive strength of RAC

- Mixing RAC with batching techniques:** the untreated recycled aggregate concrete specimen showed lower compressive strength compared to the natural aggregate concrete specimen. All the utilised batching techniques managed to enhance the compressive strength of RAC. Among all the batching techniques used, SEPP_{SF} and SEMA methods achieved the highest enhancement in the 28-day compressive strength. The observed strength enhancement achieved by SEPP_{SF} was possibly due to the addition of SF during the initial mixing stage which effectively filled and sealed the RA surface, leading to a better interlocking between the RA and the cement paste and reduced porosity which resulted in limited amount of mixing water being absorbed by RA during mixing. It was also revealed that the effects of SEMA method on enhancing the RAC mechanical properties arise from that during the first stage of mixing the RA was covered by sand-rich cement paste that effectively sealed its pores and reduced the amount of water absorbed by the RA.

6.1.3 Consistency and compressive strength of the enhanced RAC

The outcome of the initial selective analysis for the nomination of the best treatment methods presented in SCP, SE, AC, SCP+AC, SCP+SE, AC+SE, and SCP+AC+SE treatments underwent laboratory investigations in terms of workability, density, and compressive strength, at 0.4, 0.45, 0.5, 0.55, and 0.6 w/c ratios.

- **Untreated RAC (RAC1):** the untreated recycled aggregate concrete showed inferior compressive strength compared to the natural aggregate concrete at the same mix design parameters. This was due to the poor engineering properties of RA compared to NA and mainly due to the presence of two ITZs in the RAC in which the old ITZ act like a weak link in the RAC matrix.
- **Consistency and compressive strength of the enhanced RACs:** all the utilised treatment methods showed variations of enhancements in the slump, the 7-day compressive strength and the 28-day compressive strength of RAC. In addition, all the treatment methods utilised, and their combinations managed to obtain at least 30MPa which is suitable for structural applications. Among all the combination of treatment methods utilised, the combination of SCP+SE treatments exhibited the highest 28-day compressive strength of 42.3MPa at 0.4 w/c ratio, whilst the sole use of SCP treatment showed the highest the compressive strength of 38.5MPa at 0.4 w/c ratio across all the sole use of treatments. The coupled effects of SCP and SEMA method resulted in reduced porosity of RA and RAC, enhanced bond strength of RA, better interlocking, higher density of RA, lower water absorption, better compacted matrix of RAC, and higher modulus of elasticity of RA. In addition, higher C-S-H gel amount was produced as a result of soaking in cement-PFA+SF solution. All these factors resulted in higher strength RAC.

6.1.4 Flexural, tensile splitting, and modulus of elasticity of the enhanced RACs

- **Flexural strength:** the untreated recycled aggregate concrete showed inferior flexural strength performance compared to the natural aggregate concrete. All the treated RACs showed enhancements in the flexural strength of RAC. Among all the enhancement methods, the combination of SCP and SE methods achieved the best flexural strength performance.

- **Tensile splitting strength:** the untreated RACs exhibited lower tensile splitting strength performance than NAC. The combination of soaking RA in cement-PFA+SF solution prior to mixing followed by mixing using sand enveloped mixing approach exhibited the best enhancement results among all the treatment methods utilised.
- **Modulus of elasticity:** the modulus of elasticity of the untreated RAC was lower than that of the NAC. Amongst all the enhancement methods used, the combination of SCP+SE method performed the best.
- The inferior flexural strength, tensile splitting strength, and modulus of elasticity performance of RAC was mainly due to the lower bond strength and poor interlocking of RA with the cement paste because of the ITZ. In addition, the lower modulus of elasticity of RAC was associated with the lower elastic moduli of RA compared to NA. The high porous nature of RA owing to the presence of pores and micro-cracks on the RA surface along with the old ITZ were also related to the inferior mechanical performance of RAC.
- The increase (enhancements) in the flexural strength, tensile splitting strength, and the modulus of elasticity observed by the SCP treatment was mainly due to the enhanced old ITZ, the strengthened adhered mortar, and the better interlocking the treated RA. In addition, the reduced porosity because of the effects of filling and sealing of the cement-pozzolan has also contributed to improved quality of RAC. On the other hand, the reported increase in the flexural strength, tensile splitting strength, and modulus of elasticity by sand enveloped mixing approach were mainly attributed to the enhanced porosity of RA after it was covered by the pre-mixed stiff and non-porous sand-rich cement paste that sealed the RA surface, strengthened the old ITZ, and reduced the water absorbed by the RA during mixing.

6.1.5 Durability performance of the enhanced RACs

- The untreated RAC exhibited lower durability performance in terms of water absorption, freeze-thaw resistance, and sulphate attack, compared to NAC. These results were mainly ascribed to lower quality of RAC specifically the low porosity of RAC as a result of the presence of micro-pores, cavities, and micro-cracks, and the existence of the poor quality old ITZ.

- The treatments utilised presented in SCP, SE, SCP+SE achieved better durability performance compared to the untreated RAC. The sole use of soaking in cement-PFA+SF solution exhibited better durability performance compared to the sole use of sand enveloped mixing approach. The combination of SCP+SE achieved the best results in terms of resistance to freeze-thaw, resistance to sulphate attack, and water absorption. The combination of SCP+SE treatment reduced the loss in compressive strength by 4% and 6%, after 20 freeze-thaw cycles, and 140 days of sulphate attack, respectively.
- The enhanced durability performance observed by the treatments utilised was mainly due to the enhanced water absorption through the effects of treatments in filling and sealing the pores and the micro-cracks on the RA surface.
- The ACI and EC design equations for predicting the mechanical properties of the enhanced RAC are not desirable. These equations either over-estimated or underestimated the mechanical properties of RAC. This might be due to the lower mechanical properties of the enhanced RACs compared to NAC. Nonetheless, the modified models given in Section 5.7 can be used for predicting the mechanical properties of the enhanced RACs.

6.1.6 Microstructure investigations of the enhanced RACs

The microstructure and morphology of the different examined concretes, natural aggregate concrete, untreated recycled aggregate concrete, RAC produced with the sole use of soaking RA in cement-PFA+SF solution, RAC produced with sand enveloped mixing approach, and RAC produced with the combination of SCP+SE treatment showed different microstructures but relatively similar formation of cementitious hydrates (C-S-H gel, CH, and ettringite). The observed microstructure of these concretes can be summarised as follows:

- The SEM images of the untreated RAC showed a rather complicated microstructure compared to NAC. The microstructure of the RAC had two ITZs whereas the microstructure of the NAC had one ITZ. The SEM images have also indicated that the microstructure of the untreated RAC was poorly compacted with obvious pores, cavities, microcracks, and weak bonding between the RA and the cement paste due to the presence of the old ITZ, whilst the NAC microstructure was more compacted and

well-formed with excellent interlocking behaviour between the NA and the cement paste.

- The observed SEM images for the SCP, the SE, and the SCP+SE specimen showed a better microstructure compared to the untreated RAC. Soaking RA in cement-PFA+SF solution presented in the SCP RAC showed better compacted microstructure, lesser pores and microcracks, denser ITZ, and better interlocking behaviour between the RA and the cement paste. This was mainly due to filling and sealing effects of the cement-pozzolan which acted like a shield reducing the porosity and strengthening the ITZ. The sole use of sand enveloped mixing approach has also led to a better compacted and formed microstructure, but the presence of the voids and micro-cracks was more evident compared to the SCP specimen. The developed stiffed sand-rich cement paste during the early stage of mixing covering the RA surface was mainly the key factor responsible for the overall microstructure enhancement for the SE mix. The combination of the SCP+SE treatment resulted in the most desired microstructure of the RAC. The synergetic effects of these two treatments led to a relatively stronger and compacted microstructure with the fewest pores and microcracks, stronger and denser ITZs. It is also evident that the interlocking and bonding of the RA with the cement paste in the SCP+SE mix was in a relatively excellent and strong state.

Overall, it can be concluded that the proposed innovative treatments and enhancement regimes in this research (Regime A-Water treatment methods, Regime B-Enhancing the adhered mortar, Regime C-batching techniques) are powerful tools to promote the use of RA in the construction industry. These regimes can be used by either RA producers and/or end users to successfully use RA in structural applications.

6.2 Recommendations for Further Research

The present research presented comprehensive investigations on the engineering performance of the untreated RA and RAC, along with the application of various and numerous treatments in enhancing the properties of RAC in terms of a significant variety of engineering parameters. Although it was evident through the presented investigations that with the treatment methods utilised, it is possible to expand the applications of the RAC to structural and high-grade concrete applications with relatively durable concrete, significant body of research work is still required in the field of RAC and the applications of treatments. Based on

the present study, the following areas need further attention in the future works. These recommendations are believed to improve the robustness of the current work, offer more clarity, and provide more in-depth details for civil and design engineers, relevant government bodies and institutions in order to adopt these treatments to significantly promote the use of the RA in the construction industry.

- An innovative mix design method of RAC with C&DW aggregate is needed to be developed in the future research.
- Effects of the treatments utilised on the structural performance (reinforced concrete beams and columns), and durability properties of RAC such as, creep and shrinkage, fatigue, shear strength, resistance to chloride ion penetration, and alkali-silica reaction etc., are required to be extensively and judiciously investigated.
- The effects of RA and treated RA on the engineering properties of special concretes such as self-compacting RAC, aerated RAC, geopolymer RAC, precast RAC etc., are needed to be examined in detail.

REFERENCES

- Abbas, A., Fathifazal, G., Isgor, B., Razaqpur, G., Fournier, B., Foo, S., 2006. *Environmental benefits of green concrete*. s.l., EIC Climate Change Technology IEEE, pp. 1-8.
- Abukersh, S., 2009. High Quality Recycled Aggregate Concrete, Edinburgh: Edinburgh Napier University.
- ACI Committee 318, Building Code Requirements for Structural Concrete (ACI 318-02) and Commentary (ACI 318R-02), American Concrete Institute, Farmington Hills, MI, 2002.
- Agrela, F., Alaejos, P. & De Juan, M., 2013. Properties of concrete with recycled aggregates. In: F. Pacheco-Torgal, et al. eds. *Handbook of Recycled Concrete and Demolition Waste*. Sawston, Cambridge: Woodhead Publishing Series in Civil and Structural Engineering, pp. 304-329.
- Ahmad, S., Assaggaf, R., Maslehuddin, M., Al-Amoudi, O., Adkunle, S., Syed, I., 2017. Effects of carbonation pressure and duration on strength evolution of concrete subjected to accelerated carbonation curing. *Construction and Building Materials*, Volume 136, pp. 565-573.
- Ahmed, W. & Lim, C., 2021. Coupling effect assessment of vacuum based pozzolana slurry encrusted recycled aggregate and basalt fiber on mechanical performance of fiber reinforced concrete. *Construction and Building Materials*, Volume 300, p. 124032.
- Ajdukiewicz, A. & Kliszczericz, A., 2002. Influence of recycled aggregates on mechanical properties of HS/HPC. *Cement and Concrete Composites*, Volume 2, pp. 269-279.
- Ajdukiewicz, A. & Kliszczewicz, A., 2007. Comparative tests of beams and columns made of recycled aggregate concrete and natural aggregate concrete. *Journal of Advanced Concrete Technology*, 5(2), pp. 259-273.
- Al-Bayati, H. & Tighe, S., 2016. *Utilising a Different Technique for Improving Micro and Macro Characteristics of Coarse Recycled concrete Aggregate*. Toronto, Transportation Association of Canada.

- Al-Bayati, H., Das, P., Tighe, S. & Baaj, H., 2016. Evaluation of various methods for enhancing the physical and morphological properties of coarse recycled concrete aggregate. *Construction and Building Materials*, Volume 112, pp. 284-298.
- Alexandridou, C., Angelopoulos, G. N. & Coutelieris, F. A., 2018. Mechanical and durability performance of concrete produced with recycled aggregates from Greek construction and demolition waste plants. *Journal of Clean Production*, Volume 176, pp. 745-757.
- Alqarni, A. S., Abbas, H., Al-Shwikh, K. M. & Al-Salloum, Y. A., 2021. Treatment of recycled concrete aggregate to enhance concrete performance. *Construction and Building Materials*, Volume 307, p. 124960.
- Ann, K. Y., Moon, H. Y., Kim, Y. B. & Ryou, J., 2008. Durability of recycled aggregate concrete using pozzolanic materials. *Waste Management*, 28(6), pp. 993-999.
- Anstice, D., Page, C. & Page, M., 2005. The pore solution phase of carbonated cement pastes. *Cement and Concrete Research*, Volume 35, pp. 377-383.
- Arezoumandi, M., Smith, A., Volz, J. & Khayat, K., 2014. An experimental study on shear strength of reinforced concrete beams with 100% recycled concrete aggregate. *Construction and Building Materials*, Volume 53, pp. 612-620.
- Arezoumandi, M., Smith, A., Volz, J. & Khayat, K., 2015. An experimental study on flexural strength of reinforced concrete beams with 100% recycled concrete aggregate. *Engineering Structures*, Volume 88, pp. 154-162.
- Arora, S. & Singh, S., 2016. Analysis of flexural fatigue failure of concrete made with 100% coarse recycled concrete aggregate. *Construction and Building Materials*, Volume 102, pp. 782-791.
- Bai, W. & Sun, B., 2010. Experimental Study on Flexural Behavior of Recycled Coarse Aggregate Concrete Beam. *Applied Mechanics and Materials*, 29(32), pp. 543-548.
- Bairagi, N., Kishore, R. & Pareek, V., 1993. Behaviour of concrete with different proportions of natural and recycled aggregates. *Resources, Conservation, and recycling*, 9(1-2), pp. 109-126.

- Bairagi, N., Ravande, K. & Pareek, V., 1993. Behaviour of concrete with different proportions of natural and RAs. *Resources, Conservation, and Recycling*, 9(1-2), pp. 109-126.
- Bakoss, S. L. & Sri Ravindrarajah, R., 1999. *Recycled construction and demolition materials for use in roadworks and other local government activities*, Sydney: University of Technology Sydney.
- Barbudo, A., de Brito, J., Evangelista, L., Bravo, M., Agrela, F., 2013. Influence of water-reducing admixtures on the mechanical performance of recycled concrete. *Journal of Cleaner Production*, Volume 59, pp. 93-98.
- Batayneh, M., Marie, I. & Asi, I., 2007. Use of selected waste materials in concrete mixes. *Waste Management*, 27(12), pp. 1870-1876.
- Bazaz, B. & Khayati, M., 2012. Properties and Performance of Concrete Made with Recycled Low-Quality Crushed Brick. *Journal of Materials in Civil Engineering*, 24(4), pp. 330-338.
- BBC, N., 2019. *Middle East*. [Online]. Available at: <http://www.bbc.co.uk>. [Accessed 10 May 2019].
- Behera, M. et al., 2014. Recycled aggregate from C&D waste & its use in concrete - A breakthrough towards sustainability in construction sector: A review. *Construction and Building Materials*, Volume 68, pp. 501-516.
- Belen, G., Fernando, M., Diego, C. & Sindy, S., 2011. Stress-strain relationship in axial compression for concrete using recycled saturated coarse aggregate. *Construction and Building Materials*, Volume 25, pp. 2335-2342.
- Belén, G.-F. & Fernando, M.-A., 2007. Shear strength of recycled concrete beams. *Construction and Building Materials*, 21(4), pp. 887-893.
- Beltran, M., Barbudo, A., Agrela, F. & Jimenez, J., 2014. Effect of cement addition on the properties of recycled concretes to reach control concretes strengths. *Journal of Cleaner Production*, Volume 79, pp. 124-133.
- Billong, N., Oti, J. & Kinuthia, J., 2021. Using silica fume based activator in sustainable geopolymer binder for building application. *Construction and Building Materials*, Volume 275, pp. 122-177.

- Bizzozero, J., Gosselin, C. & Scrivener, K., 2014. Expansion mechanisms in calcium aluminate and sulfoaluminate systems with calcium sulfate. *Cement and Concrete Research*, Volume 56, pp. 190-202.
- Bogas, J., de Brito, J. & Ramos, D., 2016. Freeze-thaw resistance of concrete produced with fine recycled concrete aggregates. *Journal of Cleaner Production*, Volume 115, pp. 294-306.
- Borges PHR, Costa JO, Milestone NB, Lynsdale CJ, Streatfield RE. 2010. Carbonation of CH and C-S-H in composite cement pastes containing high amounts of BFS. *Cement and Concrete Research*, 40, 284-292.
- Brand, A., Roesler, J. & Salas, A., 2015. Initial Moisture and Mixing Effects on Higher Quality Recycled Coarse Aggregate Concrete. *Construction and Building Materials*, Volume 79, pp. 83-89.
- Bravo, M., de Brito, J., Evangelista, L. & Peacheco, J., 2017. Superplasticizer's efficiency on the mechanical properties of recycled aggregates concrete: Influence of recycled aggregates composition and incorporation ratio. *Construction and Building Materials*, Volume 153, pp. 129-138.
- Bravo, M., de Brito, J., Pones, J. & Evangelista, L., 2015. Mechanical performance of concrete made with aggregates from construction and demolition waste recycling plants. *Journal of Cleaner Production*, Volume 99, pp. 59-74.
- Bravo, M., de Brito, J., Pontes, J. & Evangelista, L., 2015. Durability performance of concrete with recycled aggregates from construction and demolition waste plants. *Construction and Building Materials*, Volume 77, pp. 357-369.
- BRE, 1998. *Digest 433 Recycled aggregates*, Bracknell: IHS BRE Press.
- Brecolotti, M. & Materazzi, A., 2010. Structural reliability of eccentrically-loaded sections in RC columns made of recycled aggregate concrete. *Engineering Structures*, 32(11), pp. 3704-3712.
- Bretos, M., Simons, S., Hills, C. & Carey, P., 2004. A review of accelerated carbonation technology in the treatment of cement-based materials and sequestration of CO₂. *Journal of Hazard Materials*, Volume 112, pp. 193-205.

- Bretschneider, A. & Ruhl, M., 1998. The influence of recycled aggregate concrete on the compressive strength and the elastic modulus of concrete. *Darmstadt Concrete*, Volume 13, pp. 131-141.
- British Standards Institution. BS 1881-122:2011: Testing concrete Part 122: Method for determination of water absorption; British Standards Institution: London, UK, 2011.
- British Standards Institution. BS 812-112: 1990—Testing Aggregates. Part 112: Method for Determination of Aggregate Impact Value (AIV); British Standards Institution: London, UK, 1990.
- British Standards Institution. BS 8500-2:2015 +A2: 2019—Concrete-Complementary British Standard to BS EN 206. Part 2: Specification for constituent materials and concrete; British Standards Institution: London, UK, 2019.
- British Standards Institution. BS EN 1097-2:2020—Tests for mechanical and physical properties of aggregates. Part 2: Methods for determination of resistance to fragmentation; British Standards Institution: London, UK, 2020.
- British Standards Institution. BS EN 1097-3:1998: Tests for mechanical and physical properties of aggregates. Determination of loose bulk density and voids; British Standards Institution: London, UK, 1998.
- British Standards Institution. BS EN 1097-6:2013—Tests for Mechanical and Physical Properties of Aggregates. Part 6: Determination of Particle Density and Water Absorption; British Standards Institution: London, UK, 2013.
- British Standards Institution. BS EN 12350-2:2009. Testing fresh concrete – Part 2: Slump test; British Standards Institution: London, UK, 2009.
- British Standards Institution. BS EN 12390-13:2013. Testing hardened concrete- Part 13: Determination of secant modulus of elasticity in compression; British Standards Institution: London, UK, 2013.
- British Standards Institution. BS EN 12390-2:2009: Testing hardened concrete. Making and curing specimens for strength tests; British Standards Institution: London, UK, 2009.

- British Standards Institution. BS EN 12390-3:2009: Testing hardened concrete. Compressive strength of test specimens; British Standards Institution: London, UK, 2009.
- British Standards Institution. BS EN 12390-4:2009. Testing hardened concrete- Part 4: Compressive strength – Specification for test machines; British Standards Institution: London, UK, 2009.
- British Standards Institution. BS EN 12390-5:2009. Testing hardened concrete- Part 5: Flexural strength of test specimens; British Standards Institution: London, UK, 2009.
- British Standards Institution. BS EN 12390-6: 2009: Testing hardened concrete. Tensile splitting strength of test specimens; British Standards Institution: London, UK, 2009.
- British Standards Institution. BS EN 12390-7:2009: Testing hardened concrete Part 7: Density of hardened concrete; British Standards Institution: London, UK, 2009.
- British Standards Institution. BS EN 12620: 2013—Aggregates for concrete; British Standards Institution: London, UK, 2013.
- British Standards Institution. BS EN 13242:2013—Aggregates for unbound and hydraulically bound materials for use in civil engineering work and road construction; British Standards Institution: London, UK, 2013.
- British Standards Institution. BS EN 15304:2010: Determination of the freeze-thaw resistance of autoclaved aerated concrete; British Standards Institution: London, UK, 2010.
- British Standards Institution. BS EN 1992-1-1:2004+A1:2014: UK National Annex to Eurocode 2: Design of concrete structures. General rules and rules for buildings.
- British Standards Institution. BS EN 206:2013+A1:2016: Concrete. Specification, performance, production and conformity; British Standards Institution: London, UK, 2016.
- British Standards Institution. BS EN 932-1:1997: Tests for general properties of aggregates. Methods for sampling; British Standards Institution: London, UK, 1997.

- British Standards Institution. BS EN 932-1:1997—Tests for general properties of aggregates. Part 1: Methods for sampling; British Standards Institution: London, UK, 1997.
- British Standards Institution. BS EN 932-2:1999: Tests for general properties of aggregates. Methods for reducing laboratory samples; British Standards Institution: London, UK, 1999.
- British Standards Institution. BS EN 932-5:2012: Tests for general properties of aggregates. Common equipment and calibration; British Standards Institution: London, UK, 2012.
- British Standards Institution. BS EN 933-1: 2012: Tests for geometrical properties of aggregates. Determination of particle size distribution. Sieving method; British Standards Institution: London, UK, 2012.
- British Standards Institution. BS EN 933-1:2012—Tests for geometrical properties of aggregates. Part 1: Determination of particle size distribution—Sieving method; British Standards Institution: London, UK, 2012.
- British Standards Institution. BS EN 933-3: 2012—Tests for geometrical properties of aggregates. Part 3: Determination of particle shape—Flakiness index; British Standards Institution: London, UK, 2012.
- British Standards Institution. BS EN 933-4:2008—Tests for Geometrical Properties of Aggregates. Part 4: Determination of Particle Shape—Shape Index; British Standards Institution: London, UK, 2008.

- British Standards Institution. BS EN 197-1:2011 - Cement. Composition, specifications and conformity criteria for common cements; British Standards Institution: London, UK, 2011.
- British Standards Institution. BS EN 450-1:2012 - Fly ash for concrete. Definition, specifications and conformity criteria; British Standards Institution: London, UK, 2012.
- British Standards Institution. BS EN 13263-2:2005+A1:2009 - Silica fume for concrete. Conformity evaluation; British Standards Institution: London, UK, 2009.
- British Standards Institution. BS EN 15167-1:2006 - Ground granulated blast furnace slag for use in concrete, mortar and grout. Definitions, specifications and conformity criteria; ; British Standards Institution: London, UK, 2006.
- British Standards Institution. BS EN 12620:2002+A1:2008—Aggregates for Concrete; British Standards Institution: London, UK, 2008.
- Bru, K., Touze, S., Bourgeois, F., Lippiatt, N., Menard, Y., 2014. Assessment of a microwave-assisted recycling process for the recovery of high-quality aggregates from concrete waste. *International Journal of Mineral Processing*, Volume 126, pp. 90-98.
- Bruntland, 1987. *Development and international economic co-operation: environment*, Nairobi: The World Commission on Environment and Development "Our common future".
- Buck, A., 1977. Recycled concrete as a source of aggregate. *ACI journal*, pp. 212-219.
- Bui, N., Satomi, T. & Takahashi, H., 2018. Enhancement of Recycled Aggregate Concrete Properties by a New Treatment Method. *International Journal of GEOMATE*, 14(41), pp. 68-76.

- Bulatovic, V., Melesev, M., Radeka, M., Radonjanin, V., Lukic, I., 2017. Evaluation of sulfate resistance of concrete with recycled and natural aggregates. *Construction and Building Materials*, Volume 152, pp. 614-631.
- Butler, L., West, J. & Tiegh, S., 2013. Effect of recycled concrete coarse aggregate from multiple sources on the hardened properties of concrete with equivalent compressive strength. *Construction and Building Materials*, Volume 47, pp. 1292-1301.
- Butler, L., West, J. & Tighe, S., 2011. The effect of recycled concrete aggregate properties on the bond strength between RCA concrete and steel reinforcement. *Cement and Concrete Research*, 41(2011), pp. 1037-1049.
- Cantero, B., Sáez del Bosque, I., Matías, A. & Medina, C., 2018. Statistically significant effects of mixed recycled aggregate on the physical-mechanical properties of structural concretes. *Construction and Building Materials*, Volume 185, pp. 93-101.
- Cao, Z., 2016. *The Effect of Recycled Aggregate Treated by Carbon Dioxide on Properties of Recycled Concrete*, Changsha: Hunan University.
- Casuccio, M., Torijos, M., Giaccio, G. & Zerbino, R., 2008. Failure mechanism of recycled aggregate concrete. *Construction and Building Materials*, Volume 22, pp. 1500-1506.
- Chaboki, h. R., Ghalehnove, M., Karimipour, A. & de Brito, J., 2018. Experimental study on the flexural behaviour and ductility ratio of steel fibres coarse recycled aggregate concrete beams. *Construction and Building Materials*, Volume 186, pp. 400-422.
- Chakradhara, M., Bhattacharyya, S. & Barai, S., 2010. Influence of field recycled coarse aggregate on properties of concrete. *Materials and Structures*, 44(1), pp. 205-220.
- Chen, J., Thomas, J. & Jennings, H., 2006. Decalcification shrinkage of cement paste. *Cement and Concrete Research*, 36(5), pp. 801-809.
- Chen, W., Jin, R., Xu, Y., Wanatowski, D., Li, B., Yan, L., Pan, Z., Yang, Y., 2019. Adopting recycled aggregates as sustainable construction materials: A review of the scientific literature. *Construction and Building Materials*, Volume 218, pp. 483-496.

- Choi, H. & Kang, K., 2008. Bond behaviour of deformed bars embedded in RAC. *Magazine of Concrete Reserach*, 60(6), pp. 399-410.
- Collery, D. J., Paine, K. A. & Dhir, R., 2015. Establishing rational use of recycled aggregates in concrete: a performance-related approach. *Magazine of Concrete Research*, Volume 67, pp. 559-574.
- Collins, R. J., 1997. Upgrading the Use of Recycled Material - Uk Demonstration Project. *Studies in Environmental Science* , Volume 71, pp. 185-191.
- Corinaldesi, V. & Moriconi, G., 2001. *Role of chemical and mineral admixtures on perfomance and economics of recycled aggregate concrete*. Chennai, India, s.n., pp. 869-884.
- Corinaldesi, V. & Moriconi, G., 2009. Influence of mineral additions on the performance of 100% RAC. *Construction and Building Materials*, 23(8), pp. 2869-2876.
- Corinaldesi, V., 2010. Mechanical and elastic behaviour of concretes made of recycled-concrete coarse aggregates. *Construction and Building Materials*, 24(9), pp. 1616-1620.
- Crentsil, K., Brown, T. & Taylor, A., 2001. Performance of concrete made with commercially produced coarse concrete aggregates. *Cement and Concrete Research*, Volume 31, pp. 707-712.
- Cyllok, M., 2002. *Concrete with recycled aggregateL laps and cracks*. Munch, s.n., pp. 72-72.
- Damdelen, O., 2018. Investigation of 30% recycled coarse aggregate content in sustainable concrete mixes. *Construction and Building Materials*, 408-418.
- Darmawan, K., & Napiah, M., 2012. Effect of cement coated aggregates on the creep and deformation characteristics of asphaltic concrete bituminous mixtures. *WIT Transactions on The Built Environment*, 128, 661-671.
- de Juan, M. & Gutierrez, P., 2009. Study on the influence of attached mortar content on the properties of recycled concrete aggregate. *Construction and Building Materials*, 23(2), pp. 872-877.
- De Pauw, P. & Vyncke, J., 1998. *Shrinkage and creep of concrete with recycled materials as coarse aggregate*. Scotland, Univeristy of Dundee, pp. 214-225.

- Debieb, F. & Kenai, S., 2008. The use of coarse and fine crushed bricks as aggregate in concrete. *Construction and Building Materials*, 22(5), pp. 886-893.
- Debieb, F., Courard, L., Kenai, S. & Degeimbre, R., 2010. Mechanical and durability properties of concrete using contaminated RAs. *Cement and Concrete Composites*, 32(6), pp. 421-426.
- Debieb, F., Courard, L., Kenai, S. & Degimbre, R., 2009. Roller compacted concrete with contaminated RAs. *Construction and Building Materials*, 23(11), pp. 3382-3387.
- Derwen, 2016. *Recycled Aggregate*. [Online] Available at: <https://www.derwengroup.co.uk> [Accessed 10 February 2022].
- DeVenny, A., 1999. *Recycling of demolished masonry rubble*, Edinburgh: Napier University.
- Dhir, R., Limbachiya, M. & leelawat, T., 1999. Suitability of recycled aggregate for use in BS 5328 designated mixes. *Proceedings of the Institution of Civil Engineers*, Volume 134, pp. 257-274.
- Di Niro, G., Dolara, E. & Cairns, R., 1998. *Properties of hardened recycled aggregate concrete for structural purposes*. Scotland, University of Dundee, pp. 177-187.
- Dilbas, H., Şimşek, M. & Çakır, Ö., 2014. An investigation on mechanical and physical properties of recycled aggregate concrete (RAC) with and without silica fume. *Construction and Building Materials*, Volume 61, pp. 50-59.
- Dillmann, R., 1998. *Concrete with recycled concrete aggregate*. Scotland, University of Dundee, pp. 239-253.
- Dolara, E., Di Niro, G. & Cairns, R., 1998. *Recycled aggregate concrete prestressed beams*. Scotland, University of Dundee, pp. 255-262.
- Domingo-Cabo, A., Lazaro, C., Gayarre, F., Serrano-Lopez, M., Serna, P., Castano-Tabares, J., 2009. Creep and shrinkage of RAC. *Construction and Building Materials*, 23(7), pp. 2545-2553.
- Dong, H. Song, Yu., CAO, W., Sun, W., Zhang, J., 2019. Flexural bond behavior of reinforced recycled aggregate concrete. *Construction and Building Materials*, Volume 213, pp. 514-527.

- Duan, P., Sui, Z., Chen, W. & Shen, C., 2013. Effects of metak kaolin, silica fume and slag on pore structure, interfacial transition zone and compressive strength of concrete. *Construction and Building Materials*, Volume 44, pp. 1-6.
- Duan, Z. & Poon, C., 2014. Properties of recycled aggregate concrete made with recycled aggregates with different amounts of old adhered mortars. *Materials & Design*, Volume 58, pp. 19-29.
- Elhakam, A., Mohamed, A. & Awad, E., 2012. Influence of self-healing, mixing method, and adding silica fume on mechanical properties of RAs concrete. *Construction and Building Materials*, Volume 35, pp. 421-427.
- Etxeberria, M., Vazquez, E., Mari, A. & Barra, M., 2007. Influence of amount of recycled coarse aggregates and production process on properties of recycled aggregate concrete. *Cement and Concrete Research*, 37(5), pp. 735-742.
- Etxeberria, M., Mari, A. & Vazquez, E., 2007. RAC as structural material. *Materials and Structures*, Volume 40, pp. 529-541.
- Etxeberria, M., Vazquez, E. & Mari, A., 2006. Microstructure analysis of hardened recycled aggregate concrete. *Magazine of Concrete Research*, Volume 58, pp. 683-690.
- Euml, R., Tixier, L. & Mobasher, B., 2003. Modeling of damage in cement-based materials subjected to external sulfate attack. I: formulation. *Journal of Materials and Civil Engineering*, 15(4), pp. 305-313.
- Evangelista, L. & de Brito, J., 2007. Mechanical behavior of concrete made with fine recycled concrete aggregates. *Cement and Concrete Research*, Volume 29, pp. 397-401.
- Fang, X., Xuan, D. & Poon, S., 2017. Empirical modelling of CO₂ uptake by recycled concrete aggregates under accelerated carbonation conditions. *Materials and Structures*, Volume 50, pp. 200-212.
- Fang, X., Zhan, B. & Poon, C. S., 2021. Enhancement of recycled aggregates and concrete by combined treatment of spraying Ca²⁺ rich wastewater and flow-through carbonation. *Construction and Building Materials*, Volume 277, p. 122202.

- Fang, Y. & Chang, J., 2015. Microstructure changes of waste hydrated cement paste induced by accelerated carbonation. *Construction and Building Materials*, Volume 76, pp. 360-365.
- Ferriz-Papi, J. & THomas, S., 2017. Recycled Aggregates from Construction and Demolition Waste in the Production of Concrete Blocks. *International Journal of Structural and Construction Engineering* , 11(10), pp. 1397-1402.
- Fonseca, N., de Brito, J. & Evangelista, L., 2011. The influence of curing conditions on the mechanical performance of concrete madge with recycled concrete waste. *Cement and Concrete Composites*, 33(6), pp. 637-643.
- François, B. & Hadjieva-Zaharieva, R., 2002. Influence of industrially produced RAs on flow properties of concrete. *Materials and Structures*, 35(8), pp. 504-509.
- Frondistou-Yannas, S., 1977. Waste concrete as aggregate for new concrete. *ACI journal*, pp. 373-376.
- Gagan & Agam, 2015. Flexural behavior of reinforced recycled concrete beams: a review. *International Journal of Research in Engineering and Technology*, 5(1), pp. 1-7.
- Ghanbari, M., Abbasi, A. & Ravanshadnia, M., 2017. Economic and Environmental Evaluation and Optimal Ratio of Natural and Recycled Aggregate Production. *Advances in Materials Science and Engineering*, Volume 2017, pp. 1-10.
- Gokce, A., Nagatakib, S., Saekic, T. & Hisadad, M., 2004. Freezing and thawing resistance of air-entrained concrete incorporating recycled coarse aggregate: the role of air content in demolished concrete. *Cement and COncrete Research*, 34(5), pp. 799-806.
- Gomez-Soberon, J., 2002. *Creep of concrete with sub-stitution of nomral aggregate by recycled concrete aggregate*. Cancun, s.n., pp. 461-474.
- Gomez-Soberon, J., 2002. Porosity of recycled concrete with substitution of recycled concrete aggregate: An experimental study. *Cement and Concrete Research*, 32(8), pp. 1301-1311.
- Gonzalez-Corominas, A. & Etxeberria, M., 2014. Properties of high performance concrete made with recycled fine ceramic and coarse mixed aggregates. *Construction and Building Materials*, Volume 68, pp. 618-626.

- Gonzalez-Fonteboa, B. & Martinez-Abella, F., 2007. Shear strength of recycled concrete beams. *Construction and Building Materials*, 21(4), pp. 887-893.
- González-Fonteboa, B. & Martínez-Abella, F., 2008. Concrete with aggregates from demolition waste and silica fume. Materials and Mechanical Properties. *Building and Environment*, 43(4), pp. 429-437.
- Gonzalez-Fonteboa, B., Martinez-Abella, F., Eiras-Lopez, J. & Seara-Paz, S., 2011. Effect of recycled coarse aggregate on damage of recycled concrete. *Materials and Structures*, 44(10), pp. 1759-1771.
- Gonzalez-Fonteboa, B., Martinez-Abella, F., Martinez-Lage, I. & Eiras-Lopez, J., 2009. Structural shear behaviour of recycled concrete with silica fume. *Construction and Building Materials*, 23(11), pp. 3406-3410.
- González-Fonteboa, F., 2007. Shear strength of recycled concrete beams. *Construction and Building Materials*, 21(4), pp. 887-893.
- Guo, H., Shi, C., Guan, X., Zhu, J., Ding, Y., Ling, T., Zhang, H., Wang, Y., 2018. Durability of recycled aggregate concrete - A review. *Cement and Concrete Composites*, Volume 89, pp. 251-259.
- Hadavand, B. & Imaninasab, R., 2019. Assessing the influence of construction and demolition waste materials on workability and mechanical properties of concrete using statistical analysis. *Innovative Infrastructure Solutions*, 4(29), pp. 1-11.
- Hamad, B., Dawi, A., Daou, A. & Chehab, G., 2018. Studies of the effect of recycled aggregates on flexural, shear, and bond splitting beam structural behavior. *Case Studies in Construction Materials*, Volume 9.
- Hansen, T. & Boegh, E., 1985. Elasticity and drying shrinkage of recycled aggregate concrete. *ACI Journal*, 82(5), pp. 648-652.
- Hansen, T. & Narud, H., 1983. Strength of recycled concrete made from crushed coarse aggregate. *Concrete International*, 5(1), pp. 79-83.
- Hansen, T., 1992. *Recycling of demolished concrete and masonry*. London: E & FN SPON.
- Hansen, T., 1992. *Recycling of Demolished Concrete and Masonry*. Oxfordshire, UK: Taylor and Francis.

- Hanumesh, B. Harish, N. Venkata Ramana, 2018. Influence of polypropylene fibres on recycled aggregate concrete. *Materials Today: Proceedings, Elsevier Ltd*, pp. 1147-1155.
- Henschen, J., Teramoto, A. & Lange, D., 2012. *Shrinkage and creep performance of RAC*. Springer, Netherlands, &th RILEM International Conference on Cracking in Pavements.
- Huwang, J. P., Shim, H. B., Lim, S. & Ann, K. Y., 2013. Enhancing the durability properties of concrete containing recycled aggregate by the use of pozzolanic materials. *KSCE Journal of Civil Engineering*, Volume 17, pp. 155-163.
- Hyvert, N., Sellier, A., Duprat, F., Rougeau, P., Francisco, P., 2010. Dependency of C-S-H carbonation rate on CO₂ pressure to explain transition from accelerated tests to natural carbonation. *Cement and Concrete Research*, Volume 40, pp. 1582-1589.
- ICE. (2019, November 10). Concrete Embodied Carbon Footprint Calculator. Retrieved from Circular ecology: <https://www.circularecology.com/embodied-carbon-footprint-database.html>
- Ignjatovic, I., Marinkovic, S., Miskovic, Z. & Savic, A., 2013. Flexural behavior of reinforced recycled aggregate concrete beams under short-term loading. *Materials and Structures*, Volume 46, pp. 1045-1059.
- Ikeda, T. & Yamane, S., 1988. *Strengths of concrete containing recycled aggregate*. Tokyo, Japan, RILEM, pp. 585-594.
- Ivan, I., Marinkovic, S. & Tomic, N., 2017. Shear behaviour of recycled aggregate concrete beams with and without shear reinforcement. *Engineering Structures*, Volume 141, pp. 386-401.
- Jagan, S., Neelakantan, T. & Saravanakumar, P., 2021. Mechanical properties of recycled aggregate concrete surface treated by variation in mixing approaches. *Journal of Construction*, 20(2), pp. 236-249.
- Jagan, S., Neelakantan, T. R. & Saravanakumar, P., 2021. Performance Enhancement of Recycled Aggregrate Concrete - An Experimental Study. *Applied Science and Engineering Progress*, 15(1), pp. 1-10.

- Johannesson, B. & Utgenannt, P., 2001. Microstructural changes caused by carbonation of cement mortar. *Cement and Concrete Research*, Volume 31, pp. 925-931.
- Kakizaki, M., 1988. *Strength and elastic modulus of recycled aggregate concrete*. Tokyo, Japan, RILEM, pp. 565-574.
- Kamal, M., Saafan, M., Soliman, N. & Helal, S., 2015. Behavior and Strength of Reinforced Recycled-Aggregate Concrete Beams. *International Journal of Engineering and Advanced Technology (IJEAT)* , 4(6), pp. 5-13.
- Kareem, A., Nikraz, H., & Asadi, H. (2018). Evaluation of the double coated recycled concrete aggregates for hot mix asphalt. *Construction and Building Materials*, 172, 544-552.
- Kashef-Haghighi, S., Shao, Y. & Ghoshal, S., 2015. Mathematical modeling of CO₂ uptake by concrete during accelerated carbonation curing. *Cement and Concrete Research*, Volume 67, pp. 1-10.
- Katz, A., 2003. Properties of concrete made with RA from partially hydrated old concrete. *Cement and Concrete Research*, Volume 33, pp. 703-711
- Kawai, T., Watanabe, M. & Nagataki, S., 1988. *Replaced aggregate concrete made from demolished concrete aggregates*. Tokyo, Japan, RILEM, pp. 680-689.
- Kawamura, M. & Tori, K., 1988. *Reuse of recycled concrete aggregate for pavement*. Tokyo, Japan, RILEM, pp. 726-735.
- Kazemain, F., Rooholamini, H. & Hassani, A., 2019. Mechanical and fracture properties of concrete containing treated and untreated recycled concrete aggregates. *Construction and Building Materials*, Volume 209, pp. 690-700.
- Kazmi, S., Munir, M., Wu, Y., Patnaikuni, I., Zhou, Y., Xing, F., 2019. Influence of different treatment methods on the mechanical behavior of recycled aggregate concrete: a comparative study. *Cement and Concrete Composites*, Volume 104, p. 103398.
- Kazmi, S., Munir, M., Wu, Y., Patnaikuni, I., Zhou, Y., Xing, F., 2020. Effect of different aggregate treatment techniques on the freeze-thaw and sulfate resistance of recycled aggregate concrete. *Cold Regions Science and Technology*, Volume 178, pp. 103-126.

- Khalaf, F. & DeVenny, A., 2004. Recycling of demolished masonry rubble as coarse aggregate in concrete: review. *Journal of Materials in Civil Engineering*, 16(4), pp. 331-340.
- Kheder, G. & Al-Windawi, S., 2005. Variation in mechanical properties of natural and recycled aggregate concrete as related to the strength of their binding mortar. *Materials and Structures*, 38(7), pp. 701-709.
- Kikuchi, T. & Kuroda, Y., 2011. Carbon dioxide uptake in demolished and crushed concrete. *Journal of Advanced Concrete Technology*, 9(1), pp. 115-124.
- kisku, N. et al., 2017. A critical review and assessment for usage of recycled aggregate as sustainable construction material. *Construction and Building Materials*, Volume 131, pp. 721-740.
- Kjellsen, K., Wallevik, O. & Fjalberg, L., 1998. Microstructure and microchemistry of the paste-aggregate interfacial transition zone of high-performance concrete. *Advance in Cement Research*, Volume 10, pp. 33-40.
- Kong, D., Lei, T., Zheng, J., Ma, C., Jiang, J., 2010. Effect and mechanism of surface-coating pozzalanics materials around aggregate on properties and ITZ microstructure of recycled aggregate concrete. *Construction and Building Materials*, 24(5), pp. 701-708.
- Konno, K., Sato, Y., Kakuta, Y. & Ohira, M., 1997. Property of recycled aggregate column encased by steel tube subjected to axial compression. *Transactions of the Japan Concrete*, Volume 19, pp. 231-238.
- Konrad, Z. & Frank, R., 2001. *Design of concrete structures made from recycled aggregate - a globe recommendation following the DIN 1045-1*. Berlin, s.n.
- Koren, L. & Hall, W., 2012. *Concrete*. London: Phaidon.
- Kou, S. & Poon, C., 2009. Properties of self-compacting concrete prepared with coarse and fine recycled concrete aggregates. *Cement and Concrete Composites*, 31(9), pp. 622-627.
- Kou, S. & Poon, C., 2012. Enhancing the durability properties of concrete prepared with coarse recycled aggregate. *Construction and Building Materials*, Volume 35, pp. 69-76.

- Kou, S. & Poon, C., 2013. Long-term mechanical and durability properties of RAC prepared with the incorporation of fly ash. *Cement and Concrete Composites*, Volume 37, pp. 12-19.
- Kou, S., Poon, C. & Agrela, F., 2011. Comparisons of natural and RACs prepared with the addition of different mineral admixtures. *Cement and Concrete Composites*, Volume 33, pp. 788-795.
- Kou, S., Poon, C. & Chan, D., 2004. *Properties of steam cured recycled aggregate fly ash concrete. Use of recycled materials in buildings and structures*. Barcelona, Spain, RILEM Publications, pp. 590-599.
- Kou, S., Poon, C. & Chan, D., 2008. Influence of fly ash as a cement addition on the hardened properties of RAC. *Materials and Structures*, 41(7), pp. 1191-1201.
- Kou, S., Zhan, B. & Poon, C., 2014. Use of a CO₂ curing step to improve the properties of concrete prepared with recycled aggregates. *Cement and Concrete Composites*, Volume 45, pp. 22-28.
- Kou, S.-C. & Poon, C.-S., 2010. Properties of concrete prepared with PVA-impregnated recycled concrete aggregates. *Cement and Concrete Composites*, 32(8), pp. 649-654.
- Kukadia, V., Parekh, D. & Gajar, R., 2017. Influence of Aggregate's Treatment on Properties of Recycled Aggregate Concrete. *International Journal of Civil Engineering and Technology (IJCIET)*, 8(3), pp. 351-361.
- Kurda, R., de Brito, J. & Silvestre, J., 2017. Influence of recycled concrete aggregates and high contents of fly ash on concrete fresh properties. *Cement and Concrete Composites*, Volume 84, pp. 198-213.
- Kwan, W. H., Ramli, M., Kam, K. J. & Sulieman, M., 2012. Influence of the amount of recycled coarse aggregate in concrete design and durability properties. *Construction and Building Materials*, Volume 26, pp. 565-573.
- Larbi, J., Heijnen, W., Brouwer, J. & Mulder, E., 2000. Preliminary laboratory investigation of thermally treated recycled concrete aggregate for general use in concrete. *Waste Management Series*, Volume 1, pp. 129-139.

- Lauritzen, E. & Bulletin de la, S. D., 1994. *Third International RILEM Symposium on Demolition and Reuse of Concrete and Masonry*. Odense, RILEM Publications, pp. 307-310.
- Le, H.-B. & Bui, Q.-B., 2020. Recycled aggregate concretes - A state-of-the-art from the microstructure to the structural performance. *Construction and Building Materials*, Volume 257, p. 119522.
- Lee, C.-H., Du, J.-C., & Shen, D.-H. (2011). Evaluation of pre-coated recycled concrete aggregate for hot mix asphalt. *Construction and Building Materials*, 28, 66-71.
- lee, G. C. & Choi, H. B., 2013. Study on interfacial transition zone properties of recycled aggregate by micro-hardness test. *Construction and Building Materials*, Volume 40, pp. 455-460.
- Lee, S., 2019. Effect of Nylon Fiber Addition on the Performance of Recycled Aggregate Concrete. *Applied Science* , 9(4), pp. 1-14.
- Lee, S., Park, W. & Lee, H., 2013. Life cycle CO₂ assessment method for concrete using CO₂ balance and suggestion to decrease LC CO₂ of concrete in South-Korean apartment. *Energy and Buildings*, Volume 58, pp. 93-102.
- Leemann, A., Nygaard, P., Kaufmann, J. & Loser, R., 2015. Relation between carbonation resistance, mix design and exposure of mortar and concrete. *Cement and Concrete Composites*, Volume 62, pp. 33-43.
- Levy, S. M. & Helene, P., 2004. Durability of recycled aggregate concrete: a safe way to sustainable development. *Cement and Concrete Research*, 34(11), pp. 1975-1980.
- Li W, Xiao J, Sun Z, 2012. Interfacial transition zones in recycled aggregate concrete with different mixing approaches. *Construction and Building Materials*, 35:1045–1055
- Li, J., 2004. *Study on mechanical behaviour of recycled aggregate concrete* , Shanghai: Tongji University.
- Li, J., Xiao, H. & Zhou, Y., 2009. Influence of coating recycled aggregate surface with pozzolanic powder on the properties of recycled aggregate concrete. *Construction and Building Materials*, Volume 23, pp. 1287-1291.

-
- Li, L., Sun, C., Xiao, J. & Xuan, D., 2017. Effect of carbonated recycled coarse aggregate on the dynamic compressive behaviour of recycled aggregate concrete. *Construction and Building Materials*, Volume 151, pp. 52-62.
- Li, W., Ziao, J., Sun, Z., Kawashima, S., Shah, S., 2012. Interfacial transition zones in RAC with different mixing approaches. *Construction and Building Materials*, Volume 35, pp. 1045-1055.
- Li, WG, Long, C, Tam, VWY, 2017. Effects of nano-particles on failure process and microstructural properties of recycled aggregate concrete. *Construction and Building Materials* 142: 42–50.
- Li, Y., 2014. *Improvement of Recycled Concrete Aggregate Properties by CO₂ Curing*, Changsha: Hunan University.
- Li, Y., Wang, R., LI, S. & Zhao, Y., 2017. Assessment of the freeze-thaw resistance of concrete incorporating carbonated coarse recycled concrete aggregates. *Journal of the Ceramic Society of Japan*, 125(11), pp. 837-845.
- Li, Y., Zhang, W. R., Wang, R. & Men, C., 2019. Effects of carbonation treatment on the crushing characteristics of recycled coarse aggregates. *Construction and Building Materials*, Volume 201, pp. 408-420.
- Liang, C., Pan, B., Ma, Z., He, Z., Duan, Z., 2020. Utilisation of CO₂ curing to enhance the properties of recycled aggregate and prepared concrete: A review. *Cement and Concrete Composites*, Volume 105, pp. 103-446.
- Liang, Y.-c., Ye, Z.-m., Vernerey, F. & Xi, Y., 2015. Development of Processing Methods to Improve Strength of Concrete with 100% Recycle Coarse Aggregate. *Journal of Materials in Civil Engineering*, 27(5), p. 04014163.
- Limbachiya, M., Leelawat, T. & Dhir, R., 1998. *RCA concrete: a study of properties in the fresh state, strength development and durability*. Scotland, University of Dundee, pp. 227-237.
- Limbachiya, M., Leelawat, T. & Dhir, R., 2000. Use of recycled concrete aggregate in high-strength concrete. *Materials and Structures*, Volume 33, pp. 574-590.
- Limbachiya, M., Meddah, M. & Ouchagour, Y., 2011. Use of recycled concrete aggregate in fly-ash concrete. *Construction and Building Materials*, Volume 5, pp. 564-580.
-

- Limbachiya, M., Meddah, M. & Ouchagour, Y., 2012. Use of recycled concrete aggregate in fly-ash concrete. *Construction and Building Materials*, Volume 27, pp. 439-449.
- Liu, B., Feng, C. & Deng, Z., 2019. Shear behavior of three types of recycled aggregate concrete. *Construction and Building Materials*, Volume 217, pp. 557-572.
- Lotfi, S., Deja, J., Rem, P., Mroz, R., Roekel, E., Stelt, H., 2014. Mechanical recycling of EOL concrete into high-grade aggregates. *Resources, Conservation, and Recycling*, Volume 87, pp. 117-125.
- Lotfi, S., Eggimann, M., Wagner, E., Mroz, R., Deja, J., 2015. Performance of RAC based on a new concrete recycling technology. *Construction and Building Materials*, Volume 95, pp. 243-256.
- Lotfi, S., Deja, J., Rem, P., Mroz, R., Van Roekel, E., & Van Der Stelt, H., 2014. Mechanical of EOL concrete into high-grade aggregates. *Resources, Conservation & Recycling*, 87, 117-125.
- Lotfi, S., Eggimann, W. E., Mroz, R. & Deja, J., 2015. Performance of RAC based on a new concrete recycling technology. *Construction and Building Materials*, Volume 95, pp. 243-256.
- Lotfy, A. & Al-Fayez, M., 2015. Performance evaluation of structural concrete using controlled quality coarse and fine recycled concrete aggregate. *Cement and Concrete Composites*, Volume 61, pp. 36-43.
- Lu, B., Shi, C., Cao, Z., Guo, m., Zheng, J., 2019. Effect of carbonated coarse recycled concrete aggregate on the properties and microstructure of recycled concrete. *Journal of Cleaner Production*, Volume 233, pp. 421-428.
- Lu, W., 2019. Big data analytics to identify illegal construction waste dumping: A Hong Kong study. *Resources, Conservation and Recycling*, Volume 141, pp. 264-272.
- Majhi, R., Nayak, A. & Mukharjee, B., 2018. Development of sustainable concrete using recycled coarse aggregate and ground granulated blast furnace slag. *Construction and Building Materials*, Volume 159, pp. 417-430.
- Malesev, M., Radonjanin, V. & Marinkovic, S., 2010. Recycled concrete as aggregate for structural concrete production. *Sustainability*, Volume 2, pp. 1204-1225.

- Malhotra, V., 1976. *Use of recycled concrete as a new aggregate*, Ottawa: Canada Centre for Mineral and Energy Technology.
- Manzi, S., Mazzotti, C. & Bignozzi, M., 2013. Short and long-term behaviour of structural concrete with recycled concrete aggregate. *Cement and Concrete Composites*, Volume 37, pp. 312-318.
- Maruyama, I., Sogo, M., Sogabe, T., Kawai, K., 2004. *Flexural properties of reinforced recycled concrete beams*. Barcelona, RILEM.
- Mas, B., Cladera, A., Olmo del, T. & Pitarch, F., 2012. Influence of the amount of mixed RAs on the properties of concrete for non-structural use. *Construction and Building Materials*, 27(1), pp. 612-622.
- Matias, D., de Brito, J., Rosa, A. & Pedro, D., 2013. Durability of concrete with recycled coarse aggregates: influence of super plasticizers. *Journal of Materials in Civil Engineering*, 26(7), p. 06014011.
- Matias, D., de Brito, J., Rosa, A. & Pedro, D., 2013. Mechanical properties of concrete produced with recycled coarse aggregates – influence of the use of superplasticizers. *Construction and Building Materials*, Volume 44, pp. 101-109.
- Matshei, T., lothenbach, B. & Glasser, F., 2007. The role of calcium carbonate in cement hydration. *Cement and Concrete Research*, 37(4), pp. 551-558.
- McNeil, K. & Kang, T., 2013. Recycled Concrete Aggregates: A Review. *International Journal Of Concrete Structures and Materials*, 7(1), pp. 61-69.
- Medina, C., Zhu, W., Howind, T., Rojas, M., Frias, M., 2014. Influence of mixed recycled aggregate on the physical - mechanical properties of recycled concrete. *Journal of Cleaner Production*, Volume 68, pp. 216-225.
- Medina, C., de Rojas, M. & Frias, M., 2013. Freeze-thaw durability of recycled concrete containing ceramic aggregate. *Journal of Cleaner Production*, Volume 40, pp. 151-160.
- Mefteh, H., Kebaili, O., berredjem, I., Arabi, N., 2013. Influence of moisture conditioning of recycled aggregates on the properties of fresh and hardened concrete. *Journal of Cleaner Production*, Volume 54, pp. 282-288.

- Mehta, P. & Monterio, P., 1986. *Concrete: structur, properties and materials*. Englewood Cliffs, NJ: Prentice Hall.
- Mellmann, G., 1999. *Processed Concrete rubble for the reuse as aggregate*. Scotland, Univeristy of Dundee, pp. 171-178.
- Mistri, A., Bhattacharyya, S., Dhama, N., Mukherjee, A., & Barai, S. (2020). A review on different treatment methods for enhancing the properties of recycled aggregates for sustainable construction materials. *Construction and Building Materials*, 233, 117-894.
- Mohammed, T., Das, H., Mahmood, Aziz, Rahman, M., Awal, M., 2017. Flexural Performance of RC Beams Made with Recycled Brick Aggregate. *Construction and Building Materials*, Volume 134, pp. 67-74.
- Monkman, S. & MacDonald, M., 2016. Carbon dioxide upcycling into industrially produced concrete blocks. *Construction and Building Materials*, Volume 124, pp. 127-132.
- Monkman, S., MacDonald, M., Hooton, R. & Sandberg, P., 2016. Properties and durability of concrete produced using CO₂ as an accelerating admixtures. *Cement and Concrete Composites*, Volume 74, pp. 218-224.
- Montgomery, D., 1998. *Workability and compressive strength properties of concrete containing recycled concrete aggregate*. London, Thomas Telford Publishing.
- Moon, E. & Choi, Y., 2019. Carbon dioxide fixation via accelerated carbonation of cement-based materials: potential for construction materials applications. *Construction and Building Materials*, Volume 199, pp. 676-687.
- Muduli R., Mukharjee B.B., 2020. Characteristics of Concrete Prepared with Metakaolin and Recycled Coarse Aggregates. In: Shukla S., Barai S., Mehta A. (eds) *Advances in Sustainable Construction Materials and Geotechnical Engineering. Lecture Notes in Civil Engineering*, vol 35. Springer, Singapore.
- Mukai, T., Kikuchi, M. & Ishikawa, N., 1978. *Stucy on the properties of concrete containing recycled concrete aggregate*, s.l.: Cement Association of Japan.
- Mulheron, M. & O'Mahony, M., 1988. *The durability of recycled aggregate and recycled aggregate concrete*. Tokyo, Japan, RILEM, pp. 633-642.

- Mullauer, W., Beddoe, R. & Heinz, D., 2013. Sulphate attack expansion mechanisms. *Cement and Concrete Research*, Volume 52, pp. 208-215.
- Munir, Muhammad; Kazmi, Syed; Wu, Yu-Fei; Patnaikuni, Induhushan; Wang, Junfeng; Wang, Quan, 2020. Development of a unified model to predict the axial stress-strain behavior of recycled aggregate concrete confined through spiral reinforcement. *Engineering Structures*, Volume 218, P. 110851, <https://doi.org/10.1016/j.engstruct.2020.110851>
- Nagatakia, S., Gokceb, A., Saekic, T. & Hisada, M., 2004. Assessment of recycling process induced damage sensitivity of recycled concrete aggregates. *Cement and Concrete Research*, 34(6), pp. 965-971.
- Nandhini, K., Jayakumar, S. & Kothandaraman, S., 2016. Flexural Strength Properties of Recycled Aggregate Concrete. *International Journal of Application of Innovation in Engineering and Management*, 5(5), pp. 6-11.
- Nayak, S. & Dutta, S. C., 2017. A critical review and assessment for usage of recycled aggregate as sustainable construction material. *Construction and Building Materials*, pp. 721-740.
- Nevill, A., 2012. *Properties of Concrete*. 5th Edition ed. Harlow: Pearson Education Limited.
- Neville, A., 2011. *Properties of Concrete*. 5th ed. Essex: Pearson Education Limited.
- Newman, A., 1946. The utilisation of brick rubble from demolished shelters as aggregate for concrete. *Institution of Municipal Engineers*, 72(2), pp. 113-121.
- Nuaklong, V. Sata, P. Chindapasirt, 2018. Properties of metakaolin-high calcium fly ash geopolymer concrete containing recycled aggregate from crushed concrete specimens. *Construction and Building Materials*, 161, pp. 365-373.
- Oikonomou, N., 2005. Recycled concrete aggregates. *Cement and Concrete Composite*, Volume 27, pp. 315-318.
- Oliveira, M., Assis, C. & Wanderley, A., 2004. *Study on compressed stress, water absorption and modulus of elasticity of produced concrete made by recycled aggregate*. Barcelona, Spain, Interntaional RILEM Conference , pp. 636-642.

- Olorunsogo, F. & Padayachee, N., 2002. Performance of RAC monitored by durability indexes. *Cement and Concrete Research*, 32(2), pp. 179-185.
- Olorunsogo, F. T. & Padayachee, N., 2002. Performance of recycled aggregate concrete monitored by durability indexes. *Cement and Concrete Research*, 32(2), pp. 179-185.
- Omrane, M., Kenai, S., Kadri, E.-H. & Aït-Mokhtard, A., 2017. Performance and durability of self compacting concrete using recycled concrete aggregates and natural pozzolan. *Journal of Cleaner Production*, Volume 165, pp. 415-430.
- Oti, J., Kinuthia, J., Adeleke, B. & Billong, N., 2020. Durability of Concrete Containing PFA and GGBS By-products. *Journal of Civil Engineering and Construction*, 9(3), pp. 165-174.
- Otsuki, N., Miyazato, S. & Yodsudjai, W., 2003. Influence of recycled aggregate on interfacial transition zone, strength chloride penetration and carbonation of concrete. *Journal of Materials in Civil Engineering*, 15(5), pp. 443-451.
- Pade, C. & Guimaraes, M., 2007. The CO₂ uptake of concrete in a 100 year perspective. *Cement and Concrete Research*, 37(9), pp. 1348-1356.
- Padhi, R.S., R.K. Patra, B.B. Mukharjee, T. Dey, 2018. Influence of incorporation of rice husk ash and coarse recycled concrete aggregates on properties of concrete. *Construction and Building Materials*, 173, pp. 289-297.
- Pan, G., Zhan, M., Fu, M., Wang, Y., Lu, X., 2017. Effect of CO₂ curing on demolition recycled fine aggregates enhanced by calcium hydroxide pre-soaking. *Construction and Building Materials*, Volume 154, pp. 810-818.
- PD CEN/TS 12390-9. Testing hardened concrete. Part 9: Freeze-thaw resistance with de-icing salts - Scaling. 2016
- Peng, Q., Wang, L. & Lu, Q., 2018. Influence of recycled coarse aggregate replacement percentage on fatigue performance of recycled aggregate concrete. *Construction and Building Materials*, Volume 169, pp. 347-353.
- Pepe, M., Filho, R., Koenders, E. & Martinelli, E., 2014. Alternative Processing Procedures for Recycled Aggregates in Structural Concrete. *Construction and Building Materials*, Volume 69, pp. 124-132.

- Polger, R., 1947. *An investigation of the compressive strength of concrete in which concrete rubble was used as an aggregate*, New York: Cornell Univeristy.
- Poon, C., Shui, Z., Lam, L., 2002. *Strength of concretes prepared with mineral and recycled aggregates at different moisture conditions*. Hong Kong, China, s.n., pp. 1407-1414.
- Poon, C., Shui, Z., Lam, L., Fok, H., Kou, S., 2004. Influence of moisture states of natural and recycled aggregates on the slump and compressive strength of concrete. *Cement and Concrete Composites*, Volume 34, pp. 31-36.
- Poon, C. S., 1997. Management and Recycling of Demolition Waste in Hong Kong. *Waste Management & Research*, 15(6), pp. 561-572.
- Poon, C. S., Shui, Z. H. & Lam, L., 2002. Strength of concretes prepared with natural and recycled aggregates at different moisture conditions. *Advance in Building Technology* , Volume 2, pp. 1407-1414.
- Poon, C., Azhar, S. & Kou, S., 2003. *Recycled aggregates for concrete applications*. Hong Kong, China, Proceeding of the Materials Science and Technology in Engineering Conference-Now, New, and Next.
- Poon, C., Kou, S. & Lam, L., 2007. Influence of recycled aggregate on slump and bleeding of fresh concrete. *Materials and Structures*, 40(9), pp. 981-988.
- Poon, C., Shui, Z. & Lam, L., 2004. Effect of microstructure of ITZ on compressive strength of concrete prepared with RAs. *Construction and Building Materials*, 18(6), pp. 461-468.
- Powers, M., 1953. A new roundness scale for sedimentary particles. *Journal of Seimentary Petrology*, Volume 23, pp. 117-119.
- Prince, M. & Singh, B., 2013. Bond behaviour between recycled aggregate concrete and deformed steel bars. *Materials and Structures*, 47(3), pp. 503-516.
- Pu, Y., Li, l., Wang, Q., Shi, X., Luan, C., Zhang, G., Fu, L., Abomohra, A., 2021. Accelerated carbonation technology for enhanced treatment of recycled concrete aggregates: A state-of-the-art review. *Construction and Building Materials*, Volume 282, p. 122671.

- Rahal, K., 2007. Mechanical properties of concrete with recycled coarse aggregate. *Building and Environment*, 42(1), pp. 407-415.
- Rangel, C., Amario, M., Pepe, M., Martinelli, E., Filho, R., 2020. Durability of Structural Recycled Aggregate Concrete Subjected to Freeze-Thaw Cycles. *Sustainability*, Volume 12, pp. 64-75.
- Rao, A., 2005. *Experimental investigation on use of recycled aggregate in mortar and concrete*, Kanpur: Department of Civil Engineering, Indian Institute of Technology.
- Rao, A., Kumar, N. & Misra, S., 2007. Use of aggregates from recycled construction and demolition waste in concrete. *Resources, Conservation and Recycling*, 50(1), pp. 71-81.
- Rao, M., Bhattacharyya, S. & Barai, S., 2011. Influence of field recycled coarse aggregate on properties of concrete. *Materials and Structures*, Volume 44, pp. 205-220.
- Rasheeduzzafar, K. A., 1984. Recycled concrete -a source of new aggregate. *Cement, Concrete, and Aggregates (ASTM)*, 6(1), pp. 17-27.
- Ravindarajah, R. & Tam, C., 1985. Properties of concrete made with crushed concrete as coarse aggregate. *Magazine of Concrete Research*, 37(130), pp. 29-38.
- Ravindrajah, R., Loo, Y. & Tam, C., 1987. Recycled concrete as fine and coarse aggregate in concrete. *Magazine of Concrete Research*, 39(141), pp. 214-220.
- Redling, A., 2018. *Construction and Demolition Recycling*. [Online]. Available at: <http://www.cdrecycler.com>. [Accessed 20 May 2019].
- Richardson, A., Coventry, K. & Bacon, J., 2011. Freeze/thaw durability of concrete with recycled demolition aggregate compared to virgin aggregate concrete. *Journal of Cleaner Production*, 19(2-3), pp. 272-277.
- Ridzuan, A. R. M., Diah, A. B. M., Hamir, R. & Kamarulzaman, K. B., 2001. The influence of Recycled Aggregate on the Early Compressive Strength and Drying Shrinkage of Concrete. *Structural Engineering, Mechanics and Computation*, Volume 2, pp. 1415-1422.
- Rozière, E., Loukili, A., El Hachem, R. & Grondin, F., 2009. Durability of concrete exposed to leaching and external sulphate attack. *Cement and Concrete Research*, 39(12), pp. 1188-1198.

- Sagoe-Crentsil, K., Brown, T. & Taylor, A., 2001. Performance of concrete made with commercially produced coarse recycled concrete aggregate. *Cement and Concrete Research*, 31(5), pp. 707-712.
- Salem, R., 1996. *Strength and durability characteristics of recycled aggregate concrete*, Knoxville: Univeristy of Tennessee.
- Salem, R., Burdette, E. & Jackson, N., 2003. Resistance to freezing and thawing of recycled aggregate concrete. *ACI Materials Journal*, 1100(3), pp. 216-221.
- Sanchez, d., Juan, M. & Gutierrez, P., 2004. *Influence of recycled aggregate quality on concrete properties*. Barcelona, Spain, Proceeding of the International RILEM Conference on the Use of Recycled Materials in Building and Structures, pp. 545-553.
- Sarvanakumar, P., Neelakanatan, T. & Jagan, S., 2021. Mechanical properties of recycled aggregate treated by variation in mixing approaches. *Construction Magazine*, 20(2), pp. 236-248.
- Sato, R., Maruyama, I., Sogabe, T. & Sogo, M., 2007. Flexural Behavior of Reinforced Recycled Concrete Beams. *Journal of Advanced Concrete Technology*, 5(1), pp. 43-61.
- Savija, B. & Lukovic, M., 2016. Carbonation of cement paste: understanding, challenges, and opportunities. *Construction and Building Materials*, Volume 117, pp. 285-301.
- Scrivener, K., Crumbie, A. & Laugesen, P., 2004. The Interfacial Transition Zone (ITZ) Between Cement Paste and Aggregate in Concrete. *Interface Science*, 12(4), pp. 411-421.
- Seara-Paz, S., Gonzalez-Fonteboa, B., Martinez-Abella, F., Eiras-Lopez, J., 2018. Flexural performance of reinforced concrete beams made with recycled concrete coarse aggregate. *Engineering Structures*, Volume 156, pp. 32-45.
- Seara-Paz, S., Gonzalez-Fonteboa, B., Martinez-Abella, F. & Carro-Lopez, D., 2018. Long-term flexural performance of reinforced concrete beams with recycled coarse aggregates. *Construction and Building Materials*, Volume 176, pp. 593-607.
- Seara-Paz, S., Gonzalez-Fonteboa, B., Martinez-Abella, F. & Gonzalez-Toboada, I., 2016. Time-dependent behaviour of structural concrete made with recycled coarse

- aggregates. Creep and shrinkage. *Construction and Building Materials*, Volume 122, pp. 95-109.
- Sercombe, J., Vidal, R., Galle, C. & Adenot, F., 2006. Experimental study of gas diffusion in cement paste. *Cement and Concrete Research*, 37(4), pp. 579-588.
- Shaban, W., Yang, J., Su, H., Mo, K., Li, J., Xie, J., 2019. Quality Improvement Techniques for Recycled concrete Aggregate: A review. *Journal of Advanced Concrete Technology*, Volume 17, pp. 151-167.
- Shaban, W., Yang, J., Su, H., Liu, Q., Tsang, D., Wang, L., Xie, J., Li, L., 2019. Properties of recycled concrete aggregates strengthened by different types of pozzolan slurry. *Construction and Building Materials*, Volume 216, pp. 632-647.
- Shannag, M., 2000. High strength concrete containing natural pozzolan and silica fume. *Cement and Concrete Composite*, 22(6), pp. 399-406.
- Sharman, J., 2018. *Construction Waste and materials Efficiency*. [online] Available at: <http://www.thenb.com>. [Accessed 20 February 2022].
- Shayan, A., & Xu, A. (2003). Performance and properties of structural concrete made with recycled concrete aggregate. *ACI Materials Journal*, 100(5), 371–380
- Shi, C., Li, Y., Zhang, J., Li, W., Ching, L., Xie, Z., 2016. Performance enhancement of recycled concrete aggregate - A review. *Journal of Cleaner Production*, Volume 112, pp. 466-472.
- Shi, C., Wu, Z., Cao, Z., Ling, T., Zheng, J., 2018. Performance of mortar prepared with recycled concrete aggregate enhanced by CO₂ and pozzolan slurry. *Cement and Concrete Composites*, Volume 86, pp. 130-138.
- Shinde, M., Vyawahare, M. & Modani, P., 2013. Effect of Physical Properties of Recycled Aggregate on the Strength of Concrete. *International Journal of Engineering Research & Technology*, 2(4), pp. 1655-1659.
- Silva, R., Brito, J. & Dhir, R., 2014. Properties and composition of recycled aggregates from construction and demolition waste suitable for concrete production. *Construction and Building Materials*, Volume 65, pp. 201-217.
- Silva, R., Brito, J. d. & Dhir, R., 2018. Fresh-state performance of recycled aggregate concrete: A review. *Construction and Building Materials*, Volume 178, pp. 19-31.

- Silva, R., de Brito, J. & Dhir, R. K., 2014. Properties and composition of recycled aggregates from construction and demolition waste suitable for concrete production. *Construction and Building Materials*, Volume 65, pp. 201-217.
- Silva, R., Neves, R., de Brito, J. & Dhir, R., 2015. Carbonation behaviour of RAC. *Cement and Concrete Composites*, Volume 62, pp. 22-32.
- Sim, J. & Park, C., 2011. Compressive strength and resistance to chloride ion penetration and carbonation of RAC with varying amount of fly ash and fine RA. *Waste Management*, 31(11), pp. 2352-2360.
- Singh, L.P., Karade, S.R., Bhattacharyya, M.M & Ahalawat, S., 2013. Beneficial Role of Nanosilica in Cement Based Materials - A Review. *Construction and Building Materials*, Volume 47, pp. 1069-1077.
- Singh, S. & Singh, N., 2016. Reviewing the carbonation resistance of concrete. *Journal of Materials Engineering and Structure*, Volume 3, pp. 35-57.
- Sivakumar, N., Muthukumar, S., Sivakumar, V., Gowtham, D., Muthuraj, V., 2014. Experimental studies on high strength concrete by using recycled coarse aggregate. *International Journal of Engineering and Science*, 4(1), pp. 27-36.
- Smiths & Sons, 2015. *Smiths Bletchington*. [Online] Available at: www.smithsbletchington.co.uk [Accessed 9 July 2018].
- Sogo, M., Sogabe, T., Maruyama, I., Kawai, K., 2004. *Shear behaviour of reinforced recycled concrete beams*. Barcelona, RILEM Publications, pp. 610-618.
- Sonawane, T. & Pimplikar, S., 2013. Use of recycled aggregate in concrete. *International Journal of Engineering and Research Technology*, 2(1), pp. 1-9.
- Spaeth, V. & Djerbi Tegguer, A., 2013. Improvement of recycled concrete aggregate properties by polymer treatments. *International Journal of Sustainable Built Environment*, 2(2), pp. 143-152.
- Tadayoshi, F., 1988. *Strength and drying shrinkage of concrete using concrete crushed aggregate*. Tokyo, Japan, RILEM, pp. 672-679.
- Tam, V. & Tam, C., 2007. Assessment of durability of RAC produced by two-stage mixing approach. *Journal of Material Science*, Volume 10, pp. 3592-3602.

- Tam, V. & Tam, C., 2008. Diversifying two-stage mixing approach (TSMA) for recycled aggregate concrete: TSMA and TSMA^{sc}. *Construction and Building Materials*, 22(10), pp. 2068-2077.
- Tam, V., Wattage, H., Le, K., Butera, A., Soomro, M., 2021. Methods to improve microstructural properties of recycled concrete aggregate: A critical review. *Construction and Building Materials*, Volume 270, p. 121490.
- Tam, V., 2009. Comparing the implementation of concrete recycling in the Australian and Japanese construction industries. *Journal of Cleaner Production*, 17(7), pp. 688-702.
- Tam, V., Butera, K. & Le, K., 2016. Carbon-conditioned recycled aggregate in concrete production. *Journal of Cleaner Production*, Volume 133, pp. 672-680.
- Tam, V., Gao, X. & Tam, C., 2005. Microstructural analysis of recycled aggregate concrete produced from two-stage mixing approach. *Cement and Concrete Research*, 35(6), pp. 1195-1203.
- Tam, V., Gao, X., Tam, C. & Chan, C., 2008. New approach in measuring water absorption of recycled aggregates. *Construction and Building Materials*, 22(3), pp. 364-369.
- Tam, V., Kotrayothar, D. & Xiao, J., 2015. Long-term deformation behaviour of recycled aggregate concrete. *Construction and Building Materials*, Volume 100, pp. 262-272.
- Tam, V., Soomro, M. & Evangelista, A., 2018. A review of recycled aggregate in concrete applications (2000-2017). *Construction and Building Materials*, Volume 172, pp. 272-292.
- Tam, V., Tam, C. & Le, K., 2007. Removal of cement mortar remains from recycled aggregate using pre-soaking approaches. *Resources, Conservation, and Recycled*, 50(1), pp. 82-101.
- Tam, V., Tam, C. & Wang, Y., 2007. Optimization on proportion for recycled aggregate in concrete using two-stage mixing approach. *Construction and Building Materials*, 21(10), pp.1928-1939.

- Tam, V., Tam, C., & Wang, Y. 2007. Optimization on proportion for recycled aggregate in concrete using two-stage mixing approach. *Construction and Building Materials*, 21(10), 1982-1939.
- Tangchirapat, W., Buranasing, R., Jaturapitakkul, C. & Chindaprasirt, P., 2008. Influence of rice husk–bark ash on mechanical properties of concrete containing high amount of recycled aggregates. *Construction and Building Materials*, 22(8), pp. 1812-1819.
- Tavakoli, M. & Soroushian, P., 1996. Strength of recycled aggregate concrete made using field-demolished concrete as aggregate. *ACI Materials Journal*, 93(2), pp. 182-190.
- Teranishi, K., Dosho, Y., Narikawa, M. & Kikuchi, M., 1998. *Application of recycled aggregate concrete for structural concrete*. Scotland, Univeristy of Dundee, pp. 143-156.
- Thomas, C., Setien, J., Polanco, J., Alaejos, P., Juan, M., 2013. Durability of RAC. *Construction and Building Materials*, Volume 40, pp. 1054-1065.
- Topcu, I. & Guncan, N., 1995. Using waste concrete as aggregate. *Cement and Concrete Research*, 25(7), pp. 1385-1290.
- Topçu, İ. & Şengel, S., 2004. Properties of concretes produced with waste concrete aggregate. *Properties of concretes produced with waste concrete aggregate*, 34(8), pp. 1307-1312.
- Tošić, N., Marinković, S. & Stojanović, A., 2017. Sustainability of the Concrete Industry – current Trends and Future Outlook. *TEHNIKA–NAŠE GRAĐEVINARSTVO*, 71(1), pp. 38-44.
- Tsujino, M., Noguchi, M., Tamura, M., Kanematsu, M., Maruyama, I., 2013. Application of conventionally recycled coarse aggregate to concrete structure by surface modification treatment. *J. Adv. Concr. Technol.*, 5 , pp. 13-25.
- Tuyan, M., Mardani-Aghabaglou, A. & Ramyar, K., 2014. Freeze–thaw resistance, mechanical and transport properties of self-consolidating concrete incorporating coarse recycled concrete aggregate. *Materials Design*, Volume 53, pp. 983-991.
- Verian, K., Ashraf, W. & Cao, Y., 2018. Properties of recycled concrete aggregate and their influence in new concrete production. *Resources, Conservation and Recycling*, Volume 133, pp. 30-49.

- Vieira, T., Alves, A., de Brito, J., Correia, J., Silva, R., 2016. Durability-related performance of concrete containing fine recycled aggregates from crushed bricks and sanitary ware. *Materials Design*, Volume 90, pp. 767-776.
- Villagrán-Zaccardi, Y., Zega, C. & Di Maio, A., 2008. Chloride penetration and binding in recycled concrete. *Journal of Materials in Civil Engineering*, 20(6), pp. 449-455.
- Vivian, W., Kotrayothar, D. & Xiao, J., 2015. Long-term deformation behaviour of RAC. *Construction and Building Materials*, Volume 100, pp. 262-272.
- Wang, B., Yan, L., Fu, Q. & Kasal, B., 2021. A Comprehensive Review on Recycled Aggregate and Recycled Aggregate Concrete. *Resources, Conservation and Recycling*, Volume 171, p. 105565.
- Wang, J., Zhang, J., Cao, D., Dang, H., Ding, B., 2020. Comparison of recycled aggregate treatment methods on the performance for recycled concrete. *Construction and Building Materials*, Volume 234, p. 117366.
- Wang, L., Wang, J., Qian, X., Chen, P., Xu, Y., Guo, J., 2017. An environmentally friendly method to improve the quality of recycled concrete aggregates. *Construction and Building Materials*, Volume 144, pp. 432-441.
- Wentao, Z. & Ingham, J., 2010. Using recycled concrete aggregates in New Zealand ready-mix concrete production. *Journal of Materials in Civil Engineering*, 22(5), pp. 443-450.
- Wu, J., Jing, X. & Wang, Z., 2017. Uni-axial compressive stress-strain relation of recycled coarse aggregate concrete after freezing and thawing cycles. *Construction and Building Materials*, Volume 134, pp. 210-219.
- Xiao, J. & Falkner, H., 2007. Bond behaviour between recycled aggregate concrete and steel rebars. *Construction and Building Materials*, 21(2), pp. 395-401.
- Xiao, J. et al., 2013. Properties of interfacial transition zones in recycled aggregate concrete tested by nanoindentation. *Cement and Concrete Composites*, Volume 37, pp. 276-292.
- Xiao, J., Lei, B. & Zhang, C., 2012. On carbonation behaviour of recycled aggregate concrete. *Science China Technological Sciences*, 55(9), pp. 2609-2616.

- Xiao, J., Li, J. & Zhang, C., 2005. Mechanical properties of recycled aggregate concrete under uniaxial loading. *Cement and Concrete Research*, 35(6), pp. 1187-1194.
- Xiao, J., Li, W. & Poon, C., 2012. Recent studies on mechanical properties of recycled aggregate concrete in China - A review. *Science China Technological Sciences*, 55(6), pp. 1463-1480.
- Xiao, J., Li, W., Corb, D. & Shah, S., 2013. Effects of interfacial transition zones on the stress-strain behavior of modelled RAC. *Cement and Concrete Research*, Volume 52, pp. 82-99.
- Xiao, J., Li, W., Fan, Y. & Huang, X., 2012. An overview of study on recycled aggregate concrete in China (1996-2011). *Construction and Building Materials*, Volume 31, pp. 364-383.
- Xiao, J., Sun, Y. & Falkner, H., 2006. Seismic performance of frame structures with recycled aggregate concrete. *Engineering Structures*, 28(1), pp. 1-8.
- Xiao, J.-Z., Li, J. & Zhang, C., 2005. Mechanical properties of recycled concrete under uniaxial loading. *Cement and Concrete Research*, 35(6), pp. 1187-1194.
- Xie, F., Li, J., Zhao, G., Zhou, G., Zheng, H., 2020. Experimental study on performance of cast-in-situ recycled aggregate concrete under different sulfate attack exposures. *Construction and Building Materials*, Volume 253, p. 119144.
- Xie, T., A. Gholampour, T. Ozbakkaloglu, 2018. Toward the development of sustainable concretes with recycled concrete aggregates: comprehensive review of studies on mechanical properties. *Journal of Materials and Civil Engineering*, 30, 04018211
- Xu, D., Cui, Y. & Li, H., 2015. On the further of Chinese cement industry. *Cement and Concrete Research*, Volume 78, pp. 2-13.
- Xu, G., Shen, W., Zhang, B., Li, Y., Ji, Y., Ye, Y., 2018. Properties of recycled aggregate concrete prepared with scattering-filling coarse aggregate process. *Cement and Concrete Composites*, Volume 93, pp. 19-29.
- Xuan, D., Zhan, B. & Poon, C., 2016. Assessment of mechanical properties of concrete incorporating carbonated recycled concrete aggregates. *Cement and Concrete Composites*, Volume 65, pp. 67-74.

- Xuan, D., Zhan, B. & Poon, C., 2017. Durability of recycled aggregate concrete prepared with carbonated recycled concrete aggregates. *Cement and Concrete Composites*, Volume 84, pp. 214-221.
- Xuan, D., Zhan, B. & Poon, C., 2018. A maturity approach to estimate compressive strength development of CO₂-cured concrete blocks. *Cement and Concrete Composites*, Volume 85, pp. 153-160.
- Yadav, S. & Pathak, S., 2018. Durability of Recycled Aggregate Concrete: An Experimental Study. *International Journal of Civil and Environmental Engineering*, 12(3).
- Yagishita, F., Sano, M. & Yamada, M., 1991. Properties of recycled reinforced concrete beams made from crushed concrete coarse aggregate. *Construction Materials*, pp. 41-47.
- Yagishita, F., Sano, M. & Yamada, M., 1994. *Behavior of reinforced concrete beams containing recycled coarse aggregate*. s.l., RILEM proceeding, pp. 331-342.
- Yanagi, K. & Kasai, Y., 1998. *Experimental study on the application of recycled aggregate concrete to cast-in-place concrete pile*. Scotland, Univeristy of Dundee, pp. 359-370.
- Yang, H., Xia, J., Thompson, J. & Flower, R., 2017. Urban construction and demolition waste and landfill failure in Shenzhen, China. *Waste Management*, Volume 63, pp. 393-396.
- Yang, K., Chung, H. & Ashour, A., 2008. Influence of type and replacement level of recycled aggregates on concrete properties. *ACI Materials Journal*, Volume 3, pp. 289-296.
- Yang, Y.-F. & Han, L.-H., 2006. Experimental behaviour of recycled aggregate concrete filled steel tubular columns. *Journal of Consturction and Steel Research*, 62(12), pp. 1310-1324.
- Ying, J., Men, Q. & Xia, J., 2017. The effect of cumulative aggregate treatment by carbon dioxide levels on properties of concrete. *Journal of Building Materials*, Volume 20, pp. 277-282.

- Z. Tahar, T.-T. Ngo, E.H. Kadri, A. Bouvet, F. Debieb, S. Aggoun, 2017. Effect of cement and admixture on the utilisation of recycled aggregates in concrete. *Construction and Building Materials*, 149, pp. 91-102
- Zaharieva, R., Buyle-Bodin, F., Skoczylas, F. & Wirquin, E., 2003. Assessment of the surface permeation properties of recycled aggregate concrete. *Cement and Concrete Research*, Volume 25, pp. 223-232.
- Zakaria, M. & Cabrera, J., 1996. Performance and durability of concrete made with demolition waste and artificial fly ash-clay aggregates. *Waste Management*, 16(1-3), pp. 151-158.
- Zega, C. & Di Maio, A., 2011. Use of recycled fine aggregate in concrete with durable requirements. *Waste Management*, 31(11), pp. 2336-2340.
- Zhan, B., Poon, C. & Shi, C., 2013. CO₂ curing for improving the properties of concrete blocks containing recycled aggregates. *Cement and Concrete Composites*, Volume 42, pp. 1-8.
- Zhan, B., Xuan, D., Poon, C. & Shi, C., 2016. Effect of curing parameters on CO₂ curing of concrete blocks containing recycled aggregates. *Cement and Concrete Research*, Volume 71, pp. 122-130.
- Zhan, M., Pan G., Wang, Y., Fu, M., Lu, X., 2017. Effect of presoak-accelerated carbonation factors on enhancing recycled aggregate mortars. *Magazine of Concrete Research*, Volume 69, pp. 838-849.
- Zhang, H., Ji, T., Liu, H. & Su, S., 2018. Modifying recycled aggregate concrete by aggregate surface treatment using sulphoaluminate cement and basalt powder. *Construction and Building Materials*, Volume 192, pp. 526-537.
- Zhang, J. & Shi, C., 2015. Influence of carbonated recycled concrete aggregate on properties of cement mortar. *Construction and Building Materials*, Volume 98, pp. 1-7.
- Zhang, J., Shi, C., Li, Y., Pan, X., 2015. Performance enhancement of recycled concrete aggregates through carbonation. *Journal of Materials in Civil Engineering*, 27(11), p. 04015029.

- Zhao, Z., Wang, S., Lu, L. & Gong, C., 2013. Evaluation of pre-coated recycled aggregate for concrete and mortar. *Construction and Building Materials*, Volume 43, pp. 191-196.
- Zhihui, Z., Shoude, W., Lingchao, L., & Chenchen, G., 2013. Evaluation of pre-coated recycled aggregate for concrete and mortar. *CONstruction and Building Materials*, 43, 191-196.
- Zhu, Y., Kou, Shi, Poon, C., Dai, J., Li, Q., 2013. Influence of silane-based water replent on the durability properties of RAC. *Cement and Concrete Composites*, 35(1), pp. 32-38.
- Zuo, X., Sun, W. & Yu, C., 2012. Numerical investigation on expansive volume strain in concrete subjected to sulfate attack. *Construction and Building Materials*, 36(4), pp. 404-410.

APPENDICES

APPENDIX A

Appendix A-1: data table for Figures 5.1. & 5.2

Effects of water treatment methods on the AIV and the WA of RA

Treatment Method	AIV (%)	WA (%)
NA	14	1.5
Untreated RA	17	6.1
Self-healing	18	3.6
Water-washing 1	16.5	3.7
Water-washing 2	16.7	5.1
Full saturation	18	6
Partial saturation	17	6.1

Appendix A-2: data table for Figures 5.3 & 5.4

Effects of accelerated carbonation treatment on the RA AIV and WA

AIV (%)	1 Day	2 Days	3 Days	4 Days	5 Days	6 Days	7 Days
20% CO ₂ Concentration Level	16.8	16.5	16.2	16	15.9	15.8	15.7
50% CO ₂ Concentration Level	16.5	16.2	16	15.6	15.2	15.1	15.1
100% CO ₂ Concentration Level	16	15.87	15.7	15.68	15.7	15.75	15.8
WA (%)	1 Day	2 Days	3 Days	4 Days	5 Days	6 Days	7 Days
20% CO ₂ Concentration Level	5.3	5.1	4.8	4.5	4.3	4.2	4.1
50% CO ₂ Concentration Level	4.9	4.6	4.1	3.9	3.4	3.3	3.3
100% CO ₂ Concentration Level	4.8	4.6	4.4	4.45	4.48	4.45	4.48

Appendix A-3: data table for Figures 5.6 & 5.7

Effects of soaking RA in sodium silicate-SF solution on RA AIV and WA

AIV (%)	1 hr	4 hrs	24 hrs
5% Replacement level	15.8	15.6	16.1
10% Replacement level	16	15.9	16.6
15% Replacement level	16.3	16.1	16.8
WA (%)	1 hr	4 hrs	24 hrs
5% Replacement level	4.6	4.1	4.9
10% Replacement level	4.8	4.5	5.3
15% Replacement level	5.1	4.8	5.6

Appendix A-4: data table for Figures 5.9 & 5.10***Effects of coating RA with cement and cement-SF slurry on RA AIV and WA***

Coating slurry type	AIV	WA
0.1/C	15.3	3.3
0.2 C	15.6	3.7
0.3/C	16.5	4.6
0.1/C+SF	14.9	2.8
0.2/C+SF	15.2	3.1
0.3/C+SF	16	4.1
Total RA/C	15.8	3.9
Total RA/C+SF	15.4	3.6

Appendix A-5: data table for Figures 5.11 & 5.12***Effects of soaking RA in different cement-pozzolan solutions on RA AIV and WA***

Solution type	WA (%)		AIV (%)	
	1 hr	4 hrs	1 hr	4 hrs
R05/PC+PFA+MK	3.5	3.4	15.8	15.7
R05/PC+PFA+SF	3.8	3.2	15.5	15.2
R05/PC+MK+SF	3.9	3.3	16	15.5
R10/PC+PFA+MK	3.8	3.5	15.3	15.4
R10/PC+PFA+SF	3.2	2.8	15.6	14.7
R10/PC+MK+SF	3.6	3.1	15.7	15.1
R15/PC+PFA+MK	4.5	4	16.1	16.1
R15/PC+PFA+SF	4.1	3.6	16.5	15.9
R15/PC+MK+SF	4.9	4.3	16.7	16.3

Appendix A-6: data table for Figure 5.15**Effects of different batching techniques on the compressive strength of RAC**

	NAC1	RAC2	SEMA	MMA	TSMA	SEPP _(SF)	SEPP _(GGBS)
7	32.78	26.60	31.30	29.50	28.46	32.40	30.59
14	36.40	28.70	34.44	32.70	30.80	35.70	33.86
28	38.20	29.80	36.40	34.80	33.67	37.60	35.70

APPENDIX B**Appendix B-1: data table for Figure 5.20****Effects of different treatment methods and their combination on the compressive strength of RAC at different w/c ratios**

Mix Code	28 days (MPa)	7 days (MPa)	Mix Code	28 days (MPa)	7 days (MPa)
W040/RAC2	35.95	27.15	W045/RAC2	30.55	22.10
W040/SE	37	28.20	W045/SE	31.60	22.80
W040/AC	37.15	27.75	W045/AC	31.75	22.35
W040/SCP	38.45	29.35	W045/SCP	33.05	23.95
W040/AC+SE	40.1	30.20	W045/AC+SE	34.70	24.80
W040/SCP+AC	40.75	31.35	W045/SCP+AC	35.40	25.95
W040/SCP+AC+SE	41	32.85	W045/SCP+AC+SE	35.60	27.45
W040/SCP+SE	42.25	33.15	W045/SCP+SE	36.85	27.75
W040/NAC1	46.8	36.90	W045/NAC1	41.40	31.50
Mix Code	28 days (MPa)	7 days (MPa)	Mix Code	28 days (MPa)	7 days (MPa)
W050/RAC2	25.35	16.90	W055/RAC2	20.45	12.00
W050/SE	26.40	17.60	W055/SE	21.15	12.70
W050/AC	26.55	17.15	W055/AC	21.65	12.25
W050/SCP	27.85	18.75	W055/SCP	22.95	13.85
W050/AC+SE	29.50	19.60	W055/AC+SE	24.60	14.70
W050/SCP+AC	30.15	20.75	W055/SCP+AC	25.30	15.85
W050/SCP+AC+SE	30.40	22.25	W055/SCP+AC+SE	25.50	17.35
W050/SCP+SE	31.65	22.60	W055/SCP+SE	26.75	17.65
W050/NAC1	36.00	26.10	W055/NAC1	31.11	21.20
Mix Code	28 days (MPa)	7 days (MPa)			
W060/RAC2	15.60	7.10			
W060/SE	17.20	7.80			
W060/AC	17.30	8.9			
W060/SCP	17.50	9.2			
W060/AC+SE	18.30	10			
W060/SCP+AC	19.60	11.5			
W060/SCP+AC+SE	20.90	12.1			
W060/SCP+SE	21.80	12.5			
W060/NAC1	26.21	16.40			

APPENDIX C

Appendix C-1: Data table for Figure 5.21

Effects of different treatment methods on the tensile splitting strength of RAC

Mix Code	Tensile Splitting Strength	Mix Code	Tensile Splitting Strength	Mix Code	Tensile Splitting Strength
W040/NAC1	3.80	W050/NAC1	3.40	W060/NAC1	2.80
W040/RAC2	3.30	W050/RAC2	2.85	W060/RAC2	1.90
W040/SCP	3.60	W050/SCP	3.03	W060/SCP	2.20
W040/SE	3.35	W050/SE	2.90	W060/SE	2.04
W040/SCP+SE	3.65	W050/SCP+SE	3.30	W060/SCP+SE	2.40

Appendix C-2: Data table for Figure 5.23

Effects of different treatment methods on the flexural strength of RAC

Mix Code	Flexural Strength	Mix Code	Flexural Strength	Mix Code	Flexural Strength
W040/NAC1	6.44	W050/NAC1	4.60	W060/NAC1	3.96
W040/RAC2	4.62	W050/RAC2	3.89	W060/RAC2	2.49
W040/SCP	4.96	W050/SCP	4.21	W060/SCP	2.78
W040/SE	4.72	W050/SE	4.06	W060/SE	2.65
W040/SCP+SE	5.36	W050/SCP+SE	4.46	W060/SCP+SE	3.06

Appendix C-3: Data table for Figure 5.26

Effects of different treatment methods on the modulus of elasticity of RAC

Mix Code	Flexural Strength	Mix Code	Flexural Strength	Mix Code	Flexural Strength
W040/NAC1	33.50	W050/NAC1	29.20	W060/NAC1	27.00
W040/RAC2	28.60	W050/RAC2	26.50	W060/RAC2	23.50
W040/SCP	29.10	W050/SCP	27.10	W060/SCP	25.00
W040/SE	28.90	W050/SE	26.80	W060/SE	24.80
W040/SCP+SE	31.00	W050/SCP+SE	28.50	W060/SCP+SE	26.60

APPENDIX D

Appendix D-1: Data table for Figure 5.29

Effects of different treatment methods on the water absorption of RAC

Mixture Code	Water Absorption (%)	Mixture Code	Water Absorption (%)	Mixture Code	Water Absorption (%)
W040/NAC1	0.60	W050/NAC1	0.82	W050/NAC1	1.15
W040/RAC2	1.00	W050/RAC2	1.08	W050/RAC2	1.59
W040/SCP	0.93	W050/SCP	1.01	W050/SCP	1.38
W040/SE	0.84	W050/SE	0.95	W050/SE	1.42
W040/SCP+SE	0.72	W050/SCP+SE	0.90	W050/SCP+SE	1.30

Appendix D-2: Data table for Figures 5.33 & 5.32

Effects of different treatment methods on the freeze-thaw resistance of RAC (loss in compressive strength)

	28 Days (MPa)	28 Days frost (MPa)	140 Days (MPa)	140 Days frost (MPa)
W040/NAC1	46.8	45.3	55.6	50.3
W040/RAC2	35.95	32.8	42.4	36.5
W040/SCP	38.45	36.2	45.8	40.2
W040/SE	37	34.8	43.6	38
W040/SCP+SE	42.25	40.2	52.2	46.5
W050/NAC1	36	34.3	41.2	36.1
W050/RAC2	25.35	23.1	28.9	24.2
W050/SCP	27.85	26.1	32.3	27.8
W050/SE	26.4	24.8	31.7	26.7
W050/SCP+SE	31.65	30	37.6	32.6
W060/NAC1	26.21	24.7	29.4	25.1
W060/RAC2	15.6	13.6	17.6	13.9
W060/SCP	17.5	16.1	21.9	17.5
W060/SE	17.2	15.9	20.8	16.80
W060/SCP+SE	21.8	20.3	25.8	21.50

Effects of different treatments on the freeze-thaw resistance of RAC (change in mass %)

Water to cement ratio = 0.4						Water to cement ratio = 0.5					
Cycle	NAC1	RAC2	SCP	SE	SCP+SE	Cycle	NAC	RAC	SCP	SE	SCP+SE
1	0.01	0.04	0.03	0.03	0.02	1	0.02	0.05	0.03	0.04	0.03
2	0.02	0.08	0.06	0.05	0.04	2	0.03	0.08	0.05	0.06	0.04
3	0.03	0.06	0.06	0.04	0.03	3	0.04	0.09	0.05	0.06	0.05
4	0.04	0.08	0.07	0.06	0.05	4	0	-0.02	0.00	-0.01	-0.01
5	0.05	0.09	0.08	0.09	0.06	5	-0.01	-0.08	-0.06	-0.07	-0.05
6	-0.02	0.1	-0.04	-0.05	-0.05	6	-0.05	-0.11	-0.08	-0.09	-0.09
7	-0.03	-0.05	-0.05	-0.04	-0.03	7	-0.1	-0.15	-0.12	-0.14	-0.11
8	-0.02	-0.05	-0.04	-0.04	-0.05	8	-0.12	-0.2	-0.18	-0.15	-0.13
9	-0.01	-0.06	-0.04	-0.03	-0.02	9	-0.15	-0.25	-0.20	-0.22	-0.18
10	-0.05	-0.07	-0.06	-0.05	-0.04	10	-0.21	-0.32	-0.28	-0.26	-0.24
11	-0.08	-0.12	-0.10	-0.09	-0.09	11	-0.25	-0.38	-0.33	-0.35	-0.27
12	-0.1	-0.15	-0.14	-0.15	-0.13	12	-0.27	-0.38	-0.35	-0.36	-0.34
13	-0.12	-0.19	-0.16	-0.15	-0.14	13	-0.3	-0.4	-0.38	-0.35	-0.32
14	-0.14	-0.23	-0.20	-0.18	-0.16	14	-0.32	-0.45	-0.40	-0.41	-0.36
15	-0.16	-0.28	-0.20	-0.22	-0.19	15	-0.35	-0.5	-0.46	-0.48	-0.38
16	-0.12	-0.35	-0.30	-0.24	-0.25	16	-0.4	-0.6	-0.50	-0.52	-0.46
17	-0.15	-0.4	-0.32	-0.28	-0.30	17	-0.4	-0.9	-0.60	-0.63	-0.55
18	-0.18	-0.48	-0.36	-0.38	-0.32	18	-0.5	-0.96	-0.70	-0.75	-0.62
19	-0.2	-0.6	-0.40	-0.45	-0.35	19	-0.6	-1.1	-0.78	-0.86	-0.72
20	-0.25	-0.64	-0.43	-0.50	-0.35	20	-0.70	-1.15	-0.87	-0.96	-0.82

Water to cement ratio = 0.6					
Cycle	NAC1	RAC2	SCP	SE	SCP+SE
1	0.01	0.04	0.03	0.03	0.02
2	0.02	0.08	0.06	0.05	0.04
3	0.03	0.06	0.06	0.04	0.03
4	0.04	0.08	0.07	0.06	0.05
5	0.05	0.09	0.08	0.09	0.06
6	-0.02	0.1	-0.04	-0.05	-0.05
7	-0.03	-0.05	-0.05	-0.04	-0.03
8	-0.02	-0.05	-0.04	-0.04	-0.05
9	-0.01	-0.06	-0.04	-0.03	-0.02
10	-0.05	-0.07	-0.06	-0.05	-0.04
11	-0.08	-0.12	-0.10	-0.09	-0.09
12	-0.1	-0.15	-0.14	-0.15	-0.13
13	-0.12	-0.19	-0.16	-0.15	-0.14
14	-0.14	-0.23	-0.20	-0.18	-0.16
15	-0.16	-0.28	-0.20	-0.22	-0.19
16	-0.12	-0.35	-0.30	-0.24	-0.25
17	-0.15	-0.4	-0.32	-0.28	-0.30
18	-0.18	-0.48	-0.36	-0.38	-0.32
19	-0.2	-0.6	-0.40	-0.45	-0.35
20	-0.25	-0.64	-0.43	-0.50	-0.35

Appendix D-3: Data table for Figures 5.36 & 5.35

Effects of different treatment methods on the sulphate attack resistance of RAC (loss in compressive strength)

	28 Days (MPa)	28 Days sulphate (MPa)	140 Days (MPa)	140 Days sulphate (MPa)
W040/NAC1	46.80	46.50	55.6	51.2
W040/RAC2	35.95	34.50	42.4	34.1
W040/SCP	38.45	37.60	45.8	39.6
W040/SE	37.00	36.00	43.6	36.2
W040/SCP+SE	42.25	41.20	52.2	46.5
W050/NAC1	36.00	35.20	41.2	35.3
W050/RAC2	25.35	23.70	28.9	21.8
W050/SCP	27.85	26.40	32.3	25.7
W050/SE	26.40	24.80	31.7	24.8
W050/SCP+SE	31.65	30.40	37.6	30.5
W060/NAC1	26.21	25.10	29.4	23.1
W060/RAC2	15.60	13.90	17.6	11.8
W060/SCP	17.50	16.20	21.9	16.5
W060/SE	17.20	15.70	20.8	14.80
W060/SCP+SE	21.80	20.50	25.8	19.80

Effects of different treatments on the sulphate attack resistance of RAC (change in mass %)

w/c = 0.4					
Weeks	NAC1	RAC2	SCP	SE	SCP+SE
4	0.000	0.060	0.070	0.080	0.050
8	0.040	0.100	0.078	0.089	0.065
12	0.040	0.180	0.120	0.150	0.090
16	0.165	0.270	0.210	0.260	0.180
20	0.210	0.380	0.310	0.350	0.250
w/c = 0.5					
Weeks	NAC1	RAC2	SCP	SE	SCP+SE
4	0.02	0.1	0.06	0.08	0.06
8	0.1	0.25	0.12	0.15	0.11
12	0.29	0.42	0.35	0.37	0.31
16	0.45	0.68	0.51	0.57	0.48
20	0.62	0.86	0.72	0.78	0.70
w/c = 0.5					
Weeks	NAC1	RAC2	SCP	SE	SCP+SE
4	0.2	0.7	0.50	0.67	0.50
8	0.8	1.2	0.95	1.10	0.96
12	1.3	1.8	1.50	1.60	1.40
16	1.9	2.5	2.30	2.40	2.20
20	2.6	3.8	3.1	3.50	2.90

APPENDIX E-JOURNAL PUBLICATIONS

Appendix E-1: Al-Waked, Qusai; Bai, Jiping; Kinuthia, John; Davies, Paul, 2022. Enhancing the aggregate impact value and water absorption of demolition waste coarse aggregates with various treatment methods. *Case studies in construction materials*, volume 17, p. e01267, <https://doi.org/10.1016/j.cscm.2022.e01267>

Appendix E-2: Al-Waked, Qusai; Bai, Jiping; Kinuthia, John; Davies, Paul, 2022. Enhancement of Mechanical Properties of Concrete with Treated Demolition Waste Aggregate. *Journal of Building Engineering*, p. 105047, <https://doi.org/10.1016/j.jobe.2022.105047>

Appendix E-3: Al-Waked, Qusai; Bai, Jiping; Kinuthia, John; Davies, Paul, 2022. Durability and Microstructural Analyses of Concrete Produced with Treated Demolition Waste Aggregates, *Construction and Building Materials*, volume 347, p. 128597, <https://doi.org/10.1016/j.conbuildmat.2022.128597>

1 **ENHANCING THE AGGREGATE IMPACT VALUE AND WATER ABSORPTION**
2 **OF DEMOLITION WASTE COARSE AGGREGATES WITH VARIOUS**
3 **TREATMENT METHODS**

4 Qusai Al-Waked^{1,2}, Jiping Bai¹, John Kinuthia¹, Paul Davies¹

5 ¹ Faculty of Computing, Engineering and Science, University of South Wales, Treforest
6 Campus, CF37 1DL, UK

7 ² Corresponding author

8 **ABSTRACT**

9 Recycled aggregate (RA) from construction and demolition waste can readily be used to
10 replace natural aggregate in concrete. Nonetheless, the poor quality of RA adversely affects
11 the properties of recycled aggregate concrete, limiting its use to only non-structural
12 applications. This study examined the effects of various treatment methods by testing the
13 aggregate impact value (AIV) and water absorption (WA) of recycled coarse aggregate
14 before and after treatments as an indicator to examine the efficiency of these treatments. The
15 results showed that the untreated RA achieved 17% and 6.1% for AIV and WA, respectively.
16 Accelerated carbonation treatment at 50% CO₂ concentration level for six days of CO₂
17 exposure time achieved the best results among other carbonation conditions, showing 11%
18 and 46% enhancements in the AIV and WA, respectively. The RA treated with cyclic
19 limewater combined with accelerated carbonation exhibited better improvement in the AIV
20 and WA compared to the sole use of accelerated carbonation treatment. Coating RA with
21 cement-silica fume slurry at 0.1mm coating thickness was found to be optimal, achieving
22 12% and 54% enhancements in the AIV and WA, respectively. Soaking RA in a 10%
23 Portland cement - pulverized fuel ash - silica fume solution for 4 hours was found to be

24 optimal, recording enhancements of 13% and 54% in the AIV and the WA, respectively
25 among other soaking solutions. Soaking RA in 5% sodium silicate – silica fume solution for 4
26 hours was found to be optimal, obtaining 8% and 33% enhancements in the AIV and the WA,
27 respectively. The treatment techniques proposed can be a powerful tool for promoting the use
28 of RA in the construction industry.

29 **Keywords:** Recycled aggregate, Demolition waste aggregates, Treatments, Adhered mortar,
30 Water absorption, Aggregate impact value.

31 **1. Introduction**

32 Construction industry activities generate large amounts of waste. According to Ali and
33 Samarah (2018), about 3 billion tonnes of construction and demolition waste (C&DW) is
34 annually generated worldwide until 2012, and this figure is expected to constantly increase.
35 Europe produces approximately 850 million tonnes of C&DW (Tošić et al., 2017), while,
36 nearly 18.8 and 21.2 million tonnes of hard demolition waste were generated in the UK in
37 2014 and 2015 respectively, and this quantity is predicted to continue to increase annually
38 (Sharman, 2018). The dumping and landfilling of C&DW have rapidly and enormously led to
39 a series of issues to the environment because C&DW may contain hazardous materials (Lu,
40 2019).

41 Despite that there are several countries that recycle around 80% of C&DW such as Japan, the
42 Netherlands, Germany etc., developing countries have an average rate of recycling of 20% to
43 40% (Tam et al., 2018). Accordingly, promoting the use of recycled aggregate (RA) from the
44 C&DW into new concrete as a replacement for natural aggregate (NA) is an essential
45 priority. This would lead to a reduction in carbon dioxide emissions and contribute
46 significantly towards preserving the environment by minimizing the depletion of natural
47 resources, thus leading to a sustainable and green future (Silva et al., 2014).

48 Kim (2022) stated that the recycling of concrete waste is crucial for the sustainable
49 development of the construction industry. With advances in technology in the manufacture of
50 crusher machines and the developed recycling process of plants, it is now possible to obtain
51 RA from large portions of C&DW at a reasonable cost. In line with this, recently, the
52 utilization of RA from the C&DW in civil engineering applications has gained a huge interest
53 worldwide, and studies on their possible use in new concrete have been carried out
54 extensively over the last two decades.

55 Recently, a significant number of studies examined the effects of RA on concrete (Kim,
56 2022; Katkhuda and Shatarat, 2017; Dabiri et al., 2022; Delbas et al., 2019; Dimitriou et al.,
57 2018) and revealed that replacing NA with RA in concrete adversely affects the mechanical
58 properties of concrete. This negative effect of RA on concrete performance has limited its
59 utilization in the construction industry to non-structural applications, road bases, blinding
60 concrete, and footpaths (Tam, 2009).

61 According to Gonzalez & Etxeberria (2014), the reduced attraction towards RA is mainly due
62 to their poor engineering properties as a result of numerous factors, primarily the presence of
63 the adhered mortar and the weak old interfacial transition zone on the RA surface. Other
64 factors may include, pre-loading, accelerated weathering, processing costs, and the
65 constituents of different materials with various engineering properties (i.e., bricks, glass,
66 rounded stones, and recycled concrete aggregates) (Gonzalez & Etxeberria, 2014). Therefore,
67 RA possesses low density, low aggregate impact value, low crush value, high water
68 absorption, weak ITZ, weak bonding, micropores, and microcracks compared to NA (Bru et
69 al., 2014).

70 Consequently, studies with the aim of enhancing the quality of RA have been carried out
71 extensively over the past decade to produce high-quality RA and ultimately expand RAC

72 application into structural concrete (Al-Bayati et al., 2016; Bru et al., 2014; Dilbas et al.,
73 2019; Dimitriou, 2018). The current methods used for treating RA can be categorized into
74 two main approaches; (i) removing the adhered mortar, and (ii) strengthening the adhered
75 mortar.

76 Removing the adhered mortar techniques can offer great results through practical treatment
77 procedures such as soaking in acid (Katkhuda and Shatarat, 2017), thermal or traditional
78 heating (Pawluczuk et al., 2019), microwave heating (Bru et al., 2014), and mechanical
79 treatment (Dilbas et al., 2019).

80 Although removing the adhered mortar technique has been observed to offer promising
81 results, it showed some negative side effects, for instance, soaking in acid and mechanical
82 treatments may introduce micro-cracks and damage to the RA surface (Tam et al., 2007; Al-
83 Bayati and Tighe, 2016). In addition, removing the adhered mortar methods tends to increase
84 the cost of recycled aggregates, not to mention it may result in fine aggregates which in turn
85 may be considered as another waste material generation especially if it is not utilized.

86 The approach of strengthening the adhered mortar offers greater advantages than removing
87 the adhered mortar (Tam et al., 2007). Strengthening the adhered mortar include methods
88 such as coating RA with pozzolan slurry (Kou and Poon, 2012), calcium carbonate
89 biodeposition (Grabiec et al., 2012), soaking RA in sodium silicate solution (Chen et al.,
90 2006), and accelerated carbonation (Kou et al., 2014). The latter treatment is thought to have
91 more advantages over the other treatments in terms of the environmental impact. Mazurana et
92 al, (2020) stated that RAs from the C&DW are capable of absorbing CO₂ through the reaction
93 of the available calcium hydroxide on their surface and their high surface area. Thus, the
94 utilization of carbonation treatment in the construction industry for enhancing RA can help

95 reduce the global CO₂ emission by the deployment of carbon capture of RA via carbonation
96 treatment (Mazurana, 2019).

97 There are a significant amount of studies that have dealt with the effects of different
98 treatments on the performance of recycled aggregate concrete, little attention, however, has
99 been devoted to the effects of these treatments on RA properties.

100 Aggregates as inert fillers in concrete take around 80% of the concrete volume. Its physical
101 properties, such as aggregate impact value (AIV) and water absorption (WA) affect the
102 properties of fresh and hardened concrete. To this end, the present study aims at evaluating
103 the effects of accelerated carbonation, cyclic limewater-accelerated carbonation, soaking RA
104 in sodium silicate-silica fume solution, coating RA with cement-silica fume slurry, and
105 soaking RA in cement-pozzolan solutions on the aggregate impact value (AIV) and water
106 absorption (WA) of RA.

107 **2. Materials characteristics**

108 ***2.1 Aggregates***

109 Two particle sizes of crushed limestone coarse aggregate (NA) were used throughout this
110 study, 20/10 mm, and 10/4 mm. The limestone aggregate was sourced in bulk from Jewson
111 UK Limited in Caerphilly, South Wales, UK, confirming BS EN 12620:2002+A1: 2008. The
112 untreated recycled aggregate (RA) utilized was sourced from Derwen Group, Neath Abbey,
113 UK. It is a mix of construction and demolition waste with a size range of clean 20/10 mm and
114 10/4mm. According to Derwen Group, the RA provided was produced to industry standards,
115 in accordance with WRAP Quality protocol and BS EN 13242: 2013 specifications (Derwen
116 Group, 2016). The RA consisted of different recycled materials i.e., brick, glass, bituminous,
117 rounded stones, and recycled concrete aggregates. Figure 1 shows the NA and RA utilized

118 throughout this study. Table 1 shows the compositions of RA in accordance with BS 8500-2:
 119 2015+A2: 2019. The mechanical and physical properties of the NA and RA are given in
 120 Table 2, while the particle size distribution of NA and RA is given in Figure 2.

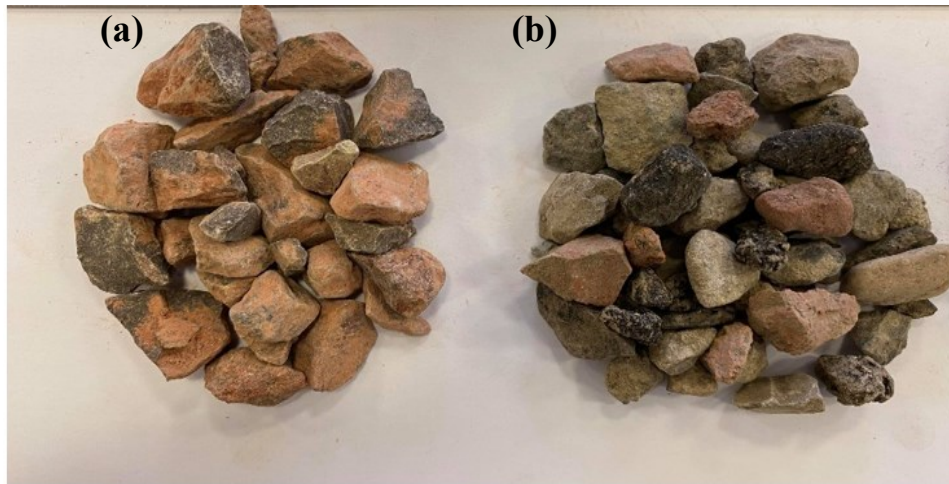


Figure 1: (a) coarse NA, (b) coarse untreated RA (URA)

121
122

	R_c (%)	R_u (%)	R_b (%)	R_g (%)	R_a (%)	X (%)
Sample 1	49.14	29.47	12.51	0.17	8.38	0.34
Sample 2	47.5	28.06	11.5	1.12	11.00	0.48
Sample 3	50.6	25.8	13.4	0.00	9.5	0.37
BS limits	–	–	–	–	≤10%	≤1%
Mean	49.08	27.78	12.47	0.42	9.6	0.39

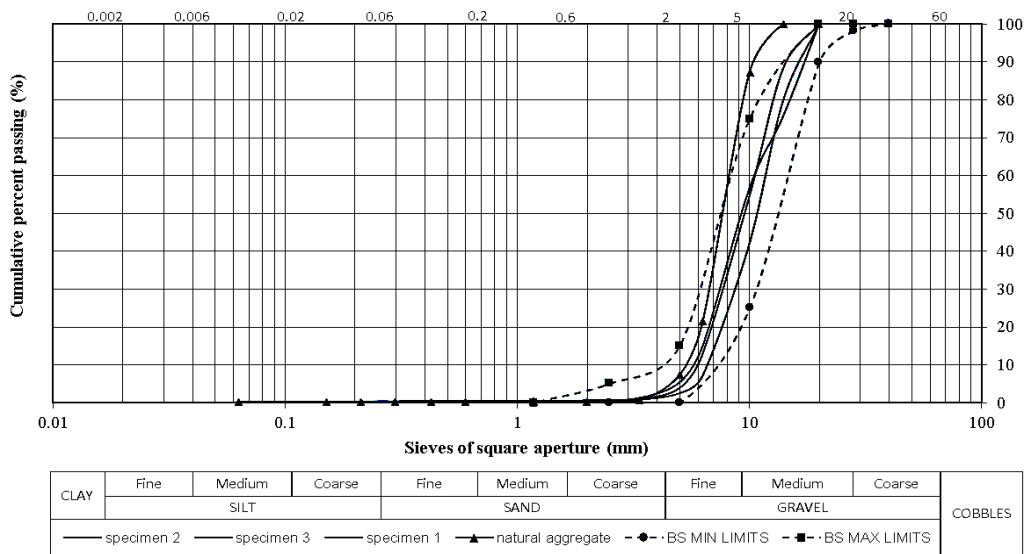
123 Notes: R_c - cement-based products, R_u - unbounded aggregates and/or natural stones, R_b -
 124 clay masonry units i.e., bricks and tiles, calcium silicate masonry unit, R_a - bituminous
 125 materials, and X - miscellaneous materials and/or non-floating wood, plastic, and rubber, R_g -
 126 crushed glass.

127 Table 1: Compositions of recycled aggregates in this study (BS 8500-2:2015 +A2: 2019)

128
129
130
131
132

Characteristic	NA	URA	BS limits	Standard
Flakiness Index (FI) (%)	18	27	< 40	BS EN 933-3:2012
Shape Index (SI) (%)	12	18	< 55	BS EN 933-4:2008
Water Absorption (WA) (%)	1.5	6.1	< 8	BS EN 1097-6:2013
Density kg/m ³	2480	2120	–	BS EN 1097-6:2013
Aggregate Impact Value (AIV) (%)	14	17	< 32	BS EN 1097-2:2020
LA (%)	18	26	< 50	BS EN 1097-2: 2020

133 Table 2: Characteristics of the untreated RA (URA) compared with NA and relevant BS EN
134 standards



135
136 Figure 2: Particle size distribution of coarse RA and coarse NA

137 **2.2 Portland cement**

138 A commercially available Portland cement (CEM I-42.5 N) which was manufactured in
139 accordance with BS EN 197-1: 2011 was used throughout the study. The CEM I was sourced
140 from Jewson UK limited based in Caerphilly, South Wales, UK. The oxide and physical
141 composition of the cement used are shown in Table 3.

142 **2.3 Pozzolanic materials**

143 The pulverized fuel ash (PFA) used throughout this study was supplied by a local supplier
144 and was compliant with BS EN 450-1:2012. The silica fume (SF) utilized throughout this
145 study was an un-densified silica fume with a commercial code 971U and was to the
146 conformity of BS EN 13263-2:2005+A1:2009. It was manufactured by Elkem Silicon

147 Materials based in Norway and had a 97.1% purity. The ground granulated blast-furnace slag
 148 (GGBS) used is a by-product material and was supplied from the Port Talbot steelworks in
 149 South Wales, UK, in compliance with BS EN 15167-1:2006. Metakaolin (MK) used was an
 150 industrial type of the Metastar 501 brand manufactured by IMERYYS company in the UK. The
 151 oxide and physical composition of the pozzolana used are given in Table 2.

152 2.4 Other materials

153 Sodium silicate also known as water-glass or sodium metasilicate was supplied by fisher
 154 scientific, Leicestershire, UK as a commercial white powder with a molar ratio $\text{SiO}_2/\text{Na}_2\text{O} =$
 155 2. Commercially available calcium hydroxide white powder with a purity of 99.995% and
 156 2.24g/mL density, was also supplied by fisher scientific, Leicestershire, UK. Limewater
 157 solution was prepared by mixing 1.65g of calcium hydroxide in 1L of water at 25° C.

Oxide	Composition by (wt%)				
	PC	SF	PFA	GGBS	MK
CaO	61.49	–	0.22	37.99	0.07
SiO ₂	18.84	97.1	59.04	35.54	52.1
Al ₂ O ₃	4.77	0.1	34.08	11.46	41.0
Fe ₂ O ₃	2.87	0.2	2.00	0.42	4.32
SO ₃	3.12	0.06	0.05	1.54	–
Na ₂ O	0.02	–	1.26	0.37	0.26
Physical properties					
Colour	Grey	Dark Grey	Light Grey	Off-white	Off-white
Bulk density (kg/m ³)	1400	120-220	800-1000	1200	500
Specific gravity (Mg/m ³)	3.16	2.20	2.90	2..85	2.50

158 Table 3: Oxide compositions and physical properties of materials used throughout this study

159 3. Experimental work of aggregate treatments

160 3.1 Testing methods

161 Aggregate impact value (AIV) and water absorption (WA) were carried out on RA before and
 162 after treatment to evaluate the effects of treatments on enhancing these two properties. AIV
 163 was carried out in accordance with BS EN 1097-2:2020. AIV was performed on coarse RA
 164 passing the 12.5 mm sieve and retaining on the 10 mm BS test sieve. The test specimen was

165 then poured into a cylindrical cup, followed by subjecting it to 25 gentle blows with a
166 tamping rod to get it compacted at three layers. Thereafter, any surplus aggregates were stuck
167 off, and the net weight of the aggregate was determined as (W1). The aggregates were then
168 poured into another cylindrical cup attached to the impact apparatus base, where 25 strokes
169 were then applied with a tamping rod to compact the test sample. The hammer of the machine
170 was raised until its lower face was 380 mm above the upper surface of the test sample in the
171 cup and was allowed to fall freely on the test sample for 15 blows. The crushed test sample
172 was then removed and sieved through the 2.36 mm BS sieve, and the passing particles were
173 weighed (W2). The Aggregate Impact Value (AIV) was calculated according to equation 1.

174
$$AIV = (W_2/W_1) \times 100\%$$
 Equation 1

175 **3.2 Treatment techniques**

176 Five treatment methods were employed in this study, accelerated carbonation, cyclic
177 limewater-accelerated carbonation, soaking in sodium silicate-silica fume solution, coating
178 with cement-silica fume slurry, and soaking in cement-pozzolan solutions.

179 ***Accelerated carbonation.*** Prior to carbonation treatment, the RA was firstly air-dried at room
180 temperature and monitored to achieve the desired moisture content of 5-7% for the required
181 experimental work as recommended by Zhan et al. (2016) and Pan et al. (2017), with a view
182 to accelerating the carbonation reaction through dissolving the CO₂ gas and Ca⁺² contained in
183 RA (especially in the adhered mortar), while reducing the moisture content of the recycled
184 aggregates. The RA was then placed into the carbonation chamber at a controlled temperature
185 and relative humidity set at 22 ± 2 °C and 50 ± 5%, respectively. Thereafter, the RA
186 underwent carbonation for 7 days at 3 different CO₂ concentration levels 20%, 50%, and
187 100% and at +0.1 bar gas pressure. A sufficient quantity of silica gel was put at the bottom of
188 the chamber and regularly replenished to remove the evaporated water from the aggregates

189 during the carbonation process. The carbonation device used in this study was a Galaxy 170
190 R CO₂ incubator as shown in Figure 3.

191



192
193

Figure 3: CO₂ incubator used for the CO₂ treatment of recycled aggregates

194 ***Cyclic limewater-accelerated carbonation.*** In this treatment approach, the following steps
195 were repeated for three cyclic periods, (i) the RA were firstly pre-soaked in limewater
196 solution for three days, and then (ii) pre-dried in a chamber at $20 \pm 2^\circ\text{C}$ and relative humidity
197 of $50 \pm 5\%$ for 3 days. (iii) The RA were then placed into the CO₂ chamber and underwent
198 carbonation at 100% CO₂ concentration level at a pressure of +0.1 bar for 24 hours.

199 ***Soaking RA in sodium silicate-silica fume solution.*** The Recycled aggregates were
200 impregnated in sodium silicate-silica fume solution for 1 hour, 4 hours, and 24 hours. The
201 solutions selected for this treatment were prepared with three different replacement levels in
202 which sodium silicate-silica fume replaced water at 5 wt%, 10 wt%, and 15wt%, and the
203 mixing proportion of these two combined materials was worked out using a ratio of 0.6 of
204 sodium silicate powder to silica fume powder. Table 4 shows a sample mix proportion design
205 of the solution for treating 1000g of recycled aggregate.

206

Replacement level %	Sodium Silicate (g)	Silica Fume (g)	Water (g)
5%	19	31	950
10%	37.5	63	900
15%	56	94	850

207 Table 4: Proposed solution ingredient for soaking RA in sodium silicate-silica fume solution

208 The methodology adopted involved the following procedures, the recycled aggregates were
209 firstly dried in an oven for 24 h at 105 °C, and then cooled at room temperature. After the
210 sodium silicate-silica fume solution was prepared, it was stirred for 2 mins to reach
211 homogeneity and ensured an appropriate diffusion of sodium silicate and silica fume
212 particles. The recycled aggregates were then immersed in the solutions prepared for 1 hour, 4
213 hours, and 24 hours. Thereafter, the RA was then drained for 10 min. Finally, the recycled
214 aggregates were dried in an oven at 105 °C for 24 hours and cooled down at room
215 temperature for one day.

216 ***Coating with cement slurry or cement-silica fume slurry.*** This treatment method involved
217 the following procedures, firstly, the cement slurry or cement-silica fume slurry was prepared
218 with the required cement or cement-silica fume and water then properly stirred. RA was then
219 added to the slurries prepared and properly mixed using a mixer machine for 10 mins. The
220 aggregates coated were then placed on trays to dry for 1 day at room temperature of $20 \pm 2^\circ\text{C}$
221 and then cured in water for 7 days holding time to ensure the cement paste of the coated RA
222 was fully hydrated. In this present study, the RA was coated with cement slurry or cement-
223 silica fume slurry to reinforce its ability in resisting impact and enhance its water absorption.
224 Two methods of coating the RA with cement and/or cement-silica fume slurry were adopted
225 in this study: (i) coating of individual RA size fractions separately, and (ii) coating of the
226 total combined RA particle sizes fraction.

227 (i) *Coating the individual particle size fractions with cement or cement-silica fume*
228 *slurry*

229 The calculation steps that were set by Lee et al., (2011) to determine the required volume of
230 the coating paste for coating the RA, were followed in this study. The water-to-binder ratio
231 for the preparation of the slurries was set at 0.45. Silica fume replaced 15% of cement weight
232 in the cement-silica fume slurry. Three different theoretical thicknesses (*t*th) were proposed
233 to coat the RA; 0.1 mm, 0.2 mm, and 0.3 mm.

234 (ii) *Coating the total combined gradation with cement or cement-silica fume slurry*

235 In this technique, the total combined gradation of RA was coated with a coating level of 5%
236 of cement content by the wight of the utilized RA. The set water-to-binder ratio for the
237 coating slurry was 0.55. Silica fume replaced 15% of the cement-silica fume slurry.

238 ***Soaking in different cement-pozzolan solutions.*** The recycled aggregates were treated by
239 soaking in different types of cement-pozzolan solutions. Different solutions were designed
240 for the RA treatment at different dosages as given in Table 5. The ingredients selected for the
241 different solutions were Portland cement (PC), silica fume (SF), metakaolin (MK), and
242 pulverised fuel ash (PFA). These pozzolan materials were selected with the aim of fulfilling
243 the environmental and economic criteria. The solutions were prepared by blending the raw
244 materials with water (twice the weight of RA) for several minutes. Then recycled aggregate
245 was added into each solution and soaked for 1 hour and 4 hours at 5%, 10% and 15%
246 concentration levels. Thereafter, the recycled aggregates were removed from the solution
247 bath and let drain for 10 min and then air-dried at room temperature for 24 hours prior to
248 testing.

249

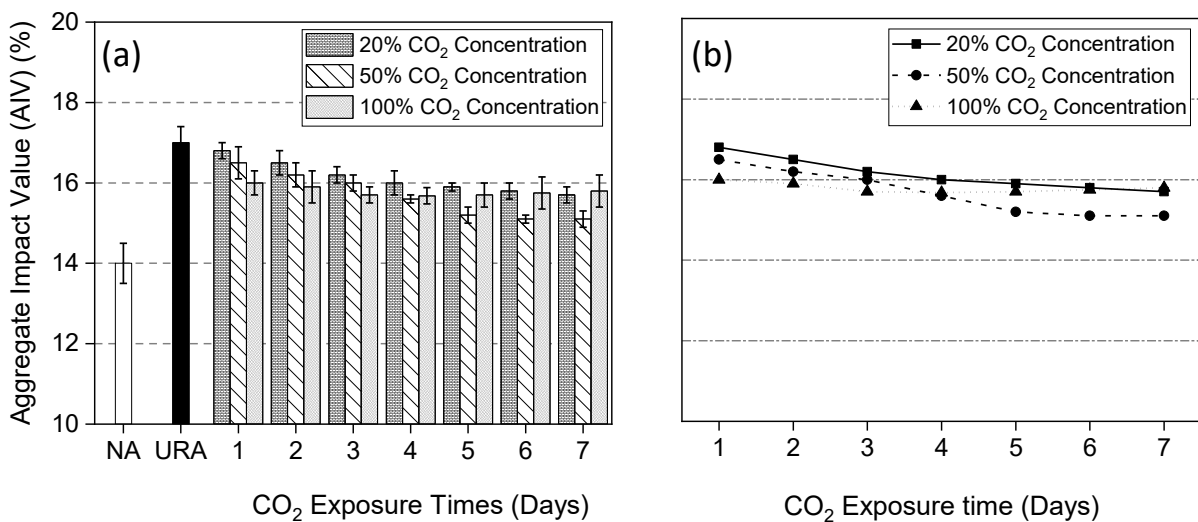
Notation	Treatment solutions PC- pozzolan	Binder (g)				Water (g)	Replacement level (Binder to water)
		PC	PFA	SF	MK		
Group 1	PFA+MK	40	30	—	30	2000	5%
	PFA+SF	40	30	30	—	2000	5%
	MK+SF	40	—	30	30	2000	5%
Group 2	PFA+MK	80	60	—	60	2000	10%
	PFA+SF	80	60	60	—	2000	10%
	MK+SF	80	—	60	60	2000	10%
Group 3	PFA+MK	120	90	—	90	2000	15%
	PFA+SF	120	90	90	—	2000	15%
	MK+SF	120	—	90	90	2000	15%

250 Table 5: Proportions of treatment solutions for 1000 g of RA prepared in this study

251 **4. Results and discussion**

252 **4.1 Effects of accelerated carbonation on the AIV and WA**

253 Figure 4 shows the effects of different CO₂ concentration levels on the aggregate impact
 254 value (AIV) of the RA. Figure 4 demonstrates that the AIV of the RA was significantly
 255 enhanced by the accelerated carbonation treatment.



256 Figure 4: The impact of carbonation treatment at different concentration levels and CO₂
 257 exposure time on the AIV of the RA shown in (a) clustered column chart, and (b) scatter
 258 chart, note: NA – natural coarse aggregate, URA – untreated recycled coarse aggregate
 259

260 During the first 3 days of carbonation treatment, the AIV of the RA treated with 100% CO₂
 261 concentration showed the highest reduction from 17% to 15.7% (7.6% enhancement). This

262 can be explained as the diffusion rate of CO₂ is influenced by the concentration level of CO₂
263 and the transport paths. Thus, a higher CO₂ concentration level such as 100% is more
264 beneficial for the diffusion of CO₂ prior to the pores being blocked up by calcium carbonates.
265 Moreover, during the initial period of reaction, carbonation occurs intensely in a rapid growth
266 stage. These two aspects contributed to a higher enhancement of 100% concentration level
267 during the first 3 days of carbonation (Pu et al., 2021).

268 Accordingly, the results demonstrate that the observed optimal CO₂ exposure time for 100%
269 CO₂ concentration was 3 days. After three days of CO₂ carbonation, there was no further
270 improvement in the AIV at a 100% CO₂ concentration level. Anstice et al. (2005) and Hyvert
271 et al. (2010) confirmed that increased concentration in CO₂ level may lead to C-S-H gel
272 decalcification, while increasing the CO₂ level up to 100% may lead to complete
273 disappearance of C-S-H gel, which results in adverse effects on the RA properties. Similarly,
274 Kashef-Haghighi et al. (2015) also observed that there was no further increase in RA
275 carbonation percentages when the CO₂ concentration level reached 100%.

276 After 3 days of carbonation, RA treated with 50% CO₂ concentration started to achieve lower
277 AIV compared to the RA treated with 100% and 20% CO₂ concentration levels. This can be
278 attributed to the high concentration level of CO₂ which increased the degree of decalcification
279 of calcium-silicate-hydrate. Thus, a large amount of CO₂ was allowed to react with C-S-H
280 which formed a phase of a lower Ca/Si ratio, hence achieving better enhancement in AIV.
281 The highest AIV enhancement at 50% CO₂ concentration level was reached at 6 days of
282 carbonation, the AIV was reduced from 17% to 15.1% (11.2% enhancement). Thus, the
283 optimal CO₂ exposure time at a 50% CO₂ concentration level is at 6 days of carbonation.

284 Treating RA with a 20% CO₂ concentration level offered better quality results over time but
285 with slow AIV enhancements because of the lower CO₂ concentration level. The highest AIV

286 enhancement at a 20% CO₂ concentration level was recorded at 7 days of CO₂ exposure time,
287 where the AIV of RA was reduced from 17% to 15.9% (6.5% enhancement). This is thought
288 to be due to carbonation treatment that led to a denser particle surface of the RA which in
289 turn reduced the rate of diffusion of CO₂ into RA pores, hence slowing down the efficiency
290 with time. This is in line with Pu et al. (2021) who reported a 9.14% reduction in the AIV of
291 the RA after carbonation treatment at a 20% CO₂ concentration level for 7 days of
292 carbonation.

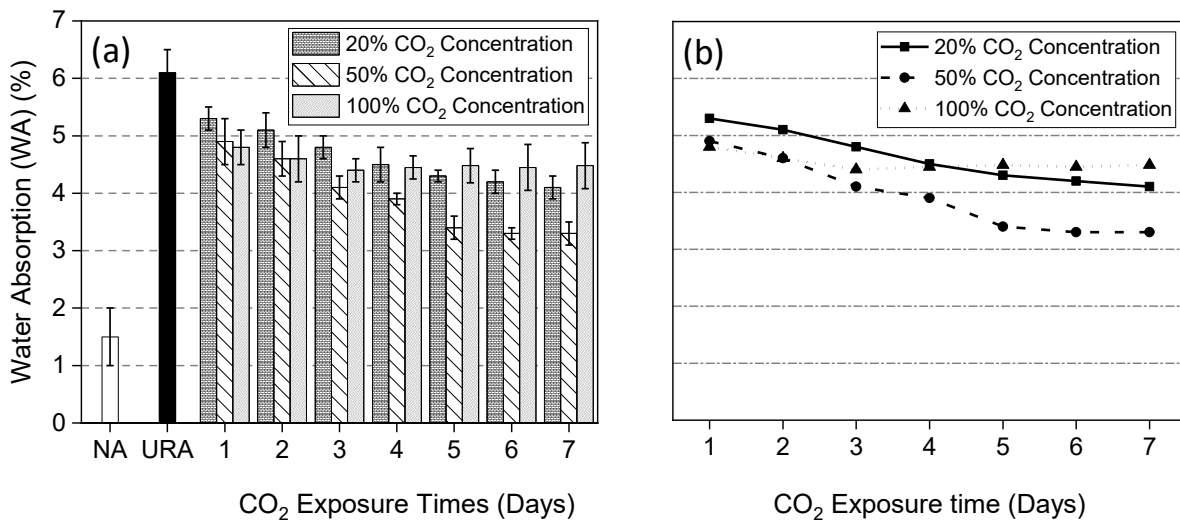
293 Generally, the main reason behind the enhancement/ reduction of the AIV value of the RA
294 after carbonation treatment is that the old ITZ was filled by the calcium carbonate that was
295 produced during the carbonation treatment. Furthermore, the efficiency of accelerated
296 carbonation treatment in enhancing the properties of the RA stems from the chemical reaction
297 of CO₂ with the hydrated products within the adhered mortar on the RA surface. The pores
298 and micro-cracks of the RA can be filled through the process of carbonation (Mistri et al.,
299 2020). At the start of carbonation, the carbonation of Ca(OH)₂ starts first, and it is rate
300 initially higher compared to that of C-S-H as it is shown in Equation 2. The reaction between
301 CO₂ and C-S-H begins (Equation 3) with decalcification, in which the Ca²⁺ reacts within the
302 interlayer with CO₃²⁻ (Borges et al., 2010).



303 Figure 5 demonstrates the effects of the different CO₂ concentration levels on the
304 enhancement of the water absorption (WA) of the RA. The RA treated at a 100% CO₂
305 concentration level achieved the highest reduction in the WA value from 6.1% to 4.4%
306 (27.9% improvement) during the first day of carbonation. The highest reduction in the WA
307 was at a 50% CO₂ concentration level at 6 days of carbonation, the WA of the RA was

308 reduced from 6.1% to 3.3% (46% enhancement). At a 20% CO₂ concentration level and 7
 309 days of carbonation, the WA was reduced from 6.1% to 4.1% (32.8% enhancement). It can be
 310 concluded that the optimal CO₂ concentration level was 50% at an optimal CO₂ exposure
 311 time of 5 days.

312 These results can be attributed to the reduction of the porosity of the cement paste after
 313 carbonation treatment, the refinement of pore structures, the transformation of portlandite
 314 into calcite, and the formation of amorphous carbonation products during accelerated
 315 carbonation treatment. A similar observation was reported by Zhang et al. (2015), Li (2014),
 316 and Ying et al. (2017), who reported a 22.6-40.3% enhancement in water absorption after
 317 carbonation treatment at various CO₂ concentration levels.



318
 319 Figure 5: The impact of carbonation treatment at different concentration levels and CO₂
 320 exposure times on the WA of RA shown in (a) clustered column chart, and (b) scatter chart,
 321 note: NA – natural aggregate, URA – untreated recycled aggregate

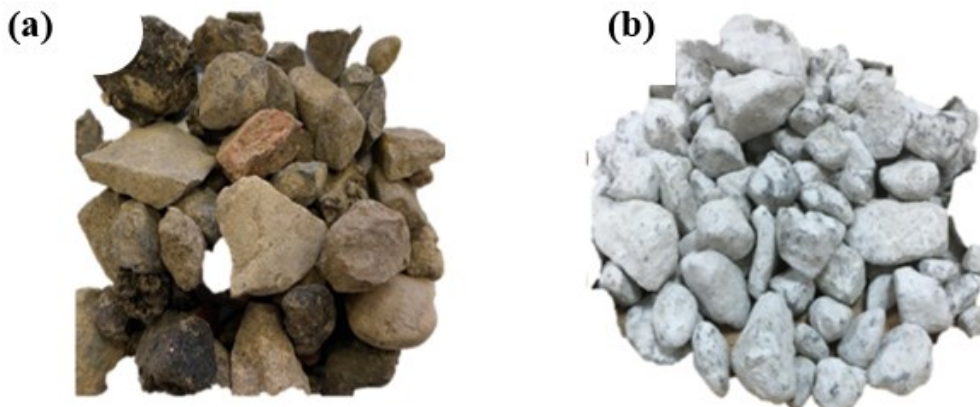
322 4.2 Effects of cyclic limewater-accelerated carbonation on the AIV and WA

323 The recycled aggregates treated with three cyclic limewater-accelerated carbonation
 324 treatment achieved further and better improvement compared to the sole use of accelerated
 325 CO₂ at 100% concentration level for 3 days. The AIV of RA was reduced by 9% (17% to

326 15.4%) and water absorption was reduced by 36% (6.1% to 3.9%). This is mainly due to the
327 introduction of the limewater pre-soaking technique resulting in additional carbonatable
328 compounds into the pores of the RA, thus leading to more CO₂ uptake and more calcium
329 carbonate precipitates, hence, resulting in a denser microstructure of the adhered mortar on
330 the RA surface (Zhan et al., 2018). These findings are in line with Zhan et al. (2017) who
331 observed that carbonated RA achieved 44% enhancement in AIV after pre-soaking followed
332 by accelerated carbonation. Simalrly, Zhan et al. (2018) reported that a 50% reduction in
333 water absorption can be achieved when cyclic lime water-carbonation treatment is repeated
334 for three cycles.

335 *4.3 Effects of Soaking RA in sodium silicate-silica fume solution on the AIV and WA*

336 Figure 6 shows the RA after soaking in sodium silicate-silica fume solution. Figures 7 and 8
337 show the effects of soaking RA in different sodium silicate-silica fume solution
338 concentrations and time on the AIV and the WA of the RA, respectively.

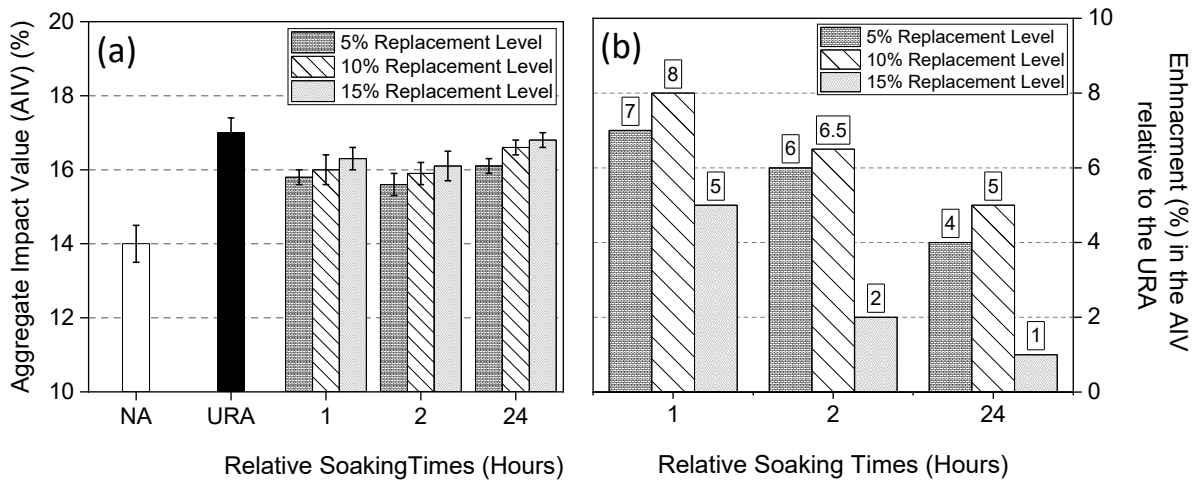


339
340 Figure 6: (a) untreated RA, (b) treated RA with soaking in sodium silicate-silica fume
341 solution

342 During the first 1 hour of soaking treatment, the AIV of the RA treated in the sodium silicate-
343 silica fume solution with a 5% replacement level showed the highest reduction from 17% to
344 15.8% (7% enhancement), whereas the AIV of the RA treated in the solution with 15%

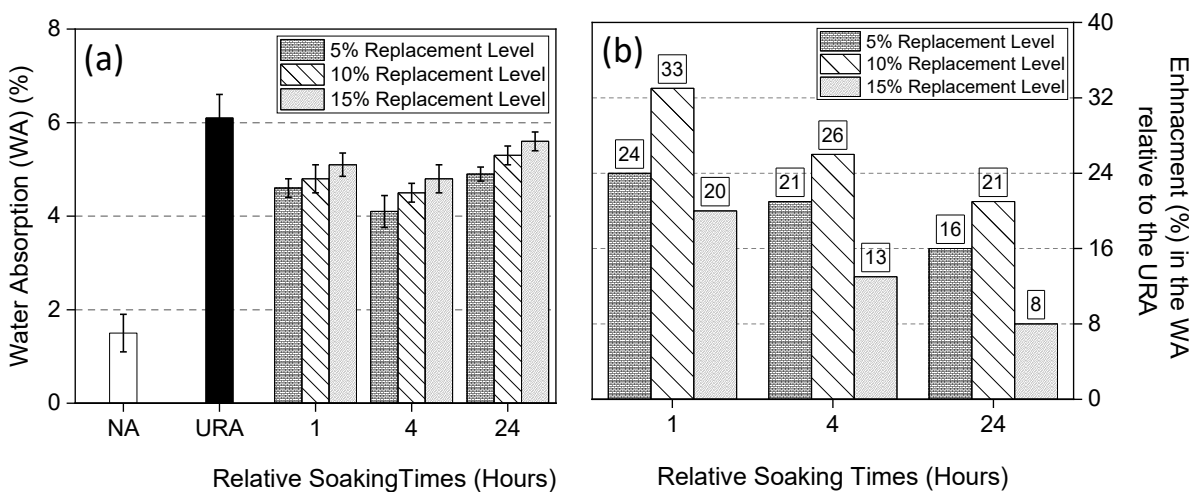
345 replacement level, recorded the lowest enhancement, the AIV was reduced from 17% to
346 16.3% (4% enhancement). After 4 hours of soaking, an increase in the reduction trend of the
347 AIV of the RA is evident for all the solutions with different replacement levels. The highest
348 AIV enhancement was obtained by the solution with a 5% replacement level, the AIV was
349 reduced from 17% to 15.6% (8% enhancement). Further soaking times of up to 24 hours
350 showed lower enhancements in the AIV of the RA compared to 1 hour and 4 hours soaking
351 times.

352 A similar trend can be seen for the WA of the RA with a significant reduction in the WA
353 after treating RA by soaking in sodium silicate – silica fume solution. At the first hour of
354 soaking, a solution with a 5% replacement level showed the highest reduction in the WA, the
355 WA of the RA treated in this solution was reduced from 6.1% to 4.6% (24.6% enhancement).
356 A significant increase in the reduction of the WA can be observed after 4 hours of soaking for
357 all the solutions with different replacement levels. The highest reduction in the WA at this
358 soaking time was obtained by the solution with a 5% replacement level, where the WA was
359 significantly reduced from 6.1% to 4.1% (33% enhancement). Further observations also
360 indicated that, after 24 hours of soaking time, lower enhancement can be seen in the WA for
361 all the prepared solutions with different sodium silicate-Silica Fume replacement levels,
362 compared to 1 hour and 4 hours soaking times. It can be concluded that, among all the
363 concentration solutions utilized, the solution with a 5% replacement level achieved the best
364 enhancements in the AIV and the WA of the RA, whereas solutions with a higher
365 replacement level of 15% achieved the lowest enhancement results. Among all the soaking
366 times, soaking for 4 hours achieved the highest enhancements. Consequently, soaking in
367 solution with a replacement level of 5% for 4 hours of soaking time is considered to be
368 optimum.



369

370 Figure 7: (a) effects of soaking the RA in sodium silicate-silica fume solution at various
 371 replacement levels and soaking times on the AIV of the RA, (b) enhancement values in the
 372 AIV relative to the untreated RA

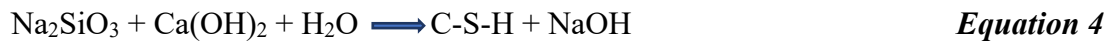


373

374 Figure 8: effects of soaking the RA in sodium silicate-Silica Fume solution at various
 375 replacement levels and soaking times on the WA of the RA, (b) enhancement values in the
 376 WA relative to the untreated RA

377 Immersing RA in a pozzolanic solution can improve the microstructure and the engineering
 378 properties of the RA in two aspects; pozzolana acts as a micro-filler that fills in the pores and
 379 micro-cracks of RA, these materials will form C-S-H gel through reacting with CH crystals in
 380 RA that fill up the voids with RA. A thin layer called water repellent is formed by
 381 impregnating the RA in sodium silicate-silica fume solution for a certain time, resulting in
 382 filling the pores and the voids within the adhered mortar when. When RA is immersed in this

383 solution, both materials can react with the calcium hydroxide existing in the adhered mortar
384 to form C-S-H gel, according to equation 4 (Yang et al., 2016):



385 Furthermore, further improvement can be achieved in this method, as a result of the
386 pozzolanic reaction between silica fume and the $\text{Ca}(\text{OH})_2$ which produces secondary C-S-H
387 gel, hence a stronger interfacial transition zone will be developed on the RA surface.

388 Soaking RA in sodium silicate-silica fume solution significantly enhanced the AIV and the
389 WA of the RA. This may be ascribed to the thin film layer formed of sodium silicate and
390 pozzolana particles on the surface of RA through consuming the CH product in the AM
391 which in return made RA a denser structure by filling up and sealing the pores and cracks of
392 RA. This is in line with the outcome of Shaban et al. (2019) study who stated that soaking
393 RA in sodium silicate solution significantly reduced the WA of the RA. They added that this
394 is attributed to the silicic acid that filled up the pores and voids of the RA surface along with
395 the chemical reaction between the sodium silicate and CH that produced C-S-H gel which
396 enhanced the bond between the adhered mortar and RA.

397 Among all the utilized concentration solutions, solutions with 5% concentration achieved the
398 best performance, whereas solutions with a higher concentration of 15% achieved the lowest
399 enhancement results. Among all the soaking periods of time, soaking for 4 hours achieved the
400 highest enhancement values in terms of RA engineering properties. This might be because the
401 pozzolan materials could not penetrate deeply into the surface of RA and efficiently
402 strengthen it in the case of short soaking times (Shaban et al., 2019). Moreover, long soaking
403 times i.e., 24 hours would result in removing the hydration products and eroding the surface
404 of RA and thus lower enhancements to the AIV and WA of RA will be achieved (Ouyang et

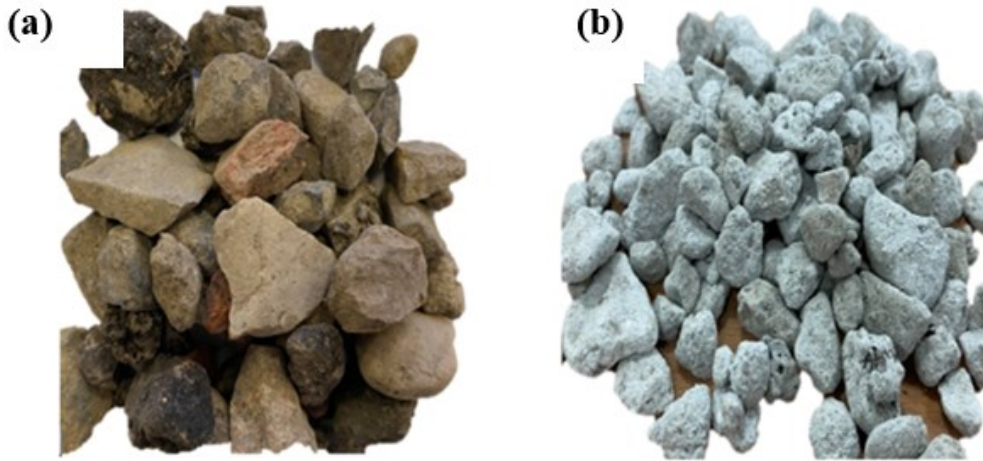
405 al., 2020). Higher concentration levels also are not beneficial to the enhancement of RA as
406 the solution may be too thick to penetrate the surface of RA and it would also reduce the
407 degree of hydration of the pozzolan products. Ouyang et al. (2020) stated that excessive
408 treatment methods should be avoided, such as high concentration of the treatment solutions,
409 and long soaking times, which could erode the surface of RA, leading to reducing the
410 efficiency of the treatment employed.

411 This is in line with Yang et al. (2016) who soaked RA in water-glass (sodium silicate)
412 solution with different concentrations of 3%, 5%, 8%, 10%, 20%, and 40% for 10 min, 1h,
413 2h, and 5h. Yang et al. (2016) found that the treated RA obtained enhanced water absorption
414 by 36% when RA was soaked in water-glass solution with 40% concentration for 1 hour,
415 whereas soaking the RA in water-glass solution with 5% for 1 hour achieved the best
416 performance in terms of concrete 3-, 7-, and 28-day compressive strength at about 22%, 28%
417 and 29% enhanced performance respectively.

418 Bui et al. (2018) soaked RA in three main solutions; solution type G, solution type S, and
419 sodium silicate SS. Solution type G included; GFA (fly ash + NaSiO_3 + NaOH), GSF (silica
420 fume + NaSiO_3 + NaOH), GMK (metakaolin + Na_2SiO_3 + NaOH). Solution type S included;
421 SFA (fly ash + Na_2SiO_3), SSF (Silica fume + Na_2SiO_3), and SMK (metakaolin + Na_2SiO_3).
422 Solution type SS was sodium silicate. RA was soaked for 24 hours and at three different
423 solution concentrations 10%, 20%, and 30%. Among all the treatment solutions, RA soaked
424 with sodium silicate (SS) solution at 30% concentration achieved the best performance in
425 terms of water absorption, RA attained 34% enhanced water absorption. Bui et al. (2018)
426 stated that, among all the utilized solutions, the combination between silica fume and sodium
427 silicate achieved the best 28-day compressive strength, whereas concrete produced with
428 treated RA in silica fume-sodium silicate solution achieved 36% enhancement.

429 **4.4 Effects of coating RA with cement or cement-silica fume slurry on the AIV and WA**

430 Figure 9 shows RA before and after coating with cement-silica fume slurry.



431

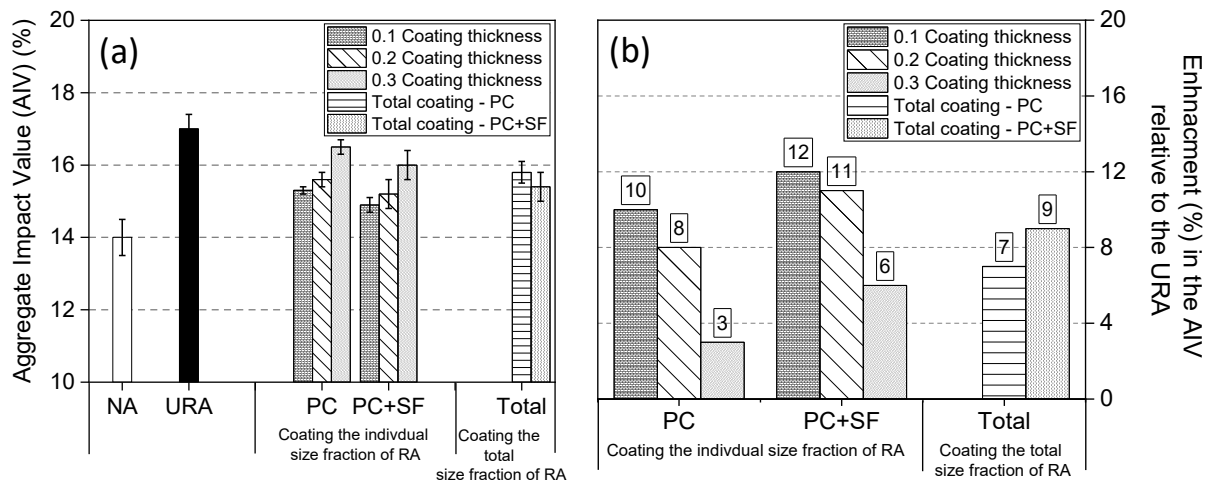
432 Figure 9: (a) untreated RA, (b) treated RA with coating with cement-silica fume slurry

433 Figures 10 and 11 show the effects of coating the individual particle size fraction with cement
434 slurry or cement-silica fume slurry, along with the effects of coating the total combined
435 gradation of RA, on the AIV and the WA of the RA, respectively. As can be seen from
436 Figures 10 and 11, among all the coating thicknesses and coating materials, the treated RA
437 with cement-silica fume slurry and coating thickness of 0.1mm recorded the highest
438 reduction in the AIV and the WA, from 17% to 14.9% (12% enhancement), and from 6.1% to
439 2.8% (54% enhancement), respectively, compared to the other coating thicknesses. In
440 addition to that, via visual inspection, coating RA particles smaller than 10 mm with a
441 thickness of 0.3 mm, results in getting the RA cemented to each other and hence, they cannot
442 be separated easily. According to Lee et al. (2011), when the coating paste around RA of
443 4.75mm size exceeds the designated theoretical thickness of 0.65 mm, then the coating paste
444 may get cemented into lumps and cannot be separated easily, while the coating paste cannot
445 entirely coat the surface of RA when the coating paste around the surface of RA of 12.5 mm
446 size is less than 0.25 mm of the coating thickness.

447 Accordingly, based on these results, it can be concluded that 0.1mm is the optimum coating
448 thickness to coat the individual RA grain sizes. This may be attributed to the small coating
449 thickness resulting in filling the pores/cracks and thus leading to strengthening the weak RA
450 particles. These findings are in line with Kareem et al. (2018) who found that coating the
451 individual RA at 0.1 mm coating thickness with cement slurry resulted in better AIV by 7%
452 enhancement compared to 0.05, 0.2, and 0.4 mm coating thicknesses. RA treated with
453 cement-silica fume slurry showed better AIV and WA compared to the ones treated with
454 cement slurry only, this may be attributed to the additional produced C-S-H gel which
455 effectively filled the pores and voids in the weak adhered mortar (Lee et al., 2011).

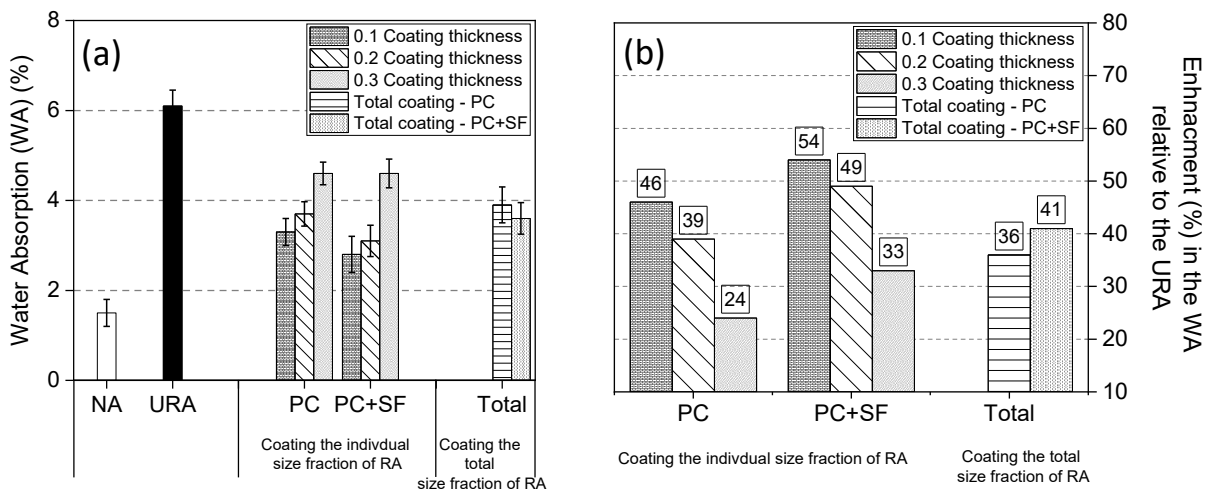
456 Coating the total combined RA with cement slurry only achieved 7% enhancement in the
457 AIV (from 17% to 15.8%) and 36% enhancement in the WA (from 6.1% to 3.9%), whereas
458 coating with cement and silica fume slurry offered slightly higher enhancement of 9% in the
459 AIV (from 17% to 15.4%) and 41% enhancement in the WA (from 6.1% to 3.6%). Overall,
460 the results of the effects of different coating methods on the AIV and the WA of the RA
461 indicated significant enhancement in the AIV and the WA for all the coated RA with cement
462 and/or cement-silica fume slurry regardless of the coating method.

463 It was also found that the increase in coating thickness layer results in adverse effects on the
464 AIV and the WA. The RA treated with cement-silica fume slurry showed better
465 enhancements in the AIV and the WA compared to the ones treated with cement slurry only.
466 The method of coating the RA particle size fraction individually performed better in
467 enhancing the AIV and the WA of the RA, in comparison with the method of coating the total
468 gradation of the RA. This is in line with Zhihui et al. (2013) who reported a 9% enhancement
469 in AIV and a 39% enhancement in the WA of RA after coating the total combined RA size
470 fraction with cement slurry.



471

472 Figure 10: (a) the effects of the different coating with cement and/or cement-SF methods on
 473 the AIV of the RA, (b) enhancement values in the AIV relative to the untreated RA



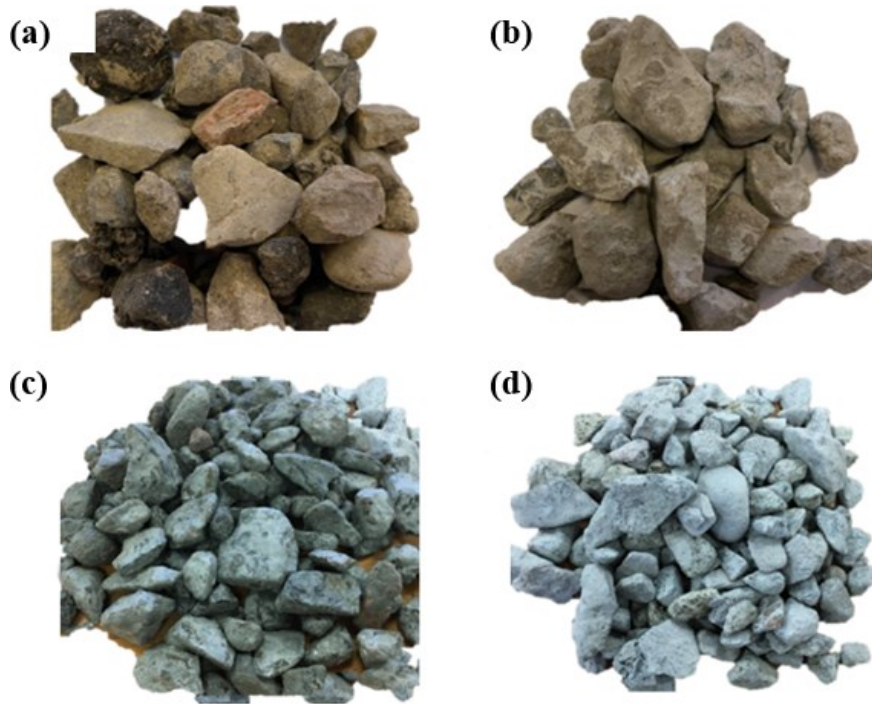
474

475 Figure 11: (a) the effects of the different coating with cement and/or cement-SF methods on
 476 the WA of the RA, (b) enhancement values in the WA relative to the untreated RA

477 Overall, this surface treatment method aims at altering the micro-surface structure of RA and
 478 then strengthen it by the touch-up of new materials (i.e., cement, silica fume, fly ash) and
 479 coating of the older material via patching and bonding of the smaller pores on the surface of
 480 RA to enhance its quality and properties, hence, reinforcing the bonding force and
 481 mechanical strength of the interface between coating materials and RA (Lee et al., 2011). It
 482 can also be added that the basic premise of this treatment is to coat RA with hydrated cement
 483 film which is thick enough to act as a shield on the surface of RA.

484 **4.5 Effects of soaking RA in different cement-pozzolan solutions on the AIV and WA**

485 Figure 12 shows RA after soaking in different cement-pozzolan solutions. The results shown
486 in Figures 13 and 14 show the effects of soaking RA in different cement-pozzolan solutions
487 on the AIV and WA of RA, respectively.



488
489 Figure 12: (a) untreated RA, (b) treated RA with soaking in PFA+SF solution, (c) treated RA
490 with soaking in PFA+MK solution, (d) treated RA with soaking in SF+MK solution

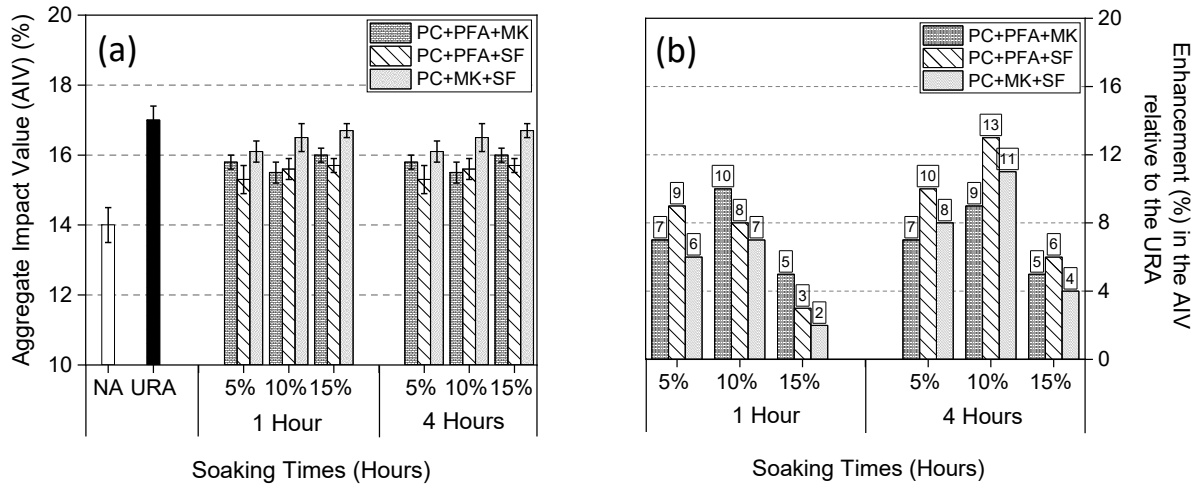
491 At the first 1 hour of soaking time, the RA treated with the combination of PFA+MK solution
492 with a 10% replacement level exhibited the highest reduction in the AIV, the AIV was
493 reduced from 17% to 15.3% (10% enhancement). Whereas the RA treated with the
494 combination of PFA+SF solution with a 10% replacement level, recorded the highest
495 reduction in the WA, the WA was reduced from 6.1% to 3.2% (47% enhancement). These
496 results are ascribed to the pozzolan thin layer formed on the RA surface after the treatment
497 which filled the pores and the micro-cracks of the RA.

498 Further soaking time of the RA for up to 4 hours resulted in better enhancement in the AIV
499 and the WA of the RA regardless of the replacement level and combination of materials,
500 compared to 1 hour of soaking. This might be because the pozzolanic materials need a longer
501 time to deeply penetrate the adhered mortar and efficiently strengthen it. This finding is in
502 line with Shaban et al. (2019) who reported a 51.4% reduction in water absorption of RA
503 after soaking in pozzolan solution. Li et al. (2009) examined the effect of soaking of RA by
504 pozzolanic powder (fly ash, silica fume, and GGBS), and found that the combination of
505 Portland cement along with fly ash and silica fume is more efficient for high strength
506 recycled aggregate concrete with better packing density and denser interfacial transition zone.

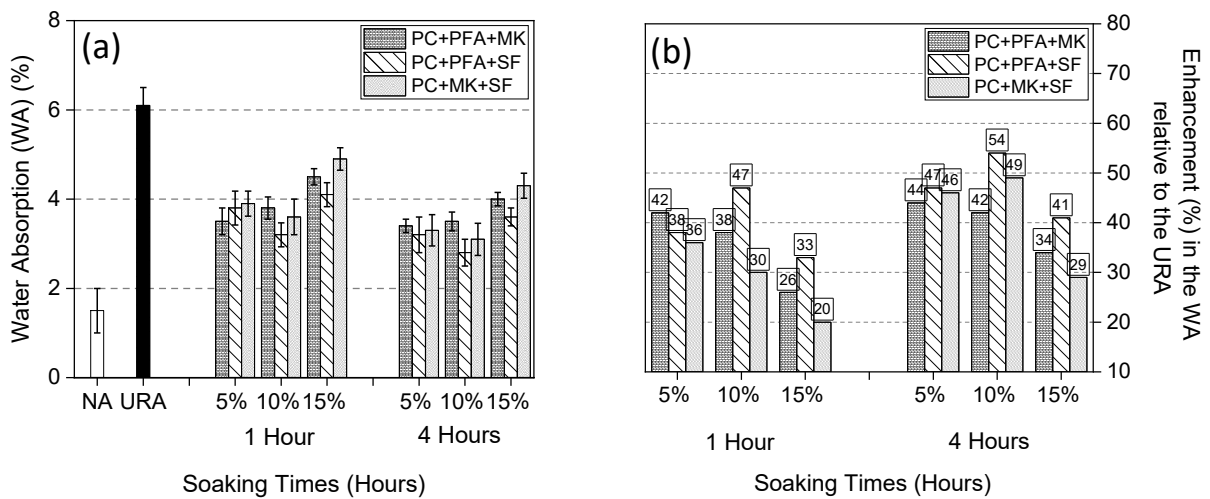
507 The highest reduction in the AIV and the WA was obtained by the PFA+SF solution at a 10%
508 replacement level. The AIV was reduced from 17% to 14.7% (13% enhancement), while the
509 WA was reduced from 6.1% to 2.8% (54% enhancement). This may be attested to the high
510 reactivity of this pozzolan solution (Mistri et al., 2020). A similar finding was observed by
511 Shaban et al. (2019), who reported an approximate reduction of 40% in AIV after soaking
512 RA in cement-pozzolan solutions.

513 Overall, it can be seen that soaking the RA in the solutions adopted for 4 hours provided
514 better enhancements in the AIV and the WA of the RA regardless of solutions replacement
515 levels, compared to the 1 hour of soaking time. Among all the replacement levels used,
516 solutions with a 10% replacement level offered higher enhancements in the AIV and the WA
517 of the RA, in comparison with solutions prepared with 5% and 15% replacement levels. In
518 addition, the AIV and the WA of the RA soaked in the solutions prepared with a 15%
519 replacement level exhibited lower enhancement values compared to solutions prepared with a
520 5% and 10% replacement levels regardless of the soaking time and the materials used.
521 Consequently, it can be concluded that the optimal soaking time is 4 hours, and the optimal

522 replacement level is 10%. Among all the combinations of materials used for solution
 523 preparation, the solution prepared with PFA+SF solution achieved somewhat the best results
 524 regardless of soaking time and replacement level.



525 Soaking Times (Hours)
 526 Figure 13: (a) the effects of different soaking solutions at different replacement levels and
 527 soaking times on the AIV of the RA, (b) enhancement values in the AIV relative to the
 528 untreated RA

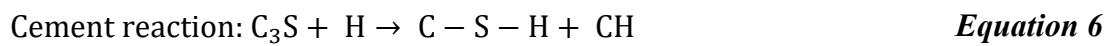
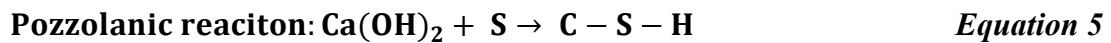


529 Soaking Times (Hours)
 530 Figure 14: (a) the effects of different soaking solutions at different replacement levels and
 531 soaking times on the WA of the RA, (b) enhancement values in the WA relative to the
 532 untreated RA

533 The main principle behind soaking RA in cement-pozzolan treatment is to cover the RA
 534 surface with a thin layer of hydration products, hence strengthening RA engineering

535 properties. After the treatment, a dense coated layer is formed around the RA surface after the
536 reaction of the pozzolanic materials with the $\text{Ca}(\text{OH})_2$ in the adhered mortar.

537 According to Singh et al. (2018), the additional hydrated calcium silicate (C-S-H) gel fills the
538 pores and voids of the adhered mortar as shown in Equation 5. The incorporation of cement
539 in the solutions is important for the treatment because it releases additional (C-S-H) gel and
540 $\text{Ca}(\text{OH})_2$ during hydration, as given in Equation 6.



541 This additional production of C-S-H gel efficiently fills the voids and pores of the weak
542 adhered mortar, resulting in a much denser microstructure of RA. Singh et al. (2018) stated
543 that particle size, the content of calcium hydroxide in the adhered mortar, the alkalinity of
544 pore solution, and the reactivity of the pozzolanic materials are the main factors affecting the
545 efficiency of the pozzolan solution treatment.

546 **4. Conclusions**

547 Recycled coarse aggregates demonstrated relatively low-quality characteristic performance
548 compared to NA due to several factors. One of the major factors is the adhered mortar that
549 results in a weak old interfacial transition zone. Other concerns include variation in
550 composition, previous loading, processing, and weathering compared to freshly crushed
551 natural aggregates. This paper has presented laboratory-based investigations on the effects of
552 different treatments including, accelerated carbonation treatment, cyclic limewater-
553 accelerated carbonation, soaking in sodium silicate-silica fume solution, coating with cement
554 and/or cement-silica fume slurry, and soaking in cement-pozzolan solutions on enhancing the

555 aggregate impact value and water absorption of RA. The following specific conclusions can
556 be drawn:

557 Accelerated carbonation treatment is an environmentally friendly viable treatment through its
558 mechanism in terms of carbon capture. Accelerated carbonation treatment at 50% CO₂
559 concentration level for six days of CO₂ exposure time achieved the best results among
560 carbonation conditions, giving 11% and 46% enhancement in the AIV and WA, respectively.
561 The recycled aggregates treated with three cyclic periods of pre-soaking in limewater
562 followed by accelerated carbonation at 100% CO₂ concentration level for 24 hours, exhibited
563 better improvement in the AIV and WA compared to the sole use of accelerated carbonation
564 treatment under the same carbonation conditions. The observed enhancements in the AIV and
565 the WA after accelerated carbonation treatment was mainly due to the carbonation process
566 through the chemical reactions between CO₂, the available calcium hydroxide, and the
567 calcium silicate hydrates on the RA surface. This carbonation process filled the pores and the
568 cracks on the RA surface and sealed its surface.

569 Coating the individual size fraction of RA with cement or cement-silica fume achieved better
570 enhancement in the AIV and WA compared with coating the whole size fraction of RA.
571 Among all the coating thicknesses, coating the individual size fraction of RA with cement-
572 silica fume slurry at 0.1mm coating thickness led to the best enhancements of 12% and 54%
573 in the AIV and the WA, respectively Coating RA with cement and silica fume slurry was
574 observed to provide better enhancement in the AIV and the WA, compared to coating RA
575 with only cement slurry. The enhancements observed in the AIV and WA were mainly due to
576 the RA surface being covered with a thick layer of hydration products and C-S-H gel that
577 acted as a shield that strengthened the adhered mortar and reduced its porosity.

578 Soaking RA in 5% sodium silicate-silica fume solution for 4 hours soaking time was found to
579 be optimal. The treated RA achieved 8% and 33% enhancement in the AIV and the WA,
580 respectively. This was ascribed to the produced C-S-H gel by the chemical reaction between
581 sodium silicate and calcium hydroxide with the presence of water and between silica fume
582 and calcium hydroxide simultaneously. The produced C-S-H gel and the secondary C-S-H
583 gel effectively filled the micro-pores, voids, and micro-cracks on the RA surface, which
584 reflected in the reduced WA and enhanced AIV.

585 Soaking RA in 10% Portland cement-pozzolan solution for 4 hours soaking time was found
586 to be optimal, among all the examined conditions, achieving enhancements of 13% and 54%
587 in the AIV and the WA, respectively. This enhancement resulted from the pore filling and
588 sealing effects of this treatment on the surface of RA.

589 **Declaration of Competing Interest**

590 The authors declare that they have no known competing financial interests or personal
591 relationships that could have appeared to influence the work reported in this paper.

592 **Funding**

593 This research did not receive any specific grant from funding agencies in the public,
594 commercial, or non-profit sectors.

595 **REFERENCES**

596 Akhtar, Ali., Samarah, Ajit., 2018. Construction and demolition waste generation and
597 properties of recycled aggregate concrete: A global perspective. Journal of cleaner
598 production, Volume 186, Pages 262-28, <https://doi.org/10.1016/j.jclepro.2018.03.085>

599 Al-Bayati, H., Das, P., Tighe, S. & Baaj, H., 2016. Evaluation of various methods for
600 enhancing the physical and morphological properties of coarse recycled concrete aggregate.
601 Construction and Building Materials, Volume 112, pp. 284-298, [https://doi.org/
602 10.1016/j.conbuildmat.2016.02.176](https://doi.org/10.1016/j.conbuildmat.2016.02.176).

603 Al-Bayati, H. & Tighe, S., 2016. Utilizing a Different Technique for Improving Micro and
604 Macro Characteristics of Coarse Recycled Concrete Aggregate. Toronto, Transportation
605 Association of Canada, [https://www.tac-atc.ca/
606 /sites/default/files/conf_papers/al-bayati](https://www.tac-atc.ca/sites/default/files/conf_papers/al-bayati).

607 Anstice, D., Page, C. & Page, M., 2005. The pore solution phase of carbonated cement
608 pastes. Cement and Concrete Research, Volume 35, pp. 377-383, [http://doi.org/
609 10.1016/j.cemconres.2004.06.041](http://doi.org/10.1016/j.cemconres.2004.06.041).

610 Borges PHR, Costa JO, Milestone NB, Lynsdale CJ, Streatfield RE. 2010. Carbonation of
611 CH and C–S–H in composite cement pastes containing high amounts of BFS. Cement and
612 Concrete Research, 40, 284-292, <http://doi.org/10.1016/j.cemconres.2009.10.020>. 25

613 British Standards Institution. BS EN 12620:2002+A1:2008—Aggregates for Concrete;
614 British Standards Institution: London, UK, 2008.

615 British Standards Institution. BS EN 1097-6:2013—Tests for Mechanical and Physical
616 Properties of Aggregates. Part 6: Determination of Particle Density and Water Absorption;
617 British Standards Institution: London, UK, 2013.

618 British Standards Institution. BS EN 933-4:2008—Tests for Geometrical Properties of
619 Aggregates. Part 4: Determination of Particle Shape—Shape Index; British Standards
620 Institution: London, UK, 2008.

620 British Standards Institution. BS EN 13242:2013—Aggregates for unbound and hydraulically
621 bound materials for use in civil engineering work and road construction; British Standards
622 Institution: London, UK, 2013.

623 British Standards Institution. BS 8500-2:2015 +A2: 2019—Concrete-Complementary British
624 Standard to BS EN 206. Part 2: Specification for constituent materials and concrete; British
625 Standards Institution: London, UK, 2019.

626 British Standards Institution. BS EN 933-3: 2012—Tests for geometrical properties of
627 aggregates. Part 3: Determination of particle shape—Flakiness index; British Standards
628 Institution: London, UK, 2012.

629 British Standards Institution. BS EN 1097-2:2020—Tests for mechanical and physical
630 properties of aggregates. Part 2: Methods for determination of resistance to fragmentation;
631 British Standards Institution: London, UK, 2020.

632 British Standards Institution. BS EN 933-1:2012—Tests for geometrical properties of
633 aggregates. Part 1: Determination of particle size distribution—Sieving method; British
634 Standards Institution: London, UK, 2012.

635 British Standards Institution. BS EN 197-1:2011 - Cement. Composition, specifications and
636 conformity criteria for common cements; British Standards Institution: London, UK, 2011.

637 British Standards Institution. BS EN 450-1:2012 - Fly ash for concrete. Definition,
638 specifications and conformity criteria; British Standards Institution: London, UK, 2012.

639 British Standards Institution. BS EN 13263-2:2005+A1:2009 - Silica fume for concrete.
640 Conformity evaluation; British Standards Institution: London, UK, 2009.

641

642 British Standards Institution. BS EN 15167-1:2006 - Ground granulated blast furnace slag for
643 use in concrete, mortar and grout. Definitions, specifications and conformity criteria; ; British
644 Standards Institution: London, UK, 2006.

645 Bru, K. et al., 2014. Assessment of a microwave-assisted recycling process for the recovery
646 of high-quality aggregates from concrete waste. *International Journal of Mineral Processing*,
647 Volume 126, pp. 90-98, <http://doi.org/10.1016/j.minpro.2013.11.009>.

648 Bui, N., Satomi, T. & Takahashi, H., 2018. Enhancement of Recycled Aggregate Concrete
649 Properties by a New Treatment Method. *International Journal of GEOMATE*, 14(41), pp. 68-
650 76. <https://doi.org/10.21660/2018.41.11484>.

651 Chen, J., Thomas, J. & Jennings, H., 2006. Decalcification shrinkage of cement paste.
652 *Cement and Concrete Research*, 36(5), pp. 801-809.
653 <http://doi.org/10.1016/j.cemconres.2005.11.003>

654 Dabiri, H. et al., 2022. Compressive strength of concrete with recycled aggregate; a machine
655 learning-based evaluation. *Cleaner Materials*, Volume 3, p. 100044.
656 <https://doi.org/10.1016/j.clema.2022.100044>.

657 Derwen, 2016. Recycled Aggregate. [Online] Available at: <https://www.derwengroup.co.uk>
658 [Accessed 10 February 2022].

659 Dilbas, H., Cakir, O. & Atis, C., 2019. Experimental investigation on properties of recycled
660 aggregate concrete with optimized Ball Milling Method. *Construction and Building*
661 *Materials*, Volume 212, pp. 716-726. <http://doi.org/10.1016/j.conbuildmat.2019.04.007>.

662 Dimitriou, G., Savva, P. & Petrou, M., 2018. Enhancing mechanical and durability properties
663 of recycled aggregate concrete. *Construction and Building Materials*, Volume 158, pp. 228-
664 235. <https://doi.org/10.1016/j.conbuildmat.2017.09.137>.

665 Gonzalez-Corominas, A. & Etxeberria, M., 2014. Properties of high-performance concrete
666 made with recycled fine ceramic and coarse mixed aggregates. *Construction and Building*
667 *Materials*, Volume 68, pp. 618-626. <http://doi.org/10.1016/J.CONBUILDMAT.2014.07.016>

668 Grabiec, A., Klama, J., Zawal, D. & Krupa, D., 2012. Modification of recycled concrete
669 aggregate by calcium carbonate bio-deposition. *Construction and Building Materials*, Volume
670 34, pp. 145-150. <https://doi.org/10.1016/j.conbuildmat.2012.02.027>.

671 Hyvert, N. et al., 2010. Dependency of C-S-H carbonation rate on CO₂ pressure to explain
672 transition from accelerated tests to natural carbonation. *Cement and Concrete Research*,
673 Volume 40, pp. 1582-1589. <https://doi.org/10.1016/j.cemconres.2010.06.010> 27

674 Kareem, A., Nikraz, H., & Asadi, H. (2018). Evaluation of the double coated recycled
675 concrete aggregates for hot mix asphalt. *Construction and Building Materials*, 172, 544-552.
676 <https://doi.org/10.1016/j.conbuildmat.2018.03.158>

677 Kashef-Haghighi, S., Shao, Y. & Ghoshal, S., 2015. Mathematical modeling of CO₂ uptake
678 by concrete during accelerated carbonation curing. *Cement and Concrete Research*, Volume
679 67, pp. 1-10. <https://doi.org/10.1016/j.cemconres.2014.07.020>

680 Katkhuda, H. & Shatarat, N., 2017. Improving the mechanical properties of recycled concrete
681 aggregate using chopped basalt fibers and acid treatment. *Construction and Building*
682 *Materials*, Volume 140, pp. 328-335. <https://doi.org/10.1016/j.conbuildmat.2017.02.128>

683 Kim, J., 2022. Influence of quality of recycled aggregates on the mechanical properties of
684 recycled aggregate concrete: An overview. *Construction and Building Materials*, Volume
685 328, p. 127071. <https://doi.org/10.1016/j.conbuildmat.2022.127071>.

686 Kou, S. & Poon, C., 2012. Enhancing the durability properties of concrete prepared with
687 coarse recycled aggregate. *Construction and Building Materials*, Volume 35, pp. 69-76.
688 <https://doi.org/10.1016/j.conbuildmat.2012.02.032>.

689 Kou, S., Zhan, B. & Poon, C., 2014. Use of a CO₂ curing step to improve the properties of
690 concrete prepared with recycled aggregates. *Cement and Concrete Composites*, Volume 45,
691 pp. 22-28. <https://doi.org/10.1016/j.cemconcomp.2013.09.008>

692 Lee, C.-H., C. Du, J. & Shen, D.-H., 2011. Evaluation of pre-coated recycled concrete
693 aggregate for hot mix asphalt. *Construction and Building Materials*, 28(1), pp. 66-71.
694 <https://doi.org/10.1016/j.conbuildmat.2011.08.025>

695 Li, J., Xiao, H. & Zhou, Y., 2009. Influence of coating recycled aggregate surface with
696 pozzolanic powder on properties of recycled aggregate concrete. *Construction and Building*
697 *Materials*, 23(3), pp. 1287-1291. <https://doi.org/10.1016/j.conbuildmat.2008.07.019>

698 Li, Y., 2014. *Improvement of Recycled Concrete Aggregate Properties by CO₂ Curing*,
699 Changsha: Hunan University. 28

700 Lu, B. et al., 2019. Effect of carbonated coarse recycled concrete aggregate on the properties
701 and microstructure of recycled concrete. *Journal of Cleaner Production*, Volume 233, pp.
702 421- 428. <https://doi.org/10.1016/j.jclepro.2019.05.350>

703 Lu, W., 2019. Big data analytics to identify illegal construction waste dumping: A Hong
704 Kong study. *Resources, Conservation and Recycling*, Volume 141, pp. 264-272.
705 <https://doi.org/10.1016/j.resconrec.2018.10.039>

706 Mistri, A., Bhattacharyya, S., Dhama, N., Mukherjee, A., & Barai, S. 2020. A review on
707 different treatment methods for enhancing the properties of recycled aggregates for
708 sustainable construction materials. *Construction and Building Materials*, 233, 117-894.
709 <https://doi.org/10.1016/j.conbuildmat.2019.117894>

710 Mazurana, L., Bittencourt, P., Scremin, F., Junior, A., Possan, E. 2020. Determination of CO₂
711 capture in rendering mortars produced with recycled construction and demolition waste
712 by thermogravimetry. *Journal of Thermal Analysis and Calorimetry*, 147, 1071–1080.
713 <https://doi.org/10.1007/s10973-020-10436-0>

714 Mazurana, L. CO₂ uptake in rendering mortars by carbonation [Internet]. Universidade
715 Tecnológica Federal do Paraná; 2019. Available from:
716 <https://repositorio.utfpr.edu.br/jspui/handle/1/4733>. Accessed 21 May 2022.

717 Ouyang, K., Shi, C., Chu, H., Guo, H., Song, B., Ding, Y., Xuemao, G., Zhu, J., Zhang, H.,
718 Wang, Y., Zheng, J. (2020). An overview on the efficiency of different pretreatment
719 techniques for recycled concrete aggregate. *Journal of Cleaner Production*, 263, 121264.
720 <https://doi.org/10.1016/j.jclepro.2020.121264>

721 Pan, G. et al., 2017. Effect of CO₂ curing on demolition recycled fine aggregates enhanced by
722 calcium hydroxide pre-soaking. *Construction and Building Materials*, Volume 154, pp. 810-
723 818. <https://doi.org/10.1016/j.conbuildmat.2017.07.079>

724 Pawluczuk, E., Wichrowska, K., Boltryk, M. & Rodriguez, J., 2019. The influence of heat
725 and mechanical treatment of concrete rubble on the properties of recycled aggregate concrete.
726 *Materials*, 12(3), pp. 1-24. <https://doi.org/10.3390/ma12030367>

727 Pu, Y., Li, L., Wang, Q., Shi, X., Luan, C., Zhang, G., Fu, L., Abomohra, A., 2021.
728 Accelerated carbonation technology for enhanced treatment of recycled concrete aggregates:
729 A state-of-the-art review. *Construction and Building Materials*, Volume 282, p. 122671.
730 <https://doi.org/10.1016/j.conbuildmat.2021.122671>

731 Sharman, J., 2018. Construction Waste and materials Efficiency. [online] Available at:
732 <http://www.thenb.com>. [Accessed 20 February 2022].

733 Shaban, W. et al., 2019. Quality Improvement Techniques for Recycled concrete Aggregate:
734 A review. *Journal of Advanced Concrete Technology*, Volume 17, pp. 151- 167.
735 <https://doi.org/10.3151/jact.17.151>

736 Silva, R., Brito, J. & Dhir, R., 2014. Properties and composition of recycled aggregates from
737 construction and demolition waste suitable for concrete production. *Construction and*
738 *Building Materials*, Volume 65, pp. 201-217.
739 <https://doi.org/10.1016/j.conbuildmat.2014.04.117>

740 Singh, L., Bisht, V., Aswathy, M.S., Chaurasia, L., Gupta, S., 2018. Studies on performance
741 enhancement of recycled aggregate by incorporating bio and nano materials. *Construction*
742 *and Building Materials*, Volume 181, PP. 217-226.
743 <https://doi.org/10.1016/j.conbuildmat.2018.05.248>.

744 Tam, V., 2009. Comparing the implementation of concrete recycling in the Australian and
745 Japanese construction industries. *Journal of Cleaner Production*, 17(7), pp. 688-702.
746 <https://doi.org/10.1016/j.jclepro.2008.11.015>

747 Tam, V., Butera, K. & Le, K., 2016. Carbon-conditioned recycled aggregate in concrete
748 production. *Journal of Cleaner Production*, Volume 133, pp. 672-680.
749 <https://doi.org/10.1016/j.jclepro.2016.06.007>

750 Tam, V., Soomro, M. & Evangelista, A., 2018. A review of recycled aggregate in concrete
751 applications (2000-2017). *Construction and Building Materials*, Volume 172, pp. 272-292.
752 <https://doi.org/10.1016/j.conbuildmat.2018.03.240>

753 Tam, V., Tam, C. & Le, K., 2007. Removal of cement mortar remains from recycled
754 aggregate using pre-soaking approaches. *Resources, Conservation & Recycling*, 50(1), pp.
755 82-101. <http://doi.org/10.1016/j.resconrec.2006.05.012>

756 Tošić, N., Marinković, S. & Stojanović, A., 2017. Sustainability of the Concrete Industry –
757 current Trends and Future Outlook. *TEHNIKA–NAŠE GRAĐEVINARSTVO*, 71(1), pp. 38-
758 44. <http://doi.org/10.5937/tehnika1701038T>

759 Yang, H., Xia, J., Thompson, J. & Flower, R., 2016. Urban construction and demolition
760 waste and landfill failure in Shenzhen, China. *Waste Management*, Volume 63, pp. 393-396.
761 <https://doi.org/10.1016/j.wasman.2017.01.026>

762 Ying, J., Men, Q. & Xia, J., 2017. The effect of cumulative aggregate treatment by carbon
763 dioxide levels on properties of concrete. *Journal of Building Materials*, Volume 20, pp. 277-
764 282.

765 Zhan, B., Xuan, D., Poon, C. & Shi, C., 2016. Effect of curing parameters on CO₂ curing of
766 concrete blocks containing recycled aggregates. *Cement and Concrete Research*, Volume 71,
767 pp. 122-130. <https://doi.org/10.1016/j.cemconcomp.2016.05.002>

768 Zhang, J. & Shi, C., 2015. Influence of carbonated recycled concrete aggregate on properties
769 of cement mortar. *Construction and Building Materials*, Volume 98, pp. 1-7.
770 <https://doi.org/10.1016/j.conbuildmat.2015.08.087>

771 Zhan, M. et al., 2018. Effect of presoak-accelerated carbonation factors on enhancing
772 recycled aggregate mortars. *Magazine of Concrete Research*, Volume 69, pp. 838-849.
773 <https://doi.org/10.1680/jmacr.16.00468>

774 Zhihui, Z., Shoude, W., Lingchao, L., & Chenchen, G., 2013. Evaluation of pre-coated
775 recycled aggregate for concrete and mortar. *Construction and Building Materials*, 43, 191-
776 196. <https://doi.org/10.1016/j.conbuildmat.2013.01.032>

1 **ENHANCEMENT OF MECHANICAL PROPERTIES OF CONCRETE WITH**
2 **TREATED DEMOLITION WASTE AGGREGATE**

3 Qusai Al-Waked^{1,2}, Jiping Bai¹, John Kinuthia¹, Paul Davies¹

4 ¹ Faculty of Computing, Engineering and Science, University of South Wales, Treforest
5 Campus, CF37 1DL, UK

6 ² Corresponding author

7 **ABSTRACT**

8 The utilization of recycled aggregate (RA) from the construction and demolition waste
9 (C&DW) in civil engineering applications, has proven to be an eco-efficient environmentally
10 friendly approach to overcome the current environmental concerns. Nevertheless, the poor
11 quality of RA has limited its utilization in high-grade civil engineering applications. To
12 maximize and promote the use of RA, it is essential that an appropriate process of treatment
13 methods is included in the production of RA to improve its properties. This research aimed to
14 examine the effects of various enhancement methods on the mechanical properties
15 (consistency, compressive strength, flexural strength, tensile splitting strength, and elastic
16 modulus) of recycled aggregate concrete (RAC). This research also included microstructure
17 investigation using Scan Electron Microscopy (SEM) images. The enhancement methods
18 used were treating RA by Soaking in Cement-Pulverized Fuel Ash-Silica Fume solution
19 (SCP), Sand Envelope Mixing Approach (SE), and their combination (SCP+SE). The
20 enhanced RACs showed an increased 28-day compressive strength of up to 46MPa suitable
21 for structural applications. The tensile splitting strength, flexural strength, and modulus
22 elasticity values of the enhanced RACs were 10%, 16%, and 6% higher than that of the
23 untreated RAC. The improved mechanical performance of the enhanced RAC was attributed
24 to the strengthened interfacial transition zone, better overall interlocking of the treated RA
25 with the new cement paste, filled-up pores and micro-cracks, reduced water absorption, and
26 improved aggregate impact value. The SEM images for the enhanced RACs showed better-
27 compacted microstructure, lesser pores and microcracks. The application of the proposed
28 innovative regime of enhancement methods is anticipated to promote the use of RA in the
29 construction industry and provide a better scientific understanding of the performance of
30 concrete produced with 100% treated RA from the C&DW for structural applications.

31

32 **Keywords:** Enhancement method, Adhered mortar, Compressive strength, Slump, Flexural
33 strength, Tensile splitting strength, Elastic modulus, Microstructure.

34 **1. Introduction**

35 The most abundant waste stream throughout Europe is the construction and demolition waste
36 (C&DW) resulting from activities of the construction industry, accounting for about 800
37 million tonnes per year [1]. According to DEFRA [2], the UK generated around 66.2 million
38 tonnes of C&DW in 2016, which is almost 30% of the total waste in the UK. In view of this,
39 recently, efforts have been made with an attempt to minimise the amount of C&DW sent to
40 landfills through recycling. For instance, the EU's Waste Framework Directive urged all the
41 European member states to achieve a minimum of 70% recycling rate of C&DW by 2020 [3].
42 Although the UK managed to achieve around a 91% recovery rate in 2016, more than 75% of
43 the recovered C&DW was used for backfilling [4]. This low-grade application is mainly due
44 to the poor and inconsistent quality of recycled aggregate (RA) from the C&DW, the
45 presence of the porous adhered mortar and the weak old interfacial transition zone. Other
46 reasons may include, pre-loading, accelerated weathering, and processing [5]. These factors
47 have caused RA to have low density, low aggregate impact value, low crushing value, and
48 high water absorption compared to natural aggregate (NA) [6].

49 Extensive studies have been carried out in the past few decades on the feasibility of
50 incorporating RA into concrete. These studies generally agreed that as the RA replacement
51 level increased the following changes in concrete properties were observed, reduced
52 consistency [7], reduced density [8], and reduced mechanical properties [8]. Given the poor
53 quality of RA, studies with the aim of improving the quality of RA and recycled aggregate
54 concrete (RAC) have been carried out extensively to expand the application of RA into
55 structural concrete [9]. The current methods used for enhancing RA and RAC can be
56 categorized into three main approaches; (i) removing the adhered mortar, (ii) strengthening
57 the adhered mortar, (iii) and batching techniques.

58 Techniques involving removing the adhered mortar can provide great improvement to RA
59 engineering properties and it may include methods such as soaking RA in acid [10], thermal
60 or traditional heating [11], microwave heating [6], and mechanical treatment [9].
61 Nevertheless, studies showed that there are some drawbacks to the use of removing the

62 adhered mortar, for instance, there is a possibility of introducing micro-cracks and damage to
63 RA surface through soaking in acid and/or mechanical treatments [12]. In addition, this
64 technique may result in fine aggregate after the treatment which in turn would increase waste
65 materials generation especially if the resulted fines are not utilized.

66 On the other hand, strengthening the adhered mortar offers greater advantages compared to
67 removing the adhered mortar [12]. It may include techniques such as coating RA with
68 pozzolanic slurry [13], soaking RA in sodium silicate solution [14], soaking in cement-
69 pozzolan solution [15], and accelerated carbonation [16]. Batching techniques may include,
70 stone envelope with pozzolanic powder [17], two-stage mixing technique [12], sand envelope
71 mixing approach [18], and mortar mixing approach [18]. Although there are a significant
72 amount of studies that dealt with the effects of different treatments on the performance of
73 recycled aggregate concrete, little attention, has been devoted to the effects of replacing
74 100% RA from the C&DW enhanced with different methods such as, strengthening the
75 adhered mortar, batching techniques, and combination of these treatments, on the mechanical
76 properties of recycled aggregate concrete (RAC). Aggregates as inert fillers play a significant
77 role in altering the properties of fresh and hardened concrete. To this end, this study aims at
78 enhancing the engineering properties of RA and the mechanical properties of RAC including
79 consistency, compressive strength, tensile splitting strength, flexural strength, and modulus of
80 elasticity. The present study also included a microstructure investigation for the treated
81 RACs. Soaking RA in cement-pulverized fuel ash – silica fume solution (SCP) was used to
82 treat RA prior to mixing, and sand envelope mixing approach (SE) was used as batching
83 technique for mixing RAC.

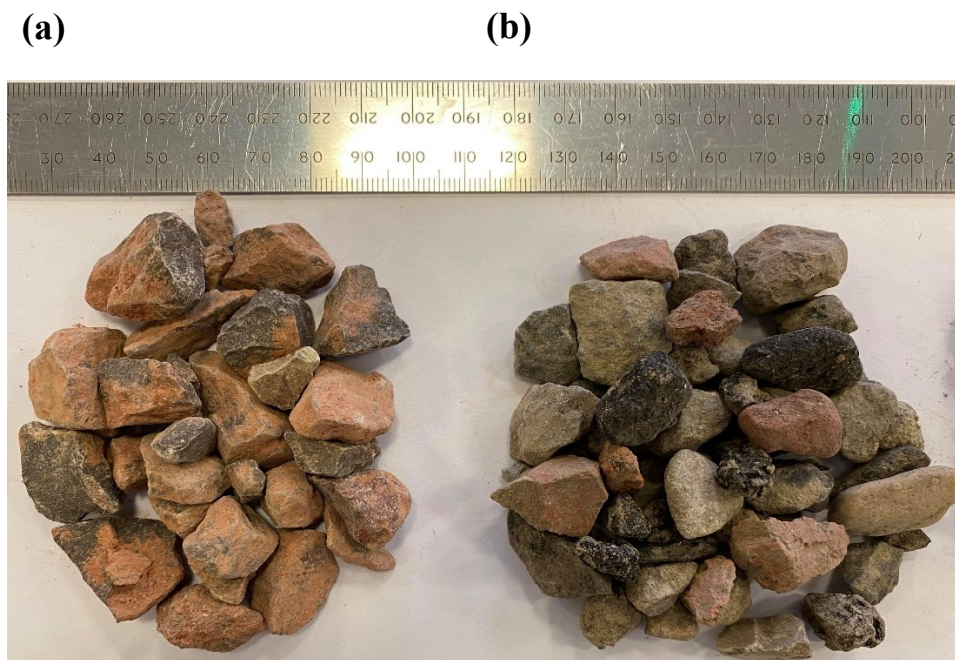
84 **2. Materials characteristics**

85 ***2.1 Aggregates***

86 Crushed limestone coarse aggregate (NA) of two particle sizes, 20/10 mm, and 10/4 mm,
87 were used throughout this study The limestone aggregate was sourced in bulk from Jewson
88 UK Limited in Caerphilly, South Wales, UK, conforming to BS EN 12620:2002+A1: 2008
89 [19]. The recycled aggregate (RA) utilized was sourced from Derwen Group, Neath Abbey,
90 UK. It is a mix of construction and demolition waste with a size range of clean 20/10 mm and
91 10/4mm. According to Derwen Group [20], the RA provided was produced to industry

92 standards, in accordance with WRAP Quality protocol and BS EN 13242: 2013 [21]
 93 specifications.

94 The RA consisted of different recycled materials i.e., brick, glass, bituminous, rounded
 95 stones, and recycled concrete aggregates. Figure 1 shows the NA and RA utilized throughout
 96 this study. Table 1 shows the compositions of RA in accordance with BS 8500-2: 2015+A2:
 97 2019 [22]. The mechanical and physical properties of the NA and RA are shown in Table 2,
 98 while the particle size distribution of NA and RA is shown in Figure 2.



99

100

Figure 1: (a) coarse NA, (b) coarse RA

	R_c (%)	R_u (%)	R_b (%)	R_g (%)	R_a (%)	X (%)
Sample 1	49.14	29.47	12.51	0.17	8.38	0.34
Sample 2	47.5	28.06	11.5	1.12	11.00	0.48
Sample 3	50.6	25.8	13.4	0.00	9.5	0.37
BS limits	–	–	–	–	≤10%	≤1%
Mean	49.08	27.78	12.47	0.42	9.6	0.39

101

102

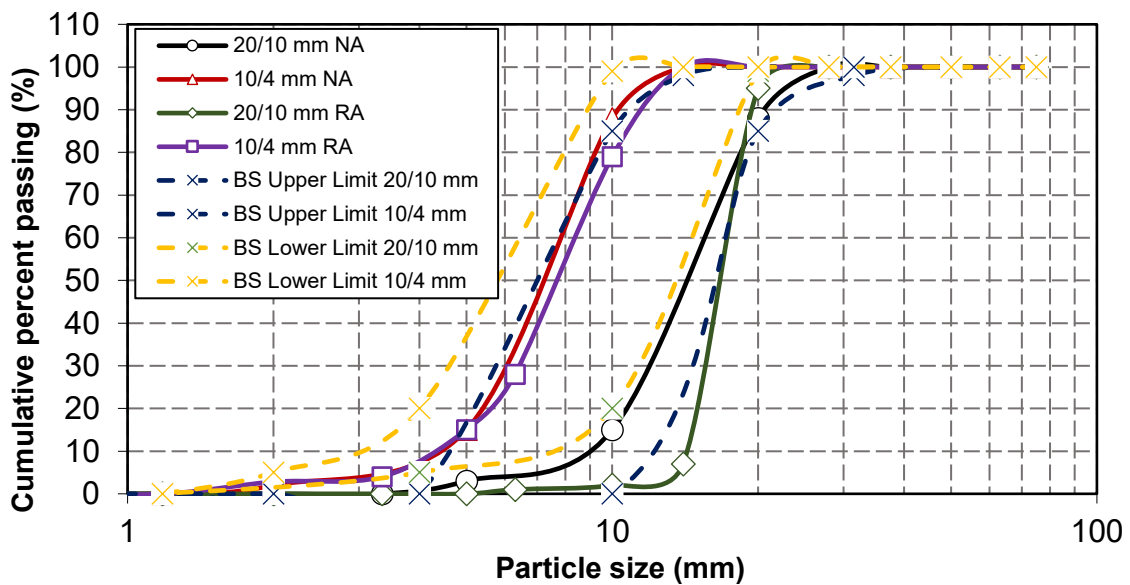
103

Notes: R_c - cement-based products, R_u - unbound aggregates and/or natural stones, R_b - clay masonry units i.e., bricks and tiles, calcium silicate masonry unit, R_a - bituminous materials, and X - miscellaneous materials and/or non-floating wood, plastic, and rubber, R_g - crushed glass.

104 Table 1: Compositions of recycled aggregates in this study (BS 8500-2:2015 +A2: 2019) [22]

Characteristic	NA	RA	BS limits	Standard
Flakiness Index (FI) (%)	18	27	< 40	BS EN 933-3:2012 [23]
Shape Index (SI) (%)	12	18	< 55	BS EN 933-4:2008 [24]
Water Absorption (WA) (%)	1.5	6.1	< 8	BS EN 1097-6:2013 [25]
Density kg/m ³	2480	2120	–	BS EN 1097-6:2013 [25]
Aggregate Impact Value (AIV) (%)	14	17	< 32	BS EN 1097-2:2020 [26]
LA (%)	18	26	< 50	BS EN 1097-2: 2020 [26]

105 Table 2: Characteristics of the RA compared with NA and relevant BS EN standards



106

107

Figure 2: Particle size distribution of coarse RA and coarse NA

108 2.2 Portland cement

109 A commercially available Portland cement (CEM I-42.5 N) which was manufactured in
 110 accordance with BS EN 197-1: 2011 [27] was used throughout the study. The CEM I was
 111 sourced from Jewson UK limited based in Caerphilly, South Wales, UK. The oxide and
 112 physical composition of the cement used are shown in Table 3.

113 2.3 Pozzolanic materials

114 The pulverized fuel ash (PFA) used throughout this study was supplied by a local supplier
 115 and was compliant with BS EN 450-1:2012 [28]. The silica fume (SF) utilized throughout
 116 this study was an un-densified silica fume with a commercial code 971U and was to the

117 conformity of BS EN 13263-2:2005+A1:2009 [29]. It was manufactured by Elkem Silicon
 118 Materials based in Norway and had a 97.1% purity.

	Oxide	Composition by (wt%)		
		PC	SF	PFA
119	CaO	61.49	–	0.22
	SiO₂	18.84	97.1	59.04
	Al₂O₃	4.77	0.1	34.08
	Fe₂O₃	2.87	0.2	2.00
	SO₃	3.12	0.06	0.05
120	Na₂O	0.02	–	1.26
		Physical properties		
	Colour	Grey	Dark Grey	Light Grey
	Bulk density (kg/m³)	1400	120-220	800-1000
	Specific gravity (Mg/m³)	3.16	2.20	2.90

Table 3: Oxide compositions and physical properties of materials used throughout this study

121

122 3. Experimental program

123 3.1 Enhancement methods for RA and RAC

124 3.1.1 Soaking RA in cement-PFA+SF solutions (SCP)

125 The recycled aggregates were treated by soaking in Portland cement - pulverized fuel ash -
 126 silica fume solution. These pozzolan materials were selected with the aim of fulfilling the
 127 environmental and economic criteria. The solution was prepared by blending the raw
 128 materials with water (twice the weight of RA) for several minutes. Then recycled aggregate
 129 was added into each solution and soaked for 4 hrs at 10% concentration level. Thereafter, the
 130 recycled aggregates were removed from the solution bath and let to drain for 10 min and then
 131 air-dried at room temperature for 24 hrs prior to testing. Table 4 shows the mix composition
 132 of the SCP treatment solution.

Treatment solution	Binder (g)			RA (g)	Water (g)	Concentration level
	PC	PFA	SF			
PC - PFA+SF	80	60	60	1000	1800	10%

133

Table 4: Proportions of the SCP treatment solution for 1000g of RA

134 3.1.2 Sand envelope mixing approach (SE)

135 Sand was firstly blended with 75% of the mixing water for 30 seconds, cement was then added to the
 136 mixture and mixed for 45 seconds. Thereafter, the recycled aggregate was added to the mixture with
 137 the rest of the mixing water and mixed for 90 seconds.

138 3.1.3 Bi-combination of SCP + SE

139 The untreated RA were firstly dried to constant mass and then soaked in pre-prepared cement-
 140 SF+PFA solution for 4 hrs, and then air-dried at room temperature for 3 days. Thereafter, the treated
 141 RA were incorporated in the mixing design of RAC and mixed via sand enveloped mixing approach
 142 (SE).

143 3.2 Concrete mix design

144 Table 5 shows concretes mix proportions produced with various enhancement methods at
 145 three different water to cement ratios, 0.4, 0.5, and 0.6.

146

Specimen designation	PC (kg/m ³)	Water (kg/m ³)	w/c ratio	NA (kg/m ³)	RA (kg/m ³)	FA (kg/m ³)	Mixing method	Notes
W040/NAC1	450	180	0.4	1257	0	677	NMA	NAC (control 1)
W040/RAC2	450	180	0.4	0	1206	677	NMA	Un-treated RAC (control 2)
W040/SCP	450	180	0.4	0	1206	677	NMA	Soaking RA in PC-SF+FA solution
W040/SE	450	180	0.4	0	1206	677	SE	Untreated RA
W040/SCP+SE	450	180	0.4	0	1206	677	SE	Soaking RA in PC-SF+FA solution
W050/NAC1	350	175	0.5	1257	0	677	NMA	NAC (control 1)
W050/RAC2	350	175	0.5	0	1206	677	NMA	Un-treated RAC (control 2)
W050/SCP	350	175	0.5	0	1206	677	NMA	Soaking RA in PC-SF+FA solution
W050/SE	350	175	0.5	0	1206	677	SE	Untreated RA
W050/SCP+SE	350	175	0.5	0	1206	677	SE	Soaking RA in PC-SF+FA solution
W060/NAC1	250	150	0.6	1257	0	677	NMA	NAC (control 1)
W060/RAC2	250	150	0.6	0	1206	677	NMA	Un-treated RAC (control 2)
W060/SCP	250	150	0.6	0	1206	677	NMA	Soaking RA in PC-SF+FA solution
W060/SE	250	150	0.6	0	1206	677	SE	Untreated RA
W060/SCP+SE	250	150	0.6	0	1206	677	SE	Soaking RA in PC-SF+FA solution

147 Note: NMA – normal mixing approach (conventional mixing approach), SE – sand envelope mixing approach, FA – fine aggregate, NA –
 148 natural aggregate, NAC – natural aggregate concrete.

149 Table 5: Concrete mix proportion for various RAC produced with different enhancement methods

150 3.3 Specimens Preparation & Testing of Concrete

151 Standard dimension of cube (100 mm × 100 mm × 100 mm), standard dimension of cylinder
 152 (150 mm × 300 mm) and (100 mm × 200 mm), and standard dimension of prismatic beam
 153 (100 mm × 100 mm × 500 mm) test specimens were utilized in the production of the
 154 concrete. The test specimens were prepared in accordance with BS EN 206:2013+A1:2016
 155 [30]. The consistency of fresh concrete was assessed using the slump test in accordance with
 156 BS EN 12350-2:2019 [31]. The de-moulding of the test specimens was carried out after 24

157 hrs of casting at room temperature. The curing of the test specimens was done in accordance
 158 with BS EN 12390-2:2019 [32]. The cube test specimens were tested for compressive
 159 strength at 7 and 28-day in accordance with BS EN 12390-3:2019 [33]. The 100 mm × 200
 160 mm concrete cylinders were tested for 28-day tensile splitting strength in accordance with BS
 161 EN 12390-6:2009 [34]. The 100 mm × 300 mm concrete cylinders were tested for 28-day
 162 modulus of elasticity in accordance with BS EN 12390-13:2021 [35]. The 100 mm × 100 mm
 163 × 500 mm prismatic concrete beams were tested for flexural strength in accordance with BS
 164 EN 12390-5: 2009 [36]. For all the mix compositions, the reported results are the average
 165 obtained from three individual test specimens for compressive strength, two for tensile
 166 splitting strength, two for flexural strength, and two for modulus of elasticity.
 167 Superplasticizer was only used for concretes produced at 0.4 w/c ratio at a 1% dosage to
 168 reach satisfactory consistency. The microstructure investigation was carried out Using a
 169 MIRA3 TESCAN Scanning Electron Microscope (SEM), fitted with a Solid-state
 170 Backscattered (electron) Detector (SBD).

171

172 4. Results and discussion

173 4.1 Effects of soaking RA in cement-PFA+SF solution on the AIV and WA

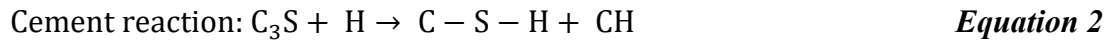
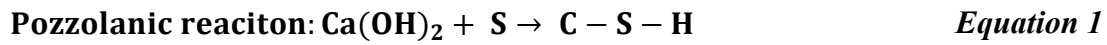
174 Table 6 shows the aggregate impact value (AIV) and water absorption (WA) of RA after
 175 treating by soaking in cement-PFA+SF solution.

Notation	AIV (%)	Enhancement (%)	WA (%)	Enhancement (%)
Un-treated RA	17	—	6.1	—
Treated RA by soaking in PC-PFA+SF	14.7	13	2.8	54

176 Table 6: Effects of soaking RA in cement-PFA+SF solution on the AIV and WA of RA

177 The main principle behind soaking RA in cement-pozzolan solution is to cover the RA
 178 surface with a thin layer of hydration products, hence improving the RA engineering
 179 properties. After the treatment, a dense coated layer was formed around the RA surface after
 180 the reaction of the pozzolanic materials with the Ca(OH)₂ in the adhered mortar. According
 181 to Singh et al. [37], the additional hydrated calcium silicate (C-S-H) gel fill the pores and
 182 voids of the adhered mortar as shown in Equation 1. The incorporation of cement in the

183 solutions is important for the treatment because it releases additional (C-S-H) gel and
184 Ca(OH)_2 during hydration, as given in Equation 2.



185 This additional production of C-S-H gel efficiently fills the voids and pores of the weak
186 adhered mortar, resulting in a much denser microstructure of RA. These findings are in
187 agreement with Shaban et al. [15] who reported 40% reduction in the AIV and 51.4%
188 reduction in water absorption of RA after soaking in pozzolan solution.

189 **4.2 Effects of SCP and SE on the consistency of fresh RACs**

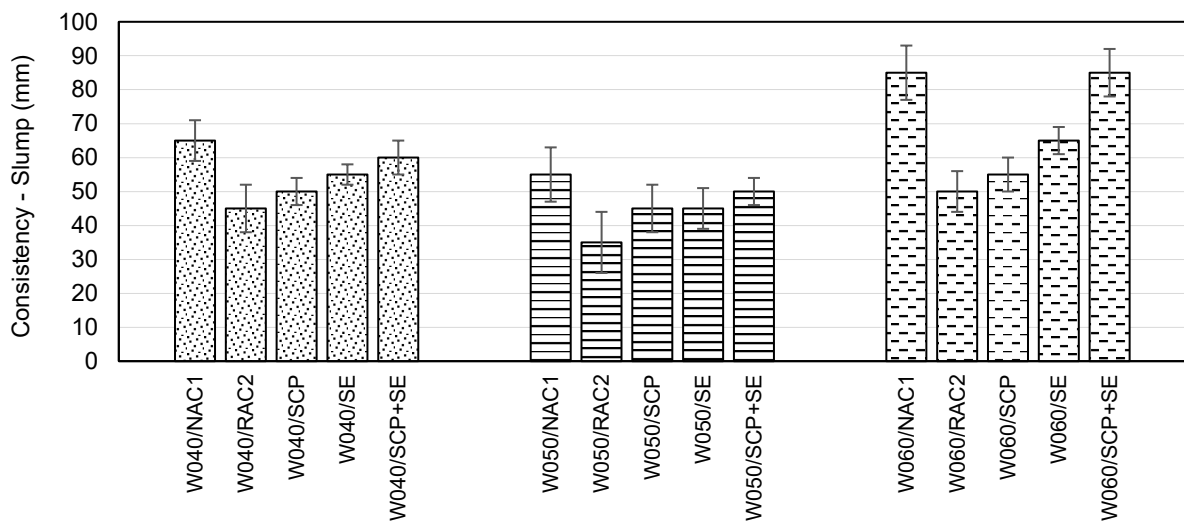
190 The results for the consistency of the fresh concrete measured using the slump test are shown
191 in Figure 3. The slump values observed for the NAC1 mix recorded the highest slump values
192 across all the concrete mixes, whereas the RAC2 mixes experienced the lowest slump values
193 among all the fresh concrete mixes irrespective of water to cement ratio. This is mainly
194 because of the porous nature of RA which reflects on its higher ability to absorb water
195 compared to NA, and hence the slump values for the RAC2 mixes are lower than for the
196 NAC1 mixes. This is in line with Malesev et al. [38] and Kou & Poon [39], who reported
197 higher slump loss for RAC compared with NAC. Kurda et al. [40] stressed that the reduced
198 consistency of RAC was mainly ascribed to the higher water absorption capacity of RA, the
199 rougher surfaces, and more angularity of RA compared to NA. Nonetheless, the poor
200 consistency of the RAC2 mixture at low w/c ratio of 0.4 was improved by the addition of
201 superplasticiser, and this is because of the efficiency of superplasticiser in increasing the
202 concrete workability.

203 The highest increase in slump values was observed with SCP+SE mix (soaking RA in
204 cement-PFA+SF solution combined with mixing via sand envelope mixing approach) across
205 all the designated enhanced RAC mixes at all the w/c ratios. The synergetic effect of the
206 combined treatments presented in SCP+SE mix increased the slump value by 33% (from
207 45mm to 60mm) at 0.4 water to cement ratios. It should be noted that, during mixing of the
208 concrete and whilst performing the slump tests, no segregation of concrete was found in any
209 of the concrete mixes. This is ascribed to firstly the effects of soaking RA in cement-PFA+SF
210 solution which strengthened the adhered mortar by the coated pozzolana layer/ film around

211 the RA particle surface, filling up the micro-pores and cracks of the RA. This ultimately
 212 prevented the RA from absorbing high amounts of mixing water, thus improving the
 213 workability [17].

214 Secondly, the utilization of sand envelope mixing approach (SE) was able to further enhance
 215 the consistency of RAC by mixing RA with the premixed cement-sand-water mixture that
 216 filled the pores and voids of RA and limited its absorption of the mixing water. This is in line
 217 with Liang et al. [18] who proposed this mixing method, and reported that the consistency of
 218 RAC was enhanced significantly after using the SE method.

219 Overall, it can be concluded that the poor consistency of untreated RAC can be overcome by
 220 the incorporation of either superplasticiser, or the treatment and batching techniques
 221 proposed. The best performed treated RAC mixes in terms of consistency are the mixes with
 222 the combination of SCP+SE treatment.



223 Figure 3: Effects of different enhancement methods on consistency - slump of RACs
 224

225 4.3 Effects of SCP and SE on the compressive strength of RACs

226 Figure 4 shows the compressive strength results for all concrete mixes at 7 and 28-day. The
 227 NAC1 mixtures showed the highest 7 and 28- day compressive strength among all the
 228 concrete mixtures of 39MPa and 49MPa, respectively, whilst the untreated RAC2 mixtures
 229 produced the lowest 7 and 28-day compressive strength of 29MPa and 37MPa, respectively.

230 This inferior compressive strength of the RAC1 stems from various factors such as the poor
 231 bonding between the adhered mortar and the RA from one side and between the RA and the

232 cement paste within the concrete matrix from another side. The presence of microcracks and
233 fissures on the RA surface due to processing. The porous nature of the adhered mortar and
234 the higher water absorption capacity of RA. The different composition of RA and the poor
235 engineering properties of RA [41]. These aspects contributed to a lower compressive strength
236 of RAC compared to NAC. Figure 5 shows SEM images for different concrete specimens.
237 Figure 5a shows the presence of two ITZ (interfacial transition zone) and the weak old ITZ in
238 the RAC2 specimen which also resulted in reduced compressive strength for RAC.

239 Similar observation of the inferior compressive strength of RAC was reported by Butler et al.
240 [42] and Xiao et al. [43] who observed a 30% reduction in compressive strength when RA
241 replaced NA at 100%. Tan et al. [44] studied the complete failure mechanism and cracking
242 mode of a modelled untreated RAC during a uniaxial compression test using digital image
243 correlation and concluded that the old ITZ was the most critical factor in controlling the
244 microcracking process of RAC. This was because the old ITZ possessed the lowest physical
245 strength in RAC compared to the old and new cement paste, aggregate, and the new ITZ. In
246 addition, Tang et al. [45] stated that, given the higher strength of the natural aggregate
247 (natural aggregate covered by old mortar) compared to the old mortar and the old ITZ, none
248 of the tensile cracks was observed in the natural aggregate region. The tensile cracks
249 observed were mostly in the old mortar region and in the old ITZ. Whereas the shear cracks
250 were observed to appear mostly along the old ITZ. This was also confirmed by Tang et al.
251 [45], who reported that it was more frequent that the cracks passed through the RA particles
252 compared to NA particles at the final pattern of cracks.

253 It can also be observed that an increase in 7- and 28-day compressive strength occurred when
254 the w/c ratio of the concrete mix was reduced for all the RAC1 mixes and the treated RACs
255 mixes specimens. This indicates that the RAC whether it was treated or untreated shows a
256 similar trend in strength development compared to natural aggregate concrete.

257 All the enhancement methods utilized, and their combinations were able to increase the 28-
258 day compressive strength of RAC to a minimum of 30MPa, hence changing the classification
259 of RAC to concrete suitable for structural application. Among all the enhanced RAC mixes,
260 the synergetic effects of soaking RA in cement-PFA+SF followed by mixing using sand
261 envelope mixing approach showed the highest increase in the 7-day and 28-day compressive
262 strength. For instance, the 7-day compressive strength of SCP+SE mixes increased from 29 to
263 36.7MPa (27% enhancement), and from 18.2 to 26.8MPa (47% enhancement), at 0.4 and 0.5

264 w/c ratios, respectively. This can be attributed to the coupled effects of these two methods
265 which led to a relatively stronger and compacted microstructure with the fewest pores and
266 microcracks, as can be seen in Figure 5d.

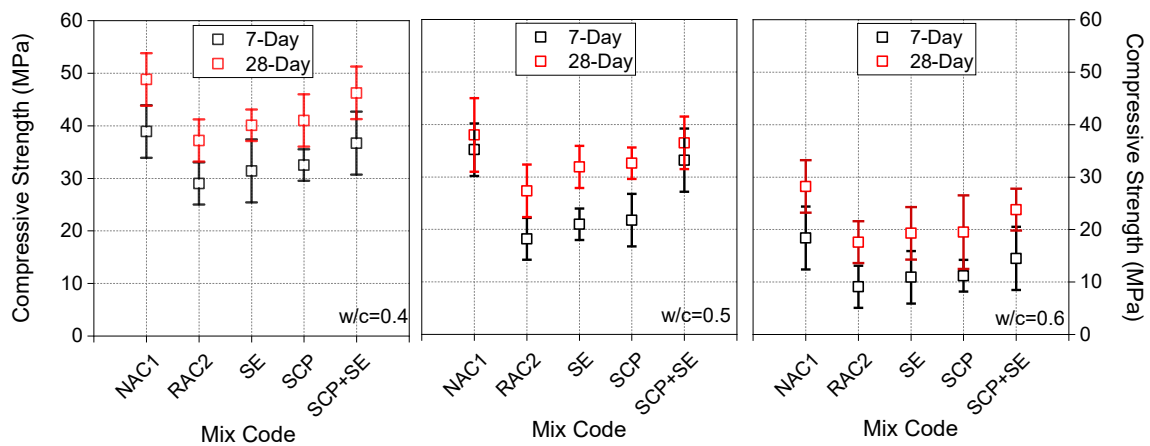
267 The enhanced 7-day and 28-day compressive strength of the SCP mixes (soaking RA in
268 cement-PFA+SF solution treatment) can be ascribed to the strengthened adhered mortar,
269 enhanced particle density, enhanced AIV, improved water absorption of RA, and
270 strengthened bond in the existing ITZ after this treatment (see Figure 5c). The enhanced
271 compressive strength of the SCP mixes can further be explained as the adhered mortar on the
272 RA surface consists of a significant amount of calcium hydroxide that can react with the
273 pozzolana materials (SF and PFA). Thus, forming a dense coating layer around the RA
274 surface. In addition, the formation of the additional calcium silicate hydrates and calcium
275 aluminate hydrates due to the presence of aluminate in PFA, leads to filling up the pores and
276 the voids of the adhered mortar [46]. The presence of cement in the treatment solution can
277 also lead to an additional formation of calcium silicate hydrates. These additional produced
278 calcium silicate products further fill up the pores and microcracks in the weak ITZ and the
279 adhered mortar on the RA surface, leading to a much denser microstructure of RA.

280 It is also worth noting that given the fine nature of SF, filler effect, high specific surface area,
281 and better packing density, it can efficiently fill the pores and voids in the adhered mortar,
282 and ultimately enhance the compressive strength of RAC [15]. Liang et al. [18] examined the
283 effects of treating RA by soaking in cement-SF solution and reported a 29% increase in the
284 28-day compressive strength of RAC, compared to the untreated RAC. This is also in line
285 with the results of Alqarni et al. [47] who reported a 32% enhancement in the 28-day
286 compressive strength for the treated RAC by soaking in cement-SF solution produced.
287 Similarly, Lei et al. [48] concluded that treating RA with cement slurry can enhance the
288 interface strength and the bonding force of RA with the new cement paste. The cement slurry
289 can fill the pores and voids of RA leading to increase RA strength and integrity. This is also
290 in line with the Lei et al. [49] study who pointed out that the pozzolan impregnation
291 treatments can lead to the pore filling and sealing of RA and enhance its interface structure
292 due to the pozzolanic reaction.

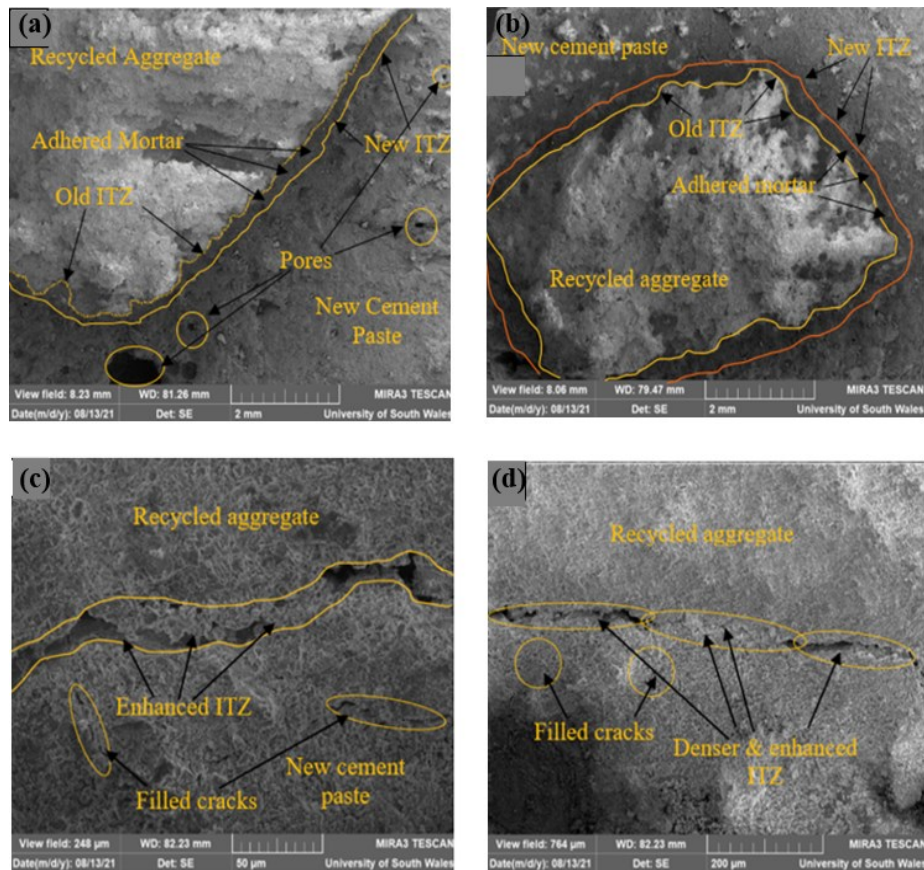
293 The enhanced compressive strength achieved by the SE mixes can be ascribed to the
294 sequential mixing process of this mixing approach, as sand and 3/4 of the total mixing and
295 cement are mixed first for a certain period of time which allow forming a cement paste prior

296 to the addition of RA, hence less water (effective mixing water) will be absorbed by the RA.
 297 The use of sand enveloped mixing approach has also led to a better compacted and formed
 298 microstructure, but the presence of the voids and micro-cracks was more evident compared to
 299 the SCP specimen as shown in Figure 5b.

300 To the best of the author's knowledge, the only study that dealt with the use of SE is the
 301 study carried out by Liang et al. [18]. Liang et al. [18] study did not show the effects of this
 302 mixing approach on the compressive strength of RAC in comparison with RAC produced
 303 with a normal/conventional mixing approach, but only reported its effects on the compressive
 304 strength of RAC compared with mortar mixing approach (MMA) and two-stage mixing
 305 approach (TSMA), in which SE performed better than both MMA and TSMA.



306
 307 Figure 4: Compressive strength development of the various concrete mixtures at 7-day, and 28-days



308
 309 Figure 5: SEM images for different test specimens, (a) RAC with untreated RA, (b) SE specimen, (c)
 310 SCP specimen, (d) SCP+SE specimen

311 4.4 Effects of SCP and SE on the tensile splitting strength of RACs

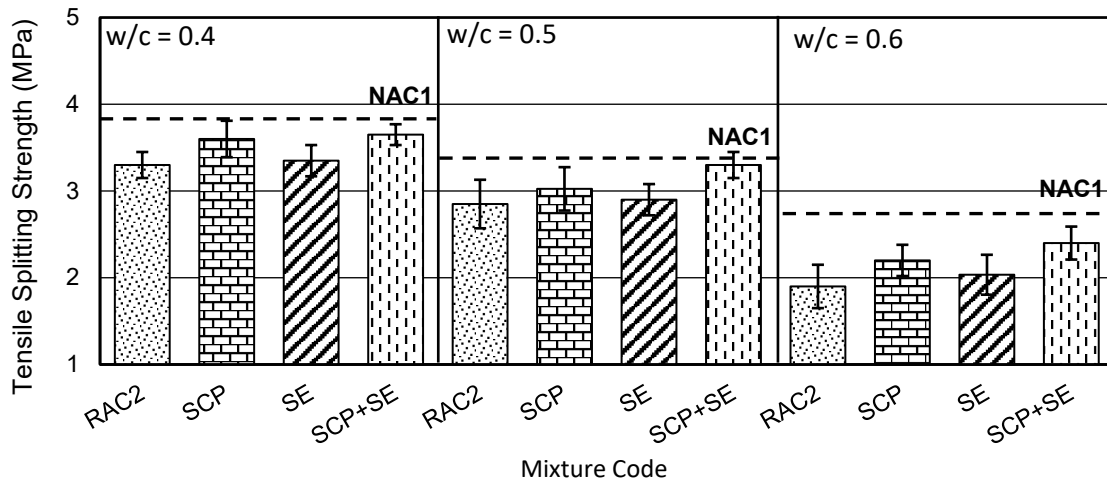
312 The tensile splitting strength results of the cylindrical enhanced RACs specimens water cured
 313 for 28 days, are shown in Figure 6. Similar to the trend observed in the compressive strength
 314 results, the highest tensile strength value across all the test concretes was recorded for the
 315 NAC1 mixes of 3.8MPa, whilst RAC2 mixes obtained the lowest tensile strength value of
 316 3.3MPa, regardless of the w/c ratio. This is ascribed to the poor quality of RA especially the
 317 adhered mortar which acts as a weak point that failed under compressive load and leads to a
 318 lower split tensile strength. This is in line with Alqarni et al. [47] who reported a reduction in
 319 the split tensile strength of 52% and 39% compared with conventional concrete, for 10mm
 320 aggregate size and 20mm aggregate size, respectively, Alqarni et al. [47] added that this
 321 reduction was due to the excessive amount of the porous adhered mortar on the RA surface.

322 Among all the enhanced mixes, RAC mixes produced with the combination of soaking in
 323 cement-PFA+SF followed by mixing using sand envelope mixing approach presented in the
 324 SCP+SE mixes achieved the highest tensile strength enhancement. SCP+SE mixes increased

325 the tensile strength of RAC from 3.3 to 3.65MPa (10% enhancement) at 0.4 w/c ratio. This is
326 can be attributed to the strengthened adhered mortar on the RA surface and especially the ITZ
327 being densified after this treatment. This is in line with Kukadia et al. [50] who treated RA by
328 soaking in cement solution, and reported a 20% enhancement in the tensile splitting strength
329 of concrete produced with 30% RA and 70% NA. Overall, all the enhanced mixes led to
330 enhancements in the tensile strength of RAC, but the enhancements were not as high as were
331 in the case of compressive strength. This might be because the efficacy of enhancement
332 methods is higher in enhancing the ability of RAC to withstand compression compared to
333 tension. In addition, one of the main factors that influence the tensile splitting strength of
334 RAC is the interlocking and bonding behavior between RA (the old ITZ to be specific) and
335 the new cement paste. Thus, another possible reason behind the lower enhancements
336 achieved in the tensile splitting strength compared to compressive strength, could be that the
337 enhancement methods utilized could not efficiently enhance the bonding strength of the old
338 ITZ with the new cement paste.

339 The SE mixes also exhibited enhancement in the split tensile strength, as the sand envelope
340 mixing approach (SE) procedures involved adding the untreated RA to the initially premixed
341 sand-rich mortar during the first stage of mixing. This sand-rich mortar coated the RA
342 surface, and ultimately strengthened the adhered mortar by sealing the RA surface [51].

343 The literature showed very limited studies were carried out on the effects of the batching
344 approaches on the tensile splitting strength of RAC. Jagan et al. [52] in their investigations,
345 mixed the RAC using sand envelope mixing approach (SE), and stated that the tensile
346 splitting tensile strength was enhanced by 14% after using SE method. The combination of
347 soaking RA in cement-PFA+SF solution prior to mixing followed by sand envelope mixing
348 approach presented in the SCP+SE mixes in enhancing the tensile splitting strength followed
349 the same trend of enhancement to the compressive strength. The SCP+SE mixes obtained the
350 highest enhancement in the tensile splitting strength of the RAC, this can be explained as the
351 coupled effects of both SCP and SE, ultimately enhancing the RA properties and the RAC
352 matrix. There are no studies to be found in the literature that examined the couple effects of
353 these treatment methods on the tensile splitting strength of the RAC.



354

355

356

Figure 6: Variation in tensile strength development at 28-day for the enhanced RACs mixes at different w/c ratios, compared to NAC1 and RAC2

357

4.5 Effects of SCP and SE on the flexural strength of RACs

358

359

360

361

362

363

364

365

366

367

368

The results of the flexural strengths of the different RACs produced with different enhancement methods are given in Figure 7. A similar trend to tensile strength development was noticed in the 28-day development of the different RACs flexural strength. The NAC1 mixes exhibited the highest flexural strength of 6.5MPa at a 0.4 w/c ratio, among all the concrete test specimens, whilst the untreated RAC2 mixes seem to develop significantly lower flexural strength compared to NAC1. The Untreated RAC2 mixes obtained 4.6MPa at a 0.4 w/c ratio. This trend of reduction in flexural strength can be attributed to the weak bonding between the RA and the new cement paste within the concrete matrix owing to the poor quality of the adhered mortar on the RA surface and the poor quality of the developed ITZ [53]. Similarly, Majhi et al. [54] concluded a 6.5% reduction in the flexural strength of the RAC in comparison with NAC.

369

370

371

372

373

374

375

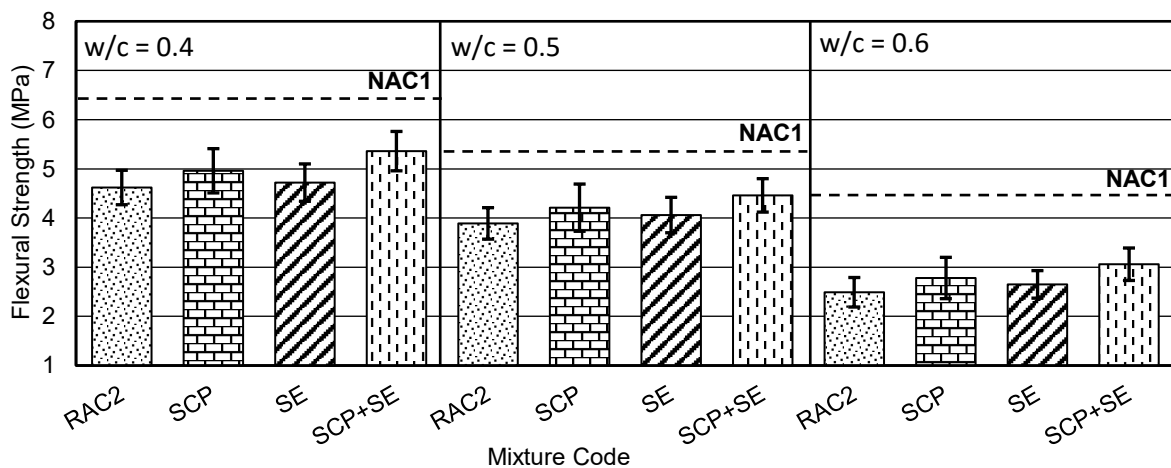
376

377

All the enhancement methods utilized were able to enhance the flexural strength of RAC. The results of the flexural strength also showed that all the enhanced RAC specimens presented in the SCP, the SE, and the SCP+SE specimens, followed similar flexural strength enhancement patterns to tensile splitting strength and compressive strength. Amongst all of these methods, the combination of soaking in cement-PFA+SF followed by mixing via sand envelope mixing approach presented in SCP+SE mixes, provided the best enhancements in the flexural strength. The synergetic effects of SCP+SE treatment resulted in a significant increase in the flexural strengths of RAC from 4.6 to 5.36MPa (16% enhancement), at a 0.4 w/c ratio. This can be ascribed to the denser developed ITZ after the treatment of the RA resulting in better

378 bonding between the RA and the cement paste. The literature showed very limited studies on
 379 the effects of coating/ soaking RA with cement-pozzolan slurry/ solution on the flexural
 380 strength of the RAC. Ahmed & Lim [55] coated the RA with pozzolan slurry and reported
 381 13% enhancement in the flexural strength of the RAC. Ahmad and Lim, pointed out that the
 382 enhancement in the flexural strength after the use of the pozzolan slurry is mainly attributed
 383 to the counteracting the microstructural deficiencies by the formation of the secondary
 384 calcium silicate hydrates which contributed to the enhancement of the flexural strength of the
 385 RAC.

386 There are very scarce studies that deal with the effects of the sand envelope mixing approach
 387 on the flexural strength of the RAC. Jagan et al. [52] reported 11% enhancement in the
 388 flexural strength of RAC after mixing using sand envelope mixing approach (SE). The
 389 combination of soaking RA in cement- PFA+SF solution prior to mixing followed by mixing
 390 using sand envelope mixing approach obtained better enhancement compared to the sole use
 391 of each method. This can be explained as the coupled effects of the two methods significantly
 392 strengthened the adhered mortar on the RA surface and densifying the ITZ resulting in a
 393 stronger bonding between the RA and the cement paste within the RAC matrix. There are no
 394 studies that examined the synergetic effect of these two methods on the flexural strength of
 395 the RAC.



396
 397 Figure 7: Flexural strength development for treated RAC mixes at different w/c ratios, compared to
 398 the NAC1 mixes and the untreated RAC2 mixes

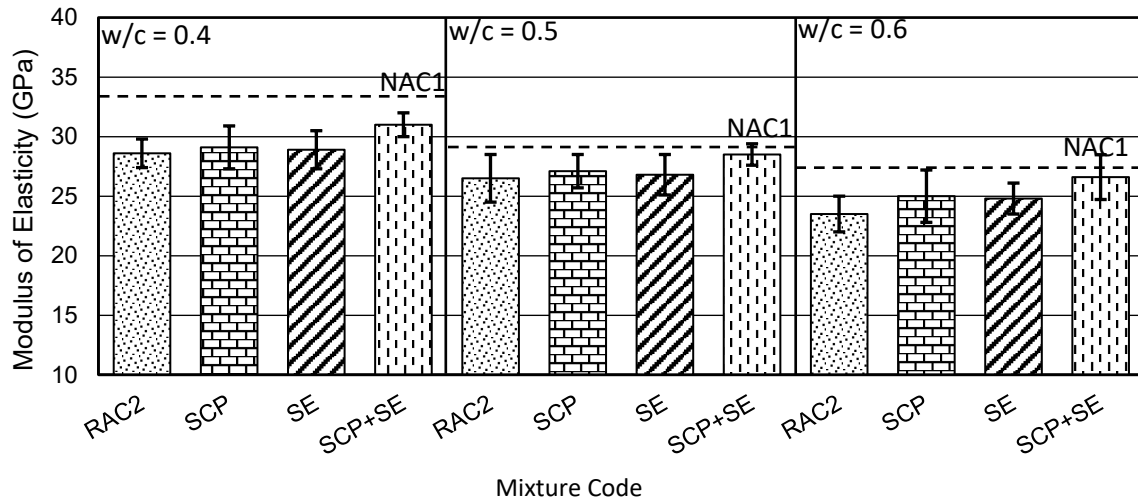
399 4.6 Effects of SCP and SE on the modulus of elasticity of RACs

400 The results of the elastic modulus of the treated RACs cylindrical specimens after 28 days of
 401 water curing are presented in Figure 8. The highest modulus of elasticity was recorded for the

402 NAC1 mixes, with ranges between 27–33.5GPa. Like the compressive strength, the tensile
403 splitting strength, and the flexural strength, a similar reduction trend has also been observed
404 for the modulus of elasticity of the RAC2 specimens compared to the NAC1 specimens. The
405 untreated RAC2 mixes exhibited the lowest modulus of elasticity values, ranging from 23.5–
406 28.6GPa. This is possibly ascribed to the higher water absorption capacity of RA due to the
407 porous adhered mortar, lower density and the weak bonding between the old ITZ and the new
408 ITZ because of the presence of pores and micro-cracks around the RA [41]. According to
409 Belen et al. [56], the RA adversely affects both the longitudinal and the transverse modulus
410 of elasticity and owing to the lower elastic moduli of the RA, the peak strain and ultimate
411 strain of RAC are increased, thus, large deformation in the RAC is endured.

412 Following the same enhancements trend observed in the compressive strength, tensile
413 strength, and flexural strength, the highest enhancements in the modulus of elasticity of RAC
414 were recorded for SCP+SE mixes. The coupled effects of SCP+SE treatment enhanced the
415 modulus of elasticity of RAC by 8%, 7%, and 9%, at 0.4, 0.5, and 0.6 w/c ratios,
416 respectively. Whereas SCP and SE mixes showed close enhancements in the modulus of
417 elasticity of RACs, but slightly lower compared to SCP+SE mixes. There are very limited
418 studies on the effects of soaking RA in cement-pozzolan solution and sand envelope mixing
419 approach on the Young's modulus of RAC. Nonetheless, the enhanced modulus of elasticity
420 of RAC achieved by the SCP specimens can be ascribed to the enhanced modulus of
421 elasticity of RA after soaking in cement-PFA+SF solution along with the enhanced
422 compressive strength and other related mechanical properties. Mixing RAC using sand
423 envelope mixing approach presented in the SE specimens has also enhanced the modulus of
424 elasticity of the RAC.

425 This is possibly attributed to the formed pre-mixed stiff matrix during the first stage of SE
426 method which filled the pores and micro-cracks of the RA, resulting in a stiffer and enhanced
427 modulus of elasticity of the RA. This is in line with Jagan et al. [60] who investigated the
428 effects of sand envelope mixing approach on the elastic modulus of RAC and reported 12%
429 and 14.8% enhancement in the modulus of elasticity of RAC at 28-day and 90-day,
430 respectively.



431

432 Figure 8: Variations in modulus of elasticity of the different treated RACs mixes in comparison with
 433 untreated RAC2 and NAC1 mixes

434 4.7 Correlation analysis of mechanical properties

435 Figure 9 shows the relationship developed between the different mechanical properties using
 436 the obtained experimental data. It can be seen from Figure 9 that a direct relationship exists
 437 between the mechanical properties of the enhanced RACs. It can be also indicated that the
 438 mechanical properties of the enhanced RACs are proportional to each other. The correlation
 439 between the different mechanical properties was obtained from the maximum correlation
 440 coefficient and can be expressed as follows:

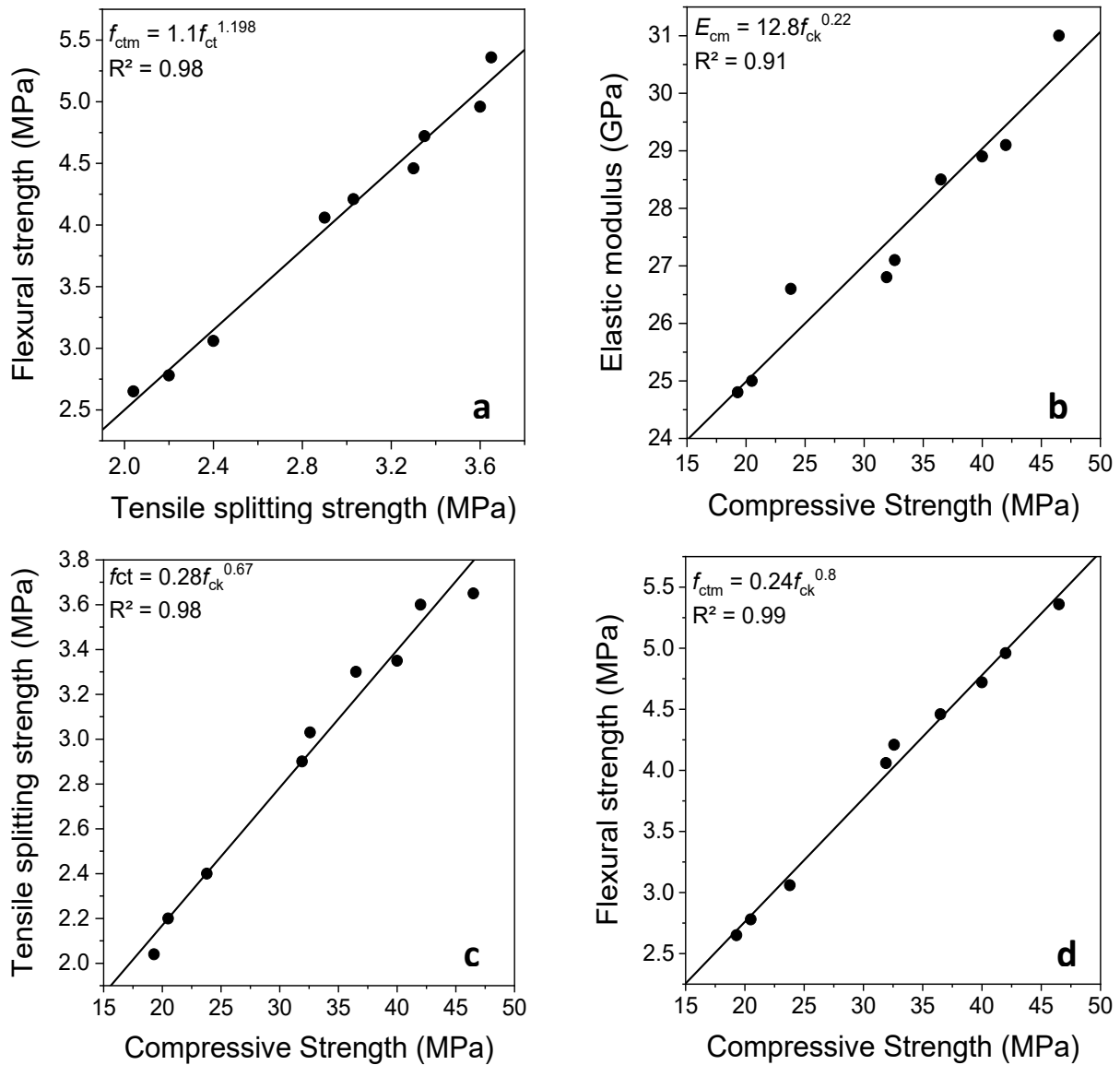
441 $f_{ctm}=1.1f_{ct}^{1.198} (R^2=0.98)$ *Equation 3*

442 $E_{cm}=12.8f_{ck}^{0.22} (R^2=0.91)$ *Equation 4*

443 $f_{ct}=0.28f_{ck}^{0.67} (R^2=0.98)$ *Equation 5*

444 $f_{ctm}=0.24f_{ck}^{0.8} (R^2=0.99)$ *Equation 6*

445 Where is f_{ct} is the flexural strength and f_{ctm} is the splitting tensile strength, E_{cm} is the
 446 modulus of elasticity, and f_{ck} is the cube compressive strength. The R-factor of all the above-
 447 derived correlations was above 0.9, which indicates that the modulus of elasticity, tensile
 448 splitting strength, and flexural strength of the enhanced RAC can be predicted with relatively
 449 reasonable accuracy if the compressive strength was known.



450

451 Figure 9: Relationship between different mechanical properties of the obtained experimental data (a)
 452 flexural strength vs. tensile splitting strength, (b) elastic modulus vs. compressive strength, (c) tensile
 453 splitting strength vs. compressive strength, (d) flexural strength vs. compressive strength

454 5. Conclusions

455 Recycled aggregate concrete with untreated RA has demonstrated low-quality engineering
 456 performance compared to NAC in terms of concrete mechanical properties due to several
 457 factors. Two of the main factors are the adhered mortar on the RA surface and the old weak
 458 ITZ which results in a weak interfacial transition zone and weak bonding within the recycled
 459 aggregate concrete matrix. Other concerns include variation in composition, previous
 460 loading, processing, and weathering compared to freshly crushed natural aggregates. This
 461 paper has presented a laboratory-based investigation of the effects of different enhancement

462 methods on enhancing the mechanical property of RAC. Accordingly, based on the data
463 presented, the following specific conclusions can be drawn.

464 **1. Recycled aggregate concrete with untreated RA:** the RAC with untreated RA showed
465 inferior consistency, lower compressive strength, lower tensile splitting strength,
466 reduced flexural strength, and inferior elastic modulus compared to the natural
467 aggregate concrete. This was due to the poor engineering properties of RA compared
468 to NA and mainly due to the presence of two ITZs in the RAC in which the old ITZ
469 acted like a weak link in the RAC matrix. The inferior flexural strength, tensile
470 splitting strength, and modulus of elasticity performance of RAC were mainly due to
471 the lower bond strength and poor interlocking of RA with the cement paste because of
472 the ITZ. In addition, the lower modulus of elasticity of RAC was associated with the
473 lower elastic moduli of RA compared to NA. The high porous nature of RA owing to
474 the presence of pores and micro-cracks on the RA surface along with the old ITZ was
475 also related to the inferior mechanical performance of RAC. The SEM images of the
476 RAC microstructure confirmed the poor mechanical performance of RAC. The
477 microstructure of RAC was full of micro-pores, voids, and micro-cracks around the
478 ITZ.

479 **2. Soaking RA in cement-PFA+SF solution (SCP):** treating RA by soaking in cement-
480 PFA+SF solution increased the consistency by 20%. The SCP achieved a minimum of
481 30MPa compressive strength suitable for structural applications. The splitting tensile
482 strength, flexural strength and modulus of elasticity were enhanced by 9%, 7%, and
483 2%, respectively, after the SCP treatment. These enhancements were due to the filling
484 and sealing effect of the SCP method. The SEM images of the SCP mix showed a
485 better and denser microstructure, lesser pores and filled micro-cracks.

486 **3. Sand Envelope mixing approach (SE):** the SE batching technique significantly
487 enhanced the consistency of RAC. A minimum of 30MPa compressive strength was
488 achieved by the SE batching technique. The splitting tensile strength, flexural
489 strength, and elastic modulus exhibited an increase of 1%, 2%, and 1%, respectively,
490 after batching using the SE method. The developed stiffed sand-rich cement paste
491 during the early stage of mixing covering the RA surface was mainly the key factor
492 responsible for the overall enhancement of the SE mix. The microstructure of the SE
493 mix was denser with lesser voids and micro-cracks compared to the untreated RAC,

494 but the presence of the voids and micro-cracks was more evident compared to the
495 SCP mix.

496 **4. *Bi-combination of SCP+SE:*** the combination of soaking RA in cement-PFA+SF
497 solution prior to mixing followed by mixing using sand envelope mixing approach
498 exhibited the highest 28-day compressive strength of 46MPa. This bi-combination of
499 the enhancement method also achieved 14%, 13%, and 7% enhancements in the
500 tensile splitting strength, flexural strength, and modulus of elasticity, respectively.
501 The coupled effects of SCP and SE method resulted in reduced water absorption of
502 RA, reduced aggregate impact value of RA, further filling of the pores and micro-
503 cracks, and a better-compacted matrix of RAC. In addition, a higher C-S-H gel
504 amount was produced as a result of soaking in cement-PFA+SF solution. All these
505 factors resulted in higher strength RAC and improved its mechanical performance.
506 The SEM images observed for the SCP+SE mix showed the most desired better-
507 compacted microstructure. The synergetic effects of these two methods led to a
508 relatively stronger and compacted microstructure with the fewest pores and
509 microcracks.

510 **5.** Overall, it can be concluded that the proposed innovative enhancement methods in
511 this research are powerful tools to promote the use of recycled aggregate in the
512 construction industry. The findings of the present research can be of great interest to
513 stakeholders, such as recycling plant owners, relevant government sectors and bodies,
514 the construction industry, design engineers, and researchers.

515 **Declaration of Competing Interest**

516 The authors declare that they have no known competing financial interests or personal
517 relationships that could have appeared to influence the work reported in this paper.

518 **Funding**

519 This research did not receive any specific grant from funding agencies in the public,
520 commercial, or non-profit sectors.

521 **REFERENCES**

- 522 [1] Deloitte, B., 2017. *Resource Efficient Use of Mixed Wastes: Improving Management*
523 *of Construction and Demolition Waste*, Brussels, Belgium: European Union.
- 524 [2] DEFRA, 2012. UK Statistics on Waste. [Online] Available at:
525 <http://www.gov.uk.com> [Accessed 15 February 2022].
- 526 [3] Commission, EU., 2019. Construction and Demolition Waste. [Online] Available at:
527 <http://www.ec.europa.eu.com> [Accessed 15 March 2022].
- 528 [4] Ferriz-Papi, J., Weekes, E., Whitehead, N. & Lee, A., 2022. A cost-effective recycled
529 aggregates classification procedure for construction and demolition waste evaluation.
530 *Construction and Build. Mater.*, Volume 324, p. 126642,
531 <http://doi.org/10.36756/JCM.v2.1.6>.
- 532 [5] Gonzalez-Corominas, A. & Etxeberria, M., 2014. Properties of high-performance
533 concrete made with recycled fine ceramic and coarse mixed aggregates. *Construction*
534 *and Build. Mater.*, Volume 68, pp. 618-626.
535 <http://doi.org/10.1016/J.CONBUILDMAT.2014.07.016>.
- 536 [6] Bru, K., Touze, S., Bourgeois, F., Lippiatt, N., Menard, Y., 2014. Assessment of a
537 microwave-assisted recycling process for the recovery of high-quality aggregates
538 from concrete waste. *International Journal of Mineral Processing*, Volume 126, pp.
539 90-98, <https://doi.org/10.1016/j.minpro.2013.11.009>.
- 540 [7] Grabiec, A. M., Zawal, D., & Rasaq, W. A., 2020. The effect of curing conditions on
541 selected properties of recycled aggregate concrete. *Applied Sciences (Switzerland)*,
542 10(13). <https://doi.org/10.3390/APP10134441>
- 543 [8] Al Ajmani, H., Suleiman, F., Abuzayed, I. & Tamimi, A., 2019. Evaluation of
544 Concrete Strength Made with Recycled Aggregate. *Buildings*, Volume 9, pp. 1-14,
545 <https://doi.org/10.3390/buildings9030056>.
- 546 [9] Dilbas, H., Cakir, O. & Atis, C., 2019. Experimental investigation on properties of
547 recycled aggregate concrete with optimized Ball Milling Method. *Construction and*
548 *Build. Mater.*, Volume 212, pp. 716-726. <http://doi.org/10.1016/j.conbuildmat.2019.04.007>.
- 550 [10] Katkhuda, H. & Shatarat, N., 2017. Improving the mechanical properties of
551 recycled concrete aggregate using chopped basalt fibers and acid treatment.
552 *Construction and Build. Mater.*, Volume 140, pp. 328-335.
553 <https://doi.org/10.1016/j.conbuildmat.2017.02.128>

- 554 [11] Pawluczuk, E., Wichrowska, K., Boltryk, M. & Rodriguez, J., 2019. The
555 influence of heat and mechanical treatment of concrete rubble on the properties of
556 recycled aggregate concrete. *Mater.*, 12(3), pp. 1-24.
557 <https://doi.org/10.3390/ma12030367>
- 558 [12] Tam, V., Tam, C. & Le, K., 2007. Removal of cement mortar remains from
559 recycled aggregate using pre-soaking approaches. *Resour., Conservation &*
560 *Recycling*, 50(1), pp. 82-101. <http://doi.org/10.1016/j.resconrec.2006.05.012>
- 561 [13] Kou, S. & Poon, C., 2012. Enhancing the durability properties of concrete
562 prepared with coarse recycled aggregate. *Construction and Build. Mater.*, Volume 35,
563 pp. 69-76. <https://doi.org/10.1016/j.conbuildmat.2012.02.032>.
- 564 [14] Chen, J., Thomas, J. & Jennings, H., 2006. Decalcification shrinkage of
565 cement paste. *Cement and Concr. Res.*, 36(5), pp. 801-809.
566 <http://doi.org/10.1016/j.cemconres.2005.11.003>
- 567 [15] Shaban, W., Yang, J., Su, H., Mo, K., Li, J., Xie, J., 2019. Quality
568 Improvement Techniques for Recycled concrete Aggregate: A review. *Journal of*
569 *Advanced Concr. Technology*, Volume 17, pp. 151-167,
570 <https://doi.org/10.3151/jact.17.151>.
- 571 [16] Kou, S., Poon, C. & Chan, D., 2008. Influence of fly ash as a cement addition
572 on the hardened properties of RAC. *Mater. and Struct.*, 41(7), pp. 1191-1201,
573 <http://doi.org/10.1617/S11527-007-9317-Y>.
- 574 [17] Li, J., Xiao, H. & Zhou, Y., 2009. Influence of coating recycled aggregate
575 surface with pozzolanic powder on properties of recycled aggregate concrete.
576 *Construction and Build. Mater.*, 23(3), pp. 1287-1291.
577 <https://doi.org/10.1016/j.conbuildmat.2008.07.019>
- 578 [18] Liang, Y., Ye, Z., Vernerey, F. & Xi, Y., 2013. Development of processing
579 methods to improve strength of concrete with 100% recycled coarse aggregate.
580 *Journal of Mater. in Civil Eng.*, 27(5), p. 130801045339002,
581 [http://doi.org/10.1061/\(ASCE\)MT.1943-5533.0000909](http://doi.org/10.1061/(ASCE)MT.1943-5533.0000909).
- 582 [19] British Standards Institution. BS EN 12620:2002+A1:2008—Aggregates for
583 Concrete; British Standards Institution: London, UK, 2008.

- 584 [20] British Standards Institution. BS EN 13242:2013—Aggregates for unbound
585 and hydraulically bound materials for use in civil engineering work and road
586 construction; British Standards Institution: London, UK, 2013.
- 587 [21] Derwen, 2016. Recycled Aggregate. [Online] Available at:
588 <https://www.derwengroup.co.uk> [Accessed 10 February 2022].
- 589 [22] British Standards Institution. BS 8500-2:2015 +A2: 2019—Concrete-
590 Complementary British Standard to BS EN 206. Part 2: Specification for constituent
591 materials and concrete; British Standards Institution: London, UK, 2019.
- 592 [23] British Standards Institution. BS EN 933-3: 2012—Tests for geometrical
593 properties of aggregates. Part 3: Determination of particle shape—Flakiness index;
594 British Standards Institution: London, UK, 2012.
- 595 [24] British Standards Institution. BS EN 933-4:2008—Tests for Geometrical
596 Properties of Aggregates. Part 4: Determination of Particle Shape—Shape Index;
597 British Standards Institution: London, UK, 2008.
- 598 [25] British Standards Institution. BS EN 1097-6:2013—Tests for Mechanical and
599 Physical Properties of Aggregates. Part 6: Determination of Particle Density and
600 Water Absorption; British Standards Institution: London, UK, 2013.
- 601 [26] British Standards Institution. BS EN 1097-2:2020—Tests for mechanical and
602 physical properties of aggregates. Part 2: Methods for determination of resistance to
603 fragmentation; British Standards Institution: London, UK, 2020.
- 604 [27] British Standard Institution. BS EN 197-1:2011 - Cement. Composition,
605 specifications and conformity criteria for common cements; British Standard
606 Institution: London, UK, 2011.
- 607 [28] British Standard Institution. BS EN 450-1:2012 – Fly ash for concrete. Part 1:
608 Definition, specifications and conformity criteria; British Standard Institution:
609 London, UK, 2012.
- 610 [29] British Standard Institution. BS EN 13263-2:2005+A1:2009 – Silica fume for
611 concrete. Part 2: conformity evaluation; British Standard Institution: London, UK,
612 2009.
- 613 [30] British Standards Institution. BS EN 206:2013+A1:2016 - Concrete.
614 Specification, performance, production and conformity; British Standards Institution:
615 London, UK, 2016.

- 616 [31] British Standards Institution. BS EN 12350-2:2019 - Testing fresh concrete.
617 Slump test; British Standards Institution: London, UK, 2019.
- 618 [32] British Standards Institution. BS EN 12390-2:2009: Testing hardened
619 concrete. Making and curing specimens for strength tests; British Standards
620 Institution: London, UK, 2009.
- 621 [33] British Standards Institution. BS EN 12390-3:2019: Testing hardened
622 concrete. Compressive strength of test specimens; British Standards Institution:
623 London, UK, 2019.
- 624 [34] British Standards Institution. BS EN 12390-6: 2009: Testing hardened
625 concrete. Tensile splitting strength of test specimens; British Standards Institution:
626 London, UK, 2009.
- 627 [35] British Standards Institution. BS EN 12390-13:2021. Testing hardened
628 concrete- Part 13: Determination of secant modulus of elasticity in compression;
629 British Standards Institution: London, UK, 2021.
- 630 [36] British Standards Institution. BS EN 12390-5:2009. Testing hardened
631 concrete- Part 5: Flexural strength of test specimens; British Standards Institution:
632 London, UK, 2009.
- 633 [37] Singh, L.P., Karade, S.R., Bhattacharyya, M.M & Ahalawat, S., 2013.
634 Beneficial Role of Nanosilica in Cement Based Materials - A Review. *Construction*
635 *and Build. Mater.*, Volume 47, pp. 1069-1077,
636 <https://doi.org/10.1016/j.conbuildmat.2013.05.052>.
- 637 [38] Malesev, M., Radonjanin, V. & Marinkovic, S., 2010. Recycled concrete as
638 aggregate for structural concrete production. *Sustainability*, Volume 2, pp. 1204-1225,
639 <https://doi.org/10.3390/su3020465>.
- 640 [39] Kou, S. C., & Poon, C. S., 2009. Properties of self-compacting concrete
641 prepared with coarse and fine recycled concrete aggregates. *Cement and Concr.*
642 *Composites*, 31(9), 622–627. <https://doi.org/10.1016/J.CEMCONCOMP.2009.06.005>
- 643 [40] R. Kurda, R., Brito, J., Silvestre, J., 2017. Influence of recycled aggregates
644 and high contents of fly ash on concrete fresh properties. *Cement and Concr.*
645 *Composites*, 84, pp. 198-213. <https://doi.org/10.1016/j.cemconcomp.2017.09.009>
- 646 [41] Behera, M., Bhattacharyya, S. K., Minocha, A. K., Deoliya, R., & Maiti, S.,
647 2014. Recycled aggregate from C&D waste & its use in concrete – A breakthrough

- 648 towards sustainability in construction sector: A review. *Construction and Build.*
649 *Mater.*, 68, 501–516. <https://doi.org/10.1016/J.CONBUILDMAT.2014.07.003>
- 650 [42] Butler, L., West, J. & Tighe, S., 2011. The effect of recycled concrete
651 aggregate properties on the bond strength between RCA concrete and steel
652 reinforcement. *Cement and Concr. Research*, 41, pp. 1037-1049,
653 <https://doi.org/10.1016/j.cemconres.2011.06.004>.
- 654 [43] Xiao, J., Li, W., Fan, Y. & Huang, X., 2012. An overview of study on
655 recycled aggregate concrete in China (1996-2011). *Construction and Build. Mater.*,
656 Volume 31, pp. 364-383, <https://doi.org/10.1016/j.conbuildmat.2011.12.074>.
- 657 [44] Tan, X., Hu, Z., Li, W., Zhou, S., & Li, T., 2020. Micromechanical Numerical
658 Modelling on Compressive Failure of Recycled Concrete using Discrete Element
659 Method (DEM). *Materials*, 13(19), 4329. doi:<https://doi.org/10.3390/ma13194329>
- 660 [45] Tang, Z., Li, W., Peng, Q., Vivian, T., & Wang, K., 2021. Study on the failure
661 mechanism of geopolymeric recycled concrete using digital image correlation
662 method. *Journal of Sustainable Cement-Based Materials*, 113-126.
663 doi:<https://doi.org/10.1080/21650373.2021.1897706>
- 664 [46] Wang, B., Yan, L., Fu, Q. & Kasal, B., 2021. A Comprehensive Review on
665 Recycled Aggregate and Recycled Aggregate Concrete. *Resour., Conservation and*
666 *Recycling*, Volume 171, p. 105565, <https://doi.org/10.1016/j.resconrec.2021.105565>.
- 667 [47] Alqarni, A. S., Abbas, H., Al-Shwikh, K. M. & Al-Salloum, Y. A., 2021.
668 Treatment of recycled concrete aggregate to enhance concrete performance.
669 *Construction and Build. Mater.*, Volume 307, p. 124960,
670 <https://doi.org/10.1016/j.conbuildmat.2021.124960>.
- 671 [48] Lei, B., Li, W., Tang, Z., Li, Z., & Tam, V., 2020. Effects of environmental
672 actions, recycled aggregate quality and modification treatments on durability
673 performance of recycled concrete. *Journal of Materials Research and Technology*,
674 9(6), 13375-13389. doi:<https://doi.org/10.1016/j.jmrt.2020.09.073>
- 675 [49] Lei, B., Wngui, L., Zhiyo, L., Vivian, T., Wenkui, D., & Kejin, W., 2020.
676 Performance Enhancement of Permeable Asphalt Mixtures with Recycled Aggregate
677 for Concrete Pavement Application. *Frontiers in Materials*, 7, 1-16.
678 doi:[10.3389/fmats.2020.00253](https://doi.org/10.3389/fmats.2020.00253)

- 679 [50] Kukadia, V., Parekh, D. & Gajar, R., 2017. Influence of Aggregate's
680 Treatment on Properties of Recycled Aggregate Concrete. *International Journal of*
681 *Civil Eng. and Tech. (IJCIET)*, 8(3), pp. 351-361.
- 682 [51] Sarvanakumar, P., Neelakanatan, T. & Jagan, S., 2021. Mechanical properties
683 of recycled aggregate treated by variation in mixing approaches. *Construction*
684 *Magazine*, 20(2), pp. 236-248.
- 685 [52] Jagan, S., Neelakantan, T. & Saravanakumar, P., 2021. Mechanical properties
686 of recycled aggregate concrete surface treated by variation in mixing approaches.
687 *Journal of Construction*, 20(2), pp. 236-249. [http://doi.org/10.1108/wje-02-2021-](http://doi.org/10.1108/wje-02-2021-0089)
688 0089
- 689 [53] Limbachiya, M., Meddah, M. & Ouchagour, Y., 2012. Use of recycled
690 concrete aggregate in fly-ash concrete. *Construction and Build. Mater.*, Volume 27,
691 pp. 439-449, <https://doi.org/10.1016/j.conbuildmat.2011.07.023>.
- 692 [54] Majhi, R., Nayak, A. & Mukharjee, B., 2018. Development of sustainable
693 concrete using recycled coarse aggregate and ground granulated blast furnace slag.
694 *Construction and Build. Mater.*, Volume 159, pp. 417-430,
695 <https://doi.org/10.1016/j.conbuildmat.2017.10.118>.
- 696 [55] Ahmed, W. & Lim, C., 2021. Coupling effect assessment of vacuum based
697 pozzolana slurry encrusted recycled aggregate and basalt fiber on mechanical
698 performance of fiber reinforced concrete. *Construction and Build. Mater.*, Volume
699 300, p. 124032, <https://doi.org/10.1016/j.conbuildmat.2021.124032>.
- 700 [56] Belen, G., Fernando, M., Diego, C. & Sindy, S., 2011. Stress-strain
701 relationship in axial compression for concrete using recycled saturated coarse
702 aggregate. *Construction and Build. Mater.*, Volume 25, pp. 2335-2342,
703 <https://doi.org/10.1016/j.conbuildmat.2010.11.031>.

704

705

706

DURABILITY AND MICROSTRUCTURAL ANALYSES OF CONCRETE PRODUCED WITH TREATED DEMOLITION WASTE AGGREGATES

Qusai Al-Waked^{1,2}, Jiping Bai¹, John Kinuthia¹, Paul Davies¹

¹ Faculty of Computing, Engineering and Science, University of South Wales, Treforest
Campus, CF37 1DL, UK

² Corresponding author

ABSTRACT

The incorporation of recycled aggregate (RA) from the construction and demolition waste (C&DW) in civil engineering applications has become a hot research topic worldwide due to the associated environmental benefits of its application. Nonetheless, the poor quality of RA reduced its attraction to be utilized widely in the construction industry. This research examined the effects of soaking RA in cement-pulverized fuel ash-silica fume method (SCP), sand envelope mixing approach (SE), and bi-combination of SCP+SE on the water absorption, resistance to freeze-thaw, and sulphate resistance of recycled aggregate concrete (RAC). This study also investigated the microstructure of the enhanced RACs using scan electron microscopy (SEM) images to validate the experimental results. In addition, a detailed cost analysis of the different enhancement methods utilized in this study was carried out. The enhanced RACs demonstrated improved durability performance which was confirmed by the SEM images. This was ascribed to the strengthened interfacial transition zone, strengthened adhered mortar, better overall interlocking of the treated RA with the new cement paste, filled-up pores and micro-cracks, reduced porosity, and compacted denser microstructure. The outcome of this study would be in a great benefit to researchers, RA producers, design engineers, and stockholders to get a better knowledge on the durability property of RAC produced with 100% treated RA, and thus promote the use of RA in the construction industry.

Keywords: Recycled aggregate, Freeze-thaw, Sulphate attack, Microstructure, Scanning electron microscopy (SEM), cost analysis.

1. Introduction

The activities of the construction industry generate large amounts of waste. In numerous countries, the amount of construction and demolition waste (C&DW) generated is rapidly increasing every year [1]. The dumping and landfilling of C&DW have rapidly led to a series of issues for the environment because C&DW may contain hazardous materials [2]. Although several countries recycle around 80% of C&DW such as Japan, the Netherlands, and Germany, there are some developing countries with an average recycling rate of 20% to 40% [3]. Accordingly, promoting the use of recycled aggregate (RA) from the C&DW into new concrete as a replacement for natural aggregate (NA) is an essential priority. This would lead to a reduction in carbon dioxide emissions and contribute significantly towards preserving the environment by minimizing the depletion of natural resources, thus leading to a sustainable and green future [4].

Nonetheless, the poor quality of RA in terms of its engineering properties has limited its use to non-structural applications such as road bases, blinding concretes, and footpaths [5]. Extensive studies on the effects of RA on concrete properties showed that as the substitution level of RA increases the following changes to concrete properties were reported, reduction in consistency

43 [6], decreased density [7], increase in permeability [8], poor chloride ion permeability [9], low
44 resistance to acid and sulfate attack [9], reduction in mechanical properties [7], and decrease
45 in elastic modulus [10]. Bahraq et al. [9] stated that the presence of the adhered mortar on RA
46 surface is the main key affecting factor that leads to higher water absorption, lower specific
47 gravity, and higher Los Angeles abrasion mass loss, compared to NA.

48 Durability of concrete can be defined as its ability to withstand various types of damage under
49 exposure to the surrounding environment while maintaining its strength and appearance for its
50 designed service period [11]. The high water absorption of RA and the presence of adhered
51 mortar on the RA surface usually lead to weaker durability performance of recycled aggregate
52 concrete (RAC) compared to natural aggregate concrete (NAC). In view of this, research to
53 enhance the quality of RA and the engineering performance of RAC has been extensively
54 conducted over the past few decades [12, 13].

55 The enhancement methods used to enhance RA and RAC by different researchers can be
56 categorized into three main methods, removing the adhered mortar, strengthening the adhered
57 mortar, and improving the whole matrix of the RAC. Removing the adhered mortar can include
58 treatments such as mechanical grinding [13], presoaking in acid solution [12], and ultrasonic
59 water cleaning [14]. Although these methods can offer great enhancement to the quality of RA,
60 they may result in adverse effects on the RA. For instance, mechanical grinding could result in
61 micro-cracks on the RA surface during the treatment process [13].

62 On the other hand, treatment techniques involving strengthening the adhered mortar might be
63 of greater benefit compared to removing the adhered mortar. Strengthening the adhered mortar
64 may include treatment techniques such as surface coating RA with pozzolan slurry [15],
65 calcium carbonate biodeposition [16], soaking RA in sodium silicate solution [17], soaking RA
66 in cement-pozzolan solution [18], and accelerated carbonation [19].

67 Improving the whole matrix of RAC can include methods such as batching techniques which
68 are modified batching procedures that generally aim at limiting the amount of mixing water
69 that is absorbed by RA during mixing. A few of these methods include stone envelope with
70 pozzolanic powder [20], two-stage mixing technique [21], sand enveloped mixing approach
71 [22], and mortar mixing approach [22].

72 **2. Research Significance**

73 Although the literature holds a large number of studies on the effects of different enhancement
74 methods on RA and RAC properties, the structural application of RAC is still limited due to
75 the inferior durability properties of RAC [23]. The literature also showed scant studies are
76 available on the effects of different treatment methods on the durability properties of RAC. The
77 vast majority of the studies in the literature focused on recycled concrete aggregate rather than
78 RA from the C&DW.

79 The quality of RA plays an important role in altering the mechanical and durability properties
80 of RAC. To this end, this research aims at evaluating the performance of three enhancement
81 methods, soaking RA in cement-pulverized fuel ash-silica fume solution (SCP), sand envelope
82 mixing approach (SE), and bi-combination of these two methods, on enhancing the durability
83 of RAC including, water absorption, resistance to freezing-thawing, and to sulphate attack.

84 The solution design of the SCP treatment was selected based on the optimal performance of
85 different solutions investigated in the previous study of Al-Waked et al. [24]. Furthermore, the

86 literature showed limited studies on the effects of SE batching technique and bi-combination
87 of SCP and SE method on the durability properties of concrete produced with 100% RA from
88 construction and demolition waste.

89 This study also includes microstructural analyses using Scan Electron Microscopy (SEM)
90 images to report any changes to the microstructure of RAC after the application of these
91 enhancement methods. In addition, a comprehensive analysis of cost and other influencing
92 factors is provided in this study for comparison purposes. Accordingly, it is anticipated that
93 this study would undoubtedly enrich the literature and provide better understanding of the
94 durability performance of enhanced RAC with the overall aim of expanding the application of
95 RA in the construction industry.

96 **3. Materials characteristics**

97 *3.1 Aggregates*

98 20/10 mm and 10/4 mm crushed limestone aggregates (NA) were utilized throughout this study
99 (Figure 1a). NA conforming BS EN 12620:2002+A1: 2008 [25] was supplied from Jewson UK
100 Caerphilly, South Wales, UK. The recycled aggregates (RA) (Figure 1b) used were a mix of
101 construction and demolition waste with a clean size range of 20/10 mm and 10/4 mm
102 confirming BS EN 13242: 2013 [26] and were processed in accordance with WRAP quality
103 protocol [27]. The RA were supplied by Derwen Group, Neath Abbey, UK. RA consisted of
104 different construction materials, brick, glass, bituminous, rounded stones, and recycled
105 concrete aggregate. Table 1 shows the compositions of RA in accordance with BS 8500-2:
106 2015+A2: 2019 [28]. The mechanical and physical properties of the NA and RA are provided
107 in Table 2, while the particle size distribution of NA and RA in accordance with BS EN 933-
108 1:2012 [29] is shown in Figure 2.

109 As can be observed in Table 2, untreated RA showed inferior characteristics compared to NA
110 due to the presence of the adhered mortar [23]. Nevertheless, treated RA with cement-PFA+SF
111 solution showed enhanced Aggregate Impact Value (AIV) and Water Absorption (WA). For
112 instance, the AIV was reduced by 13% while the WA was reduced by 54%. This can be
113 attributed to the filling and sealing effect of the pozzolan used in the treatment [24].

114 It is thought that the source of RA plays a vital role in the quality of RA. For instance, Munir
115 et al. [30] investigated different characteristics of RA with 5% impurities (i.e., glass, asphalt,
116 bricks, and ceramic) and found that the WA of RA is 6.85% and the crushing value was 31%.
117 Munir et al. [30] also stressed that the treatment methods utilized such as carbonation treatment
118 directly affects the water absorption property of RA through effectively filling or sealing the
119 voids and pores on RA surface.

120 On the other hand, the crushing value or the impact value of RA is mainly controlled by several
121 aspects, such as the strength of the parent concrete (source), and the type of crusher used on
122 site [30]. Accordingly, this can explain the higher enhancement observed in the WA compared
123 to the AIV after the treatment utilized in the current study.

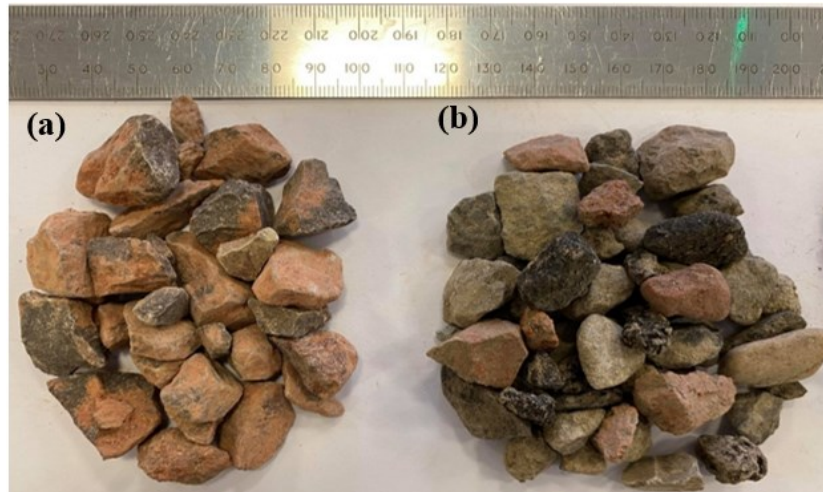


Figure 1: Coarse aggregates used in this study (a) coarse natural aggregate, (b) coarse recycled aggregate

124
125
126

Table 1: Compositions of recycled aggregates in this study (BS 8500-2:2015 +A2: 2019)

	R_c (%)	R_u (%)	R_b (%)	R_g (%)	R_a (%)	X (%)
Sample 1	49.14	29.47	12.51	0.17	8.38	0.34
Sample 2	47.5	28.06	11.5	1.12	11.00	0.48
Sample 3	50.6	25.8	13.4	0.00	9.5	0.37
BS limits	–	–	–	–	≤10%	≤1%
Mean	49.08	27.78	12.47	0.42	9.6	0.39

Notes: R_c - cement-based products, R_u - unbounded aggregates and/or natural stones, R_b - clay masonry units i.e., bricks and tiles, calcium silicate masonry unit, R_a - bituminous materials, and X - miscellaneous materials and/or non-floating wood, plastic, and rubber, R_g - crushed glass.

Table 2: Characteristics of the RA compared with NA and relevant BS EN standards

Characteristic	NA	RA	TRA	BS limits	Standard
Flakiness Index (%)	18	27	–	< 40	BS EN 933-3:2012 [31]
Shape Index (%)	12	18	–	< 55	BS EN 933-4:2008 [32]
Water Absorption (%)	1.5	6.1	3	< 8	BS EN 1097-6:2013 [33]
Density kg/m ³	2480	2120	–	–	BS EN 1097-6:2013 [33]
Impact Value (%)	14	17	14.7	< 32	BS EN 1097-2:2020 [34]
LA (%)	18	26	–	< 50	BS EN 1097-2: 2020 [34]

Note, TRA – treated RA by soaking in cement-PFA+SF solution

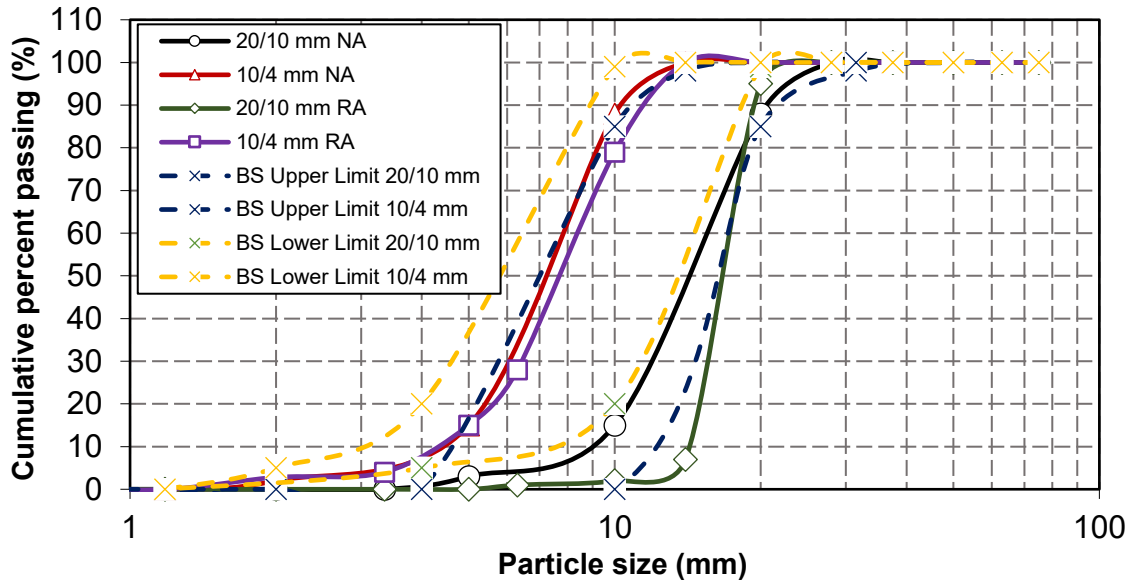


Figure 2: Particle size distribution of coarse RA and coarse NA (BS EN 933-1:2012)

133
134

135 3.2 Portland cement

136 A commercially available Portland cement (CEM I-42.5 N) conforming BS EN 197-1: 2011
137 [35] was used throughout this study. The CEM I was also supplied from Jewson UK limited,
138 Caerphilly, South Wales, UK. The oxide and physical composition of CEM I are provided in
139 Table 3.

140 3.3 Pozzolan

141 The pulverized fuel ash (PFA) used throughout this study compliant with BS EN 450-1:2012
142 [36] was sourced from a local supplier. Un-densified silica fume (SF) with a commercial code
143 971U and 97.1% purity conforming BS EN 13263-2:2005+A1:2009 [37] was used throughout
144 this study. It was manufactured by Elkem Silicon Materials, Norway.

145 Table 3: Oxide compositions and physical properties of powder materials used throughout
146 this study

Oxide	Composition by (wt%)		
	PC	SF	PFA
CaO	61.49	–	0.22
SiO ₂	18.84	97.1	59.04
Al ₂ O ₃	4.77	0.1	34.08
Fe ₂ O ₃	2.87	0.2	2.00
SO ₃	3.12	0.06	0.05
Na ₂ O	0.02	–	1.26
	Physical properties		
Colour	Grey	Dark Grey	Light Grey
Bulk density (kg/m ³)	1400	120-220	800-1000
Specific gravity (Mg/m ³)	3.16	2.20	2.90

147 **4. Experimental program**

148 **4.1 Enhancement methods**

149 *4.1.1 Soaking RA in cement-PFA+SF solution (SCP)*

150 The recycled aggregates were treated by soaking in Portland cement - pulverized fuel ash -
151 silica fume solution. These pozzolan materials were selected to fulfil the environmental and
152 economic criteria. The solution was prepared by mixing the raw materials with water for
153 several minutes (see Table 4). Then the recycled aggregates were added to the solution and
154 soaked for 4 hrs at a 10% concentration level. Thereafter, the recycled aggregates were
155 removed from the solution bath and let to drain for 10 min and then air-dried at room
156 temperature for 24 hrs prior to casting. The design of the solution compositions, selection of
157 soaking time, and concentration level were based on several trial formulations of solutions with
158 different concentration levels. Four hours of soaking time and 10% solution concentration level
159 were found to be optimal.

160 Table 4: Proportions of treatment solution for 1000g of RA

Treatment solution	Binder (g)			RA (g)	Water (g)	Concentration level (binder to water ratio)
	PC	PFA	SF			
PC - PFA+SF	80	60	60	1000	2000	10%

161 *4.1.2 Sand envelope mixing approach (SE)*

162 The sand was firstly mixed with 75% of the mixing water for 30 seconds, cement was then
163 added to the mixture and mixed for 45 seconds. Thereafter, the untreated recycled aggregate
164 were added to the mixture with the rest of the mixing water and mixed for 90 seconds. This
165 technique aimed at minimizing the amount of mixing water to be absorbed by RA during
166 mixing.

167 *4.1.3 Bi-combination of SCP + SE*

168 The untreated RA were firstly dried to constant mass and then soaked in the pre-prepared
169 cement-SF+PFA solution for 4 hrs, and then air-dried at room temperature for 3 days.
170 Thereafter, the treated RA were incorporated into the mixing design of RAC and mixed using
171 sand envelope batching technique.

172 **4.2 Concrete mix design**

173 Table 5 shows concrete mix proportions produced with the enhancement methods utilized at
174 three different water to cement ratios, 0.4, 0.5, and 0.6.

175

176

177
178

Table 5: Concrete mix proportion for various RAC produced with different enhancement methods

Specimen designation	PC (kg/m ³)	Water (kg/m ³)	w/c ratio	NA (kg/m ³)	RA (kg/m ³)	FA (kg/m ³)	Mixing method	Notes
W040/NAC1	450	180	0.4	1257	0	677	NMA	NAC (control 1)
W040/RAC2	450	180	0.4	0	1257	677	NMA	Un-treated RAC (control 2)
W040/SCP	450	180	0.4	0	1257	677	NMA	Soaking RA in PC-SF+FA solution
W040/SE	450	180	0.4	0	1257	677	SE	Untreated RA
W040/SCP+SE	450	180	0.4	0	1257	677	SE	Soaking RA in PC-SF+FA solution
W050/NAC1	350	175	0.5	1257	0	677	NMA	NAC (control 1)
W050/RAC2	350	175	0.5	0	1257	677	NMA	Un-treated RAC (control 2)
W050/SCP	350	175	0.5	0	1257	677	NMA	Soaking RA in PC-SF+FA solution
W050/SE	350	175	0.5	0	1257	677	SE	Untreated RA
W050/SCP+SE	350	175	0.5	0	1257	677	SE	Soaking RA in PC-SF+FA solution
W060/NAC1	250	150	0.6	1257	0	677	NMA	NAC (control 1)
W060/RAC2	250	150	0.6	0	1257	677	NMA	Un-treated RAC (control 2)
W060/SCP	250	150	0.6	0	1257	677	NMA	Soaking RA in PC-SF+FA solution
W060/SE	250	150	0.6	0	1257	677	SE	Untreated RA
W060/SCP+SE	250	150	0.6	0	1257	677	SE	Soaking RA in PC-SF+FA solution

179
180

NMA – normal mixing approach/ conventional mixing, SE – sand envelope mixing approach, FA – fine aggregate, NA – natural aggregate, NAC – natural aggregate concrete.

181 4.3 Specimens Preparation & Testing of Concrete

182 Cube test specimens of dimension of (100 mm × 100 mm × 100 mm) were utilized in the
183 production of all the concrete. The test specimens were prepared in accordance with BS EN
184 206:2013+A1:2016 [38]. The de-moulding of the test specimens was carried out after 24 hrs
185 of casting at room temperature, and curing done in accordance with BS EN 12390-2:2019 [39].

186 The assessment of the durability performance of the concrete in terms of resistance to freeze-
187 thaw was carried out in a Prior Clave chamber LCH/600/25 model of 0.7m³ volume capacity,
188 in accordance with PD CEN/TS 12390-9:2016 [40]. The test hardened concrete cube specimens
189 were firstly left in the freezing chamber for seven days at -17°C temperature and then thawed
190 for 1 hr in a controlled temperature water bath set at 20 ± 2°C. This cycle of freezing and
191 thawing was repeated 20 times while the weight change was recorded after each cycle, and the
192 compressive strength loss recorded after 4 and 20 cycles.

193 Water absorption was carried out in accordance with BS 1881-122:2011+A1:2020 [41].
194 Testing for sulphate attack involved the concrete test specimens being first cured in a water
195 bath at a controlled temperature of 20±2 °C for 7 days. Seawater saline solution was selected
196 for concrete specimen immersion. The immersion was carried out in lidded plastic containers
197 in accordance with BS EN 206:2013+A2: 2021 [42].

198 After 7 days of water curing, the concrete specimens were removed and placed into the lidded
199 container for sulphate attack investigations. A visual inspection was undertaken to report any
200 scaling, spalling, cracking, or chipping that occurred to any of the concrete specimens after
201 freeze-thaw and sulphate attack tests. The microstructure investigation was carried out Using
202 a MIRA3 TESCAN Scanning Electron Microscope (SEM), fitted with a Solid-state
203 Backscattered (electron) Detector (SBD).

204

205

206

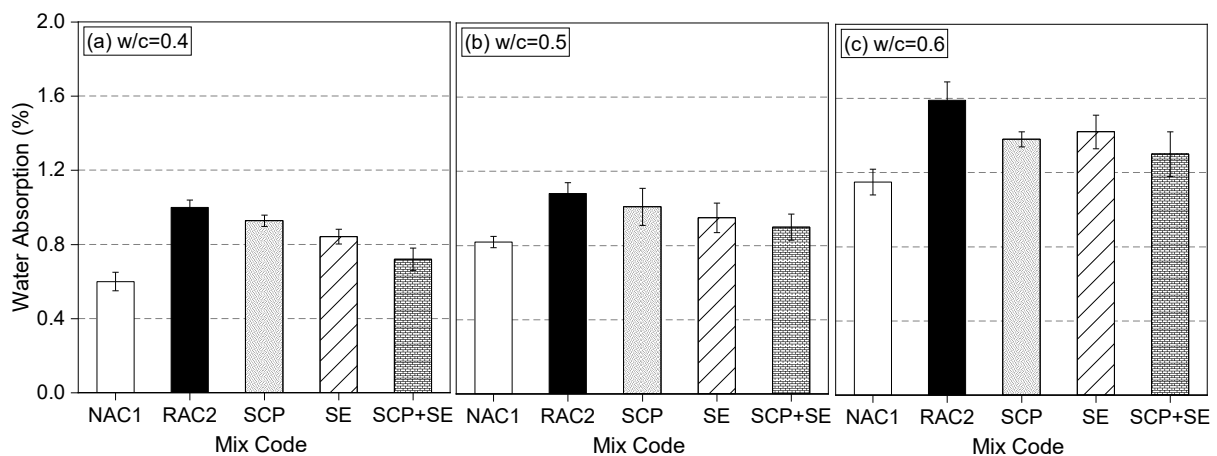
207 5. Results and discussion

208 5.1 Effects of SCP and SE on water absorption of RACs

209 Figures 3 shows the results of the water absorption of the treated RACs in comparison with
210 untreated RAC2 and NAC1 mixes, at 0.4, 0.5, and 0.6 w/c ratios. As a general trend for all the
211 test concretes specimens, the lower the w/c ratio the lower was the water absorption.

212 NAC1 mixes recorded the lowest water absorption values across all the test concrete mix
213 specimens, at all w/c ratios, whilst RAC2 mixes exhibited the highest water absorption values
214 at all w/c ratios. It can also be seen that all the treatment methods varied in the enhancement of
215 the water absorption of RAC.

216 The bi-combination of soaking RA in cement-PFA+SF prior to mixing and batching using the
217 sand envelope mixing approach, presented in SCP+SE mixes, produced the highest
218 enhancement in water absorption.



219

220 Figure 3: Results of the water absorption of the treated RACs in comparison with RAC2 and
221 NAC1

222 The water absorption of a given test concrete specimen reflects on its porosity state, hence the
223 higher the porosity of concrete, the higher its water absorption property [43]. The water
224 absorption for all the designed concrete in general increased with an increase in w/c ratio. This
225 is mainly ascribed to the increased pores and voids and lesser dense microstructure of lower
226 strength concrete. This is in line with the work of Thomas et al. [44] who stated that higher-
227 strength concrete tends to show lower water absorption compared to concrete of lower-strength.
228 According to Lotfi et al. [45], designing concrete with a low water/cement ratio and higher
229 cement content reduces the capillary voids, and thus a reduction in the water absorption can be
230 achieved. The current test results showed higher water absorption of the untreated RAC2 mixes
231 compared to NAC1 mixes, this is because of the porous nature of RA given to the attached

232 adhered mortar around the RA surface which consists of micro-cracks and pores that are
233 formed during the preparation of RA.

234 Similar observations were given in the study of Debieb et al. [46] who argued that the water
235 absorption of RAC is significantly lower than that of NAC by 0.4% to 0.6%. Kwan et al. [47]
236 stated that due to the porous nature of RA and the developed micro-cracks during the crushing
237 process, its incorporation in concrete significantly increases the permeability.

238 Lotfi et al. [45] stated that the adverse effects of RA on the high water absorption of the RAC
239 can be mitigated by utilizing lower water to binder ratio. Tam & Tam [48] stressed that mixing
240 RAC using batching approach increase the RAC resistance to water absorption due to the
241 reduced water absorption. In this study, the enhanced water absorption by SE mixes using the
242 SE method (sand enveloped mixing approach) can be ascribed to the process of the SE mixing
243 approach, in which the RA is covered with premixed cement/ mortar slurry that filled up the
244 cracks and pores of RAC, hence enhancing its resistance to water absorption [49].

245 The enhanced water absorption provided by the SCP mixes (soaking RA in cement-PFA+SF
246 solution) can be explained by the formation of a thin coated pozzolanic layer that blocked the
247 pores and micro-cracks, thus enhancing the ITZ of RA, and lowering the porosity of RAC [21].

248 **5.2 Effects of SCP and SE on resistance to freeze-thaw cycles of RACs**

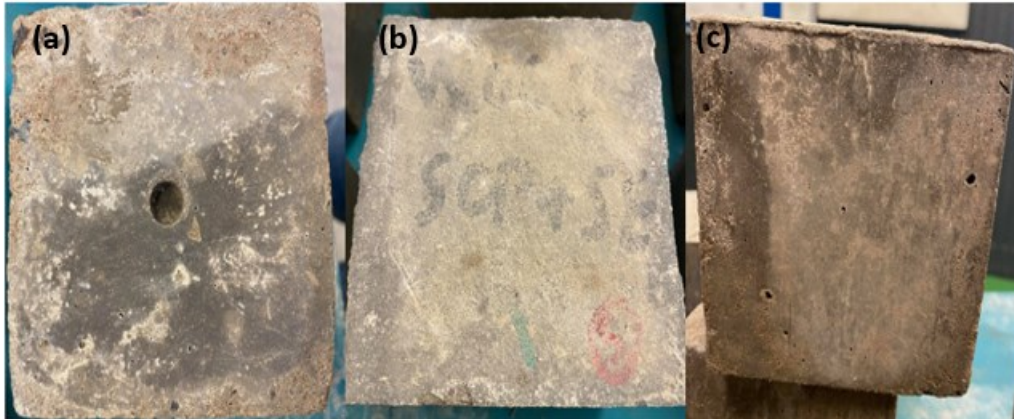
249 **5.2.1 Visual inspection**

250 Table 6 shows the description of defect/damage endured by the different concrete mixes after
251 visual inspection after the freezing and thawing repeated cycles. Figure 4 shows some of the
252 test specimens after 20 successive freeze-thaw cycles. As a general trend, the visual inspection
253 showed the damage/ defect phenomena of the RAC2 specimens were similar to those of the
254 NAC1 specimens, but the extent and degree of the damage were different. At the end of the
255 20th freeze-thaw cycle, all the concrete specimens experienced chipping and scaling, the
256 intensity of chipping and scaling was being more prominent with increase in w/c ratio and
257 increase in freeze-thaw cycles.

258 Table 6: Description of the visual inspection of damage/defects endured by the different
259 concrete cube specimens during and at the end of the freeze and thaw cycles

Description of Damage	Visual Remarks
Fractures	No fractures were encountered for all the concrete specimens investigated after the end of the 20 th freeze-thaw cycle.
Scaling/ Peeling	Minimal scaling was observed on all the NAC1 specimens during and after the end of the freeze-thaw cycles. RAC2 specimens exhibited prominent scaling after the 8 th freeze-thaw cycle. The treated RAC specimens experienced minor to medium scaling on all the concrete cubes faces during the freeze-thaw cycles.
Hairline Cracks <0.2mm	No hairline cracks were noticed on any of the concrete test specimens throughout the freeze-thaw cycles.
Surface Crack >0.2mm	No surface cracks were observed on any of the concrete specimens throughout the freeze-thaw cycles up to 20 cycles.
Chipping	Chipping of concrete edges was observed on all the concrete specimens throughout the freeze-thaw cycles. Minor chippings were observed on the NAC1 specimens, whilst the RAC2 specimen exhibited prominent chippings along its edges. Treated

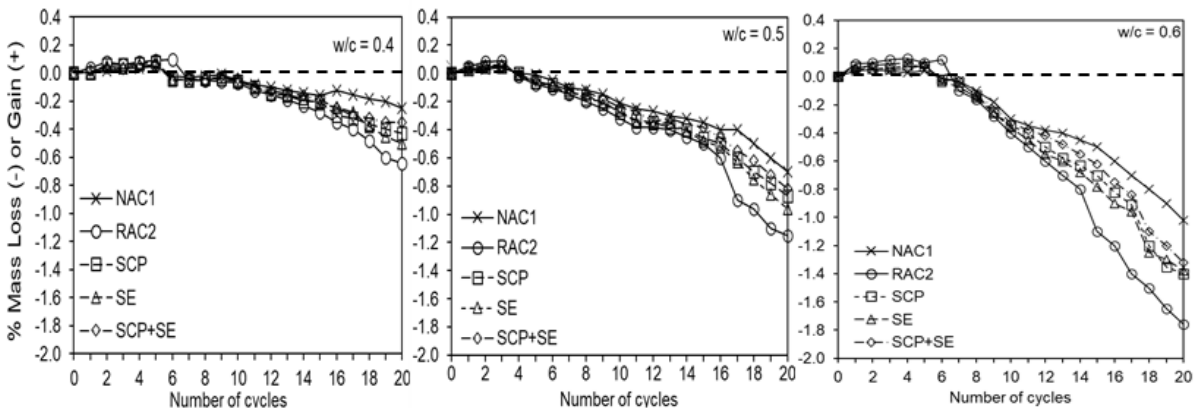
	RAC specimens showed somewhat minor chippings along the edges throughout the freeze-thaw cycles.
Craters	Visual inspections showed no craters in any of the concrete specimens throughout the freeze-thaw cycles.
Major Spalling/ Delamination	Observations showed no major spalling nor delamination occurred on any of the concrete specimens during the freeze-thaw cycles.



260
261 Figure 4: Concrete cube test specimens after 20 successive freeze-thaw cycles, (a) RAC2
262 specimen, (b) SCP+SE specimen, (c) NAC1 specimen

263 **5.2.2 Mass change due to freeze-thaw cycles**

264 A typical profile of the effects of freezing and the thawing cycles on the mass change of the
265 NAC1, RAC2 and the enhanced RAC specimens is shown in Figure 5.



266
267 Figure 5: Mass change (Loss or gain) due to freeze-thaw cycles

268 At the start of the freezing and thawing cycles, all the concrete specimens showed mass gain
269 regardless of the w/c ratio, with no further mass gain after the 4th and 6th cycles. This can be
270 explained by the filling of the enclosed pores with water within the concrete matrix caused by
271 the freezing action of water. At the end of the 6th cycle, the highest mass gain was observed for
272 RAC2 specimens across all the concrete specimens, whilst the lowest recorded mass gain was
273 for the NAC1 specimens. This is in line with the study of Salem et al. [50] who stated that the

274 higher mass gain of the untreated RAC2 specimens at the start of the freeze-thaw cycles can
 275 be ascribed to the penetrated water into the inner cracks and pores of the RAC after exposure
 276 to freeze-thaw filling all the pores and interfacial transition zone (ITZ). The enhanced RAC
 277 specimens given in SCP, SE, and SCP+SE mixes showed reductions in mass gain compared to
 278 the RAC2 specimens. This can be ascribed to the enhanced water absorption of RAC after these
 279 enhancement methods.

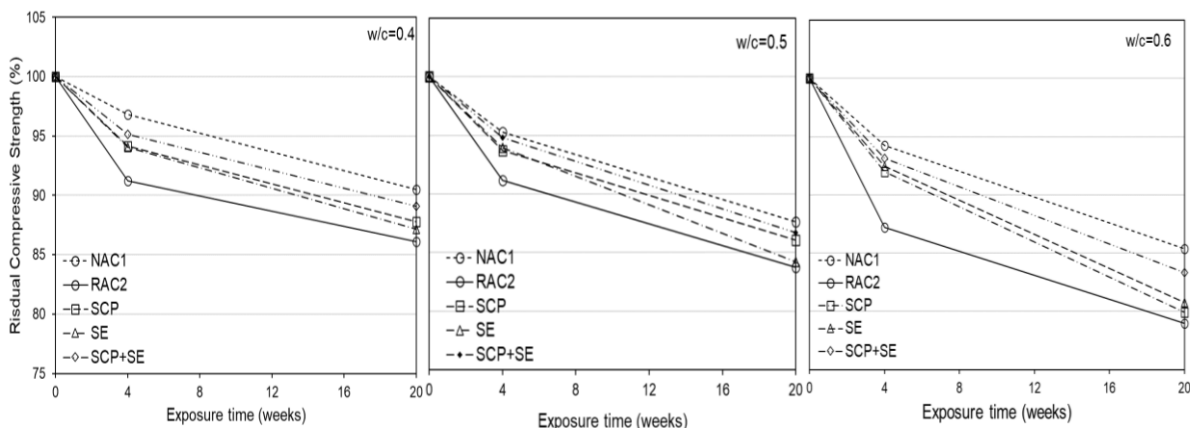
280 A general trend of mass loss occurred after around 4 to 6 freeze-thaw cycles for all the concrete
 281 specimens, and the degree of the mass loss increased with increase in w/c ratio and increased
 282 in the freezing and thawing cycles. This is attributed to the higher number of capillary pores,
 283 average aperture and porosity of higher w/c ratios. The NAC1 specimens recorded the lowest
 284 mass loss across all the concrete specimens after the end of the 20th freezing and thawing cycles.
 285 Whereas the RAC2 specimens experienced the highest mass loss.

286 This is mainly attributed to the high water absorption of RA which can drain into the cement
 287 paste and then lead to more intense frost damage. The absorbed water within the concrete
 288 matrix gets frozen upon exposure to freeze-thaw cycles, leading to internal cracks and pressure,
 289 hence resulting in the spalling of mortar and loss of mass [51]. Wu et al. [52] concluded that
 290 the RAC specimens endured lower resistance to freeze and thaw cycles in terms of mass loss,
 291 compared to NAC specimens due to internal cracks developed and pressure endured. This is
 292 also in line with the work of Kazmi et al. [51] who stated that the higher mass loss for RAC
 293 specimens is ascribed to the additional pores of RAC compared to NAC, which results in a rise
 294 in the water ingress through these pores leading to further internal pressure and micro-cracks
 295 of RAC.

296 All the treated RAC specimens showed a reduction in mass loss compared to RAC2 mixes.
 297 Among all the treated RAC specimens, the SCP+SE mixes showed the lowest mass loss. This
 298 is mainly attributed to the strengthening of the attached adhered mortar via these treatments,
 299 which resulted in reduced porosity, lesser cracks and denser microstructure of the enhanced
 300 RAC specimens [51]. It should be noted that scant studies are available on the effects of
 301 treatment methods on the resistance to freeze-thaw of RAC.

302 5.2.3 Strength loss due to freeze-thaw cycles

303 Figure 6 shows the effects of freezing and thawing cycles on the compressive strength of the
 304 NAC1 specimens, RAC2 specimens and the treated RAC specimens at 4 weeks and 20 weeks.



305
 306 Figure 6: Residual compressive strength of the different concretes at 4 weeks and 20 weeks
 307 due to freeze-thaw cycles, (a) w/c ratio of 0.4, (b) w/c ratio of 0.5, and (c) w/c ratio of 0.6

308 Observations showed a general trend of strength loss across all the concrete specimens after 4
309 weeks of freeze-thaw cycles. The strength loss was more prominent in higher w/c ratio concrete
310 mixes and at higher freeze-thaw cycles. According to Kisku et al. [53], the phenomenon of
311 concrete strength loss during freeze-thaw cycles is attributed to the exposure of concrete to
312 frost action before the development of desirable strength, the occurred expansion is associated
313 with the formation of ice which leads to disruption and hence, irreparable strength loss. At the
314 end of the 20th freezing and thawing cycles, all the concrete specimens endured higher
315 compressive strength loss compared to the 4 weeks strength loss.

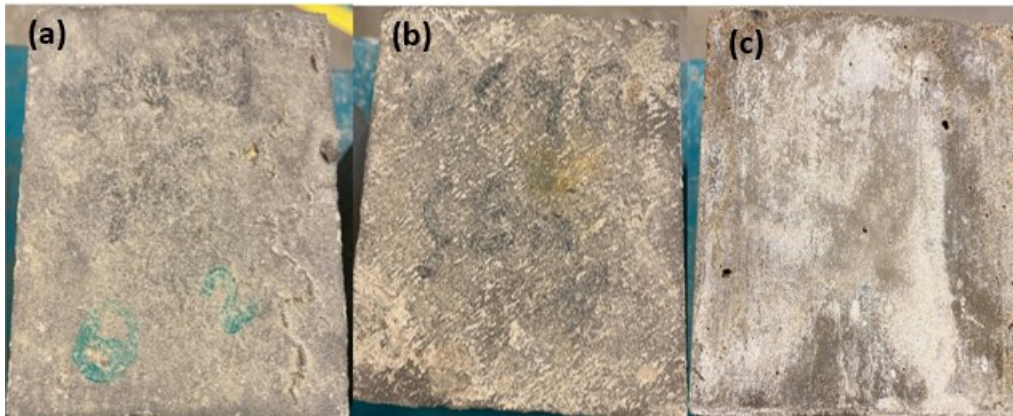
316 The highest strength losses at the end of the freezing and thawing cycles were exhibited by the
317 RAC2 specimens. All the treated RAC specimens were able to minimize the strength losses of
318 the untreated RAC. The best-performed treatment in terms of enhancing the frost resistance of
319 untreated RAC was for the SCP+SE mixes. The higher reduction observed in the strength of
320 the RAC specimen is mainly ascribed to the inner cracks evolved in the cement paste and the
321 ITZ, which loosened the paste and weakened the bond between the aggregates and the cement
322 paste. Kazmi et al. [51] stated that the higher strength loss in RAC compared to NAC after
323 freezing and thawing cycles could be the results of many factors, i.e., higher water absorption
324 of RA, mineralogical types of aggregates, higher porosity of RAC, w/c ratio, and air content.

325 The improved frost resistance of the SCP mixes is mainly attributed to the formation of a thin
326 coating film of pozzolanic powder around the RA surface that occupied all the pores and
327 reduced the high water absorption of RA [23]. The reduction in strength and mass loss of the
328 SE mixes can be ascribed to the use of this batching technique (SE) which stems from allowing
329 the sand particles in the mixture to mix more readily with water and cement, thus reducing the
330 water absorbed by the RA. This is in line with the work of Liang et al. [25] who reported
331 improved properties of the untreated RAC after using the SE mixing method.

332 **5.3 Effects of SCP and SE on sulphate resistance of RACs**

333 **5.3.1 Visual inspection**

334 Figure 7 shows some of the test specimens after 20 weeks of exposure to sulphate attack. The
335 results of the visual inspection for any physical change to the test specimens showed that there
336 were no observed changes in terms of expansion in dimension or any spalling in any of the test
337 specimens after immersing in sodium sulphate solution for 20 weeks. Crystallized salt and
338 efflorescence were observed covering the upper surface of the test specimens after exposure to
339 the sulphate environment. The degree of the crystallized salt was observed to increase with
340 increased time of immersion in a sulphate solution.



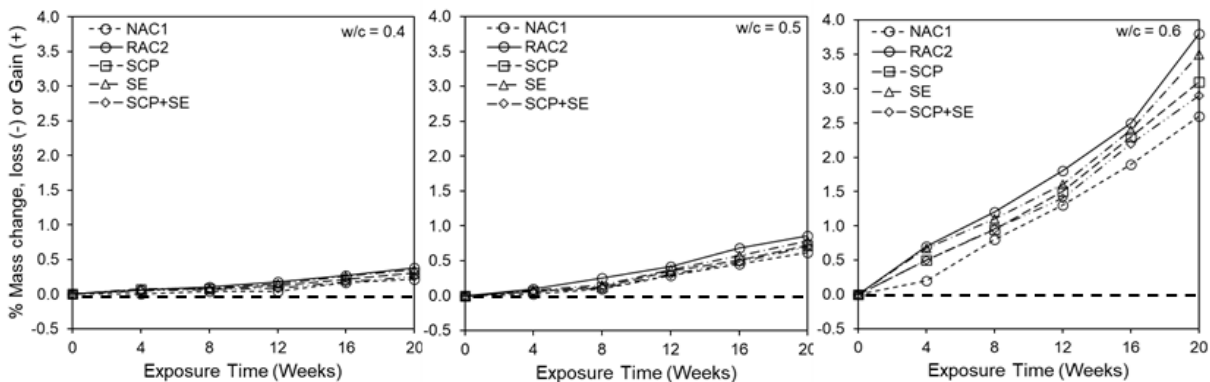
341

342 Figure 7: Some of the test specimens after 20 weeks of exposure to sulphate, (a) NAC1
 343 specimen, (b) SCP+SE specimen, (c) RAC2 specimen

344

345 **5.3.2 Mass change due to sulphate attack**

346 The results of the mass change rate of the NAC1, RAC2, SCP, SE, SCP+SE concrete specimens
 347 under sulphate attack for 20 weeks are shown in Figure 8.



348

349 Figure 8: Mass change (loss or gain) of the enhanced RACs due to sulphate attack

350 The results showed a general trend of mass increase for all the concrete specimens after
 351 exposure to sulphate solution at all w/c ratios. This is due to the formed ettringite within the
 352 concrete structure that causes internal stresses that leads to the loss of strength. Ettringite
 353 formed as the result of the occurred reaction between the hydrated cement products and the
 354 sulphate ions in the sulphate solutions, leading to the production of gypsum. This produced
 355 gypsum converts the tricalcium aluminate (C_3A) to ettringite [54,55]. It also can be indicated
 356 that an increase in w/c ratio and exposure time to sulphate attack resulted in a mass gain
 357 increase for all the concrete specimens. This can be explained as the concentration of sulphate
 358 within concrete structure increasing with time during exposure and decreasing with the depth
 359 of concrete. The decrease in sulphate content with depth of concrete is because sulphate ions
 360 need to transfer to the interior structure of the unsaturated concrete by either diffusion, capillary
 361 sorption, and penetration [56].

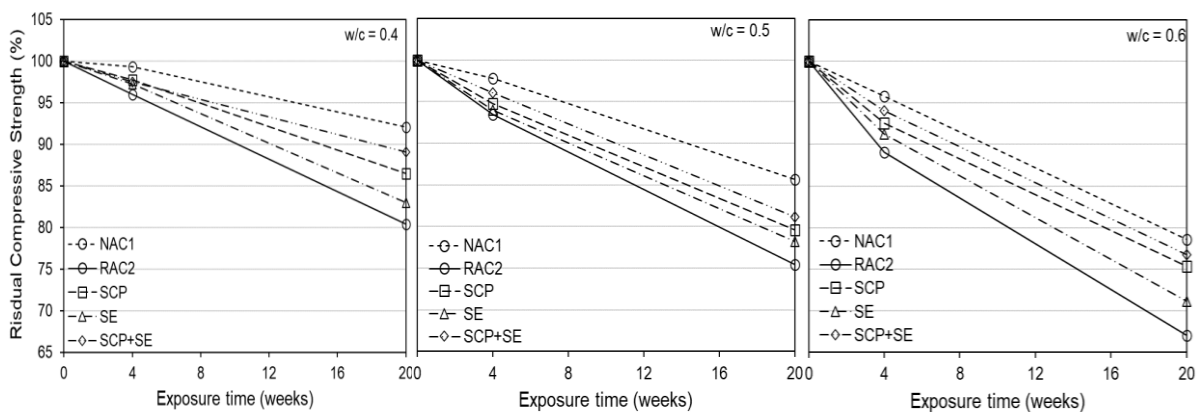
362 The growth rate of sulphate concentration by penetration through the micropores in the first 4
 363 weeks is low and slow because of the low water absorption of concrete, and then it increases
 364 with time, as the porosity of concrete decreases due to the occurred reaction between the
 365 sulphate ions and the hydrated cementitious products. The gypsum and ettringite formed in the
 366 micropores of concrete via this chemical reaction can delay the diffusion process during the
 367 first 4 weeks of sulphate exposure. Nonetheless, this diffusion process accelerates with time as
 368 a result of increased concrete porosity due to the generated micro-cracks because of the internal
 369 crystallisation pressure applied on the pore walls of concrete by the ettringite formed.
 370 Additionally, another reason that could accelerate the diffusion process is the leaching of
 371 calcium [57,58].

372 After 20 weeks of sulphate exposure, the NAC1 specimens exhibited the lowest mass gain
 373 across all the concrete specimens, whilst the untreated RAC2 specimens endured the highest
 374 mass gain. This can be ascribed to the poor quality of RA compared to NA. RA is porous in
 375 nature, hence it absorbed a significant amount of water during mixing. This resulted in higher
 376 porosity of concrete which in turn leads to higher penetration of sulphate ion. Thus, higher
 377 uptake of gypsum and greater formation of ettringite was obtained, and ultimately greater
 378 damage to sulphate attack. This is in line with the results of Xie et al. [59] study, which showed
 379 that the mass gain of RACs increased slightly up to 0.69% by 40 weeks of exposure to sulphate
 380 due to the ettringite and gypsum (expansion products) formed by the chemical reaction between
 381 the sulphate ions and the hydrated cement products

382 All the enhanced RACs showed a lesser gain in mass and enhanced sulphate resistance after
 383 20 weeks of exposure to sulphate, compared to the untreated RAC2 specimens. The enhanced
 384 sulphate resistance of the SCP specimens could be explained by the enhanced porosity due to
 385 the pozzolan coated layer formed around the RA surface that filled the micropores and the
 386 micro-cracks of RA. The enhanced resistance to sulphate attack of the SE specimens can be
 387 ascribed to the efficiency of the sand enveloped batching technique in reducing the water
 388 absorption of RA during mixing, and hence strengthening the whole matrix [60]. Similarly,
 389 Kazmi et al. [61] reported lesser mass gain for treated RACs compared with untreated RACs,
 390 after 10 weeks of sulphate exposure.

391 5.3.3 Strength loss due to sulphate attack

392 Figure 9 shows the residual compressive strength of the NAC1, the untreated RAC2, and the
 393 enhanced RACs after exposure to sulphate solution for up to 20 weeks.



394

395 Figure 9: Residual compressive strength of the treated RACs due to sulphate exposure

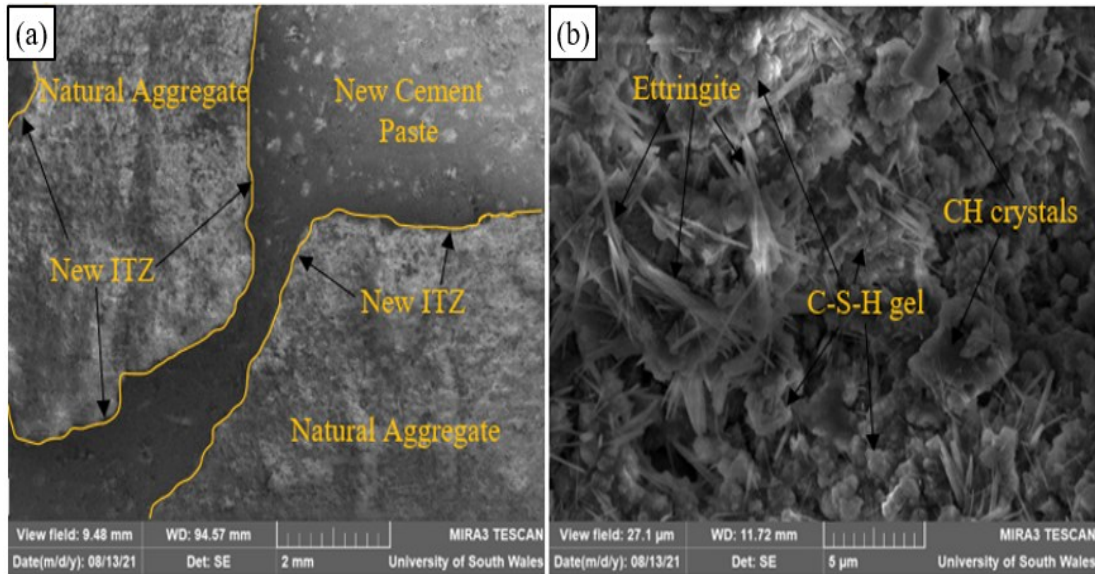
396 Overall, all the test concrete specimens endured compressive strength loss after exposure to
397 sulphate solution. The strength loss rate is higher at the end of the 20 weeks exposure at higher
398 w/c ratios. None of the test concrete specimens showed a significant reduction in compressive
399 strength after 4 weeks of exposure to sulphate solution except for the untreated RAC2
400 specimen. Xie et al. [59] examined the effects of sulphate attack on untreated recycled
401 aggregate concrete for up to 40 weeks, the results showed that the RACs exposed to sulphate
402 attack showed higher strength loss by 20% compared RACs without sulphate, after 40 weeks
403 of exposure time. In addition, the RACs started to exhibit a loss in strength after 22 weeks of
404 exposure time. Xie et al. [59] explained these results as the internal pressure caused by the
405 crystallisation of ettringite exceeded the tensile strength capacity of concrete, resulting in
406 internal propagated microcracks and damage. All the treated RACs specimens showed a lesser
407 reduction in the 4 weeks strength compared to the untreated RAC2 specimens. The combined
408 treatments given in SCP+SE specimens showed the lowest reduction in compressive strength
409 after 4 weeks of exposure time compared to the SE and SCP specimens.

410 After 20 weeks of immersion in sulphate solution, all the concrete specimens showed a higher
411 reduction in compressive strength loss compared to the 4 weeks of sulphate attack. Amongst
412 all the concrete specimens, the NAC1 specimens recorded the lowest loss in compressive
413 strength after 20 weeks of exposure to sulphate solution, whereas the RAC2 specimens
414 exhibited the highest strength loss. The results also indicated enhanced sulphate resistance
415 achieved by the treated RACs in terms of strength loss after 20 weeks of sulphate exposure.
416 The SCP+SE showed the lowest reduction in compressive strength after 20 weeks of exposure
417 to sulphate. The enhanced sulphate resistance of the SCP specimens could be explained by the
418 enhanced water absorption due to the pozzolan coated layer formed around the RA surface that
419 filled the micropores and the micro-cracks of RA. The enhanced resistance to sulphate attack
420 of the SE specimens can be attributed to the efficacy of the sand envelope batching technique
421 in reducing the water absorption of RA during mixing, and hence densifying the whole matrix
422 [60].

423 The literature shows that concrete under sulphate exposure exhibited a higher increase in its
424 compressive strength up to 22 to 25 weeks compared to water cured concretes, and then the
425 compressive strength tends to decrease rapidly at later ages of exposure to sulphate. Xie et al.
426 [59] reported about a 10% to 12% higher increase in compressive strength for recycled
427 aggregate concrete exposed to sulphate solution compared with concretes cured in water after
428 22 weeks of curing age. This higher increase in compressive strength can be ascribed due to
429 the pore structure being filled by the expansion products. Nonetheless, this was not observed
430 in the current study and this could be because the present study has only examined the
431 compressive strength loss of the concrete test specimens after 4 weeks and 20 weeks of sulphate
432 attack.

433 **5.4 Microstructure investigations**

434 Figures 10 and 11 show the SEM images of the microstructure of NAC1 and untreated RAC2
435 samples, respectively.

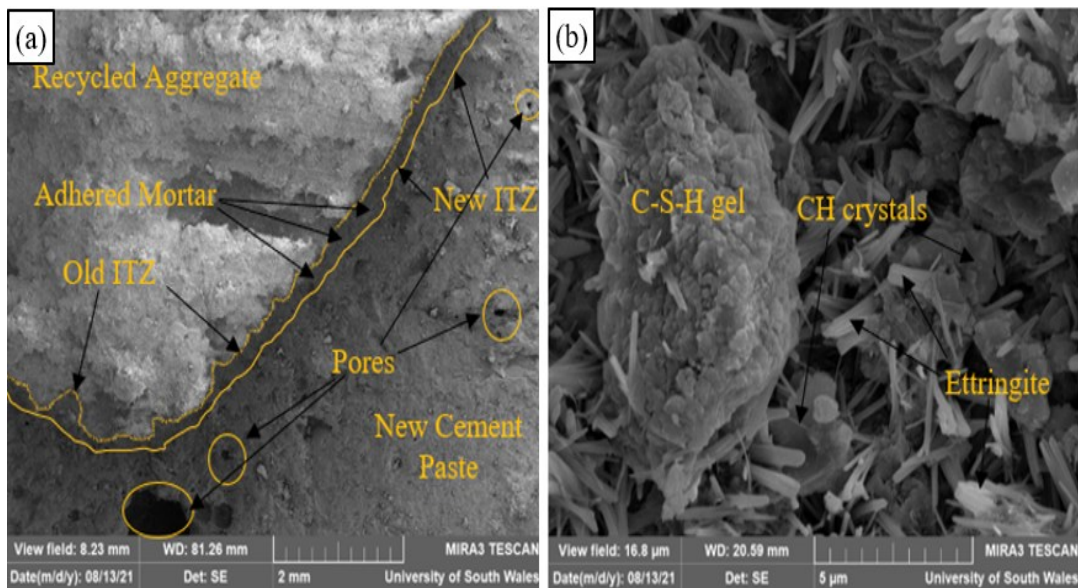


436

437

438

Figure 10: SEM images of NAC1 sample, (a) microstructure of NAC1 sample, (b) SEM image for the hydrated compounds developed in NAC1 sample



439

440

441

Figure 11: SEM images of RAC2 sample, (a) microstructure of RAC2 sample, (b) SEM image for the hydrated compounds developed in RAC2 sample

442

443

444

445

446

447

448

449

450

The SEM observations for the NAC1 specimen revealed that the structure of the NAC1 is a well-formed, dense, and well-compacted structure of the aggregate-cement paste matrix, specifically at the interfacial zones. Whereas the SEM observations for the untreated RAC2 specimens show that the microstructure of the RAC2 specimen is quite different and complicated structure than that of the NAC1 specimen, due to the presence of the adhered mortar on the RA surface which leads to the formation of two interfacial transition zones (ITZ), the first one is between the RA (virgin aggregate) and the adhered mortar and another one between the adhered mortar and the new cement paste. This is in line with the studies of Poon et al. [62], Otsuki et al. [63], and Li et al. [64].

451 The SEM observation for the NAC1 specimen shows that the expansion of crack around the
452 joint boundary between the NA and the cement paste indicates that the constructed cement
453 paste in the designed mix possesses strong coherence and was able to withstand the target load,
454 whilst the SEM observation for RAC2 specimen indicates the appearance of large pores, voids,
455 cavities, and hollow spaces, as well as the presence of the clustered pores, and micro-cracks
456 around the ITZ, indicating that the cement paste was not sufficiently compacted. These porous
457 zones and cavities ultimately weaken the bond between the aggregates and the cement paste,
458 which may possibly explain the lowered strength of RAC2 specimens compared to the NAC1
459 specimen. Similar findings were observed by Poon et al. [62].

460 The old ITZ in the RAC plays a vital role in defining the quality of the RAC compared to the
461 new ITZ. Otsuki et al. [63] stated that at high water to cement ratios, if the characteristics of
462 the old ITZ are better than the new ITZ, the strength of the RAC is comparable to the of NAC,
463 whilst at low water to cement ratios, a weaker old ITZ results in lower strength of RAC
464 compared to NAC. According to Xiao et al. [65], an increase in the ratio of the mechanical
465 properties of the old ITZ (i.e., elastic modulus and strength), leads to higher strength but
466 reduced ductility. Nonetheless, the new ITZ was found to have minimal effects on the
467 properties of the RAC.

468 Accordingly, it can be seen that the old ITZ forms the weakest link in the RAC matrix and
469 results in a more fragile microstructure of RAC due to its porous nature, weak bonding with
470 the new cement paste, the presence of the loose particles, voids, pores, and micro-cracks [66].
471 In addition, the adhered mortar has a lower modulus of elasticity than that of the RA, which
472 results in a lower modulus of elasticity of the RAC compared to NAC [63].

473 The characteristics of ITZ are governed by the quality of the adhered mortar, and the type of
474 aggregate, as it was found to be thicker and better for recycled limestone aggregate than
475 recycled gravel aggregate [65]. It was argued that the old ITZ acts as the weakest link that
476 limits the strength phase in RAC as it forms a barrier wall between the cement paste phase and
477 the RA phase within concrete. It also prevents transferring the loads as the cracks develop first
478 near the ITZ [63].

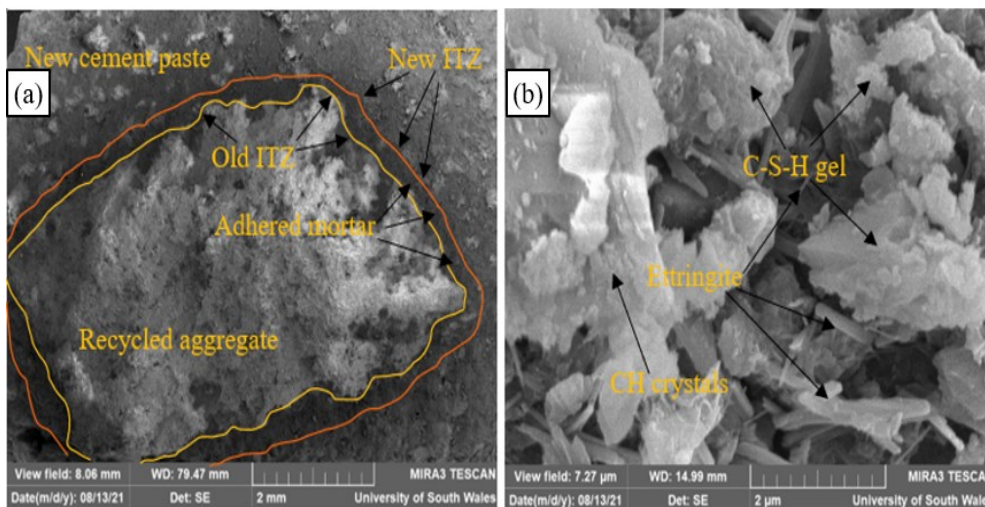
479 Poon et al. [62] pointed out that the ITZ acts as a gradual transition zone in which its thickness
480 is influenced by the degree of hydration and the content of the adhered mortar on the RA
481 surface. Behera et al. [68] argued that the ITZ is highly porous and consists of less unhydrated
482 products, a higher concentration of calcium hydroxide, and ettringite. Behera et al. [68] pointed
483 out that the ITZ is comprised of numerous minute intrinsic pores, voids, micro-cracks, and
484 fissures.

485 According to Thomas et al. [44] and Xiao et al. [65], the porous nature of ITZ leads to lower
486 strength and reduced modulus of elasticity around the surrounded cement paste matrix. The
487 authors added that owing to the very poor microstructure of ITZ, the RAC stiffness is lowered
488 and does not withstand the transferred stresses. Khalaf & DeVenny [69] argued that the cement
489 paste can only partially penetrate the RA surface due to the variation in sizes of the existing
490 pores and cracks on the RA surface, however, water can easily penetrate these pores which
491 explains the higher water absorption of RA.

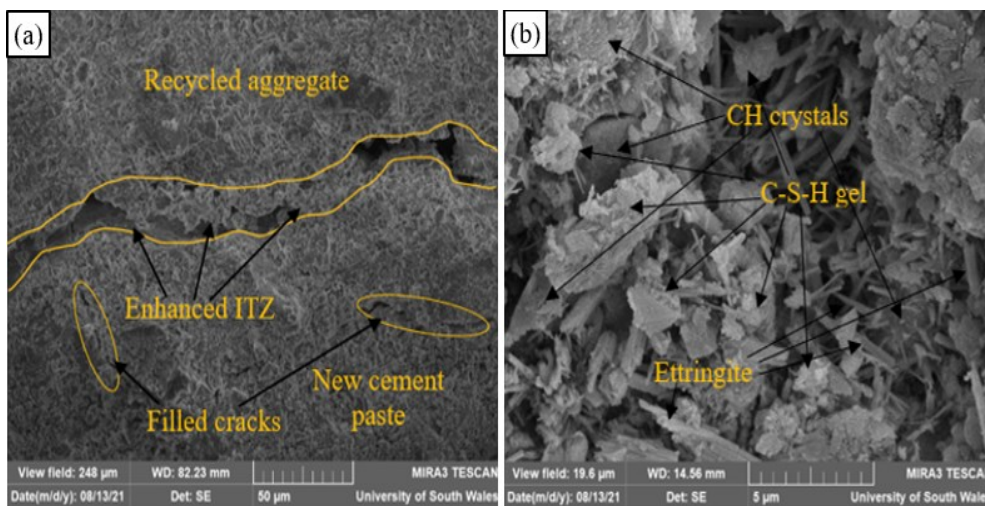
492 Khalaf & DeVenny [69] also stated that several fine flake-like and whisker-like crystals were
493 observed in the pores and voids of the ITZ. Behera et al. [68] revealed that the formed
494 incomplete hydration calcium hydroxide crystals attached to the surface of the RA lead to the
495 development of a highly porous structure in the ITZ as a result of the accumulation of water

496 film in the surrounding area to the RA surface. This may explain the poor durability
 497 performance of the RAC2 specimen, as it is associated with the porous nature of RA, the higher
 498 absorption capacity, and the poor ITZ.

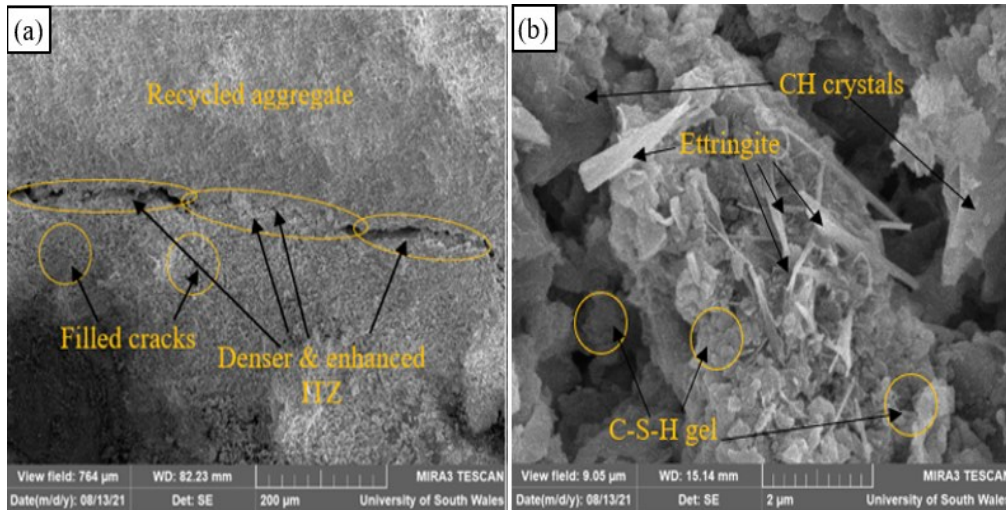
499 Le & Bui [43] observed that there is a gradient of porosity in the ITZ zone, and this porosity
 500 increases from the cement paste to the RA surface. The reason behind this complicated
 501 microstructure can be explained as follows, as the water content increases and the cement
 502 content decreases, at the boundary of the RA. It was also observed that this zone initial
 503 thickness is several dozens of microns. During the curing phase, the thickness of the ITZ
 504 decreases due to the reduced porosity as a result of the formed hydrated products. In addition,
 505 during this phase, a transmission of hydration products occurs between the new cement paste
 506 and the adhered mortar [69]. Figures 12, 13, and 14 show the SEM images of the SE concrete
 507 sample, the SCP concrete sample, and the SCP+SE concrete sample, respectively.



508
 509 Figure 12: SEM images for SE sample, (a) microstructure of SE sample, (b) SEM image for
 510 the hydrated compounds developed in SE sample



511
 512 Figure 13: SEM images for SCP sample, (a) microstructure of SCP sample, (b) SEM image
 513 for the hydrated compounds developed in SCP sample



514
 515 Figure 14: SEM images for SCP+SE sample, (a) microstructure of SCP+SE sample, (b) SEM image
 516 for the hydrated compounds developed in SCP+SE sample

517 The SEM observations for the SE specimen in Figure 12 showed a better-compacted structure
 518 of RAC. It also showed fewer cracks and lesser pores around the ITZ due to the coated RA
 519 with the sand-rich mortar during the initial stage of mixing. The literature showed limited
 520 studies on the microstructure investigations of RAC produced with sand enveloped mixing
 521 approach, nonetheless, Jagan et al. [70] studied the effects of mixing RAC using sand
 522 enveloped mixing approach on the microstructure of RAC. The results of the SEM
 523 investigations showed that the microstructure of RAC was enhanced with lesser cracks and
 524 pores and better bonding behaviour due to the non-porous stiff sand-rich mortar that was
 525 produced in the early stage of the mixing process which covered the RA surface.

526 The SEM observations for the SCP specimen in Figure 13 showed that the ITZ was much
 527 tighter and more compact, the width and number of the micro-cracks were reduced, and the
 528 cement paste was relatively denser, compared to the untreated RAC2 specimen. It was also
 529 observed that the number of pores and voids was reduced which reflects on the reduced
 530 porosity, which was possibly related to the larger amount of calcium silicate hydrates and
 531 calcium hydroxide products that filled the pores and the micro-cracks.

532 The possible reasons behind the microstructure enhancement of RAC (SCP specimen) with
 533 treated RA by coating with cement-PFA+SF solution are as follow, (i) the relatively lower
 534 water to binder ratio of coated layer on the RA surface leads to denser and stronger ITZ, thus
 535 higher strength of RAC, (ii) the use of micro-fillers SF and PFA tend to flocculate due to their
 536 overwhelming specific area and better packing density, (iii) the coated cement- pozzolan layer
 537 on the RA surface forms a barrier that reduces inner bleeding of water, (iv) and the
 538 incorporation of the treated RA in RAC limits the amount of the absorbed effective mixing
 539 water during mixing. This is in line with the study of Wang et al. [71] who treated RA with
 540 cement and fly ash slurry and the results of the SEM observations still showed the presence of
 541 micro-cracks and pores at the ITZ zone, but the micro-cracks were much smaller compared to
 542 the untreated RAC specimen. The authors added that the new ITZ was filled with overlaid
 543 hydration products, the micro-cracks got disappeared and the ITZ was enhanced.

544 The SEM images for the SCP+SE specimen in Figure 14 showed the best enhanced higher
 545 quality microstructure compared to SCP and SE specimens. This is the result of the synergetic
 546 effects of soaking RA in cement-pozzolan solution followed by mixing using sand enveloped

547 mixing approach. The SCP+SE specimen showed the fewest cracks and pores and the densest
 548 ITZ. In addition, the microstructure of the SCP+SE specimen achieved excellent compaction,
 549 and highly strengthened ITZ with excellent interlock and bonding between the RA and the
 550 cement paste.

551 The findings of the microstructure investigations support and validate the durability test results
 552 which demonstrated that the SCP+SE mixes achieved the highest enhancements in water
 553 absorption, freeze-thaw resistance, and sulphate attack. It is worth noting that, no study in the
 554 literature examined the microstructure investigations of RAC produced with treated RA by
 555 soaking in cement-PFA+SF solution combined with sand enveloped mixing approach.

556

557

558

559

560 6. Cost analysis

561 Several factors play significant role in promoting the use of recycled aggregate in the
 562 construction industry in comparison with natural aggregate. These are cost efficiency,
 563 environmental impact, performance, sustainability, and durability. Table 7 shows the price
 564 breakdown per concrete mix. It is clearly notable that the untreated RAC mix have a lower
 565 carbon footprint and lower price per cubic meter compared to NAC. Nevertheless, based on
 566 the durability performance in this study, the untreated RAC exhibited poor durability properties
 567 compared to NAC. Therefore, there was a need to carry out treatment/ enhancement methods
 568 in order to enhance the quality of RAC. However, several factors should be considered when
 569 selecting the type of the enhancement methods. As shown in Table 7, soaking RA in cement-
 570 pozzolan solution prior to mixing (SCP mix) increased the cost and the associated carbon
 571 footprint of the end product by 93% and 17%, respectively, compared to the untreated RAC.
 572 In the contrary, the utilization of sand envelop batching technique (SE mix) kept the same cost
 573 and the same carbon footprint compared to the untreated RAC.

574 Table 7: Price breakdown of the different concrete mixes and the associated embodied carbon
 575 dioxide footprint

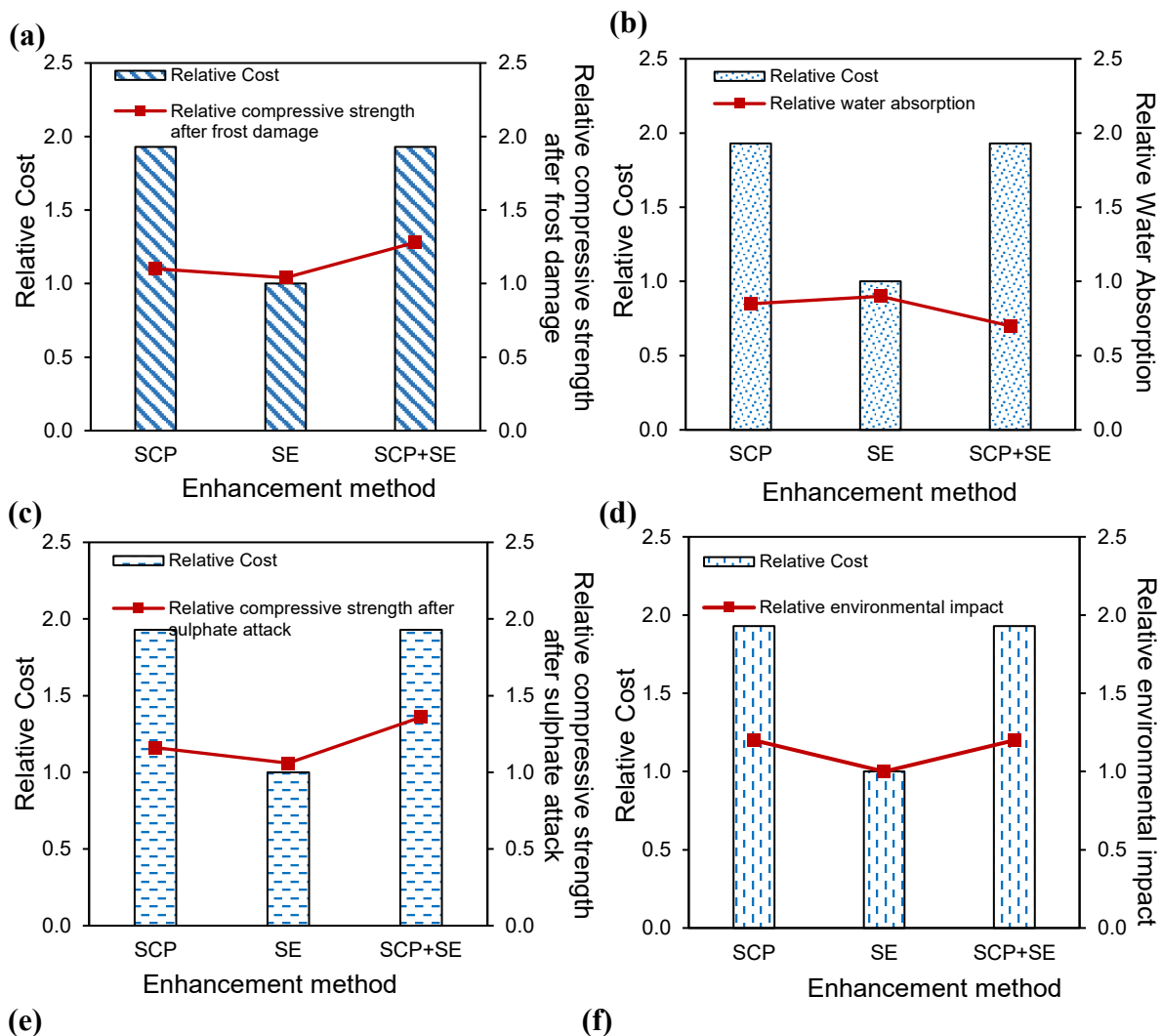
Mix	Constituent						Concrete cost (£/m ³) ^a	Cost /NAC1	Cost/ RAC2	kg CO _{2e} / m ³ concrete ^b
	OPC	PFA	SF	NA	Sand	RA				
Estimated Price (£/t)	150	650	550	40	40	15	-	-	-	-
NAC1 (£/m ³)	67	-	-	58	27	-	152	100%	-	450
RAC2 (£/m ³)	67	-	-	-	27	19	113	74%	100%	437
SCP (£/m ³)	83	48	41	-	27	19	218	143%	193%	530
SE (£/m ³)	67	-	-	-	27	19	113	74%	100%	437
SCP+SE (£/m ³)	83	48	41	-	27	19	218	143%	193%	530

576 ^a Tentative price for each concrete ingredient including SF and PFA were obtained from
 577 searching through trading local suppliers.

578 ^b The estimated embodied carbon footprint was calculated based on the data given in [72] and
 579 excluding transportation.

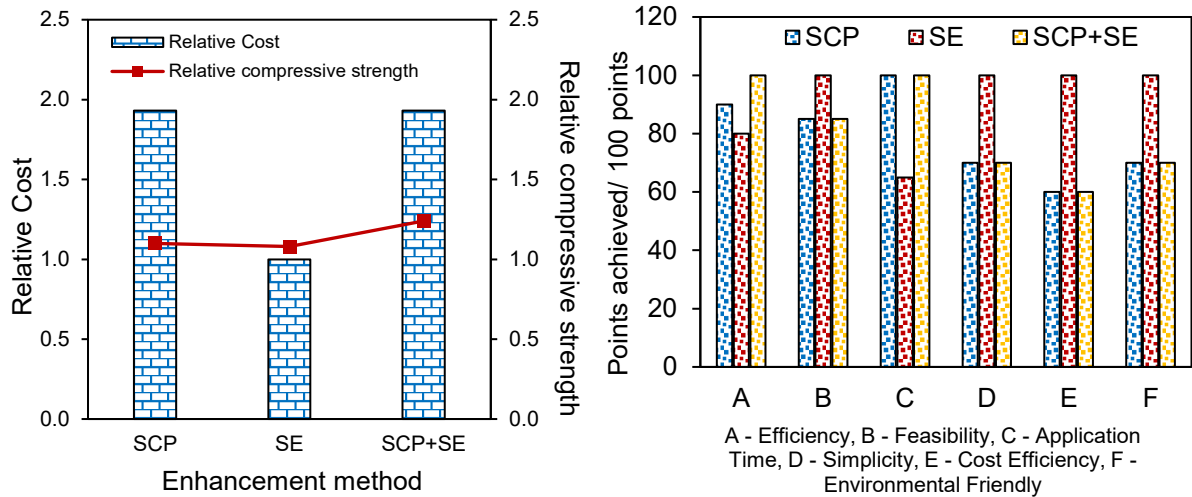
580 Figure 8 shows the cost analysis of the various enhancement methods against different factors
 581 related to untreated RAC. It can be seen the use of bi-combination of enhancement methods
 582 (SCP+SE) obtained the best performance in terms of durability properties and compressive
 583 strength at 28-days. Nevertheless, the sole use of batching technique (SE) seemed a better
 584 choice in terms of other influencing factors such as cost efficiency, carbon dioxide footprint,
 585 simplicity, application time, and feasibility.

586 In view of this discussion, it is quite important to consider the cost-efficiency, sustainability,
 587 and efficiency of enhancement method for RA and RAC. Although treatments such as soaking
 588 RA in cement-pozzolan may increase the cost and CO₂ emission for RAC, it is still a better
 589 choice compared to other treatments utilized by other researchers [9]. To this end, in order to
 590 successfully promote the use of RA in the construction industry, several factors should be
 591 considered specifically the feasibility of the treatment method to be used in practice at bulk
 592 production.



593

594



595

596 Figure 15: Cost analysis of the various enhancement methods: (a) cost vs. compressive
 597 strength after 20 cycles of freezing-thawing, (b) cost vs. water absorption, (c) cost vs.
 598 compressive strength after exposure to sulphate attack, (d) cost vs. environmental impact, (e)
 599 cost vs. 28-day compressive strength, (f) other influencing factors.

600

601

602 7. Conclusions

603 Concrete with untreated recycled aggregate demonstrated low-quality durability performance
 604 compared to natural aggregate concrete due to several factors. Two of the main factors are the
 605 weak porous adhered mortar on the RA surface and the old weak interfacial transition zone
 606 which resulted in a weak interfacial transition zone and weak bonding within the recycled
 607 aggregate concrete matrix. Other concerns include variation in composition, previous loading,
 608 processing, and weathering compared to freshly crushed natural aggregates. This paper has
 609 presented laboratory-based investigations on the effects of different enhancement methods on
 610 the durability properties of concretes with untreated RA and treated RA. The following specific
 611 conclusions can be drawn:

612 1. **Recycled aggregate concrete with untreated RA:** RAC with untreated RA showed poor
 613 durability performance in terms of water absorption, resistance to freeze-thaw cycles, and
 614 sulphate attack compared to NAC. This was ascribed mainly to the lower quality of the
 615 untreated RA, the high-water absorption of the untreated RA, the presence of micro-pores,
 616 cavities, micro-cracks, and the poor quality of the old ITZ in the RAC with untreated RA. The
 617 microstructure of the RAC had two ITZs whereas the microstructure of the NAC had one ITZ.
 618 The SEM images have also indicated that the microstructure of the RAC with untreated RA
 619 was poorly compacted with obvious pores, cavities, microcracks, and weak bonding between
 620 the RA and the new cement paste.

621 2. **Soaking RA in cement-PFA+SF solution (SCP):** RAC with treated RA by the SCP
 622 method achieved enhanced water absorption compared to RAC with untreated RA. The SCP
 623 enhanced the resistance to freeze-thaw and sulphate attack showing reduced mass losses/gains
 624 and lower strength losses compared to the untreated RAC. This was mainly due to the enhanced
 625 water absorption through the effects of the SCP treatment in filling and sealing the pores and
 626 the micro-cracks on the RA surface. The SEM images observed for the SCP specimen showed

627 a better microstructure compared to the untreated RAC. The SCP specimen exhibited better-
628 compacted microstructure, lesser pores and microcracks, denser ITZ, and better interlocking
629 behaviour between the RA and the cement paste.

630 3. **Sand envelope mixing approach (SE):** the sole use of this batching technique also
631 demonstrated enhanced water absorption, resistance to freezing-thawing, and enhanced
632 resistance to sulphate attack. The enhancement observed in the durability properties of the SE
633 mixe can be ascribed to the use of this batching technique (SE) which stems from allowing the
634 sand particles in the mixture to mix more readily with water and cement. This resulted in
635 covering the RA with premixed cement/ mortar slurry that filled up the cracks and pores of
636 RAC, hence enhancing its resistance to water absorption and ultimately improving the
637 durability performance. The sole use of the sand enveloped mixing approach has also led to a
638 better compacted and formed microstructure, but the presence of the voids and micro-cracks
639 was more evident compared to the SCP specimen.

640 4. **Bi-combination of SCP+SE:** the combination of treating RA by soaking in cement-
641 PFA+SF solution followed by mixing using sand envelop batching technique achieved higher
642 durability performance compared to the sole use of the SCP and SE methods. The combination
643 of the SCP+SE treatment resulted in the most desired microstructure of the RAC. The
644 synergetic effects of these two treatments led to a relatively stronger and compacted
645 microstructure with the fewest pores and microcracks, stronger and denser ITZs.

646 5. **Cost analysis:** several factors may influence the selection of the best treatment methods.
647 The efficiency, cost-effectiveness, feasibility, and the environmental impact are the most
648 influence factors that should be carefully considered prior to application of any treatment.

649 **Declaration of Competing Interest**

650 The authors declare that they have no known competing financial interests or personal
651 relationships that could have appeared to influence the work reported in this paper.

652 **Funding**

653 This research did not receive any specific grant from funding agencies in the public,
654 commercial, or non-profit sectors.

655 **REFERENCES**

- 656 [1] Kim, J., 2022. Influence of quality of recycled aggregate on the mechanical properties
657 of recycled aggregate concrete: An overview. *Construction and Building Materials*,
658 Volume 328m P. 127071. <https://doi.org/10.1016/j.conbuildmat.2022.127071>
- 659 [2] Lu, W., 2019. Big data analytics to identify illegal construction waste dumping: A Hong
660 Kong study. *Resources, Conservation and Recycling*, Volume 141, pp. 264-272.
661 <https://doi.org/10.1016/j.resconrec.2018.10.039>
- 662 [3] Tam, V., Soomro, M. & Evangelista, A., 2018. A review of recycled aggregate in
663 concrete applications (2000-2017). *Construction and Building Materials*, Volume 172,
664 pp. 272-292. <https://doi.org/10.1016/j.conbuildmat.2018.03.240>
- 665 [4] Silva, R., Brito, J. & Dhir, R., 2014. Properties and composition of recycled
666 aggregates from construction and demolition waste suitable for concrete production.

- 667 *Construction and Building Materials*, Volume 65, pp. 201-217.
668 <https://doi.org/10.1016/j.conbuildmat.2014.04.117>
- 669 [5] Tam, V., 2009. Comparing the implementation of concrete recycling in the Australian
670 and Japanese construction industries. *Journal of Cleaner Production*, 17(7), pp. 688-
671 702. <https://doi.org/10.1016/j.jclepro.2008.11.015>
- 672 [6] Grabiec, A., Zawal, D. & Rasaq, W., 2020. The Effect of Curing Conditions on Selected
673 Properties of Recycled Aggregate Concrete. *Applied Sciences*, Volume 10, pp. 1-15.
674 DOI: 10.3390/app10134441
- 675 [7] Al Ajmani, H., Suleiman, F., Abuzayed, I. & Tamimi, A., 2019. Evaluation of Concrete
676 Strength Made with Recycled Aggregate. *Buildings*, Volume 9, pp. 1-14,
677 <https://doi.org/10.3390/buildings9030056>.
- 678 [8] Vieira, G. et al., 2020. Influence of recycled aggregate replacement and fly ash content
679 in performance of pervious concrete mixtures. *Journal of Cleaner Production*, Volume
680 271, p. 122665, <https://doi.org/10.1016/j.jclepro.2020.122665>.
- 681 [9] Bahraq, Ashraf; Jose, Jobin; Shameem, Mohammed; Maslehuiddin, Mohammed, 2022.
682 A review on treatment techniques to improve the durability of recycled aggregate
683 concrete: Enhancement mechanisms, performance, and cost analysis. *Journal of*
684 *Building Engineering*, Volume 55, p. 104713,
685 <https://doi.org/10.1016/j.jobe.2022.104713>
- 686
- 687 [10] Etxeberria, M., Vazquez, E., Mari, A. & Barra, M., 2007. Influence of amount
688 of recycled coarse aggregates and production process on properties of recycled
689 aggregate concrete. *Cement and Concrete Research*, 37(5), pp. 735-742,
690 <https://doi.org/10.1016/j.cemconres.2007.02.002>.
- 691 [11] Guo, H. et al., 2018. Durability of recycled aggregate concrete - A review.
692 *Cement and Concrete Composites*, Volume 89, pp. 251-259.
693 <https://doi.org/10.1016/j.cemconcomp.2018.03.008>
- 694 [12] Al-Bayati, H., Das, P., Tighe, S. & Baaj, H., 2016. Evaluation of various
695 methods for enhancing the physical and morphological properties of coarse recycled
696 concrete aggregate. *Construction and Building Materials*, Volume 112, pp. 284-298,
697 <https://doi.org/10.1016/j.conbuildmat.2016.02.176>.
- 698 [13] Bru, K. et al., 2014. Assessment of a microwave-assisted recycling process for
699 the recovery of high-quality aggregates from concrete waste. *International Journal of*
700 *Mineral Processing*, Volume 126, pp. 90-98,
701 <http://doi.org/10.1016/j.minpro.2013.11.009>.
- 702 [14] Gonzalez-Corominas, A. & Etxeberria, M., 2014. Properties of high-
703 performance concrete made with recycled fine ceramic and coarse mixed aggregates.
704 *Construction and Building Materials*, Volume 68, pp. 618-626.
705 <http://doi.org/10.1016/J.CONBUILDMAT.2014.07.016>
- 706 [15] Kou, S. & Poon, C., 2012. Enhancing the durability properties of concrete
707 prepared with coarse recycled aggregate. *Construction and Building Materials*, Volume
708 35, pp. 69-76. <https://doi.org/10.1016/j.conbuildmat.2012.02.032>.
- 709 [16] Grabiec, A., Klama, J., Zawal, D. & Krupa, D., 2012. Modification of recycled
710 concrete aggregate by calcium carbonate bio-deposition. *Construction and Building*
711 *Materials*, Volume 34, pp. 145-150.
712 <https://doi.org/10.1016/j.conbuildmat.2012.02.027>.

- 713 [17] Chen, J., Thomas, J. & Jennings, H., 2006. Decalcification shrinkage of cement
714 paste. *Cement and Concrete Research*, 36(5), pp. 801-809.
715 <http://doi.org/10.1016/j.cemconres.2005.11.003>
- 716 [18] Shaban, W., Yang, J., Su, H., Mo, K., Li, J., Xie, J., 2019. Quality Improvement
717 Techniques for Recycled concrete Aggregate: A review. *Journal of Advanced Concrete*
718 *Technology*, Volume 17, pp. 151-167, <https://doi.org/10.3151/jact.17.151>.
- 719 [19] Kou, S., Zhan, B. & Poon, C., 2014. Use of a CO₂ curing step to improve the
720 properties of concrete prepared with recycled aggregates. *Cement and Concrete*
721 *Composites*, Volume 45, pp. 22-28.
722 <https://doi.org/10.1016/j.cemconcomp.2013.09.008>
- 723 [20] Li, J., Xiao, H. & Zhou, Y., 2009. Influence of coating recycled aggregate
724 surface with pozzolanic powder on properties of recycled aggregate concrete.
725 *Construction and Building Materials*, 23(3), pp. 1287-1291.
726 <https://doi.org/10.1016/j.conbuildmat.2008.07.019>.
- 727 [21] Tam, V., Tam, C. & Wang, Y., 2007. Optimization on proportion for recycled
728 aggregate in concrete using two-stage mixing approach. *Construction and Building*
729 *Materials*, 21(10), pp. 1928-1939. <https://doi.org/10.1016/j.conbuildmat.2006.05.040>
- 730 [22] Liang, Y., Ye, Z., Vernerey, F. & Xi, Y., 2015. Development of processing
731 methods to improve strength of concrete with 100% recycled coarse aggregate. *Journal*
732 *of Materials in Civil Engineering*, 27(5), p. 130801045339002,
733 [http://doi.org/10.1061/\(ASCE\)MT.1943-5533.0000909](http://doi.org/10.1061/(ASCE)MT.1943-5533.0000909).
- 734 [23] Kazmi, Syed; Munir, Muhammad; Wu, Yu-Fei; Patnaikuni, Indubhushan;
735 Zhou, Yingwu; Xing, Feng, 2020. Effect of recycled aggregate treatment techniques on
736 the durability of concrete: A comparative evaluation. *Construction and Building*
737 *Materials*, Volume 264, p. 120284, <https://doi.org/10.1016/j.conbuildmat.2020.120284>
- 738 [24] Al-Waked, Qusai; Bai, Jiping; Kinuthia, John; Davies, Paul, 2022. Enhancing
739 the aggregate impact value and water absorption of demolition waste coarse aggregates
740 with various treatment methods. *Case studies in construction materials*, volume 17, p.
741 e01267, <https://doi.org/10.1016/j.cscm.2022.e01267>
- 742 [25] British Standards Institution. BS EN 12620:2002+A1:2008—Aggregates for
743 Concrete; British Standards Institution: London, UK, 2008.
- 744 [26] British Standards Institution. BS EN 13242:2013—Aggregates for unbound and
745 hydraulically bound materials for use in civil engineering work and road construction;
746 British Standards Institution: London, UK, 2013.
- 747 [27] Derwen, 2016. Recycled Aggregate. [Online] Available at:
748 <https://www.derwengroup.co.uk> [Accessed 10 February 2022].
- 749 [28] British Standards Institution. BS 8500-2:2015 +A2: 2019—Concrete-
750 Complementary British Standard to BS EN 206. Part 2: Specification for constituent
751 materials and concrete; British Standards Institution: London, UK, 2019.
- 752 [29] British Standards Institution. BS EN 933-1:2012—Tests for geometrical
753 properties of aggregates. Part 1: Determination of particle size distribution—Sieving
754 method; British Standards Institution: London, UK, 2012.
- 755 [30] Munir, Muhammad; Kazmi, Syed; Wu, Yu-Fei; Patnaikuni, Indubhushan; Wang,
756 Junfeng; Wang, Quan, 2020. Development of a unified model to predict the axial stress-
757 strain behavior of recycled aggregate concrete confined through spiral reinforcement.
758 *Engineering Structures*, Volume 218, P. 110851,
759 <https://doi.org/10.1016/j.engstruct.2020.110851>

- 760 [31] British Standards Institution. BS EN 933-3: 2012—Tests for geometrical
761 properties of aggregates. Part 3: Determination of particle shape—Flakiness index;
762 British Standards Institution: London, UK, 2012.
- 763 [32] British Standards Institution. BS EN 933-4:2008—Tests for Geometrical
764 Properties of Aggregates. Part 4: Determination of Particle Shape—Shape Index;
765 British Standards Institution: London, UK, 2008.
- 766 [33] British Standards Institution. BS EN 1097-6:2013—Tests for Mechanical and
767 Physical Properties of Aggregates. Part 6: Determination of Particle Density and Water
768 Absorption; British Standards Institution: London, UK, 2013.
- 769 [34] British Standards Institution. BS EN 1097-2:2020—Tests for mechanical and
770 physical properties of aggregates. Part 2: Methods for determination of resistance to
771 fragmentation; British Standards Institution: London, UK, 2020.
- 772 [35] British Standard Institution. BS EN 197-1:2011 - Cement. Composition,
773 specifications and conformity criteria for common cements; British Standard
774 Institution: London, UK, 2011.
- 775 [36] British Standard Institution. BS EN 450-1:2012 – Fly ash for concrete. Part 1:
776 Definition, specifications and conformity criteria; British Standard Institution: London,
777 UK, 2012.
- 778 [37] British Standard Institution. BS EN 13263-2:2005+A1:2009 – Silica fume for
779 concrete. Part 2: conformity evaluation; British Standard Institution: London, UK,
780 2009.
- 781 [38] British Standards Institution. BS EN 206:2013+A1:2016: Concrete.
782 Specification, performance, production and conformity; British Standards Institution:
783 London, UK, 2016.
- 784 [39] British Standards Institution. BS EN 12390-2:2009: Testing hardened concrete.
785 Making and curing specimens for strength tests; British Standards Institution: London,
786 UK, 2009.
- 787 [40] PD CEN/TS 12390-9. Testing hardened concrete. Part 9: Freeze-thaw resistance
788 with de-icing salts - Scaling. 2016
- 789 [41] British Standards Institution. BS 1881-122:2011+A1:2020: Testing concrete.
790 Method for determination of water absorption; British Standards Institution: London,
791 UK, 2020.
- 792 [42] British Standards Institution. BS EN 206:2013+A2:2021: Concrete.
793 Specification, performance, production and conformity; British Standards Institution:
794 London, UK, 2021.
- 795 [43] Le, H.-B. & Bui, Q.-B., 2020. Recycled aggregate concretes - A state-of-the-art
796 from the microstructure to the structural performance. *Construction and Building*
797 *Materials*, Volume 257, p. 119522. <https://doi.org/10.1016/j.conbuildmat.2020.119522>
- 798 [44] Thomas, C., Setien, J., Polanco, J., Alaejos, P., Juan, M., 2013. Durability of
799 RAC. *Construction and Building Materials*, Volume 40, pp. 1054-1065.
800 <https://doi.org/10.1016/j.conbuildmat.2012.11.106>
- 801 [45] Lotfi, S., Eggimann, M., Wagner, E., Mroz, R., Deja, J., 2015. Performance of
802 RAC based on a new concrete recycling technology. *Construction and Building*
803 *Materials*, Volume 95, pp. 243-256. <https://doi.org/10.1016/j.conbuildmat.2015.07.021>
- 804 [46] Debieb, F., Courard, L., Kenai, S. & Degimbre, R., 2010. Roller compacted
805 concrete with contaminated RAs. *Construction and Building Materials*, 23(11), pp.
806 3382-3387. <https://doi.org/10.1016/j.conbuildmat.2009.06.031>

- 807 [47] Kwan, W. H., Ramli, M., Kam, K. J. & Sulieman, M., 2012. Influence of the
808 amount of recycled coarse aggregate in concrete design and durability properties.
809 *Construction and Building Materials*, Volume 26, pp. 565-573.
810 <https://doi.org/10.1016/j.conbuildmat.2011.06.059>
- 811 [48] Tam, V., Tam, C. & Le, K., 2007. Removal of cement mortar remains from
812 recycled aggregate using pre-soaking approaches. *Resources, Conservation, and*
813 *Recycled*, 50(1), pp. 82-101. <https://doi.org/10.1016/j.resconrec.2006.05.012>
- 814 [49] Wang, B., Yan, L., Fu, Q. & Kasal, B., 2021. A Comprehensive Review on
815 Recycled Aggregate and Recycled Aggregate Concrete. *Resources, Conservation and*
816 *Recycling*, Volume 171, p. 105565, <https://doi.org/10.1016/j.resconrec.2021.105565>.
- 817 [50] Salem, R., Burdette, E. & Jackson, N., 2003. Resistance to freezing and thawing
818 of recycled aggregate concrete. *ACI Materials Journal*, 1100(3), pp. 216-221.
- 819 [51] Kazmi, S., Munir, M., Wu, Y., Patnaikuni, I., Zhou, Y., Xing, F., 2020. Effect
820 of different aggregate treatment techniques on the freeze-thaw and sulfate resistance of
821 recycled aggregate concrete. *Cold Regions Science and Technology*, Volume 178, pp.
822 103-126. <https://doi.org/10.1016/j.coldregions.2020.103126>
- 823 [52] Wu, C.-R., Zhu, Y.-G., Zhang, X.-T. & Kou, S.-C., 2017. Improving the
824 properties of recycled concrete aggregate with bio-deposition approach. *Cement and*
825 *Concrete composites*, Volume 94, pp. 248-254.
826 <https://doi.org/10.1016/j.cemconcomp.2018.09.012>
- 827 [53] Kisku, N. et al., 2017. A critical review and assessment for usage of recycled
828 aggregate as sustainable construction material. *Construction and Building Materials*,
829 Volume 131, pp. 721-740. <https://doi.org/10.1016/j.conbuildmat.2016.11.029>
- 830 [54] Mullauer, W., Beddoe, R. & Heinz, D., 2013. Sulphate attack expansion
831 mechanisms. *Cement and Concrete Research*, Volume 52, pp. 208-215.
832 <https://doi.org/10.1016/j.cemconres.2013.07.005>
- 833 [55] Bizzozero, J., Gosselin, C. & Scrivener, K., 2014. Expansion mechanisms in
834 calcium aluminate and sulfoaluminate systems with calcium sulfate. *Cement and*
835 *Concrete Research*, Volume 56, pp. 190-202.
836 <https://doi.org/10.1016/j.cemconres.2013.11.011>
- 837 [56] Zuo, X., Sun, W. & Yu, C., 2012. Numerical investigation on expansive volume
838 strain in concrete subjected to sulfate attack. *Construction and Building Materials*,
839 36(4), pp. 404-410. <https://doi.org/10.1016/j.conbuildmat.2012.05.020>
- 840 [57] Euml, R., Tixier, L. & Mobasher, B., 2003. Modeling of damage in cement-
841 based materials subjected to external sulfate attack. I: formulation. *Journal of Materials*
842 *and Civil Engineering*, 15(4), pp. 305-313. [https://doi.org/10.1061/\(ASCE\)0899-1561\(2003\)15:4\(305\)](https://doi.org/10.1061/(ASCE)0899-1561(2003)15:4(305))
- 844 [58] Rozière, E., loukili, A., El Hachem, R. & Grondin, F., 2009. Durability of
845 concrete exposed to leaching and external sulphate attack. *Cement and Concrete*
846 *Research*, 39(12), pp. 1188-1198. <https://doi.org/10.1016/j.cemconres.2009.07.021>
- 847 [59] Xie, F., Li, J., Zhao, G., Zhou, G., Zheng, H., 2020. Experimental study on
848 performance of cast-in-situ recycled aggregate concrete under different sulfate attack
849 exposures. *Construction and Building Materials*, Volume 253, p. 119144.
850 <https://doi.org/10.1016/j.conbuildmat.2020.119144>

- 851 [60] Wang, J. et al., 2017. Microbial carbonate precipitation for the improvement of
852 quality of recycled aggregates. *Journal of Cleaner Production*, Volume 156, pp. 355-
853 366. <https://doi.org/10.1016/j.jclepro.2017.04.051>
- 854 [61] Kazmi, S., Munir, M., Wu, Y., Patnaikuni, I., Zhou, Y., Xing, F., 2019.
855 Influence of different treatment methods on the mechanical behavior of recycled
856 aggregate concrete: a comparative study. *Cement and Concrete Composites*, Volume
857 104, p. 103398. <https://doi.org/10.1016/j.cemconcomp.2019.103398>
- 858 [62] Poon, C., Shui, Z. & Lam, L., 2004. Effect of microstructure of ITZ on
859 compressive strength of concrete prepared with RAs. *Construction and Building*
860 *Materials*, 18(6), pp. 461-468. <https://doi.org/10.1016/j.conbuildmat.2004.03.005>
- 861 [63] Otsuki, N., Miyazato, S. & Yodsudjai, W., 2003. Influence of recycled
862 aggregate on interfacial transition zone, strength chloride penetration and carbonation
863 of concrete. *Journal of Materials in Civil Engineering*, 15(5), pp. 443-451.
864 [https://doi.org/10.1061/\(ASCE\)0899-1561\(2003\)15:5\(443\)](https://doi.org/10.1061/(ASCE)0899-1561(2003)15:5(443))
- 865 [64] Li, W., Ziao, J., Sun, Z., Kawashima, S., Shah, S., 2012. Interfacial transition
866 zones in RAC with different mixing approaches. *Construction and Building Materials*,
867 Volume 35, pp. 1045-1055. <https://doi.org/10.1016/j.conbuildmat.2012.06.022>
- 868 [65] Xiao, J., Li, W., Fan, Y. & Huang, X., 2013. An overview of study on recycled
869 aggregate concrete in China (1996-2011). *Construction and Building Materials*,
870 Volume 31, pp. 364-383, <https://doi.org/10.1016/j.conbuildmat.2011.12.074>.
- 871 [66] Nayak, S. & Dutta, S. C., 2017. A critical review and assessment for usage of
872 recycled aggregate as sustainable construction material. *Construction and Building*
873 *Materials*, pp. 721-740. <https://doi.org/10.1016/j.conbuildmat.2016.11.029>
- 874 [67] Khalaf, F. & DeVenny, A., 2004. Recycling of demolished masonry rubble as
875 coarse aggregate in concrete: review. *Journal of Materials in Civil Engineering*, 16(4),
876 pp. 331-340. [http://dx.doi.org/10.1061/\(ASCE\)0899-1561](http://dx.doi.org/10.1061/(ASCE)0899-1561)
- 877 [68] Behera, M. et al., 2014. Recycled aggregate from C&D waste & its use in
878 concrete - A breakthrough towards sustainability in construction sector: A review.
879 *Construction and Building Materials*, Volume 68, pp. 501-516,
880 <https://doi.org/10.1016/j.conbuildmat.2014.07.003>.
- 881 [69] Kjellsen, K., Wallevik, O. & Fjalberg, L., 1998. Microstructure and
882 microchemistry of the paste-aggregate interfacial transition zone of high-performance
883 concrete. *Advance in Cement Research*, Volume 10, pp. 33-40.
884 <https://doi.org/10.1680/adcr.1998.10.1.33>
- 885 [70] Jagan, S., Neelakantan, T. & Saravanakumar, P., 2021. Mechanical properties
886 of recycled aggregate concrete surface treated by variation in mixing approaches.
887 *Journal of Construction*, 20(2), pp. 236-249. <http://doi.org/10.1108/wje-02-2021-0089>
- 888 [71] Wang, B., Yan, L., Fu, Q. & Kasal, B., 2021. A Comprehensive Review on
889 Recycled Aggregate and Recycled Aggregate Concrete. *Resources, Conservation and*
890 *Recycling*, Volume 171, p. 105565, <https://doi.org/10.1016/j.resconrec.2021.105565>.
- 891 [72] ICE. (2019, November 10). Concrete Embodied Carbon Footprint Calculator.
892 Retrieved from Circular ecology: [https://www.circularecology.com/embodied-carbon-](https://www.circularecology.com/embodied-carbon-footprint-database.html)
893 [footprint-database.html](https://www.circularecology.com/embodied-carbon-footprint-database.html)